



DEPARTMENT OF HEALTH & HUMAN SERVICES

Public Health Service

Food and Drug Administration
Rockville, MD 20857

February 28, 2022

Kathryn Blankenberg
Paul J. Orfanedes
Judicial Watch, Inc.
425 Third Street SW
Suite 800
Washington, DC 20024

Sent via email: kblankenberg@judicialwatch.org
porfanedes@judicialwatch.org

Re: FDA FOIA Request 2021-4379; *Judicial Watch, Inc. v. U.S. Department of Health and Human Services*, 21-cv-2418

Dear Ms. Blankenberg and Mr. Orfanedes,

This is a partial response to the Freedom of Information Act (FOIA) request number **2021-4379** that is the subject of the Complaint filed in *Judicial Watch, Inc. v. U.S. Department of Health and Human Services*, 21-cv-2418, now pending in the U.S. District Court for the District of Columbia.

Enclosed are 466 pages of records, some of which contain redaction. Please note, the pages with Bates numbers FDA-CBER-2021-4379-0000752 to -0000753 and FDA-CBER-2021-4379-0000931 to -0000932 contain what appears to be blacked out content; these markings were in the records received by FDA and are not redactions made by FDA.

We have withheld portions of pages under Exemption (b)(4), 5 U.S.C. § 552(b)(4). That exemption permits the withholding of trade secrets and commercial or financial information that was obtained from a person outside the government and that is privileged or confidential.

In addition, we have withheld portions of pages under Exemption (b)(6), 5 U.S.C. § 552(b)(6). That exemption protects information from disclosure when its release would cause a clearly unwarranted invasion of personal privacy. FOIA Exemption 6 is available to protect information in personnel or medical files and similar files. This requires a balancing of the public's right to disclosure against the individual's right to privacy.

Please direct any questions regarding this response to Jonathan Silberman, Associate Chief Counsel, Food and Drug Administration, telephone number (240) 731-9982 or email Jonathan.Silberman@fda.hhs.gov.

Sincerely,

Beth Brockner Ryan
Chief, Access Litigation and Freedom of Information Branch
Division of Disclosure and Oversight Management
Office of Communication Outreach and Development
Center for Biologics Evaluation and Research

Enclosure(s)

2.4 NONCLINICAL OVERVIEW

090177e1962c108d\Approved\Approved On: 08-Feb-2021 15:26 (GMT)

CONFIDENTIAL

Page 1

FDA-CBER-2021-4379-0000664

TABLE OF CONTENTS

2.4 NONCLINICAL OVERVIEW 1

 LIST OF ABBREVIATIONS AND DEFINITION OF TERMS 4

 2.4.1. OVERVIEW OF NONCLINICAL TESTING STRATEGY 6

 Table 2.4.1-1. Nomenclature of the Vaccine Candidates 6

 Table 2.4.1-2. Nonclinical Studies 8

 2.4.2. PHARMACOLOGY10

 2.4.2.1. Primary Pharmacodynamics10

 2.4.2.1.1. Summary10

 2.4.2.1.2. BNT162b2, A Lipid Nanoparticle Encapsulated RNA Vaccine Encoding the SARS-CoV-2 P2 S as a Vaccine Antigen.....10

 Figure 2.4.2-1. Schematic of the Organization of the SARS-CoV-2 S Glycoprotein11

 2.4.2.1.3. Immunogenicity of BNT162b2 (V9) in Mice11

 2.4.2.1.4. Evaluation of BNT162b2 (V9) Immunogenicity and Protection Against SARS-CoV-2 Challenge in Rhesus Macaques.....12

 2.4.2.1.5. Immunogenicity Testing After Weekly Immunization of Rats in GLP Compliant Repeat Dose Toxicology Studies and a Developmental and Reproductive Toxicity Study..... 13

 2.4.2.2. Secondary Pharmacodynamics 14

 2.4.2.3. Safety Pharmacology 14

 2.4.2.4. Pharmacodynamic Drug Interactions 14

 2.4.3. PHARMACOKINETICS 15

 2.4.3.1. Brief Summary 15

 2.4.3.2. Methods of Analysis 15

 2.4.3.3. Absorption 16

 2.4.3.3.1. In Vitro Absorption 16

 2.4.3.3.2. Single-Dose Pharmacokinetics 16

 Table 2.4.3-1. PK of ALC-0315 and ALC-0159 in Wistar Han Rats After IV Administration of LNPs Containing Surrogate Luciferase RNA at 1 mg/kg..... 16

 Figure 2.4.3-1. Plasma and Liver Concentrations of ALC-0315 and ALC-0159 in Wistar Han Rats After IV Administration of LNPs Containing Surrogate Luciferase RNA at 1 mg/kg..... 16

 2.4.3.4. Distribution 17

 Figure 2.4.3-2. Bioluminescence Emission in BALB/c Mice after IM Injection of an LNP Formulation of modRNA Encoding Luciferase..... 17

090177e1962c108d\Approved\Approved On: 08-Feb-2021 15:26 (GMT)

2.4.3.5. Metabolism 18

Figure 2.4.3-3. Proposed Biotransformation Pathway of ALC-0315 in Various Species 19

Figure 2.4.3-4. Proposed Biotransformation Pathway of ALC-0159 in Various Species 20

2.4.3.6. Excretion 20

2.4.3.7. Pharmacokinetic Drug Interactions 20

2.4.4. TOXICOLOGY 21

2.4.4.1. Brief Summary 21

Table 2.4.4-1. Overview of Toxicity Testing Program 22

2.4.4.2. Single-Dose Toxicity 23

2.4.4.3. Repeat-Dose Toxicity 23

 2.4.4.3.1. Repeat-Dose Toxicity Study of Three LNP-Formulated RNA Platforms
 Encoding for Viral Proteins by Repeated Intramuscular Administration to Wistar Han
 Rats..... 23

 2.4.4.3.2. 17-Day Intramuscular Toxicity Study of BNT162b2 (V9) in Wistar Han
 Rats with a 3-week Recovery..... 26

2.4.4.4. Genotoxicity 29

2.4.4.5. Carcinogenicity 29

2.4.4.6. Reproductive and Developmental Toxicity 29

2.4.4.7. Local Tolerance 30

2.4.4.8. Other Toxicity Studies 30

 2.4.4.8.1. Phototoxicity 30

 2.4.4.8.2. Antigenicity 30

 2.4.4.8.3. Immunotoxicity 30

 2.4.4.8.4. Mechanistic Studies 30

 2.4.4.8.5. Dependence 31

 2.4.4.8.6. Studies on Metabolites 31

 2.4.4.8.7. Studies on Impurities 31

 2.4.4.8.8. Other Studies 31

2.4.4.9. Target Organ Toxicity 31

2.4.5. INTEGRATED OVERVIEW AND CONCLUSIONS 32

2.4.6. LIST OF LITERATURE REFERENCES 34

090177e1962c108d\Approved\Approved On: 08-Feb-2021 15:26 (GMT)

LIST OF ABBREVIATIONS AND DEFINITION OF TERMS

A:G	Albumin:globulin ratio
ACE	Angiotension-converting enzyme
ADME	Absorption, distribution, metabolism, excretion
ALC-0159	Proprietary PEG-lipid included as an excipient in the LNP formulation used in BNT162b2
ALC-0315	Proprietary amino-lipid included as an excipient in the LNP formulation used in BNT162b2
ALT	Alanine aminotransferase
AST	Aspartate aminotransferase
BAL	Bronchoalveolar lavage
CAS	Chemical abstracts service
CBER	Center for Biologics Evaluation and Research
CD	Cluster of differentiation
COVID-19	Coronavirus Disease 2019
DART	Developmental and reproductive toxicity
DNA	Deoxyribonucleic acid
DSPC	1,2-distearoyl-sn-glycero-3-phosphocholine
ELISA	Enzyme-linked immunosorbent assay
EUA	Emergency Use Authorization
F0	Parental generation administered vaccine
F1	First generation offspring of F0 generation
GD	Gestation day
GGT	Gamma-glutamyl transferase
GLP	Good Laboratory Practice
H	Human (in metabolite scheme)
[³ H]-CHE	Radiolabeled [Cholesteryl-1,2- ³ H(N)]-Cholesteryl Hexadecyl Ether
HGB	Hemoglobin
IFN	Interferon
IgG	Immunoglobulin G
IL	Interleukin
IM	Intramuscular(ly)
IND	Investigational New Drug Application
IV	Intravenous(ly)
LC/MS	Liquid chromatography-tandem mass spectrometry
LD	Lactation day
LNP	Lipid-nanoparticle
Luc	Luciferase (from firefly <i>Pyroactomena lucifera</i>)
LUC	Large unstained cell
Mk	Monkey (in metabolite scheme)
Mo	Mouse (in metabolite scheme)
modRNA	Nucleoside-modified mRNA
mRNA	Messenger RNA
NA	Not applicable

090177e1962c108d\Approved\Approved On: 08-Feb-2021 15:26 (GMT)

LIST OF ABBREVIATIONS AND DEFINITION OF TERMS - CONTINUED

NHP	Nonhuman primate
OECD	Organisation for Economic Co-operation and Development
P2 S	Spike protein P2 mutant
PEG	Polyethylene glycol
PK	Pharmacokinetics
PLT	Platelet
PND	Postnatal day
PT	Prothrombin time
QC	Quality control review
QW	Once weekly
R	Rat (in metabolite scheme)
RBC	Red blood cell
RBD	Receptor binding domain
RdRp	RNA-dependent RNA-polymerase
RDW	Red cell distribution width
RETIC	Reticulocyte
RNA	Ribonucleic acid
RT-PCR	Reverse transcription-polymerase chain reaction
S	SARS-CoV-2 spike glycoprotein
S1	S1 domain of the SARS-CoV-2 spike glycoprotein
S9	Supernatant fraction obtained from liver homogenate by centrifuging at 9000 g
SARS	Severe Acute Respiratory Syndrome
SARS-CoV-2	Severe acute respiratory syndrome coronavirus 2; coronavirus causing COVID-19
Tfh	T follicular helper cell
Th1	Type 1 T helper cells
TK	Toxicokinetic
TNF	Tumor necrosis factor
V8	Variant 8; P2 S
V9	Variant 9; P2 S
WBC	White blood cell
WHO	World Health Organization

090177e1962c108d\Approved\Approved On: 08-Feb-2021 15:26 (GMT)

2.4.1. OVERVIEW OF NONCLINICAL TESTING STRATEGY

BNT162b2 (BioNTech code number BNT162, Pfizer code number PF-07302048) is an investigational vaccine intended to prevent COVID-19, which is caused by SARS-CoV-2. BNT162b2 is a nucleoside modified mRNA (modRNA) expressing full-length S with two proline mutations (P2) to lock the transmembrane protein in an antigenically optimal prefusion conformation (Pallesen et al, 2017; Wrapp et al, 2020). The vaccine is formulated in lipid nanoparticles (LNPs). The LNP is composed of 4 lipids: ALC-0315, ALC-0159, DSPC, and cholesterol. Other excipients in the formulation include sucrose, NaCl, KCl, Na₂HPO₄, and KH₂PO₄. The dose selected for BNT162b2, with efficacy demonstrated in Phase 2/3 clinical evaluation and intended for commercial use, is 30 µg administered IM as two doses given 21 days apart.

In nonclinical studies, two variants of BNT162b2 were tested; designated “variant 8” and “variant 9” (V8 and V9, respectively). The variants differ only in their codon optimization sequences which are designed to improve antigen expression, otherwise the amino acid sequences of the encoded antigens are identical. Only BNT162b2 (V9) has been evaluated in the clinic, is currently authorized under EUA, and is the subject of this BLA application. The characteristics of each variant are described in the table below (Table 2.4.1-1).

Table 2.4.1-1. Nomenclature of the Vaccine Candidates

Product Code	RNA Platform	Antigen Variant	Description/Translated Protein	Variant Code	GLP Tox Data	Clinical Candidate
BNT162b2	modRNA	V8 ^a	P2 S	RBP020.1	Yes	No
BNT162b2	modRNA	V9^a	P2 S	RBP020.2	Yes	Yes

a. The V8 and V9 variants of the P2 S antigen have the same amino acid sequence. Different codon optimizations were used for their ribonucleotide sequences.

Bold: BNT162b2 (V9) vaccine candidate submitted for licensure.

The primary pharmacology, distribution, metabolism, and safety of BNT162b2 were evaluated in nonclinical pharmacology, pharmacokinetic, and toxicity studies in vitro and in vivo (Table 2.4.1-2).

Immunogenicity of BNT162b2 was evaluated in mice (2.4.2.1.3), rats (2.4.2.1.5) and nonhuman primates (2.4.2.1.4). For assessment of serum antibody responses in mice and rats, S1 and RBD-binding IgG responses were tested by an ELISA. Functional antibody responses were tested by a SARS-CoV-2 pseudotype neutralization assay (pVNT). In nonhuman primate studies, S1-binding IgG responses were tested in a direct Luminex-based immunoassay (dLIA) and functional antibody responses were assessed in a SARS-CoV-2 neutralization assay. S-specific T cell responses were assessed in mouse and nonhuman primate studies in an IFNγ ELISpot and by intracellular cytokine staining flow cytometry-based analysis of the Th1/Th2 profile using splenocytes.

A SARS-CoV-2 challenge study in BNT162b2 (V9)-immunized nonhuman primates was also conducted to assess protection against infection and to demonstrate lack of disease enhancement ([Section 2.4.2.1.4.2](#)).

Platform properties that support BNT162b2 were initially demonstrated with non-SARS-CoV-2 antigens. Non-GLP in vivo testing of an LNP-formulated modRNA encoding luciferase examined biodistribution in BALB/c mice and Wistar Han rats after IM injection ([Section 2.4.3.4](#)) and the PK of the two novel excipients in the LNP formulation, ALC-0315 and ALC-0159, in Wistar Han rats ([Section 2.4.3.3](#)). In addition, the metabolism of ALC-0315 and ALC-0159 was evaluated in mouse, rat, monkey, and human blood, liver microsomes, S9 fractions, and hepatocytes and in vivo in rat plasma, urine, feces, and liver samples from the PK study ([Table 2.4.1-2](#); [Section 2.4.3.5](#)).

BNT162b2 (V8) and (V9) have been studied in GLP-compliant repeat-dose toxicity studies in rats ([Table 2.4.1-2](#)). Two GLP repeat-dose toxicity studies for BNT162b2 (V8) and BNT162b2 (V9), one study for each variant, have been completed. The study designs are described in [Section 2.4.4](#) and are based on WHO guidelines for vaccine development ([WHO, 2005](#)). A DART study with BNT162b2 (V9) in rats has also been completed. No additional toxicity studies are planned for BNT162b2.

IM administration was chosen for the toxicity studies as this is the intended route of administration. Rats were chosen for toxicity assessments as they are a commonly used animal species for the evaluation of toxicity, and they mount an antigen-specific immune response to vaccination with BNT162b2.

The design of the nonclinical repeat-dose toxicity studies was consistent with the WHO Guidelines on Nonclinical Evaluation of Vaccines, the EMA Note for Guidance on Preclinical Pharmacological and Toxicological Testing of Vaccines, and Japan guidance on the nonclinical safety assessment of vaccines. In addition, the 2020 CBER guidance on “Development and Licensure of Vaccines to Prevent COVID-19” ([US FDA, 2020](#)) was considered when assembling the nonclinical safety licensure package as well as feedback from regulatory agencies. All GLP-compliant studies were conducted in accordance with Good Laboratory Practice for Nonclinical Laboratory Studies, Code of US Federal Regulations (21 CFR Part 58), in an OECD Mutual Acceptance of Data member state. All nonclinical studies described herein were conducted by or for Pfizer Inc or BioNTech RNA Pharmaceuticals GmbH. The location of records for inspection is included in each final study report.

BNT162b2

Module 2.4. Nonclinical Overview

Table 2.4.1-2. Nonclinical Studies

Study Number	Study Type	Species / Test System	Test Item	Dose [RNA]	Cross reference
Pharmacology - BNT162b2 studies					
R-20-0085	In vivo immunogenicity	BALB/c mice	BNT162b2 (V9)	0.2, 1, 5 µg	Section 2.4.2.1.3
R-20-0112	In vivo immunogenicity	BALB/c mice	BNT162a1, BNT162b1, BNT162b2 (V9), BNT162c2	5 µg	Section 2.4.2.1.3
R-20-0211	In vitro protein expression	Cell culture	BNT162b2 (V9)	varied	Section 2.4.2.1.2
VR-VTR-10741	In vitro protein expression	Cell culture	BNT162b2 (V9)	varied	Section 2.4.2.1.2
VR-VTR-10671	In vivo immunogenicity and SARS-CoV-2 challenge	Rhesus macaques	BNT162b2 (V9)	30 and 100 µg	Section 2.4.2.1.4
ADME					
PF-07302048_06Jul20_072424	PK of ALC-0315 and ALC-0159	Wistar Han Rats	modRNA encoding luciferase formulated in LNP comparable to BNT162b2	1 mg/kg	Section 2.4.3.3
R-20-0072	In vivo distribution	BALB/c mice	modRNA encoding luciferase formulated in LNP comparable to BNT162b2	2 µg	Section 2.4.3.4
185350	In vivo distribution	Wistar Han Rats	modRNA encoding luciferase formulated in LNP comparable to BNT162b2 with trace amounts of [³ H]-CHE as non-diffusible label	50 µg	Section 2.4.3.4
01049-20008	In vitro metabolism	CD-1/ICR mouse, Wistar Han and/or Sprague Dawley rat, cynomolgus monkey and human liver microsomes, S9 fraction, hepatocytes	ALC-0315	NA	Section 2.4.3.5
01049-20009					
01049-20010					
01049-20020			ALC-0159	NA	
01049-20021					
01049-20022					

090177e1962c108d\Approved\Approved On: 08-Feb-2021 15:26 (GMT)

Table 2.4.1-2. Nonclinical Studies - Continued

Study Number	Study Type	Species / Test System	Test Item	Dose [RNA]	Cross reference
PF-07302048 _05Aug20_043725	In vitro and in vivo metabolism	Blood, liver S9 fractions and hepatocytes from CD-1 mouse, Wistar Han rat, cynomolgus monkey and human. In vivo samples from Wistar Han rat plasma, urine, feces, and liver	In vitro: ALC-0315 and ALC-0159 In vivo: modRNA encoding luciferase formulated in LNP comparable to BNT162b2	1 mg/kg modRNA (in vivo samples)	Section 2.4.3.5
Toxicology – Studies with BNT162b2 variants					
38166	Repeat-dose toxicity	Wistar Han Rats	BNT162b2 (V8)	100 µg	Section 2.4.4.3
20GR142	Repeat-dose toxicity	Wistar Han Rats	BNT162b2 (V9)	30 µg	Section 2.4.4.3
20256434	Development and Reproductive Toxicity	Wistar Han Rats	BNT162b2 (V9)	30 µg	Section 2.4.4.6

090177e1962c108d\Approved\Approved On: 08-Feb-2021 15:26 (GMT)

2.4.2. PHARMACOLOGY

2.4.2.1. Primary Pharmacodynamics

2.4.2.1.1. Summary

BNT162b2 (BioNTech code number BNT162, Pfizer code number PF-07302048) is a nucleoside-modified mRNA (modRNA) vaccine that encodes the SARS-CoV-2 full-length spike glycoprotein (S). The glycoprotein encoded by both BNT162b2 variants includes two amino acid substitutions to proline (P2 S) locking the transmembrane protein in an antigenically optimal prefusion conformation (Wrapp et al, 2020; Pallesen et al, 2017). The RNA is formulated with functional and structural lipids, which protect the RNA from degradation and enable transfection of the RNA into host cells after IM injection. S is a major target of virus neutralizing antibodies and is a key antigen for vaccine development. The well-resolved trimeric prefusion structure and the high affinity binding to ACE2 and human neutralizing antibodies demonstrate that the recombinant P2 S authentically presents the ACE2 binding site and other epitopes targeted by many SARS-CoV-2 neutralizing antibodies.

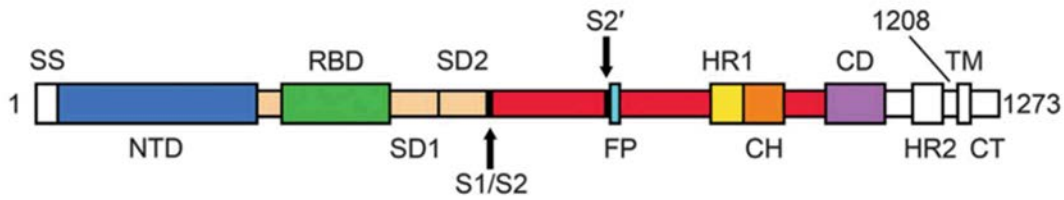
In vitro studies and in vivo studies in mice and nonhuman primates demonstrate the mechanism of action for this RNA-based vaccine, which is to encode SARS-CoV-2 S that induces an immune response characterized by both a strong neutralizing antibody response and Th1-type CD4⁺ and an IFN γ ⁺ CD8⁺ T-cell response. BNT162b2 immunization protected rhesus macaques from infectious SARS-CoV-2 challenge, with reduced detection of viral RNA in vaccine-immunized animals compared to saline-immunized animals and with no evidence of clinical exacerbation.

2.4.2.1.2. BNT162b2, A Lipid Nanoparticle Encapsulated RNA Vaccine Encoding the SARS-CoV-2 P2 S as a Vaccine Antigen

BNT162b2 is based on a nucleoside-modified mRNA (modRNA) platform technology. Vaccination with modRNA formulated in LNPs is characterized by strong expansion of Th1-skewed antigen-specific T follicular helper (Tfh) cells, which stimulate and expand germinal center B cells, thereby resulting in particularly strong, long lived, high-affinity antibody responses (Sahin et al, 2014; Pardi et al, 2018). ModRNA vaccine candidates against other infectious diseases induce strong antibody responses and prime and expand multifunctional CD4⁺ and CD8⁺ T cells (Pardi et al, 2017; Pardi et al, 2018).

SARS-CoV-2 S is a large, trimeric glycoprotein that exists predominantly in a prefusion conformation on the virion (Ke et al, 2020). It is cleaved by furin into an N-terminal S1 and a C-terminal S2 fragment. S attaches to the host cell receptor, ACE2, by its receptor binding domain which is contained in the S1 furin cleavage fragment. Spontaneously and during cell entry, the S1 fragment dissociates, and the S2 fragment undergoes a fold-back rearrangement to the post-fusion conformation in a process that facilitates fusion of viral and host cell membranes. S is the main target of virus neutralizing antibodies (Zakhartchouk et al, 2007; Yong et al, 2019). Most of the antibodies with SARS-CoV-2 neutralizing activity are directed against the RBD (Jiang et al, 2020; Zost et al, 2020).

090177e1962c108d\Approved\Approved On: 08-Feb-2021 15:26 (GMT)

Figure 2.4.2-1. Schematic of the Organization of the SARS-CoV-2 S Glycoprotein

The S1 furin cleavage fragment includes the signal sequence (SS), the N terminal domain (NTD), the receptor binding domain (RBD, which binds the human cellular receptor, ACE-2), subdomain 1 (SD1), and subdomain 2 (SD2). The furin cleavage site (S1/S2) separates S1 from the S2 fragment, which contains the S2 protease cleavage site (S2') followed by a fusion peptide (FP), heptad repeats (HR1 and HR2), a central helix (CH) domain, the connector domain (CD), the transmembrane domain (TM) and a cytoplasmic tail (CT).

Source: modified from [Wrapp et al, 2020](#).

BNT162b2 (V9) encodes a full-length P2 S transmembrane protein that contains two consecutive prolines introduced at amino acid positions 986 and 987, between the central helix (CH) and heptad repeat 1 (HR1) (Figure 2.4.2-1) ([Wrapp et al, 2020](#); [Pallesen et al, 2017](#)). Two codon optimized forms of the coding sequence for this antigen were tested preclinically and were designated “variant 8” and “variant 9” (V8 and V9), with the vaccine candidate tested clinically and being proposed for licensure or authorization, V9, expressed from a codon optimized RNA gene with a higher content of cytosine ribonucleotides for increased protein expression. The RNA-expressed P2 S is membrane bound and elicits a potent humoral neutralizing antibody response and Th1-type CD4⁺ and CD8⁺ cellular response to block virus infection and kill virus infected cells, respectively.

Efficient in vitro expression of the P2 S protein was demonstrated following in vitro transfection of cells with BNT162b2 RNA drug substance and BNT162b2 drug product. Electron cryomicroscopy analysis of purified recombinant P2 S, expressed from DNA encoding the same S amino acid sequence as BNT162b2 RNA (except for the addition of a C-terminal tag for protein purification) revealed high similarity to previously reported structures ([Cai et al, 2020](#)). The well-resolved trimeric prefusion structure and the high affinity binding to ACE2 and human neutralizing antibodies demonstrate that the recombinant full-length P2 S protein authentically presents the ACE-2 binding site.

2.4.2.1.3. Immunogenicity of BNT162b2 (V9) in Mice

BNT162b2 was highly immunogenic in mice with strong antigen-binding IgG and high titer neutralizing antibody responses together with a Th1-phenotype CD4⁺ response as well as an IFN γ ⁺, IL-2⁺ CD8⁺ T-cell response after a single immunization. Total IgG ELISA showed that the vaccine induced a strong, dose-dependent IgG response that recognizes S1 and the RBD and elicited high neutralizing titers in a pseudotype neutralization assay.

Stimulation of fresh splenocytes, collected 28 days after immunization, with an S protein specific overlapping peptide pool demonstrated robust CD4⁺ and CD8⁺ T-cell IFN γ responses and a Th1-dominant profile was demonstrated in quantification of cytokines (IL-2 and IFN γ) in the corresponding culture supernatants.

In summary, BNT162b2 induced a strong, neutralizing antibody response. CD4⁺ and CD8⁺ T-cell responses were detectable 12 and 28 days after one immunization and exhibited a Th1-dominant T cell response characteristic of RNA-based vaccines.

2.4.2.1.4. Evaluation of BNT162b2 (V9) Immunogenicity and Protection Against SARS-CoV-2 Challenge in Rhesus Macaques

BNT162b2 was assessed for immunogenicity and for protection against an infectious SARS-CoV-2 challenge in rhesus macaques. SARS-CoV-2 infection in humans manifests as both asymptomatic infection and as the disease COVID-19, with diverse signs, symptoms, and levels of severity. Based on published reports, SARS-CoV-2 challenged rhesus macaques develop an acute, transient infection in the upper and lower respiratory tract and have evidence of viral replication in the gastrointestinal tract, similar to humans (Zou et al, 2020; Kim et al, 2020). Varying degrees of pulmonary inflammation, primarily at the peak of infection at approximately Day 2 to 4 post-challenge, have been reported in the literature (Munster et al, 2020). The human and rhesus ACE-2 receptor have 100% amino acid identity at the critical binding residues, which may account for the fidelity of this SARS-CoV-2 animal model (Zhou et al, 2020).

2.4.2.1.4.1. Immunogenicity in Rhesus Macaques

Rhesus macaques immunized IM with 30 µg or 100 µg of BNT162b2 on Days 0 and 21 had readily detectable S1-binding IgG and SARS-CoV-2 neutralizing titers (NT50) as early as 14 days after a single immunization, with substantial increases following the second immunization. On Day 28, seven days after Dose 2 at the 30 µg dose level, the neutralizing geometric mean titer (GMT) reached 8-fold the GMT of a 38 member panel of human convalescent sera (HCS); at the 100 µg dose level, the neutralizing GMT was 18-fold the HCS GMT. The HCS sera were drawn from SARS-CoV-2 infected individuals 18 to 83 years of age, at least 14 days after PCR-confirmed diagnosis and at a time when individuals were asymptomatic. The HCS panel provides a currently accessible benchmark to judge the quality of the humoral immune response to the vaccine. A decline of both, S1-binding IgG levels and neutralizing titers, was observed out to the latest measured time point (Day 56) but remained above the neutralizing GMT and the S1-binding geometric mean concentration (GMC) of the HCS.

As seen following mouse immunization, strong S-specific Th1-dominant IFN γ ⁺ T-cell responses were detected in all immunized rhesus macaques. By intracellular cytokine staining analysis, there was a dose-dependent increase in S-specific CD4⁺ T cell responses with a strong Th1-bias evidenced by high frequency of IFN γ ⁺, IL-2⁺, or TNF- α ⁺ cells. Notably, CD8⁺ T-cell responses were also detectable in BNT162b2-immunized animals.

2.4.2.1.4.2. SARS-CoV-2 Challenge of BNT162b2 (V9)-Immunized Nonhuman Primates

Groups of 2-4 year old male rhesus macaques that had received two IM immunizations with 100 µg BNT162b2 V9 (n=6) or saline (Control; n=3) 21 days apart were challenged 55 days after the second immunization with 1.05×10^6 plaque forming units of SARS-CoV-2 (strain USA-WA1/2020), split equally between the intranasal (IN) and intratracheal (IT) routes, as

090177e1962c108d\Approved\Approved On: 08-Feb-2021 15:26 (GMT)

previously described (Singh et al, 2020) (VR-VTR-10671). SARS-CoV-2 RNA was measured by reverse transcription- quantitative polymerase chain reaction (RT-qPCR) in bronchoalveolar lavage fluid, nasal swabs, and oropharyngeal swabs. The difference in viral RNA detection in BAL fluid between BNT162b2-immunised and control-immunised rhesus macaques after challenge is highly statistically significant (by a nonparametric test, $p=0.0014$). None of the challenged animals showed clinical signs of significant illness, indicating that the 2-4 years old male rhesus challenge model is primarily an infection model for SARS-CoV-2, not a COVID-19 disease model. No radiographic or histological evidence of vaccine-elicited enhanced disease was observed. In summary, BNT162b2 provided complete protection from the presence of detectable viral RNA in the lungs compared to the saline control with no evidence of vaccine-elicited disease enhancement.

2.4.2.1.5. Immunogenicity Testing After Weekly Immunization of Rats in GLP Compliant Repeat Dose Toxicology Studies and a Developmental and Reproductive Toxicity Study

The nonclinical safety data package consists of two GLP-compliant repeat-dose rat toxicity studies, in which both BNT162b2 variants (V8 and V9) were evaluated, and a DART study, in which BNT162b2 (V9) was evaluated (Section 2.4.4). In all studies, Study 38166 (evaluating V8) as well as Study 20GR142 and Study 20256434 (evaluating V9), the vaccine candidates were immunogenic.

In Study 38166, male and female rats received three weekly IM doses of BNT162b2 (V8). Serum samples were collected from main study animals on Day 17 (two days after the third dose) at the end of the dosing phase and on Day 38 at the end of a 3-week recovery phase. The sera were analyzed by ELISA for IgG that bound S1 and RBD as well as for SARS-CoV-2-S pseudovirus neutralizing antibodies. The vaccine candidates elicited IgG that recognized S1 and RBD. After immunization, animals developed high titers of antigen-specific antibodies as well as pseudovirus neutralization titers.

In Study 20GR142, male and female rats received three weekly IM doses of BNT162b2 (V9). Serum samples were collected from study animals prior to vaccine administration, at the end of the dosing phase on Day 17 (two days after the third dose), and at the end of the 3-week recovery phase on Recovery Phase Day 21. Sera were analyzed for SARS-CoV-2 neutralizing antibodies. After immunization, BNT162b2 (V9) elicited SARS-CoV-2 neutralizing antibody responses in males and females at the end of the dosing and recovery phases of the study. SARS-CoV-2 neutralizing antibody responses were not observed in animals prior to vaccine administration or in saline-administered control animals.

In Study 20256434, female rats were administered 4 total IM doses of BNT162b2 (V9) 21 and 14 days prior to mating and on GD9 and GD20. Serum samples were collected from females prior to vaccine administration, just prior to mating (M0), at the end of gestation (GD21), and at the end of lactation (LD21) and offspring (fetuses on GD21 and pups on PND21). Sera were analyzed for SARS-CoV-2 neutralizing antibodies. After immunization, SARS-CoV-2 neutralizing titers were detected in all maternal females as well as in their offspring (fetuses and pups). SARS-CoV-2 neutralizing antibody titers were not observed in animals prior to vaccine administration or in saline-administered control animals.

2.4.2.2. Secondary Pharmacodynamics

No secondary pharmacodynamics studies were conducted with BNT162b2.

2.4.2.3. Safety Pharmacology

No safety pharmacology studies were conducted with BNT162b2 as they are not considered necessary for the development of vaccines according to the WHO guideline ([WHO, 2005](#)).

2.4.2.4. Pharmacodynamic Drug Interactions

Nonclinical studies evaluating pharmacodynamic drug interactions with BNT162b2 were not conducted as they are generally not considered necessary to support development and licensure of vaccine products for infectious diseases (WHO, 2005).

2.4.3. PHARMACOKINETICS

2.4.3.1. Brief Summary

Assessment of the ADME profile of BNT162b2 (BioNTech code number BNT162, Pfizer code number PF-07302048) included evaluating the PK and metabolism of two novel lipid excipients (ALC-0315 and ALC-0159) in the LNP and potential biodistribution of BNT162b2 using luciferase expression as a surrogate reporter. The luciferase reporter was used as it was a readily available reporter that has been widely used to develop an understanding of protein/organ expression (Chen et al, 2020; Elia et al, 2020; Fukuchi et al, 2020; Hassett et al, 2019; Truong et al, 2019; Barry et al, 2012; Jeon et al, 2006). An intravenous rat PK study, using LNPs with the identical lipid composition as BNT162b2, demonstrated that ALC-0315 and ALC-0159 distribute from the plasma to the liver. While there was no detectable excretion of either lipid in the urine, the percent of dose excreted unchanged in feces was ~1% for ALC-0315 and ~50% for ALC-0159.

The biodistribution of BNT162b2 was evaluated using luciferase expression as a surrogate reporter in BALB/c mice. Mice were administered a luciferase expressing modRNA formulated like BNT162b2, with the identical lipid composition. Luciferase expression was measured in vivo following luciferin application. Luciferase expression was identified at the injection site at 6 hours after injection and was not detected after 9 days. Expression in the liver was also present to a lesser extent at 6 hours after injection and was not detected by 48 hours after injection. The distribution was also examined in male and female Wistar Han rats using LNPs with a comparable lipid composition to BNT162b2 but with a surrogate luciferase RNA and containing trace amounts of radiolabeled [³H]-CHE, a non-exchangeable, non-metabolizable lipid marker. The greatest mean concentration of LNP was found remaining in the injection site in both sexes. Total recovery (% of injected dose) of LNP outside the injection site was greatest in the liver and was much less in the spleen, adrenal glands, and ovaries.

The in vitro metabolism of ALC-0315 and ALC-0159 was evaluated in blood, liver microsomes, S9 fractions, and hepatocytes from mice, rats, monkeys, and humans. The in vivo metabolism was examined in rat plasma, urine, feces, and liver samples from the PK study. Metabolism of ALC-0315 and ALC-0159 appears to occur slowly in vitro and in vivo. ALC-0315 and ALC-0159 are metabolized by hydrolytic metabolism of the ester and amide functionalities, respectively, and this hydrolytic metabolism is observed across the species evaluated.

In summary, the nonclinical ADME studies indicate that the LNP distributes to the liver. Approximately 50% of ALC-0159 is excreted unchanged in feces, while metabolism played a role in the elimination of ALC-0315.

2.4.3.2. Methods of Analysis

No methods of analysis have been validated to support GLP TK studies of components of BNT162b2; however, a qualified LC/MS method was developed to support quantitation of the two novel LNP excipients for the non-GLP IV PK study in rats

090177e1962c108d\Approved\Approved On: 08-Feb-2021 15:26 (GMT)

(Study PF-07302048_06Jul20_072424). Methods for immunogenicity and efficacy studies are described in Section 2.6.2.12.

2.4.3.3. Absorption

2.4.3.3.1. In Vitro Absorption

No absorption studies were conducted for BNT162b2, as the administration route is IM.

2.4.3.3.2. Single-Dose Pharmacokinetics

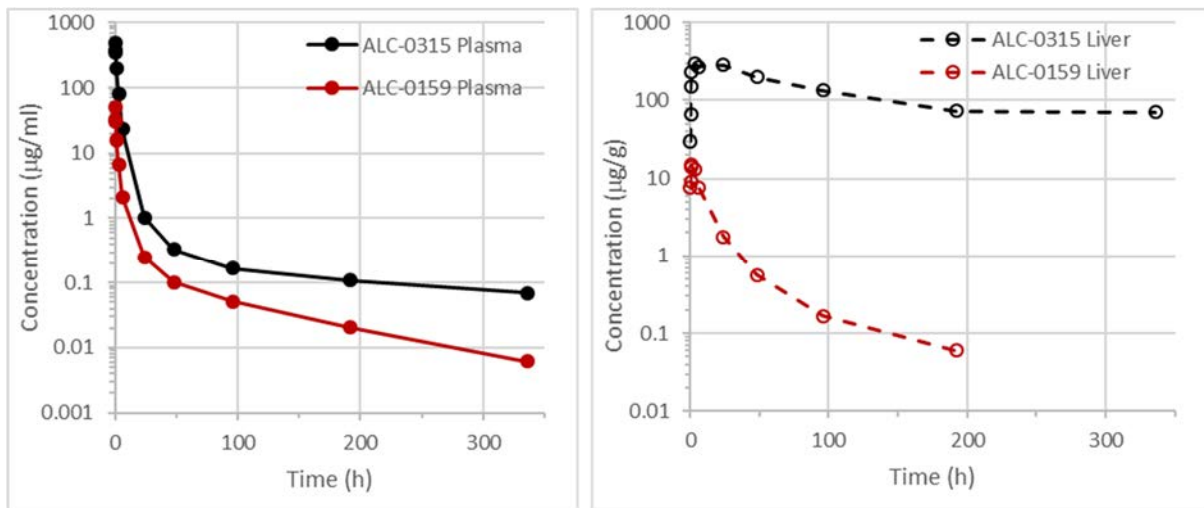
An intravenous rat PK study (PF-07302048_06Jul20_072424; Tabulated Summary 2.6.5.3) was performed using LNPs containing surrogate luciferase RNA, with the identical lipid composition as BNT162b2. This study was conducted to explore the disposition of ALC-0315 and ALC-0159 that had reached the systemic circulation following IM administration; thus, the IV route was felt to be appropriate. The findings are depicted in Table 2.4.3-1 and Figure 2.4.3-1.

Table 2.4.3-1. PK of ALC-0315 and ALC-0159 in Wistar Han Rats After IV Administration of LNPs Containing Surrogate Luciferase RNA at 1 mg/kg

Analyte	Dose of Analyte (mg/kg)	Gender /N	t _{1/2} (h)	AUC _{inf} (µg•h/mL)	AUC _{last} (µg•h/mL)	Estimated fraction of dose distributed to liver (%) ^a
ALC-0315	15.3	Male/3 ^b	139	1030	1020	60
ALC-0159	1.96	Male/3 ^b	72.7	99.2	98.6	20

a. Calculated as highest mean amount in the liver (µg)/total mean dose (µg) of ALC-0315 or ALC-0159.
b. 3 animals per timepoint; non-serial sampling.

Figure 2.4.3-1. Plasma and Liver Concentrations of ALC-0315 and ALC-0159 in Wistar Han Rats After IV Administration of LNPs Containing Surrogate Luciferase RNA at 1 mg/kg



090177e1962c108d\Approved\Approved On: 08-Feb-2021 15:26 (GMT)

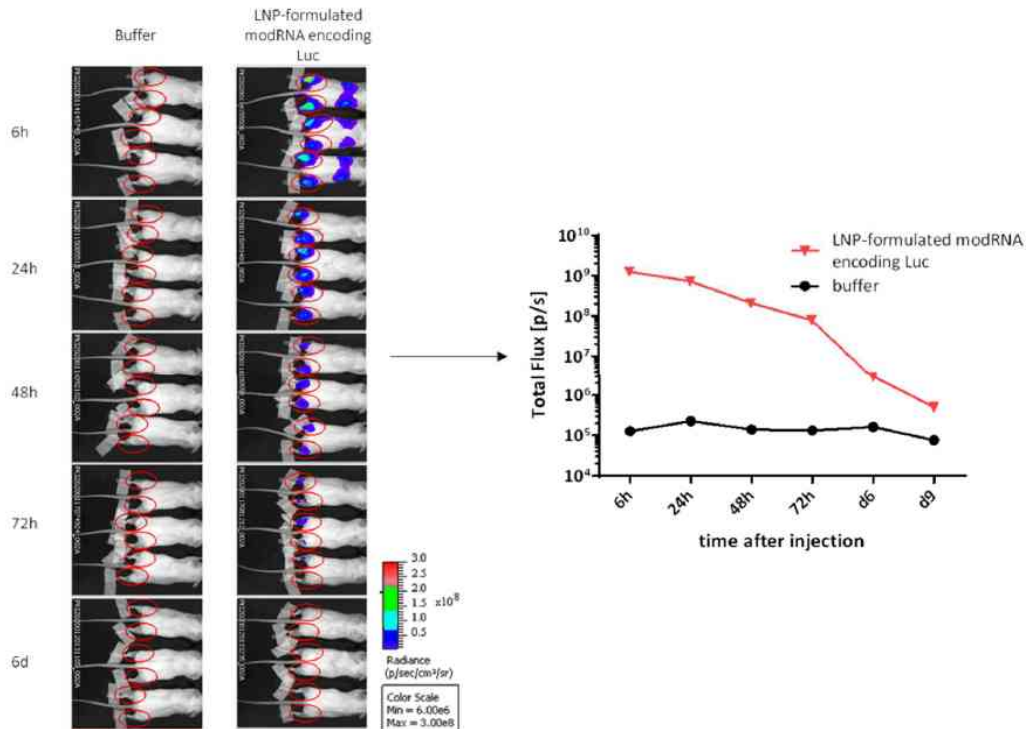
Pharmacokinetic studies have not been conducted with BNT162b2 and are generally not considered necessary to support the development and licensure of vaccine products for infectious diseases (WHO, 2005; WHO, 2014).

2.4.3.4. Distribution

In an in vivo study (R-20-0072; Tabulated Summary 2.6.5.5A), biodistribution was assessed using luciferase as a surrogate marker protein, with RNA encoding luciferase formulated like BNT162b2, with the identical lipid composition. The LNP-formulated luciferase-encoding modRNA was administered to BALB/c mice by IM injection of 1 µg each in the right and left hind leg (for a total of 2 µg). Using in vivo bioluminescence after injection of luciferin substrate, luciferase protein expression was detected at different timepoints at the site of injection and to a lesser extent, and more transiently, in the liver (Figure 2.4.3-2. Distribution to the liver is likely mediated by LNPs entering the blood stream. The luciferase expression at the injection sites dropped to background levels after 9 days. The repeat-dose toxicity study in rats showed no evidence of liver injury (Section 2.4.4.3).

The biodistribution of the antigen encoded by the RNA component of BNT162b2 is expected to be dependent on the LNP distribution and the results presented should be representative for the vaccine RNA platform, as the LNP-formulated luciferase-encoding modRNA had the same lipid composition.

Figure 2.4.3-2. Bioluminescence Emission in BALB/c Mice after IM Injection of an LNP Formulation of modRNA Encoding Luciferase



090177e1962c108d\Approved\Approved On: 08-Feb-2021 15:26 (GMT)

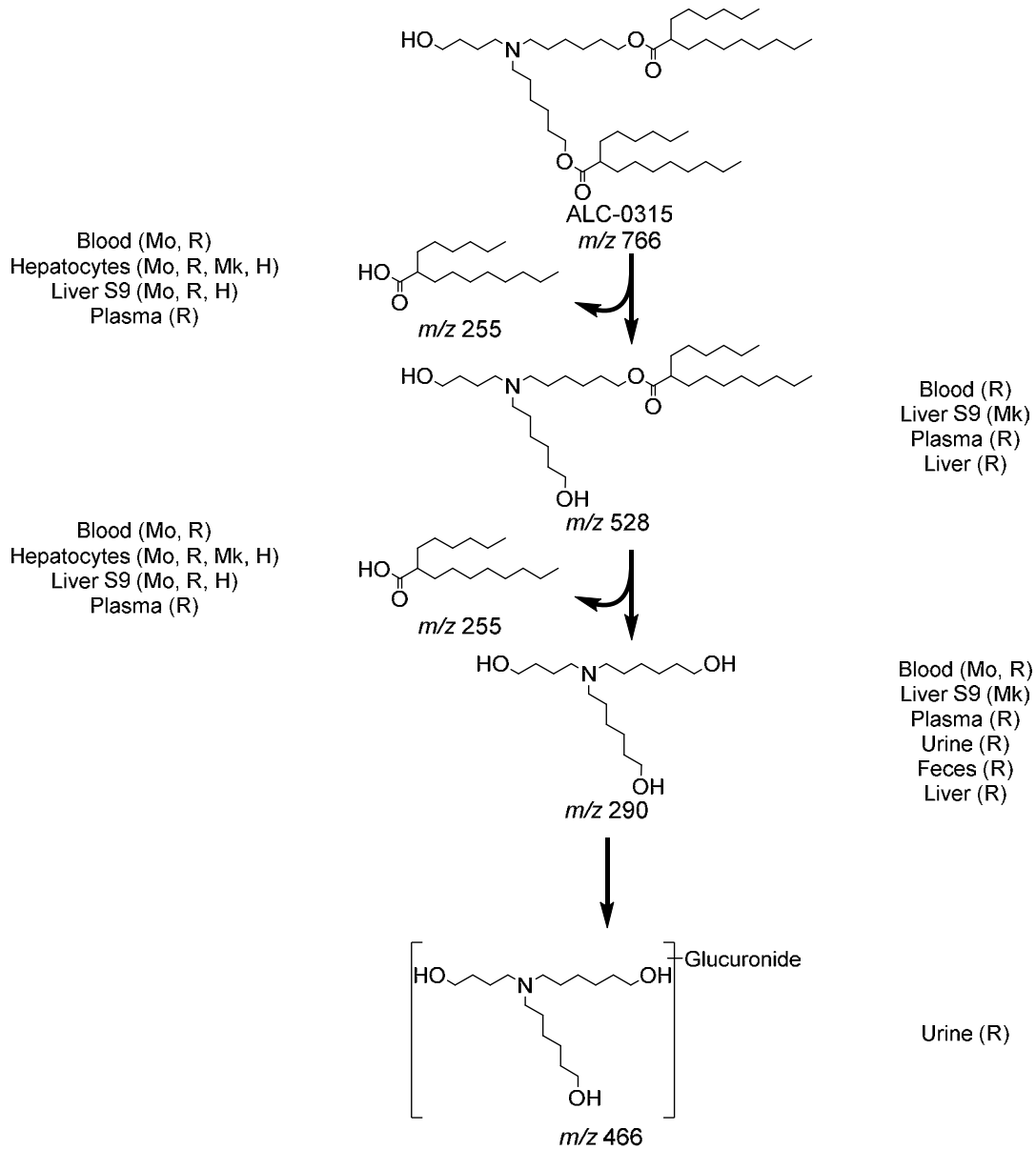
The distribution of a LNP with a comparable lipid composition to BNT162b2 but with a surrogate luciferase RNA (monitoring the ^3H -CHE lipid label), was investigated in blood, plasma and selected tissues in male and female Wistar Han rats over 48 hours after a single IM injection at 50 μg mRNA/animal (Study 185350; Tabulated Summary 2.6.5.5B). The greatest mean concentration of LNP was found remaining in the injection site at each time point in both sexes. Outside the injection site, low levels of radioactivity were detected in most tissues, with the greatest levels in plasma observed 1-4 hours post-dose. Over 48 hours, the LNP distributed mainly to liver, adrenal glands, spleen and ovaries, with maximum concentrations observed at 8-48 hours post-dose. Total recovery (% of injected dose) of LNP, for combined male and female animals, outside of the injection site was greatest in the liver (up to 18%) and was much less in the spleen ($\leq 1.0\%$), adrenal glands ($\leq 0.11\%$) and ovaries ($\leq 0.095\%$). The mean concentrations and tissue distribution pattern were broadly similar between the sexes.

2.4.3.5. Metabolism

Of the four lipids used as excipients in the LNP formulation, two are naturally occurring (cholesterol and DSPC) and will be metabolized and excreted like their endogenous counterparts. The in vitro metabolic stability of the two novel lipids, ALC-0315 (aminolipid) and ALC-0159 (PEG-lipid), were evaluated in mouse, rat, monkey, and human liver microsomes, S9 fractions, and hepatocytes. ALC-0315 and ALC-0159 were stable ($>82\%$ remaining) over 120 min in liver microsomes and S9 fractions and over 240 min in hepatocytes in all species and test systems (Studies 01049-20008, 01049-20009, 01049-20010, 01049-20020, 01049-20021, and 01049-20022; Tabulated Summaries 2.6.5.10A and 2.6.5.10B).

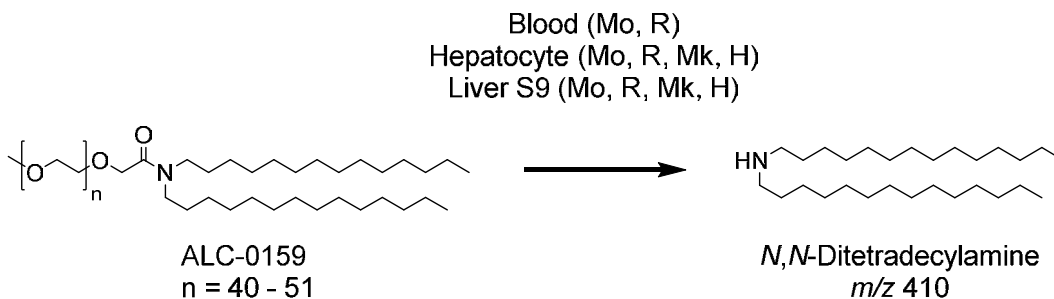
Further study of the metabolism of ALC-0315 and ALC-0159 in vitro and in vivo evaluating the plasma, urine, feces, and liver from the rat PK study (Section 2.4.3.3.2) determined ALC-0315 and ALC-0159 are metabolized slowly (Study PF-07302048_05Aug20_043725; Tabulated Summaries 2.6.5.9, 2.6.5.10C, and 2.6.5.10D). ALC-0315 and ALC-0159 underwent hydrolytic metabolism of the ester and amide functionalities, respectively, and this hydrolytic metabolism was observed across the species evaluated (Figure 2.4.3-3 and Figure 2.4.3-4).

Figure 2.4.3-3. Proposed Biotransformation Pathway of ALC-0315 in Various Species



Metabolism of ALC-0315 occurs via two sequential ester hydrolysis reactions, first yielding the monoester metabolite (m/z 528) followed by the doubly deesterified metabolite (m/z 290). Subsequent metabolism of the doubly deesterified metabolite resulted in a glucuronide metabolite (m/z 466), which was only observed in urine from the rat PK study. Additionally, 6-hexyldecanoic acid (m/z 255), the acid product of both hydrolysis reactions of ALC-0315, was identified.

090177e1962c108d\Approved\Approved On: 08-Feb-2021 15:26 (GMT)

Figure 2.4.3-4. Proposed Biotransformation Pathway of ALC-0159 in Various Species

The primary route of metabolism identified for ALC-0159 involves amide bond hydrolysis yielding *N,N*-ditetradecylamine (*m/z* 410).

The protein encoded by the RNA in BNT162b2 is expected to be proteolytically degraded like other endogenous proteins. RNA is degraded by cellular RNases and subjected to nucleic acid metabolism. Nucleotide metabolism occurs continuously within the cell, with the nucleoside being degraded to waste products and excreted or recycled for nucleotide synthesis. Therefore, no RNA or protein metabolism or excretion studies will be conducted.

2.4.3.6. Excretion

In the rat PK study ([Section 2.4.3.3.2](#)), there was no detectable excretion of ALC-0315 and ALC-0159 in urine after IV administration of LNPs containing surrogate luciferase RNA at 1 mg/kg. The percent excreted unchanged in feces was ~1% for ALC-0315 and ~50% for ALC-0159. Metabolites of ALC-0315 were detected in the urine of rats ([Figure 2.4.3-3](#)). No excretion studies have been conducted with BNT162b2 for the reasons described in [Section 2.4.3.5](#).

2.4.3.7. Pharmacokinetic Drug Interactions

No PK drug interaction studies have been conducted with BNT162b2.

2.4.4. TOXICOLOGY

2.4.4.1. Brief Summary

The nonclinical toxicity assessment of BNT162b2 (BioNTech code number BNT162, Pfizer code number PF-07302048) includes 2 GLP-compliant repeat-dose toxicity studies and a developmental and reproductive toxicity (DART) study in Wistar Han rats, outlined below in [Table 2.4.4-1](#). The nonclinical safety evaluation included 2 variants of BNT162b2: V8 and V9. BNT162b2 (V9), the candidate submitted for licensure, differs from BNT162b2 (V8) only in the presence of optimized codons to improve antigen expression, but the amino acid sequences of the encoded antigens are identical. Two GLP repeat-dose toxicity studies for BNT162b2 (V8) and BNT162b2 (V9), one study for each variant, have been completed. In both studies, the nonclinical toxicology findings were similar between BNT162b2 (V9) and BNT162b2 (V8). BNT162b2 (V9) was assessed for development and reproductive toxicity in rats.

The IM route of exposure was selected as it is the intended route of clinical administration. The selection of rats as the toxicology test species is consistent with the WHO guidance documents on nonclinical evaluation of vaccines ([WHO, 2005](#)), which recommend that vaccine toxicity studies be conducted in a species in which an immune response is induced by the vaccine. Generation of an immune response to BNT162b2 has been confirmed in rats in both repeat-dose toxicity studies and the DART study. The Wistar Han rat is used routinely for regulatory toxicity studies, and there is an extensive historical safety database on this strain of rat.

Table 2.4.4-1. Overview of Toxicity Testing Program

Study ^a	Study (Sponsor) No.	Group/ Dose, µg RNA	Total Volume (µL) ^b	No. of Animals/ Group	Study Status
Repeat-Dose Toxicity					
17-Day, 2 or 3 Dose (1 Dose/Week) IM Toxicity With a 3 Week Recovery Phase in Rats ^{c,d}	38166	Control ^e , 0	200 ^f	15/sex	Completed
		BNT162b2 (V8) ⁱ , 100	200 ^f	15/sex	
17-Day, 3 Dose (1 Dose/Week) IM Toxicity With a 3 Week Recovery Phase in Rats ^g	20GR142	Saline ^h , 0	60	15/sex	Completed
		BNT162b2 (V9) ⁱ , 30	60	15/sex	
Developmental and Reproductive Toxicity					
Combined Fertility and Developmental Study (Including Teratogenicity and Postnatal Investigations) by the IM route in Rats ^j	20256434 (RN9391 R58)	Saline ^h , 0	60	44 F	Completed
		BNT162b2 (V9) ⁱ , 30	60	44 F	

a. All studies are GLP-compliant and were conducted in an OECD mutual acceptance of data-compliant member state.

b. Doses were administered as 1 application at 1 site unless otherwise indicated.

c. Study also evaluated the BNT162a1, BNT162b1, and BNT162c1 vaccine candidates.

d. QW x 3 (Days 1, 8, 15) for BNT162a1, BNT162b1, and BNT162b2 (V8); QW x 2 (Days 1, 8) for BNT162c1.

e. Phosphate buffered saline, 300 mM sucrose.

f. One application (100 µL) at 2 sites for a total dose volume of 200 µL.

g. Study also evaluated BNT162b3.

h. Sterile saline (0.9% NaCl).

i. BNT162b2 (V8) and BNT162b2 (V9) both encode the same amino acid sequence of the spike protein antigen with two prefusion conformation-stabilizing amino acids in the stalk.

j. Study also evaluated BNT162b1 and BNT162b3.

Administration of BNT162b2 by IM injection to male and female Wistar Han rats once every week for a total of 3 weekly cycles of dosing was tolerated without evidence of systemic toxicity in GLP-compliant repeat-dose toxicity studies. Expected inflammatory responses to the vaccine were evident such as edema and erythema at the injection sites, transient elevation in body temperature, elevations in WBCs and acute phase reactants, and lower A:G ratios. A transient elevation in GGT was noted in animals vaccinated with BNT162b2 (V8) in Study 38166 without evidence of microscopic changes in the biliary system or other hepatobiliary biomarkers but was not recapitulated in Study 20GR142. Injection site reactions were common in all vaccine-administered animals and were greater after boost immunizations. Changes secondary to inflammation included slight and transient reduction in body weights and transient reductions in RETIC, PLT, and RBC mass parameters. All changes in clinical pathology parameters and acute phase proteins were reversed at the end of

the recovery phase for BNT162b2 with the exception of higher RDW, higher globulins, and lower A:G ratios in animals administered BNT162b2 (V9). The higher RDW reflects prior RETIC increases. The higher A:G is due to low magnitude increases in globulins, which is an expected immune response to vaccine administration (Sellers et al, 2020).

Macroscopic pathology and organ weight changes were also consistent with immune activation and inflammatory response and included increased size of draining iliac lymph nodes and increased size and weight of spleen. Vaccine-related microscopic findings at the end of the dosing phase consisted of edema and inflammation in injection sites and surrounding tissues; increased cellularity in the draining (iliac) lymph nodes, bone marrow, and spleen; and hepatocyte vacuolation in the liver. Periportal vacuolation of hepatocytes was not associated with any microscopic evidence of hepatic injury or alterations in liver function tests and is interpreted to reflect hepatocyte uptake of the LNP lipids (Sedic et al, 2018). Microscopic findings at the end of the dosing phase were partially or completely recovered in all animals at the end of the recovery phase for BNT162b2. A robust immune response was elicited to the BNT162b2 antigen.

In the DART study, administration of BNT162b2 to female rats twice before the start of mating and twice during gestation at the human clinical dose (30 µg RNA/dosing day) was associated with nonadverse effects (body weight, food consumption, and localized effects in the injection site) after each dose administration. There were no effects of BNT162b2 administration on mating performance, fertility, or any ovarian or uterine parameters in the F0 female rats nor on embryo-fetal or postnatal survival, growth, or development in the F1 offspring through the end of lactation. A SARS-CoV-2 neutralizing antibody response to the vaccine was confirmed in F0 female rats prior to mating, at the end of gestation, and at the end of lactation and these neutralizing antibodies were also detectable in the F1 offspring (fetuses and pups).

2.4.4.2. Single-Dose Toxicity

A separate single-dose toxicity study with BNT162b2 has not been conducted.

2.4.4.3. Repeat-Dose Toxicity

2.4.4.3.1. Repeat-Dose Toxicity Study of Three LNP-Formulated RNA Platforms Encoding for Viral Proteins by Repeated Intramuscular Administration to Wistar Han Rats

The vaccine candidate BNT162b2 (V8), an LNP-formulated modified RNA vaccine expressing SARS-CoV-2 P2 S, was assessed in a GLP-compliant repeat-dose toxicity study in Wistar Han rats (Study 38166). This study also included assessment of 3 other LNP-formulated RNA vaccines, encoding either the SARS-CoV-2 P2 S or RBD antigens, which were not selected for licensure. For the purpose of this submission, only the study findings from the 100 µg BNT162b2 (V8) vaccine group are summarized; findings from the other vaccine candidates were generally similar.

Administration of BNT162b2 (V8) via IM injections once weekly for 3 administrations to male and female Wistar Han rats was tolerated without evidence of systemic toxicity. The

vaccine elicited a robust antigen-specific immune response and produced nonadverse macroscopic changes at the injection sites, spleen, and the draining lymph nodes; increased hematopoiesis in the bone marrow and spleen; periportal hepatocyte vacuolation; and clinical pathology changes consistent with an immune response. The findings in this study were fully recovered or showed evidence of ongoing recovery at the end of the 3-week recovery phase, and were consistent with those typically associated with the IM administration of LNP-encapsulated mRNA vaccines (Hassett et al, 2019).

Body weights were lower 24 hours after each BNT162b2 (V8) vaccine administration compared with predose values (down to 0.92x versus baseline) with evidence of weight gain (1.22x to 1.37x versus baseline) by the end of recovery. Body weight gain between the administrations was comparable to the buffer control group. There were no noteworthy effects on body weight at the end of the recovery phase. There were no effects on food consumption.

BNT162b2 (V8)-administered animals generally had higher body temperatures compared with buffer control animals at 4 and 24 hours postdose. Group mean temperatures in rats administered the BNT162b2 (V8) vaccine were higher, but within approximately 1°C of the group mean body temperature of buffer-administered animals. Individual rats administered BNT162b2 (V8) did not have body temperatures >40.0°C after administration.

Local reactions were observed in male and female animals dosed IM with BNT162b2 (V8). The incidence and severity of the reactions were higher after the second or third injections compared with the first injection. The majority of animals had very slight edema or rarely slight erythema after the first dose. After the second or third dose, the severity of edema and erythema increased up to moderate or rarely, severe grades. These observations resolved prior to the next injection or for recovery animals resolved during the 3-week recovery phase.

Most BNT162b2 (V8)-related changes in clinical pathology were consistent with an acute phase response and anticipated inflammation. Minor and variable alterations in other clinical pathology parameters were considered secondary effects of vaccination.

Expected immune responses to BNT162b2 (V8) were evident in hematology, such as elevations in mean neutrophil (up to 7.8x) eosinophil (up to 5.1x controls), basophil (1.47x controls), and LUC counts (up to 7.7x controls) and were highest on Day 17, 48 hours after the last injection. WBCs were higher (up to 2.2x controls) in the BNT162b2 (V8) vaccinated group on Day 17. PLT counts were slightly decreased on Day 17 (down to 0.66x controls). A transient reduction in RETIC counts (down to 0.28x controls) was only observed after the administration of the first dose on Day 4. Decreased RETICs were similarly observed in rats treated with the licensed LNP-siRNA pharmaceutical Onpattro™ (NDA # 210922) but have not been observed in humans treated with this biotherapeutic (Kozauer et al, 2018), suggesting this is a species-specific effect. A slight reduction in red blood cell mass (HGB down to 0.87x controls) was observed on Day 17. RETIC and RBC mass parameter decreases were likely secondary to the inflammation.

BNT162b2 (V8)-related changes in clinical chemistry included slightly higher GGT (a biomarker of biliary and not hepatocellular injury [Boone et al, 2005]) on Days 4 (up to 4.6x

090177e1962c108d\Approved\Approved On: 08-Feb-2021 15:26 (GMT)

controls) and 17 (up to 4.2x controls) without evidence of microscopic changes in the biliary system or other hepatobiliary biomarkers. Additionally, higher GGT was not observed in the second repeat-dose toxicity study (20GR142), conducted with the clinical candidate submitted for licensure. Albumin was slightly lower on Days 4 (down to 0.87x controls) and 17 (down to 0.89x controls) and globulin slightly higher on Day 17 (up to 1.2x controls). This resulted in the A:G ratio being slightly lower on Days 4 (down to 0.84x controls) and 17 (down to 0.76x controls). The effect on albumin and globulin were related to the vaccine-mediated inflammatory response as part of the negative and positive acute phase response, respectively (Sellers et al, 2020).

The acute phase proteins alpha-1-acid glycoprotein (up to 21x controls on Day 17) and alpha-2-macroglobulin (up to 217x controls on Day 17) were elevated in both males and females in the BNT162b2 (V8)-administered group on Days 4 and 17. Fibrinogen was higher in the vaccine-administered group (up to 3.1x controls), consistent with an acute phase response. Higher concentrations of acute phase proteins are an anticipated response to vaccination.

All changes in clinical pathology parameters and acute phase proteins were reversed at the end of the recovery phase.

Compared with the buffer control, there were no test-article related differences in the concentration of serum cytokines evaluated, in urinalysis parameters, or in ophthalmoscopic or auditory parameters.

BNT162b2 (V8)-related higher absolute and relative (to body) spleen weights (up to 1.62x controls) were evident and correlated with the macroscopic observation of increased spleen size and the increased hematopoiesis. This is likely secondary to immune responses induced by the BNT162b2 (V8) vaccine.

The most common macroscopic observation in the BNT162b2 (V8) group was a thickened injection site and/or induration noted for nearly all animals (16/20) at necropsy. This finding correlated with microscopic inflammation at the injection site. Macroscopic findings at the injection site were resolved at the end of the recovery phase. Enlarged spleen and iliac lymph nodes were noted in several animals in the BNT162b2 (V8)-administered group, which correlated microscopically to expansion of lymphoid and/or hematopoietic cells. The effects on the lymphoid organs are consistent with immune responses to the BNT162b2 (V8).

Vaccine-related microscopic findings at the end of dosing were evident in injection sites and surrounding tissues, in the draining (iliac) lymph nodes, bone marrow, spleen, and liver.

The inflammation at the injection site was characterized by infiltrates of macrophages, granulocytes, and lymphocytes into the muscle, and variably into the dermis and subcutis. Injection site inflammation was associated with moderate edema, mild myofiber degeneration, occasional muscle necrosis, and mild fibrosis. Injection site findings were consistent with an immune/inflammatory response to an IM vaccine administration.

In the draining (iliac) lymph node, increased cellularity of the follicular germinal centers and increased plasma cells (plasmacytosis) were variably present for all BNT162b2 (V8)-dosed animals. In addition, minimal to mild increases in the cellularity of bone marrow and

hematopoiesis in the spleen likely related to increased granulopoiesis and correlated with increased circulating neutrophils (which correlated with increased spleen size and weight) were present in BNT162b2 (V8)-dosed animals.

Vacuolation of hepatocytes (minimal to mild) in the portal regions of the liver were present for all BNT162b2 (V8)-dosed animals. The liver findings were not associated with changes in markers of hepatocyte injury (eg, AST or ALT). While GGT was elevated in vaccine-administered animals, it was not considered to be associated with the vacuolation of hepatocytes (Enmulat et al, 2010). The microscopic observation of liver vacuolation is believed to be associated with hepatocyte uptake of the LNP lipids (Section 2.4.3.4; Sedic et al, 2018).

Microscopic findings at the end of the dosing phase were partially or completely resolved in all animals at the end of the recovery phase. Inflammation at the injection site and surrounding tissues was less severe (minimal to mild) in animals administered BNT162b2 (V8) at the end of the 3-week recovery phase, indicating partial recovery. In the iliac lymph node, plasmacytosis was less severe, and macrophage infiltrates were present at the end of the 3-week recovery phase and reflect resolution of the inflammation noted at the end of the dosing phase.

All other observations in the bone marrow, spleen, and liver were fully resolved at the end of the 3-week recovery phase.

The immune response to the vaccine antigen was evaluated by S1-binding IgG and RBD-binding IgG ELISAs, and a SARS-CoV-2 S pseudotype neutralization (pVNT) assay on Days 17 and 38 (Section 2.4.2.1.4). The data demonstrate that BNT162b2 (V8) elicited a SARS-CoV-2 S-specific antibody response with high neutralizing activity.

In conclusion, administration of BNT162b2 (V8) by IM injection to male and female Wistar Han rats once every week for 3 doses, was tolerated at 100 µg RNA/dosing day without evidence of systemic toxicity.

2.4.4.3.2. 17-Day Intramuscular Toxicity Study of BNT162b2 (V9) in Wistar Han Rats with a 3-week Recovery

The vaccine candidate BNT162b2 (V9), an LNP-formulated modified RNA vaccine expressing SARS-CoV-2 P2 S, was assessed in a GLP-compliant repeat-dose toxicity study in Wistar Han rats (Study 20GR142). This study also included assessment of another LNP-formulated RNA vaccine candidate (BNT162b3) that will not be included in the licensure application. For the purpose of this submission, the study findings from the BNT162b2 (V9) vaccine are summarized; findings from the BNT162b3 vaccine candidate also tested in this study were generally similar. BNT162b2 (V9) was administered at 30 µg once weekly for 3 doses (Days 1, 8, and 15) followed by a 3-week recovery phase.

Administration of BNT162b2 (V9) via IM injections once weekly for 3 administrations to male and female Wistar Han rats was tolerated without evidence of systemic toxicity. The vaccine elicited a robust antigen-specific immune response and produced nonadverse macroscopic changes at the injection sites, spleen, and the draining lymph nodes; increased

hematopoiesis in the bone marrow and spleen; liver vacuolation; and clinical pathology changes consistent with an immune response. The findings in this study were either fully recovered or showed evidence of ongoing recovery at the end of the 3-week recovery phase, and were consistent with those typically associated with the IM administration of LNP-encapsulated mRNA vaccines ([Hassett et al, 2019](#)).

All animals administered BNT162b2 (V9) survived to scheduled necropsy. There were no test article-related clinical signs or body weight changes noted. Test article-related reduced mean food consumption was noted on Days 4 and 11 (down to 0.83x controls). Test article-related higher mean body temperature (maximum increase post each dose) compared with control animals was noted on Day 1 (up to 0.54°C), Day 8 (up to 0.98°C), and Day 15 (up to 1.03°C) postdose.

BNT162b2 (V9)-related injection site edema and erythema were noted on Days 1 (up to slight edema and very slight erythema), 8 (up to moderate edema and very slight erythema), and 15 (up to moderate edema and very slight erythema). The incidence and severity of the reactions were higher after the second or third injections compared with the first injection. Test article-related erythema and edema fully resolved prior to dose administration on Days 8 and 15. Injection site erythema and edema were fully resolved at the end of the recovery phase.

All clinical pathology changes (type and magnitude) were generally consistent with expected immune responses to the vaccine or secondary to inflammation.

There were higher WBCs (up to 2.95x controls), primarily involving neutrophils (up to 6.60x controls), monocytes (up to 3.30x controls), and LUC (up to 13.2x controls) and slightly higher eosinophils and basophils on Days 4 and 17. WBCs were higher on Day 17 as compared with Day 4. There were transiently lower RETICs on Day 4 (down to 0.27x controls) in both sexes and higher RETICs on Day 17 (up to 1.31x controls) in females only. Lower RBC mass parameters (down to 0.90x controls) were present on Days 4 and 17. All test article-related hematology and coagulation changes noted in the dosing phase were fully reversed after a 3-week recovery phase, with the exception of higher red cell distribution width (up to 1.21x controls) in animals administered BNT162b2 (V9). The higher RDW reflects prior reticulocyte increases.

There were lower A:G ratios (down to 0.82x) on Days 4 and 17. Higher fibrinogen levels were observed on Day 17 (up to 2.49x) when compared with control animals, consistent with an acute phase response. The acute phase proteins alpha-1-acid glycoprotein (up to 39x on Day 17) and alpha-2-macroglobulin (up to 71x on Day 17) were elevated in both males and females in the BNT162b2 (V9)-administered group on Days 4 and 17 with higher concentrations generally observed in males. All other changes in clinical pathology parameters were considered incidental. All test article-related clinical chemistry changes noted in the dosing phase were fully reversed after a 3-week recovery phase, except higher globulins (up to 1.08x controls) in animals administered BNT162b2 (V9) and lower A:G ratio (down to 0.91x controls) in females administered BNT162b2 (V9), reflecting vaccine-related immune response.

Test article-related higher group mean absolute and relative spleen weights (compared to body weight) were noted in males that had received BNT162b2 (V9) (up to 1.42x) and females (up to 1.59x) relative to control group means. There were no other test article-related changes in organ weights. At the end of the recovery phase, spleen weights were within normal limits.

Test article-related macroscopic findings included the observation of enlarged draining lymph nodes (2/20 animals) and pale/dark (5/20 animals) or firm (6/20 animals) injection sites in animals administered BNT162b2 (V9). These changes fully recovered, except for partial recovery of enlarged draining nodes, suggesting recovery in progress.

Test article-related microscopic pathology findings were observed at the injection site and in the draining (iliac) and inguinal lymph nodes, spleen, bone marrow, and liver for both vaccine candidates. All microscopic findings were nonadverse, as there was no evidence of systemic toxicity or clinical signs of illness or lameness.

At the end of the dosing phase, test article-related mixed cell inflammation (mild to moderate) and edema (mild to moderate) at the injection site were consistent with findings typically associated with the IM administration of LNP-encapsulated mRNA vaccines (Hassett et al, 2019). These findings correlated with macroscopic observations of abnormal color (dark/pale) and consistency (firm). At the end of the 3-week recovery phase, there was full recovery for injection site edema and partial recovery for injection site inflammation, suggesting recovery in progress.

At the end of the dosing phase, test article-related findings in the draining (iliac) and inguinal lymph nodes (up to moderately increased cellularity of plasma cells and germinal centers), spleen (minimally increased cellularity of hematopoietic cells and germinal centers), and the bone marrow (minimal increased cellularity of hematopoietic cells) were present. These changes are secondary to immune activation and/or inflammation at the injection site. The presence of plasma cells (interpreted as plasmablasts) in the draining (iliac) and inguinal lymph nodes is consistent with a robust immunological response to the vaccines. These observations correlated with macroscopic observations of abnormal size (enlarged) in the lymph nodes and spleen and increased spleen weights. At the end of the 3-week recovery phase, full recovery of increased cellularity of hematopoietic cells in the spleen and bone marrow, with partial recovery (recovery in progress) of increased cellularity of plasma cells and germinal centers in the draining and inguinal lymph nodes, and increased cellularity of the germinal centers in the spleen.

At the end of the dosing phase, the test article-related microscopic finding of minimal periportal hepatocyte vacuolation was not associated with hepatocellular damage or alterations in liver function tests. The liver vacuolation is believed to be associated with hepatocyte uptake of the LNP lipids (Section 2.4.3.4; Sedic et al, 2018). At the end of 3-week recovery phase, this finding was completely recovered.

Administration of 3 once weekly doses of BNT162b2 (V9) elicited SARS-CoV-2 neutralizing antibody responses in males and females at the end of the dosing (Day 17) and recovery phases (Day 21) of the study. SARS-CoV-2 neutralizing antibody responses were

090177e1962c108d\Approved\Approved On: 08-Feb-2021 15:26 (GMT)

not observed in animals prior to vaccine administration or in saline-administered control animals.

In conclusion, administration of BNT162b2 (V9) at 30 µg RNA/dosing day via IM injections weekly for 3 administrations to male and female Wistar Han rats was tolerated without evidence of systemic toxicity. Dosing of BNT162b2 (V9) produced changes consistent with an inflammatory response and immune activation. The findings in this study are consistent with those typically associated with the IM administration of LNP-encapsulated mRNA vaccines.

2.4.4.4. Genotoxicity

No genotoxicity studies are planned for BNT162b2 as the components of the vaccine construct are lipids and RNA and are not expected to have genotoxic potential (WHO, 2005).

2.4.4.5. Carcinogenicity

Carcinogenicity studies with BNT162b2 have not been conducted as the components of the vaccine construct are lipids and RNA and are not expected to have carcinogenic or tumorigenic potential. Carcinogenicity testing is generally not considered necessary to support the development and licensure of vaccine products for infectious diseases (WHO, 2005).

2.4.4.6. Reproductive and Developmental Toxicity

Reproductive and developmental toxicity assessments were made with BNT162b2 (V9) (Study 20256434). BNT162b2 was administered by IM injection at the human clinical dose (30 µg RNA/dosing day) to 44 female Wistar Han rats (F0) 21 and 14 days prior to mating with untreated males and on GD 9 and 20, for a total of 4 dosing days. A separate control group of 44 F0 females received saline by the same route and regimen.

Following completion of a mating phase with untreated males, 22 rats/group underwent caesarean-section on GD 21 and were submitted to routine embryo-fetal development evaluations. The remaining 22 rats/group were allowed to litter and development of the offspring was observed until PND 21.

There were no BNT162b2-related deaths during the study. IM administration of BNT162b2 before and during gestation to female Wistar rats resulted in nonadverse clinical signs and macroscopic findings localized to the injection site as well as transient, nonadverse body weight and food consumption effects after each dose administration. These maternal findings are all consistent with administration of a vaccine and an inflammatory/immune response.

There were no BNT162b2-related effects on any mating or fertility parameters. There were no BNT162b2-related effects on any ovarian, uterine, or litter parameters, including embryo-fetal survival, growth, or external, visceral, or skeletal malformations, anomalies, or variations. There were no effects of BNT162b2 administration on postnatal offspring (F1) development, including postnatal growth, physical development (pinna unfolding and eye

opening), reflex ontogeny (pre-weaning auditory and visual function tests), macroscopic observations, and survival.

All F0 females administered BNT162b2 developed SARS-CoV-2 neutralizing antibodies and these antibodies were also detectable in all fetuses and pups from the caesarean and littering groups, respectively. The animals in the saline control group did not exhibit an immune response to BNT162b2.

In conclusion, administration of BNT162b2 to female rats twice before the start of mating and twice during gestation at the human clinical dose was associated with nonadverse effects (body weight, food consumption, and effects localized to the injection site) after each dose administration. However, there were no effects of BNT162b2 administration on mating performance, fertility, or any ovarian or uterine parameters in the F0 female rats nor on embryo-fetal or postnatal survival, growth, or development in the F1 offspring. An immune response was confirmed in F0 female rats following administration of each vaccine candidate and these responses were also detectable in the F1 offspring (fetuses and pups).

Macroscopic and microscopic evaluation of male and female reproductive tissues from the repeat-dose toxicity studies with BNT162b2 showed no evidence of toxicity.

2.4.4.7. Local Tolerance

Local tolerance of IM administration of BNT162b2 was evaluated by injection site observations and macroscopic and microscopic examination of injection sites in the repeat-dose toxicity studies and is described in [Section 2.4.4.3](#).

2.4.4.8. Other Toxicity Studies

2.4.4.8.1. Phototoxicity

Phototoxicity studies with BNT162b2 have not been conducted.

2.4.4.8.2. Antigenicity

Immunogenicity was evaluated as part of the primary pharmacodynamic studies ([Section 2.4.2.1](#)). Serology data from the repeat-dose toxicity studies shows a robust antigen-specific immune response to BNT162b2.

2.4.4.8.3. Immunotoxicity

Stand-alone immunotoxicity studies with BNT162b2 have not been conducted. However, immunotoxicological endpoints were collected as part of the repeat-dose toxicity studies; there were no adverse effects observed and no significant effects on measured cytokines.

2.4.4.8.4. Mechanistic Studies

Mechanistic studies with BNT162b2 have not been conducted.

2.4.4.8.5. Dependence

Dependence studies with BNT162b2 have not been conducted.

2.4.4.8.6. Studies on Metabolites

Stand-alone studies with administration of metabolites of BNT162b2 have not been conducted.

2.4.4.8.7. Studies on Impurities

Stand-alone studies with administration of impurities of BNT162b2 have not been conducted.

2.4.4.8.8. Other Studies

No other studies with BNT162b2 evaluated in this submission have been conducted.

2.4.4.9. Target Organ Toxicity

Based on data from the GLP repeat-dose toxicity studies ([Section 2.4.4.3](#)), administration of BNT162b2 was well tolerated without any evidence of systemic toxicity. BNT162b2 administration was associated with local reactogenicity at the injection site and expected inflammatory responses, including increases in lymphoid cells in draining lymph nodes and spleen. Microscopic findings within injection sites, which were partially reversed by the end of recovery, support this conclusion. The liver finding was reversible, not associated with changes in markers of hepatocyte injury and not considered adverse. The elevated levels of GGT in [Study 38166](#) were not recapitulated in [Study 20GR142](#) and were not associated with hepatobiliary changes microscopically. Elevated GGT was not attributed to the hepatocyte vacuolation ([Enmulat et al, 2010](#)).

090177e1962c108d\Approved\Approved On: 08-Feb-2021 15:26 (GMT)

2.4.5. INTEGRATED OVERVIEW AND CONCLUSIONS

The nonclinical program demonstrates that BNT162b2 is immunogenic in mice, rats, and nonhuman primates, and the toxicity studies support the licensure of this vaccine. Preclinical assessments in mice and nonhuman primates demonstrate that BNT162b2 elicits a rapid antibody response with measurable SARS-CoV-2 neutralizing titers after a single dose and substantial increases in titers after a second dose that exceed titers in sera from SARS-CoV-2/COVID-19-recovered patients. A Th1-dominant T cell response was evident in both mice and nonhuman primates. In a SARS-CoV-2 rhesus challenge model, BNT162b2 provided complete protection in the lungs, as determined by lack of detectable viral RNA, and there was no evidence of vaccine-elicited disease enhancement.

An IV rat PK study, using an LNP with the identical lipid composition as BNT162b2, demonstrated that the novel lipid excipients in the LNP formulation, ALC-0315 and ALC-0159, distribute from the plasma to the liver. While there was no detectable excretion of either lipid in the urine, the percent of dose excreted unchanged in feces was ~1% for ALC-0315 and ~50% for ALC-0159. Further studies indicated metabolism played a role in the elimination of ALC-0315. Biodistribution was assessed using luciferase expression as a surrogate reporter formulated like BNT162b2, with the identical lipid composition. After IM injection of the LNP-formulated RNA encoding luciferase in BALB/c mice, luciferase protein expression was demonstrated at the site of injection 6 hours post dose and was not detected after 9 days. Luciferase was detected to a lesser extent in the liver; expression was present at 6 hours after injection and was not detected by 48 hours after injection. After IM administration of a radiolabeled LNP-mRNA formulation containing ALC-0315 and ALC-0159 to rats, the percent of administered dose was also greatest at the injection site. Outside of the injection site, total recovery of radioactivity was greatest in the liver and much lower in the spleen, with very little recovery in the adrenal glands and ovaries. The metabolism of ALC-0315 and ALC-0159 was evaluated in blood, liver microsomes, S9 fractions, and hepatocytes from mice, rats, monkeys, and humans. The *in vivo* metabolism was examined in rat plasma, urine, feces, and liver samples from the PK study. Metabolism of ALC-0315 and ALC-0159 appears to occur slowly *in vitro* and *in vivo*. ALC-0315 and ALC-0159 are metabolized by hydrolytic metabolism of the ester and amide functionalities, respectively, and this hydrolytic metabolism is observed across the species evaluated.

Administration of BNT162b2 by IM injection to male and female Wistar Han rats once every week for a total of 3 weekly cycles of dosing was tolerated without evidence of systemic toxicity in GLP-compliant repeat-dose toxicity studies. Expected immune responses to the vaccine were evident such as edema and erythema at the injection sites, transient elevation in body temperature, elevations in WBCs and acute phase reactants, and decreased A:G ratios. Injection site reactions were common in all vaccine-administered animals and were greater after boost immunizations. Changes secondary to inflammation included slight and transient reductions in body weights and transient reductions in RETIC, PLT, and RBC mass parameters. All changes in hematology parameters and acute phase proteins were similar to control at the end of the recovery phase for BNT162b2 with the exception of higher RDW and lower A:G ratios in animals administered BNT162b2 (V9). Macroscopic pathology and organ weight changes were also consistent with immune activation and inflammatory response and included increased size of draining iliac lymph nodes and increased size and

090177e1962c108d\Approved\Approved On: 08-Feb-2021 15:26 (GMT)

BNT162b2

Module 2.4. Nonclinical Overview

weight of spleen. Vaccine-related microscopic findings at the end of dosing for BNT162b2 were evident in injection sites and surrounding tissues, in the draining iliac lymph nodes, bone marrow, spleen, and liver. Microscopic findings at the end of the dosing phase were partially (recovery in progress) or completely recovered in all animals at the end of the recovery phase for BNT162b2. A robust immune response was elicited to the BNT162b2 vaccine antigen.

Administration of BNT162b2 to female rats twice before the start of mating and twice during gestation at the human clinical dose (30 µg RNA/dosing day) was associated with nonadverse effects (body weight, food consumption and effects localized to the injection site) after each dose administration. There were no effects of BNT162b2 administration on mating performance, fertility, or any ovarian or uterine parameters in the F0 female rats nor on embryo-fetal or postnatal survival, growth, or development in the F1 offspring. An immune response was confirmed in F0 female rats following administration of BNT162b2 and this response was also detectable in the F1 offspring (fetuses and pups).

In summary, the nonclinical package summarized above supports the BLA of BNT162b2 administered twice by IM injection at a dose of 30 µg RNA.

090177e1962c108d\Approved\Approved On: 08-Feb-2021 15:26 (GMT)

CONFIDENTIAL

Page 33

FDA-CBER-2021-4379-0000696

2.4.6. LIST OF LITERATURE REFERENCES

Barry MA, May S, Weaver EA. Imaging luciferase-expressing viruses. *Methods Mol Biol* 2012;797:79-87.

Boone L, Meyer D, Cusick P, et al. Selection and interpretation of clinical pathology indicators of hepatic injury in preclinical studies. *Vet Clin Pathol* 2005;34(3):182-8.

Cai Y, Zhang J, Xiao T, et al. Distinct conformational states of SARS-CoV-2 spike protein. *Science* 2020;10.1126/science.abd4251.

Chen C-Y, Tran DM, Cavedon A, et al. Treatment of Hemophilia A Using Factor VIII Messenger RNA Lipid Nanoparticles. *Mol Ther Nucleic Acids* 2020;20:534-44.

Elia U, Ramishetti S, Dammes N, et al. Design of SARS-CoV-2 RBD mRNA Vaccine Using Novel Ionizable Lipids. *bioRxiv* 2020.10.15.341537.

Ennulat D, Magid-Slav M, Rehm S, et al. Diagnostic performance of traditional hepatobiliary biomarkers of drug-induced liver injury in the rat. *Toxicol Sci* 2010;116(2):397-412.

Fukuchi M, Saito R, Maki S, et al. Visualization of activity-regulated BDNF expression in the living mouse brain using non-invasive near-infrared bioluminescence imaging. *Mol Brain* 2020;13(1):122.

Hassett KJ, Benenato KE, Jacquinet E et al. Optimization of lipid nanoparticles for intramuscular administration of mRNA vaccines. *Molecular Therapy Nucleic Acids* 2019;15:1-11.

Jeon YH, Choi Y, Kang JH, et al. In vivo monitoring of DNA vaccine gene expression using firefly luciferase as a naked DNA. *Vaccine* 2006;24(16):3057-62.

Jiang S, Hyllyer C, Du L. Neutralizing antibodies against SARS-CoV-2 and other human coronaviruses. *Science and society. Trends Immunol* 2020;41(5)(May):355-9.

Ke Z, Oton J, Qu K, et al. Structures, conformations and distributions of SARS-CoV-2 spike protein trimers on intact virions. *Nature* 2020;10.1038/s41586-020-2665-2.

Kim JY, Ko JH, Kim Y, et al. Viral load kinetics of SARS-CoV-2 infection in first two patients in Korea. *J Korean Med Sci* 2020;35(7)(Feb):e86.

Kozauer NA, Dunn WH, Unger EF, et al. CBER multi-discipline review of Onpattro. NDA 210922. 10 Aug 2018. Available at: https://www.accessdata.fda.gov/drugsatfda_docs/nda/2018/210922Orig1s000MultiR.pdf. 02 Aug 2020.

Munster VJ, Feldmann F, Williamson BN, et al. Respiratory disease in rhesus macaques inoculated with SARS-CoV-2. *Nature* 2020 (May). Available from: <https://doi.org/10.1101/2020.03.21.001628>. Accessed: 24 Sep 2020.

Pallesen J, Wang N, Corbett KS, et al. Immunogenicity and structures of a rationally designed prefusion MERS-CoV spike antigen. *Proc Natl Acad Sci USA* 2017;114(35):E7348-57.

Pardi N, Hogan MJ, Pelc RS, et al. Zika virus protection by a single low-dose nucleoside-modified mRNA vaccination. *Nature* 2017;543(7644):248-51.

Pardi N, Parkhouse K, Kirkpatrick E, et al. Nucleoside-modified mRNA immunization elicits influenza virus hemagglutinin stalk-specific antibodies. *Nat Comm* 2018;9(1)(08):3361.

Sahin U, Karikó K, Türeci Ö. mRNA-based therapeutics - developing a new class of drugs. *Nat Rev Drug Discov* 2014;13(10):759-80.

Sedic M, Senn J, Lynn A, et al. Safety Evaluation of Lipid Nanoparticle–Formulated Modified mRNA in the Sprague- Dawley Rat and Cynomolgus Monkey. *Vet Path* 2018;55(2):341-54.

Sellers RS, Nelson K, Bennet B, et al. Scientific and regulatory policy committee points to consider*: approaches to the conduct and interpretation of vaccine safety studies for clinical and anatomic pathologists. *Toxicol Pathol* 2020;48(2):257-76.

Singh DK, Ganatra SR, Singh B, et al. SARS-CoV-2 infection leads to acute infection with dynamic cellular and inflammatory flux in the lung that varies across nonhuman primate species. *bioRxiv* 2020:06.05.136481. Accessed: 24 Sep 2020.

Truong B, Allegri G, Liu X-B, et al. Lipid nanoparticle-targeted mRNA therapy as a treatment for the inherited metabolic liver disorder arginase deficiency. *Proc Natl Acad Sci USA* 2019;116(42):21150-9.

US Department of Health and Human Services, Food and Drug Administration, Center for Biologics Evaluation and Research. Development and licensure of vaccines to prevent COVID-19. In: *Guidance for industry*. Rockville, MD: Food and Drug Administration; 2020: 21 pages.

World Health Organization. WHO guidelines on nonclinical evaluation of vaccines. Annex 1. In: *World Health Organization. WHO technical report series, no. 927*. Geneva, Switzerland; World Health Organization; 2005:31-63.

World Health Organization. Annex 2. Guidelines on the nonclinical evaluation of vaccine adjuvants and adjuvanted vaccines. In: *WHO technical report series no. 987*. Geneva, Switzerland: World Health Organization; 2014: p. 59-100.

Wrapp D, Wang N, Corbett KS, et al. Cryo-EM structure of the 2019-nCoV spike in the prefusion conformation. *Science* 2020;367(6483):1260-3.

Yong CY, Ong HK, Yeap SK, et al. Recent advances in the vaccine development against middle east respiratory syndrome-coronavirus. *Front Microbiol* 2019;10:1781.

Zakhartchouk AN, Sharon C, Satkunarajah M, et al. Immunogenicity of a receptor-binding domain of SARS coronavirus spike protein in mice: implications for a subunit vaccine. *Vaccine* 2007;25(1):136-43.

Zhou M, Zhang X, Qu J. Coronavirus disease 2019 (COVID-19): a clinical update. *Front Med* 2020(Apr):1-10.

Zost S, Gilchuk P, Chen R, et al. Rapid isolation and profiling of a diverse panel of human monoclonal antibodies targeting the SARS-CoV-2 spike protein. *BioRxiv* posted May13, 2020, www.biorxiv.org/content/10.1101/2020.05.12.091462v1.

Zou L, Ruan F, Huang M, et al. SARS-CoV-2 viral load in upper respiratory specimens of infected patients. *N Engl J Med* 2020;382(12)(03):1177-9.

MODULE 2.6.4. PHARMACOKINETICS WRITTEN SUMMARY

This document contains confidential information belonging to BioNTech/Pfizer. Except as may be otherwise agreed to in writing, by accepting or reviewing these materials, you agree to hold such information in confidence and not to disclose it to others (except where required by applicable law), nor to use it for unauthorized purposes. In the event of actual or suspected breach of this obligation, BioNTech/Pfizer should be promptly notified.

090177e1961d1c83\Approved\Approved On: 08-Feb-2021 17:49 (GMT)

CONFIDENTIAL

Page 1

TABLE OF CONTENTS

LIST OF ABBREVIATIONS AND DEFINITION OF TERMS3

2.6.4. PHARMACOKINETICS WRITTEN SUMMARY4

 2.6.4.1. Brief Summary4

 2.6.4.2. Methods of Analysis.....4

 2.6.4.3. Absorption4

 2.6.4.4. Distribution.....5

 2.6.4.5. Metabolism.....7

 2.6.4.6. Excretion9

 2.6.4.7. Pharmacokinetic Drug Interactions9

 2.6.4.8. Discussion and Conclusions9

 2.6.4.9. References10

090177e1961d1c83\Approved\Approved On: 08-Feb-2021 17:49 (GMT)

BNT162b2

Module 2.6.4. Pharmacokinetics Written Summary

LIST OF ABBREVIATIONS AND DEFINITION OF TERMS

ADME	Absorption, distribution, metabolism, excretion
ALC-0159	Proprietary PEG-lipid included as an excipient in the LNP formulation used in BNT162b2
ALC-0315	Proprietary amino-lipid included as an excipient in the LNP formulation used in BNT162b2
[³ H]-CHE	Radiolabeled [Cholesteryl-1,2- ³ H(N)]-Cholesteryl Hexadecyl Ether
DSPC	1,2-distearoyl-sn-glycero-3-phosphocholine
GLP	Good Laboratory Practice
H	Human (in metabolite scheme)
IM	Intramuscular(ly)
IV	Intravenous(ly)
LNP	Lipid-nanoparticle
Luc	Luciferase (from firefly <i>Pyroactomena lucifera</i>)
Mk	Monkey (in metabolite scheme)
Mo	Mouse (in metabolite scheme)
modRNA	Nucleoside-modified mRNA
mRNA	Messenger RNA
PEG	Polyethylene glycol
PK	Pharmacokinetics
R	Rat (in metabolite scheme)
RNA	Ribonucleic acid
S9	Supernatant fraction obtained from liver homogenate by centrifuging at 9000 g
WHO	World Health Organization

090177e1961d1c83\Approved\Approved On: 08-Feb-2021 17:49 (GMT)

CONFIDENTIAL

Page 3

FDA-CBER-2021-4379-0000702

2.6.4. PHARMACOKINETICS WRITTEN SUMMARY

2.6.4.1. Brief Summary

The ADME profile of BNT162b2 (BioNTech code number BNT162, Pfizer code number PF-07302048) included evaluation of the PK and metabolism of two novel lipid excipients (ALC-0315 and ALC-0159) in the LNP and potential biodistribution using luciferase expression as a surrogate reporter or a radiolabeled lipid marker. The PK study showed the LNP distributes from the blood to the liver, ~1% of ALC-0315 and ~50% of ALC-0159 were excreted unchanged in feces, and there was no detectable excretion of unchanged ALC-0315 and ALC-0159 in the urine.

In a mouse biodistribution study, protein expression was demonstrated at the site of injection and to a lesser extent in the liver after BALB/c mice received an IM injection of modRNA encoding luciferase in an LNP formulation, with the identical lipid composition as BNT162b2. Luciferase expression was identified at the injection site at 6 hours after injection and was not detected after 9 days. Liver expression was also present at 6 hours after injection and was no longer detected by 48 hours after injection. A quantitative biodistribution study was also carried out in Wistar Han rats using a radiolabeled lipid marker and a luciferase modRNA in the same LNP formulation as BNT162b2. Following IM administration, the greatest mean concentration remained at the injection site, while up to 18% of the administered dose was found in the liver.

The metabolism of ALC-0315 (aminolipid) and ALC-0159 (PEG-lipid) was evaluated in vitro using blood, liver microsomes, S9 fractions, and hepatocytes from mice, rats, monkeys, and humans. The in vivo metabolism was examined in rat plasma, urine, feces, and liver samples collected during the PK study. In vitro and in vivo studies indicated ALC-0315 and ALC-0159 are metabolized slowly by hydrolytic metabolism of the ester and amide functionalities, respectively, across the species evaluated.

2.6.4.2. Methods of Analysis

No methods of analysis have been validated to support GLP TK studies of components of BNT162b2; however, a qualified LC/MS method was developed to support quantitation of the two novel LNP excipients for the non-GLP IV PK study in rats ([PF-07302048_06Jul20_072424](#)). Methods for immunogenicity and efficacy studies are described in [Section 2.6.2.12](#).

2.6.4.3. Absorption

An intravenous rat PK study was performed using LNPs containing surrogate luciferase RNA, with the identical lipid composition as BNT162b2, to explore the disposition of ALC-0159 and ALC-0315 ([Table 2.6.4-1](#), Study [PF-07302048_06Jul20_072424](#); [Tabulated Summary 2.6.5.3](#)). The distribution of the LNP from the blood to the liver was rapid and essentially complete by 24 h, with <1% of the maximum observed plasma concentrations remaining ([Figure 2.6.4-1](#)). The liver appears to be the major site of drug uptake from the blood.

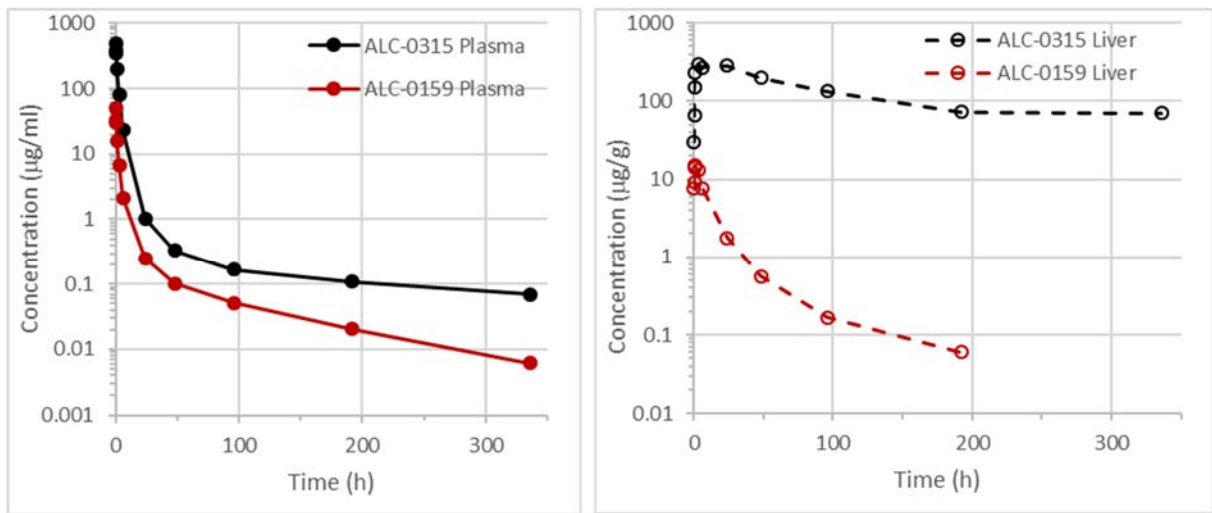
Table 2.6.4-1. PK of ALC-0315 and ALC-0159 in Wistar Han Rats After IV Administration of LNPs Containing Surrogate Luciferase RNA at 1 mg/kg

Analyte	Dose of Analyte (mg/kg)	Gender /N	t _{1/2} (h)	AUC _{inf} (µg•h/mL)	AUC _{last} (µg•h/mL)	Estimated fraction of dose distributed to liver (%) ^a
ALC-0315	15.3	Male/3 ^b	139	1030	1020	60
ALC-0159	1.96	Male/3 ^b	72.7	99.2	98.6	20

a. Calculated as highest mean amount in the liver (µg)/total mean dose (µg) of ALC-0315 or ALC-0159.

b. 3 animals per timepoint; non-serial sampling.

Figure 2.6.4-1. Plasma and Liver Concentrations of ALC-0315 and ALC-0159 in Wistar Han Rats After IV Administration of LNPs Containing Surrogate Luciferase RNA at 1 mg/kg



No absorption studies were conducted for BNT162b2, as the administration route is IM. Pharmacokinetic studies have not been conducted with BNT162b2 and are generally not considered necessary to support the development and licensure of vaccine products for infectious diseases (WHO, 2005; WHO, 2014).

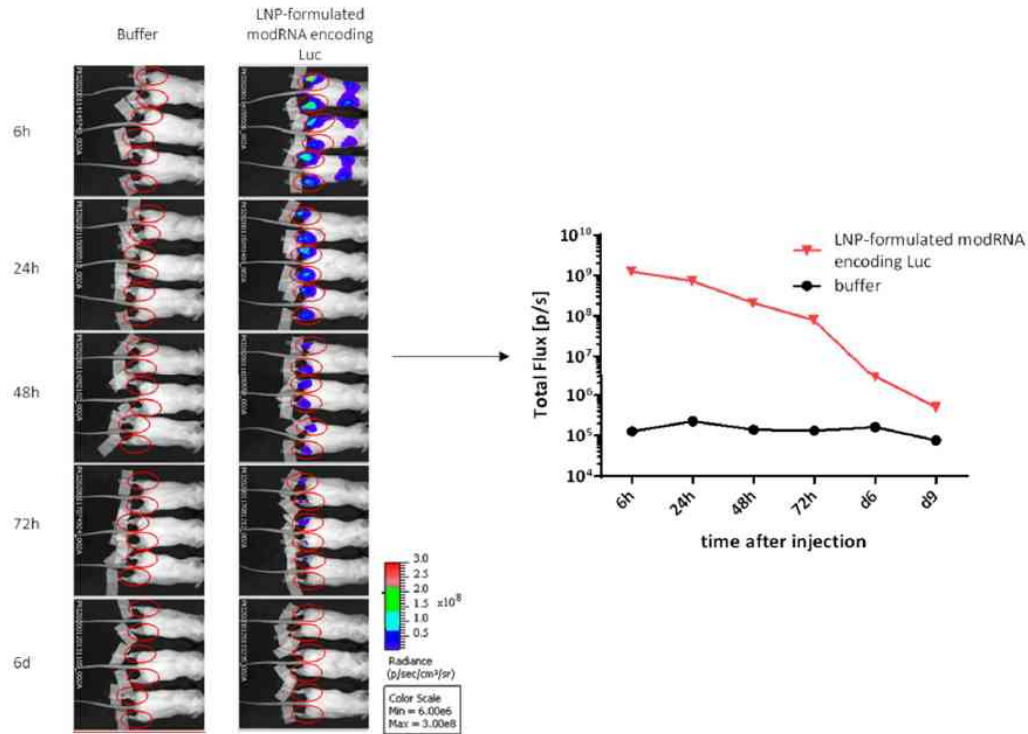
2.6.4.4. Distribution

In an in vivo study in BALB/c mice (Study R-20-0072; Tabulated Summary 2.6.5.5A), the biodistribution of BNT162b2 was assessed using luciferase as a surrogate marker protein. RNA encoding luciferase was formulated like BNT162b2, with the identical lipid composition, and mice received IM injections of 1 µg each in the right and left hind leg (for a total of 2 µg) of LNP-formulated modRNA encoding luciferase. Luciferase protein expression was detected at different timepoints, by measuring the in vivo bioluminescence (Figure 2.6.4-2) after injection of luciferin substrate, at the site of injection and to a lesser extent in the liver. Distribution to the liver is likely mediated by LNPs entering the blood stream. The repeat-dose toxicity studies in rats showed no evidence of liver injury (Section 2.6.6.3). The luciferase expression at the injection site, the tissue with the highest

090177e1961d1c83\Approved\Approved On: 08-Feb-2021 17:49 (GMT)

bioluminescence, dropped to background levels after 9 days. As detailed in Section 2.6.4.3, following systemic (IV) administration the liver appears to be the major organ into which the LNPs distribute, this is consistent with the observations made following IM administration.

Figure 2.6.4-2. Bioluminescence Emission in BALB/c Mice after IM Injection of an LNP Formulation of modRNA Encoding Luciferase



These qualitative data are supported by a biodistribution study (Study 185350; Tabulated Summary 2.6.5.5B) carried out with LNPs with a comparable lipid composition as BNT162b2 but with a luciferase mRNA and a [³H]-CHE lipid radiolabel. Following IM administration to male and female Wistar Han rats at a dose of 50 µg (1.29 mg total lipid), the greatest mean concentration was found remaining in the injection site at each time point in both sexes. Outside the injection site, the highest levels of radioactivity were observed in plasma at 1-4 hours post-dose. Over 48 hours, the radiolabel distributed mainly to the liver, adrenal glands, spleen and ovaries, with maximum concentrations observed at 8-48 hours post-dose. Total recovery of radioactivity (% of injected dose) outside the injection site was greatest in the liver (up to 18%) and was much less in the spleen (≤1.0%), adrenal glands (≤0.11%) and ovaries (≤0.095%). The mean concentrations and tissue distribution pattern were broadly similar between sexes.

The biodistribution of the expression of the antigen encoded by the RNA component of BNT162b2 is expected to be dependent on the LNP distribution. Therefore, results of these biodistribution studies should be representative for BNT162b2, as the LNP-formulated luciferase-encoding modRNA had the same lipid composition.

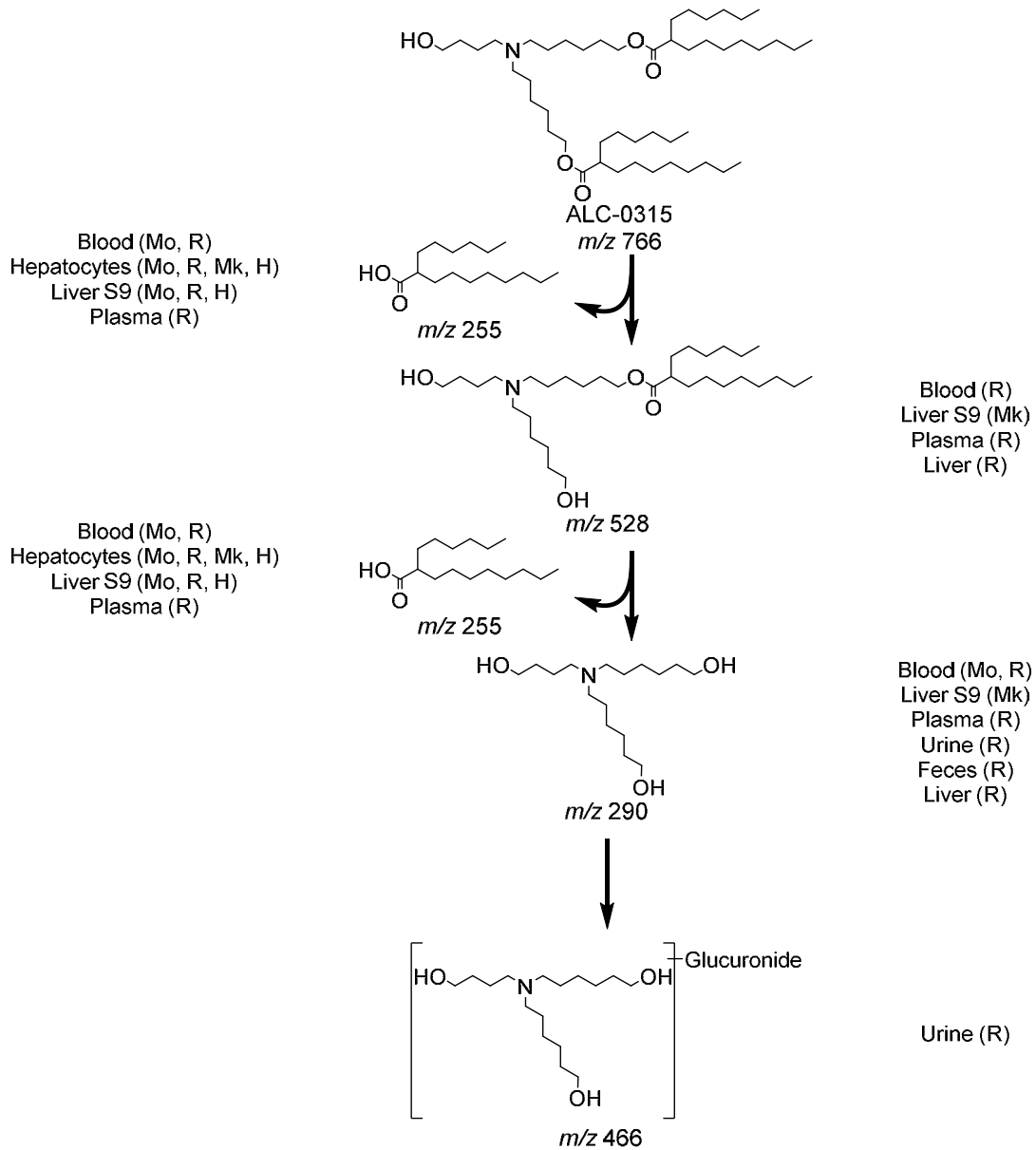
090177e1961d1c83\Approved\Approved On: 08-Feb-2021 17:49 (GMT)

2.6.4.5. Metabolism

Metabolism studies were conducted to evaluate ALC-0315 (aminolipid) and ALC-0159 (PEG-lipid). These novel lipids were evaluated for in vitro metabolic stability in CD-1/ICR mouse, Wistar Han and/or Sprague Dawley rat, cynomolgus monkey, and human liver microsomes, S9 fractions, and hepatocytes. ALC-0315 and ALC-0159 were stable (>82% remaining) over 120 min in liver microsomes and S9 fractions and over 240 min in hepatocytes in all species and test systems (Studies [01049-20008](#), [01049-20009](#), [01049-20010](#), [01049-20020](#), [01049-20021](#), and [01049-20022](#); [Tabulated Summaries 2.6.5.10A](#) and [2.6.5.10B](#)).

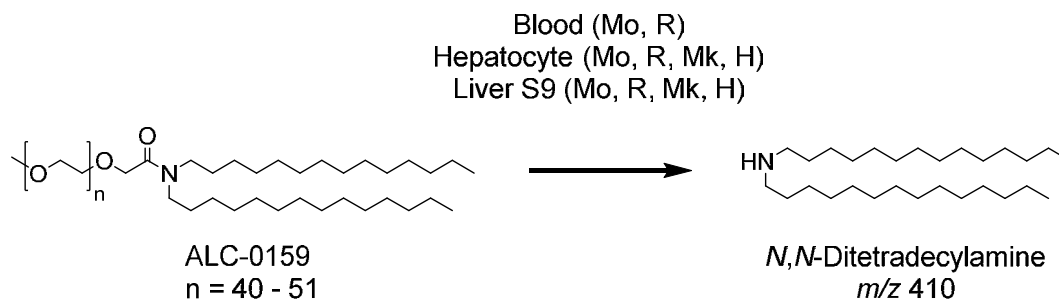
The metabolism of ALC-0315 and ALC-0159 was further evaluated (Study [PF-07302048_05Aug20_043725](#); [Tabulated Summaries 2.6.5.9](#), [2.6.5.10C](#), and [2.6.5.10D](#)) in vitro using blood, liver S9 fractions, and hepatocytes from CD-1 mice, Wistar Han rats, cynomolgus monkeys, and humans and in vivo using the rat plasma, urine, feces, and liver from the PK study ([Section 2.6.4.3](#)). This study determined ALC-0315 and ALC-0159 are metabolized slowly and undergo hydrolytic metabolism of the ester and amide functionalities, respectively. This hydrolytic metabolism was observed across the species evaluated, as shown in [Figure 2.6.4-3](#) and [Figure 2.6.4-4](#).

Figure 2.6.4-3. Proposed Biotransformation Pathway of ALC-0315 in Various Species



Metabolism of ALC-0315 occurs via two sequential ester hydrolysis reactions, first yielding the monoester metabolite (m/z 528) followed by the doubly deesterified metabolite (m/z 290). Subsequent metabolism of the doubly deesterified metabolite resulted in a glucuronide metabolite (m/z 466), which was only observed in urine from the rat PK study. The acid product of both hydrolysis reactions of ALC-0315, 6-hexyldecanoic acid (m/z 255), was also identified.

090177e1961d1c83\Approved\Approved On: 08-Feb-2021 17:49 (GMT)

Figure 2.6.4-4. Proposed Biotransformation Pathway of ALC-0159 in Various Species

The primary route of metabolism identified for ALC-0159 involves amide bond hydrolysis yielding *N,N*-ditetradecylamine (*m/z* 410). This metabolite was identified in mouse and rat blood, as well as hepatocytes and liver S9 from mouse, rat, monkey, and human. No metabolites of ALC-0159 were identified from in vivo samples.

The other two lipids in the LNP are naturally occurring (cholesterol and DSPC) and will be metabolized and excreted like other endogenous lipids. As the protein encoded by the mRNA in BNT162b2 is expected to be proteolytically degraded and RNA is degraded by cellular RNases and subjected to nucleic acid metabolism, no RNA or protein metabolism or excretion studies will be conducted.

2.6.4.6. Excretion

In the rat PK study (Section 2.6.4.3), there was no detectable excretion ALC-0315 and ALC-0159 in urine after IV administration of LNPs containing surrogate luciferase RNA at 1 mg/kg. The percent excreted unchanged in feces was ~1% for ALC-0315 and ~50% for ALC-0159. Metabolites of ALC-0315 were detected in the urine of rats (Figure 2.6.4-3). No excretion studies have been conducted with BNT162b2 for the reasons described in Section 2.6.4.5.

2.6.4.7. Pharmacokinetic Drug Interactions

No PK drug interaction studies have been conducted with BNT162b2.

2.6.4.8. Discussion and Conclusions

In the rat PK study, concentrations of ALC-0159 dropped approximately 8000- and >250-fold in plasma and liver, respectively, during this 2-week study. For ALC-0315, the elimination of the molecule from plasma and liver was slower, but concentrations fell approximately 7000- and 4-fold in two weeks for plasma and liver, respectively. Overall, the apparent terminal $t_{1/2}$ in plasma and liver were similar in both tissues and were 2-3 and 6-8 days for ALC-0159 and ALC-0315, respectively. The apparent terminal $t_{1/2}$ in plasma likely represents the re-distribution of the respective lipids from the tissues into which they have distributed as the LNP back to plasma where they are eliminated.

Overall, it appears that 50% of ALC-0159 was eliminated unchanged in feces. Metabolism played a role in the elimination of ALC-0315, as little to no unchanged material was detected in either urine or feces. Investigations of urine, feces and plasma from the rat PK study

identified a series of ester cleavage products of ALC-0315; this likely represents the primary clearance mechanism acting on this molecule, although no quantitative data is available to confirm this hypothesis. In vitro, ALC-0159 was metabolized slowly by hydrolytic metabolism of the amide functionality.

The potential biodistribution of BNT162b2 was assessed using luciferase expression as a surrogate reporter. Protein expression was demonstrated at the site of injection and to a lesser extent, and more transiently, in the liver after BALB/c mice received an IM injection of RNA encoding luciferase in an LNP formulation like BNT162b2. Luciferase expression was identified at the injection site at 6 hours after injection and was not detected by 9 days. Expression in the liver was also present at 6 hours after injection and was not detected by 48 hours after injection. These findings are supported by a quantitative biodistribution study in Wistar Han rats. After IM administration of a radiolabeled lipid marker and a luciferase modRNA in the same LNP formulation as BNT162b2 to rats, the percent of administered dose was greatest at the injection site. Outside of the injection site, total recovery of radioactivity was highest in the liver and much lower in the spleen, with very little recovery in the adrenal glands and ovaries.

2.6.4.9. References

1. World Health Organization. Annex 1. Guidelines on the nonclinical evaluation of vaccines. In: WHO Technical Report Series No. 927, Geneva, Switzerland. World Health Organization; 2005:31-63.
2. World Health Organization. Annex 2. Guidelines on the nonclinical evaluation of vaccine adjuvants and adjuvanted vaccines. In: WHO Technical Report Series No. 987, Geneva, Switzerland. World Health Organization 2014:59-100.

MODULE 2.6.5. PHARMACOKINETICS TABULATED SUMMARY

This document contains confidential information belonging to BioNTech/Pfizer. Except as may be otherwise agreed to in writing, by accepting or reviewing these materials, you agree to hold such information in confidence and not to disclose it to others (except where required by applicable law), nor to use it for unauthorized purposes. In the event of actual or suspected breach of this obligation, BioNTech/Pfizer should be promptly notified.

CONFIDENTIAL

Page 1

BNT162b2

2.6.5 Pharmacokinetics Tabulated Summary

2.6.5.1. PHARMACOKINETICS OVERVIEW

Test Article: BNT162b2

Type of Study	Test System	Test item	Method of Administration	Testing Facility	Report Number
Single Dose Pharmacokinetics					
Single Dose Pharmacokinetics and Excretion in Urine and Feces of ALC-0159 and ALC-0315	Rat (Wistar Han)	modRNA encoding luciferase formulated in LNP comparable to BNT162b2	IV bolus	Pfizer Inc ^a	PF-07302048_06Jul20_072424
Distribution					
In Vivo Distribution	Mice (BALB/c)	modRNA encoding luciferase formulated in LNP comparable to BNT162b2	IM Injection	BioNTech ^b	R-20-0072
In Vivo Distribution	Rat (Wistar Han)	modRNA encoding luciferase formulated in LNP comparable to BNT162b2 with trace amounts of [³ H]-CHE as non-diffusible label	IM Injection	(b) (4)	185350
Metabolism					
In Vitro and In Vivo Metabolism					
In Vitro Metabolic Stability of ALC-0315 in Liver Microsomes	Mouse (CD-1/ICR), rat (Sprague Dawley and Wistar Han), monkey (Cynomolgus), and human liver microsomes	ALC-0315	In vitro	(b) (4)	01049-20008
In Vitro Metabolic Stability of ALC-0315 in Liver S9	Mouse (CD-1/ICR), rat (Sprague Dawley), monkey (Cynomolgus), and human S9 liver fractions	ALC-0315	In vitro	(b) (4)	01049-20009

090177e196137069\Approved\Approved On: 21-Jan-2021 23:22 (GMT)

BNT162b2

2.6.5 Pharmacokinetics Tabulated Summary

2.6.5.1. PHARMACOKINETICS OVERVIEW

Test Article: BNT162b2

Type of Study	Test System	Test item	Method of Administration	Testing Facility	Report Number
In Vitro Metabolic Stability of ALC-0315 in Hepatocytes	Mouse (CD-1/ICR), rat (Sprague Dawley and Wistar Han), monkey (Cynomolgus), and human hepatocytes	ALC-0315	In vitro	(b) (4)	01049-20010
In Vitro Metabolic Stability of ALC-0159 in Liver Microsomes	Mouse (CD-1/ICR), rat (Sprague Dawley and Wistar Han), monkey (Cynomolgus), and human liver microsomes	ALC-0159	In vitro	(b) (4)	01049-20020
In Vitro Metabolic Stability of ALC-0159 in Liver S9	Mouse (CD-1/ICR), rat (Sprague Dawley), monkey (Cynomolgus), and human S9 fractions	ALC-0159	In vitro	(b) (4)	01049-20021
In Vitro Metabolic Stability of ALC-0159 in Hepatocytes	Mouse (CD-1/ICR), rat (Sprague Dawley and Wistar Han), monkey (Cynomolgus), and human hepatocytes	ALC-0159	In vitro	(b) (4)	01049-20022
Biotransformation of ALC-0159 and ALC-0315 In Vitro and In Vivo in Rats	In vitro: CD-1 mouse, Wistar Han rat, cynomolgus monkey, and human blood, liver S9 fractions and hepatocytes In vivo: male Wistar Han rats	ALC-0315 and ALC-0159	In vitro or IV (in vivo in rats)	Pfizer Inc ^e	PF-07302048_05Aug20_043725

090177e196137069\Approved\Approved On: 21-Jan-2021 23:22 (GMT)

BNT162b2

2.6.5 Pharmacokinetics Tabulated Summary

2.6.5.1. PHARMACOKINETICS OVERVIEW

Test Article: BNT162b2

Type of Study	Test System	Test item	Method of Administration	Testing Facility	Report Number
<p>ALC-0159 = 2-[(polyethylene glycol)-2000]-N,N-ditetradecylacetamide), a proprietary polyethylene glycol-lipid included as an excipient in the LNP formulation used in BNT162b2; ALC-0315 = (4-hydroxybutyl)azanediylbis(hexane-6,1-diyl)bis(2-hexyldecanoate), a proprietary aminolipid included as an excipient in the LNP formulation used in BNT162b2; [³H]-CHE = radiolabeled [cholesteryl-1,2-³H(N)]-cholesteryl hexadecyl ether; IM = Intramuscular; IV = Intravenous; LNP = lipid nanoparticles; S9 = Supernatant fraction obtained from liver homogenate by centrifuging at 9000 g.</p>					
<p>a. La Jolla, California. b. Mainz, Germany. (b) (4) e. Groton, Connecticut.</p>					

090177e196137069\Approved\Approved On: 21-Jan-2021 23:22 (GMT)

BNT162b2

2.6.5 Pharmacokinetics Tabulated Summary

**2.6.5.3. PHARMACOKINETICS:
PHARMACOKINETICS AFTER A SINGLE DOSE****Test Article: modRNA encoding luciferase in LNP
Report Number: PF-07302048_06Jul20_072424**

Species (Strain)	Rat (Wistar Han)	
Sex/Number of Animals	Male/ 3 animals per timepoint ^a	
Feeding Condition	Fasted	
Method of Administration	IV	
Dose modRNA (mg/kg)	1	
Dose ALC-0159 (mg/kg)	1.96	
Dose ALC-0315 (mg/kg)	15.3	
Sample Matrix	Plasma, liver, urine and feces	
Sampling Time Points (h post dose):	Predose, 0.1, 0.25, 0.5, 1, 3, 6, 24, 48, 96, 192, 336	
Analyte	ALC-0315	ALC-0159
PK Parameters:	Mean ^b	Mean ^b
AUC _{inf} (µg•h/mL) ^c	1030	99.2
AUC _{last} (µg•h/mL)	1020	98.6
Initial t _{1/2} (h) ^d	1.62	1.74
Terminal elimination t _{1/2} (h) ^e	139	72.7
Estimated fraction of dose distributed to liver (%) ^f	59.5	20.3
Dose in Urine (%)	NC ^g	NC ^g
Dose in Feces (%) ^h	1.05	47.2

ALC-0159 = 2-[(polyethylene glycol)-2000]-N,N-ditetradecylacetamide), a proprietary polyethylene glycol-lipid included as an excipient in the LNP formulation used in BNT162b2; ALC-0315 = (4-hydroxybutyl)azanediylbis(hexane-6,1-diyl)bis(2-hexyldecanoate), a proprietary aminolipid included as an excipient in the LNP formulation used in BNT162b2; AUC_{inf} = Area under the plasma drug concentration-time curve from 0 to infinite time; AUC_{last} = Area under the plasma drug concentration-time curve from 0 to the last quantifiable time point; BLQ = Below the limit of quantitation; LNP = Lipid nanoparticle; modRNA = Nucleoside modified messenger RNA; PK = Pharmacokinetics; t_{1/2} = Half-life.

- Non-serial sampling, 36 animals total.
- Only mean PK parameters are reported due to non-serial sampling.
- Calculated using the terminal log-linear phase (determined using 48, 96, 192, and 336 h for regression calculation).
- ln(2)/initial elimination rate constant (determined using 1, 3, and 6 h for regression calculation).
- ln(2)/terminal elimination rate constant (determined using 48, 96, 192, and 336 h for regression calculation).
- Calculated as follows: highest mean amount in the liver (µg)/total mean dose (µg) of ALC-0315 or ALC-0159.
- Not calculated due to BLQ data.
- Fecal excretion, calculated as: (mean µg of analyte in feces/ mean µg of analyte administered) × 100

CONFIDENTIAL

Page 5

FDA-CBER-2021-4379-0000714

090177e196137069\Approved\Approved On: 21-Jan-2021 23:22 (GMT)

BNT162b2

2.6.5 Pharmacokinetics Tabulated Summary

2.6.5.5A. PHARMACOKINETICS: ORGAN DISTRIBUTION

Test Article: modRNA encoding luciferase in LNP
Report Number: R-20-0072

Species (Strain):	Mice (BALB/c)
Sex/Number of Animals:	Female/3 per group
Feeding Condition:	Fed ad libitum
Vehicle/Formulation:	Phosphate-buffered saline
Method of Administration:	Intramuscular injection
Dose (mg/kg):	1 µg/hind leg in gastrocnemius muscle (2 µg total)
Number of Doses:	1
Detection:	Bioluminescence measurement
Sampling Time (hour):	6, 24, 48, 72 hours; 6 and 9 days post-injection

Time point	Total Mean Bioluminescence signal (photons/second)		Mean Bioluminescence signal in the liver (photons/second)
	Buffer control	modRNA Luciferase in LNP	modRNA Luciferase in LNP
6 hours	1.28×10 ⁵	1.26×10 ⁹	4.94×10 ⁷
24 hours	2.28×10 ⁵	7.31×10 ⁸	2.4×10 ⁶
48 hours	1.40×10 ⁵	2.10×10 ⁸	Below detection ^a
72 hours	1.33×10 ⁵	7.87×10 ⁷	Below detection ^a
6 days	1.62×10 ⁵	2.92×10 ⁶	Below detection ^a
9 days	7.66×10 ⁴	5.09×10 ⁵	Below detection ^a

LNP = Lipid nanoparticle; modRNA = Nucleoside modified messenger RNA.

a. At or below the background level of the buffer control.

090177e196137069\Approved\Approved On: 21-Jan-2021 23:22 (GMT)

BNT162b2

2.6.5 Pharmacokinetics Tabulated Summary

2.6.5.5B. PHARMACOKINETICS: ORGAN DISTRIBUTION CONTINUED

**Test Article: [³H]-Labelled LNP-mRNA formulation containing ALC-0315 and ALC-0159
Report Number: 185350**

Species (Strain):	Rat (Wistar Han)
Sex/Number of Animals:	Male and female/3 animals/sex/timepoint (21 animals/sex total for the 50 µg dose)
Feeding Condition:	Fed ad libitum
Method of Administration:	Intramuscular injection
Dose:	50 µg [³ H]-08-A01-C0 (lot # NC-0552-1)
Number of Doses:	1
Detection:	Radioactivity quantitation using liquid scintillation counting
Sampling Time (hour):	0.25, 1, 2, 4, 8, 24, and 48 hours post-injection

Sample	Mean total lipid concentration (µg lipid equivalent/g (or mL) (males and females combined))							% of administered dose (males and females combined)						
	0.25 min	1 h	2 h	4 h	8 h	24 h	48 h	0.25 min	1 h	2 h	4 h	8 h	24 h	48 h
Adipose tissue	0.057	0.100	0.126	0.128	0.093	0.084	0.181	--	--	--	--	--	--	--
Adrenal glands	0.271	1.48	2.72	2.89	6.80	13.8	18.2	0.001	0.007	0.010	0.015	0.035	0.066	0.106
Bladder	0.041	0.130	0.146	0.167	0.148	0.247	0.365	0.000	0.001	0.001	0.001	0.001	0.002	0.002
Bone (femur)	0.091	0.195	0.266	0.276	0.340	0.342	0.687	--	--	--	--	--	--	--
Bone marrow (femur)	0.479	0.960	1.24	1.24	1.84	2.49	3.77	--	--	--	--	--	--	--
Brain	0.045	0.100	0.138	0.115	0.073	0.069	0.068	0.007	0.013	0.020	0.016	0.011	0.010	0.009
Eyes	0.010	0.035	0.052	0.067	0.059	0.091	0.112	0.000	0.001	0.001	0.002	0.002	0.002	0.003
Heart	0.282	1.03	1.40	0.987	0.790	0.451	0.546	0.018	0.056	0.084	0.060	0.042	0.027	0.030
Injection site	128	394	311	338	213	195	165	19.9	52.6	31.6	28.4	21.9	29.1	24.6
Kidneys	0.391	1.16	2.05	0.924	0.590	0.426	0.425	0.050	0.124	0.211	0.109	0.075	0.054	0.057
Large intestine	0.013	0.048	0.093	0.287	0.649	1.10	1.34	0.008	0.025	0.065	0.192	0.405	0.692	0.762
Liver	0.737	4.63	11.0	16.5	26.5	19.2	24.3	0.602	2.87	7.33	11.9	18.1	15.4	16.2
Lung	0.492	1.21	1.83	1.50	1.15	1.04	1.09	0.052	0.101	0.178	0.169	0.122	0.101	0.101

090177e196137069Approved On: 21-Jan-2021 23:22 (GMT)

BNT162b2

2.6.5 Pharmacokinetics Tabulated Summary

2.6.5.5B. PHARMACOKINETICS: ORGAN DISTRIBUTION CONTINUED

**Test Article: [³H]-Labelled LNP-mRNA formulation containing ALC-0315 and ALC-0159
Report Number: 185350**

Sample	Total Lipid concentration (µg lipid equivalent/g [or mL]) (males and females combined)							% of Administered Dose (males and females combined)						
	0.25 min	1 h	2 h	4 h	8 h	24 h	48 h	0.25 min	1 h	2 h	4 h	8 h	24 h	48 h
Lymph node (mandibular)	0.064	0.189	0.290	0.408	0.534	0.554	0.727	--	--	--	--	--	--	--
Lymph node (mesenteric)	0.050	0.146	0.530	0.489	0.689	0.985	1.37	--	--	--	--	--	--	--
Muscle	0.021	0.061	0.084	0.103	0.096	0.095	0.192	--	--	--	--	--	--	--
Ovaries (females)	0.104	1.34	1.64	2.34	3.09	5.24	12.3	0.001	0.009	0.008	0.016	0.025	0.037	0.095
Pancreas	0.081	0.207	0.414	0.380	0.294	0.358	0.599	0.003	0.007	0.014	0.015	0.015	0.011	0.019
Pituitary gland	0.339	0.645	0.868	0.854	0.405	0.478	0.694	0.000	0.001	0.001	0.001	0.000	0.000	0.001
Prostate (males)	0.061	0.091	0.128	0.157	0.150	0.183	0.170	0.001	0.001	0.002	0.003	0.003	0.004	0.003
Salivary glands	0.084	0.193	0.255	0.220	0.135	0.170	0.264	0.003	0.007	0.008	0.008	0.005	0.006	0.009
Skin	0.013	0.208	0.159	0.145	0.119	0.157	0.253	--	--	--	--	--	--	--
Small intestine	0.030	0.221	0.476	0.879	1.28	1.30	1.47	0.024	0.130	0.319	0.543	0.776	0.906	0.835
Spinal cord	0.043	0.097	0.169	0.250	0.106	0.085	0.112	0.001	0.002	0.002	0.003	0.001	0.001	0.001
Spleen	0.334	2.47	7.73	10.3	22.1	20.1	23.4	0.013	0.093	0.325	0.385	0.982	0.821	1.03
Stomach	0.017	0.065	0.115	0.144	0.268	0.152	0.215	0.006	0.019	0.034	0.030	0.040	0.037	0.039
Testes (males)	0.031	0.042	0.079	0.129	0.146	0.304	0.320	0.007	0.010	0.017	0.030	0.034	0.074	0.074
Thymus	0.088	0.243	0.340	0.335	0.196	0.207	0.331	0.004	0.007	0.010	0.012	0.008	0.007	0.008
Thyroid	0.155	0.536	0.842	0.851	0.544	0.578	1.00	0.000	0.001	0.001	0.001	0.001	0.001	0.001
Uterus (females)	0.043	0.203	0.305	0.140	0.287	0.289	0.456	0.002	0.011	0.015	0.008	0.016	0.018	0.022
Whole blood	1.97	4.37	5.40	3.05	1.31	0.909	0.420	--	--	--	--	--	--	--
Plasma	3.97	8.13	8.90	6.50	2.36	1.78	0.805	--	--	--	--	--	--	--
Blood:Plasma ratio ^a	0.815	0.515	0.550	0.510	0.555	0.530	0.540	--	--	--	--	--	--	--

090177e196137069\Approved\Approved On: 21-Jan-2021 23:22 (GMT)

BNT162b2

2.6.5 Pharmacokinetics Tabulated Summary

**2.6.5.5B. PHARMACOKINETICS: ORGAN
DISTRIBUTION CONTINUED**

**Test Article: [³H]-Labelled LNP-mRNA formulation containing
ALC-0315 and ALC-0159
Report Number: 185350**

-- = Not applicable, partial tissue taken; [³H]-08-A01-C0 = An aqueous dispersion of LNPs, including ALC-0315, ALC-0159, distearoylphosphatidylcholine, cholesterol, mRNA encoding luciferase and trace amounts of radiolabeled [Cholesteryl-1,2-3H(N)]-Cholesteryl Hexadecyl Ether, a nonexchangeable, non-metabolizable lipid marker used to monitor the disposition of the LNPs; ALC-0159 = 2-[(polyethylene glycol)-2000]-N,N--ditetradecylacetamide), a proprietary polyethylene glycol-lipid included as an excipient in the LNP formulation used in BNT162b2; ALC-0315 = (4--hydroxybutyl)azanediyl)bis(hexane-6,1-diyl)bis(2-hexyldecanoate), a proprietary aminolipid included as an excipient in the LNP formulation used in BNT162b2; LNP = Lipid nanoparticle; mRNA = messenger RNA.

a. The mean male and female blood:plasma values were first calculated separately and this value represents the mean of the two values.

090177e196137069\Approved\Approved On: 21-Jan-2021 23:22 (GMT)

BNT162b2

2.6.5 Pharmacokinetics Tabulated Summary

2.6.5.9. PHARMACOKINETICS: METABOLISM IN VIVO, RAT

Test Article: modRNA encoding luciferase in LNP
Report Number: PF-07302048_05Aug20_043725

Species (Strain): Rat (Wistar Han)
 Sex/ Number of animals: Male/ 36 animals total for plasma and liver, 3 animals for urine and feces
 Method of Administration: Intravenous
 Dose (mg/kg): 1
 Test System: Plasma, Urine, Feces, Liver
 Analysis Method: Ultrahigh performance liquid chromatography/ mass spectrometry

Biotransformation	m/z	Metabolites of ALC-0315 Detected			
		Plasma	Urine	Feces	Liver
N-dealkylation, oxidation	102.0561 ^a	ND	ND	ND	ND
N-Dealkylation, oxidation	104.0706 ^b	ND	ND	ND	ND
N-dealkylation, oxidation	130.0874 ^a	ND	ND	ND	ND
N-Dealkylation, oxidation	132.1019 ^b	ND	ND	ND	ND
N-dealkylation, hydrolysis, oxidation	145.0506 ^a	ND	ND	ND	ND
Hydrolysis (acid)	255.2330 ^a	+	ND	ND	ND
Hydrolysis, hydroxylation	271.2279 ^a	ND	ND	ND	ND
Bis-hydrolysis (amine)	290.2690 ^b	+	+	+	+
Hydrolysis, glucuronidation	431.2650 ^a	ND	ND	ND	ND
Bis-hydrolysis (amine), glucuronidation	464.2865 ^a	ND	ND	ND	ND
Bis-hydrolysis (amine), glucuronidation	466.3011 ^b	ND	+	ND	ND
Hydrolysis (amine)	528.4986 ^b	+	ND	ND	+
Hydrolysis (amine), Glucuronidation	704.5307 ^b	ND	ND	ND	ND
Oxidation to acid	778.6930 ^a	ND	ND	ND	ND
Oxidation to acid	780.7076 ^b	ND	ND	ND	ND
Hydroxylation	782.7232 ^b	ND	ND	ND	ND
Sulfation	844.6706 ^a	ND	ND	ND	ND
Sulfation	846.6851 ^b	ND	ND	ND	ND
Glucuronidation	940.7458 ^a	ND	ND	ND	ND
Glucuronidation	942.7604 ^b	ND	ND	ND	ND

Note: Both theoretical and observed metabolites are included.

m/z = mass to charge ratio; ND = Not detected; + = minor metabolite as assessed by ultraviolet detection.

a. Negative ion mode.

b. Positive ion mode.

CONFIDENTIAL

Page 10

090177e196137069Approved\Approved On: 21-Jan-2021 23:22 (GMT)

BNT162b2

2.6.5 Pharmacokinetics Tabulated Summary

2.6.5.10A. PHARMACOKINETICS: METABOLISM IN VITRO

Test Article: ALC-0315
 Report Numbers: 01049-20008
 01049-20009
 01049-20010

Type of Study:	Liver Microsomes + NADPH		Stability of ALC-0315 In Vitro S9 Fraction + NADPH, UDPGA, and alamethicin		Hepatocytes
Study System:	Liver Microsomes + NADPH		Stability of ALC-0315 In Vitro S9 Fraction + NADPH, UDPGA, and alamethicin		Hepatocytes
ALC-0315 Concentration:	1 µM		1 µM		1 µM
Duration of Incubation (min):	120 min		120 min		240 min
Analysis Method:	Ultra-high performance liquid chromatography-tandem mass spectrometry				

Incubation time (min)	Percent ALC-0315 remaining													
	Liver Microsomes					Liver S9 Fraction				Hepatocytes				
	Mouse (CD-1/ICR)	Rat (SD)	Rat (WH)	Monkey (Cyno)	Human	Mouse (CD-1/ICR)	Rat (SD)	Monkey (Cyno)	Human	Mouse (CD-1/ICR)	Rat (SD)	Rat (WH)	Monkey (Cyno)	Human
0	100.00	100.00	100.00	100.00	100.00	100.00	100.00	100.00	100.00	100.00	100.00	100.00	100.00	100.00
15	98.77	94.39	96.34	97.96	100.24	97.69	98.85	99.57	95.99	--	--	--	--	--
30	97.78	96.26	97.32	96.18	99.76	97.22	99.62	96.96	97.32	101.15	97.75	102.70	96.36	100.72
60	100.49	99.73	98.54	100.00	101.45	98.61	99.62	99.13	94.98	100.77	98.50	102.32	97.82	101.44
90	97.78	98.66	94.15	97.96	100.48	98.15	98.85	98.70	98.33	101.92	99.25	103.09	100.0	100.36
120	96.54	95.99	93.66	97.71	98.31	96.76	98.46	99.57	99.33	98.85	97.38	99.61	96.36	100.72
180	--	--	--	--	--	--	--	--	--	101.15	98.88	103.47	95.64	98.92
240	--	--	--	--	--	--	--	--	--	99.62	101.12	100.00	93.82	99.64
t½ (min)	>120	>120	>120	>120	>120	>120	>120	>120	>120	>240	>240	>240	>240	>240

-- = Data not available; ALC-0315 = (4-hydroxybutyl)azanediylbis(hexane-6,1-diyl)bis(2-hexyldecanoate), a proprietary aminolipid included as an excipient in the lipid nanoparticle formulation used in BNT162b2; Cyno = Cynomolgus; NADPH = Reduced form of nicotinamide adenine dinucleotide phosphate; NC = not calculated; SD = Sprague Dawley; t½ = half-life; WH = Wistar-Han; UDPGA= uridine-diphosphate-glucuronic acid trisodium salt.

090177e196137069\Approved On: 21-Jan-2021 23:22 (GMT)

BNT162b2

2.6.5 Pharmacokinetics Tabulated Summary

2.6.5.10B. PHARMACOKINETICS: METABOLISM IN VITRO CONTINUED

Test Article: ALC-0159
 Report Numbers: **01049-20020**
01049-20021
01049-20022

Type of Study:	Liver Microsomes + NADPH		Stability of ALC-0159 In Vitro S9 Fraction + NADPH, UDPGA, and alamethicin		Hepatocytes
Study System:	Liver Microsomes + NADPH		Stability of ALC-0159 In Vitro S9 Fraction + NADPH, UDPGA, and alamethicin		Hepatocytes
ALC-0159 Concentration:	1 µM		1 µM		1 µM
Duration of Incubation (min):	120 min		120 min		240 min
Analysis Method:	Ultra-high performance liquid chromatography-tandem mass spectrometry				

Incubation time (min)	Percent ALC-0159 remaining													
	Liver Microsomes					Liver S9 Fraction				Hepatocytes				
	Mouse (CD-1/ICR)	Rat (SD)	Rat (WH)	Monkey (Cyno)	Human	Mouse (CD-1/ICR)	Rat (SD)	Monkey (Cyno)	Human	Mouse (CD-1/ICR)	Rat (SD)	Rat (WH)	Monkey (Cyno)	Human
0	100.00	100.00	100.00	100.00	100.00	100.00	100.00	100.00	100.00	100.00	100.00	100.00	100.00	100.00
15	82.27	101.24	112.11	100.83	99.59	98.93	84.38	91.30	106.73	--	--	--	--	--
30	86.40	93.78	102.69	85.12	92.28	91.10	90.87	97.96	107.60	100.85	93.37	113.04	90.23	106.34
60	85.54	98.34	105.38	86.36	95.53	102.85	97.97	105.56	104.97	94.92	91.81	105.07	92.93	101.58
90	85.41	95.44	100.90	94.63	97.97	90.75	93.51	108.33	109.36	94.28	90.25	112.80	94.59	92.67
120	95.87	97.10	108.97	93.39	93.09	106.76	92.70	105.74	119.59	87.08	89.47	104.11	97.51	96.04
180	--	--	--	--	--	--	--	--	--	94.92	93.96	102.90	89.81	93.66
240	--	--	--	--	--	--	--	--	--	102.75	94.93	98.79	92.93	102.57
t½ (min)	>120	>120	>120	>120	>120	>120	>120	>120	>120	>240	>240	>240	>240	>240

-- = Data not available; ALC-0159 = 2-[(polyethylene glycol)-2000]-N,N-ditetradecylacetamide), a proprietary polyethylene glycol-lipid included as an excipient in the lipid nanoparticle formulation used in BNT162b2; Cyno = Cynomolgus; NADPH = Reduced form of nicotinamide adenine dinucleotide phosphate; NC = not calculated; SD = Sprague Dawley; WH = Wistar-Han; UDPGA= uridine-diphosphate-glucuronic acid trisodium salt.

090177e196137069\Approved On: 21-Jan-2021 23:22 (GMT)

BNT162b2

2.6.5 Pharmacokinetics Tabulated Summary

**2.6.5.10C. PHARMACOKINETICS: METABOLISM
IN VITRO CONTINUED**

Test Article: ALC-0315
Report Number: PF-07302048_05Aug20_043725

Type of study		Metabolism of ALC-0315 In Vitro											
Study system		Blood				Hepatocytes				Liver S9 Fraction			
ALC-0315 concentration		10 µM				10 µM				10 µM			
Duration of incubation		24 h				4 h				24 h			
Analysis Method:		Ultrahigh performance liquid chromatography/ mass spectrometry											
Biotransformation	m/z	Blood				Hepatocytes				Liver S9 Fraction			
		Mouse	Rat	Monkey	Human	Mouse	Rat	Monkey	Human	Mouse	Rat	Monkey	Human
<i>N</i> -dealkylation, oxidation	102.0561 ^a	ND	ND	ND	ND	ND	ND	ND	ND	ND	ND	ND	ND
<i>N</i> -Dealkylation, oxidation	104.0706 ^b	ND	ND	ND	ND	ND	ND	ND	ND	ND	ND	ND	ND
<i>N</i> -dealkylation, oxidation	130.0874 ^a	ND	ND	ND	ND	ND	ND	ND	ND	ND	ND	ND	ND
<i>N</i> -Dealkylation, oxidation	132.1019 ^b	ND	ND	ND	ND	ND	ND	ND	ND	ND	ND	ND	ND
<i>N</i> -dealkylation, hydrolysis, oxidation	145.0506 ^a	ND	ND	ND	ND	ND	ND	ND	ND	ND	ND	ND	ND
Hydrolysis (acid)	255.2330 ^a	+	+	ND	ND	+	+	+	+	+	+	ND	+
Hydrolysis, hydroxylation	271.2279 ^a	ND	ND	ND	ND	ND	ND	ND	ND	ND	ND	ND	ND
Bis-hydrolysis (amine)	290.2690 ^b	+	+	ND	ND	ND	ND	ND	ND	ND	ND	+	ND
Hydrolysis, glucuronidation	431.2650 ^a	ND	ND	ND	ND	ND	ND	ND	ND	ND	ND	ND	ND
Bis-hydrolysis (amine), glucuronidation	464.2865 ^a	ND	ND	ND	ND	ND	ND	ND	ND	ND	ND	ND	ND
Bis-hydrolysis (amine), glucuronidation	466.3011 ^b	ND	ND	ND	ND	ND	ND	ND	ND	ND	ND	ND	ND
Hydrolysis (amine)	528.4986 ^b	ND	+	ND	ND	ND	ND	ND	ND	ND	ND	+	ND
Hydrolysis (amine), glucuronidation	704.5307 ^b	ND	ND	ND	ND	ND	ND	ND	ND	ND	ND	ND	ND
Oxidation to acid	778.6930 ^a	ND	ND	ND	ND	ND	ND	ND	ND	ND	ND	ND	ND
Oxidation to acid	780.7076 ^b	ND	ND	ND	ND	ND	ND	ND	ND	ND	ND	ND	ND
Hydroxylation	782.7232 ^b	ND	ND	ND	ND	ND	ND	ND	ND	ND	ND	ND	ND
Sulfation	844.6706 ^a	ND	ND	ND	ND	ND	ND	ND	ND	ND	ND	ND	ND
Sulfation	846.6851 ^b	ND	ND	ND	ND	ND	ND	ND	ND	ND	ND	ND	ND
Glucuronidation	940.7458 ^a	ND	ND	ND	ND	ND	ND	ND	ND	ND	ND	ND	ND
Glucuronidation	942.7604 ^b	ND	ND	ND	ND	ND	ND	ND	ND	ND	ND	ND	ND

Note: Both theoretical and observed metabolites are included.
 m/z = mass to charge ratio; ND = Not detected; + = metabolite present.
 a. Negative ion mode.
 b. Positive ion mode.

090177e196137069\Approved\Approved On: 21-Jan-2021 23:22 (GMT)

BNT162b2

2.6.5 Pharmacokinetics Tabulated Summary

**2.6.5.10D. PHARMACOKINETICS: METABOLISM
IN VITRO CONTINUED**

**Test Article: ALC-0159
Report Number: PF-07302048_05Aug20_043725**

Type of study		Metabolism of ALC-0159 In Vitro											
Study system		Blood				Hepatocytes				Liver S9 Fraction			
ALC-0159 concentration		10 µM				10 µM				10 µM			
Duration of incubation		24 h				4 h				24 h			
Analysis Method:		Ultrahigh performance liquid chromatography/ mass spectrometry											
Biotransformation	m/z	Blood				Hepatocytes				Liver S9 Fraction			
		Mouse	Rat	Monkey	Human	Mouse	Rat	Monkey	Human	Mouse	Rat	Monkey	Human
<i>O</i> -Demethylation, <i>O</i> -dealkylation	107.0703 ^b	ND	ND	ND	ND	ND	ND	ND	ND	ND	ND	ND	ND
<i>O</i> -Demethylation, <i>O</i> -dealkylation	151.0965 ^b	ND	ND	ND	ND	ND	ND	ND	ND	ND	ND	ND	ND
<i>O</i> -Demethylation, <i>O</i> -dealkylation	195.1227 ^b	ND	ND	ND	ND	ND	ND	ND	ND	ND	ND	ND	ND
Hydrolysis, <i>N</i> -Dealkylation	214.2529 ^b	ND	ND	ND	ND	ND	ND	ND	ND	ND	ND	ND	ND
<i>N</i> -Dealkylation, oxidation	227.2017 ^a	ND	ND	ND	ND	ND	ND	ND	ND	ND	ND	ND	ND
Hydrolysis (amine)	410.4720 ^b	+	+	ND	ND	+	+	+	+	+	+	+	+
<i>N,N</i> -Didealkylation	531.5849 ^b	ND	ND	ND	ND	ND	ND	ND	ND	ND	ND	ND	ND
<i>N</i> -Dealkylation	580.6396 ^b	ND	ND	ND	ND	ND	ND	ND	ND	ND	ND	ND	ND
<i>O</i> -Demethylation, oxidation	629.6853 ^b	ND	ND	ND	ND	ND	ND	ND	ND	ND	ND	ND	ND
Hydroxylation	633.6931 ^b	ND	ND	ND	ND	ND	ND	ND	ND	ND	ND	ND	ND
ω -Hydroxylation, Oxidation	637.1880 ^b	ND	ND	ND	ND	ND	ND	ND	ND	ND	ND	ND	ND
Hydrolysis (acid)	708.7721 ^b	ND	ND	ND	ND	ND	ND	ND	ND	ND	ND	ND	ND

Note: Both theoretical and observed metabolites are included.
 m/z = mass to charge ratio; ND = Not detected; + = metabolite present.
 a. Negative ion mode.
 b. Positive ion mode.

090177e196137069\Approved\Approved On: 21-Jan-2021 23:22 (GMT)

(b) (4)

FINAL REPORT

Test Facility Study No. 185350
Sponsor Reference No. ALC-NC-0552

**A Tissue Distribution Study of a [³H]-Labelled Lipid Nanoparticle-mRNA
Formulation Containing ALC-0315 and ALC-0159 Following
Intramuscular Administration in Wistar Han Rats**

TEST FACILITY:

(b) (4)

SPONSOR:

Acuitas Therapeutics Inc.
6190 Agronomy Road, Suite 402
Vancouver, British Columbia
V6T 1Z3 Canada

TABLE OF CONTENTS

1 COMPLIANCE STATEMENT 6

2 QUALITY ASSURANCE STATEMENT 7

3 RESPONSIBLE PERSONNEL 8

4 SUMMARY 9

5 INTRODUCTION..... 11

5.1 Study Location..... 11

5.2 Study Dates 11

5.3 Archiving..... 12

6 EXPERIMENTAL PROCEDURE..... 12

6.1 Test Item 12

6.2 Other Materials 13

6.3 Animals and Husbandry..... 14

6.4 Specific Activity..... 14

6.5 Dose Formulation 14

6.6 Dose Administration and Determination 15

6.7 Collection of Biological Samples 15

6.8 Sample Storage 16

6.9 Preparation of Samples for Total Radioactivity Analysis..... 16

6.9.1 Dose Formulation 16

6.9.2 Blood and Plasma 16

6.9.3 Tissues 16

6.9.4 Urine, Faeces and Cage Wash..... 17

6.10 Quantification of Radioactivity..... 17

090177e195794698\Approved\Approved On: 09-Nov-2020 21:23 (GMT)

6.10.1 Liquid Scintillation Counting 17

6.10.2 Data Presentation 17

6.11 Protocol Deviations 18

7 RESULTS 19

7.1 Clinical Observations..... 19

7.2 Body Weights..... 19

7.3 Tissue Distribution Following Intramuscular Administration 19

8 CONCLUSIONS 22

9 TABLES..... 23

10 APPENDICES 28

090177e195794698\Approved\Approved On: 09-Nov-2020 21:23 (GMT)

LIST OF TABLES

Table 1 Mean (Sexes-Combined) Concentration and Recovery of Total Radioactivity in Whole Blood, Plasma and Tissues Following Single Intramuscular Administration of [³H]-08-A01-C01 to Wistar Han Rats 23

Table 2 Mean Concentration of Total Radioactivity in Whole Blood, Plasma and Tissues Following Single Intramuscular Administration of [³H]-08-A01-C01 to Wistar Han Rats 25

Table 3 Mean Recovery of Total Radioactivity in Tissues Following Single Intramuscular Administration of [³H]-08-A01-C01 to Wistar Han Rats 27

090177e195794698\Approved\Approved On: 09-Nov-2020 21:23 (GMT)

LIST OF APPENDICES

Appendix 1 Certificates of Analysis for [³H]-08-A01-C01 and [³H]-CHE 28
Appendix 2 Individual Animal Dosing Summary 30
Appendix 3 Urine and Faeces Sample Weights 33
Appendix 4 Individual Male Concentration Data 36
Appendix 5 Individual Female Concentration Data 43
Appendix 6 Individual Male Recovery Data 50
Appendix 7 Individual Female Recovery Data 57
Appendix 8 Individual Male 100 µg mRNA data 64

090177e195794698\Approved\Approved On: 09-Nov-2020 21:23 (GMT)

1 COMPLIANCE STATEMENT

Study Title: A Tissue Distribution Study of a [³H]-Labelled Lipid Nanoparticle-mRNA Formulation Containing ALC-0315 and ALC-0159 Following Intramuscular Administration in Wistar Han Rats

GLP regulations are not applicable to studies of this nature therefore no claim of GLP compliance is made. Nevertheless, as Study Director, I confirm that this study was conducted in a GLP compliant facility and that the practices and procedures adopted during its conduct were consistent with the OECD Principles of Good Laboratory Practice as incorporated into the United Kingdom Statutory Instrument for GLP.

The study was conducted according to the procedures herein described and this report represents a true and accurate record of the results obtained.

DocuSigned by: (b) (4) Signer Name: (b) (4) Signing Reason: I approve this document Signing Time: 05-Nov-2020 11:52:33 EST CD262FA0424043DEB85DE525652AC3BD
--

(b) (4)
Study Director

090177e195794698\Approved\Approved On: 09-Nov-2020 21:23 (GMT)

2 QUALITY ASSURANCE STATEMENT

Study Title: A Tissue Distribution Study of a [³H]-Labelled Lipid Nanoparticle-mRNA Formulation Containing ALC-0315 and ALC-0159 Following Intramuscular Administration in Wistar Han Rats

This study has not been subjected to any study specific Quality Assurance procedures.

3 RESPONSIBLE PERSONNEL

Study Director: (b) (4)

Sponsor Representative: (b) (6)

Test Facility Management: (b) (4)

090177e195794698\Approved\Approved On: 09-Nov-2020 21:23 (GMT)

4 SUMMARY

The test item, 08-A01-C01, is an aqueous dispersion of lipid nanoparticles (LNP), comprised of a proprietary mixture of lipid components (including ALC-0315, ALC-0159, distearoylphosphatidylcholine, and cholesterol) and mRNA. The mRNA encodes a model protein (luciferase) and is not pharmacologically active. The test item contains trace amounts of radiolabelled [Cholesteryl-1,2-³H(N)]-Cholesteryl Hexadecyl Ether (³H)-CHE), a non-exchangeable, non-metabolisable lipid marker used to monitor the disposition of the lipid nanoparticles (containing encapsulated mRNA). Once intracellular, the [³H]-CHE does not recirculate and therefore allows assessment of distribution of the particles.

The objectives of this study were to:

1. Characterise the disposition of 08-A01-C01 containing a radiolabelled lipid marker in male and female Wistar Han rats following a single intramuscular administration.
2. Determine the concentration and content of radioactivity in blood, plasma and tissues of rats (expressed as µg lipid eq/mL (or per g for tissue), and % administered (injected dose)/tissue, where appropriate).

Wistar Han rats (21 male and 21 female) each received a single intramuscular dose of [³H]-08-A01-C01 at a target mRNA total dose of 50 µg/animal (1.29 mg/animal total lipid dose). The content and concentration of total radioactivity in blood, plasma and tissues were determined at pre-defined time points following administration.

Whole blood and tissue samples were collected at 0.25, 1, 2, 4, 8, 24 and 48 hours post-dose (three animals/sex/timepoint) and plasma was subsequently separated from blood by centrifugation. The concentration of total radioactivity was measured by liquid scintillation counting (LSC).

Following intramuscular administration of [³H]-08-A01-C01 to male and female Wistar Han rats at a target dose level of 50 µg/animal (1.29 mg/animal total lipid dose), the greatest mean concentration was found remaining in the injection site at each time point in both sexes. Outside the injection site, low levels of radioactivity were detected in most tissues, with the greatest levels in plasma observed 1-4 hours post-dose. Over 48 hours, [³H]-08-A01-C01 distributed mainly to liver, adrenal glands, spleen and ovaries, with maximum concentrations observed at 8-48 hours post-dose. Total recovery (% of injected dose) of [³H]-08-A01-C01 outside the injection site was greatest in the liver (up to 21.5%) and was much less in spleen (≤1.1%), adrenal glands (≤0.1%) and ovaries (≤0.1%). The mean concentrations and tissue distribution pattern were broadly similar between the sexes.

Blood:plasma ratios were generally between 0.5-0.6, indicating that the majority of the total radioactivity is associated with the plasma fraction and that [³H]-08-A01-C01 does not undergo appreciable accumulation in red blood cells.

In conclusion, the distribution of [³H]-08-A01-C01 (monitoring the [³H]-CHE lipid label) in blood, plasma and selected tissues was determined in male and female Wistar Han rats over 48 hours after a single intramuscular injection at 50 µg mRNA/animal (1.29 mg/animal lipid dose). The concentrations of [³H]-08-A01-C01 were greatest in the injection site at all time points, with levels peaking in the plasma by 1-4 hours post-dose and distribution mainly into liver, adrenal glands, spleen and ovaries over 48 hours. Total recovery of radioactivity outside of the injection site was greatest in the liver, with much lower total recovery in spleen, and very little recovery in adrenals glands and ovaries. The mean plasma, blood and tissue concentrations and tissue distribution patterns were broadly similar between the sexes and [³H]-08-A01-C01 did not associate with red blood cells.

5 INTRODUCTION

The objectives of this study were to:

1. Characterise the disposition of 08-A01-C01 containing a radiolabelled lipid marker in male and female Wistar Han rats following a single intramuscular administration
2. Determine the concentration and content of radioactivity in blood, plasma and tissues of rats (expressed as µg lipid eq/g (or per mL for plasma) and % injected dose/tissue, where appropriate)

The Wistar Han rat was chosen as the animal model for this study as it is an accepted rodent species for preclinical toxicity testing by regulatory agencies and has been used in all regulatory toxicology studies by the Sponsor.

The study was designed to be appropriate for submission to regulatory authorities. However, it is recognised that no detailed test guidelines for the conduct of drug distribution and pharmacokinetic studies are currently available.

Initially, 21 male rats were dosed at 100 µg mRNA/animal. Some adverse clinical signs were observed after approximately 24 hours post-dose and a subsequent review of the data showed concentrations were well detected in tissues. After discussions with the Sponsor, the target dose level was lowered to 50 µg mRNA/animal by amendment for the remainder of the study. Reference is made to the 100 µg mRNA /animal group in some sections of the report, however, the results are not discussed.

5.1 Study Location

The study was carried out at (b) (4) according to (b) (4) Protocol No. 185350 and Amendments 1 and 2.

5.2 Study Dates

The study was conducted according to the following timetable:

Study Initiation:	16 July 2020
Experimental Start Date:	17 July 2020
Experimental Completion Date:	24 September 2020
Study Completion Date:	See compliance page for date of Study Director's signature.

090177e195794698\Approved\Approved On: 09-Nov-2020 21:23 (GMT)

5.3 Archiving

All raw data generated and recorded during this study will be stored in the Scientific Archive of (b) (4) for 2 years after issue of the final report. After the 2-year period the Sponsor will be consulted regarding the disposal, transfer, or continued storage of the raw data. Electronic data generated by the Test Facility were archived as noted above, except reporting files stored on Shared Document Management System (SDMS), which were archived at the (b) (4)

The original signed copy of the final report will be stored indefinitely in the Scientific Archive of (b) (4)

The residual [³H]-08-A01-C01 dose (approximately 5 MBq) will be retained and stored in a fridge set to maintain 4°C at (b) (4)

Biological samples generated during the course of this study were held deep frozen until issue of the final report. (b) (4) will contact the Sponsor to discuss the fate of the samples (disposal, return or retain at (b) (4)) on issue of the final report. Samples will be disposed of unless (b) (4) receives written instruction regarding shipment of the samples to the Sponsor or continued storage at (b) (4)

6 EXPERIMENTAL PROCEDURE

6.1 Test Item

Identification:	[³ H]-08-A01-C01
Supplier:	Acuitas Therapeutics Inc
Lot Number:	NC-0552-1
Expiration Date:	July 7, 2021
Physical Description:	White to off-white, homogenous, opalescent liquid; no foreign particles
Concentration (mRNA):	1.0 mg/mL
Radioactive Concentration	0.864 mCi/mL, 1,900,000 dpm/μL

090177e195794698\Approved\Approved On: 09-Nov-2020 21:23 (GMT)

Concentration (Total Lipid)	25.7 mg/mL
Molecular weight	Not applicable for LNP
Purity:	94%
Radiochemical Purity	>97%
Specific Activity (mRNA):	0.864 mCi/mg (32.0 MBq/mg)
Correction Factor	None
Storage Conditions:	Frozen (-60°C to -90°C)

The test item contains trace amounts of radiolabelled [Cholesteryl-1,2-³H(N)]-Cholesteryl Hexadecyl Ether (³H]-CHE), a non-exchangeable, non-metabolisable lipid marker used to monitor the disposition of the lipid nanoparticles (containing encapsulated mRNA). Per the manufacturer's information, the radiochemical purity of [³H]-CHE was found to be >97% and the rate of decomposition is initially 2% for 6 months from the date of purification (16 December 2019). No radiochemical purity assessments were made as part of this study.

The Certificates of Analysis for [³H]-08-A01-C01 and [³H]-CHE are presented in [Appendix 1](#).

6.2 Other Materials

AquaSafe 500 Plus liquid scintillation fluid was obtained from Zinsser Inc.

Monophase® was used in conjunction with the Perkin Elmer Model 307 Automatic Sample Oxidiser and was supplied by Perkin Elmer Life Science and Analytical Instruments Inc, UK.

Spec-Chec™-³H used to estimate efficiencies of combustion was also obtained from Perkin Elmer Life Science and Analytical Instruments Inc, UK.

All other materials and chemicals used were of analytical grade where available and supplied by standard commercial suppliers.

6.3 Animals and Husbandry

Forty-two male and 21 female Wistar Han rats (8-11 weeks and body weight 179-270 g at the time of dosing) were used in the study and were supplied by (b) (4). The animals were acclimatised to the experimental unit for at least 5 days prior to use on the study. During the acclimatisation periods, the animals were closely observed by the animal technicians to ensure that they were in good health and suitable for inclusion in the study. During the study period the animals were closely observed twice daily by the animal technicians to ensure that they were in good health.

During the study period, the rats were housed in groups in polycarbonate and stainless steel cages with wire mesh floors. Animals used for excretion collection were housed singly in all-glass metabolism cages for the separate collection of urine and faeces.

A standard laboratory diet of known formulation (SDS Rat and Rat Maintenance Diet No.1, Special Diet Services, 1 Stepfield, Witham, Essex) and domestic mains tap water were available *ad libitum*.

Holding and study areas had automatic control of light cycles and temperature. Automatic 12 hours light and 12 hours dark. Ranges of temperature and humidity measured during the study were 21-23°C and 44-67%, respectively, with the exception of 31 July 2020 where the room temperature reached a maximum of 25°C.

6.4 Specific Activity

The specific activity value of 1.24 MBq/mg lipid (as calculated from the 0.864 mCi/mg mRNA specific activity value supplied and converted to per mg lipid) was used to calculate the amount of [³H]-08-A01-C01 dispensed in the dose formulation.

6.5 Dose Formulation

[³H]-08-A01-C01 was provided in PBS/sucrose buffer at the required dose concentration (1 mg mRNA/mL). No dilutions were therefore required. Four dose formulation vials were provided (3 x 1.5 mL and 1 x 1.2 mL).

The appropriate number of vials for each dosing occasion were defrosted for at least 30 minutes prior to dosing. Prior to use, each vial was inverted 3 times to mix. Once dosing was complete, each vial was stored in a fridge within 4 hours of removal from the -80°C freezer.

The radioactive concentration of the supplied dose formulation was determined by the removal of triplicate aliquots (50 µL) prior to and after the first dosing occasion. Appropriate

dilutions of each aliquot were prepared in distilled water and duplicate aliquots of each dilution were analysed by liquid scintillation counting (LSC).

The radioactive concentration determined by LSC was within 10% of the target value provided in the supplied Certificate of Analysis and was used in the dose determination calculations.

6.6 Dose Administration and Determination

Each animal received a single (one site) intramuscular administration of [³H]-08-A01-C01 at either 50 or 100 µL volume for the 50 and 100 µg mRNA/animal dose groups, respectively (target doses of 1.29 or 2.57 mg total lipid/animal, respectively).

The actual dose received by each animal was determined with reference to the dose concentration, the volume of dose administered and the specific activity of [³H]-08-A01-C01 in the formulated dose. Any undosed residue was also taken in to account. The actual dose received by each animal is documented in [Appendix 2](#).

6.7 Collection of Biological Samples

Three male and three female rats were sacrificed at the following times:

0.25, 1, 2, 4, 8, 24 and 48 hours post dose

From each animal, a terminal blood sample (*ca.* 5-10 mL) was collected by cardiac puncture into heparinised tubes. A portion (*ca.* 0.5 mL) was retained and plasma separated from the remainder of each sample by centrifugation (3000 rpm for 10 minutes in a centrifuge set to maintain a temperature of 4°C). Blood cells were discarded.

The following tissues were collected (where relevant for sex):

Adipose tissue	Ovaries
Adrenal glands	Pancreas
Bladder	Pituitary gland
Bone (femur)	Prostate
Bone marrow (femur)	Salivary glands
Brain	Skin
Eyes	Muscle
Heart	Small intestine
Injection site	Spinal cord
Kidneys	Spleen
Large intestine	Stomach
Liver	Testes
Lung	Thymus
Lymph node (mandibular)	Thyroid

Lymph node (mesenteric)

Uterus

Additionally, for animals 043M, 045M, 046M, 048M, 051M, 052M, 055M and 058M, the tibia/fibula bone was also collected but not analysed (refer to Section 6.11).

6.8 Sample Storage

Samples not analysed immediately were stored frozen in a freezer set to maintain a temperature of -20°C until taken for analysis, with the exception of urine and faeces samples which were stored at -80°C. After analysis, samples were returned to storage in a freezer set to maintain a temperature of -20°C.

Samples of cage wash, dose determinations and dose residues were stored at room temperature prior to and following analysis. These samples were discarded at the Study Director's discretion following acceptance of the study results.

6.9 Preparation of Samples for Total Radioactivity Analysis

Volumes or weights of all samples were measured where appropriate

6.9.1 Dose Formulation

Duplicate aliquots (0.1 mL) of each dilution of the dose formulation were diluted with water and dissolved in scintillation fluid (Aquasafe 500 Plus, Zinsser Inc.) and analysed directly by liquid scintillation counting.

6.9.2 Blood and Plasma

Duplicate weighed aliquots of whole blood (2 x ca. 0.15 g) were taken and then combusted using a Perkin Elmer Model 307 Sample Oxidiser. The resultant $^3\text{H}_2\text{O}$ generated was collected by absorption in Monophase® (15 mL).

Duplicate aliquots (100 µL) of plasma were allowed to air dry, diluted with water and dissolved in scintillation fluid (Aquasafe 500 Plus, Zinsser Inc.) and analysed directly by LSC.

6.9.3 Tissues

Tissue samples were finely chopped with scissors and duplicate, where appropriate, portions were combusted using a Perkin Elmer Model 307 Sample Oxidiser. Smaller tissues were aliquoted directly. The resultant $^3\text{H}_2\text{O}$ generated was collected by absorption in Monophase® S (15 mL).

Combustion of standards showed that recovery efficiencies were in excess of 95% throughout.

6.9.4 Urine, Faeces and Cage Wash

Urine, faeces and cage wash samples were collected but not analysed for total radioactivity. Urine and faeces sample weights were taken prior to storage. Urine and faeces samples were retained at -80°C for possible analysis of specific lipids by LC-MS/MS conducted and reported separately. The sample weights are presented in [Appendix 3](#).

6.10 Quantification of Radioactivity

6.10.1 Liquid Scintillation Counting

All samples prepared in scintillation fluid were subjected to liquid scintillation counting for 5 min, together with representative blank samples, using a Liquid Scintillation Analyser with automatic quench correction by an external standard method. Prior to analysis, samples were allowed to stabilise with regard to light and temperature. Self-normalisation and calibration (SNC) were conducted once a day. An unquenched tritium standard was used to initially calibrate the system to obtain optimal performance by adjusting the voltage on the photo-multiplier tubes. Representative blank sample values were subtracted from sample count rates to give net disintegrations per minute (dpm) per sample. A limit of reliable measurement of 30 counts per minute (cpm) above background was instituted in these laboratories. Any results arising from data below the limit of reliable measurement were noted in the Results section of the report. Sample repeat analysis were in accordance with Standard Operating Procedures.

6.10.2 Data Presentation

Levels of radioactivity in all samples were quantified by LSC and the data captured into DEBRA® management software, Version 5.7 (LabLogic Ltd, UK). Plasma, blood and tissues concentrations of radioactivity in dpm/g and mass eq/g were calculated based on the measured specific activity (1.24 MBq/mg lipid) of radiolabelled test item in the dose formulation.

Individual and mean data were tabulated. The following information was reported:

- Radioactive content in tissues where a total organ weight is applicable was calculated as % administered (injected) dose
- Radioactive content in tissues, whole blood and plasma as µg equiv/g (or mL).
- Blood/plasma ratio

Data presented in results tables are computer generated in DEBRA and rounded appropriately for inclusion in the report. As a consequence, calculation of individual and mean values from data presented will, in some instances, yield slight differences from the results presented.

6.11 Protocol Deviations

Due to the unavailability of rats within specification at (b) (4) the rat supplier used in this study was Envigo, UK, deviating from Section 11 of the Protocol. In the opinion of the Study Director this had no impact on the study outcome since the correct age and strain of rats were used on this study.

In error, tibia/fibula bone were collected at necropsy for animals 043M, 045M, 046M, 048M, 051M, 052M, 055M, and 058M instead of femur bone, deviating from Section 14.1 of the Protocol. Once noticed, the femur bone was retrieved from the residual carcass stored in the -20°C freezer pending disposal and analysed after discussions with the Sponsor. The results appeared similar to the other animals in each timepoint and therefore this had no impact on the study outcome.

7 RESULTS

7.1 Clinical Observations

In the 100 µg mRNA male group, approximately 24 h following administration, animal 021M was noted to have decreased activity, ungroomed, brown staining on muzzle and irregular respiration. A decrease in bodyweight was noted in all remaining animals (approximately 16 g, equivalent to *ca.* 7% reduction of bodyweight) and food hoppers appeared untouched. By approximately 30 hours post-dose, animal 021M was also piloerect, hunched, and was hypersensitive to noise stimulus. Animal 021M was humanely killed and the diagnostic necropsy carried out showed one finding in the liver (prominent lobular architecture). Additionally, animals 019M and 020M were hunched and piloerect from approximately 30 h post-dose onwards.

In the 50 µg mRNA male group, following administration and for the duration of the study, no adverse effects were noted in any animal.

In the 50 µg mRNA female group, approximately 30 h following administration, animal 042F was noted to have decreased activity, and irregular respiration. At 48 h post dose animal 042F was additionally hunched and piloerect.

7.2 Body Weights

At the time of dosing, body weights were in the range of 217-270 g (males) and 179-224 g (females).

7.3 Tissue Distribution Following Intramuscular Administration

The mean (sex combined) concentration and recovery of total radioactivity in whole blood, plasma, injection site and tissues following a single intramuscular administration of [³H]-08-A01-C01 to Wistar Han rats at a target dose level of 50 µg mRNA/animal (1.29 mg/animal lipid) is presented in [Table 1](#). The mean concentration of total radioactivity in whole blood, plasma, injection site and tissues following a single intramuscular administration of [³H]-08-A01-C01 to male and female Wistar Han rats at a target dose level of 50 µg mRNA/animal (1.29 mg/animal lipid) is presented in [Table 2](#). The mean recovery in male and female individual tissues is presented in [Table 3](#).

Individual male and female concentration data is presented in [Appendix 4](#) and [Appendix 5](#), respectively. Individual male and female recovery data is presented in [Appendix 6](#) and [Appendix 7](#), respectively. The male 100 µg data is presented in [Appendix 8](#).

When analysing the injection site, there was often high inter-animal variability in concentration and % injected dose values at each time point. This may have been due to

difficulty in collecting the entirety of this sample since the total area that the injected bolus dose migrated to within the muscle was not visible. When dosing the male 50 µg mRNA group, the injection site was circled using a marker pen to help aid dissection of the injection area. The overall injection site concentrations and % dose values were higher in males than in females. Since concentrations in other tissues were broadly similar between the sexes, it is likely that the higher injection site values in males were a result of its more consistent identification and collection in males.

Following a single intramuscular administration of [³H]-08-A01-C01, the greatest mean tissue concentration and, in most instances, % of injected dose was found remaining in the injection site at each time point in both sexes. The injection site mean concentration and equivalent % dose values are presented in the table below.

Timepoint (h)	Injection site (µg equiv lipid/g)		Injection site (% dose)	
	Male	Female	Male	Female
0.25	219.940	36.566	32.887	6.815
1	587.670	199.950	68.829	36.411
2	529.210	93.144	39.053	24.094
4	619.850	56.227	47.710	9.056
8	299.590	125.930	18.731	24.993
24	267.170	122.540	31.957	26.295
48	268.770	61.088	32.823	16.426

The highest mean recovery of total radioactivity observed was 68.8% of the administered dose at 1-hour post-dose in males.

Low levels of radioactivity were detected in most tissues from the first time point (0.25 h), with the greatest level found circulating in plasma between 1-4 hours post-dose. The plasma and blood mean concentrations and blood:plasma ratios are presented in the table below.

Timepoint (h)	Blood (µg equiv lipid/g)		Plasma (µg equiv lipid/mL)		Blood:plasma ratio	
	Male	Female	Male	Female	Male	Female
0.25	3.003	0.936	6.035	1.894	0.48	1.15
1	2.809	5.928	5.379	10.884	0.49	0.54
2	4.028	6.773	8.714	9.091	0.46	0.64
4	3.400	2.698	8.755	4.251	0.42	0.60
8	2.000	0.628	3.573	1.147	0.56	0.55
24	1.274	0.544	2.621	0.945	0.49	0.57
48	0.535	0.305	1.085	0.524	0.50	0.58

Mean plasma concentrations peaked by 4 hours post-dose in males (8.755 µg equiv lipid/mL) and by 1 hour post-dose in females (10.884 µg equiv lipid/mL), before steadily decreasing. Concentrations were higher in plasma than in blood, with mean blood:plasma ratios generally

ca. 0.5-0.6, indicating that the majority of the total radioactivity is associated with the plasma fraction.

Over 48 hours, [³H]-08-A01-C01 distributed from the injection site to most tissues, with the majority of tissues exhibiting low levels of radioactivity. The highest mean concentrations observed, and the equivalent % dose, are presented in the tables below.

Timepoint (h)	Values expressed as µg equiv lipid/g)						
	Liver		Spleen		Adrenal glands		Ovaries
	Male	Female	Male	Female	Male	Female	Female
0.25	1.151	0.323	0.354	0.313	0.302	0.240	0.104
1	4.006	5.244	2.140	2.801	0.580	2.388	1.339
2	9.574	12.370	5.255	10.213	1.206	4.232	1.638
4	18.525	14.569	8.945	11.646	2.569	3.206	2.341
8	27.916	25.172	24.434	19.747	6.387	7.218	3.088
24	23.360	15.119	22.819	17.341	19.948	7.595	5.240
48	18.164	30.411	19.550	27.155	21.476	14.942	12.261

=Mean includes results calculated from data less than 30 cpm above background

Timepoint (h)	Liver		Spleen		Adrenal glands		Ovaries
	Male	Female	Male	Female	Male	Female	Female
0.25	0.995	0.209	0.014	0.011	0.001	0.001	0.001
1	2.834	2.907	0.087	0.098	0.002	0.012	0.009
2	7.629	7.030	0.232	0.418	0.005	0.015	0.008
4	15.027	8.699	0.351	0.419	0.012	0.018	0.016
8	21.519	14.580	1.118	0.845	0.026	0.043	0.025
24	19.901	10.977	0.957	0.685	0.083	0.049	0.037
48	13.953	18.357	0.914	1.146	0.104	0.108	0.095

=Mean includes results calculated from data less than 30 cpm above background

Maximum concentrations (C_{max}) in liver and spleen were observed at 8 hours post-dose in males and 48 hours post dose in females, but were broadly similar and appeared to plateau at 8 hours post-dose when considering variability. The greatest mean concentration outside the injection site was observed in the liver, with values of 27.916 µg equiv lipid/g (equivalent to 21.5 % dose) in males and 30.411 µg equiv lipid/g (equivalent to 18.4 % dose) in females. In the spleen the highest concentrations were 24.434 µg equiv lipid/g in males and 27.155 µg equiv lipid/g (equivalent to 1.1% dose in both sexes).

In the adrenal glands and ovaries, the highest mean concentrations were observed at 48 hours post-dose. The highest mean concentrations in the adrenal glands were 21.476 and 14.942 µg equiv lipid/g in males and females, respectively (equivalent to 0.1% dose in both sexes). The highest mean ovaries concentration was 12.261 µg equiv lipid/g (equivalent to 0.1 % dose).

090177e195794698\Approved\Approved On: 09-Nov-2020 21:23 (GMT)

8 CONCLUSIONS

In conclusion, the distribution of [³H]-08-A01-C01 (monitoring the [³H]-CHE lipid label) in blood, plasma and selected tissues was determined in male and female Wistar Han rats over 48 hours after a single intramuscular injection at 50 µg mRNA/animal (1.29 mg/animal lipid dose). The concentrations of [³H]-08-A01-C01 were greatest in the injection site at all time points, with levels peaking in the plasma by 1-4 hours post-dose and distribution mainly into liver, adrenal glands, spleen and ovaries over 48 hours. Total recovery of radioactivity outside of the injection site was greatest in the liver, with much lower total recovery in spleen, and very little recovery in adrenals glands and ovaries. The mean plasma, blood and tissue concentrations and tissue distribution patterns were broadly similar between the sexes and [³H]-08-A01-C01 did not associate with red blood cells.

9 TABLES

Table 1 Mean (Sexes-Combined) Concentration and Recovery of Total Radioactivity in Whole Blood, Plasma and Tissues Following Single Intramuscular Administration of [³H]-08-A01-C01 to Wistar Han Rats

Target Dose Level: 50 µg mRNA/Animal; 1.29 mg Total Lipid/Animal

Results expressed as total lipid concentration (µg lipid equiv/g (mL)) and % of administered dose

Sample	Total Lipid Concentration (µg lipid equiv/g (or mL))							% of Administered Dose						
	0.25 min	1 h	2 h	4 h	8 h	24 h	48 h	0.25 min	1 h	2 h	4 h	8 h	24 h	48 h
Adipose tissue	0.057	0.100	0.126	0.128	0.093	0.084	0.181	-	-	-	-	-	-	-
Adrenal glands	0.271	1.484	2.719	2.888	6.803	13.772	18.209	0.001	0.007	0.010	0.015	0.035	0.066	0.106
Bladder	0.041	0.130	0.146	0.167	0.148	0.247	0.365	0.000	0.001	0.001	0.001	0.001	0.002	0.002
Bone (femur)	0.091	0.195	0.266	0.276	0.340	0.342	0.687	-	-	-	-	-	-	-
Bone marrow (femur)	0.479	0.960	1.237	1.236	1.836	2.492	3.771	-	-	-	-	-	-	-
Brain	0.045	0.100	0.138	0.115	0.073	0.069	0.068	0.007	0.013	0.020	0.016	0.011	0.010	0.009
Eyes	0.010	0.035	0.052	0.067	0.059	0.091	0.112	0.000	0.001	0.001	0.002	0.002	0.002	0.003
Heart	0.282	1.029	1.402	0.987	0.790	0.451	0.546	0.018	0.056	0.084	0.060	0.042	0.027	0.030
Injection site	128.253	393.810	311.177	338.039	212.760	194.855	164.929	19.851	52.620	31.574	28.383	21.862	29.126	24.625
Kidneys	0.391	1.161	2.046	0.924	0.590	0.426	0.425	0.050	0.124	0.211	0.109	0.075	0.054	0.057
Large intestine	0.013	0.048	0.093	0.287	0.649	1.104	1.338	0.008	0.025	0.065	0.192	0.405	0.692	0.762
Liver	0.737	4.625	10.972	16.547	26.544	19.240	24.288	0.602	2.871	7.330	11.863	18.050	15.439	16.155
Lung	0.492	1.210	1.834	1.497	1.151	1.039	1.093	0.052	0.101	0.178	0.169	0.122	0.101	0.101
Lymph node (man)	0.064	0.189	0.290	0.408	0.534	0.554	0.727	-	-	-	-	-	-	-
Lymph node (mes)	0.050	0.146	0.530	0.489	0.689	0.985	1.366	-	-	-	-	-	-	-
Muscle	0.021	0.061	0.084	0.103	0.096	0.095	0.192	-	-	-	-	-	-	-
Ovaries (females)	0.104	1.339	1.638	2.341	3.088	5.240	12.261	0.001	0.009	0.008	0.016	0.025	0.037	0.095
Pancreas	0.081	0.207	0.414	0.380	0.294	0.358	0.599	0.003	0.007	0.014	0.015	0.015	0.011	0.019
Pituitary gland	0.339	0.645	0.868	0.854	0.405	0.478	0.694	0.000	0.001	0.001	0.001	0.000	0.000	0.001
Prostate (males)	0.061	0.091	0.128	0.157	0.150	0.183	0.170	0.001	0.001	0.002	0.003	0.003	0.004	0.003
Salivary glands	0.084	0.193	0.255	0.220	0.135	0.170	0.264	0.003	0.007	0.008	0.008	0.005	0.006	0.009
Skin	0.013	0.208	0.159	0.145	0.119	0.157	0.253	-	-	-	-	-	-	-

- =Partial tissue taken therefore not applicable

090177e195794698\Approved\Approved On: 09-Nov-2020 21:23 (GMT)

Table 1 Mean (Sexes-Combined) Concentration of Total Radioactivity in Whole Blood, Plasma and
 (Continued) Tissues Following Single Intramuscular Administration of [³H]-08-A01-C01 to Wistar Han Rats

Target Dose Level: 50 µg mRNA/Animal; 1.29 mg Total Lipid/Animal

Results expressed as total lipid concentration (µg lipid equiv/g (mL)) and % of administered dose

Sample	Total Lipid Concentration (µg lipid equiv/g (or mL))							% of Administered Dose						
	0.25 min	1 h	2 h	4 h	8 h	24 h	48 h	0.25 min	1 h	2 h	4 h	8 h	24 h	48 h
Small intestine	0.030	0.221	0.476	0.879	1.279	1.302	1.472	0.024	0.130	0.319	0.543	0.776	0.906	0.835
Spinal cord	0.043	0.097	0.169	0.250	0.106	0.085	0.112	0.001	0.002	0.002	0.003	0.001	0.001	0.001
Spleen	0.334	2.471	7.734	10.296	22.091	20.080	23.353	0.013	0.093	0.325	0.385	0.982	0.821	1.030
Stomach	0.017	0.065	0.115	0.144	0.268	0.152	0.215	0.006	0.019	0.034	0.030	0.040	0.037	0.039
Testes (males)	0.031	0.042	0.079	0.129	0.146	0.304	0.320	0.007	0.010	0.017	0.030	0.034	0.074	0.074
Thymus	0.088	0.243	0.340	0.335	0.196	0.207	0.331	0.004	0.007	0.010	0.012	0.008	0.007	0.008
Thyroid	0.155	0.536	0.842	0.851	0.544	0.578	1.000	0.000	0.001	0.001	0.001	0.001	0.001	0.001
Uterus (females)	0.043	0.203	0.305	0.140	0.287	0.289	0.456	0.002	0.011	0.015	0.008	0.016	0.018	0.022
Whole blood	1.970	4.369	5.401	3.049	1.314	0.909	0.420	-	-	-	-	-	-	-
Plasma	3.965	8.132	8.903	6.503	2.360	1.783	0.805	-	-	-	-	-	-	-
Blood:plasma ratio	0.815	0.515	0.550	0.510	0.555	0.530	0.540	-	-	-	-	-	-	-

- =Partial tissue taken therefore not applicable/not applicable

090177e195794698\Approved\Approved On: 09-Nov-2020 21:23 (GMT)

Table 2 Mean Concentration of Total Radioactivity in Whole Blood, Plasma and Tissues Following Single Intramuscular Administration of [³H]-08-A01-C01 to Wistar Han Rats

Target Dose Level: 50 µg mRNA/Animal; 1.29 mg Total Lipid/Animal

Results expressed as µg lipid equiv/g (mL)

Sample	0.25 min		1 h		2 h		4 h		8 h		24 h		48 h	
	Male	Female	Male	Female	Male	Female	Male	Female	Male	Female	Male	Female	Male	Female
Adipose tissue	0.040	°0.073	0.050	0.149	0.070	0.182	0.093	0.163	0.116	0.069	0.126	0.042	0.129	0.232
Adrenal glands	0.302	°0.240	0.580	2.388	1.206	4.232	2.569	3.206	6.387	7.218	19.948	7.595	21.476	14.942
Bladder	0.049	°0.033	0.095	0.165	0.137	0.155	0.227	0.106	0.211	0.085	0.323	0.171	0.340	0.389
Bone (femur)	0.126	0.056	0.148	0.241	0.235	0.296	0.335	0.217	0.502	0.177	0.504	0.180	0.520	0.854
Bone marrow (femur)	0.761	°0.196	0.910	1.010	1.136	1.337	1.557	0.915	2.397	1.274	3.579	1.405	3.690	3.851
Brain	0.073	°0.016	0.083	0.117	0.143	0.133	0.155	0.075	0.101	0.045	0.090	0.047	0.083	0.052
Eyes	0.014	°0.006	0.027	0.043	0.046	0.058	0.095	0.038	0.088	0.030	0.129	0.052	0.127	0.097
Heart	0.419	°0.144	0.631	1.426	1.122	1.682	1.049	0.925	1.189	0.391	0.583	0.318	0.672	0.420
Injection site	219.940	36.566	587.670	199.950	529.210	93.144	619.850	56.227	299.590	125.930	267.170	122.540	268.770	61.088
Kidneys	0.511	0.271	0.630	1.692	1.124	2.967	1.033	0.814	0.837	0.342	0.504	0.348	0.482	0.368
Large intestine	0.017	°0.008	0.031	0.065	0.080	0.106	0.350	0.224	0.690	0.608	1.741	0.466	1.426	1.249
Liver	1.151	0.323	4.006	5.244	9.574	12.370	18.525	14.569	27.916	25.172	23.360	15.119	18.164	30.411
Lung	0.737	0.247	0.845	1.574	1.594	2.074	1.772	1.222	1.674	0.628	1.316	0.762	1.288	0.898
Lymph node (man)	0.090	°0.038	0.154	0.223	0.217	0.362	0.424	0.391	0.695	0.372	0.744	0.363	0.820	0.633
Lymph node (mes)	0.052	°0.048	0.095	0.196	0.229	0.831	0.441	0.536	0.649	0.729	1.106	0.863	1.057	1.675
Muscle	°0.029	0.012	0.039	0.082	0.067	0.100	0.075	0.130	0.101	0.091	0.098	0.092	0.280	0.104
Ovaries (females)	-	°0.104	-	1.339	-	1.638	-	2.341	-	3.088	-	5.240	-	12.261
Pancreas	0.125	0.037	0.153	0.261	0.423	0.404	0.361	0.398	0.349	0.239	0.396	0.320	0.587	0.611
Pituitary gland	0.537	°0.141	0.446	0.844	0.781	0.955	1.249	0.458	0.669	0.141	0.656	0.300	0.543	0.845
Prostate (males)	0.061	-	0.091	-	0.128	-	0.157	-	0.150	-	0.183	-	0.170	-
Salivary glands	0.114	°0.054	0.148	0.237	0.214	0.295	0.270	0.169	0.176	0.094	0.243	0.096	0.297	0.231
Skin	°0.016	0.010	0.028	0.387	0.054	0.263	0.085	0.204	0.122	0.116	0.195	0.118	0.209	0.297

°=Mean includes results calculated from data less than 30 cpm above background

090177e195794698\Approved\Approved On: 09-Nov-2020 21:23 (GMT)

Table 2 Mean Concentration of Total Radioactivity in Whole Blood, Plasma and Tissues Following Single (Continued) Intramuscular Administration of [³H]-08-A01-C01 to Wistar Han Rats

Target Dose Level: 50 µg mRNA/Animal; 1.29 mg Total Lipid/Animal

Results expressed as µg lipid equiv/g (mL)

Sample	0.25 min		1 h		2 h		4 h		8 h		24 h		48 h	
	Male	Female	Male	Female	Male	Female	Male	Female	Male	Female	Male	Female	Male	Female
Small intestine	0.038	°0.021	0.194	0.247	0.471	0.481	0.919	0.838	1.525	1.033	1.878	0.726	1.630	1.314
Spinal cord	0.061	°0.024	0.072	0.122	0.166	0.172	0.375	0.124	0.168	0.044	0.121	0.048	0.162	0.062
Spleen	0.354	°0.313	2.140	2.801	5.255	10.213	8.945	11.646	24.434	19.747	22.819	17.341	19.550	27.155
Stomach	0.018	°0.015	0.039	0.091	0.104	0.126	0.186	0.101	0.410	0.126	0.222	0.081	0.235	0.195
Testes (males)	0.031	-	0.042	-	0.079	-	0.129	-	0.146	-	0.304	-	0.320	-
Thymus	0.106	°0.069	0.187	0.298	0.220	0.459	0.461	0.209	0.292	0.100	0.255	0.159	0.296	0.366
Thyroid	0.217	°0.093	0.391	0.680	0.575	1.109	1.097	0.604	0.781	0.307	0.820	0.335	1.344	0.655
Uterus (females)	-	°0.043	-	0.203	-	0.305	-	0.140	-	0.287	-	0.289	-	0.456
Whole Blood	3.003	0.936	2.809	5.928	4.028	6.773	3.400	2.698	2.000	0.628	1.274	0.544	0.535	0.305
Plasma	6.035	1.894	5.379	10.884	8.714	9.091	8.755	4.251	3.573	1.147	2.621	0.945	1.085	0.524
Blood:plasma ratio	0.48	1.15	0.49	0.54	0.46	0.64	0.42	0.60	0.56	0.55	0.49	0.57	0.50	0.58

°=Mean includes results calculated from data less than 30 cpm above background

090177e195794698\Approved\Approved On: 09-Nov-2020 21:23 (GMT)

Table 3 Mean Recovery of Total Radioactivity in Tissues Following Single Intramuscular Administration of [³H]-08-A01-C01 to Wistar Han Rats

Target Dose Level: 50 µg mRNA/Animal; 1.29 mg Total Lipid/Animal

Results expressed as % administered dose

Sample	0.25 min		1 h		2 h		4 h		8 h		24 h		48 h	
	Male	Female	Male	Female	Male	Female	Male	Female	Male	Female	Male	Female	Male	Female
Adrenal glands	0.001	°0.001	0.002	0.012	0.005	0.015	0.012	0.018	0.026	0.043	0.083	0.049	0.104	0.108
Bladder	0.000	°0.000	0.001	0.001	0.001	0.001	0.001	0.001	0.002	0.000	0.002	0.001	0.002	0.002
Brain	0.011	°0.002	0.010	0.016	0.021	0.019	0.021	0.011	0.014	0.007	0.012	0.007	0.011	0.007
Eyes	0.000	°0.000	0.000	0.001	0.001	0.001	0.002	0.001	0.002	0.001	0.002	0.001	0.003	0.002
Heart	0.028	°0.008	0.032	0.079	0.065	0.102	0.067	0.052	0.061	0.022	0.035	0.018	0.039	0.020
Injection site	32.887	6.815	68.829	36.411	39.053	24.094	47.710	9.056	18.731	24.993	31.957	26.295	32.823	16.426
Kidneys	0.069	0.030	0.077	0.171	0.149	0.272	0.136	0.082	0.109	0.040	0.068	0.039	0.071	0.042
Large intestine	0.011	°0.004	0.018	0.032	0.054	0.075	0.236	0.148	0.463	0.346	1.091	0.293	0.810	0.714
Liver	0.995	0.209	2.834	2.907	7.629	7.030	15.027	8.699	21.519	14.580	19.901	10.977	13.953	18.357
Lung	0.082	0.022	0.085	0.117	0.189	0.167	0.226	0.112	0.180	0.064	0.136	0.065	0.131	0.070
Ovaries (females)	-	°0.001	-	0.009	-	0.008	-	0.016	-	0.025	-	0.037	-	0.095
Pancreas	0.005	0.001	0.006	0.008	0.015	0.012	0.013	0.017	0.014	0.016	0.013	0.009	0.015	0.023
Pituitary gland	0.000	°0.000	0.000	0.001	0.000	0.001	0.001	0.000	0.000	0.000	0.000	0.000	0.000	0.001
Prostate (males)	0.001	-	0.001	-	0.002	-	0.003	-	0.003	-	0.004	-	0.003	-
Salivary glands	0.004	°0.002	0.005	0.008	0.007	0.009	0.009	0.006	0.007	0.003	0.008	0.003	0.010	0.007
Small intestine	0.032	°0.015	0.124	0.135	0.353	0.285	0.623	0.462	0.972	0.580	1.275	0.536	0.971	0.698
Spinal cord	0.001	°0.000	0.001	0.002	0.001	0.002	0.003	0.002	0.001	0.001	0.001	0.001	0.001	0.001
Spleen	0.014	°0.011	0.087	0.098	0.232	0.418	0.351	0.419	1.118	0.845	0.957	0.685	0.914	1.146
Stomach	0.008	°0.003	0.016	0.022	0.033	0.035	0.037	0.022	0.055	0.024	0.054	0.020	0.049	0.029
Testes (males)	0.007	-	0.010	-	0.017	-	0.030	-	0.034	-	0.074	-	0.074	-
Thymus	0.005	°0.002	0.006	0.008	0.008	0.012	0.018	0.006	0.012	0.003	0.009	0.004	0.008	0.007
Thyroid	0.000	°0.000	0.000	0.001	0.001	0.001	0.001	0.001	0.001	0.000	0.001	0.000	0.001	0.001
Uterus (females)	-	°0.002	-	0.011	-	0.015	-	0.008	-	0.016	-	0.018	-	0.022

°=Mean includes results calculated from data less than 30 cpm above background

090177e195794698\Approved\Approved On: 09-Nov-2020 21:23 (GMT)

10 APPENDICES

Appendix 1 Certificates of Analysis for [³H]-08-A01-C01 and [³H]-CHE

Confidential



R&D Formulation Characterization Report

Batch ID	LNP ID	Specific Activity	[Lipid]	Encaps	Encapsulated mRNA	Yield	mRNA/Lipid Ratio	Particle Diameter	Poly-dispersity
		dpm/uL	mg/mL	%	mg/mL	mg	mg/mg	nm	
NC-0552-1	08-A01-C01	1,900,000	25.7	94	1.0	6.05	0.039	89	0.062

Notes

Formulated July 6, 2020 for NC-0552 using BioNTech mRNA (AnSo luc 1041 CorVac) and trace labeled with 3H-CHE. Endotoxin below detection limit (<0.5 EU/mL). Sterile filtered using 0.2 µm pore-size filters.

Stored at -70°C. Thaw at room temperature and dilute on the day of use.

(b) (6)

(b) (6)

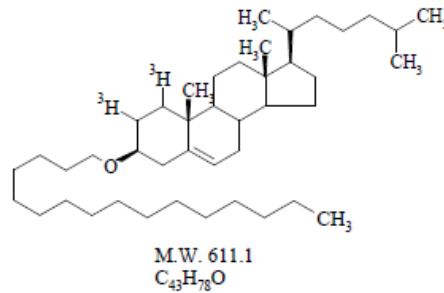
08-July-20
Date

Appendix 1 Certificates of Analysis for [³H]-08-A01-C01 and [³H]-CHE
(continued)

TECHNICAL DATA SHEET	³ H
Research Use Only. Not for use in diagnostic procedures	
CHOLESTERYL HEXADECYL ETHER, [CHOLESTERYL-1,2-³H(N)]-	
Product Number: NET859	

LOT SPECIFIC INFORMATION

Lot Number:	2656317
Specific Activity:	51.9 Ci/mmol
	1920 GBq/mmol
Production Date:	16-Dec-2019



PACKAGING: 1.0 mCi/ml (37 MBq/ml) in toluene, under argon in an ampoule. Shipped on dry ice.

STABILITY AND STORAGE RECOMMENDATIONS: When cholesteryl hexadecyl ether, [cholesteryl-1,2-³H(N)]- is stored at -20°C in its original solvent and at its original concentration, the rate of decomposition is initially 2% for 6 months from date of purification. Stability is nonlinear and not correlated to isotope half-life. Lot to lot variation may occur.

SPECIFIC ACTIVITY RANGE: 40-60 Ci/mmol (1480-2220 GBq/mmol)

RADIOCHEMICAL PURITY: This product was initially found to be greater than 97% when determined by the following methods. The rate of decomposition can accelerate. It is advisable to check purity prior to use:

High pressure liquid chromatography on a Zorbax C-8 column using the following mobile phase:
acetonitrile : isopropanol, (35:65).

Thin layer chromatography on silica gel using the following solvent system:
toluene : hexane, (1:9).

QUALITY CONTROL: The radiochemical purity of cholesteryl hexadecyl ether, [cholesteryl-1,2-³H(N)]- is checked at appropriate intervals using the first listed chromatography method.

The precursor used in the synthesis of NET-859 is synthetic.

HAZARD INFORMATION: WARNING: This product contains a chemical known to the state of California to cause cancer.

PerkinElmer, Inc.
549 Albany Street
Boston, MA 02118 USA
P: (800) 762-4000 or (+1) 203-925-4602
www.perkinelmer.com/nenradiochemicals
For a complete listing of our global offices, visit www.perkinelmer.com/ContactUs
Copyright ©2010, PerkinElmer, Inc. All rights reserved. PerkinElmer® is a registered trademark of PerkinElmer, Inc.
All other trademarks are the property of their respective owners.
NET859-REV-02



Appendix 2 Individual Animal Dosing Summary

Males

Target Dose Level: 50 µg mRNA/Animal; 1.29 mg Total Lipid/Animal

Animal ID	Body weight (g)	Dose Received		
		mg mRNA	mg lipid	MBq
043M	270	0.0514	1.32	1.63
044M	264	0.0518	1.33	1.65
045M	244	0.0521	1.34	1.66
046M	263	0.0525	1.35	1.68
047M	232	0.0514	1.32	1.64
048M	228	0.0525	1.35	1.67
049M	259	0.0514	1.32	1.64
050M	249	0.0518	1.33	1.66
051M	257	0.0533	1.37	1.70
052M	258	0.0521	1.34	1.66
053M	249	0.0529	1.36	1.69
054M	235	0.0525	1.35	1.68
055M	247	0.0502	1.29	1.60
056M	256	0.0514	1.32	1.64
057M	266	0.0521	1.34	1.66
058M	263	0.0521	1.34	1.66
059M	243	0.0525	1.35	1.67
060M	248	0.0518	1.33	1.65
061M	240	0.0521	1.34	1.66
062M	259	0.0521	1.34	1.66
063M	238	0.0521	1.34	1.66

090177e195794698\Approved\Approved On: 09-Nov-2020 21:23 (GMT)

**Appendix 2 Individual Animal Dosing Summary
 (continued)**

Females

Target Dose Level: 50 µg mRNA/Animal; 1.29 mg Total Lipid/Animal

Animal ID	Body weight (g)	Dose Received		
		mg mRNA	mg lipid	MBq
022F	215	0.0521	1.34	1.66
023F	206	0.0529	1.36	1.68
024F	206	0.0514	1.32	1.64
025F	212	0.0533	1.37	1.70
026F	213	0.0525	1.35	1.68
027F	207	0.0529	1.36	1.69
028F	198	0.0529	1.36	1.68
029F	208	0.0529	1.36	1.69
030F	214	0.0518	1.33	1.64
031F	204	0.0537	1.38	1.71
032F	207	0.0533	1.37	1.70
033F	209	0.0521	1.34	1.66
034F	224	0.0510	1.31	1.62
035F	179	0.0482	1.24	1.53
036F	211	0.0467	1.20	1.49
037F	205	0.0506	1.30	1.61
038F	225	0.0502	1.29	1.60
039F	213	0.0525	1.35	1.67
040F	199	0.0533	1.37	1.69
041F	218	0.0529	1.36	1.69
042F	193	0.0533	1.37	1.70

090177e195794698\Approved\Approved On: 09-Nov-2020 21:23 (GMT)

**Appendix 2 Individual Animal Dosing Summary
 (continued)**

Males

Target Dose Level: 100 µg mRNA/Animal; 2.57 mg Total Lipid/Animal

Animal ID	Body weight (g)	Dose Received		
		mg mRNA	mg lipid	MBq
001M	240	0.104	2.66	3.30
002M	243	0.106	2.73	3.38
003M	277	0.107	2.74	3.40
004M	247	0.106	2.72	3.37
005M	243	0.107	2.76	3.42
006M	237	0.107	2.74	3.39
007M	245	0.107	2.75	3.41
008M	237	0.106	2.73	3.39
009M	248	0.106	2.73	3.39
010M	227	0.101	2.60	3.22
011M	267	0.105	2.71	3.36
012M	237	0.106	2.72	3.37
013M	241	0.105	2.69	3.34
014M	264	0.107	2.76	3.42
015M	264	0.105	2.71	3.36
043M	241	0.106	2.73	3.39
017M	252	0.106	2.73	3.39
018M	263	0.105	2.70	3.35
019M	248	0.106	2.72	3.37
020M	246	0.106	2.73	3.39
021M	217	0.107	2.75	3.41

090177e195794698\Approved\Approved On: 09-Nov-2020 21:23 (GMT)

Appendix 3 Urine and Faeces Sample Weights

Males

Target Dose Level: 50 µg mRNA/Animal; 1.29 mg Total Lipid/Animal

Results expressed in g

Sample	Timepoint	061M	062M	063M
Urine	Pre-dose	6.860	18.617	14.228
	6 h	6.139	8.101	8.153
	24 h	21.208	29.766	40.276
	48 h	28.317	28.566	36.902
Faeces	Pre-dose	11.324	7.893	6.070
	24 h	4.716	14.327	8.659
	48 h	6.968	8.398	7.007

Appendix 3 Urine and Faeces Sample Weights
(continued)

Females

Target Dose Level: 50 µg mRNA/Animal; 1.29 mg Total Lipid/Animal

Results expressed in g

Sample	Timepoint	040F	041F	042F
Urine	Pre-dose	3.963	9.453	7.513
	6 h	4.844	5.664	9.719
	24 h	20.736	29.176	21.294
	48 h	30.371	33.928	23.141
Faeces	Pre-dose	6.110	2.679	6.010
	24 h	8.887	9.193	5.619
	48 h	4.565	6.139	4.834

090177e195794698\Approved\Approved On: 09-Nov-2020 21:23 (GMT)

Appendix 3 Urine and Faeces Sample Weights
(continued)

Males

Target Dose Level: 100 µg mRNA/Animal; 2.57 mg Total Lipid/Animal

Results expressed in g

Sample	Timepoint	019M	020M	021M
Urine	Pre-dose	7.519	4.094	13.159
	6 h	8.883	8.835	10.517
	24 h	29.916	22.983	12.664
	48 h	37.860	35.653	*6.931
Faeces	Pre-dose	9.491	9.292	4.882
	24 h	11.197	14.005	8.769
	48 h	6.950	8.229	*2.449

Note that for animal 021M the collection period was approximately 24-31 h.

Appendix 4 Individual Male Concentration Data

Concentration of Total Radioactivity in Whole Blood, Plasma and Tissues 0.25 min Following Single Intramuscular Administration of [³H]-08-A01-C01 to Male Wistar Han Rats

Target Dose Level: 50 µg mRNA/Animal; 1.29 mg Total Lipid/Animal

Results expressed as µg lipid equiv/g (mL)

Sample	043M	044M	045M	Mean	SD
Adipose tissue	0.056	0.045	0.019	0.040	0.019
Adrenal glands	0.380	0.480	0.046	0.302	0.227
Bladder	0.096	0.045	0.007	0.049	0.045
Bone (femur)	0.172	0.085	0.119	0.126	0.044
Bone marrow (femur)	0.775	0.326	1.182	0.761	0.428
Brain	0.093	0.092	0.033	0.073	0.034
Eyes	0.025	0.013	0.005	0.014	0.010
Heart	0.710	0.474	0.074	0.419	0.322
Injection site	436.090	159.310	64.429	219.940	193.100
Kidneys	0.808	0.600	0.123	0.511	0.351
Large intestine	0.020	0.027	0.003	0.017	0.012
Liver	2.035	1.226	0.193	1.151	0.923
Lung	1.050	0.826	0.334	0.737	0.366
Lymph node (Man)	0.152	0.069	0.049	0.090	0.055
Lymph node (Mes)	0.087	0.054	0.016	0.052	0.036
Muscle	0.049	0.035	*0.003	°0.029	°0.024
Pancreas	0.156	0.201	0.019	0.125	0.095
Pituitary gland	0.962	0.535	0.115	0.537	0.424
Prostate	0.098	0.074	0.012	0.061	0.044
Salivary glands	0.169	0.145	0.028	0.114	0.076
Skin	0.030	0.015	*0.002	°0.016	°0.014
Small intestine	0.064	0.043	0.008	0.038	0.028
Spinal cord	0.108	0.063	0.013	0.061	0.047
Spleen	0.519	0.450	0.094	0.354	0.228
Stomach	0.022	0.027	0.005	0.018	0.012
Testes	0.053	0.036	0.006	0.031	0.024
Thymus	0.119	0.169	0.030	0.106	0.071
Thyroid	0.292	0.307	0.053	0.217	0.142
Whole Blood	5.631	2.526	0.852	3.003	2.425
Plasma	9.854	6.519	1.732	6.035	4.083
Blood:plasma ratio	0.57	0.39	0.49	0.48	0.09

*=Results calculated from data less than 30 cpm above background

°=Mean includes results calculated from data less than 30 cpm above background

090177e195794698\Approved\Approved On: 09-Nov-2020 21:23 (GMT)

Appendix 4 Individual Male Concentration Data
 (continued)

Concentration of Total Radioactivity in Whole Blood, Plasma and Tissues 1 hour Following Single Intramuscular Administration of [³H]-08-A01-C01 to Male Wistar Han Rats

Target Dose Level: 50 µg mRNA/Animal; 1.29 mg Total Lipid/Animal

Results expressed as µg lipid equiv/g (mL)

Sample	046M	047M	048M	Mean	SD
Adipose tissue	0.037	0.073	0.040	0.050	0.020
Adrenal glands	0.293	0.647	0.800	0.580	0.260
Bladder	0.111	0.087	0.088	0.095	0.013
Bone (femur)	0.115	0.085	0.246	0.148	0.085
Bone marrow (femur)	0.561	1.150	1.021	0.910	0.310
Brain	0.033	0.108	0.107	0.083	0.043
Eyes	0.014	0.019	0.049	0.027	0.019
Heart	0.266	0.780	0.847	0.631	0.318
Injection site	503.490	593.230	666.280	587.670	81.536
Kidneys	0.322	0.710	0.857	0.630	0.276
Large intestine	0.026	0.032	0.037	0.031	0.005
Liver	2.667	3.571	5.780	4.006	1.602
Lung	0.428	1.203	0.903	0.845	0.391
Lymph node (Man)	0.151	0.166	0.145	0.154	0.011
Lymph node (Mes)	0.076	0.100	0.109	0.095	0.017
Muscle	0.030	0.036	0.050	0.039	0.010
Pancreas	0.076	0.189	0.193	0.153	0.067
Pituitary gland	0.202	0.502	0.634	0.446	0.221
Prostate	0.063	0.105	0.105	0.091	0.024
Salivary glands	0.084	0.151	0.208	0.148	0.062
Skin	0.020	0.027	0.039	0.028	0.010
Small intestine	0.144	0.214	0.223	0.194	0.043
Spinal cord	0.062	0.070	0.084	0.072	0.011
Spleen	3.314	1.388	1.720	2.140	1.029
Stomach	0.024	0.043	0.049	0.039	0.013
Testes	0.026	0.041	0.057	0.042	0.015
Thymus	0.201	0.133	0.226	0.187	0.048
Thyroid	0.126	0.599	0.448	0.391	0.241
Whole Blood	0.873	4.534	3.018	2.809	1.840
Plasma	2.937	6.047	7.153	5.379	2.186
Blood:plasma ratio	0.30	0.75	0.42	0.49	0.23

090177e195794698\Approved\Approved On: 09-Nov-2020 21:23 (GMT)

**Appendix 4 Individual Male Concentration Data
(continued)****Concentration of Total Radioactivity in Whole Blood, Plasma and
Tissues 2 hours Following Single Intramuscular Administration of
[³H]-08-A01-C01 to Male Wistar Han Rats****Target Dose Level: 50 µg mRNA/Animal; 1.29 mg Total Lipid/Animal****Results expressed as µg lipid equiv/g (mL)**

Sample	049M	050M	051M	Mean	SD
Adipose tissue	0.084	0.034	0.090	0.070	0.031
Adrenal glands	1.809	0.584	1.226	1.206	0.613
Bladder	0.152	0.080	0.179	0.137	0.051
Bone (femur)	0.250	0.180	0.273	0.235	0.048
Bone marrow (femur)	1.526	0.559	1.323	1.136	0.510
Brain	0.220	0.088	0.121	0.143	0.069
Eyes	0.036	0.023	0.077	0.046	0.028
Heart	1.782	0.682	0.901	1.122	0.582
Injection site	445.930	1052.800	88.843	529.210	487.370
Kidneys	1.467	0.785	1.120	1.124	0.341
Large intestine	0.074	0.056	0.109	0.080	0.027
Liver	12.023	5.816	10.885	9.574	3.304
Lung	2.397	0.968	1.419	1.594	0.730
Lymph node (Man)	0.328	0.112	0.210	0.217	0.108
Lymph node (Mes)	0.312	0.180	0.194	0.229	0.073
Muscle	0.083	0.060	0.057	0.067	0.014
Pancreas	0.296	0.179	0.792	0.423	0.325
Pituitary gland	1.175	0.405	0.764	0.781	0.385
Prostate	0.150	0.095	0.139	0.128	0.029
Salivary glands	0.279	0.113	0.251	0.214	0.089
Skin	0.083	0.032	0.048	0.054	0.026
Small intestine	0.455	0.458	0.500	0.471	0.025
Spinal cord	0.184	0.150	0.163	0.166	0.017
Spleen	6.771	2.590	6.403	5.255	2.315
Stomach	0.121	0.059	0.133	0.104	0.040
Testes	0.120	0.039	0.077	0.079	0.040
Thymus	0.248	0.146	0.265	0.220	0.065
Thyroid	0.749	0.361	0.615	0.575	0.197
Whole Blood	4.913	2.788	4.384	4.028	1.106
Plasma	10.623	6.177	9.341	8.714	2.288
Blood:plasma ratio	0.46	0.45	0.47	0.46	0.01

090177e195794698\Approved\Approved On: 09-Nov-2020 21:23 (GMT)

**Appendix 4 Individual Male Concentration Data
(continued)****Concentration of Total Radioactivity in Whole Blood, Plasma and Tissues 4 hours Following Single Intramuscular Administration of [³H]-08-A01-C01 to Male Wistar Han Rats****Target Dose Level: 50 µg mRNA/Animal; 1.29 mg Total Lipid/Animal****Results expressed as µg lipid equiv/g (mL)**

Sample	052M	053M	054M	Mean	SD
Adipose tissue	0.062	0.092	0.124	0.093	0.031
Adrenal glands	2.252	1.999	3.456	2.569	0.779
Bladder	0.207	0.239	0.234	0.227	0.017
Bone (femur)	0.264	0.234	0.506	0.335	0.149
Bone marrow (femur)	1.318	1.364	1.987	1.557	0.374
Brain	0.136	0.112	0.217	0.155	0.055
Eyes	0.084	0.133	0.067	0.095	0.034
Heart	0.993	0.669	1.484	1.049	0.411
Injection site	445.970	1001.000	412.620	619.850	330.480
Kidneys	0.967	0.737	1.395	1.033	0.334
Large intestine	0.413	0.311	0.327	0.350	0.055
Liver	14.739	16.391	24.445	18.525	5.193
Lung	2.047	1.003	2.265	1.772	0.675
Lymph node (Man)	0.283	0.564	0.426	0.424	0.140
Lymph node (Mes)	0.287	0.258	0.780	0.441	0.293
Muscle	0.064	0.057	0.104	0.075	0.025
Pancreas	0.277	0.413	0.393	0.361	0.073
Pituitary gland	0.933	2.418	0.397	1.249	1.047
Prostate	0.161	0.121	0.190	0.157	0.035
Salivary glands	0.232	0.197	0.380	0.270	0.097
Skin	0.073	0.052	0.131	0.085	0.041
Small intestine	0.822	0.698	1.235	0.919	0.281
Spinal cord	0.193	0.745	0.188	0.375	0.320
Spleen	6.146	11.159	9.529	8.945	2.557
Stomach	0.324	0.058	0.176	0.186	0.134
Testes	0.105	0.098	0.185	0.129	0.049
Thymus	0.210	0.371	0.800	0.461	0.305
Thyroid	1.055	1.301	0.936	1.097	0.186
Whole Blood	3.547	2.519	4.133	3.400	0.817
Plasma	8.820	4.802	12.644	8.755	3.922
Blood:plasma ratio	0.40	0.52	0.33	0.42	0.10

090177e195794698\Approved\Approved On: 09-Nov-2020 21:23 (GMT)

**Appendix 4 Individual Male Concentration Data
(continued)****Concentration of Total Radioactivity in Whole Blood, Plasma and
Tissues 8 hours Following Single Intramuscular Administration of
[³H]-08-A01-C01 to Male Wistar Han Rats****Target Dose Level: 50 µg mRNA/Animal; 1.29 mg Total Lipid/Animal****Results expressed as µg lipid equiv/g (mL)**

Sample	055M	056M	057M	Mean	SD
Adipose tissue	0.076	0.163	0.109	0.116	0.044
Adrenal glands	4.440	4.886	9.835	6.387	2.995
Bladder	N.S.	0.198	0.224	0.211	N.A.
Bone (femur)	0.510	0.355	0.639	0.502	0.142
Bone marrow (femur)	3.050	1.943	2.199	2.397	0.579
Brain	0.105	0.096	0.103	0.101	0.005
Eyes	N.S.	0.071	0.104	0.088	N.A.
Heart	1.418	1.008	1.142	1.189	0.209
Injection site	181.620	497.270	219.870	299.590	172.260
Kidneys	0.934	0.795	0.783	0.837	0.084
Large intestine	0.735	0.665	0.672	0.690	0.039
Liver	23.158	22.178	38.412	27.916	9.103
Lung	1.679	1.643	1.701	1.674	0.029
Lymph node (Man)	0.432	1.053	0.601	0.695	0.321
Lymph node (Mes)	0.444	0.609	0.892	0.649	0.226
Muscle	0.082	0.096	0.127	0.101	0.023
Pancreas	0.352	0.418	0.276	0.349	0.071
Pituitary gland	0.635	0.477	0.894	0.669	0.211
Prostate	0.184	0.127	0.139	0.150	0.030
Salivary glands	0.170	0.157	0.202	0.176	0.023
Skin	0.138	0.111	0.117	0.122	0.014
Small intestine	1.423	1.518	1.634	1.525	0.106
Spinal cord	0.146	0.119	0.239	0.168	0.063
Spleen	21.122	24.073	28.107	24.434	3.507
Stomach	0.345	0.107	0.777	0.410	0.340
Testes	0.153	0.107	0.179	0.146	0.037
Thymus	0.317	0.278	0.282	0.292	0.021
Thyroid	0.940	0.611	0.792	0.781	0.165
Whole Blood	2.215	1.968	1.817	2.000	0.201
Plasma	3.978	3.465	3.275	3.573	0.364
Blood:plasma ratio	0.56	0.57	0.55	0.56	0.01

N.S. = No sample due to oxidiser failure

N.A. = Not applicable

**Appendix 4 Individual Male Concentration Data
(continued)****Concentration of Total Radioactivity in Whole Blood, Plasma and Tissues 24 hours Following Single Intramuscular Administration of [³H]-08-A01-C01 to Male Wistar Han Rats****Target Dose Level: 50 µg mRNA/Animal; 1.29 mg Total Lipid/Animal****Results expressed as µg lipid equiv/g (mL)**

Sample	058M	059M	060M	Mean	SD
Adipose tissue	0.079	0.116	0.182	0.126	0.053
Adrenal glands	10.795	21.060	27.988	19.948	8.650
Bladder	0.211	0.394	0.365	0.323	0.099
Bone (femur)	0.456	0.408	0.649	0.504	0.127
Bone marrow (femur)	2.286	3.625	4.824	3.579	1.270
Brain	0.049	0.099	0.124	0.090	0.038
Eyes	0.098	0.113	0.178	0.129	0.042
Heart	0.640	0.590	0.520	0.583	0.060
Injection site	178.010	330.550	292.960	267.170	79.471
Kidneys	0.522	0.407	0.584	0.504	0.090
Large intestine	0.592	1.611	3.019	1.741	1.219
Liver	17.750	21.966	30.365	23.360	6.422
Lung	0.942	1.334	1.672	1.316	0.365
Lymph node (Man)	0.577	0.689	0.965	0.744	0.200
Lymph node (Mes)	0.905	1.040	1.373	1.106	0.241
Muscle	0.092	0.068	0.133	0.098	0.033
Pancreas	0.294	0.382	0.513	0.396	0.110
Pituitary gland	0.489	0.768	0.711	0.656	0.147
Prostate	0.150	0.183	0.215	0.183	0.032
Salivary glands	0.168	0.243	0.317	0.243	0.075
Skin	0.134	0.166	0.287	0.195	0.081
Small intestine	0.971	1.994	2.670	1.878	0.855
Spinal cord	0.091	0.144	0.127	0.121	0.027
Spleen	19.140	15.796	33.523	22.819	9.419
Stomach	0.110	0.168	0.386	0.222	0.145
Testes	0.234	0.286	0.392	0.304	0.080
Thymus	0.163	0.235	0.368	0.255	0.104
Thyroid	0.721	0.660	1.081	0.820	0.228
Whole Blood	1.473	1.237	1.112	1.274	0.183
Plasma	2.584	2.935	2.345	2.621	0.297
Blood:plasma ratio	0.57	0.42	0.47	0.49	0.08

090177e195794698\Approved\Approved On: 09-Nov-2020 21:23 (GMT)

**Appendix 4 Individual Male Concentration Data
(continued)****Concentration of Total Radioactivity in Whole Blood, Plasma and Tissues 48 hours Following Single Intramuscular Administration of [³H]-08-A01-C01 to Male Wistar Han Rats****Target Dose Level: 50 µg mRNA/Animal; 1.29 mg Total Lipid/Animal****Results expressed as µg lipid equiv/g (mL)**

Sample	061M	062M	063M	Mean	SD
Adipose tissue	0.104	0.162	0.121	0.129	0.030
Adrenal glands	13.913	35.091	15.424	21.476	11.815
Bladder	0.274	0.447	0.298	0.340	0.094
Bone (femur)	0.344	0.577	0.639	0.520	0.155
Bone marrow (femur)	2.566	5.049	3.455	3.690	1.258
Brain	0.051	0.112	0.087	0.083	0.031
Eyes	0.100	0.121	0.160	0.127	0.031
Heart	0.418	0.955	0.642	0.672	0.270
Injection site	292.370	196.910	317.030	268.770	63.446
Kidneys	0.309	0.673	0.463	0.482	0.182
Large intestine	0.998	1.235	2.045	1.426	0.549
Liver	17.734	20.580	16.177	18.164	2.233
Lung	0.809	1.885	1.170	1.288	0.548
Lymph node (Man)	0.728	1.078	0.656	0.820	0.226
Lymph node (Mes)	0.924	1.620	0.626	1.057	0.510
Muscle	0.078	0.115	0.647	0.280	0.318
Pancreas	0.291	0.506	0.964	0.587	0.344
Pituitary gland	0.431	0.610	0.588	0.543	0.098
Prostate	0.110	0.265	0.135	0.170	0.083
Salivary glands	0.286	0.370	0.234	0.297	0.069
Skin	0.177	0.267	0.183	0.209	0.051
Small intestine	1.178	2.030	1.681	1.630	0.428
Spinal cord	0.089	0.129	0.267	0.162	0.093
Spleen	12.073	25.689	20.887	19.550	6.906
Stomach	0.122	0.315	0.268	0.235	0.101
Testes	0.214	0.471	0.275	0.320	0.134
Thymus	0.226	0.362	0.299	0.296	0.068
Thyroid	0.830	1.797	1.406	1.344	0.486
Whole Blood	0.594	0.473	0.536	0.535	0.060
Plasma	1.021	1.003	1.230	1.085	0.126
Blood:plasma ratio	0.58	0.47	0.44	0.50	0.08

090177e195794698\Approved\Approved On: 09-Nov-2020 21:23 (GMT)

Appendix 5 Individual Female Concentration Data**Concentration of Total Radioactivity in Whole Blood, Plasma and Tissues 0.25 min Following Single Intramuscular Administration of [³H]-08-A01-C01 to Female Wistar Han Rats****Target Dose Level: 50 µg mRNA/Animal; 1.29 mg Total Lipid/Animal****Results expressed as µg lipid equiv/g (mL)**

Sample	022F	023F ^A	024F	Mean	SD
Adipose tissue	0.203	*0.002	0.015	°0.073	°0.113
Adrenal glands	0.578	*0.000	0.143	°0.240	°0.301
Bladder	0.050	*0.000	0.048	°0.033	°0.029
Bone (femur)	0.146	0.003	0.019	0.056	0.079
Bone marrow (femur)	N.S.	0.264	*0.128	°0.196	N.A.
Brain	0.036	*0.002	0.011	°0.016	°0.018
Eyes	0.015	*0.000	0.004	°0.006	°0.008
Injection site	27.519	77.480	4.697	36.566	37.225
Heart	0.310	*0.001	0.121	°0.144	°0.156
Kidneys	0.544	0.126	0.143	0.271	0.236
Large intestine	0.019	*0.001	0.004	°0.008	°0.010
Liver	0.635	0.018	0.316	0.323	0.309
Lung	0.550	0.012	0.177	0.247	0.275
Lymph node (Man)	0.088	*0.000	0.025	°0.038	°0.045
Lymph node (Mes)	0.127	*0.000	0.018	°0.048	°0.069
Muscle	0.024	0.006	0.007	0.012	0.010
Ovaries	0.206	*0.000	0.106	°0.104	°0.103
Pancreas	0.072	0.008	0.030	0.037	0.033
Pituitary gland	0.310	*0.000	0.113	°0.141	°0.157
Salivary glands	0.133	*0.000	0.028	°0.054	°0.070
Skin	0.018	0.004	0.009	0.010	0.007
Small intestine	0.051	*0.001	0.010	°0.021	°0.026
Spinal cord	0.057	*0.000	0.016	°0.024	°0.029
Spleen	0.366	*0.004	0.570	°0.313	°0.287
Stomach	0.032	*0.001	0.013	°0.015	°0.016
Thymus	0.159	*0.003	0.047	°0.069	°0.080
Thyroid	0.181	*0.000	0.097	°0.093	°0.091
Uterus	0.090	*0.000	0.037	°0.043	°0.045
Whole Blood	2.016	0.013	0.778	0.936	1.011
Plasma	4.189	0.005	1.487	1.894	2.121
Blood:plasma ratio	0.48	2.43	0.52	1.15	1.12

N.S. = No sample due to analysis error (the bone marrow was not able to be removed from the bone since the bone was initially crushed for analysis)

A = Animal 023F appeared to have a slow distribution compared with the other animals

* = Results calculated from data less than 30 cpm above background

° = Mean includes results calculated from data less than 30 cpm above background

Appendix 5 Individual Female Concentration Data
 (continued)

Concentration of Total Radioactivity in Whole Blood, Plasma and Tissues 1 hour Following Single Intramuscular Administration of [³H]-08-A01-C01 to Female Wistar Han Rats

Target Dose Level: 50 µg mRNA/Animal; 1.29 mg Total Lipid/Animal

Results expressed as µg lipid equiv/g (mL)

Sample	025F	026F	027F	Mean	SD
Adipose tissue	0.145	0.234	0.069	0.149	0.083
Adrenal glands	1.779	2.131	3.254	2.388	0.770
Bladder	0.123	0.206	0.166	0.165	0.042
Bone (femur)	0.216	0.285	0.223	0.241	0.038
Bone marrow (femur)	0.886	1.219	0.926	1.010	0.182
Brain	0.096	0.139	0.115	0.117	0.022
Eyes	0.052	0.052	0.027	0.043	0.015
Heart	1.273	1.884	1.120	1.426	0.404
Injection site	31.021	202.720	366.100	199.950	167.560
Kidneys	1.568	2.396	1.112	1.692	0.651
Large intestine	0.060	0.065	0.070	0.065	0.005
Liver	6.342	4.717	4.674	5.244	0.951
Lung	1.455	1.954	1.313	1.574	0.336
Lymph node (Man)	0.226	0.266	0.176	0.223	0.045
Lymph node (Mes)	0.207	0.226	0.155	0.196	0.037
Muscle	0.080	0.093	0.072	0.082	0.011
Ovaries	1.630	1.650	0.736	1.339	0.522
Pancreas	0.208	0.343	0.234	0.261	0.072
Pituitary gland	0.607	1.114	0.810	0.844	0.255
Salivary glands	0.245	0.327	0.140	0.237	0.094
Skin	0.056	0.956	0.148	0.387	0.495
Small intestine	0.281	0.223	0.235	0.247	0.031
Spinal cord	0.111	0.119	0.137	0.122	0.013
Spleen	2.423	2.626	3.355	2.801	0.490
Stomach	0.085	0.118	0.070	0.091	0.025
Thymus	0.248	0.483	0.164	0.298	0.165
Thyroid	0.510	0.997	0.533	0.680	0.275
Uterus	0.194	0.251	0.164	0.203	0.044
Whole Blood	5.057	8.484	4.243	5.928	2.251
Plasma	9.655	14.318	8.680	10.884	3.014
Blood:plasma ratio	0.52	0.59	0.49	0.54	0.05

090177e195794698\Approved\Approved On: 09-Nov-2020 21:23 (GMT)

Appendix 5 Individual Female Concentration Data
 (continued)

Concentration of Total Radioactivity in Whole Blood, Plasma and Tissues 2 hours Following Single Intramuscular Administration of [³H]-08-A01-C01 to Female Wistar Han Rats

Target Dose Level: 50 µg mRNA/Animal; 1.29 mg Total Lipid/Animal

Results expressed as µg lipid equiv/g (mL)

Sample	028F	029F	030F	Mean	SD
Adipose tissue	0.110	0.274	0.162	0.182	0.084
Adrenal glands	1.429	8.981	2.285	4.232	4.135
Bladder	0.062	0.289	0.114	0.155	0.119
Bone (femur)	0.132	0.566	0.189	0.296	0.236
Bone marrow (femur)	0.575	1.722	1.714	1.337	0.660
Brain	0.063	0.241	0.095	0.133	0.095
Eyes	0.034	0.117	0.023	0.058	0.051
Heart	0.554	3.221	1.272	1.682	1.380
Injection site	0.092	1.744	277.600	93.144	159.740
Kidneys	0.623	2.870	5.408	2.967	2.394
Large intestine	0.027	0.198	0.092	0.106	0.086
Liver	5.209	21.794	10.108	12.370	8.521
Lung	0.908	4.000	1.313	2.074	1.681
Lymph node (Man)	0.198	0.701	0.188	0.362	0.293
Lymph node (Mes)	1.473	0.640	0.381	0.831	0.571
Muscle	0.045	0.140	0.114	0.100	0.049
Ovaries	0.474	2.683	1.756	1.638	1.109
Pancreas	0.116	0.825	0.270	0.404	0.373
Pituitary gland	0.414	1.853	0.599	0.955	0.783
Salivary glands	0.141	0.562	0.182	0.295	0.232
Skin	0.040	0.263	0.486	0.263	0.223
Small intestine	0.305	0.664	0.473	0.481	0.180
Spinal cord	0.109	0.289	0.118	0.172	0.102
Spleen	2.066	23.785	4.788	10.213	11.832
Stomach	0.088	0.211	0.077	0.126	0.074
Thymus	0.109	1.108	0.160	0.459	0.562
Thyroid	0.371	1.791	1.163	1.109	0.711
Uterus	0.169	0.568	0.178	0.305	0.228
Whole Blood	2.194	14.470	3.655	6.773	6.706
Plasma	4.442	15.480	7.350	9.091	5.721
Blood:plasma ratio	0.49	0.93	0.50	0.64	0.25

090177e195794698\Approved\Approved On: 09-Nov-2020 21:23 (GMT)

Appendix 5 Individual Female Concentration Data
 (continued)

Concentration of Total Radioactivity in Whole Blood, Plasma and Tissues 4 hours Following Single Intramuscular Administration of [³H]-08-A01-C01 to Female Wistar Han Rats

Target Dose Level: 50 µg mRNA/Animal; 1.29 mg Total Lipid/Animal

Results expressed as µg lipid equiv/g (mL)

Sample	031F	032F	033F	Mean	SD
Adipose tissue	0.134	0.061	0.296	0.163	0.121
Adrenal glands	1.879	3.483	4.255	3.206	1.212
Bladder	0.043	0.101	0.175	0.106	0.066
Bone (femur)	0.136	0.194	0.321	0.217	0.095
Bone marrow (femur)	0.448	0.818	1.480	0.915	0.522
Brain	0.033	0.058	0.133	0.075	0.052
Eyes	0.022	0.046	0.048	0.038	0.015
Heart	0.296	0.746	1.734	0.925	0.735
Injection site	8.920	103.630	56.133	56.227	47.355
Kidneys	0.328	0.627	1.486	0.814	0.601
Large intestine	0.165	0.222	0.283	0.224	0.059
Liver	8.503	14.685	20.519	14.569	6.009
Lung	0.610	1.159	1.898	1.222	0.646
Lymph node (Man)	0.173	0.454	0.546	0.391	0.194
Lymph node (Mes)	0.316	0.598	0.695	0.536	0.197
Muscle	0.033	0.057	0.301	0.130	0.148
Ovaries	0.555	2.916	3.552	2.341	1.579
Pancreas	0.358	0.270	0.568	0.398	0.153
Pituitary gland	0.251	0.317	0.805	0.458	0.303
Salivary glands	0.087	0.156	0.262	0.169	0.088
Skin	0.043	0.371	0.197	0.204	0.164
Small intestine	0.684	0.739	1.089	0.838	0.220
Spinal cord	0.073	0.061	0.236	0.124	0.098
Spleen	9.910	11.442	13.587	11.646	1.847
Stomach	0.050	0.113	0.141	0.101	0.047
Thymus	0.130	0.267	0.231	0.209	0.071
Thyroid	0.225	0.718	0.867	0.604	0.336
Uterus	0.080	0.096	0.246	0.140	0.091
Whole Blood	1.090	1.981	5.022	2.698	2.062
Plasma	2.037	3.442	7.274	4.251	2.711
Blood:plasma ratio	0.53	0.58	0.69	0.60	0.08

090177e195794698\Approved\Approved On: 09-Nov-2020 21:23 (GMT)

Appendix 5 Individual Female Concentration Data
 (continued)

Concentration of Total Radioactivity in Whole Blood, Plasma and Tissues 8 hours Following Single Intramuscular Administration of [³H]-08-A01-C01 to Female Wistar Han Rats

Target Dose Level: 50 µg mRNA/Animal; 1.29 mg Total Lipid/Animal

Results expressed as µg lipid equiv/g (mL)

Sample	034F	035F	036F	Mean	SD
Adipose tissue	0.095	0.041	0.072	0.069	0.027
Adrenal glands	7.562	6.554	7.538	7.218	0.575
Bladder	0.047	0.080	0.127	0.085	0.040
Bone (femur)	0.243	0.143	0.144	0.177	0.057
Bone marrow (femur)	1.262	1.350	1.210	1.274	0.071
Brain	0.047	0.030	0.058	0.045	0.014
Eyes	0.046	0.013	0.032	0.030	0.016
Heart	0.532	0.193	0.448	0.391	0.177
Injection site	30.227	174.950	172.620	125.930	82.890
Kidneys	0.416	0.239	0.372	0.342	0.092
Large intestine	0.679	0.381	0.764	0.608	0.201
Liver	22.242	25.442	27.834	25.172	2.806
Lung	0.661	0.378	0.846	0.628	0.236
Lymph node (Man)	0.315	0.251	0.551	0.372	0.158
Lymph node (Mes)	0.790	0.481	0.915	0.729	0.223
Muscle	0.040	0.160	0.075	0.091	0.062
Ovaries	2.960	1.276	5.029	3.088	1.880
Pancreas	0.390	0.087	0.241	0.239	0.151
Pituitary gland	0.169	0.099	0.157	0.141	0.037
Salivary glands	0.124	0.074	0.082	0.094	0.027
Skin	0.137	0.057	0.155	0.116	0.052
Small intestine	1.162	0.839	1.098	1.033	0.171
Spinal cord	0.051	0.021	0.060	0.044	0.020
Spleen	19.387	16.090	23.763	19.747	3.849
Stomach	0.243	0.040	0.094	0.126	0.105
Thymus	0.111	0.086	0.102	0.100	0.013
Thyroid	0.395	0.131	0.395	0.307	0.152
Uterus	0.584	0.055	0.223	0.287	0.270
Whole Blood	0.731	0.319	0.833	0.628	0.272
Plasma	1.421	0.574	1.447	1.147	0.496
Blood:plasma ratio	0.51	0.56	0.58	0.55	0.03

090177e195794698\Approved\Approved On: 09-Nov-2020 21:23 (GMT)

Appendix 5 Individual Female Concentration Data
(continued)**Concentration of Total Radioactivity in Whole Blood, Plasma and Tissues 24 hours Following Single Intramuscular Administration of [³H]-08-A01-C01 to Female Wistar Han Rats****Target Dose Level: 50 µg mRNA/Animal; 1.29 mg Total Lipid/Animal****Results expressed as µg lipid equiv/g (mL)**

Sample	037F	038F	039F	Mean	SD
Adipose tissue	0.031	0.042	0.053	0.042	0.011
Adrenal glands	9.718	3.981	9.084	7.595	3.145
Bladder	0.141	0.135	0.235	0.171	0.056
Bone (femur)	0.158	0.105	0.278	0.180	0.089
Bone marrow (femur)	1.180	1.058	1.978	1.405	0.500
Brain	0.040	0.039	0.063	0.047	0.014
Eyes	0.063	0.037	0.057	0.052	0.014
Heart	0.342	0.259	0.355	0.318	0.052
Injection site	2.568	202.540	162.510	122.540	105.810
Kidneys	0.270	0.412	0.361	0.348	0.072
Large intestine	0.561	0.370	0.465	0.466	0.095
Liver	13.368	10.520	21.469	15.119	5.681
Lung	0.519	0.822	0.945	0.762	0.219
Lymph node (Man)	0.259	0.242	0.589	0.363	0.195
Lymph node (Mes)	0.944	0.550	1.095	0.863	0.281
Muscle	0.028	0.114	0.133	0.092	0.056
Ovaries	4.091	5.266	6.363	5.240	1.136
Pancreas	0.176	0.362	0.422	0.320	0.128
Pituitary gland	0.309	0.213	0.379	0.300	0.083
Salivary glands	0.084	0.083	0.119	0.096	0.021
Skin	0.047	0.156	0.151	0.118	0.062
Small intestine	0.748	0.661	0.769	0.726	0.057
Spinal cord	0.047	0.034	0.064	0.048	0.015
Spleen	15.606	12.977	23.440	17.341	5.443
Stomach	0.094	0.054	0.096	0.081	0.024
Thymus	0.154	0.190	0.135	0.159	0.028
Thyroid	0.302	0.294	0.410	0.335	0.065
Uterus	0.307	0.207	0.354	0.289	0.075
Whole Blood	0.475	0.380	0.779	0.544	0.208
Plasma	0.930	0.681	1.223	0.945	0.271
Blood:plasma ratio	0.51	0.56	0.64	0.57	0.06

090177e195794698\Approved\Approved On: 09-Nov-2020 21:23 (GMT)

**Appendix 5 Individual Female Concentration Data
(continued)****Concentration of Total Radioactivity in Whole Blood, Plasma and Tissues 48 hours Following Single Intramuscular Administration of [³H]-08-A01-C01 to Female Wistar Han Rats****Target Dose Level: 50 µg mRNA/Animal; 1.29 mg Total Lipid/Animal****Results expressed as µg lipid equiv/g (mL)**

Sample	040F	041F	042F	Mean	SD
Adipose tissue	0.081	0.201	0.414	0.232	0.168
Adrenal glands	12.979	15.142	16.707	14.942	1.872
Bladder	0.234	0.640	0.293	0.389	0.219
Bone (femur)	0.299	1.911	0.351	0.854	0.916
Bone marrow (femur)	2.096	1.993	7.463	3.851	3.129
Brain	0.038	0.046	0.072	0.052	0.018
Eyes	0.064	0.105	0.121	0.097	0.029
Heart	0.352	0.369	0.539	0.420	0.103
Injection site	93.643	27.547	62.073	61.088	33.059
Kidneys	0.314	0.378	0.412	0.368	0.050
Large intestine	1.210	1.507	1.031	1.249	0.241
Liver	24.416	20.707	46.111	30.411	13.722
Lung	0.921	0.719	1.053	0.898	0.168
Lymph node (Man)	0.600	0.516	0.784	0.633	0.137
Lymph node (Mes)	1.557	1.669	1.800	1.675	0.122
Muscle	0.126	0.068	0.119	0.104	0.032
Ovaries	9.305	13.544	13.933	12.261	2.567
Pancreas	0.364	0.298	1.170	0.611	0.485
Pituitary gland	0.910	0.816	0.810	0.845	0.056
Salivary glands	0.200	0.204	0.288	0.231	0.049
Skin	0.303	0.173	0.416	0.297	0.122
Small intestine	1.142	1.461	1.339	1.314	0.161
Spinal cord	0.043	0.075	0.069	0.062	0.017
Spleen	19.456	16.775	45.234	27.155	15.714
Stomach	0.154	0.197	0.233	0.195	0.040
Thymus	0.314	0.248	0.536	0.366	0.151
Thyroid	0.584	0.870	0.512	0.655	0.190
Uterus	0.267	0.521	0.581	0.456	0.167
Whole Blood	0.258	0.338	0.320	0.305	0.042
Plasma	0.429	0.598	0.546	0.524	0.087
Blood:plasma ratio	0.60	0.57	0.59	0.58	0.02

090177e195794698\Approved\Approved On: 09-Nov-2020 21:23 (GMT)

Appendix 6 Individual Male Recovery Data**Recovery of Total Radioactivity in Tissues 0.25 min Following Single Intramuscular Administration of [³H]-08-A01-C01 to Male Wistar Han Rats****Target Dose Level: 50 µg mRNA/Animal; 1.29 mg Total Lipid/Animal****Results expressed as % administered dose**

Sample	043M	044M	045M	Mean	SD
Adrenal glands	0.002	0.002	0.000	0.001	0.001
Bladder	0.001	0.000	0.000	0.000	0.000
Brain	0.013	0.014	0.005	0.011	0.005
Eyes	0.001	0.000	0.000	0.000	0.000
Heart	0.056	0.024	0.004	0.028	0.026
Injection site	82.460	6.097	10.103	32.887	42.978
Kidneys	0.103	0.087	0.016	0.069	0.046
Large intestine	0.012	0.018	0.002	0.011	0.008
Liver	1.735	1.083	0.167	0.995	0.787
Lung	0.133	0.082	0.031	0.082	0.051
Pancreas	0.004	0.010	0.001	0.005	0.005
Pituitary gland	0.001	0.000	0.000	0.000	0.000
Prostate	0.002	0.002	0.000	0.001	0.001
Salivary glands	0.007	0.005	0.001	0.004	0.003
Small intestine	0.051	0.040	0.005	0.032	0.024
Spinal cord	0.002	0.001	0.000	0.001	0.001
Spleen	0.020	0.019	0.003	0.014	0.009
Stomach	0.008	0.013	0.002	0.008	0.006
Testes	0.012	0.008	0.001	0.007	0.005
Thymus	0.005	0.010	0.001	0.005	0.005
Thyroid	0.000	0.000	0.000	0.000	0.000

**Appendix 6 Individual Male Recovery Data
 (continued)**

**Recovery of Total Radioactivity in Tissues 1 hour Following Single
 Intramuscular Administration of [³H]-08-A01-C01 to Male Wistar Han
 Rats**

Target Dose Level: 50 µg mRNA/Animal; 1.29 mg Total Lipid/Animal

Results expressed as % administered dose

Sample	046M	047M	048M	Mean	SD
Adrenal glands	0.001	0.003	0.002	0.002	0.001
Bladder	0.001	0.001	0.000	0.001	0.000
Brain	0.005	0.014	0.013	0.010	0.005
Eyes	0.000	0.000	0.001	0.000	0.000
Heart	0.015	0.036	0.045	0.032	0.015
Injection site	74.148	46.614	85.725	68.829	20.090
Kidneys	0.047	0.086	0.098	0.077	0.027
Large intestine	0.016	0.017	0.021	0.018	0.002
Liver	2.218	2.607	3.676	2.834	0.755
Lung	0.043	0.131	0.081	0.085	0.044
Pancreas	0.004	0.009	0.006	0.006	0.003
Pituitary gland	0.000	0.000	0.000	0.000	0.000
Prostate	0.001	0.002	0.001	0.001	0.001
Salivary glands	0.003	0.005	0.006	0.005	0.002
Small intestine	0.102	0.133	0.136	0.124	0.019
Spinal cord	0.001	0.000	0.001	0.001	0.000
Spleen	0.115	0.063	0.082	0.087	0.026
Stomach	0.007	0.019	0.023	0.016	0.008
Testes	0.007	0.009	0.013	0.010	0.003
Thymus	0.008	0.004	0.007	0.006	0.002
Thyroid	0.000	0.001	0.000	0.000	0.000

090177e195794698\Approved\Approved On: 09-Nov-2020 21:23 (GMT)

**Appendix 6 Individual Male Recovery Data
 (continued)**

**Recovery of Total Radioactivity in Tissues 2 hours Following Single
 Intramuscular Administration of [³H]-08-A01-C01 to Male Wistar Han
 Rats**

Target Dose Level: 50 µg mRNA/Animal; 1.29 mg Total Lipid/Animal

Results expressed as % administered dose

Sample	049M	050M	051M	Mean	SD
Adrenal glands	0.006	0.003	0.005	0.005	0.001
Bladder	0.001	0.001	0.001	0.001	0.000
Brain	0.033	0.013	0.016	0.021	0.011
Eyes	0.001	0.000	0.002	0.001	0.001
Heart	0.109	0.036	0.051	0.065	0.039
Injection site	53.157	53.477	10.525	39.053	24.707
Kidneys	0.203	0.096	0.148	0.149	0.054
Large intestine	0.063	0.035	0.063	0.054	0.016
Liver	10.166	4.262	8.460	7.629	3.038
Lung	0.313	0.094	0.160	0.189	0.113
Pancreas	0.011	0.006	0.028	0.015	0.012
Pituitary gland	0.000	0.000	0.000	0.000	0.000
Prostate	0.002	0.002	0.003	0.002	0.000
Salivary glands	0.010	0.004	0.008	0.007	0.003
Small intestine	0.418	0.305	0.336	0.353	0.058
Spinal cord	0.001	0.001	0.002	0.001	0.001
Spleen	0.296	0.101	0.299	0.232	0.114
Stomach	0.034	0.017	0.047	0.033	0.015
Testes	0.027	0.008	0.017	0.017	0.009
Thymus	0.010	0.005	0.008	0.008	0.002
Thyroid	0.001	0.001	0.000	0.001	0.000

090177e195794698\Approved\Approved On: 09-Nov-2020 21:23 (GMT)

**Appendix 6 Individual Male Recovery Data
(continued)****Recovery of Total Radioactivity in Tissues 4 hours Following Single
Intramuscular Administration of [³H]-08-A01-C01 to Male Wistar Han
Rats****Target Dose Level: 50 µg mRNA/Animal; 1.29 mg Total Lipid/Animal****Results expressed as % administered dose**

Sample	052M	053M	054M	Mean	SD
Adrenal glands	0.013	0.009	0.014	0.012	0.002
Bladder	0.001	0.002	0.001	0.001	0.000
Brain	0.019	0.015	0.029	0.021	0.007
Eyes	0.002	0.002	0.001	0.002	0.001
Heart	0.071	0.033	0.096	0.067	0.032
Injection site	61.619	36.450	45.061	47.710	12.792
Kidneys	0.151	0.088	0.169	0.136	0.042
Large intestine	0.271	0.219	0.216	0.236	0.031
Liver	12.655	13.898	18.528	15.027	3.095
Lung	0.356	0.080	0.241	0.226	0.139
Pancreas	0.007	0.020	0.011	0.013	0.007
Pituitary gland	0.001	0.001	0.000	0.001	0.000
Prostate	0.003	0.002	0.003	0.003	0.001
Salivary glands	0.009	0.007	0.012	0.009	0.002
Small intestine	0.632	0.499	0.737	0.623	0.120
Spinal cord	0.002	0.004	0.002	0.003	0.001
Spleen	0.309	0.410	0.334	0.351	0.052
Stomach	0.053	0.027	0.033	0.037	0.013
Testes	0.028	0.021	0.039	0.030	0.009
Thymus	0.010	0.011	0.033	0.018	0.013
Thyroid	0.001	0.001	0.001	0.001	0.000

090177e195794698\Approved\Approved On: 09-Nov-2020 21:23 (GMT)

**Appendix 6 Individual Male Recovery Data
(continued)****Recovery of Total Radioactivity in Tissues 8 hours Following Single Intramuscular Administration of [³H]-08-A01-C01 to Male Wistar Han Rats****Target Dose Level: 50 µg mRNA/Animal; 1.29 mg Total Lipid/Animal****Results expressed as % administered dose**

Sample	055M	056M	057M	Mean	SD
Adrenal glands	0.013	0.023	0.042	0.026	0.015
Bladder	N.S.	0.001	0.002	0.002	N.A.
Brain	0.014	0.013	0.014	0.014	0.001
Eyes	N.S.	0.001	0.002	0.002	N.A.
Heart	0.071	0.051	0.061	0.061	0.010
Injection site	18.863	19.984	17.346	18.731	1.324
Kidneys	0.114	0.107	0.108	0.109	0.004
Large intestine	0.536	0.424	0.430	0.463	0.063
Liver	17.280	17.862	29.414	21.519	6.844
Lung	0.226	0.146	0.169	0.180	0.042
Pancreas	0.010	0.021	0.012	0.014	0.006
Pituitary gland	0.000	0.000	0.001	0.000	0.000
Prostate	0.004	0.002	0.001	0.003	0.001
Salivary glands	0.008	0.006	0.007	0.007	0.001
Small intestine	0.850	1.034	1.031	0.972	0.106
Spinal cord	0.001	0.001	0.001	0.001	0.000
Spleen	1.037	1.022	1.293	1.118	0.152
Stomach	0.043	0.026	0.097	0.055	0.037
Testes	0.034	0.022	0.045	0.034	0.012
Thymus	0.013	0.010	0.012	0.012	0.001
Thyroid	0.001	0.001	0.001	0.001	0.000

N.S. = No sample due to oxidiser failure

N.A. = Not applicable

**Appendix 6 Individual Male Recovery Data
 (continued)**

Recovery of Total Radioactivity in Tissues 24 hours Following Single Intramuscular Administration of [³H]-08-A01-C01 to Male Wistar Han Rats

Target Dose Level: 50 µg mRNA/Animal; 1.29 mg Total Lipid/Animal

Results expressed as % administered dose

Sample	058M	059M	060M	Mean	SD
Adrenal glands	0.052	0.059	0.137	0.083	0.047
Bladder	0.002	0.002	0.002	0.002	0.000
Brain	0.006	0.013	0.017	0.012	0.006
Eyes	0.002	0.002	0.004	0.002	0.001
Heart	0.051	0.026	0.026	0.035	0.014
Injection site	39.854	26.623	29.394	31.957	6.978
Kidneys	0.075	0.053	0.075	0.068	0.012
Large intestine	0.332	0.895	2.045	1.091	0.873
Liver	14.444	16.303	28.957	19.901	7.897
Lung	0.109	0.118	0.179	0.136	0.038
Pancreas	0.007	0.017	0.015	0.013	0.005
Pituitary gland	0.000	0.000	0.000	0.000	0.000
Prostate	0.003	0.004	0.005	0.004	0.001
Salivary glands	0.005	0.008	0.012	0.008	0.004
Small intestine	0.693	1.198	1.934	1.275	0.624
Spinal cord	0.001	0.002	0.002	0.001	0.001
Spleen	0.977	0.660	1.234	0.957	0.287
Stomach	0.021	0.033	0.107	0.054	0.046
Testes	0.057	0.058	0.105	0.074	0.028
Thymus	0.007	0.010	0.009	0.009	0.002
Thyroid	0.001	0.001	0.001	0.001	0.000

090177e195794698\Approved\Approved On: 09-Nov-2020 21:23 (GMT)

**Appendix 6 Individual Male Recovery Data
 (continued)**

Recovery of Total Radioactivity in Tissues 48 hours Following Single Intramuscular Administration of [³H]-08-A01-C01 to Male Wistar Han Rats

Target Dose Level: 50 µg mRNA/Animal; 1.29 mg Total Lipid/Animal

Results expressed as % administered dose

Sample	061M	062M	063M	Mean	SD
Adrenal glands	0.078	0.157	0.078	0.104	0.046
Bladder	0.001	0.002	0.002	0.002	0.000
Brain	0.006	0.016	0.012	0.011	0.005
Eyes	0.002	0.003	0.003	0.003	0.000
Heart	0.024	0.055	0.037	0.039	0.016
Injection site	49.053	18.355	31.059	32.823	15.425
Kidneys	0.045	0.104	0.063	0.071	0.031
Large intestine	0.541	0.624	1.264	0.810	0.395
Liver	12.962	17.164	11.734	13.953	2.848
Lung	0.088	0.173	0.133	0.131	0.043
Pancreas	0.010	0.013	0.023	0.015	0.007
Pituitary gland	0.000	0.000	0.000	0.000	0.000
Prostate	0.002	0.004	0.004	0.003	0.001
Salivary glands	0.010	0.012	0.008	0.010	0.002
Small intestine	0.635	1.258	1.020	0.971	0.314
Spinal cord	0.001	0.001	0.002	0.001	0.001
Spleen	0.544	1.271	0.926	0.914	0.364
Stomach	0.027	0.065	0.056	0.049	0.019
Testes	0.053	0.109	0.060	0.074	0.030
Thymus	0.004	0.012	0.009	0.008	0.004
Thyroid	0.001	0.002	0.001	0.001	0.001

090177e195794698\Approved\Approved On: 09-Nov-2020 21:23 (GMT)

Appendix 7 Individual Female Recovery Data

Recovery of Total Radioactivity in Tissues 0.25 min Following Single Intramuscular Administration of [³H]-08-A01-C01 to Female Wistar Han Rats

Target Dose Level: 50 µg mRNA/Animal; 1.29 mg Total Lipid/Animal

Results expressed as % administered dose

Sample	022F	023F	024F	Mean	SD
Adrenal glands	0.003	*0.000	0.001	°0.001	°0.002
Bladder	0.000	*0.000	0.000	°0.000	°0.000
Brain	0.005	*0.000	0.002	°0.002	°0.002
Eyes	0.000	*0.000	0.000	°0.000	°0.000
Heart	0.017	*0.000	0.006	°0.008	°0.008
Injection site	8.145	11.578	0.723	6.815	5.549
Kidneys	0.063	0.012	0.014	0.030	0.028
Large intestine	0.010	*0.000	0.002	°0.004	°0.005
Liver	0.435	0.010	0.180	0.209	0.214
Lung	0.051	0.001	0.013	0.022	0.026
Ovaries	0.002	*0.000	0.001	°0.001	°0.001
Pancreas	0.002	0.000	0.001	0.001	0.001
Pituitary gland	0.000	*0.000	0.000	°0.000	°0.000
Salivary glands	0.004	*0.000	0.001	°0.002	°0.002
Small intestine	0.038	*0.001	0.005	°0.015	°0.020
Spinal cord	0.000	*0.000	0.000	°0.000	°0.000
Spleen	0.014	*0.000	0.017	°0.011	°0.009
Stomach	0.007	*0.000	0.002	°0.003	°0.003
Thymus	0.005	*0.000	0.002	°0.002	°0.002
Thyroid	0.000	*0.000	0.000	°0.000	°0.000
Uterus	0.004	*0.000	0.002	°0.002	°0.002

*=Results calculated from data less than 30 cpm above background

°=Mean includes results calculated from data less than 30 cpm above background

090177e195794698\Approved\Approved On: 09-Nov-2020 21:23 (GMT)

**Appendix 7 Individual Female Recovery Data
(continued)****Recovery of Total Radioactivity in Tissues 1 hour Following Single
Intramuscular Administration of [³H]-08-A01-C01 to Female Wistar
Han Rats****Target Dose Level: 50 µg mRNA/Animal; 1.29 mg Total Lipid/Animal****Results expressed as % administered dose**

Sample	025F	026F	027F	Mean	SD
Adrenal glands	0.010	0.011	0.015	0.012	0.003
Bladder	0.001	0.001	0.001	0.001	0.000
Brain	0.013	0.019	0.015	0.016	0.003
Eyes	0.001	0.001	0.001	0.001	0.000
Heart	0.066	0.109	0.062	0.079	0.026
Injection site	10.609	47.776	50.847	36.411	22.398
Kidneys	0.162	0.250	0.102	0.171	0.074
Large intestine	0.030	0.035	0.029	0.032	0.003
Liver	3.586	2.713	2.421	2.907	0.606
Lung	0.112	0.131	0.106	0.117	0.013
Ovaries	0.012	0.010	0.004	0.009	0.004
Pancreas	0.009	0.009	0.007	0.008	0.001
Pituitary gland	0.000	0.001	0.001	0.001	0.000
Salivary glands	0.008	0.009	0.006	0.008	0.002
Small intestine	0.153	0.130	0.121	0.135	0.017
Spinal cord	0.002	0.002	0.001	0.002	0.001
Spleen	0.082	0.099	0.112	0.098	0.015
Stomach	0.024	0.021	0.023	0.022	0.002
Thymus	0.007	0.013	0.004	0.008	0.005
Thyroid	0.001	0.001	0.001	0.001	0.000
Uterus	0.008	0.010	0.015	0.011	0.004

**Appendix 7 Individual Female Recovery Data
(continued)****Recovery of Total Radioactivity in Tissues 2 hours Following Single Intramuscular Administration of [³H]-08-A01-C01 to Female Wistar Han Rats****Target Dose Level: 50 µg mRNA/Animal; 1.29 mg Total Lipid/Animal****Results expressed as % administered dose**

Sample	028F	029F	030F	Mean	SD
Adrenal glands	0.010	0.022	0.012	0.015	0.006
Bladder	0.000	0.001	0.001	0.001	0.001
Brain	0.008	0.034	0.014	0.019	0.014
Eyes	0.001	0.003	0.000	0.001	0.001
Heart	0.028	0.201	0.077	0.102	0.089
Injection site	0.018	0.236	72.027	24.094	41.511
Kidneys	0.056	0.264	0.497	0.272	0.221
Large intestine	0.018	0.142	0.065	0.075	0.063
Liver	3.203	12.436	5.452	7.030	4.815
Lung	0.080	0.311	0.110	0.167	0.125
Ovaries	0.003	0.012	0.009	0.008	0.004
Pancreas	0.003	0.022	0.010	0.012	0.010
Pituitary gland	0.000	0.002	0.000	0.001	0.001
Salivary glands	0.005	0.015	0.007	0.009	0.006
Small intestine	0.205	0.367	0.283	0.285	0.081
Spinal cord	0.002	0.004	0.001	0.002	0.002
Spleen	0.063	1.010	0.180	0.418	0.516
Stomach	0.027	0.057	0.022	0.035	0.019
Thymus	0.003	0.028	0.004	0.012	0.014
Thyroid	0.000	0.002	0.001	0.001	0.001
Uterus	0.008	0.025	0.011	0.015	0.009

**Appendix 7 Individual Female Recovery Data
(continued)****Recovery of Total Radioactivity in Tissues 4 hours Following Single Intramuscular Administration of [³H]-08-A01-C01 to Female Wistar Han Rats****Target Dose Level: 50 µg mRNA/Animal; 1.29 mg Total Lipid/Animal****Results expressed as % administered dose**

Sample	031F	032F	033F	Mean	SD
Adrenal glands	0.011	0.019	0.023	0.018	0.006
Bladder	0.000	0.001	0.001	0.001	0.000
Brain	0.005	0.007	0.020	0.011	0.008
Eyes	0.001	0.001	0.001	0.001	0.000
Heart	0.013	0.046	0.097	0.052	0.042
Injection site	2.619	19.042	5.508	9.056	8.768
Kidneys	0.031	0.062	0.154	0.082	0.064
Large intestine	0.111	0.136	0.198	0.148	0.045
Liver	5.207	8.846	12.045	8.699	3.421
Lung	0.054	0.093	0.188	0.112	0.069
Ovaries	0.003	0.022	0.022	0.016	0.011
Pancreas	0.016	0.009	0.027	0.017	0.009
Pituitary gland	0.000	0.000	0.001	0.000	0.000
Salivary glands	0.003	0.005	0.011	0.006	0.005
Small intestine	0.354	0.435	0.596	0.462	0.123
Spinal cord	0.001	0.001	0.003	0.002	0.001
Spleen	0.390	0.421	0.447	0.419	0.028
Stomach	0.014	0.022	0.029	0.022	0.008
Thymus	0.004	0.007	0.006	0.006	0.002
Thyroid	0.000	0.001	0.001	0.001	0.000
Uterus	0.005	0.004	0.016	0.008	0.007

**Appendix 7 Individual Female Recovery Data
(continued)****Recovery of Total Radioactivity in Tissues 8 hours Following Single Intramuscular Administration of [³H]-08-A01-C01 to Female Wistar Han Rats****Target Dose Level: 50 µg mRNA/Animal; 1.29 mg Total Lipid/Animal****Results expressed as % administered dose**

Sample	034F	035F	036F	Mean	SD
Adrenal glands	0.048	0.031	0.051	0.043	0.011
Bladder	0.000	0.000	0.001	0.000	0.000
Brain	0.007	0.004	0.009	0.007	0.002
Eyes	0.001	0.000	0.001	0.001	0.000
Heart	0.029	0.010	0.027	0.022	0.011
Injection site	10.296	26.182	38.500	24.993	14.139
Kidneys	0.056	0.022	0.042	0.040	0.017
Large intestine	0.409	0.233	0.397	0.346	0.098
Liver	13.264	12.033	18.443	14.580	3.402
Lung	0.089	0.028	0.074	0.064	0.031
Ovaries	0.022	0.010	0.042	0.025	0.016
Pancreas	0.034	0.002	0.011	0.016	0.016
Pituitary gland	0.000	0.000	0.000	0.000	0.000
Salivary glands	0.005	0.002	0.003	0.003	0.001
Small intestine	0.718	0.308	0.714	0.580	0.235
Spinal cord	0.001	0.000	0.001	0.001	0.000
Spleen	0.853	0.601	1.082	0.845	0.241
Stomach	0.043	0.005	0.023	0.024	0.019
Thymus	0.004	0.002	0.003	0.003	0.001
Thyroid	0.001	0.000	0.001	0.000	0.000
Uterus	0.030	0.004	0.014	0.016	0.013

**Appendix 7 Individual Female Recovery Data
 (continued)**

Recovery of Total Radioactivity in Tissues 24 hours Following Single Intramuscular Administration of [³H]-08-A01-C01 to Female Wistar Han Rats

Target Dose Level: 50 µg mRNA/Animal; 1.29 mg Total Lipid/Animal

Results expressed as % administered dose

Sample	037F	038F	039F	Mean	SD
Adrenal glands	0.064	0.032	0.050	0.049	0.016
Bladder	0.001	0.001	0.001	0.001	0.000
Brain	0.005	0.006	0.009	0.007	0.002
Eyes	0.001	0.001	0.001	0.001	0.000
Heart	0.019	0.014	0.020	0.018	0.003
Injection site	0.444	39.677	38.765	26.295	22.392
Kidneys	0.029	0.053	0.035	0.039	0.013
Large intestine	0.334	0.283	0.263	0.293	0.037
Liver	9.112	9.776	14.042	10.977	2.675
Lung	0.053	0.071	0.072	0.065	0.010
Ovaries	0.031	0.038	0.043	0.037	0.006
Pancreas	0.005	0.007	0.014	0.009	0.004
Pituitary gland	0.000	0.000	0.000	0.000	0.000
Salivary glands	0.003	0.003	0.004	0.003	0.001
Small intestine	0.575	0.601	0.432	0.536	0.091
Spinal cord	0.001	0.001	0.001	0.001	0.000
Spleen	0.591	0.508	0.955	0.685	0.237
Stomach	0.019	0.011	0.029	0.020	0.009
Thymus	0.003	0.005	0.003	0.004	0.001
Thyroid	0.000	0.000	0.001	0.000	0.000
Uterus	0.027	0.009	0.017	0.018	0.009

090177e195794698\Approved\Approved On: 09-Nov-2020 21:23 (GMT)

**Appendix 7 Individual Female Recovery Data
(continued)****Recovery of Total Radioactivity in Tissues 48 hours Following Single Intramuscular Administration of [³H]-08-A01-C01 to Female Wistar Han Rats****Target Dose Level: 50 µg mRNA/Animal; 1.29 mg Total Lipid/Animal****Results expressed as % administered dose**

Sample	040F	041F	042F	Mean	SD
Adrenal glands	0.085	0.126	0.114	0.108	0.021
Bladder	0.001	0.004	0.002	0.002	0.001
Brain	0.005	0.006	0.010	0.007	0.002
Eyes	0.001	0.003	0.003	0.002	0.001
Heart	0.018	0.017	0.024	0.020	0.004
Injection site	20.139	5.852	23.287	16.426	9.292
Kidneys	0.036	0.045	0.044	0.042	0.005
Large intestine	0.570	0.928	0.644	0.714	0.189
Liver	15.122	13.811	26.137	18.357	6.770
Lung	0.066	0.066	0.076	0.070	0.006
Ovaries	0.075	0.113	0.097	0.095	0.019
Pancreas	0.011	0.007	0.050	0.023	0.024
Pituitary gland	0.001	0.001	0.000	0.001	0.000
Salivary glands	0.007	0.005	0.009	0.007	0.002
Small intestine	0.540	0.825	0.729	0.698	0.145
Spinal cord	0.001	0.002	0.001	0.001	0.000
Spleen	0.772	0.848	1.818	1.146	0.583
Stomach	0.023	0.028	0.035	0.029	0.006
Thymus	0.007	0.005	0.009	0.007	0.002
Thyroid	0.001	0.001	0.001	0.001	0.000
Uterus	0.010	0.031	0.025	0.022	0.010

Appendix 8 Individual Male 100 µg mRNA data

Concentration of Total Radioactivity in Whole Blood, Plasma and Tissues 0.25 min Following Single Intramuscular Administration of [³H]-08-A01-C01 to Male Wistar Han Rats

Target Dose Level: 100 µg mRNA/Animal; 2.57 mg Total Lipid/Animal

Results expressed as µg lipid equiv/g (mL)

Sample	001M	002M	003M	Mean	SD
Adipose tissue	0.075	0.108	0.018	0.067	0.046
Adrenal glands	0.193	0.192	0.184	0.190	0.005
Bladder	0.035	0.079	0.026	0.047	0.028
Bone (femur)	0.195	0.054	0.044	0.098	0.085
Bone marrow (femur)	0.312	0.163	0.229	0.234	0.075
Brain	0.050	0.047	0.046	0.048	0.002
Eyes	0.015	0.021	0.007	0.014	0.007
Heart	0.394	0.365	0.460	0.406	0.048
Injection site	16.832	24.313	179.840	73.662	92.030
Kidneys	0.576	0.552	0.273	0.467	0.169
Large intestine	0.016	0.012	0.051	0.026	0.022
Liver	0.963	0.503	0.670	0.712	0.233
Lung	0.689	0.497	0.410	0.532	0.143
Lymph node (Man)	0.043	0.046	0.042	0.044	0.002
Lymph node (Mes)	0.045	0.020	0.018	0.028	0.015
Muscle	0.035	0.040	0.285	0.120	0.143
Pancreas	0.088	0.068	0.068	0.075	0.012
Pituitary gland	0.787	0.796	0.225	0.603	0.327
Prostate	0.035	0.045	0.047	0.042	0.006
Salivary glands	0.087	0.087	0.049	0.074	0.022
Skin	2.094	3.233	12.691	6.499	6.668
Small intestine	0.046	0.030	0.016	0.031	0.015
Spinal cord	0.091	0.064	0.068	0.074	0.015
Spleen	0.426	1.463	0.221	0.704	0.666
Stomach	0.032	0.026	*0.007	°0.022	°0.013
Testes	0.033	0.030	0.020	0.028	0.007
Thymus	0.121	0.161	0.216	0.166	0.048
Thyroid	0.175	0.498	0.105	0.259	0.209
Whole Blood	2.291	2.426	1.678	2.132	0.398
Plasma	5.640	5.530	3.924	5.031	0.960
Blood:plasma ratio	0.41	0.44	0.43	0.42	0.02

*=Results calculated from data less than 30 cpm above background

°=Mean includes results calculated from data less than 30 cpm above background

090177e195794698\Approved\Approved On: 09-Nov-2020 21:23 (GMT)

**Appendix 8 Individual Male 100 µg mRNA Data
 (continued)**

**Concentration of Total Radioactivity in Whole Blood, Plasma and
 Tissues 1 hour Following Single Intramuscular Administration of
 [³H]-08-A01-C01 to Male Wistar Han Rats**

Target Dose Level: 100 µg mRNA/Animal; 2.57 mg Total Lipid/Animal

Results expressed as µg lipid equiv/g (mL)

Sample	004M	005M	006M	Mean	SD
Adipose tissue	0.193	0.307	0.350	0.283	0.081
Adrenal glands	1.775	1.877	2.208	1.953	0.227
Bladder	0.224	0.098	0.264	0.195	0.086
Bone (femur)	1.102	0.530	0.566	0.733	0.320
Bone marrow (femur)	2.111	4.732	2.456	3.100	1.424
Brain	0.253	0.297	0.296	0.282	0.025
Eyes	0.229	0.070	0.093	0.131	0.086
Heart	1.948	3.461	2.496	2.635	0.766
Injection site	152.370	78.654	150.890	127.300	42.139
Kidneys	3.017	3.096	3.170	3.094	0.077
Large intestine	0.090	0.091	0.152	0.111	0.035
Liver	13.805	10.906	16.323	13.678	2.711
Lung	3.523	3.532	2.901	3.319	0.362
Lymph node (Man)	0.366	0.379	0.437	0.394	0.038
Lymph node (Mes)	0.268	0.412	0.389	0.356	0.077
Muscle	0.184	0.213	0.195	0.198	0.015
Pancreas	0.335	0.375	0.469	0.393	0.069
Pituitary gland	1.389	1.810	1.717	1.639	0.221
Prostate	0.328	0.363	0.380	0.357	0.027
Salivary glands	0.471	0.613	0.493	0.526	0.076
Skin	3.043	0.407	1.179	1.543	1.355
Small intestine	0.393	3.191	3.563	2.382	1.733
Spinal cord	0.216	0.356	0.303	0.292	0.071
Spleen	4.066	4.402	4.868	4.445	0.402
Stomach	0.332	2.377	8.099	3.603	4.026
Testes	0.185	0.196	0.486	0.289	0.171
Thymus	0.332	0.343	0.596	0.424	0.149
Thyroid	1.219	1.909	1.266	1.465	0.385
Whole Blood	7.985	11.835	10.357	10.059	1.942
Plasma	23.703	26.782	26.070	25.518	1.612
Blood:plasma ratio	0.34	0.44	0.40	0.39	0.05

090177e195794698\Approved\Approved On: 09-Nov-2020 21:23 (GMT)

Appendix 8 Individual Male 100 µg mRNA Data
 (continued)

Concentration of Total Radioactivity in Whole Blood, Plasma and Tissues 2 hours Following Single Intramuscular Administration of [³H]-08-A01-C01 to Male Wistar Han Rats

Target Dose Level: 100 µg mRNA/Animal; 2.57 mg Total Lipid/Animal

Results expressed as µg lipid equiv/g (mL)

Sample	007M	008M	009M	Mean	SD
Adipose tissue	0.311	0.211	0.486	0.336	0.140
Adrenal glands	3.152	3.337	2.559	3.016	0.406
Bladder	0.310	0.241	0.479	0.343	0.122
Bone (femur)	0.835	0.462	0.385	0.561	0.241
Bone marrow (femur)	3.322	2.694	2.057	2.691	0.632
Brain	0.348	0.310	0.250	0.302	0.049
Eyes	0.126	0.104	0.064	0.098	0.031
Heart	2.866	3.359	3.481	3.235	0.326
Injection site	6.971	61.485	30.751	33.069	27.331
Kidneys	2.887	2.858	2.679	2.808	0.113
Large intestine	0.283	0.125	0.148	0.185	0.085
Liver	33.320	24.542	22.034	26.632	5.926
Lung	3.839	2.982	3.769	3.530	0.476
Lymph node (Man)	0.784	0.413	0.474	0.557	0.199
Lymph node (Mes)	0.859	0.503	0.333	0.565	0.268
Muscle	0.220	0.182	0.189	0.197	0.020
Pancreas	0.595	0.512	0.557	0.554	0.041
Pituitary gland	1.998	1.921	1.729	1.883	0.139
Prostate	0.458	0.354	0.461	0.424	0.061
Salivary glands	0.740	0.597	0.539	0.625	0.104
Skin	0.524	0.353	0.454	0.444	0.086
Small intestine	1.147	0.887	0.755	0.930	0.199
Spinal cord	0.396	0.373	0.360	0.377	0.018
Spleen	14.103	8.227	7.803	10.044	3.521
Stomach	0.234	0.142	0.143	0.173	0.053
Testes	0.239	0.402	0.317	0.320	0.081
Thymus	0.447	0.424	0.371	0.414	0.039
Thyroid	1.906	1.397	1.481	1.595	0.273
Whole Blood	11.413	10.005	10.736	10.718	0.704
Plasma	25.479	22.927	22.340	23.582	1.669
Blood:plasma ratio	0.45	0.44	0.48	0.45	0.02

090177e195794698\Approved\Approved On: 09-Nov-2020 21:23 (GMT)

**Appendix 8 Individual Male 100 µg mRNA Data
(continued)****Concentration of Total Radioactivity in Whole Blood, Plasma and
Tissues 4 hours Following Single Intramuscular Administration of
[³H]-08-A01-C01 to Male Wistar Han Rats****Target Dose Level: 100 µg mRNA/Animal; 2.57 mg Total Lipid/Animal****Results expressed as µg lipid equiv/g (mL)**

Sample	010M	011M	012M	Mean	SD
Adipose tissue	0.222	0.262	0.105	0.196	0.082
Adrenal glands	5.481	2.469	2.491	3.480	1.732
Bladder	0.237	0.151	0.156	0.181	0.048
Bone (femur)	1.452	1.249	0.348	1.016	0.588
Bone marrow (femur)	1.880	3.875	1.459	2.405	1.291
Brain	0.373	0.123	0.090	0.195	0.155
Eyes	0.095	0.056	0.042	0.065	0.027
Heart	1.233	1.095	1.064	1.131	0.090
Injection site	55.286	464.630	257.860	259.260	204.680
Kidneys	2.190	1.607	1.007	1.601	0.591
Large intestine	0.180	0.713	0.338	0.410	0.274
Liver	38.606	14.955	19.426	24.329	12.565
Lung	1.255	3.060	1.398	1.904	1.003
Lymph node (Man)	0.694	0.271	0.242	0.402	0.253
Lymph node (Mes)	0.970	0.427	0.502	0.633	0.294
Muscle	0.129	0.076	0.085	0.097	0.029
Pancreas	0.189	0.419	0.299	0.302	0.115
Pituitary gland	0.870	0.599	0.480	0.649	0.200
Prostate	0.244	0.133	0.133	0.170	0.064
Salivary glands	0.334	0.192	0.170	0.232	0.089
Skin	0.931	0.178	2.172	1.094	1.007
Small intestine	0.758	1.381	1.189	1.110	0.319
Spinal cord	0.154	0.094	0.111	0.120	0.031
Spleen	9.286	27.731	9.780	15.599	10.510
Stomach	0.057	0.131	0.302	0.163	0.125
Testes	0.397	0.134	0.110	0.214	0.159
Thymus	0.164	0.229	0.185	0.193	0.033
Thyroid	1.256	0.565	0.742	0.854	0.359
Whole Blood	4.741	2.416	2.502	3.220	1.318
Plasma	11.200	5.253	5.862	7.438	3.272
Blood:plasma ratio	0.42	0.46	0.43	0.44	0.02

090177e195794698\Approved\Approved On: 09-Nov-2020 21:23 (GMT)

Appendix 8 Individual Male 100 µg mRNA Data
(continued)**Concentration of Total Radioactivity in Whole Blood, Plasma and Tissues 8 hours Following Single Intramuscular Administration of [³H]-08-A01-C01 to Male Wistar Han Rats****Target Dose Level: 100 µg mRNA/Animal; 2.57 mg Total Lipid/Animal****Results expressed as µg lipid equiv/g (mL)**

Sample	013M	014M	015M	Mean	SD
Adipose tissue	0.134	0.147	0.269	0.184	0.075
Adrenal glands	6.445	9.564	32.615	16.208	14.294
Bladder	0.741	0.264	0.499	0.501	0.238
Bone (femur)	0.835	0.274	0.855	0.655	0.330
Bone marrow (femur)	1.920	1.495	2.225	1.880	0.367
Brain	0.165	0.120	0.214	0.166	0.047
Eyes	0.188	0.146	0.229	0.188	0.041
Heart	2.084	1.104	2.398	1.862	0.675
Injection site	126.340	106.800	2.416	78.521	66.629
Kidneys	2.145	1.122	1.472	1.580	0.520
Large intestine	1.713	1.199	1.781	1.564	0.318
Liver	34.463	41.789	61.002	45.751	13.706
Lung	2.999	1.707	3.360	2.689	0.869
Lymph node (Man)	1.158	0.644	1.099	0.967	0.282
Lymph node (Mes)	1.076	1.409	1.701	1.395	0.313
Muscle	0.158	0.096	0.196	0.150	0.051
Pancreas	0.433	0.326	0.579	0.446	0.127
Pituitary gland	0.858	0.517	0.994	0.790	0.246
Prostate	0.314	0.176	0.386	0.292	0.107
Salivary glands	0.242	0.168	0.386	0.265	0.111
Skin	0.295	0.285	0.547	0.376	0.148
Small intestine	2.012	1.963	1.865	1.946	0.075
Spinal cord	0.185	0.148	0.252	0.195	0.053
Spleen	24.956	16.693	35.344	25.664	9.345
Stomach	0.113	0.187	2.187	0.829	1.177
Testes	0.269	0.328	0.361	0.319	0.047
Thymus	0.110	0.295	0.481	0.295	0.185
Thyroid	1.544	0.885	2.170	1.533	0.642
Whole Blood	3.450	2.106	4.202	3.253	1.062
Plasma	7.541	4.597	8.168	6.768	1.907
Blood:plasma ratio	0.46	0.46	0.51	0.48	0.03

090177e195794698\Approved\Approved On: 09-Nov-2020 21:23 (GMT)

**Appendix 8 Individual Male 100 µg mRNA Data
 (continued)**

**Concentration of Total Radioactivity in Whole Blood, Plasma and
 Tissues 24 hours Following Single Intramuscular Administration of
 [³H]-08-A01-C01 to Male Wistar Han Rats**

Target Dose Level: 100 µg mRNA/Animal; 2.57 mg Total Lipid/Animal

Results expressed as µg lipid equiv/g (mL)

Sample	016M	017M	018M	Mean	SD
Adipose tissue	0.268	0.219	0.261	0.249	0.027
Adrenal glands	63.795	42.538	52.924	53.085	10.629
Bladder	0.609	0.643	0.373	0.542	0.147
Bone (femur)	1.254	2.075	0.950	1.426	0.582
Bone marrow (femur)	5.002	4.711	7.513	5.742	1.541
Brain	0.186	0.221	0.255	0.221	0.034
Eyes	0.342	0.247	0.360	0.316	0.061
Heart	1.613	1.877	1.760	1.750	0.132
Injection site	50.606	70.405	268.240	129.750	120.340
Kidneys	1.971	1.774	2.460	2.068	0.353
Large intestine	5.083	2.282	3.210	3.525	1.427
Liver	51.485	71.224	45.827	56.179	13.334
Lung	3.831	3.615	3.360	3.602	0.236
Lymph node (Man)	3.227	1.555	1.570	2.117	0.961
Lymph node (Mes)	5.835	3.496	3.765	4.366	1.279
Muscle	0.208	0.263	0.247	0.239	0.028
Pancreas	0.767	0.966	0.781	0.838	0.111
Pituitary gland	1.320	1.362	1.603	1.428	0.152
Prostate	0.407	0.446	0.481	0.445	0.037
Salivary glands	0.617	0.561	0.701	0.626	0.071
Skin	0.833	0.937	0.645	0.805	0.148
Small intestine	3.736	3.157	3.433	3.442	0.289
Spinal cord	0.229	0.200	0.326	0.252	0.066
Spleen	47.746	74.940	44.431	55.706	16.739
Stomach	0.572	0.802	0.489	0.621	0.162
Testes	0.638	0.502	0.616	0.585	0.073
Thymus	0.473	0.568	0.506	0.516	0.048
Thyroid	1.845	1.890	2.651	2.129	0.453
Whole Blood	2.448	1.756	3.404	2.536	0.827
Plasma	5.639	5.297	8.191	6.376	1.581
Blood:plasma ratio	0.43	0.33	0.42	0.39	0.05

090177e195794698\Approved\Approved On: 09-Nov-2020 21:23 (GMT)

**Appendix 8
(continued)****Individual Male 100 µg mRNA Data****Concentration of Total Radioactivity in Whole Blood, Plasma and Tissues 48 hours Following Single Intramuscular Administration of [³H]-08-A01-C01 to Male Wistar Han Rats****Target Dose Level: 100 µg mRNA/Animal; 2.57 mg Total Lipid/Animal****Results expressed as µg lipid equiv/g (mL)**

Sample	019M	020M	Mean
Adipose tissue	0.276	0.234	0.255
Adrenal glands	52.496	45.684	49.090
Bladder	0.779	0.849	0.814
Bone (femur)	0.639	0.867	0.753
Bone marrow (femur)	3.233	2.890	3.062
Brain	0.477	0.173	0.325
Eyes	0.239	0.260	0.249
Heart	1.132	1.158	1.145
Injection site	48.800	59.876	54.338
Kidneys	0.971	1.131	1.051
Large intestine	4.144	2.190	3.167
Liver	48.512	36.690	42.601
Lung	1.853	2.477	2.165
Lymph node (Man)	2.418	1.157	1.788
Lymph node (Mes)	5.067	3.297	4.182
Muscle	0.166	0.926	0.546
Pancreas	0.540	0.701	0.620
Pituitary gland	0.987	0.884	0.936
Prostate	0.308	0.285	0.296
Salivary glands	0.488	0.588	0.538
Skin	0.640	0.699	0.670
Small intestine	3.644	3.750	3.697
Spinal cord	0.212	0.237	0.224
Spleen	35.545	33.899	34.722
Stomach	0.794	1.011	0.903
Testes	0.523	0.555	0.539
Thymus	0.514	0.655	0.584
Thyroid	1.604	1.523	1.564
Whole Blood	0.967	1.011	0.989
Plasma	1.451	1.493	1.472
Blood:plasma ratio	0.67	0.68	0.67

090177e195794698\Approved\Approved On: 09-Nov-2020 21:23 (GMT)

Appendix 8 Individual Male 100 µg mRNA Data
(continued)**Recovery of Total Radioactivity in Tissues 0.25 min Following Single Intramuscular Administration of [³H]-08-A01-C01 to Male Wistar Han Rats****Target Dose Level: 100 µg mRNA/Animal; 2.57 mg Total Lipid/Animal****Results expressed as % administered dose**

Sample	001M	002M	003M	Mean	SD
Adrenal glands	0.000	0.000	0.000	0.000	0.000
Bladder	0.000	0.000	0.000	0.000	0.000
Brain	0.003	0.003	0.003	0.003	0.000
Eyes	0.000	0.000	0.000	0.000	0.000
Heart	0.011	0.009	0.017	0.013	0.004
Injection site	1.865	3.345	18.252	7.821	9.064
Kidneys	0.037	0.033	0.019	0.030	0.010
Large intestine	0.006	0.004	0.018	0.009	0.008
Liver	0.368	0.185	0.278	0.277	0.091
Lung	0.028	0.017	0.023	0.023	0.005
Pancreas	0.001	0.001	0.002	0.001	0.000
Pituitary gland	0.000	0.000	0.000	0.000	0.000
Prostate	0.000	0.000	0.000	0.000	0.000
Salivary glands	0.001	0.002	0.001	0.001	0.000
Small intestine	0.016	0.009	0.006	0.010	0.005
Spinal cord	0.001	0.001	0.000	0.001	0.000
Spleen	0.010	0.026	0.006	0.014	0.011
Stomach	0.005	0.004	*0.002	°0.003	°0.002
Testes	0.004	0.003	0.003	0.003	0.001
Thymus	0.003	0.003	0.004	0.003	0.001
Thyroid	0.000	0.000	0.000	0.000	0.000

* = Results calculated from data less than 30 cpm above background

° = Mean includes results calculated from data less than 30 cpm above background

**Appendix 8 Individual Male 100 µg mRNA Data
 (continued)**

**Recovery of Total Radioactivity in Tissues 1 hour Following Single
 Intramuscular Administration of [³H]-08-A01-C01 to Male Wistar Han
 Rats**

Target Dose Level: 100 µg mRNA/Animal; 2.57 mg Total Lipid/Animal

Results expressed as % administered dose

Sample	004M	005M	006M	Mean	SD
Adrenal glands	0.005	0.003	0.004	0.004	0.001
Bladder	0.001	0.000	0.001	0.001	0.000
Brain	0.019	0.020	0.020	0.019	0.001
Eyes	0.002	0.001	0.001	0.001	0.001
Heart	0.049	0.103	0.074	0.075	0.027
Injection site	15.619	13.609	16.094	15.107	1.319
Kidneys	0.191	0.176	0.188	0.185	0.008
Large intestine	0.024	0.027	0.050	0.034	0.014
Liver	5.198	3.856	5.564	4.873	0.899
Lung	0.148	0.159	0.103	0.137	0.030
Pancreas	0.004	0.006	0.007	0.006	0.002
Pituitary gland	0.000	0.000	0.000	0.000	0.000
Prostate	0.003	0.003	0.003	0.003	0.000
Salivary glands	0.007	0.009	0.011	0.009	0.002
Small intestine	0.132	1.003	1.062	0.732	0.521
Spinal cord	0.001	0.003	0.001	0.002	0.001
Spleen	0.090	0.087	0.089	0.089	0.001
Stomach	0.075	0.362	1.259	0.565	0.618
Testes	0.020	0.021	0.057	0.033	0.021
Thymus	0.007	0.005	0.006	0.006	0.001
Thyroid	0.001	0.001	0.001	0.001	0.000

090177e195794698\Approved\Approved On: 09-Nov-2020 21:23 (GMT)

**Appendix 8 Individual Male Recovery Data
 (continued)**

Recovery of Total Radioactivity in Tissues 2 hours Following Single Intramuscular Administration of [³H]-08-A01-C01 to Male Wistar Han Rats

Target Dose Level: 100 µg mRNA/Animal; 2.57 mg Total Lipid/Animal

Results expressed as % administered dose

Sample	007M	008M	009M	Mean	SD
Adrenal glands	0.008	0.006	0.007	0.007	0.001
Bladder	0.001	0.001	0.001	0.001	0.000
Brain	0.024	0.021	0.018	0.021	0.003
Eyes	0.001	0.001	0.001	0.001	0.000
Heart	0.078	0.095	0.115	0.096	0.019
Injection site	0.598	9.070	3.532	4.400	4.302
Kidneys	0.180	0.148	0.160	0.163	0.016
Large intestine	0.088	0.038	0.055	0.061	0.025
Liver	11.802	8.114	8.654	9.523	1.992
Lung	0.147	0.112	0.153	0.137	0.022
Pancreas	0.008	0.007	0.011	0.009	0.002
Pituitary gland	0.001	0.000	0.000	0.000	0.000
Prostate	0.003	0.004	0.004	0.004	0.001
Salivary glands	0.012	0.010	0.013	0.011	0.002
Small intestine	0.434	0.294	0.281	0.336	0.085
Spinal cord	0.003	0.004	0.002	0.003	0.001
Spleen	0.271	0.155	0.192	0.206	0.059
Stomach	0.036	0.023	0.026	0.028	0.007
Testes	0.025	0.045	0.036	0.035	0.010
Thymus	0.010	0.008	0.007	0.008	0.001
Thyroid	0.001	0.001	0.001	0.001	0.000

090177e195794698\Approved\Approved On: 09-Nov-2020 21:23 (GMT)

**Appendix 8 Individual Male Recovery Data
 (continued)**

Recovery of Total Radioactivity in Tissues 4 hours Following Single Intramuscular Administration of [³H]-08-A01-C01 to Male Wistar Han Rats

Target Dose Level: 100 µg mRNA/Animal; 2.57 mg Total Lipid/Animal

Results expressed as % administered dose

Sample	010M	011M	012M	Mean	SD
Adrenal glands	0.010	0.005	0.005	0.007	0.003
Bladder	0.001	0.000	0.000	0.001	0.000
Brain	0.027	0.009	0.006	0.014	0.011
Eyes	0.001	0.001	0.000	0.001	0.000
Heart	0.031	0.043	0.033	0.036	0.007
Injection site	5.231	59.191	24.168	29.530	27.377
Kidneys	0.141	0.101	0.058	0.100	0.041
Large intestine	0.062	0.258	0.123	0.147	0.100
Liver	13.675	6.428	7.436	9.180	3.926
Lung	0.079	0.141	0.069	0.096	0.039
Pancreas	0.003	0.008	0.006	0.006	0.003
Pituitary gland	0.000	0.000	0.000	0.000	0.000
Prostate	0.002	0.001	0.001	0.001	0.001
Salivary glands	0.005	0.003	0.003	0.004	0.001
Small intestine	0.234	0.614	0.356	0.401	0.194
Spinal cord	0.001	0.001	0.001	0.001	0.000
Spleen	0.177	0.530	0.167	0.291	0.207
Stomach	0.007	0.035	0.043	0.028	0.019
Testes	0.048	0.017	0.012	0.026	0.019
Thymus	0.003	0.005	0.003	0.003	0.001
Thyroid	0.001	0.000	0.001	0.001	0.000

090177e195794698\Approved\Approved On: 09-Nov-2020 21:23 (GMT)

**Appendix 8 Individual Male Recovery Data
(continued)****Recovery of Total Radioactivity in Tissues 8 hours Following Single Intramuscular Administration of [³H]-08-A01-C01 to Male Wistar Han Rats****Target Dose Level: 100 µg mRNA/Animal; 2.57 mg Total Lipid/Animal****Results expressed as % administered dose**

Sample	013M	014M	015M	Mean	SD
Adrenal glands	0.025	0.021	0.080	0.042	0.033
Bladder	0.002	0.001	0.001	0.001	0.001
Brain	0.012	0.009	0.014	0.012	0.003
Eyes	0.002	0.001	0.002	0.002	0.001
Heart	0.058	0.035	0.081	0.058	0.023
Injection site	8.806	17.803	0.313	8.974	8.746
Kidneys	0.134	0.073	0.091	0.099	0.031
Large intestine	0.511	0.398	0.634	0.514	0.118
Liver	11.864	16.293	24.504	17.553	6.414
Lung	0.192	0.129	0.197	0.172	0.038
Pancreas	0.005	0.006	0.012	0.007	0.004
Pituitary gland	0.000	0.000	0.000	0.000	0.000
Prostate	0.002	0.001	0.003	0.002	0.001
Salivary glands	0.004	0.003	0.008	0.005	0.003
Small intestine	0.585	0.529	0.633	0.582	0.052
Spinal cord	0.002	0.001	0.002	0.002	0.000
Spleen	0.560	0.369	0.848	0.592	0.241
Stomach	0.021	0.019	0.288	0.109	0.155
Testes	0.031	0.036	0.038	0.035	0.004
Thymus	0.002	0.004	0.007	0.004	0.002
Thyroid	0.001	0.001	0.001	0.001	0.000

**Appendix 8 Individual Male Recovery Data
 (continued)**

Recovery of Total Radioactivity in Tissues 24 hours Following Single Intramuscular Administration of [³H]-08-A01-C01 to Male Wistar Han Rats

Target Dose Level: 100 µg mRNA/Animal; 2.57 mg Total Lipid/Animal

Results expressed as % administered dose

Sample	016M	017M	018M	Mean	SD
Adrenal glands	0.137	0.095	0.106	0.113	0.022
Bladder	0.003	0.002	0.001	0.002	0.001
Brain	0.012	0.015	0.019	0.015	0.003
Eyes	0.004	0.002	0.004	0.003	0.001
Heart	0.038	0.052	0.051	0.047	0.008
Injection site	3.590	15.406	29.435	16.144	12.938
Kidneys	0.107	0.104	0.165	0.125	0.034
Large intestine	1.668	0.752	0.996	1.139	0.475
Liver	22.736	26.544	20.865	23.382	2.894
Lung	0.170	0.160	0.226	0.185	0.036
Pancreas	0.010	0.016	0.012	0.013	0.003
Pituitary gland	0.000	0.000	0.000	0.000	0.000
Prostate	0.003	0.004	0.004	0.004	0.000
Salivary glands	0.011	0.010	0.011	0.010	0.001
Small intestine	1.194	0.896	1.321	1.137	0.218
Spinal cord	0.002	0.001	0.002	0.002	0.001
Spleen	1.003	1.590	1.111	1.234	0.312
Stomach	0.066	0.099	0.065	0.077	0.019
Testes	0.070	0.056	0.075	0.067	0.010
Thymus	0.007	0.009	0.007	0.008	0.002
Thyroid	0.001	0.001	0.001	0.001	0.000

090177e195794698\Approved\Approved On: 09-Nov-2020 21:23 (GMT)

**Appendix 8 Individual Male Recovery Data
(continued)****Recovery of Total Radioactivity in Tissues 48 hours Following Single Intramuscular Administration of [³H]-08-A01-C01 to Male Wistar Han Rats****Target Dose Level: 100 µg mRNA/Animal; 2.57 mg Total Lipid/Animal****Results expressed as % administered dose**

Sample	019M	020M	Mean
Adrenal glands	0.155	0.112	0.134
Bladder	0.002	0.002	0.002
Brain	0.034	0.012	0.023
Eyes	0.002	0.003	0.002
Heart	0.030	0.031	0.030
Injection site	2.978	10.414	6.696
Kidneys	0.063	0.076	0.070
Large intestine	1.070	0.719	0.894
Liver	17.436	16.159	16.797
Lung	0.071	0.132	0.102
Pancreas	0.007	0.006	0.006
Pituitary gland	0.000	0.000	0.000
Prostate	0.003	0.002	0.003
Salivary glands	0.008	0.009	0.008
Small intestine	0.790	1.021	0.905
Spinal cord	0.002	0.002	0.002
Spleen	0.886	0.649	0.768
Stomach	0.044	0.047	0.046
Testes	0.064	0.054	0.059
Thymus	0.006	0.005	0.006
Thyroid	0.001	0.001	0.001



BioNTech SE
An der Goldgrube 12
55131 Mainz, Germany
Phone: +49 (0)6131 9084-0
Telefax: +49 (0)6131 9084-390

R&D STUDY REPORT No. R-20-0072

EXPRESSION OF LUCIFERASE-ENCODING MODRNA AFTER I.M. APPLICATION OF GMP- READY ACUITAS LIPID NANOPARTICLE FORMULATION

Version 03

Date: 27 Nov 2020

Reported by (b) (6)

Test item: modRNA encoding luciferase

Key words: COVID-19, modRNA, biodistribution, mouse, bioluminescence assay

This R&D report consists of 36 pages.

Confidentiality Statement: The information contained in this document is the property and copyright of BioNTech RNA Pharmaceuticals GmbH. Therefore, this document is provided in confidence to the recipient (e.g., regulatory authorities, IECs/IRBs, investigators, auditors, inspectors). No information contained herein shall be published, disclosed, or reproduced without prior written approval of the proprietors.

090177e195a2e6f3\Approved\Approved On: 27-Nov-2020 16:30 (GMT)

TABLE OF CONTENTS

TABLE OF CONTENTS	2
LIST OF FIGURES	3
LIST OF TABLES	3
LIST OF ABBREVIATIONS	4
RESPONSIBILITIES	5
1 SUMMARY	6
2 GENERAL INFORMATION	8
2.1 Sponsor and Test Facilities	8
2.2 Participating Personnel	8
2.3 Study Dates	8
2.4 Guidelines and Regulations	9
2.5 Changes and Deviations	9
2.6 Documentation and Archive	9
3 INTRODUCTION	10
3.1 Background	10
3.2 Objectives	10
3.3 Study Design	11
4 MATERIALS AND METHODS	12
4.1 Test Item	12
4.2 Control Item	12
4.3 Test System	12
4.4 Materials	13
4.5 Methods	14
4.5.1 Animal Care	14
4.5.2 Animal Monitoring	15
4.5.3 Endpoint of Experiment / Termination Criteria	15
4.5.4 Injection of Test and Control Items	15
4.5.5 Bioluminescence Measurements	16
4.5.6 Blood Sampling via the <i>Vena Facialis</i>	16
4.5.7 Luminex-based Multiplex Assay (ProcartaPlex Multiplex Immunoassay)	16
4.5.8 Luciferase-specific ELISA	17
4.5.9 ELISpot Analysis	17
4.5.10 Statistical Analysis	18
5 RESULTS	19
5.1 Bioluminescence Measurements	19
5.2 Liver Expression (b) (4) vs LNP8	21
5.3 Luminex-based Multiplex Assay	21
5.4 Luciferase-specific ELISA	23
5.5 IFN- γ ELISpot Assay	23
6 CONCLUSION	25
7 DOCUMENT HISTORY	26

090177e195a2e6f3\Approved\Approved On: 27-Nov-2020 16:30 (GMT)

8 REFERENCES27

9 APPENDIX28

Appendix 1: Animal Observations.....28

Appendix 2: Certificates of Analysis29

Appendix 3: Raw Data IFN- γ ELISpot.....32

Appendix 4: Statistical Analysis33

LIST OF FIGURES

Figure 1: Bioluminescence measurement using the LNP-formulated modRNA encoding for luciferase20

Figure 2: Bioluminescence measurement in the liver using the LNP-formulated modRNA encoding for luciferase21

Figure 3: Activation of the innate immune system by LNP-formulated modRNA encoding for luciferase22

Figure 4: Luciferase-specific IgG ELISA on days -1 and 923

Figure 5: ELISpot analysis using splenocytes on day 9.....24

LIST OF TABLES

Table 1: Study design11

Table 2: Lipid component formulations12

Table 3: Materials13

Table 4: Software14

Table 5: Peptide pool for stimulation of splenocytes.....14

090177e195a2e6f3\Approved\Approved On: 27-Nov-2020 16:30 (GMT)

LIST OF ABBREVIATIONS

ALC-0159	Proprietary PEG-lipid included as an excipient in the LNP formulation from Acuitas
ALC-0315	Proprietary amino-lipid included as an excipient in the LNP formulation from Acuitas
ALP	Alkaline phosphatase
ANOVA	Analysis of variance
AUC	Area under the curve
BALB/c	Mouse strain used in this study
BCIP	5-Bromo-4-chloro-3-indolyl-phosphate
BNT162	BioNTech's vaccine program against COVID-19
ConA	Concanavalin A
COVID-19	Coronavirus disease 2019
DPBS	Dulbecco's phosphate-buffered saline
ELISA	Enzyme-linked immunosorbent assay
ELISpot	Enzyme-linked immunosorbent spot
FELASA	Federation of European Laboratory Animal Science Associations
GMP	Good manufacturing practice
HRP	Horseradish peroxidase
IFN	Interferon
IgG	Immunoglobulin G
IL	Interleukin
i.m.	Intramuscularly
IP-10	Interferon-gamma induced protein 10
IVIS	<i>In vivo</i> imaging system
LNP	Lipid nanoparticle
Luc	Luciferase (from firefly <i>Pyroactomena lucifera</i>)
MCP-1	Monocyte chemotactic protein 1
MHC	Major histocompatibility complex
MIP-1 β	Macrophage inflammatory protein 1 β
modRNA	Nucleoside-modified mRNA
NBT	Nitro blue tetrazolium
OD	Optical density
p/s	Photons per second
SD	Standard deviation
SOP	Standard operating procedure
S protein	Spike protein
saRNA	Self-amplifying mRNA
SARS-CoV-2	Severe acute respiratory syndrome coronavirus 2
TNF	Tumor necrosis factor

090177e195a2e6f3\Approved\Approved On: 27-Nov-2020 16:30 (GMT)

RESPONSIBILITIES

Person responsible for the study:	(b) (6)	26 NOV 2020
	(b) (6) BioNTech (b) (6)	Date
Author:	(b) (6)	
	BioNTech SE	Date
Reviewer:	(b) (6)	26 NOV 2020
	(b) (6) BioNTech (b) (6)	Date
QA representative:	(b) (6)	27 NOV 2020
	BioNTech SE (b) (6)	Date

Meaning of the signatures:

Person responsible for the study: I am responsible for the content of the R&D report and confirm that it represents an accurate record of the results. This study was performed according to the SOPs and methods as well as the rules and regulations described in the report.

Author: I am the author of this document.

Reviewer: I reviewed the R&D report and confirm that this document complies with the scientific and technical standards and requirements.

QA representative: I confirm that this document complies with the relevant quality assurance requirements.

Approval of the author via email according to CC-20-0087 (see attachment).
 erg (b) (6) 27 NOV 2020

090177e195a2e6f3\Approved\Approved On: 27-Nov-2020 16:30 (GMT)

1 SUMMARY

BioNTech is developing RNA-based vaccines designed to protect against the novel coronavirus disease that emerged in 2019 (COVID-19). The BNT162 project involves testing three RNA platforms, which are under development at BioNTech with the surface or spike protein (S protein) of the novel coronavirus (SARS-CoV-2) as the viral antigen. These RNAs will be formulated with a GMP-compatible LNP formulation provided by Acuitas.

In this study, the GMP-ready formulation containing the amino-lipid ALC-0315 and the PEG-lipid ALC-0159 (in this report referred to as LNP 8 which is the identical composition as used in BNT162) was tested in comparison with a (b) (4) (b) (4) by Acuitas, (b) (4) and an in-house formulation, (b) (4) to characterize the biodistribution of luciferase expressed by LNP-formulated nucleoside-modified mRNA (modRNA). Activation of the innate immune system, formation of antibodies against luciferase, and T-cell activation were also assessed.

Four groups of three BALB/c mice were injected intramuscularly (i.m.) with a total dose of 2 µg/animal of (b) (4) LNP8- or (b) (4) -formulated modRNA encoding luciferase or with buffer (DPBS) as control. At 6 h, 24 h, 48 h, 72 h, 6 d, and 9 d after injection, the *in vivo* luciferase expression was measured by luciferin application. Serum samples were taken 1 day before and 6 h after immunization as well as on day 9 for quantification of the activation of the innate immune system in a Luminex-based multiplex assay and antigen-binding antibody analysis in an IgG-specific ELISA. Splenocytes were isolated on 9 d to assess the T-cell response by IFN-γ ELISpot Assay.

An approximately 20-fold higher luciferase expression at the injections site was observed for modRNA-Luciferase (b) (4) and the GMP-ready modRNA-Luciferase LNP8 when compared to modRNA formulated with (b) (4). The difference between the area under the curve for (b) (4) and LNP8-formulated modRNA compared to buffer control as well as to (b) (4) formulated modRNA was statistically significant. In addition, luciferase expressed from the (b) (4)-formulated modRNA showed limited drainage to the liver compared to LNP8-formulated modRNA.

A multiplex assay showed that the innate immune system was temporally activated by (b) (4) and LNP8-formulated modRNA. The activation was more pronounced for (b) (4) formulated modRNA than for modRNA formulated with LNP8, indicating a formulation-related effect rather than a payload or expression level effect.

Treatment with modRNA with all tested LNP formulations did not induce the formation of luciferase-specific IgGs on day 9. However, a strong antigen-specific IFN-γ T-cell response was measured by ELISpot assay on day 9 for (b) (4) and LNP8-formulated modRNAs, with statistically significant differences between these test groups, the buffer control, and the (b) (4) group.

090177e195a2e6f3\Approved\Approved On: 27-Nov-2020 16:30 (GMT)

In conclusion, despite different biodistribution characteristics, both Acuitas LNPs allowed a high antigen expression level thereby inducing a strong T- but not B-cell response on day 9 post immunization.

(b) (6)		
Responsible Person:	(b) (6)	26 Nov 2020
(b) (6) BioNTech	(b) (6)	Date

090177e195a2e6f3\Approved\Approved On: 27-Nov-2020 16:30 (GMT)

2 GENERAL INFORMATION

2.1 Sponsor and Test Facilities

Sponsor

BioNTech RNA Pharmaceuticals GmbH
 An der Goldgrube 12
 55131 Mainz
 Germany

Test Facility

BioNTech SE
 An der Goldgrube 12
 55131 Mainz
 Germany

2.2 Participating Personnel

Responsible person: (as defined in SOP-100-024)	(b) (6) (b) (6) BioNTech (b) (6)
Author:	(b) (6) BioNTech SE
Experimenter: Immunization, blood sampling, ELISA, ELISpot	(b) (6) BioNTech (b) (6)
Experimenter: Luminex-based multiplex assay	(b) (6) BioNTech (b) (6)

2.3 Study Dates

Start of experiments: 14 JAN 2020

Completion of experiments: 23 JAN 2020

090177e195a2e6f3\Approved\Approved On: 27-Nov-2020 16:30 (GMT)

2.4 Guidelines and Regulations

All experiments are executed in accordance with the existing standard operating procedures and described processes from BioNTech SE. Applicable documents are listed below.

- Animal test application approval number: G18-12-007
- SOP-030-071 Abtöten von Mäusen
- SOP-030-072 Fixiergriff und Ohrmarkierung bei Mäusen
- SOP-030-073 Betäubung bei Mäusen
- SOP-030-074 Blutentnahme bei Mäusen
- SOP-030-078 Isolierung muriner Splenozyten
- SOP-030-079 Intramuskuläre Applikation bei Mäusen
- SOP-030-110 IFN- γ ELISpot murin
- SOP-090-013 Biological safety in laboratories

2.5 Changes and Deviations

Not applicable. There is no formal R&D plan available.

2.6 Documentation and Archive

Study reports are stored and archived according to SOP-100-003 Archiving of Paper-Based Documents.

Raw data and evaluated data are saved at:

- P:\BioNTechRNA\RN_R0030_AIRVAC\24_Preclinic\01_Vakzine Testing in vivo Luc\IM#88 GMP ready LNP Acuitas modRNA
- Lab books:
 - No. 1455 (complete study plan including results)
 - No. 1835 (IVIS images and quantification, Luciferase ELISA, ELISpot)
 - No. 1593 page 71-84 (Luminex-based multiplex assay)

3 INTRODUCTION

3.1 Background

In December 2019, an outbreak of pneumonia of unknown cause in Wuhan, Hubei province in China started. The disease spread rapidly and in January 2020, the agent was identified. By 1 April 2020, infection with the novel coronavirus (SARS-CoV-2) was confirmed in approximately 820,000 people with more than 40,000 casualties¹. A vaccine is urgently needed and BioNTech decided to develop a rapid vaccine project (BNT162) with the surface or spike protein (S protein) of the virus as the viral antigen.

The development of *in vitro* transcribed RNA as an active platform for the use in infectious disease vaccines is based on the extensive knowledge of the company in RNA technology, which has been gained over the last decade. The core innovation is based on *in vivo* delivery of a pharmacologically optimized, antigen-coding RNA vaccine to induce robust neutralizing Abs and accompanying/concomitant T-cell responses to achieve protective immunization with minimal vaccine doses (Vogel et al. 2017, Moyo et al. 2018, Pardi et al. 2017).

At BioNTech, three different RNA platforms formulated with lipid nanoparticles (LNPs) are under development, namely non-modified uridine-containing mRNA (uRNA), nucleoside-modified mRNA (modRNA) and self-amplifying RNA (saRNA). In the present study, an LNP-formulated modRNA encoding luciferase was used representatively to investigate the *in vivo* biodistribution and the immune response of the vaccine candidates.

LNP formulations from a third party provider (Acuitas) were tested in comparison to the in-house formulation (b) (4) Acuitas (b) (4)

(b) (4)

(b) (4)

Acuitas also provided an LNP

formulation that is cGMP-ready, namely LNP8, which contains two proprietary lipids (ALC-0159 and ALC-0315) and has the identical composition as the LNP formulation used in the BNT162 program.

3.2 Objectives

The objective of this study was to investigate the biodistribution of luciferase expressed by the LNP-formulated modRNA using bioluminescence measurements in BALB/c mice, as well as innate immune system activation, formation of antibodies against luciferase and T-cell activation.

¹ Coronavirus disease (COVID-2019) situation report 72, World Health Organization; www.who.int/emergencies/diseases/novel-coronavirus-2019/situation-reports

3.3 Study Design

Four groups of three BALB/c mice were injected intramuscularly (i.m.) in the right and left hind leg with each 1 µg of LNP-formulated modRNA encoding luciferase or with buffer as control on day 0. At 6 h, 24 h, 48 h, 72 h, 6 d, and 9 d after injection, the *in vivo* luciferase expression was measured by luciferin application.

In addition, serum samples were collected on day -1 and 6 h and 9 d post immunization and cytokine/chemokine level determination (multiple) and on day 1 and 9 for luciferase-specific ELISA. On day 9, spleens were resected for immunological analysis using IFN-γ ELISpot assays.

Table 1: Study design

Group	Treatment	Dose [µg/mouse]	Formulation	Treatment schedule	End of experiment	Sample collection
1	Buffer control	N/A	N/A	Day 0	Day 9	Serum ELISA on days -1 and 9, serum for Multiplex assay on day -1, 6 h, and 9 d; splenocytes for ELISpot on day 9
2	modRNA-Luciferase (b) (4)	2 µg (1 µg/leg)	(b) (4)	Day 0	Day 9	
3	modRNA-Luciferase (b) (4)	2 µg (1 µg/leg)	Acuitas proprietary	Day 0	Day 9	
4	modRNA-Luciferase LNP8 (GMP-ready)	2 µg (1 µg/leg)	ALC-0315:ALC-0159:DSPC:Chol	Day 0	Day 9	

090177e195a2e6f3\Approved\Approved On: 27-Nov-2020 16:30 (GMT)

4 MATERIALS AND METHODS

4.1 Test Item

- LNP-formulated modRNA encoding luciferase diluted to 0.05 mg/mL to obtain a dose of 1 µg in 20 µL application volume. For CoAs see [Appendix 2: Certificates of Analysis](#) of RNA and LNPs.
- Acuitas LNPs:
 - (b) (4)
 - LNP8 modRNA Luc, RNA-EH190611-01c, batch FM-1074-D, 90% encapsulation, 1.0 mg/mL encapsulated RNA, diameter 71 nm, polydispersity 0.053, storage temperature -80°C.
- BioNTech LNP:
 - (b) (4)

Table 2: Lipid component formulations

Formulation	Lipids			
	Functional lipid 1	Functional lipid 2	Structural lipid 1	Structural lipid 2
(b) (4)	Acuitas proprietary	Acuitas proprietary	Acuitas proprietary	Acuitas proprietary
LNP8	ALC-0315	ALC-0159	DSPC	Cholesterol
(b) (4)	(b) (4)	(b) (4)	(b) (4)	(b) (4)

4.2 Control Item

- DPBS

4.3 Test System

- *Mus musculus*: 12 female BALB/c mice at an age of 9 weeks at study start with a body weight of approximately 25 g

090177e195a2e6f3\Approved\Approved On: 27-Nov-2020 16:30 (GMT)

4.4 Materials

Table 3: Materials

Product name	Application/specification	Article no.	Working dilution	Provider
Dulbecco's phosphate-buffered saline (DPBS)	Buffer control	14190-094	1×	Thermo Fisher Scientific
Syringes 0.3 mL 30 G	Insulin syringes for i.m. application	4144150	N/A	BD
Syringes 0.5 mL 29 G	Insulin syringes for i.p. application	324824	N/A	BD
Luciferin	Substrate for <i>in vivo</i> luciferase imaging	122799-10	150 mg/kg	Perkin-Elmer
Microvette 500 Z-gel tubes	Blood sampling	2021-01-31	N/A	Sarstedt
Xenogen IVIS® Spectrum	<i>In vivo</i> BLI imager	-	N/A	Caliper Life Sciences
MaxiSorp plate	ELISA	439454	N/A	Thermo Fisher Scientific
QuantiLum recombinant luciferase	Positive control	E1701	100 ng/μL	Promega
Casein blocking buffer	10×	B6429	1×	Sigma-Aldrich
TMB ONE ECO-TEK	Chromogenic substrate for horseradish peroxidase	4380H	N/A	BIOTREND
Sodium bicarbonate	7.5% NaHCO ₃	S8761-100 ml	N/A	Sigma-Aldrich
HCl	Hydrochloric acid solution volumetric, 0.1 M HCl	2104-50 ml	N/A	Sigma-Aldrich
RPMI1640 medium	Cell culture medium	61870	N/A	Gibco
Biotek Epoch	ELISA plate reader	-	N/A	Biotek
Mouse IFN-γ ELISpotPLUS kit	Kit for enumeration of cells secreting mouse IFN-γ	3321-4APT-2	N/A	Mabtech
ImmunoSpot® S5 Versa Analyzer	ELISpot plate reader	-	N/A	Cellular Technology Ltd.
RPMI1640 medium	Cell culture medium	61870	N/A	Gibco
Multiplex	PROCARTAPLEX 10 PLEX	PPX-10 - MXU63C9	N/A	Life Technologies GmbH
Bio-Plex 200	Multiplex reader	-	N/A	Bio-Rad
Anti-firefly luciferase antibody (mAb21),	Assay control ELISA	ab64564	1:1,000	Abcam
Mouse IgG isotype	Assay control ELISA	0107-08	1:100 as starting dilution	Southern Biotech
Goat anti-mouse IgG HRP	Secondary antibody ELISA	115-035-071	1:15,000 (if stored in 50% glycerol 1:7,500)	Jackson

090177e195a2e6f3\Approved\Approved On: 27-Nov-2020 16:30 (GMT)

Table 4: Software

Product name	Application	Provider
Living image	<i>In vivo</i> BLI quantification	Perkin-Elmer
Prism	Analysis	GraphPad Software Inc.
Excel	Animal monitoring, raw data ELISA	Microsoft Corp.
Bio-Plex Manager (6.1)	Bio-Plex reader	Bio-Rad
Gen5	Absorbance reader	Biotek
ImmunoCapture V6.3	ELISpot analysis	Cellular Technology Ltd.

Table 5: Peptide pool for stimulation of splenocytes

Peptide pool MHC-I	
Name	Sequence
Firefly luciferase-1	GFQSMYTFV
Firefly luciferase-2	VPFHGFGM
Firefly luciferase-3	VALPHRTAC

Consensus sequences from [Limberis et al. 2009](#)

4.5 Methods

4.5.1 Animal Care

4.5.1.1 General Information

BALB/c mice were delivered at the age of at least six weeks. Delivered mice were used for experiments after approximately one week of acclimatization. All experiments and protocols were approved by the local authorities (local welfare committee), conducted according to the FELASA recommendations and in compliance with the German animal welfare act and Directive 2010/63/EU. Only animals with an unobjectionable health status were selected for testing procedures.

All animals were registered upon arrival in the lab animal colony management system PyRAT (Scionics Computer Innovation GmbH, Dresden, Germany) and tracked until death. Each cage was labeled with a cage card indicating the mouse strain, gender, date of birth, and number of animals per cage. At the start of an experiment additional information was added such as the project and license number, the start of the experiment and details on interventions. Where necessary for identification, animals were arbitrarily numbered with earmarks.

4.5.1.2 Housing Condition and Husbandry

Mice were housed at BioNTech SE's animal facility under barrier and SPF conditions (An der Goldgrube 12, 55131 Mainz) in individually ventilated cages (Sealsafe GM500 IVC Green Line, TECNIPLAST, Hohenpeißenberg, Germany; 500 cm²) with a maximum of five animals per cage. The temperature and relative humidity in the cages and animal unit was kept at 20-24°C and 45-55%, respectively, and the air change (AC) rate in the cages at 75 AC/hour. The cages with dust-free bedding made of

debarked chopped aspen wood (Abedd LAB & VET Service GmbH, Vienna, Austria, product code: LTE E-001) and additional nesting material were changed weekly. Autoclaved sniff M-Z food (sniff Spezialdiäten GmbH, Soest, Germany; product code: V1124) and autoclaved water (tap water) were provided *ad libitum* and changed at least once weekly. All materials were autoclaved prior to use.

4.5.2 Animal Monitoring

Routine animal monitoring was carried out daily and included inpection for dead animals and control of food and water supplies. Each animal's health was closely assessed at least once weekly. The general physical condition was assessed with regard to the following parameters:

- Body weight change
- Macroscopic assessment of activity level/ behavior
- Macroscopic assessment of general discomfort: drop in body temperature determined by touch and by visual inspection of ears and paws. Ears and paws appear pink in a healthy mouse, white in a mouse with discomfort indicated by reduced blood circulation
- Macroscopic assessment of fur condition and appearance of eyes, inspection of body cavities/ fluids
- Macroscopic assessment of irregularities in breathing ability
- Indication of pain
- Macroscopic assessment for signs of automutilation and or fighting

4.5.3 Endpoint of Experiment / Termination Criteria

Animals were euthanized in accordance with §4 of the German animal welfare act and the recommendation of GV-SOLAS by cervical dislocation or by exposure to carbon dioxide. Additionally, termination criteria applied according to the specification within the respective animal test approval as listed below. Body weight losses exceeding 20%, or a high severity level in any of the parameters found in Section 4.5.2 were on their own sufficient reason for immediate euthanasia.

4.5.4 Injection of Test and Control Items

Animals were anesthetized by inhalation of 2.5% isoflurane in oxygen and the injection site (hind leg) was shaved. Buffer or dissolved test item was applied i.m. into the *musculus gastrocnemius* at a volume of 20 µL. All mice received 1 µg in each leg. After injection and a short recovery phase from anesthesia, the animals were observed for any signs of discomfort due to the injection procedure.

090177e195a2e6f3\Approved\Approved On: 27-Nov-2020 16:30 (GMT)

4.5.5 Bioluminescence Measurements

The mice were monitored over a period of 9 days using *in vivo* imaging system (IVIS) measurements. Briefly, the Xenogen IVIS® Spectrum device was used for *in vivo* imaging according to the manufacturer's instruction. Approximately 6 h after LNP administration and 5 min prior to imaging, animals were injected for the first time intraperitoneally (i.p.) with luciferin (150 mg/kg, dosing volume: 300 µL, 29 G needle). Mice were anesthetized (2.5% isoflurane/O₂) and placed in the imager, first with the dorsal side exposed and then with the ventral side exposed, and luciferase activity was measured. Images were taken with exposure time and sensitivity set to 1 s, 10 s, and 1 min and bin 2, bin 4, or bin 8, respectively. The dorsal and ventral images were analyzed by visual inspection after aligning of sensitivities of each picture and used for illustration of findings. The images were analyzed using Living Image *in vivo* imaging 3.0 software, where the regions to be quantified (radiance) were drawn manually and calculated automatically (region of interest, ROI), to follow kinetics of the total fluxes (p/s) over time in a GraphPad file.

4.5.6 Blood Sampling via the *Vena Facialis*

Blood was sampled via the *vena facialis* according to SOP-030-074. In short, without prior anesthesia, mice were held tightly and using a lancet, the *v. facialis* was punctured in a precise and short movement. Blood was collected into Microvette 500 Z-gel tubes, subsequently the restraining grip was loosened. Blood samples were centrifuged at 10,000 ×g (room temperature) for 5 min and serum transferred to a pre-labeled 1.5 mL reagent tube before storage at -20°C.

4.5.7 Luminex-based Multiplex Assay (ProcartaPlex Multiplex Immunoassay)

The assay was performed according to manufacturer's protocol. Briefly, magnetic beads were added to the provided 96-well flat bottom plate and the beads were washed (wash buffer 1×) with the help of a hand-held magnetic plate washer. The antigen standard was reconstituted in universal assay buffer (1×), pooled in one tube, the volume adjusted to a final volume of 250 µL, serial diluted (4-fold serial dilution steps), and 50 µL was added to the designated wells. Serum samples were diluted 1:1 with the universal assay buffer and 50 µL added to the wells. The standard was measured in duplicates and the serum samples in triplicates. The plate was incubated on a plate shaker at 500 rpm) for 2 h covered with a black lid. After three wash steps, 25 µL of the ready-to-use detection antibody was added, incubated for 30 min on the shaker and washed three times. Streptavidin-PE (50 µL) were added and the plate incubated for 30 min on the shaker and washed three times. The beads were resuspended in 120 µL reading buffer, the plate was sealed, and data were acquired in the Bio-Plex 200 Luminex system.

090177e195a2e6f3\Approved\Approved On: 27-Nov-2020 16:30 (GMT)

4.5.8 Luciferase-specific ELISA

Luciferase-specific IgGs in serum samples obtained on study days 1 and 9 were detected using ELISA. Recombinant luciferase (100 ng/100 μ L) protein was utilized to coat MaxiSorp plates at 4°C overnight. Upon washing and blocking using casein-based blocking buffer, serum samples were screened for luciferase-specific antibodies by incubation on plates for 1 h at 37°C. An anti-firefly luciferase antibody (mAb21) as well as a mouse IgG isotype were included as assay controls. Subsequently, plates were incubated with horseradish peroxidase (HRP)-labeled secondary anti-mouse IgG antibody for another 45 min at 37°C before 3, 3', 5, 5'-tetramethylbenzidine (TMB) ONE substrate was applied. Colorimetric detection was monitored and optical density read at 450 nm calculated to a wavelength reference of 620 nm (Δ OD 450–620 nm).

4.5.9 ELISpot Analysis

4.5.9.1 T-cell epitope prediction

The respective peptides for stimulation of splenocytes ([Table 5](#)) were used as published by [Limberis et al. 2009](#), where the authors mapped the dominant and minor T-cell epitopes in BALB/c mice (GFQSMYTFV and VPFHHGFGM, VALPHRTAC, respectively) for monitoring cellular responses *in vivo*. No modifications have been added to the published peptides before peptide synthesis by JPT technologies GmbH.

4.5.9.2 Sample Collection and Processing

Spleens were removed on day 9 after euthanizing the mice, and single-cell suspensions were prepared (SOP-030-078). In brief, the removed organs were pressed through a 70 μ m cell mesh using the plunger of a syringe to release the cells from the organ into a tube. After washing with PBS the cell pellet was incubated with erythrocyte lysis buffer, washed in PBS, and passed again through a 70 μ m cell mesh. Resulting cells were resuspended in medium and counted.

4.5.9.3 IFN- γ ELISpot Assay

The IFN- γ ELISpot assay was used to measure IFN- γ release after *in vitro* stimulation of T cells as an indicator for the induction of antigen-specific T cells. ELISpot analysis was performed using the Mabtech Mouse IFN- γ ELISpot^{PLUS} kit. Isolated splenocytes were seeded to pre-coated ELISpot plates at 5×10^5 cells/well in 200 μ L medium and stimulated with antigen-specific peptide pools composed of single peptides and a final concentration of 2 μ g/mL per peptide, predicted as described in [Section 4.5.9.1](#) overnight in a humidified incubator at 37°C. As peptide controls, splenocytes were incubated with 6 μ g/mL of an irrelevant AH1 peptide derived from the endogenous retroviral gene product envelope glycoprotein 70 (gp70; AH1: amino acids 6 to 14). Splenocytes were incubated with medium alone as a negative control or with 2 μ g/mL Concanavalin A (ConA) as an internal positive control, confirming the functionality of

the assay. Spots were visualized with a biotin-conjugated anti-IFN- γ antibody followed by incubation with streptavidin-alkaline phosphatase (ALP) and 5-bromo-4-chloro-3-indolyl-phosphate/nitro blue tetrazolium (BCIP/NBT) substrate. Spot numbers were counted and analyzed using the ImmunoSpot® S5 Versa ELISpot Analyzer, the ImmunoCapture™ image acquisition software, and the ImmunoSpot® Analysis software version 5. The quality control (QC) function of ImmunoSpot analysis software was used to limit false positive spot counts. All tests were performed in triplicate and spot counts were summarized as median values for each triplicate.

4.5.10 Statistical Analysis

GraphPad Prism 8 software (La Jolla, USA) was used for statistical analysis and figure generation. All groups were compared by a one-way ANOVA with Tukey's multiple comparison post-test on each measurement day (area under the curve for bioluminescence assay, ELISA, and ELISpot analysis).

090177e195a2e6f3\Approved\Approved On: 27-Nov-2020 16:30 (GMT)

5 RESULTS

5.1 Bioluminescence Measurements

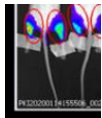
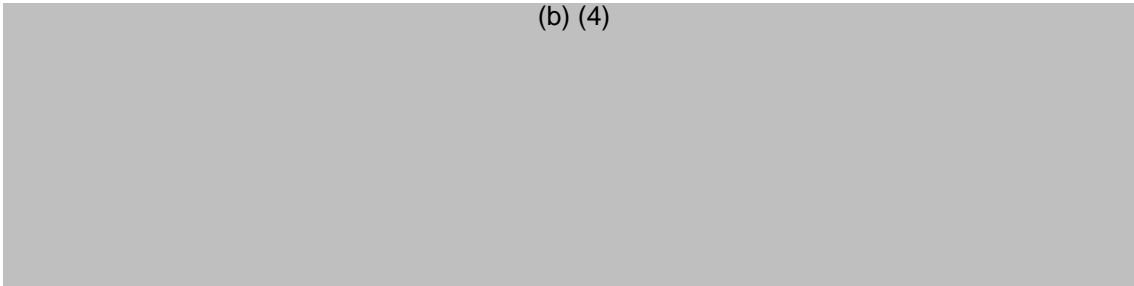
The biodistribution of luciferase expressed by the LNP-formulated modRNA after i.m. injection was assessed by bioluminescence measurements. Mice received a total dose of 2 µg (b) (4) LNP8, or (b) (4) -formulated modRNA, the control group received 20 µL DPBS only.

Mice were monitored over nine days and Luciferase signal was recorded and quantified (Figure 1).

A Time

6 h	24 h	48 h	72 h	6 d	9 d
-----	------	------	------	-----	-----

Buffer control



modRNA-Luciferase LNP8

090177e195a2e6f3\Approved\Approved On: 27-Nov-2020 16:30 (GMT)

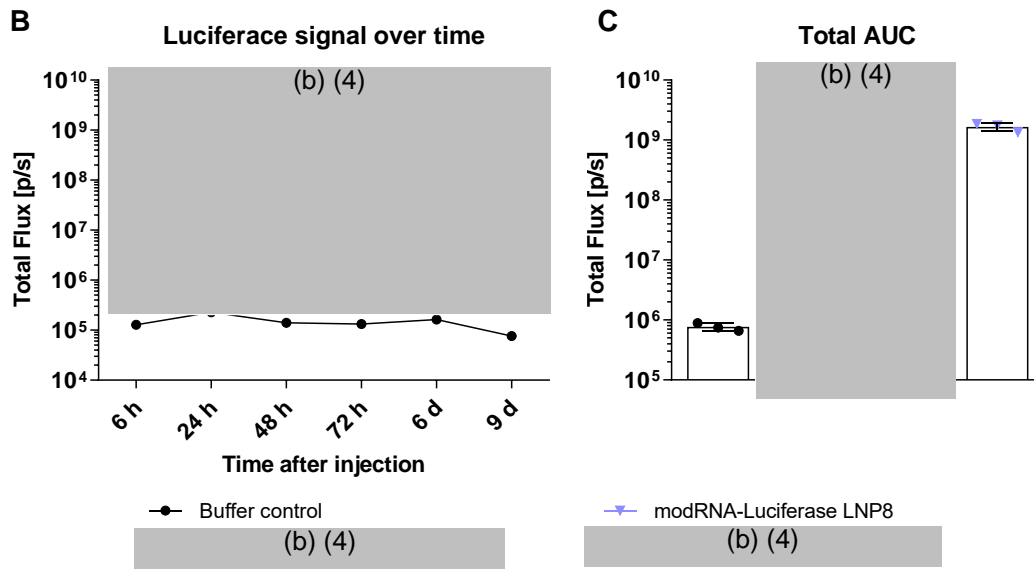


Figure 1: Bioluminescence measurement using the LNP-formulated modRNA encoding for luciferase

BALB/c mice were injected i.m. in the right and left hind leg with each 1 µg of LNP-formulated modRNA encoding luciferase or DPBS only. A) At different time points after injection, the luciferase expression *in vivo* was measured by luciferin application. After 9 d, the reporter expression dropped to background levels. B) Quantification of luciferase signal over time and C) as total area under the curve (AUC, ±SD). p/s: photons per second

All formulations resulted in a modRNA-typical expression over time (Figure 1). Highest signal was detected at the first time points after immunization at the injection site and the signal declined slowly over time until day 9 (Figure 1B). Luciferase expressed by the modRNA formulated with Acuitas LNP8 drained to the liver as visualized by luciferase expression at 6 h in the liver region (b) (4). (b) (4) Acuitas (b) (4) formulations (Figure 1A and Figure 2). Group mean luciferase expression from RNA formulated with Acuitas (b) (4) LNP8 in the muscle at 6 h was approximately 1 × 10⁹ p/s, (b) (4). (b) (4) Hence, Acuitas-formulated modRNA started at about 20-fold higher signal levels, stayed more than 20-fold higher until 72 h (~7 × 10⁷ p/s for (b) (4) LNP8 vs (b) (4)) and declined then to a low level (b) (4) on day 9 (~3–5 × 10⁵ p/s).

Area under the curve calculation allowed comparing overall expression levels over the course of the experiment (Figure 1C). Statistical significance was assessed by one-way ANOVA with Tukey’s multiple comparison post-test comparing all groups with each other. Total luciferase expression from modRNA formulated with (b) (4) (b) (4) while total luciferase expression from modRNA formulated with (b) (4) LNP8 was approximately (b) (4) 1.5 × 10⁹ p/s, respectively. The difference between the area under the curve for (b) (4) LNP8-formulated modRNA compared to buffer control (b) (4) was

090177e195a2e6f3\Approved\Approved On: 27-Nov-2020 16:30 (GMT)

statistically significant ($p < 0.0001$). (b) (4)
 (b) (4)

5.2 Liver Expression (b) (4) LNP8

As mentioned in Section 5.1, luciferase expressed by the modRNA formulated with Acuitas LNP8 drained to the liver as visualized by luciferase expression at 6 h in the liver region (b) (4) Acuita (b) (4) (Figure 2A). Here the luciferase signal of modRNA formulated with (b) (4) LNP8 was quantified for better comparison. Group mean luciferase expression from RNA formulated with Acuitas (b) (4) in the liver at 6 h was (b) (4) while luciferase expression of RNA formulated with LNP8 was at about 4.94×10^7 p/s. Hence, luciferase expression from (b) (4) Acuitas (b) (4) (b) (4) compared to LNP8 (Figure 2B). The liver luciferase expression from RNA formulated with Acuitas LNP8 dropped to 2.4×10^6 p/s at 24 h, while the luciferase signal from RNA formulated with Acuitas (b) (4) No liver signal was detected at 48 h post immunization. Statistical analysis was not performed.

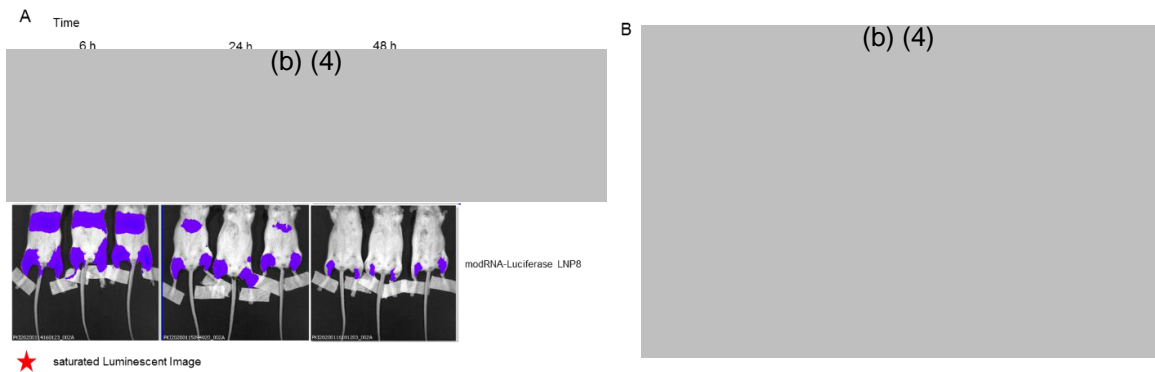


Figure 2: Bioluminescence measurement in the liver using the LNP-formulated modRNA encoding for luciferase

BALB/c mice were injected i.m. in the right and left hind leg with each 1 μ g of LNP-formulated modRNA encoding luciferase. A) At 6 h, 24 h, and 48 h after injection, the luciferase expression *in vivo* was measured by luciferin application. B) Quantification of luciferase signal in the liver over time (mean \pm SD). p/s: photons per second.

5.3 Luminex-based Multiplex Assay

Activation of the innate immune system was assessed in a Luminex-based multiplex assay (Procarta immunoassays). Serum samples (day -1 (pre), 6 h, and day 9) were tested for levels of the following chemokines and cytokines: MCP-1, MIP-1 β , TNF- α , IFN- α , IFN- γ , IL-2, IL-6, IL-10, IL-1 β , IP-10 (Figure 3). No cytokines/chemokines were detected in the pre-serum. (b) (4)

(b) (4) Immunization with LNP8 induced slightly increased levels of MCP-1, IL-6, and IP-10 at 6 h post immunization (b) (4)

090177e195a2e6f3\Approved\Approved On: 27-Nov-2020 16:30 (GMT)

(b) (4) All chemokine/cytokine levels dropped to background levels at day 9. Statistical analysis was not performed for this assay.

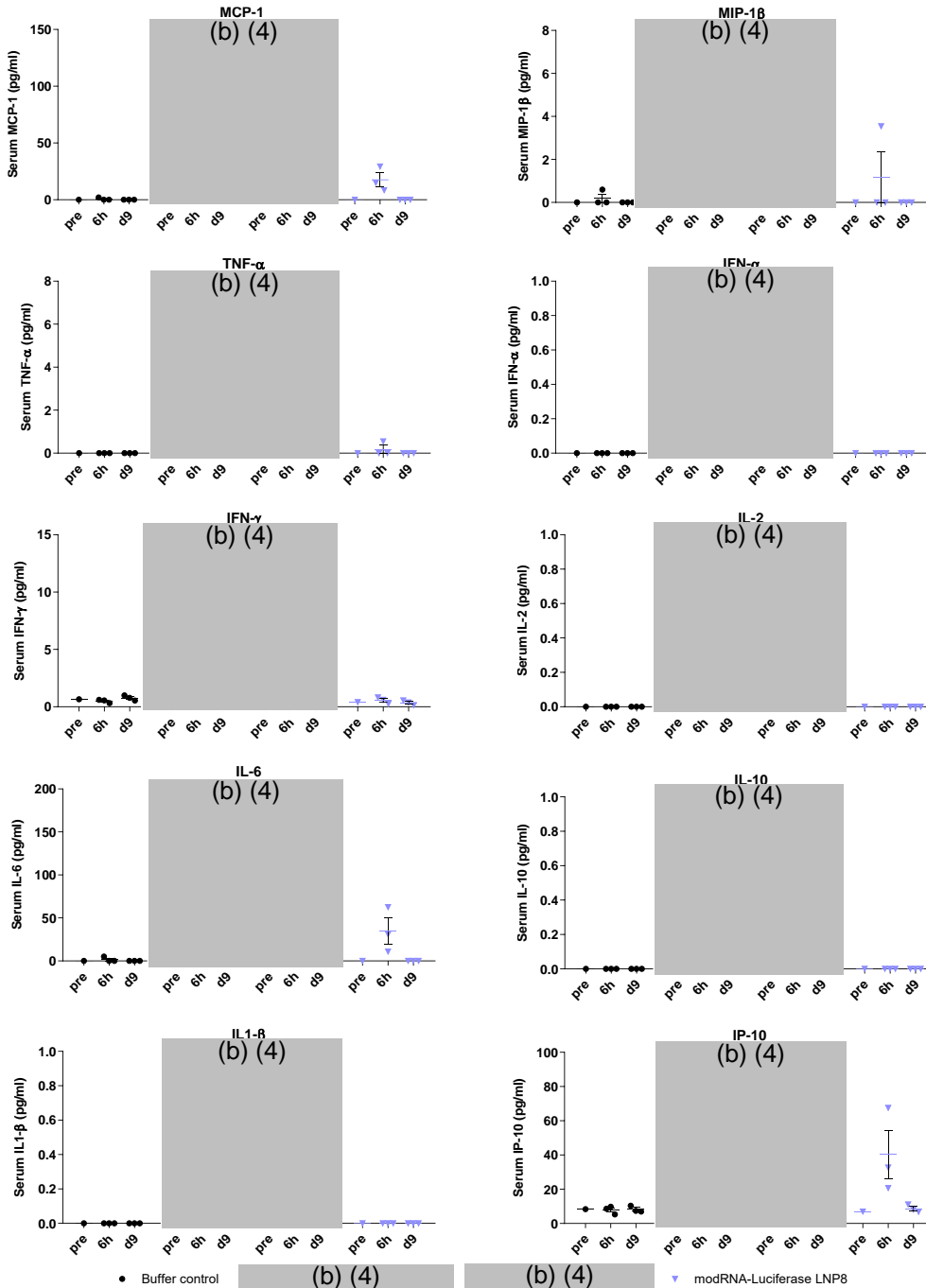


Figure 3: Activation of the innate immune system by LNP-formulated modRNA encoding for luciferase
 BALB/c mice were injected i.m. in the right and left hind leg with each 1 µg of LNP-formulated modRNA encoding luciferase or DPBS only. Serum samples (day -1 (pre), 6 h, and 9 d) were assessed for presence of indicated chemokines/cytokines in a Luminex-based multiplex immunoassay.

090177e195a2e6f3\Approved\Approved On: 27-Nov-2020 16:30 (GMT)

5.4 Luciferase-specific ELISA

Luciferase-specific IgGs in serum samples obtained on study days -1 and 9 were investigated by ELISA.

Before immunization, no luciferase-specific IgGs were detected (day -1, [Figure 4](#)). Treatment with modRNA with all tested LNP formulations did not induce the formation of luciferase-specific IgGs on day 9 post immunization.

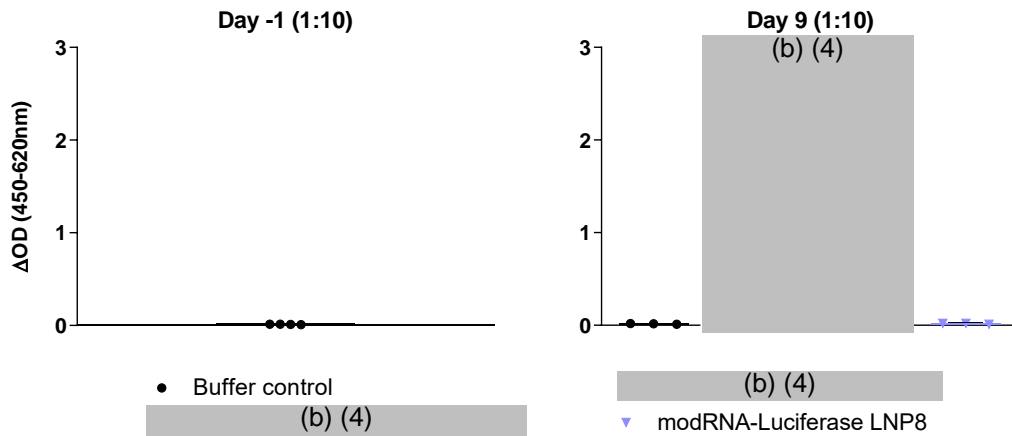


Figure 4: Luciferase-specific IgG ELISA on days -1 and 9

BALB/c mice were immunized with 1 $\mu\text{g}/\text{leg}$ luciferase-encoding modRNA on day 0. Serum samples were collected on days -1 and 9 and the total amount of antigen-specific immunoglobulin G (IgG) was measured via ELISA. The serum 1:10 diluted. Individual ΔOD values are shown by dots; group mean values are indicated by horizontal bars ($\pm\text{SD}$).

5.5 IFN- γ ELISpot Assay

Mice were euthanized on day 9 and splenocytes were isolated to assess T-cell responses by ELISpot analysis. Splenocytes were stimulated with luciferase-specific peptide pools ([Table 5](#)) and IFN- γ secretion was detected. Statistical significance was assessed by one-way ANOVA with Tukey's multiple comparison post-test comparing all groups with each other. Control measurements were performed using an irrelevant peptide pool, medium only, or Concanavalin A.

Stimulation of splenocytes with MHC I-specific peptide pools induced IFN- γ responses in T cells of animals immunized with all modRNA LNP candidates ([Figure 5](#)). Group mean values of 53 spots per 5×10^5 cells were counted for animals injected with buffer control after stimulation with MHC I-specific luciferase peptide pools. The high spot count in can be attributed to reactivity of T cells of one mouse in group 1. Splenocytes of this mouse react also to the stimulation with AH1, the negative control. The group mean values are also 44 spots be 5×10^5 cells for the AH1 control, thus the response

of the control group to the luciferase-specific peptide pool can be considered unspecific. Group mean spot counts after stimulation with MHC I-specific peptide pools were (b) (4)

(b) (4) 519 spots per 5×10^5 cells for the group treated with LNP8-formulated modRNA. The reactivity of splenocytes of the treatment groups to the negative control was very low (6-8 spots per 5×10^5 cells), thus activation of T-cells with luciferase peptides is highly specific in the treatment groups.

(b) (4)

(b) (4) The differences between the groups treated (b) (4) LNP8-formulated modRNAs compared to buffer control were statistically significant ((b) (4) $p = 0.0051$ for modRNA-luciferase LNP8). The (b) (4) and LNP8 groups displayed significantly higher MHC I-specific $IFN-\gamma$ secretion (b) (4)

(b) (4) $p = 0.0163$ for modRNA-luciferase LNP8). (b) (4)

(b) (4)

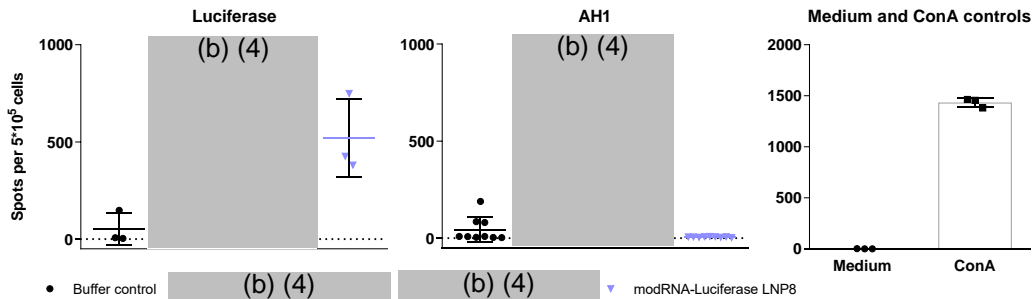


Figure 5: ELISpot analysis using splenocytes on day 9

ELISpot assay was performed using splenocytes isolated on day 9 after prime immunization. Splenocytes were stimulated with MHC I-specific luciferase peptide pools and $IFN-\gamma$ secretion was measured to assess T-cell responses. Individual spot counts are shown by dots; group mean values are indicated by horizontal bars (\pm SD).

090177e195a2e6f3\Approved\Approved On: 27-Nov-2020 16:30 (GMT)

6 CONCLUSION

After injection of LNP-formulated modRNAs, an approximately 20-fold higher luciferase expression at the injections site was observed in a bioluminescence assay for (b) (4) the GMP-ready modRNA-Luciferase LNP8 (b) (4) (b) (4). The difference between the area under the curve for (b) (4) LNP8-formulated modRNA compared to buffer control (b) (4) was statistically significant. (b) (4) (b) (4)

A multiplex assay showed that the innate immune system was temporally activated by (b) (4) LNP8-formulated modRNA. (b) (4) (b) (4) (b) (4)

Treatment with modRNA with all tested LNP formulations did not induce the formation of luciferase-specific IgGs on day 9 as measured by ELISA.

However, a strong antigen-specific IFN- γ T-cell response measured by ELISpot assay on day 9 for (b) (4) LNP8-formulated modRNAs, with statistically significant differences between these test groups and the buffer control (b) (4)

7 DOCUMENT HISTORY

Reasons for changes compared to previous version:

Minor editorial changes, such as the correction of typing errors, are not listed.

Sections	Version 01	Version 02	Reason for change
1	-	More detailed information about LNP8 added	Clarification that LNP8 contains ALC-0159 and ALC-0315
3.1			
6			
4.1		Table added	Details of LNP lipid component formulations

Sections	Version 02	Version 03	Reason for change
4.1	-	Test item information updated	Diameter of LNP8 modRNA was corrected to 71 nm

8 REFERENCES

Limberis MP, Bell CL, Wilson JM. Identification of the murine firefly luciferase-specific CD8 T-cell epitopes. *Gene Ther.* 2009;16(3):441-7.

Moyo N, Vogel AB, Buus S, Erbar S, Wee EG, Sahin U et al. Efficient Induction of T Cells against Conserved HIV-1 Regions by Mosaic Vaccines Delivered as Self-Amplifying mRNA. *Molecular therapy. Methods & clinical development.* 2018; 12, 32-46.

Pardi N, Hogan MJ, Pelc RS, Muramasu H, Andersen H, DeMaso CR et al. Zika virus protection by a single low-dose nucleoside-modified mRNA vaccination. *Nature.* 2017; 543 (7644), 248-251.

Vogel AB, Lambert L, Kinnear E, Busse D, Erbar S, Reuter KC et al. Self-amplifying RNA vaccines give equivalent protection against influenza to mRNA vaccines but at much lower doses. *Molecular therapy: the journal of the American Society of Gene Therapy.* 2017; 26 (2), 446-455.

090177e195a2e6f3\Approved\Approved On: 27-Nov-2020 16:30 (GMT)

9 APPENDIX

Appendix 1: Animal Observations

		-5 days p.a. 09.01.2020		1 days p.a. 15.01.2020			3 days p.a. 17.01.2020			6 days p.a. 20.01.2020		
treatment	Lab ID	weight in g	health	weight in g	% change weight	health	weight in g	% change weight	health	weight in g	% change weight	health
Buffer control	1-1	21.4	No observations	21.7	101.0	No observations	21.5	100.4	No observations	21.7	101.3	No observations
	1-2	22.5	No observations	22.8	101.2	No observations	22.2	98.6	No observations	22.7	100.8	No observations
	1-3	23.0	No observations	23.3	101.4	No observations	23.5	102.3	No observations	23.4	101.5	No observations
modRNA- Luciferase (b) (4)	2-1	20.7	No observations	21.0	101.4	No observations	20.9	100.7	No observations	20.8	100.3	No observations
	2-2	21.5	No observations	22.5	104.6	No observations	22.3	103.8	No observations	23.2	107.9	No observations
	2-3	21.2	No observations	21.4	100.8	No observations	21.3	100.4	No observations	21.3	100.5	No observations
Acuitas LNPs modRNA luciferase	3-1	21.3	No observations	21.5	100.8	No observations	21.4	100.5	No observations	21.0	98.4	No observations
	3-2	21.2	No observations	21.2	99.9	No observations	21.0	99.1	No observations	21.0	99.2	No observations
	3-3	20.9	No observations	21.1	101.0	No observations	22.3	107.0	No observations	21.7	104.1	No observations
modRNA- Luciferase LNP8 (GMP-ready)	4-1	22.2	No observations	23.2	104.7	No observations	22.9	103.2	No observations	23.5	106.1	No observations
	4-2	21.6	No observations	22.4	103.8	No observations	22.5	104.3	No observations	21.9	101.6	No observations
	4-3	20.5	No observations	20.8	101.3	No observations	20.9	101.7	No observations	20.9	101.9	No observations

090177e195a2e6f3\Approved\Approved On: 27-Nov-2020 16:30 (GMT)

Strictly Confidential

Appendix 2: Certificates of Analysis

Confidential



R&D Formulation Characterization Summary:

Batch ID	LNP ID	mRNA ID	Encaps (%)	Encaps mRNA (mg/mL)	Yield (mg)	mRNA/Lipid Ratio (mg/umol)	Particle Diameter (nm)	Poly-dispersity
FM-1074 -D	LNP 8	mod Luc RNA-EH190611-01c	90%	1	0.36	0.025	71	0.053

Notes

Formulated 09-Dec-19
 Diluent: 300 mM sucrose in PBS
 Recommended storage at approximately -80 °C. Avoid repeated freeze/thaw cycles.

(b) (6)

(b) (6) Research Associate

11-Dec-19
Date

090177e195a2e6f3\Approved\Approved On: 27-Nov-2020 16:30 (GMT)

Confidential



R&D Formulation Characterization Summary:

Batch ID	LNP Variant	mRNA ID	Encaps (%)	Encaps mRNA (mg/ml)	Yield (mg)	mRNA/Lipid Ratio (mg/umol)	Particle Diameter (nm)	Poly-dispersity
----------	-------------	---------	------------	---------------------	------------	----------------------------	------------------------	-----------------

(b) (4)

Notes

(b) (4)

(b) (6)
(b) (6) Research Associate

26-Nov-19
Date

1 | Analytical Datasheet

Test items – Formulation: Analytical Data Sheet

Formulation experiment number: FSU-I#029
 Responsible: MeSc, JaKs
 Experimenter: MnSt, JaKs
 Date of preparation: 06Jan20

Physicochemical characterisation:

Sample batch number	Formulation			pH	Osmolality (mOsmol/kg)	Size		Zeta (mV)	Encapsulation efficiency (%)	RNA conc. (mg/mL)	LNP are conform ?
	Lipid Mix	Batch	RNA Batch			Z-Av (nm)	PDI				

(b) (4)

(b) (4)

(b) (4)

090177e195a2e6f3\Approved\Approved On: 27-Nov-2020 16:30 (GMT)

RNA Certificate of Analysis

(Version 17)



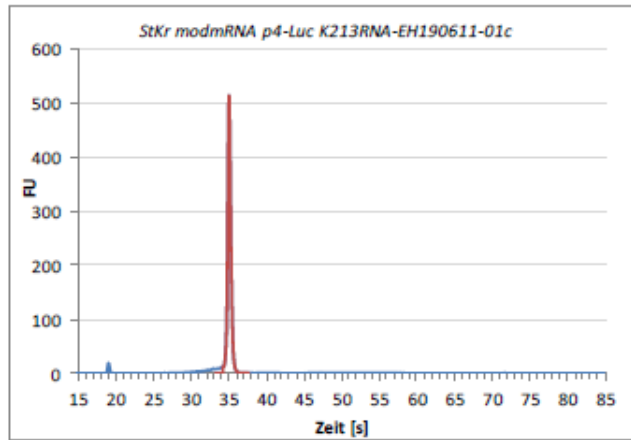
Customer (b) (6)	Date of Order 27.05.2019	RNA-ID RNA-EH190611-01c	Project Number RN9095R00
Cap (b) (4)	Construct modmRNA p4-Luc		
Purification dsRNA removal	Storage Buffer H2O		
Modification m1Y	Concentration [µg/µl] 5,75	Aliquot volume [µl] 10600	Total amount [µg] 60950

Quality Control:

Instrument: Agilent 2100 Bioanalyzer
 Run: mRNA Nano_2019-06-14_001

Results:

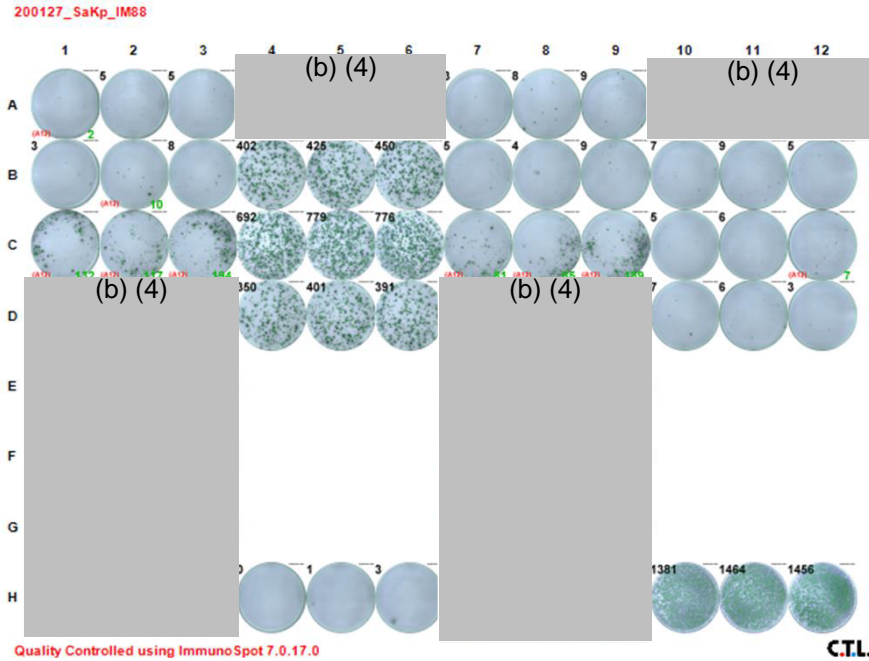
Peak height (FU): 514.963
 Integral (%): 90



090177e195a2e6f3\Approved\Approved On: 27-Nov-2020 16:30 (GMT)

Appendix 3: Raw Data IFN- γ ELISpot

Plate 1: Left, luciferase peptides; right, AH1 ELISpot (irrelevant peptide)



Luc

AH1

	1	2	3	4	5	6	7	8	9	10	11	12
A	Group 1, animal 1			Group 3, animal 3			Group 1, animal 1			Group 3, animal 3		
B	Group 1, animal 2			Group 4, animal 1			Group 1, animal 2			Group 4, animal 1		
C	Group 1, animal 3			Group 4, animal 2			Group 1, animal 3			Group 4, animal 2		
D	Group 2, animal 1			Group 4, animal 3			Group 2, animal 1			Group 4, animal 3		
E	Group 2, animal 2						Group 2, animal 2					
F	Group 2, animal 3						Group 2, animal 3					
G	Group 3, animal 1						Group 3, animal 1					
H	Group 3, animal 2			Medium			Group 3, animal 2			ConA		

Group 1: Buffer control; Group 2: (b) (4) (2x1 μ g); Group 3: (b) (4) (2x1 μ g); Group 4: modRNA-luciferase LNP8 (GMP-ready) (2x1 μ g)

090177e195a2ef3\Approved\Approved On: 27-Nov-2020 16:30 (GMT)

Appendix 4: Statistical Analysis

Bioluminescence assay

Group mean values, bioluminescence assay, luciferase signal over time

Time point	Buffer control	(b) (4)	(b) (4)	modRNA-Luciferase LNP8
	N = 3			N = 3
6 h	128046,667			1,2589e+009
24 h	227766,667			7,310667e+008
48 h	139995			2,1038333e+008
72 h	132585			7,8667e+007
6 d	162383,333			2920333,333
9 d	76573,333			509000

Please note that commas are used as decimal separators.

Descriptive statistics, bioluminescence assay, area under the curve

	Buffer control	(b) (4)	(b) (4)	modRNA-Luciferase LNP8
Number of values	3			3
Minimum	657790			1352000000
Maximum	889908			1848000000
Range	232118			496000000
Mean	765040			1652666667
SD	117058			264244836
SEM	67583			152561827

Please note that commas are used as decimal separators. SD: Standard deviation. SEM: Standard error of the mean.

One-way ANOVA with Tukey's multiple comparisons post-test, bioluminescence assay, area under the curve

ANOVA summary	
F	80,68
P value	<0,0001
P value summary	****
Significant diff. among means (P < 0.05)?	Yes
R square	0,9680

090177e195a2e6f3\Approved\Approved On: 27-Nov-2020 16:30 (GMT)

Tukey's multiple comparisons test	Mean diff.	95,00% CI of diff.	Significant?	Summary	Adjusted P value
(b) (4)					
(b) (4)					
Buffer control vs. modRNA-Luciferase LNP8	-1651901626	-2072407467 to -1231395786	Yes	****	<0,0001
(b) (4)					
(b) (4)					
(b) (4)					

Please note that commas are used as decimal separators. F: F-statistic. P values ≤ 0.05 indicate statistically significant difference. R square: Coefficient of determination. CI: Confidence interval. n.s.: Not significant.

Luciferase-Specific ELISA

Descriptive statistics, luciferase-specific ELISA, day 9

	Buffer control	(b) (4)	(b) (4)	modRNA-Luciferase LNP8
Number of values	3			3
Minimum	0,0110			0,0100
Maximum	0,0190			0,0220
Range	0,00800			0,0120
Mean	0,0153			0,0177
SD	0,00404			0,00666
SEM	0,00233			0,00384

Please note that commas are used as decimal separators. SD: Standard deviation. SEM: Standard error of the mean.

090177e195a2e6f3\Approved\Approved On: 27-Nov-2020 16:30 (GMT)

One-way ANOVA with Tukey's multiple comparisons post-test, bioluminescence assay, area under the curve

ANOVA summary	
F	0,4597
P value	0,6520
P value summary	ns
Significant diff. among means (P < 0.05)?	No
R square	0,1209

No post-test for non-significant main test.

ELISpot analysis

Descriptive statistics, ELISpot analysis, day 9

	Buffer control	(b) (4)	(b) (4)	modRNA-Luciferase LNP8
Number of values	3			3
Minimum	4,00			381
Maximum	148			749
Range	144			368
Mean	53,0			519
SD	82,3			201
SEM	47,5			116

Please note that commas are used as decimal separators. SD: Standard deviation. SEM: Standard error of the mean.

One-way ANOVA with Tukey's multiple comparisons post-test, bioluminescence assay, area under the curve

ANOVA summary	
F	19,90
P value	0,0005
P value summary	***
Significant diff. among means (P < 0.05)?	Yes
R square	0,8819

090177e195a2e6f3\Approved\Approved On: 27-Nov-2020 16:30 (GMT)

Tukey's multiple comparisons test	Mean diff.	95,00% CI of diff.	Significant?	Summary	Adjusted P value
		(b) (4)			
		(b) (4)			
Buffer control vs. modRNA-Luciferase LNP8	-465,7	-769,0 to -162,3	Yes	**	0,0051
		(b) (4)			
		(b) (4)			
		(b) (4)			

Please note that commas are used as decimal separators. F: F-statistic. P values ≤ 0.05 indicate statistically significant difference. R square: Coefficient of determination. CI: Confidence interval. n.s.: Not significant.

090177e195a2e6f3\Approved\Approved On: 27-Nov-2020 16:30 (GMT)

(b) (6)

Von: (b) (6)
Gesendet: Freitag, 27. November 2020 07:24
An: (b) (6)
Cc: (b) (6)
Betreff: signatures: R-20-0072v3.0 (BNT162)
Anlagen: R-20-0072 Report V3.0 Bioluminescence in vivo_final_sig.pdf

Kennzeichnung: Zur Nachverfolgung
Kennzeichnungsstatus: Gekennzeichnet

Hello (b) (6)

With this email I'm giving my approval for the R&D report R-20-0072 version 3 update.

Best,
(b) (6)

(b) (6)
BioNTech SE
(b) (6)

090177e195a2e6f3\Approved\Approved On: 27-Nov-2020 16:30 (GMT)

MODULE 2.6.5. PHARMACOKINETICS TABULATED SUMMARY

This document contains confidential information belonging to BioNTech/Pfizer. Except as may be otherwise agreed to in writing, by accepting or reviewing these materials, you agree to hold such information in confidence and not to disclose it to others (except where required by applicable law), nor to use it for unauthorized purposes. In the event of actual or suspected breach of this obligation, BioNTech/Pfizer should be promptly notified.

CONFIDENTIAL

Page 1

BNT162b2

2.6.5 Pharmacokinetics Tabulated Summary

2.6.5.1. PHARMACOKINETICS OVERVIEW

Test Article: BNT162b2

Type of Study	Test System	Test item	Method of Administration	Testing Facility	Report Number
Single Dose Pharmacokinetics					
Single Dose Pharmacokinetics and Excretion in Urine and Feces of ALC-0159 and ALC-0315	Rat (Wistar Han)	modRNA encoding luciferase formulated in LNP comparable to BNT162b2	IV bolus	Pfizer Inc ^a	PF-07302048_06Jul20_072424
Distribution					
In Vivo Distribution	Mice BALB/c	modRNA encoding luciferase formulated in LNP comparable to BNT162b2	IM Injection	BioNTech ^b	R-20-0072
Metabolism					
In Vitro and In Vivo Metabolism					
In Vitro Metabolic Stability of ALC-0315 in Liver Microsomes	Mouse (CD-1/ICR), rat (Sprague Dawley and Wistar Han), monkey (Cynomolgus), and human liver microsomes	ALC-0315	In vitro	(b) (4)	01049-20008
In Vitro Metabolic Stability of ALC-0315 in Liver S9	Mouse (CD-1/ICR), rat (Sprague Dawley), monkey (Cynomolgus), and human S9 liver fractions	ALC-0315	In vitro	(b) (4)	01049-20009
In Vitro Metabolic Stability of ALC-0315 in Hepatocytes	Mouse (CD-1/ICR), rat (Sprague Dawley and Wistar Han), monkey (Cynomolgus), and human hepatocytes	ALC-0315	In vitro	(b) (4)	01049-20010

090177e1950bbf6fApproved\Approved On: 29-Sep-2020 20:17 (GMT)

BNT162b2

2.6.5 Pharmacokinetics Tabulated Summary

2.6.5.1. PHARMACOKINETICS OVERVIEW

Test Article: BNT162b2

Type of Study	Test System	Test item	Method of Administration	Testing Facility	Report Number
In Vitro Metabolic Stability of ALC-0159 in Liver Microsomes	Mouse (CD-1/ICR), rat (Sprague Dawley and Wistar Han), monkey (Cynomolgus), and human liver microsomes	ALC-0159	In vitro	(b) (4)	01049-20020
In Vitro Metabolic Stability of ALC-0159 in Liver S9	Mouse (CD-1/ICR), rat (Sprague Dawley), monkey (Cynomolgus), and human S9 fractions	ALC-0159	In vitro	(b) (4)	01049-20021
In Vitro Metabolic Stability of ALC-0159 in Hepatocytes	Mouse (CD-1/ICR), rat (Sprague Dawley and Wistar Han), monkey (Cynomolgus), and human hepatocytes	ALC-0159	In vitro	(b) (4)	01049-20022
Biotransformation of ALC-0159 and ALC-0315 In Vitro and In Vivo in Rats	In vitro: CD-1 mouse, Wistar Han rat, cynomolgus monkey, and human blood, liver S9 fractions and hepatocytes In vivo: male Wistar Han rats	ALC-0315 and ALC-0159	In vitro or IV (in vivo in rats)	Pfizer Inc ^d	PF-07302048_05Aug20_043725

ALC-0159 = 2-[(polyethylene glycol)-2000]-N,N-ditetradecylacetamide), a proprietary polyethylene glycol-lipid included as an excipient in the LNP formulation used in BNT162b2; ALC-0315 = (4-hydroxybutyl)azanediylbis(hexane-6,1-diyl)bis(2-hexyldecanoate), a proprietary aminolipid included as an excipient in the LNP formulation used in BNT162b2; IM = Intramuscular; IV = Intravenous; LNP = lipid nanoparticles; S9 = Supernatant fraction obtained from liver homogenate by centrifuging at 9000 g.

a. La Jolla, California.

b. Mainz, Germany.

(b) (4)

d. Groton, Connecticut.

CONFIDENTIAL

Page 3

090177e1950bbf6fApprovedApproved On: 29-Sep-2020 20:17 (GMT)

BNT162b2

2.6.5 Pharmacokinetics Tabulated Summary

**2.6.5.3. PHARMACOKINETICS:
PHARMACOKINETICS AFTER A SINGLE DOSE****Test Article: modRNA encoding luciferase in LNP
Report Number: PF-07302048_06Jul20_072424**

Species (Strain)	Rat (Wistar Han)	
Sex/Number of Animals	Male/ 3 animals per timepoint ^a	
Feeding Condition	Fasted	
Method of Administration	IV	
Dose modRNA (mg/kg)	1	
Dose ALC-0159 (mg/kg)	1.96	
Dose ALC-0315 (mg/kg)	15.3	
Sample Matrix	Plasma	
Sampling Time Points (h post dose):	Predose, 0.1, 0.25, 0.5, 1, 3, 6, 24, 48, 96, 192, 336	
Analyte	ALC-0315	ALC-0159
PK Parameters:	Mean ^b	Mean ^b
AUC _{inf} (µg•h/mL) ^c	1030	99.2
AUC _{last} (µg•h/mL)	1020	98.6
Initial t _{1/2} (h) ^d	1.62	1.74
Terminal elimination t _{1/2} (h) ^e	139	72.7
Estimated fraction of dose distributed to liver (%) ^f	59.5	20.3
Dose in Urine (%)	NC ^g	NC ^g
Dose in Feces (%) ^h	1.05	47.2

ALC-0159 = 2-[(polyethylene glycol)-2000]-N,N-ditetradecylacetamide), a proprietary polyethylene glycol-lipid included as an excipient in the LNP formulation used in BNT162b2; ALC-0315 = (4-hydroxybutyl)azanediylbis(hexane-6,1-diyl)bis(2-hexyldecanoate), a proprietary aminolipid included as an excipient in the LNP formulation used in BNT162b2; AUC_{inf} = Area under the plasma drug concentration-time curve from 0 to infinite time; AUC_{last} = Area under the plasma drug concentration-time curve from 0 to the last quantifiable time point; BLQ = Below the limit of quantitation; LNP = Lipid nanoparticle; modRNA = Nucleoside modified messenger RNA; PK = Pharmacokinetics; t_{1/2} = Half-life.

- Non-serial sampling, 36 animals total.
- Only mean PK parameters are reported due to non-serial sampling.
- Calculated using the terminal log-linear phase (determined using 48, 96, 192, and 336 h for regression calculation).
- ln(2)/initial elimination rate constant (determined using 1, 3, and 6 h for regression calculation).
- ln(2)/terminal elimination rate constant (determined using 48, 96, 192, and 336 h for regression calculation).
- Calculated as follows: highest mean amount in the liver (µg)/total mean dose (µg) of ALC-0315 or ALC-0159.
- Not calculated due to BLQ data.
- Fecal excretion, calculated as: (mean µg of analyte in feces/ mean µg of analyte administered) × 100

CONFIDENTIAL

Page 4

BNT162b2

2.6.5 Pharmacokinetics Tabulated Summary

2.6.5.5. PHARMACOKINETICS: ORGAN DISTRIBUTION

**Test Article: modRNA encoding luciferase in LNP
Report Number: R-20-0072**

Species (Strain):	Mice (BALB/c)
Sex/Number of Animals:	Female/3 per group
Feeding Condition:	Fed ad libitum
Vehicle/Formulation:	Phosphate-buffered saline
Method of Administration:	Intramuscular injection
Dose (mg/kg):	1 µg/hind leg in gastrocnemius muscle (2 µg total)
Number of Doses:	1
Detection:	Bioluminescence measurement
Sampling Time (hour):	6, 24, 48, 72 hours; 6 and 9 days post-injection

Time point	Total Mean Bioluminescence signal (photons/second)		Mean Bioluminescence signal in the liver (photons/second)
	Buffer control	modRNALuciferase in LNP	modRNALuciferase in LNP
6 hours	1.28×10 ⁵	1.26×10 ⁹	4.94×10 ⁷
24 hours	2.28×10 ⁵	7.31×10 ⁸	2.4×10 ⁶
48 hours	1.40×10 ⁵	2.10×10 ⁸	Below detection ^a
72 hours	1.32×10 ⁵	7.87×10 ⁷	Below detection ^a
6 days	1.62×10 ⁵	2.02×10 ⁶	Below detection ^a
9 days	7.66×10 ⁴	5.09×10 ⁵	Below detection ^a

LNP = Lipid nanoparticle; modRNA = Nucleoside modified messenger RNA.

a. At or below the background level of the buffer control.

090177e1950bbf6f\Approved\Approved On: 29-Sep-2020 20:17 (GMT)

BNT162b2

2.6.5 Pharmacokinetics Tabulated Summary

2.6.5.9. PHARMACOKINETICS: METABOLISM IN VIVO, RAT

Test Article: modRNA encoding luciferase in LNP
Report Number: PF-07302048_05Aug20_043725

Species (Strain): Rat (Wistar Han)
 Sex/ Number of animals: Male/ 36 animals total for plasma and urine, 3 animals for urine and feces
 Method of Administration: Intravenous
 Dose (mg/kg): 1
 Test System: Plasma, Urine, Feces, Liver
 Analysis Method: Ultrahigh performance liquid chromatography/ mass spectrometry

Biotransformation	m/z	Metabolites of ALC-0315 Detected			
		Plasma	Urine	Feces	Liver
N-dealkylation, oxidation	102.0561 ^a	ND	ND	ND	ND
N-Dealkylation, oxidation	104.0706 ^b	ND	ND	ND	ND
N-dealkylation, oxidation	130.0874 ^a	ND	ND	ND	ND
N-Dealkylation, oxidation	132.1019 ^b	ND	ND	ND	ND
N-dealkylation, hydrolysis, oxidation	145.0506 ^a	ND	ND	ND	ND
Hydrolysis (acid)	255.2330 ^a	+	ND	ND	ND
Hydrolysis, hydroxylation	271.2279 ^a	ND	ND	ND	ND
Bis-hydrolysis (amine)	290.2690 ^b	+	+	+	+
Hydrolysis, glucuronidation	431.2650 ^a	ND	ND	ND	ND
Bis-hydrolysis (amine), glucuronidation	464.2865 ^a	ND	ND	ND	ND
Bis-hydrolysis (amine), glucuronidation	466.3011 ^b	ND	+	ND	ND
Hydrolysis (amine)	528.4986 ^b	+	ND	ND	+
Hydrolysis (amine), Glucuronidation	704.5307 ^b	ND	ND	ND	ND
Oxidation to acid	778.6930 ^a	ND	ND	ND	ND
Oxidation to acid	780.7076 ^b	ND	ND	ND	ND
Hydroxylation	782.7232 ^b	ND	ND	ND	ND
Sulfation	844.6706 ^a	ND	ND	ND	ND
Sulfation	846.6851 ^b	ND	ND	ND	ND
Glucuronidation	940.7458 ^a	ND	ND	ND	ND
Glucuronidation	942.7604 ^b	ND	ND	ND	ND

Note: Both theoretical and observed metabolites are included.

m/z = mass to charge ratio; ND = Not detected; + = minor metabolite as assessed by ultraviolet detection.

a. Negative ion mode.

b. Positive ion mode.

CONFIDENTIAL

Page 6

090177e1950bbf6f\Approved\Approved On: 29-Sep-2020 20:17 (GMT)

BNT162b2

2.6.5 Pharmacokinetics Tabulated Summary

2.6.5.10A. PHARMACOKINETICS: METABOLISM IN VITRO

Test Article: **ALC-0315**
 Report Numbers: **01049-20008**
01049-20009
01049-20010

Type of Study:	Liver Microsomes + NADPH		Stability of ALC-0315 In Vitro S9 Fraction + NADPH, UDPGA, and alamethicin				Hepatocytes							
Study System:														
ALC-0315 Concentration:	1 µM		1 µM				1 µM							
Duration of Incubation (min):	120 min		120 min				240 min							
Analysis Method:	Ultra-high performance liquid chromatography-tandem mass spectrometry													
Incubation time (min)	Percent ALC-0315 remaining													
	Liver Microsomes					Liver S9 Fraction				Hepatocytes				
	Mouse (CD-1/ICR)	Rat (SD)	Rat (WH)	Monkey (Cyno)	Human	Mouse (CD-1/ICR)	Rat (SD)	Monkey (Cyno)	Human	Mouse (CD-1/ICR)	Rat (SD)	Rat (WH)	Monkey (Cyno)	Human
0	100.00	100.00	100.00	100.00	100.00	100.00	100.00	100.00	100.00	100.00	100.00	100.00	100.00	100.00
15	98.77	94.39	96.34	97.96	100.24	97.69	98.85	99.57	95.99	--	--	--	--	--
30	97.78	96.26	97.32	96.18	99.76	97.22	99.62	96.96	97.32	101.15	97.75	102.70	96.36	100.72
60	100.49	99.73	98.54	100.00	101.45	98.61	99.62	99.13	94.98	100.77	98.50	102.32	97.82	101.44
90	97.78	98.66	94.15	97.96	100.48	98.15	98.85	98.70	98.33	101.92	99.25	103.09	100.0	100.36
120	96.54	95.99	93.66	97.71	98.31	96.76	98.46	99.57	99.33	98.85	97.38	99.61	96.36	100.72
180	--	--	--	--	--	--	--	--	--	101.15	98.88	103.47	95.64	98.92
240	--	--	--	--	--	--	--	--	--	99.62	101.12	100.00	93.82	99.64
t _½ (min)	>120	>120	>120	>120	>120	>120	>120	>120	>120	>240	>240	>240	>240	>240

-- = Data not available; ALC-0315 = (4-hydroxybutyl)azanediylbis(hexane-6,1-diyl)bis(2-hexyldecanoate), a proprietary aminolipid included as an excipient in the lipid nanoparticle formulation used in BNT162b2; Cyno = Cynomolgus; NADPH = Reduced form of nicotinamide adenine dinucleotide phosphate; NC = not calculated; SD = Sprague Dawley; t_½ = half-life; WH = Wistar-Han; UDPGA= uridine-diphosphate-glucuronic acid trisodium salt.

090177e1950bbf6fApproved On: 29-Sep-2020 20:17 (GMT)

BNT162b2

2.6.5 Pharmacokinetics Tabulated Summary

**2.6.5.10B. PHARMACOKINETICS: METABOLISM IN VITRO
CONTINUED**

Test Article: ALC-0159
Report Numbers: **01049-20020**
01049-20021
01049-20022

Type of Study:	Liver Microsomes + NADPH	Stability of ALC-0159 In Vitro S9 Fraction + NADPH, UDPGA, and alamethicin	Hepatocytes
Study System:			
ALC-0159 Concentration:	1 µM	1 µM	1 µM
Duration of Incubation (min):	120 min	120 min	240 min
Analysis Method:	Ultra-high performance liquid chromatography-tandem mass spectrometry		

Incubation time (min)	Percent ALC-0159 remaining													
	Liver Microsomes					Liver S9 Fraction				Hepatocytes				
	Mouse (CD- 1/ICR)	Rat (SD)	Rat (WH)	Monkey (Cyno)	Human	Mouse (CD-1/ICR)	Rat (SD)	Monkey (Cyno)	Human	Mouse (CD- 1/ICR)	Rat (SD)	Rat (WH)	Monkey (Cyno)	Human
0	100.00	100.00	100.00	100.00	100.00	100.00	100.00	100.00	100.00	100.00	100.00	100.00	100.00	100.00
15	82.27	101.24	112.11	100.83	99.59	98.93	84.38	91.30	106.73	--	--	--	--	--
30	86.40	93.78	102.69	85.12	92.28	91.10	90.87	97.96	107.60	100.85	93.37	113.04	90.23	106.34
60	85.54	98.34	105.38	86.36	95.53	102.85	97.97	105.56	104.97	94.92	91.81	105.07	92.93	101.58
90	85.41	95.44	100.90	94.63	97.97	90.75	93.51	108.33	109.36	94.28	90.25	112.80	94.59	92.67
120	95.87	97.10	108.97	93.39	93.09	106.76	92.70	105.74	119.59	87.08	89.47	104.11	97.51	96.04
180	--	--	--	--	--	--	--	--	--	94.92	93.96	102.90	89.81	93.66
240	--	--	--	--	--	--	--	--	--	102.75	94.93	98.79	92.93	102.57
t _{1/2} (min)	NC	>120	NC	>120	>120	>120	>120	>120	>120	>240	>240	>240	>240	>240

-- = Data not available; ALC-0159 = 2-[(polyethylene glycol)-2000]-N,N-ditetradecylacetamide), a proprietary polyethylene glycol-lipid included as an excipient in the lipid nanoparticle formulation used in BNT162b2; Cyno = Cynomolgus; NADPH = Reduced form of nicotinamide adenine dinucleotide phosphate; NC = not calculated; SD = Sprague Dawley; WH = Wistar-Han; UDPGA= uridine-diphosphate-glucuronic acid trisodium salt.

090177e1950bbf6f\Approved\Approved On: 29-Sep-2020 20:17 (GMT)

BNT162b2

2.6.5 Pharmacokinetics Tabulated Summary

**2.6.5.10C. PHARMACOKINETICS: METABOLISM
IN VITRO CONTINUED**

**Test Article: ALC-0315
Report Number: PF-07302048_05Aug20_043725**

Type of study		Metabolism of ALC-0315 In Vitro											
Study system		Blood				Hepatocytes				Liver S9 Fraction			
ALC-0315 concentration		10 µM				10 µM				10 µM			
Duration of incubation		24 h				4 h				24 h			
Analysis Method:		Ultrahigh performance liquid chromatography/ mass spectrometry											
Biotransformation	m/z	Blood				Hepatocytes				Liver S9 Fraction			
		Mouse	Rat	Monkey	Human	Mouse	Rat	Monkey	Human	Mouse	Rat	Monkey	Human
<i>N</i> -dealkylation, oxidation	102.0561 ^a	ND	ND	ND	ND	ND	ND	ND	ND	ND	ND	ND	ND
<i>N</i> -Dealkylation, oxidation	104.0706 ^b	ND	ND	ND	ND	ND	ND	ND	ND	ND	ND	ND	ND
<i>N</i> -dealkylation, oxidation	130.0874 ^a	ND	ND	ND	ND	ND	ND	ND	ND	ND	ND	ND	ND
<i>N</i> -Dealkylation, oxidation	132.1019 ^b	ND	ND	ND	ND	ND	ND	ND	ND	ND	ND	ND	ND
<i>N</i> -dealkylation, hydrolysis, oxidation	145.0506 ^a	ND	ND	ND	ND	ND	ND	ND	ND	ND	ND	ND	ND
Hydrolysis (acid)	255.2330 ^a	+	+	ND	ND	+	+	+	+	+	+	ND	+
Hydrolysis, hydroxylation	271.2279 ^a	ND	ND	ND	ND	ND	ND	ND	ND	ND	ND	ND	ND
Bis-hydrolysis (amine)	290.2690 ^b	+	+	ND	ND	ND	ND	ND	ND	ND	ND	+	ND
Hydrolysis, glucuronidation	431.2650 ^a	ND	ND	ND	ND	ND	ND	ND	ND	ND	ND	ND	ND
Bis-hydrolysis (amine), glucuronidation	464.2865 ^a	ND	ND	ND	ND	ND	ND	ND	ND	ND	ND	ND	ND
Bis-hydrolysis (amine), glucuronidation	466.3011 ^b	ND	ND	ND	ND	ND	ND	ND	ND	ND	ND	ND	ND
Hydrolysis (amine)	528.4986 ^b	ND	+	ND	ND	ND	ND	ND	ND	ND	ND	+	ND
Hydrolysis (amine), glucuronidation	704.5307 ^b	ND	ND	ND	ND	ND	ND	ND	ND	ND	ND	ND	ND
Oxidation to acid	778.6930 ^a	ND	ND	ND	ND	ND	ND	ND	ND	ND	ND	ND	ND
Oxidation to acid	780.7076 ^b	ND	ND	ND	ND	ND	ND	ND	ND	ND	ND	ND	ND
Hydroxylation	782.7232 ^b	ND	ND	ND	ND	ND	ND	ND	ND	ND	ND	ND	ND
Sulfation	844.6706 ^a	ND	ND	ND	ND	ND	ND	ND	ND	ND	ND	ND	ND
Sulfation	846.6851 ^b	ND	ND	ND	ND	ND	ND	ND	ND	ND	ND	ND	ND
Glucuronidation	940.7458 ^a	ND	ND	ND	ND	ND	ND	ND	ND	ND	ND	ND	ND
Glucuronidation	942.7604 ^b	ND	ND	ND	ND	ND	ND	ND	ND	ND	ND	ND	ND

Note: Both theoretical and observed metabolites are included.
 m/z = mass to charge ratio; ND = Not detected; + = metabolite present.
 a. Negative ion mode.
 b. Positive ion mode.

090177e1950bbf6fApproved\Approved On: 29-Sep-2020 20:17 (GMT)

BNT162b2

2.6.5 Pharmacokinetics Tabulated Summary

**2.6.5.10D. PHARMACOKINETICS: METABOLISM
IN VITRO CONTINUED**

Test Article: ALC-0159
Report Number: PF-07302048_05Aug20_043725

Type of study		Metabolism of ALC-0159 In Vitro											
Study system		Blood				Hepatocytes				Liver S9 Fraction			
ALC-0159 concentration		10 µM				10 µM				10 µM			
Duration of incubation		24 h				4 h				24 h			
Analysis Method:		Ultrahigh performance liquid chromatography/ mass spectrometry											
Biotransformation	m/z	Blood				Hepatocytes				Liver S9 Fraction			
		Mouse	Rat	Monkey	Human	Mouse	Rat	Monkey	Human	Mouse	Rat	Monkey	Human
<i>O</i> -Demethylation, <i>O</i> -dealkylation	107.0703 ^b	ND	ND	ND	ND	ND	ND	ND	ND	ND	ND	ND	ND
<i>O</i> -Demethylation, <i>O</i> -dealkylation	151.0965 ^b	ND	ND	ND	ND	ND	ND	ND	ND	ND	ND	ND	ND
<i>O</i> -Demethylation, <i>O</i> -dealkylation	195.1227 ^b	ND	ND	ND	ND	ND	ND	ND	ND	ND	ND	ND	ND
Hydrolysis, <i>N</i> -Dealkylation	214.2529 ^b	ND	ND	ND	ND	ND	ND	ND	ND	ND	ND	ND	ND
<i>N</i> -Dealkylation, oxidation	227.2017 ^a	ND	ND	ND	ND	ND	ND	ND	ND	ND	ND	ND	ND
Hydrolysis (amine)	410.4720 ^b	+	+	ND	ND	+	+	+	+	+	+	+	+
<i>N,N</i> -Didealkylation	531.5849 ^b	ND	ND	ND	ND	ND	ND	ND	ND	ND	ND	ND	ND
<i>N</i> -Dealkylation	580.6396 ^b	ND	ND	ND	ND	ND	ND	ND	ND	ND	ND	ND	ND
<i>O</i> -Demethylation, oxidation	629.6853 ^b	ND	ND	ND	ND	ND	ND	ND	ND	ND	ND	ND	ND
Hydroxylation	633.6931 ^b	ND	ND	ND	ND	ND	ND	ND	ND	ND	ND	ND	ND
ω -Hydroxylation, Oxidation	637.1880 ^b	ND	ND	ND	ND	ND	ND	ND	ND	ND	ND	ND	ND
Hydrolysis (acid)	708.7721 ^b	ND	ND	ND	ND	ND	ND	ND	ND	ND	ND	ND	ND

Note: Both theoretical and observed metabolites are included.
 m/z = mass to charge ratio; ND = Not detected; + = metabolite present.
 a. Negative ion mode.
 b. Positive ion mode.

090177e1950bbf6f\Approved\Approved On: 29-Sep-2020 20:17 (GMT)

**Appendix 1: Justification for the absence of studies in CTD Module 4
(part of 2.4)**

CTD Section	Title	Reason not included in the dossier
4.2.1	Pharmacology	
4.2.1.1	Primary Pharmacodynamics	Study reports included.
4.2.1.2	Secondary Pharmacodynamics	No secondary pharmacodynamics studies were conducted with BNT162b2.
4.2.1.3	Safety Pharmacology	No safety pharmacology studies were conducted as they are not considered necessary according to the WHO guideline (WHO, 2005).
4.2.1.4	Pharmacodynamic Drug Interactions	Nonclinical studies evaluating pharmacodynamic drug interactions were not conducted as they are generally not considered necessary to support development and licensure of vaccine products for infectious diseases (WHO, 2005).
4.2.2	Pharmacokinetics	
4.2.2.1	Analytical Methods and Validation Reports (if separate reports are available)	No methods of analysis have been validated to support GLP TK studies of components of the BNT162b2; however, a qualified LCMS method was developed to support quantitation of the two novel LNP excipients for the non-GLP IV PK study (PF-07302048 06Jul20 072424).
4.2.2.2	Absorption	No specific absorption studies have been carried out with BNT162b2 or the novel lipid excipients as the vaccine is dosed IM. Study report included for PK of novel lipid excipients.
4.2.2.3	Distribution	Study report included.
4.2.2.4	Metabolism	Study reports included for metabolic stability and biotransformation of the novel lipid excipients.
4.2.2.5	Excretion	Study report included for excretion of novel lipid excipients.
4.2.2.6	Pharmacokinetic Drug Interactions (nonclinical)	No PK drug interaction studies have been conducted with BNT162b2.
4.2.2.7	Other Pharmacokinetic Studies	No other PK studies have been conducted with BNT162b2.
4.2.3	Toxicology	
4.2.3.1	Single-Dose Toxicity (in order by species, by route)	A separate single-dose toxicity study with BNT162b2 has not been conducted. Studies using N+1 dosing strategy was incorporated into the repeat dose studies (WHO, 2005).

090177e1950ad582\Approved\Approved On: 29-Sep-2020 15:49 (GMT)

CTD Section	Title	Reason not included in the dossier
4.2.3.2	Repeat-Dose Toxicity (in order by species, by route, by duration; including supportive toxicokinetics evaluations)	Study report included for BNT162b2 (V8) (Study38166). Dosing phase summary and data report included for BNT162b2 (V9) (Study 20GR142).
4.2.3.3	Genotoxicity	No genotoxicity studies are planned for BNT162b2 as the components of the vaccine constructs are lipids and RNA that are not expected to have genotoxic potential (WHO, 2005).
4.2.3.3.1	In vitro	See above.
4.2.3.3.2	In vivo (including supportive toxicokinetics evaluations)	See above.
4.2.3.4	Carcinogenicity (including supportive toxicokinetics evaluations)	Carcinogenicity studies with BNT162b2 have not been conducted as the components of the vaccine constructs are lipids and RNA that are not expected to have carcinogenic or tumorigenic potential. Carcinogenicity testing is generally not considered necessary to support the development and licensure of vaccine products for infectious diseases (WHO, 2005).
4.2.3.4.1	Long-term studies (in order by species; including range-finding studies that cannot appropriately be included under repeat-dose toxicity or pharmacokinetics)	See above.
4.2.3.4.2	Short- or medium-term studies (including range-finding studies that cannot appropriately be included under repeat-dose toxicity or pharmacokinetics)	See above.
4.2.3.4.3	Other studies	See above.

090177e1950ad582\Approved\Approved On: 29-Sep-2020 15:49 (GMT)

CTD Section	Title	Reason not included in the dossier
4.2.3.5	Reproductive and Developmental Toxicity (including range-finding studies and supportive TK evaluations)	Reproductive and developmental toxicity assessments are ongoing with BNT162b2 (V9) (Study 20256434). Macroscopic and microscopic evaluation of male and female reproductive tissues from the repeat-dose toxicity study with BNT162b2 (V8) showed no evidence of toxicity (Study 38166).
4.2.3.5.1	Fertility and early embryonic development	See above
4.2.3.5.2	Embryo-fetal development	See above
4.2.3.5.3	Prenatal and postnatal development, including maternal function	See above
4.2.3.5.4	Studies in which the offspring (juvenile animals) are dosed and/or further evaluated.	Pre-weaning evaluations are included in the DART study (Study 20256434) indicated above.
4.2.3.6	Local Tolerance	Local tolerance of IM administration was evaluated in the repeat-dose toxicity studies (Study 38166 and Study 20GR142).
4.2.3.7	Other Toxicity Studies (if available)	See below
4.2.3.7.1	Antigenicity	Immunogenicity was evaluated as part of the primary pharmacology studies and the repeat-dose toxicity study (Study 38166).
4.2.3.7.2	Immunotoxicity	Stand-alone immunotoxicity studies BNT162b2 have not been conducted. However, immunotoxicological endpoints have been collected as part of the repeat-dose toxicity studies (Study 38166 and Study 20GR142).
4.2.3.7.3	Mechanistic studies (if not included elsewhere)	Mechanistic studies with BNT162b2 have not been conducted. Mechanistic studies are generally not required for vaccines (WHO, 2005).
4.2.3.7.4	Dependence	Dependence studies with BNT162b2 have not been conducted. Dependence studies are generally not required for vaccines (WHO, 2005).
4.2.3.7.5	Metabolites	Stand-alone studies with administration of metabolites of BNT162b2 have not been conducted and are generally not required for vaccines (WHO, 2005).
4.2.3.7.6	Impurities	Stand-alone studies with administration of impurities of BNT162b2 have not been conducted.

090177e1950ad582\Approved\Approved On: 29-Sep-2020 15:49 (GMT)

CTD Section	Title	Reason not included in the dossier
4.2.3.7.7	Other	No other studies with BNT162b2 evaluated in this submission have been conducted.

GLP = Good Laboratory Practice; IV = Intravenous; LCMS = Liquid chromatography mass spectrometry; PK = Pharmacokinetic; TK = Toxicokinetic; WHO = World Health Organization.

REFERENCES:

Study 38166. Engel L. Repeat-Dose Toxicity Study of Three LNP-Formulated RNA Platforms Encoding for Viral Proteins by Repeated Intramuscular Administration to Wistar Han Rats. 01 Jul 2020.

Study 20GR142. Giovanelli M. 17-Day Intramuscular Toxicity Study of BNT162B2 (V9) and BNT162B3C in Wistar Han Rats with a 3-Week Recovery. Study ongoing.

Study 20256434 (RN9391R58). Bouressam M. Combined Fertility and Developmental Study (Including Teratogenicity and Postnatal Investigations) of BNT162b1, BNT162b2 and BNT162b3 by the Intramuscular Route in the Wistar Rat GLP Study. Study ongoing.

PF-07302048_06Jul20_072424. Kraynov E. A Single Dose Pharmacokinetics Study of ALC-0315 and ALC-0159 Following Intravenous Bolus Injection of PF-07302048 Nanoparticle Formulation in Wistar Han Rats. TBD.

World Health Organization. WHO guidelines on nonclinical evaluation of vaccines. Annex 1. In: World Health Organization. WHO technical report series, no. 927. Geneva, Switzerland; World Health Organization; 2005:31-63.

090177e1950ad582\Approved\Approved On: 29-Sep-2020 15:49 (GMT)



BioNTech SE
An der Goldgrube 12
55131 Mainz, Germany
Phone: +49 (0)6131 9084-0
Telefax: +49 (0)6131 9084-390

R&D STUDY REPORT No. R-20-0072

EXPRESSION OF LUCIFERASE-ENCODING MODRNA AFTER I.M. APPLICATION OF GMP- READY ACUITAS LNP FORMULATION

Version 01

Date: 16 APR 2020

Reported by (b) (6)

Test item: modRNA encoding luciferase

Key words: COVID-19, modRNA, biodistribution, mouse, bioluminescence assay

This R&D report consists of 37 pages.

Confidentiality Statement: The information contained in this document is the property and copyright of BioNTech RNA Pharmaceuticals GmbH. Therefore, this document is provided in confidence to the recipient (e.g. regulatory authorities, IECs/IRBs, investigators, auditors, inspectors). No information contained herein shall be published, disclosed, or reproduced without prior written approval of the proprietors.

090177e19346f093\Approved\Approved On: 20-Apr-2020 13:17 (GMT)

TABLE OF CONTENTS

LIST OF FIGURES 4

LIST OF TABLES 4

LIST OF ABBREVIATIONS 5

RESPONSIBILITIES 6

1 SUMMARY 7

2 GENERAL INFORMATION 9

2.1 Sponsor and Test Facilities 9

2.2 Participating Personnel 9

2.3 Study Dates 9

2.4 Guidelines and Regulations 10

2.5 Changes and Deviations 10

2.6 Documentation and Archive 10

3 INTRODUCTION 11

3.1 Background 11

3.2 Objectives 11

3.3 Study Design 12

4 MATERIALS AND METHODS 12

4.1 Test Item 12

4.2 Control Item 13

4.3 Test System 13

4.4 Materials 13

4.5 Methods 14

4.5.1 Animal Care 14

4.5.1.1 General Information 14

4.5.1.2 Housing Condition and Husbandry 15

4.5.2 Animal Monitoring 15

4.5.3 Endpoint of Experiment / Termination Criteria 16

4.5.4 Injection of Test and Control Items 16

4.5.5 Bioluminescence Measurements 16

4.5.6 Blood Sampling via the *Vena Facialis* 16

4.5.7 Luminex-based multiplex assay (ProcartaPlex Multiplex Immunoassay) 17

4.5.8 Luciferase-specific ELISA 17

4.5.9 ELISpot Analysis 17

4.5.9.1 T-cell epitope prediction 17

4.5.9.2 Sample Collection and Processing 18

4.5.9.3 IFN-γ ELISpot Assay 18

4.5.10 Statistical Analysis 18

5 RESULTS 19

5.1 Bioluminescence measurements 19

5.2 Liver expression (b) (4) vs LNP8 21

5.3 Luminex-based multiplex assay 22

090177e19346f093\Approved\Approved On: 20-Apr-2020 13:17 (GMT)

5.4 Luciferase-specific ELISA 24

5.5 IFN- γ ELISpot Assay 24

6 CONCLUSION..... 26

7 DOCUMENT HISTORY 27

8 REFERENCES 28

9 APPENDIX 29

Appendix 1: Animal Observations 29

Appendix 2: Certificates of Analysis..... 30

Appendix 3: Raw Data IFN- γ ELISpot..... 33

Appendix 4: Statistical Analysis 34

090177e19346f093\Approved\Approved On: 20-Apr-2020 13:17 (GMT)

LIST OF FIGURES

Figure 1: Bioluminescence measurement using the LNP-formulated modRNA encoding for luciferase20

Figure 2: Bioluminescence measurement in the liver using the LNP-formulated modRNA encoding for luciferase22

Figure 3: Activation of the innate immune system by LNP-formulated modRNA encoding for luciferase23

Figure 4: Luciferase-specific IgG ELISA on days -1 and 924

Figure 5: ELISpot analysis using splenocytes on day 9.....25

LIST OF TABLES

Table 1: Study design 12

Table 2: Materials 13

Table 3: Software 14

Table 4: Peptide pool for stimulation of splenocytes..... 14

090177e19346f093\Approved\Approved On: 20-Apr-2020 13:17 (GMT)

LIST OF ABBREVIATIONS

ALP	Alkaline phosphatase
ANOVA	Analysis of variance
AUC	Area under the curve
BALB/c	Mouse strain used in this study
BCIP	5-Bromo-4-chloro-3-indolyl-phosphate
ConA	Concanavalin A
COVID-19	Coronavirus disease emerged 2019
DPBS	Dulbecco's phosphate-buffered saline
ELISA	Enzyme-linked immunosorbent assay
ELISpot	Enzyme-linked immunospot
FELASA	Federation of European Laboratory Animal Science Associations
GMP	Good manufacturing practice
HRP	Horseradish peroxidase
IFN	Interferon
IgG	Immunoglobulin
IL	Interleukin
i.m.	Intramuscularly
IP-10	Interferon-gamma induced protein 10
IVIS	In Vivo Imaging System
LNP	Lipid nanoparticle
Luc	Luciferase (from firefly <i>Pyroactomena lucifera</i>)
MCP-1	Monocyte chemotactic protein 1
MHC	Major histocompatibility complex
MIP-1 β	Macrophage inflammatory protein 1 β
modRNA	Nucleoside modified mRNA
NBT	Nitro blue tetrazolium
OD	Optical density
p/s	Photons per second
RNA	Ribonucleic Acid
SD	Standard deviation
SOP	Standard operating procedure
S protein	Spike protein
saRNA	Self-amplifying mRNA
SARS-CoV-2	Severe Acute Respiratory Syndrome-Coronavirus-2
TNF- α	Tumor necrosis factor α

090177e19346f093\Approved\Approved On: 20-Apr-2020 13:17 (GMT)

RESPONSIBILITIES

Person responsible for the study:	(b) (6)	15 APR 2020
	(b) (6) BioNTech (b) (6)	Date
Author:	(b) (6)	15 APR 2020
	(b) (6) BioNTech SE	Date
Reviewer:	(b) (6)	16 APR 2020
	(b) (6) BioNTech (b) (6)	Date
QA representative:	(b) (6)	16 APR 2020
	(b) (6) BioNTech SE	Date

Meaning of the signatures:

Person responsible for the study: I am responsible for the content of the R&D report and confirm that it represents an accurate record of the results. This study was performed according to the SOPs and methods as well as the rules and regulations described in the report.

Author: I am the author of this document.

Reviewer: I reviewed the R&D report and confirm that this document complies with the scientific and technical standards and requirements.

QA representative: I confirm that this document complies with the relevant quality assurance requirements.

Strictly Confidential

090177e19346f093\Approved\Approved On: 20-Apr-2020 13:17 (GMT)

1 SUMMARY

BioNTech is developing RNA-based vaccines designed to protect against the novel coronavirus disease that emerged in 2019 (COVID-19). The project involves testing three RNA platforms, which are under development at BioNTech with the surface or spike protein (S protein) of the novel Coronavirus (SARS-CoV-2) as the viral antigen. These RNAs will be formulated with a GMP-compatible LNP formulation provided by Acuitas (LNP8).

In this study, LNP 8 was tested in comparison with a (b) (4) by Acuitas, (b) (4) and an in-house formulation, (b) (4) to characterize the biodistribution of luciferase expressed by LNP-formulated nucleoside-modified mRNA (modRNA) as well as innate immune system activation, formation of antibodies against luciferase and T-cell activation.

Four groups of three BALB/c mice were injected intramuscularly (i.m.) with a total dose of 2 µg/animal of (b) (4) LNP8- or (b) (4)-formulated modRNA encoding luciferase or with buffer (DPBS) as control. At 6 h, 24 h, 48 h, 72 h, 6 d and 9 d after injection, the *in vivo* luciferase expression was measured by luciferin application. Serum samples were taken 1 day before and 6 h after immunization as well as on day 9 for quantification of the activation of the innate immune system in a Luminex-based multiplex assay and antigen-binding antibody analysis in an IgG-specific ELISA. Splenocytes were isolated on 9 d to assess the T-cell response by IFN-γ ELISpot Assay.

An approximately 20-fold higher luciferase expression at the injections site was observed for modRNA-Luciferase (b) (4) and the GMP-ready modRNA-Luciferase LNP8 when compared to modRNA formulated with (b) (4). The difference between the area under the curve for (b) (4) and LNP8-formulated modRNA compared to buffer control as well as to (b) (4)-formulated modRNA was statistically significant. In addition, luciferase expressed from the (b) (4)-formulated modRNA showed limited drainage to the liver compared to LNP8-formulated modRNA.

A multiplex assay showed that the innate immune system was temporally activated by (b) (4) and LNP8-formulated modRNA. The activation was more pronounced for (b) (4) formulated modRNA than for modRNA formulated with LNP8, indicating a formulation-related effect rather than a payload or expression level effect.

Treatment with modRNA with all tested LNP formulations did not induce the formation of luciferase-specific IgGs on day 9. However, a strong antigen-specific IFN-γ T-cell response was measured by ELISpot assay on day 9 for (b) (4) and LNP8-formulated modRNAs, with statistically significant differences between these test groups, the buffer control and the (b) (4) group.

090177e19346f093\Approved\Approved On: 20-Apr-2020 13:17 (GMT)

In conclusion, despite different biodistribution characteristics, both Acuitas LNPs allowed a high antigen expression level thereby inducing a strong T-, but not B-cell response on day 9 post immunization.

	(b) (6)		15 APR 2020
Responsible Person:	(b) (6)	(b) (6)	Date
(b) (6) BioNTech	(b) (6)		

090177e19346f093\Approved\Approved On: 20-Apr-2020 13:17 (GMT)

2 GENERAL INFORMATION

2.1 Sponsor and Test Facilities

Sponsor

BioNTech RNA Pharmaceuticals GmbH
 An der Goldgrube 12
 55131 Mainz
 Germany

Test Facility

BioNTech SE
 An der Goldgrube 12
 55131 Mainz
 Germany

2.2 Participating Personnel

Responsible person: (as defined in SOP-100-024)	(b) (6) BioNTech (b) (6) An der Goldgrube 12 55131 Mainz
Author:	(b) (6) BioNTech SE
Experimenter: Immunization, blood sampling, ELISA, ELISpot	(b) (6) BioNTech (b) (6)
Experimenter: Luminex-based multiplex assay	(b) (6) BioNTech (b) (6)

2.3 Study Dates

Start of experiments: 14 JAN 2020

Completion of experiments: 23 JAN 2020

090177e19346f093\Approved\Approved On: 20-Apr-2020 13:17 (GMT)

2.4 Guidelines and Regulations

All experiments are executed in accordance with the existing standard operating procedures and described processes from BioNTech SE. Applicable documents are listed below.

- Animal test application approval number: G18-12-007
- SOP-030-071 Abtöten von Mäusen
- SOP-030-072 Fixiergriff und Ohrmarkierung bei Mäusen
- SOP-030-073 Betäubung bei Mäusen
- SOP-030-074 Blutentnahme bei Mäusen
- SOP-030-078 Isolierung muriner Splenozyten
- SOP-030-079 Intramuskuläre Applikation bei Mäusen
- SOP-030-110 IFN- γ ELISpot murin
- SOP-090-013 Biological safety in laboratories

2.5 Changes and Deviations

Not applicable. There is no formal R&D plan available.

2.6 Documentation and Archive

Study reports are stored and archived according to SOP-100-003 Archiving of Paper-Based Documents.

Raw data and evaluated data are saved at:

- P:\BioNTechRNA\RN_R0030_AIRVAC\24_Preclinic\01_Vakzine Testing in vivo Luc\IM#88 GMP ready LNP Acuitas modRNA
- Labbooks:
 - No. 1455 (complete study plan including results)
 - No. 1835 (IVIS images and quantification, Luciferase ELISA, ELISpot)
 - No. 1593 page 71-84 (Luminex based multiplex assay)

090177e19346f093\Approved\Approved On: 20-Apr-2020 13:17 (GMT)

3 INTRODUCTION

3.1 Background

In December 2019, an outbreak of pneumonia of unknown cause in Wuhan, Hubei province in China started. The disease spread rapidly and in January 2020, the agent was identified. By April 1st 2020, infection with the novel Coronavirus (SARS-CoV-2) was confirmed in approximately 820,000 people with more than 40,000 casualties¹. A vaccine is urgently needed and BioNTech decided to develop a rapid vaccine project with the surface or spike protein (S protein) of the virus as the viral antigen.

The development of *in vitro* transcribed RNA as an active platform for the use in infectious disease vaccines is based on the extensive knowledge of the company in RNA technology, which has been gained over the last decade. The core innovation is based on *in vivo* delivery of a pharmacologically optimized, antigen-coding RNA vaccine to induce robust neutralizing Abs and accompanying/concomitant T-cell responses to achieve protective immunization with minimal vaccine doses (Vogel et al. 2017, Moyo et al. 2018, Pardi et al. 2017).

At BioNTech, three different RNA platforms formulated with lipid nanoparticles (LNPs) are under development, namely non-modified uridine-containing mRNA (uRNA), nucleoside-modified mRNA (modRNA) and self-amplifying RNA (saRNA). In the present study, an LNP-formulated modRNA encoding luciferase was used representatively to investigate the *in vivo* biodistribution and the immune response of the vaccine candidates.

LNP formulations from a third party provider (Acuitas) were tested in comparison to the in-house formulation (b) (4) Acuitas (b) (4) (b) (4) (b) (4) Acuitas also provided an LNP formulation that is cGMP-ready (LNP8).

3.2 Objectives

The objective of this study was to investigate the biodistribution of luciferase expressed by the LNP-formulated modRNA using bioluminescence measurements in BALB/c mice, as well as innate immune system activation, formation of antibodies against luciferase and T-cell activation.

¹ Coronavirus disease (COVID-2019) situation report 72, World Health Organization; <https://www.who.int/emergencies/diseases/novel-coronavirus-2019/situation-reports>

3.3 Study Design

Four groups of three BALB/c mice were injected intramuscularly (i.m.) in the right and left hind leg with each 1 µg of LNP-formulated modRNA encoding luciferase or with buffer as control on day 0. At 6 h, 24 h, 48 h, 72 h, 6 d and 9 d after injection, the *in vivo* luciferase expression was measured by luciferin application.

In addition, serum samples were collected on day -1 and 6 h and 9 d post immunization and cytokine/chemokine level determination (multiplex) and on days -1 and 9 for luciferase-specific ELISA. On day 9, spleens were resected for immunological analysis using IFN-γ ELISpot assays.

Table 1: Study design

Group	Treatment	Dose [µg/mouse]	Formulation	Treatment schedule	End of experiment	Sample collection
1	Buffer control	N/A	N/A	Day 0	Day 9	Serum ELISA on days -1 and 9, serum for Multiplex assay on day -1, 6 h and 9 d; splenocytes for ELISpot on day 9.
2	modRNA-Luciferase (b) (4)	2 µg (1 µg/leg)	(b) (4)	Day 0	Day 9	
3	modRNA-Luciferase (b) (4)	2 µg (1 µg/leg)	Acuitas proprietary	Day 0	Day 9	
4	modRNA-Luciferase LNP8 (GMP-ready)	2 µg (1 µg/leg)	GMP-ready Acuitas formulation	Day 0	Day 9	

4 MATERIALS AND METHODS

4.1 Test Item

- LNP-formulated modRNA encoding luciferase diluted to 0.05 mg/ml to obtain a dose of 1 µg in 20 µL application volume. For CoA see [Appendix 2: Certificates of Analysis](#) of RNA and LNPs.
- Acuitas LNPs:
 - (b) (4)
 - LNP8 modRNA Luc, RNA-EH190611-01c, batch FM-1074-D, 90% encapsulation, 1.0 mg/ml encapsulated RNA, diameter 171 nm, polydispersity 0.053, storage temperature -80°C.

090177e19346f093\Approved\Approved On: 20-Apr-2020 13:17 (GMT)

- BioNTech LNP:

-

(b) (4)

4.2 Control Item

- DPBS

4.3 Test System

- *Mus musculus*: 12 female BALB/c mice at an age of 9 weeks at study start with a body weight of approximately 25 g.

4.4 Materials

Table 2: Materials

Product name	Application/specification	Article no.	Working dilution	Provider
DPBS	Buffer control	14190-094	1x	Thermo Fisher Scientific
Syringes 0.3 ml 30 G	Insulin syringes for i.m. application	4144150	N/A	BD
Syringes 0.5 ml 29 G	Insulin syringes for i.p. application	324824	N/A	BD
Luciferin	Substrate for in vivo luciferase imaging	122799-10	150mg/kg	Perkin-Elmer
Mircovette 500 Z-gel tubes	Blood sampling	2021-01-31	N/A	Sarstedt
Xenogen IVIS® Spectrum	In vivo BLI imager	-	N/A	Caliper Life Sciences
MaxiSorp plate	ELISA	439454	N/A	Thermo Fisher Scientific
rec. QuantiLum Recombinant Luciferase	Positive control	E1701	100 ng/μl	Promega
Casein Blocking Buffer	10x	B6429	1x	Sigma-Aldrich
TMB ONE ECO-TEK	Chromogenic substrate for horseradish peroxidase	4380H	N/A	BIOTREND, Cologne, Germany
Sodium carbonate	7.5% NaHCO ₃	S8761-100 ml	N/A	Sigma-Aldrich
HCl	Hydrochloric acid solution volumetric, 0.1 M HCl	2104-50 ml	N/A	Sigma-Aldrich
RPMI1640 medium	Cell culture medium	61870	N/A	Gibco
Biotek Epoch	ELISA plate reader	-	N/A	Biotek
Mouse IFN-γ ELISpotPLUS kit	Kit for enumeration of cells secreting mouse IFN-γ	3321-4APT-2	N/A	Mabtech

090177e19346f093\Approved\Approved On: 20-Apr-2020 13:17 (GMT)

Product name	Application/specification	Article no.	Working dilution	Provider
ImmunoSpot® S5 Versa Analyzer	ELISpot plate reader	-	N/A	Cellular Technology Ltd
RPMI1640 medium	Cell culture medium	61870	N/A	Gibco
Multiplex	PROCARTAPLEX 10 PLEX	PPX-10 - MXU63C9	N/A	Life Technologies GmbH
Bio-Plex 200	Multiplex reader	-	N/A	Bio-Rad
Anti-firefly luciferase antibody (mAb21),	Assay control ELISA	ab64564	1:1000	Abcam
Mouse IgG isotype	Assay control ELISA	0107-08	1:100 as starting dilution	Southern Biotech
goat anti-mouse IgG HRP	Secondary antibody ELISA	115-035-071	1:15000 (If stored in 50% glycerol 1:7500)	Jackson

Table 3: Software

Product name	Application	Provider
Living image	In vivo BLI quantification	Perkin Elmer
Prism	Analysis	Graphpad Software Inc.
Excel	Animal monitoring, raw data ELISA	Microsoft Corp.
Bio-Plex Manager (6.1)	Bio-Plex reader	Bio-Rad
Gen5	Absorbance reader	Biotek
ImmunoCapture V6.3	ELISpot analysis	Cellular Technology Ltd

Table 4: Peptide pool for stimulation of splenocytes

Consensus sequences from Limberis et al., 2009 Gene Therapy)

Peptide pool MHC-I	
Name	Sequence
Firefly luciferase-1	GFQSMYTFV
Firefly luciferase-2	VPFHHGFGM
Firefly luciferase-3	VALPHRTAC

4.5 Methods

4.5.1 Animal Care

4.5.1.1 General Information

BALB/c mice were delivered at the age of at least six weeks. Delivered mice were used for experiments after approximately one week of acclimatization. All experiments and protocols were approved by the local authorities (local welfare committee), conducted

090177e19346f093\Approved\Approved On: 20-Apr-2020 13:17 (GMT)

according to the FELASA recommendations and in compliance with the German animal welfare act and Directive 2010/63/EU. Only animals with an unobjectionable health status were selected for testing procedures.

All animals were registered upon arrival in the lab animal colony management system PyRAT (Scionics Computer Innovation GmbH, Dresden, Germany) and tracked until death. Each cage was labelled with a cage card indicating the mouse strain, gender, date of birth and number of animals per cage. At the start of an experiment additional information was added such as the project and license number, the start of the experiment and details on interventions. Where necessary for identification, animals were arbitrarily numbered with earmarks.

4.5.1.2 Housing Condition and Husbandry

Mice were housed at BioNTech SE's animal facility under barrier and SPF conditions (An der Goldgrube 12, 55131 Mainz) in individually ventilated cages (Sealsafe GM500 IVC Green Line, TECNIPLAST, Hohenpeißenberg, Germany; 500 cm²) with a maximum of five animals per cage. The temperature and relative humidity in the cages and animal unit was kept at 20-24°C and 45-55%, respectively, and the air change (AC) rate in the cages at 75 AC/hour. The cages with dust-free bedding made of debarked chopped aspen wood (Abedd LAB & VET Service GmbH, Vienna, Austria, product code: LTE E-001) and additional nesting material were changed weekly. Autoclaved sniff M-Z food (sniff Spezialdiäten GmbH, Soest, Germany; product code: V1124) and autoclaved water (tap water) were provided ad libitum and changed at least once weekly. All materials were autoclaved prior to use.

4.5.2 Animal Monitoring

Routine animal monitoring was carried out daily and included inspection for dead animals and control of food and water supplies. Each animal's health was closely assessed at least once weekly. The general physical condition was assessed with regard to the following parameters:

- Body weight change
- Macroscopic assessment of activity level/ behavior
- Macroscopic assessment of general discomfort: drop in body temperature determined by touch and by visual inspection of ears and paws. Ears and paws appear pink in a healthy mouse, white in a mouse with discomfort indicated by reduced blood circulation
- Macroscopic assessment of fur condition and appearance of eyes, inspection of body cavities/ fluids
- Macroscopic assessment of irregularities in breathing ability
- Indication of pain
- Macroscopic assessment for signs of automutilation and or fighting

4.5.3 Endpoint of Experiment / Termination Criteria

Animals were euthanized in accordance with §4 of the German animal welfare act and the recommendation of GV-SOLAS by cervical dislocation or by exposure to carbon dioxide. Additionally, termination criteria applied according to the specification within the respective animal test approval as listed below. Body weight losses exceeding 20%, or a high severity level in any of the parameters found in Section 4.5.2 were on their own sufficient reason for immediate euthanasia.

4.5.4 Injection of Test and Control Items

Animals were anesthetized by inhalation of 2.5% isoflurane in oxygen and the injection site (hind leg) was shaved. Buffer or dissolved test item was applied i.m. into the *musculus gastrocnemius* at a volume of 20 µL. All mice received 1 µg in each leg. After injection and a short recovery phase from anesthesia, the animals were observed for any signs of discomfort due to the injection procedure.

4.5.5 Bioluminescence Measurements

The mice were monitored over a period of 9 days using In Vivo Imaging System (IVIS) measurements. Briefly, the Xenogen IVIS® Spectrum device was used for *in vivo* imaging according to the manufacturer's instruction. Approximately 6 h after LNP administration and 5 min prior to imaging, animals were injected for the first time intraperitoneally (i.p.) with luciferin (150 mg/kg, dosing volume: 300 µl, 29 G needle). Mice were anesthetized (2.5% isoflurane/O₂) and placed in the imager, first with the dorsal side exposed and then with the ventral side exposed, and luciferase activity was measured. Images were taken with exposure time and sensitivity set to 1 sec, 10 sec and 1 min and bin 2, bin 4 or bin 8, respectively. The dorsal and ventral images were analyzed by visual inspection after aligning of sensitivities of each picture and used for illustration of findings. The images were analyzed using Living Image *in vivo* imaging 3.0 software, where the regions to be quantified (radiance) were drawn manually and calculated automatically (region of interest, ROI), to follow kinetics of the total fluxes (p/s) over time in a GraphPad file.

4.5.6 Blood Sampling via the *Vena Facialis*

Blood was sampled via the *vena facialis* according to SOP-030-074. In short, without prior anesthesia, mice were held tightly and using a lancet, the *v. facialis* was punctured in a precise and short movement. Blood was collected into Microvette 500 Z-gel tubes, subsequently the restraining grip was loosened. Blood samples were centrifuged at 10000 × g and RT for 5 min and serum transferred to a pre-labeled 1.5 mL reagent tube before storage at -20°C.

4.5.7 Luminex-based multiplex assay (ProcartaPlex Multiplex Immunoassay)

The assay was performed according to manufacturer's protocol. Briefly, magnetic beads were added to the provided 96-well flat bottom plate and the beads were washed (wash buffer 1x) with the help of a hand-held magnetic plate washer. The antigen standard was reconstituted in universal assay buffer (1x), pooled in one tube, the volume adjusted to a final volume of 250 μ l, serial diluted (4-fold serial dilution steps) and 50 μ l added to the designated wells. Serum samples were diluted 1:1 with the universal assay buffer and 50 μ l added to the wells. The standard was measured in duplicates and the serum samples in triplicates. The plate was incubated on a plate shaker at 500 rpm) for 2 h covered with a black lid. After three wash steps, 25 μ l of the ready-to-use detection antibody was added, incubated for 30 min on the shaker and washed three times. Streptavidin-PE (50 μ l) were added and the plate incubated for 30 min on the shaker and washed three times. The beads were resuspended in 120 μ l reading buffer, the plate was sealed and the data were acquired in the Bio-Plex 200 luminex system.

4.5.8 Luciferase-specific ELISA

Luciferase-specific IgGs in serum samples obtained on study days -1 and 9 were detected using ELISA. Recombinant luciferase (100 ng/100 μ L) protein was utilized to coat MaxiSorp plates at 4°C overnight. Upon washing and blocking using casein-based blocking buffer, serum samples were screened for luciferase-specific antibodies by incubation on plates for 1 h at 37°C. An anti-firefly luciferase antibody (mAb21) as well as a mouse IgG isotype were included as assay controls. Subsequently, plates were incubated with horseradish peroxidase (HRP)-labeled secondary anti-mouse IgG antibody for another 45 min at 37°C before 3, 3', 5, 5'-tetramethylbenzidine (TMB) ONE substrate was applied. Colorimetric detection was monitored and optical density read at 450 nm calculated to a wavelength reference of 620 nm (Δ OD 450–620 nm).

4.5.9 ELISpot Analysis

4.5.9.1 T-cell epitope prediction

The respective peptides for stimulation of splenocytes (Table 4) were used as published by [Limberis et al. 2009](#). The authors mapped the dominant and minor T-cell epitopes in BALB/c mice (GFQSMYTFV and VPFHHGFGM, VALPHRTAC, respectively) for the monitoring of cellular responses *in vivo*. No modifications have been added to the published peptides before peptide synthesis by JPT technologies GmbH.

4.5.9.2 Sample Collection and Processing

Spleens were removed on day 9 after euthanizing the mice and single cell suspensions were prepared (SOP-030-078). In brief, the removed organs were pressed through a 70 µm cell mesh using the plunger of a syringe to release the cells from the organ into a tube. After washing with PBS the cell pellet was incubated with erythrocyte lysis buffer, washed in PBS and passed again through a 70 µm cell mesh. Resulting cells were resuspended in medium and counted.

4.5.9.3 IFN-γ ELISpot Assay

The IFN-γ ELISpot assay was used to measure IFN-γ release after *in vitro* stimulation of T cells as an indicator for the induction of antigen-specific T cells. ELISpot analysis was performed using the Mabtech Mouse IFN-γ ELISpot^{PLUS} kit. Isolated splenocytes were seeded to pre-coated ELISpot plates at 5×10^5 cells/well in 200 µL medium and stimulated with antigen-specific peptide pools composed of single peptides and a final concentration of 2 µg/mL per peptide, predicted as described in Section 4.5.9.1 overnight in a humidified incubator at 37°C. As peptide controls, splenocytes were incubated with 6 µg/mL of an irrelevant AH1 peptide derived from the endogenous retroviral gene product envelope glycoprotein 70 (gp70; AH1: amino acids 6 to 14). Splenocytes were incubated with medium alone as a negative control or with 2 µg/mL Concanavalin A (ConA) as an internal positive control, confirming the functionality of the assay. Spots were visualized with a biotin-conjugated anti-IFN-γ antibody followed by incubation with streptavidin-alkaline phosphatase (ALP) and 5-bromo-4-chloro-3-indolyl-phosphate/nitro blue tetrazolium (BCIP/NBT) substrate. Spot numbers were counted and analyzed using the ImmunoSpot® S5 Versa ELISpot Analyzer, the ImmunoCaptureTM image acquisition software, and the ImmunoSpot® Analysis software Version 5. The QC function of ImmunoSpot analysis software was used to limit false positive spot counts. All tests were performed in triplicate and spot counts were summarized as median values for each triplicate.

4.5.10 Statistical Analysis

GraphPad Prism 8 Software (La Jolla, USA) was used for statistical analysis and figure generation. All groups were compared by a one-way ANOVA test with Tukey's multiple comparison post-test on each measurement day (area under the curve for bioluminescence assay, ELISA and ELISpot analysis).

5 RESULTS

5.1 Bioluminescence measurements

The biodistribution of luciferase expressed by the LNP-formulated modRNA after i.m. injection was assessed by bioluminescence measurements. Mice received a total dose of 2 µg (b) (4) LNP8 or (b) (4) -formulated modRNA, the control group received 20 µl DPBS only.

Mice were monitored over nine days and Luciferase signal was recorded and quantified (Figure 1).

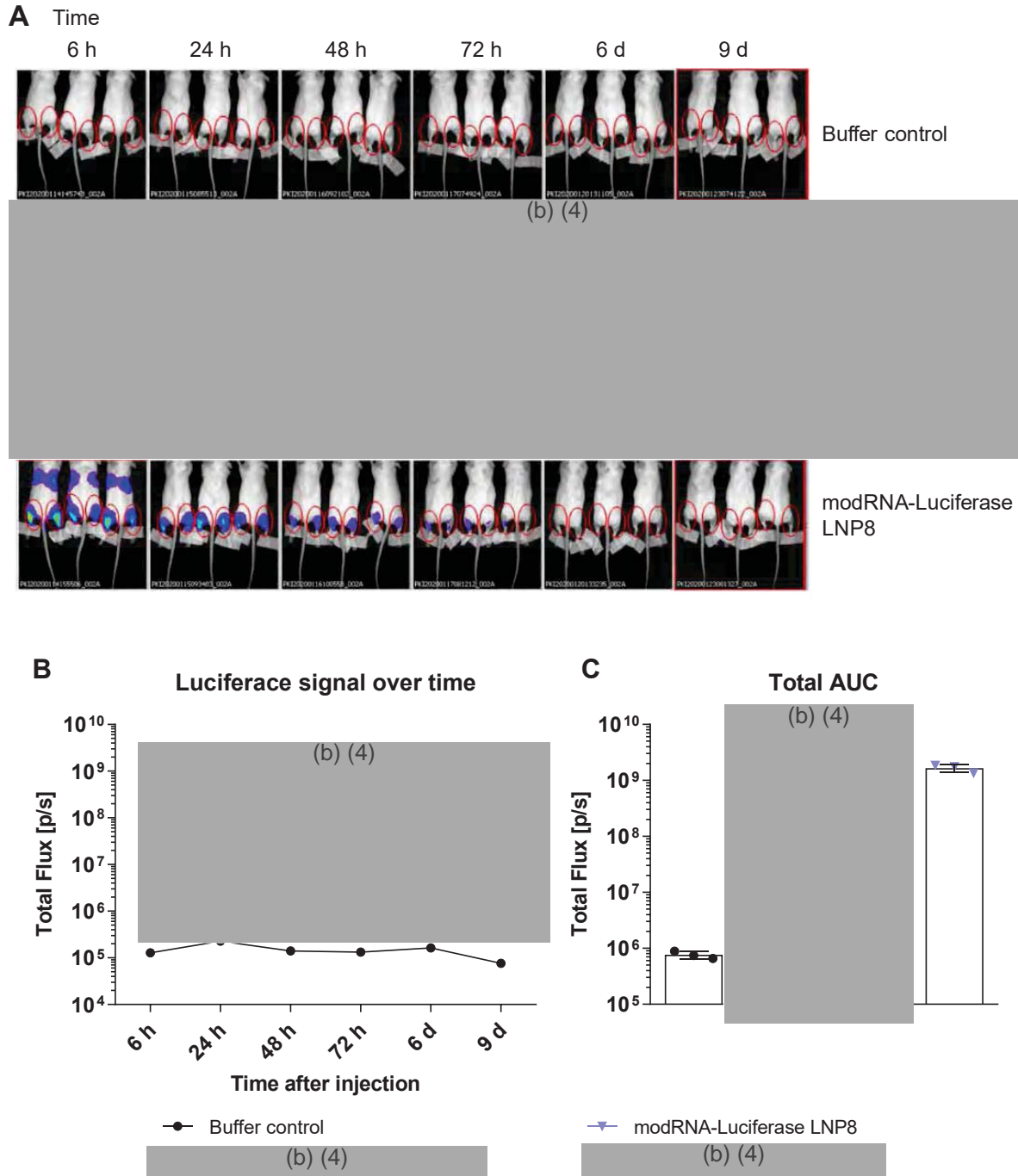


Figure 1: Bioluminescence measurement using the LNP-formulated modRNA encoding for luciferase

BALB/c mice were injected i.m. in the right and left hind leg with each 1 µg of LNP-formulated modRNA encoding luciferase or DPBS only. A) At different time points after injection, the luciferase expression *in vivo* was measured by luciferin application. After 9 d, the reporter expression dropped to background levels. B) Quantification of luciferase signal over time and C) as total area under the curve (AUC, ±SD). p/s: photons per second

All formulations resulted in a modRNA-typical expression over time (Figure 1). Highest signal was detected at the first time points after immunization at the injection site and the signal declined slowly over time until day 9 (Figure 1B). Luciferase expressed by

090177e19346f093\Approved\Approved On: 20-Apr-2020 13:17 (GMT)

the modRNA formulated with Acuitas LNP8 drained to the liver as visualized by luciferase expression at 6 h in the liver region (b) (4). (b) (4) Acuitas (b) (4) formulations (Figure 1A and Figure 2). Group mean luciferase expression from RNA formulated with Acuitas (b) (4) LNP8 in the muscle at 6 h was approximately 1×10^9 p/s, (b) (4). (b) (4) Hence, Acuitas-formulated modRNA started at about 20-fold higher signal levels, stayed more than 20-fold higher until 72 h ($\sim 7 \times 10^7$ p/s for (b) (4) LNP8 vs (b) (4) and declined then to a low level (b) (4) on day 9 ($\sim 3\text{--}5 \times 10^5$ p/s).

Area under the curve calculation allowed comparing overall expression levels over the course of the experiment (Figure 1C). Statistical significance was assessed by one-way ANOVA test with Tukey's multiple comparison post-test comparing all groups with each other. Total luciferase expression from modRNA formulated with (b) (4) (b) (4) while total luciferase expression from modRNA formulated with (b) (4) LNP8 was approximately (b) (4) 1.5×10^9 p/s, respectively. The difference between the area under the curve for (b) (4) LNP8-formulated modRNA compared to buffer control (b) (4) was statistically significant ($p < 0.0001$). (b) (4)

5.2 Liver expression (b) (4) LNP8

As mentioned in Section 5.1, luciferase expressed by the modRNA formulated with Acuitas LNP8 drained to the liver as visualized by luciferase expression at 6 h in the liver region (b) (4) Acuitas (b) (4) (Figure 2A). Here the luciferase signal of modRNA formulated with (b) (4) LNP8 was quantified for better comparison. Group mean luciferase expression from RNA formulated with Acuitas (b) (4) in the liver at 6 h was (b) (4) while luciferase expression of RNA formulated with LNP8 was at about 4.94×10^7 p/s. Hence, luciferase expression from (b) (4) Acuitas (b) (4) (b) (4) compared to LNP8 (Figure 2B). The liver luciferase expression from RNA formulated with Acuitas LNP8 dropped to 2.4×10^6 p/s at 24 h, while the luciferase signal from RNA formulated with Acuitas (b) (4). No liver signal was detected at 48 h post immunization. Statistical analysis was not performed.

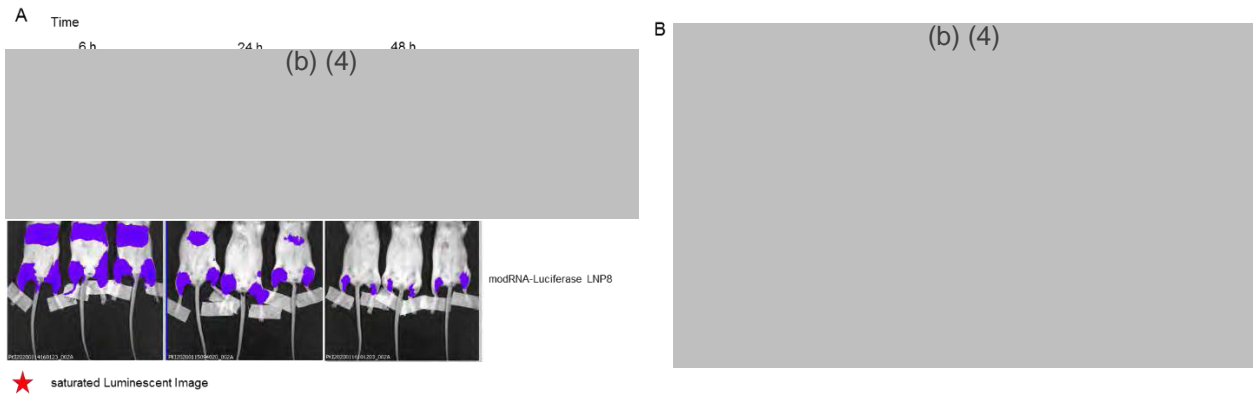


Figure 2: Bioluminescence measurement in the liver using the LNP-formulated modRNA encoding for luciferase

BALB/c mice were injected i.m. in the right and left hind leg with each 1 µg of LNP-formulated modRNA encoding luciferase. A) At 6 h, 24 h and 48 h after injection, the luciferase expression *in vivo* was measured by luciferin application. B) Quantification of luciferase signal in the liver over time (mean ±SD). p/s: photons per second.

5.3 Luminex-based multiplex assay

Activation of the innate immune system was assessed in a Luminex-based multiplex assay (Procarata immunoassays). Serum samples (day -1 (pre), 6 h and day 9) were tested for levels of the following chemokines and cytokines: MCP-1, MIP-1β, TNF-α, IFN-α, IFN- γ, IL-2, IL-6, IL-10, IL1-β, IP-10 (Figure 3). No cytokines/chemokines were detected in the pre-serum. (b) (4)

Immunization with LNP8 induced slightly increased levels of MCP-1, IL-6, IP-10 at 6 h post immunization (b) (4)

(b) (4) All chemokine/cytokine levels dropped to background levels at day 9. Statistical analysis was not performed for this assay.

090177e19346f093\Approved\Approved On: 20-Apr-2020 13:17 (GMT)

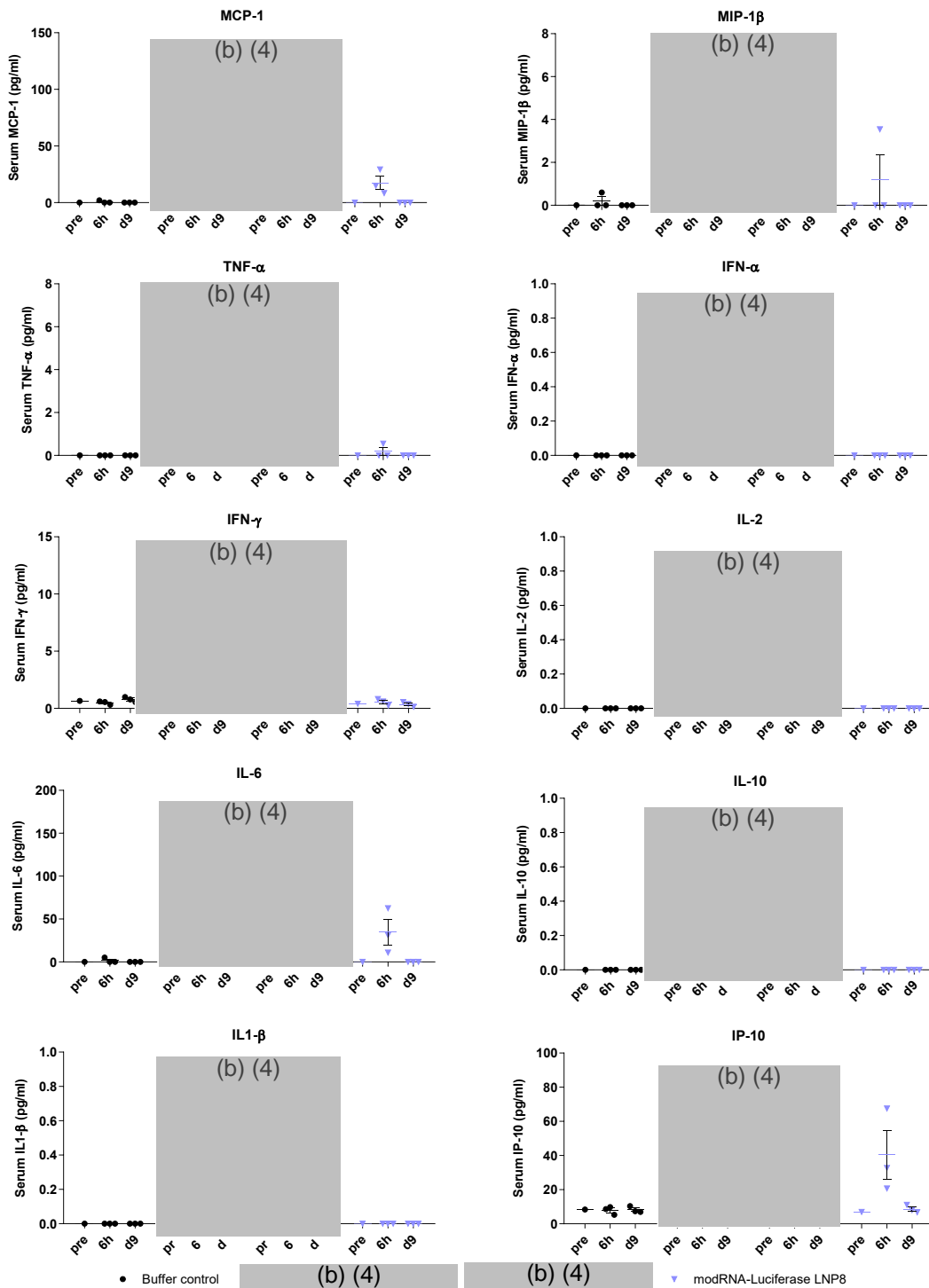


Figure 3: Activation of the innate immune system by LNP-formulated modRNA encoding for luciferase

BALB/c mice were injected i.m. in the right and left hind leg with each 1 µg of LNP-formulated modRNA encoding luciferase or DPBS only. Serum samples (day -1 (pre), 6 h, 9 d) were assessed for presence of indicated chemokines/cytokines in a Luminex-based multiplex immunoassay.

090177e19346f093\Approved\Approved On: 20-Apr-2020 13:17 (GMT)

5.4 Luciferase-specific ELISA

Luciferase-specific IgGs in serum samples obtained on study days -1 and 9 were investigated by ELISA.

Before immunization, no luciferase-specific IgGs were detected (Day -1, Figure 4). Treatment with modRNA with all tested LNP formulations did not induce the formation of luciferase-specific IgGs on day 9 post immunization.

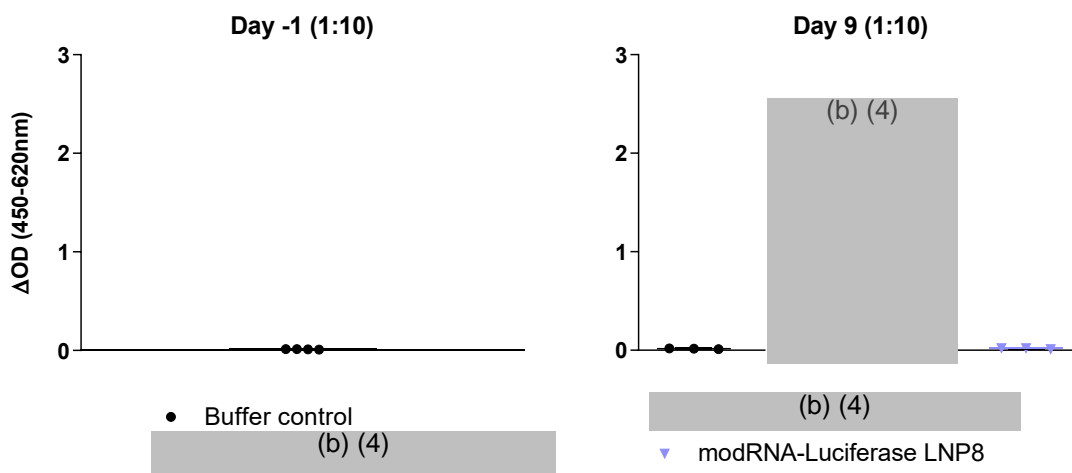


Figure 4: Luciferase-specific IgG ELISA on days -1 and 9

BALB/c mice were immunized 1 $\mu\text{g}/\text{leg}$ luciferase encoding modRNA on day 0. Serum samples were collected on days -1 and 9 and the total amount of antigen-specific immunoglobulin G (IgG) was measured via ELISA. The serum 1:10 diluted. Individual ΔOD values are shown by dots; group mean values are indicated by horizontal bars ($\pm\text{SD}$).

5.5 IFN- γ ELISpot Assay

Mice were euthanized on day 9 and splenocytes were isolated to assess T-cell responses by ELISpot analysis. Splenocytes were stimulated with luciferase-specific peptide pools (Table 4) and IFN- γ secretion was detected. Statistical significance was assessed by one-way ANOVA test with Tukey's multiple comparison post-test comparing all groups with each other. Control measurements were performed using an irrelevant peptide pool, medium only or Concanavalin A.

Stimulation of splenocytes with MHC I-specific peptide pools induced IFN- γ responses in T cells of animals immunized with all modRNA LNP candidates (Figure 5). Group mean values of 53 spots per 5×10^5 cells were counted for animals injected with buffer control after stimulation with MHC I-specific luciferase peptide pools. The high spot count in can be attributed to reactivity of T cells of one mouse in group 1. Splenocytes of this mouse react also to the stimulation with AH1, the negative control. The group

mean values are also 44 spots per 5×10^5 cells for the AH1 control, thus the response of the control group to the luciferase specific peptide pool can be considered unspecific. Group mean spot counts after stimulation with MHC I-specific peptide pools were (b) (4)

(b) (4) 519 spots per 5×10^5 cells for the group treated with LNP8-formulated modRNA. The reactivity of splenocytes of the treatment groups to the negative control was very low (6-8 spots per 5×10^5 cells), thus activation of T-cells with luciferase peptides is highly specific in the treatment groups.

(b) (4)

(b) (4) The differences between the groups treated (b) (4) LNP8-formulated modRNAs compared to buffer control were statistically significant ((b) (4) p = 0.0051 for modRNA-luciferase LNP8). The (b) (4) and LNP8 groups displayed significantly higher MHC I-specific IFN- γ secretion (b) (4) p = 0.0163 for modRNA-luciferase LNP8). (b) (4)

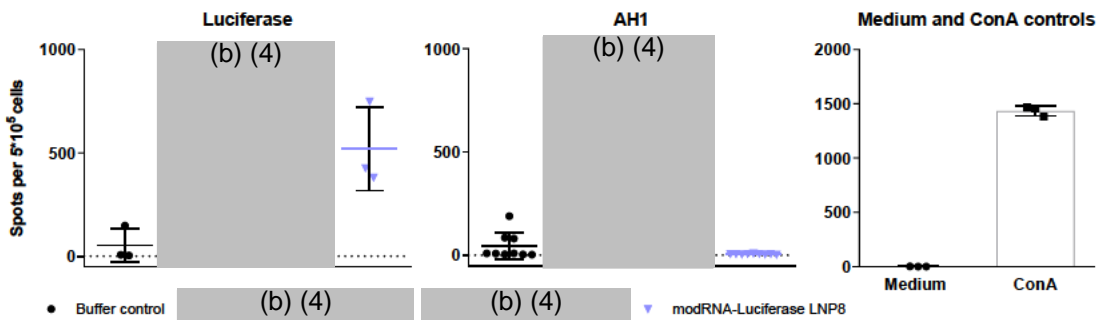


Figure 5: ELISpot analysis using splenocytes on day 9

ELISpot assay was performed using splenocytes isolated on day 9 after prime immunization. Splenocytes were stimulated with MHC I-specific luciferase peptide pools and IFN- γ secretion was measured to assess T-cell responses. Individual spot counts are shown by dots; group mean values are indicated by horizontal bars (\pm SD).

090177e19346f093\Approved\Approved On: 20-Apr-2020 13:17 (GMT)

6 CONCLUSION

After injection of LNP-formulated modRNAs, an approximately 20-fold higher luciferase expression at the injections site was observed in a bioluminescence assay for (b) (4) the GMP-ready modRNA-Luciferase LNP8 (b) (4) (b) (4). The difference between the area under the curve for (b) (4) LNP8-formulated modRNA compared to buffer control (b) (4) was statistically significant. (b) (4) (b) (4)

A multiplex assay showed that the innate immune system was temporally activated by (b) (4) LNP8-formulated modRNA. (b) (4) (b) (4)

Treatment with modRNA with all tested LNP formulations did not induce the formation of luciferase-specific IgGs on day 9 as measured by ELISA.

However, a strong antigen-specific IFN-γ T-cell response measured by ELISpot assay on day 9 for (b) (4) LNP8-formulated modRNAs, with statistically significant differences between these test groups and the buffer control (b) (4)

090177e19346f093\Approved\Approved On: 20-Apr-2020 13:17 (GMT)

7 DOCUMENT HISTORY

First version / no change.

090177e19346f093\Approved\Approved On: 20-Apr-2020 13:17 (GMT)

8 REFERENCES

Limberis MP, Bell CL, Wilson JM. Identification of the murine firefly luciferase-specific CD8 T-cell epitopes. *Gene Ther.* 2009;16(3):441-7.

Moyo N, Vogel AB, Buus S, Erbar S, Wee EG, Sahin U, et al. Efficient Induction of T Cells against Conserved HIV-1 Regions by Mosaic Vaccines Delivered as Self-Amplifying mRNA. *Molecular therapy. Methods & clinical development.* 2018; 12, 32–46.

Pardi N, Hogan MJ, Pelc RS, Muramasu H, Andersen H, DeMaso CR et al. Zika virus protection by a single low-dose nucleoside-modified mRNA vaccination. *Nature.* 2017; 543 (7644), 248–251.

Vogel AB, Lambert L, Kinnear E, Busse D, Erbar S, Reuter KC, et al. Self-amplifying RNA vaccines give equivalent protection against influenza to mRNA vaccines but at much lower doses. *Molecular therapy: the journal of the American Society of Gene Therapy.* 2017; 26 (2), 446–455.

090177e19346f093\Approved\Approved On: 20-Apr-2020 13:17 (GMT)

9 APPENDIX

Appendix 1: Animal Observations

		-5 days p.a. 09.01.2020		1 days p.a. 15.01.2020			3 days p.a. 17.01.2020			6 days p.a. 20.01.2020		
treatment	Lab ID	weight in g	health	weight in g	% change weight	health	weight in g	% change weight	health	weight in g	% change weight	health
Buffer control	1-1	21.4	No observations	21.7	101.0	No observations	21.5	100.4	No observations	21.7	101.3	No observations
	1-2	22.5	No observations	22.8	101.2	No observations	22.2	98.6	No observations	22.7	100.8	No observations
	1-3	23.0	No observations	23.3	101.4	No observations	23.5	102.3	No observations	23.4	101.5	No observations
modRNA- Luciferase (b) (4)	2-1	20.7	No observations	21.0	101.4	No observations	20.9	100.7	No observations	20.8	100.3	No observations
	2-2	21.5	No observations	22.5	104.6	No observations	22.3	103.8	No observations	23.2	107.9	No observations
	2-3	21.2	No observations	21.4	100.8	No observations	21.3	100.4	No observations	21.3	100.5	No observations
Acuitas LNPs modRNA luciferase	3-1	21.3	No observations	21.5	100.8	No observations	21.4	100.5	No observations	21.0	98.4	No observations
	3-2	21.2	No observations	21.2	99.9	No observations	21.0	99.1	No observations	21.0	99.2	No observations
	3-3	20.9	No observations	21.1	101.0	No observations	22.3	107.0	No observations	21.7	104.1	No observations
modRNA- Luciferase LNP8 (GMP-ready)	4-1	22.2	No observations	23.2	104.7	No observations	22.9	103.2	No observations	23.5	106.1	No observations
	4-2	21.6	No observations	22.4	103.8	No observations	22.5	104.3	No observations	21.9	101.6	No observations
	4-3	20.5	No observations	20.8	101.3	No observations	20.9	101.7	No observations	20.9	101.9	No observations

090177e19346f093\Approved\Approved On: 20-Apr-2020 13:17 (GMT)

Appendix 2: Certificates of Analysis

Confidential



R&D Formulation Characterization Summary:

Batch ID	LNP ID	mRNA ID	Encaps (%)	Encaps mRNA (mg/mL)	Yield (mg)	mRNA/Lipid Ratio (mg/umol)	Particle Diameter (nm)	Poly-dispersity
FM-1074 -D	LNP 8	mod Luc RNA-EH190611-01c	90%	1	0.36	0.025	71	0.053

Notes

Formulated 09-Dec-19
 Diluent: 300 mM sucrose in PBS
 Recommended storage at approximately -80 °C. Avoid repeated freeze/thaw cycles.

(b) (6)
 (b) (6) Research Associate

11-Dec-19
 Date

090177e19346f093\Approved\Approved On: 20-Apr-2020 13:17 (GMT)

Confidential



R&D Formulation Characterization Summary:

Batch ID	LNP Variant	mRNA ID	Encaps (%)	Encaps mRNA (mg/ml)	Yield (mg)	mRNA/Lipid Ratio (mg/μmol)	Particle Diameter (nm)	Poly-dispersity
----------	-------------	---------	------------	---------------------	------------	----------------------------	------------------------	-----------------

[Redacted data row]

(b) (4)

Notes

[Redacted notes]

(b) (4)

(b) (6)

(b) (6) Research Associate

26-Nov-19

Date

1 | Analytical Datasheet

Test items – Formulation: Analytical Data Sheet

Formulation experiment number: FSU-I#029
 Responsible: MeSc, JaKs
 Experimenter: MnSt, JaKs
 Date of preparation: 06Jan20

Physicochemical characterisation:

Sample batch number	Formulation				pH	Osmolality (mOsmol/kg)	Size		Zeta (mV)	Encapsulation efficiency (%)	RNA conc. (mg/ml)	LNP are conform?
	Lipid Mix	Batch	RNA	Batch			Z-Av (nm)	PDI				

[Redacted data row]

(b) (4)

[Redacted data row]

(b) (4)

[Redacted notes]

090177e19346f093\Approved\Approved On: 20-Apr-2020 13:17 (GMT)

RNA Certificate of Analysis

(Version 17)



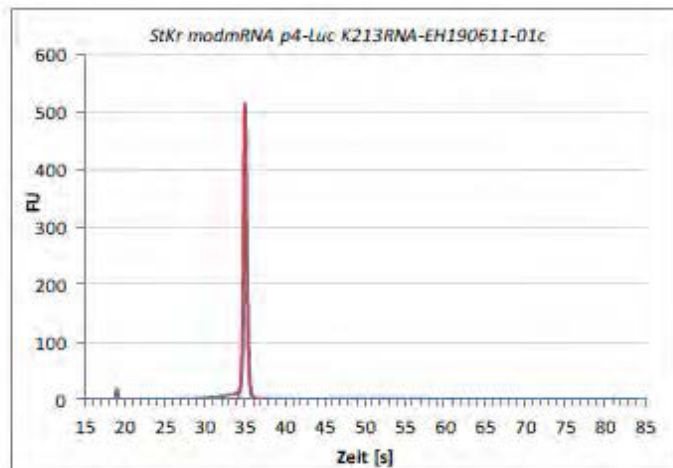
Customer (b) (6)	Date of Order 27.05.2019	RNA-ID RNA-EH190611-01c	Project Number RN0095R00
Cap (b) (4)	Construct modmRNA p4-Luc		
Purification dsRNA removal	Storage Buffer H2O		
Modification m1Y	Concentration [µg/µl] 5,75	Aliquot volume [µl] 10600	Total amount [µg] 60950

Quality Control:

Instrument: Agilent 2100 Bioanalyzer
Run: mRNA Nano_2019-06-14_001

Results:

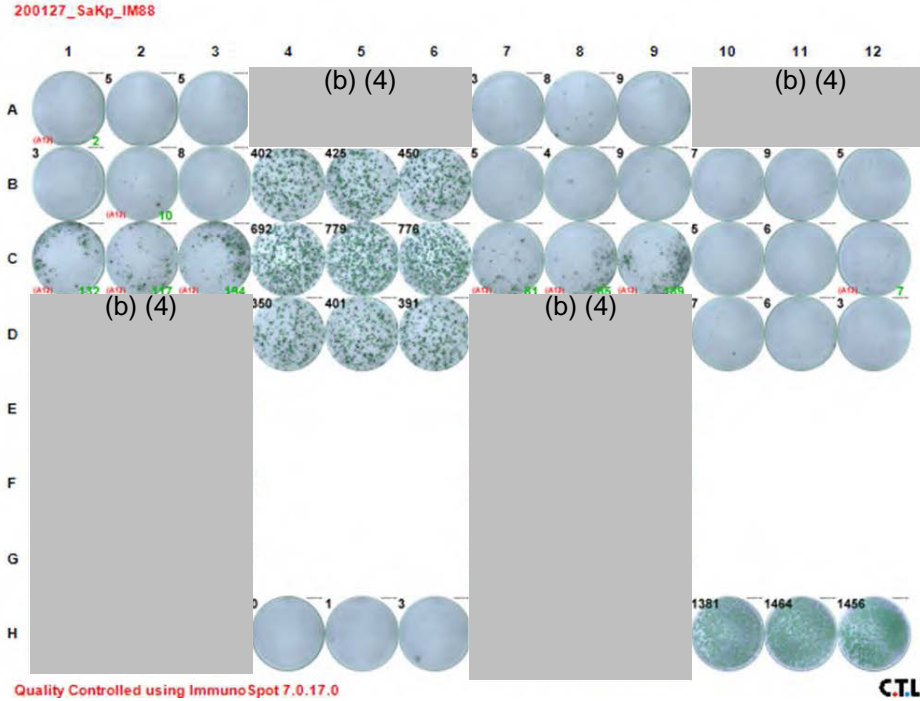
Peak height (FU): 514,963
Integral (%): 90



090177e19346f093\Approved\Approved On: 20-Apr-2020 13:17 (GMT)

Appendix 3: Raw Data IFN-γ ELISpot

Plate 1: Left, luciferase peptides; right, AH1 ELISpot (irrelevant peptide)



Luc

AH1

	1	2	3	4	5	6	7	8	9	10	11	12
A	Group 1, animal 1			Group 3, animal 3			Group 1, animal 1			Group 3, animal 3		
B	Group 1, animal 2			Group 4, animal 1			Group 1, animal 2			Group 4, animal 1		
C	Group 1, animal 3			Group 4, animal 2			Group 1, animal 3			Group 4, animal 2		
D	Group 2, animal 1			Group 4, animal 3			Group 2, animal 1			Group 4, animal 3		
E	Group 2, animal 2						Group 2, animal 2					
F	Group 2, animal 3						Group 2, animal 3					
G	Group 3, animal 1						Group 3, animal 1					
H	Group 3, animal 2			Medium			Group 3, animal 2			ConA		

Group 1: Buffer control; Group 2: (b) (4) (2x1 µg); Group 3: (b) (4) (2x1 µg); Group 4: modRNA-luciferase LNP8 (GMP-ready) (2x1 µg)

090177e19346f093\Approved\Approved On: 20-Apr-2020 13:17 (GMT)

Appendix 4: Statistical Analysis

Bioluminescence assay

Group mean values, bioluminescence assay, luciferase signal over time.

Time point	Buffer control	(b) (4)	(b) (4)	modRNA-Luciferase LNP8
	N = 3			N = 3
6 h	128046,667			1,2589e+009
24 h	227766,667			7,310667e+008
48 h	139995			2,1038333e+008
72 h	132585			7,8667e+007
6 d	162383,333			2920333,333
9 d	76573,333			509000

Please note that commas are used as decimal separators.

Descriptive statistics, bioluminescence assay, area under the curve.

	Buffer control	(b) (4)	(b) (4)	modRNA-Luciferase LNP8
Number of values	3			3
Minimum	657790			1352000000
Maximum	889908			1848000000
Range	232118			496000000
Mean	765040			1652666667
SD	117058			264244836
SEM	67583			152561827

Please note that commas are used as decimal separators. SD: Standard deviation. SEM: Standard error of the mean.

One-way ANOVA with Tukey's multiple comparisons post-test, bioluminescence assay, area under the curve.

ANOVA summary	
F	80,68
P value	<0,0001
P value summary	****
Significant diff. among means (P < 0.05)?	Yes
R square	0,9680

090177e19346f093\Approved\Approved On: 20-Apr-2020 13:17 (GMT)

Tukey's multiple comparisons test	Mean Diff.	95,00% CI of diff.	Significant?	Summary	Adjusted P Value
(b) (4)					
(b) (4)					
Buffer control vs. modRNA-Luciferase LNP8	-1651901626	-2072407467 to -1231395786	Yes	****	<0,0001
(b) (4)					
(b) (4)					
(b) (4)					

Please note that commas are used as decimal separators. F: F-statistic. P values ≤ 0.05 indicate statistically significant difference. R square: Coefficient of determination. CI: Confidence interval. n.s.: Not significant.

Luciferase-Specific ELISA

Descriptive statistics, luciferase-specific ELISA, day 9.

	Buffer control	(b) (4)	(b) (4)	modRNA-Luciferase LNP8
Number of values	3			3
Minimum	0,0110			0,0100
Maximum	0,0190			0,0220
Range	0,00800			0,0120
Mean	0,0153			0,0177
SD	0,00404			0,00666
SEM	0,00233			0,00384

Please note that commas are used as decimal separators. SD: Standard deviation. SEM: Standard error of the mean.

090177e19346f093\Approved\Approved On: 20-Apr-2020 13:17 (GMT)

One-way ANOVA with Tukey's multiple comparisons post-test, bioluminescence assay, area under the curve.

ANOVA summary	
F	0,4597
P value	0,6520
P value summary	ns
Significant diff. among means (P < 0.05)?	No
R square	0,1209

No post-test for insignificant main test.

ELISpot analysis

Descriptive statistics, ELISpot analysis, day 9.

	Buffer control	(b) (4)	(b) (4)	modRNA-Luciferase LNP8
Number of values	3			3
Minimum	4,00			381
Maximum	148			749
Range	144			368
Mean	53,0			519
SD	82,3			201
SEM	47,5			116

Please note that commas are used as decimal separators. SD: Standard deviation. SEM: Standard error of the mean.

One-way ANOVA with Tukey's multiple comparisons post-test, bioluminescence assay, area under the curve.

ANOVA summary	
F	19,90
P value	0,0005
P value summary	***
Significant diff. among means (P < 0.05)?	Yes
R square	0,8819

090177e19346f093\Approved\Approved On: 20-Apr-2020 13:17 (GMT)

Tukey's multiple comparisons test	Mean Diff.	95,00% CI of diff.	Significant?	Summary	Adjusted P Value
(b) (4)					
(b) (4)					
Buffer control vs. modRNA-Luciferase LNP8	-465,7	-769,0 to -162,3	Yes	**	0,0051
(b) (4)					
(b) (4)					
(b) (4)					

Please note that commas are used as decimal separators. F: F-statistic. P values ≤ 0.05 indicate statistically significant difference. R square: Coefficient of determination. CI: Confidence interval. n.s.: Not significant.

090177e19346f093\Approved\Approved On: 20-Apr-2020 13:17 (GMT)

MODULE 2.6.4. PHARMACOKINETICS WRITTEN SUMMARY

This document contains confidential information belonging to BioNTech/Pfizer. Except as may be otherwise agreed to in writing, by accepting or reviewing these materials, you agree to hold such information in confidence and not to disclose it to others (except where required by applicable law), nor to use it for unauthorized purposes. In the event of actual or suspected breach of this obligation, BioNTech/Pfizer should be promptly notified.

090177e1950b5f8d\Approved\Approved On: 29-Sep-2020 20:20 (GMT)

TABLE OF CONTENTS

LIST OF ABBREVIATIONS AND DEFINITION OF TERMS3

2.6.4. PHARMACOKINETICS WRITTEN SUMMARY4

 2.6.4.1. Brief Summary4

 2.6.4.2. Methods of Analysis.....4

 2.6.4.3. Absorption4

 2.6.4.4. Distribution.....5

 2.6.4.5. Metabolism.....6

 2.6.4.6. Excretion8

 2.6.4.7. Pharmacokinetic Drug Interactions8

 2.6.4.8. Discussion and Conclusions8

 2.6.4.9. References9

090177e1950b5f8d\Approved\Approved On: 29-Sep-2020 20:20 (GMT)

BNT162b2

Module 2.6.4. Pharmacokinetics Written Summary

LIST OF ABBREVIATIONS AND DEFINITION OF TERMS

ADME	Absorption, distribution, metabolism, excretion
ALC-0159	Proprietary PEG-lipid included as an excipient in the LNP formulation used in BNT162b2
ALC-0315	Proprietary amino-lipid included as an excipient in the LNP formulation used in BNT162b2
DSPC	1,2-distearoyl-sn-glycero-3-phosphocholine
GLP	Good Laboratory Practice
H	Human (in metabolite scheme)
IM	Intramuscular(ly)
IV	Intravenous(ly)
LNP	Lipid-nanoparticle
Luc	Luciferase (from firefly <i>Pyroactomena lucifera</i>)
Mk	Monkey (in metabolite scheme)
Mo	Mouse (in metabolite scheme)
modRNA	Nucleoside-modified mRNA
mRNA	Messenger RNA
PEG	Polyethylene glycol
PK	Pharmacokinetics
R	Rat (in metabolite scheme)
RNA	Ribonucleic acid
S9	Supernatant fraction obtained from liver homogenate by centrifuging at 9000 g
WHO	World Health Organization

090177e1950b5f8d\Approved\Approved On: 29-Sep-2020 20:20 (GMT)

CONFIDENTIAL

Page 3

FDA-CBER-2021-4379-0000976

2.6.4. PHARMACOKINETICS WRITTEN SUMMARY

2.6.4.1. Brief Summary

The ADME profile of BNT162b2 (BioNTech code number BNT162, Pfizer code number PF-07302048) included evaluation of the PK and metabolism of two novel lipid excipients (ALC-0315 and ALC-0159) in the LNP and potential biodistribution using luciferase expression as a surrogate reporter. The PK study showed the LNP distributes from the blood to the liver, ~1% of ALC-0315 and ~50% of ALC-0159 were excreted unchanged in feces, and there was no detectable excretion of unchanged ALC-0315 and ALC-0159 in the urine.

In the biodistribution study, protein expression was demonstrated at the site of injection and to a lesser extent in the liver after BALB/c mice received an IM injection of modRNA encoding luciferase in an LNP formulation comparable to BNT162b2, with the identical lipid composition. Luciferase expression was identified at the injection site at 6 hours after injection and was not detected after 9 days. Liver expression was also present at 6 hours after injection and was no longer detected by 48 hours after injection.

The metabolism of ALC-0315 (aminolipid) and ALC-0159 (PEG-lipid) was evaluated in vitro using blood, liver microsomes, S9 fractions, and hepatocytes from mice, rats, monkeys, and humans. The in vivo metabolism was examined in rat plasma, urine, feces, and liver samples collected during the PK study. In vitro and in vivo studies indicated ALC-0315 and ALC-0159 are metabolized slowly by hydrolytic metabolism of the ester and amide functionalities, respectively, across the species evaluated.

2.6.4.2. Methods of Analysis

No methods of analysis have been validated to support GLP TK studies of components of BNT162b2; however, a qualified LC/MS method was developed to support quantitation of the two novel LNP excipients for the non-GLP IV PK study in rats (PF-07302048_06Jul20_072424). Methods for immunogenicity and efficacy studies are described in [Section 2.6.2.12](#).

2.6.4.3. Absorption

An intravenous rat PK study was performed using LNPs containing surrogate luciferase RNA, with the identical lipid composition as BNT162b2, to explore the disposition of ALC-0159 and ALC-0315 ([Table 2.6.4-1](#), Study PF-07302048_06Jul20_072424; [Tabulated Summary 2.6.5.3](#)). The distribution of the LNP from the blood to the liver was rapid and essentially complete by 24 h, with <1% of the maximum observed plasma concentrations remaining ([Figure 2.6.4-1](#)). The liver appears to be the major site of drug uptake from the blood.

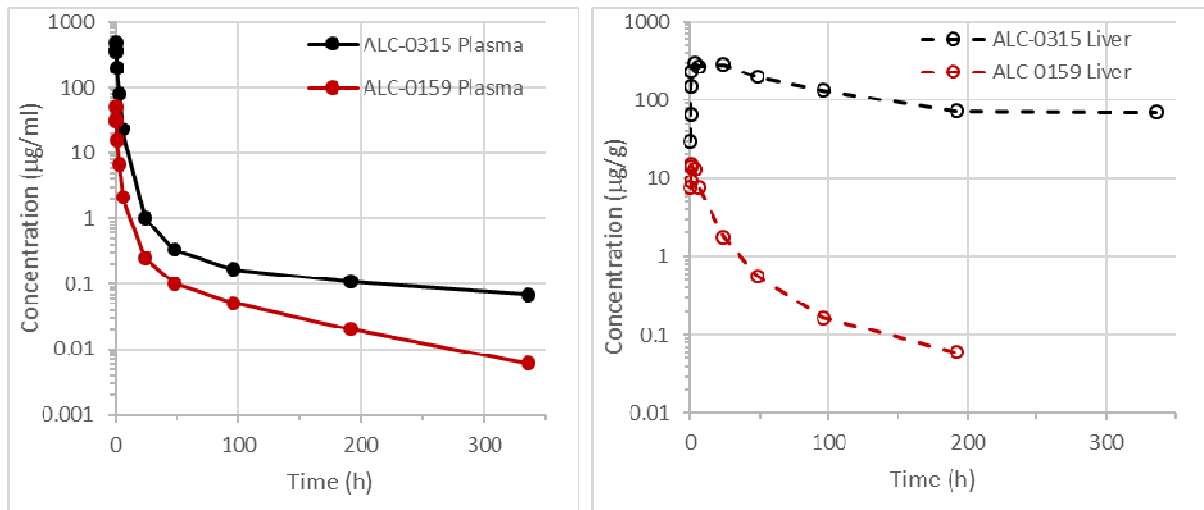
Table 2.6.4-1. PK of ALC-0315 and ALC-0159 in Wistar Han Rats After IV Administration of LNPs Containing Surrogate Luciferase RNA at 1 mg/kg

Analyte	Dose of Analyte (mg/kg)	Gender /N	t _{1/2} (h)	AUC _{inf} (µg•h/mL)	AUC _{last} (µg•h/mL)	Estimated fraction of dose distributed to liver (%) ^a
ALC-0315	15.3	Male/3 ^b	139	1030	1020	60
ALC-0159	1.96	Male/3 ^b	72.7	99.2	98.6	20

a. Calculated as highest mean amount in the liver (µg)/total mean dose (µg) of ALC-0315 or ALC-0159.

b. 3 animals per timepoint; non-serial sampling.

Figure 2.6.4-1. Plasma and Liver Concentrations of ALC-0315 and ALC-0159 in Wistar Han Rats After IV Administration of LNPs Containing Surrogate Luciferase RNA at 1 mg/kg



No absorption studies were conducted for BNT162b2, as the administration route is IM. Pharmacokinetic studies have not been conducted with BNT162b2 and are generally not considered necessary to support the development and licensure of vaccine products for infectious diseases (WHO, 2005; WHO, 2014).

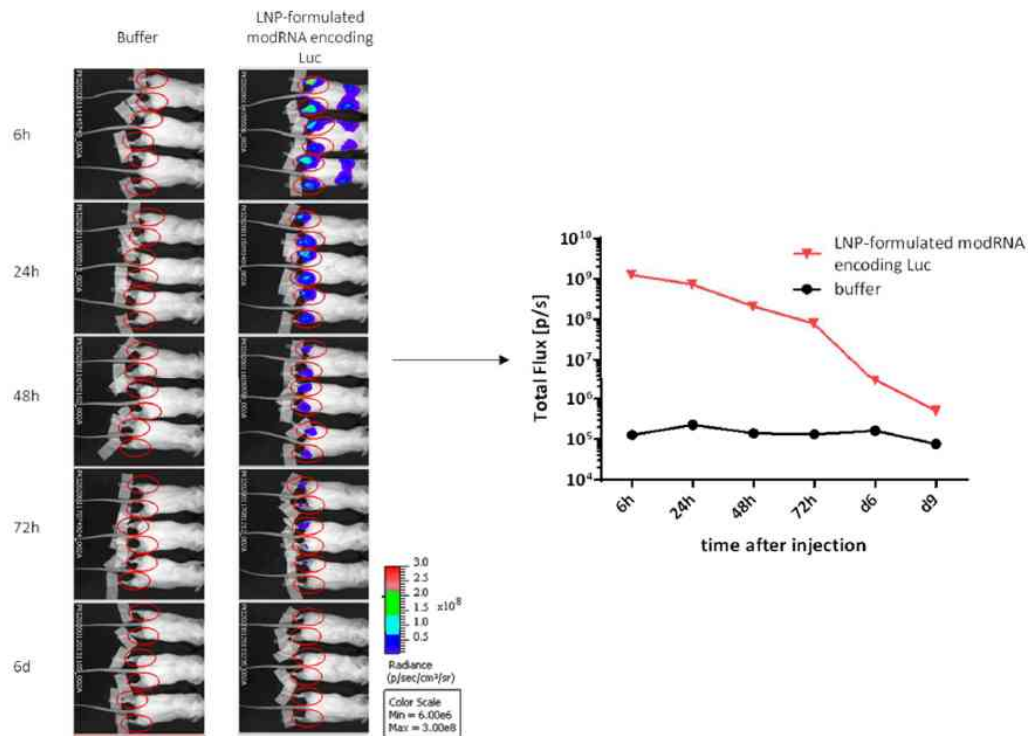
2.6.4.4. Distribution

In an in vivo study in BALB/c mice (Study R-20-0072), the biodistribution of BNT162b2 was assessed using luciferase as a surrogate marker protein. RNA encoding luciferase was formulated like BNT162b2, with the identical lipid composition, and mice received IM injections of 1 µg each in the right and left hind leg (for a total of 2 µg) of LNP-formulated modRNA encoding luciferase. Luciferase protein expression was detected at different timepoints, by measuring the in vivo bioluminescence (Figure 2.6.4-2; Tabulated Summary 2.6.5.5) after injection of luciferin substrate, at the site of injection and to a lesser extent in the liver. Distribution to the liver is likely mediated by LNPs entering the blood stream. The repeat-dose toxicity study in rats showed no evidence of liver injury (Section 2.6.6.3.1). The luciferase expression at the injection site, the tissue with the highest bioluminescence, dropped to background levels after 9 days. As detailed in Section 2.6.4.3, following systemic

090177e1950b5f8d\Approved\Approved On: 29-Sep-2020 20:20 (GMT)

(IV) administration the liver appears to be the major organ into which the LNPs distribute, this is consistent with the observations made following IM administration.

Figure 2.6.4-2. Bioluminescence Emission in BALB/c Mice after IM Injection of an LNP Formulation of modRNA Encoding Luciferase



The biodistribution of the expression of the antigen encoded by the RNA component of BNT162b2 is expected to be dependent on the LNP distribution. Therefore, results of these biodistribution studies should be representative for BNT162b2, as the LNP-formulated luciferase-encoding modRNA had the exact same lipid composition.

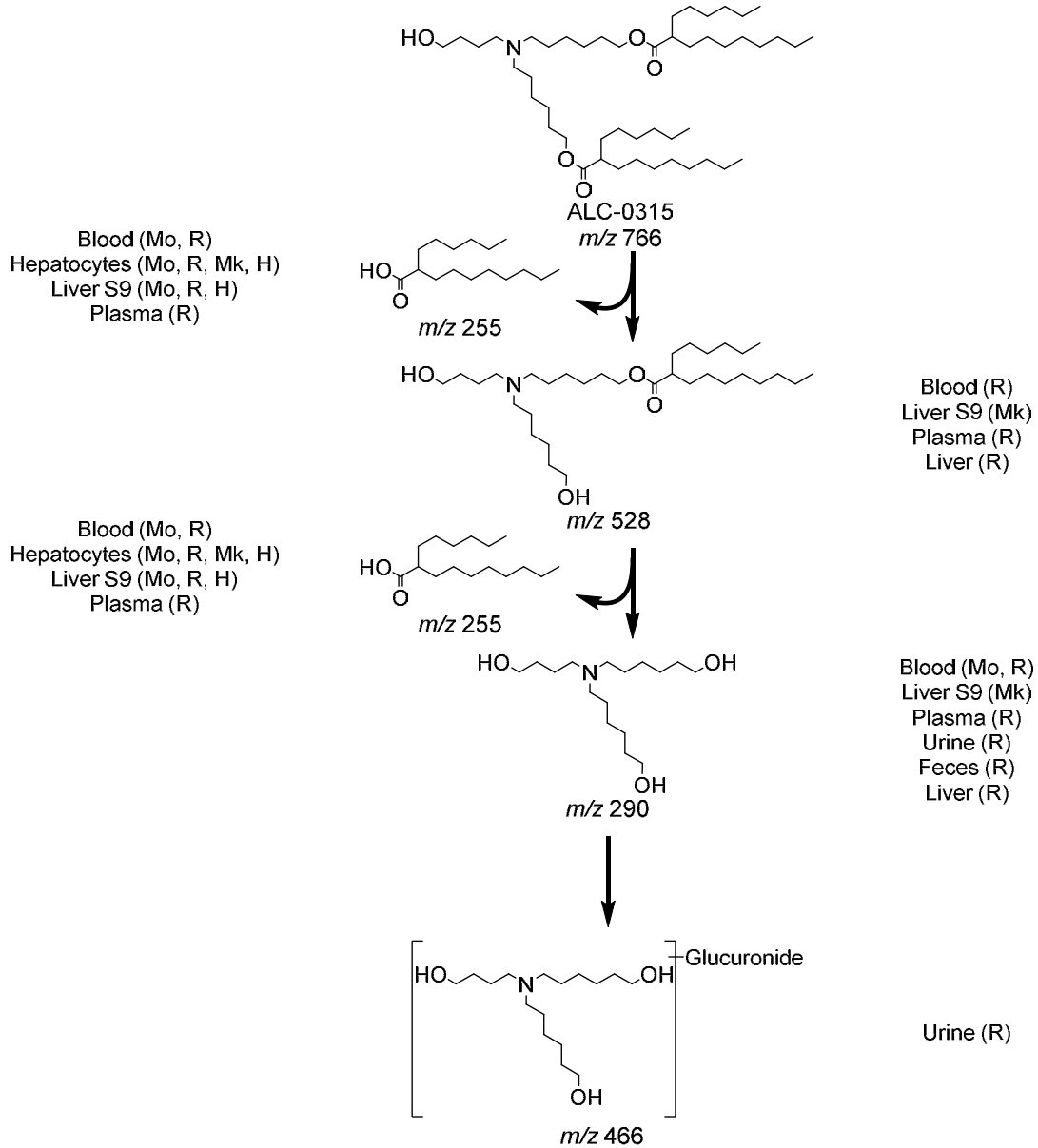
2.6.4.5. Metabolism

Metabolism studies were conducted to evaluate ALC-0315 (aminolipid) and ALC-0159 (PEG-lipid). These novel lipids were evaluated for in vitro metabolic stability in CD-1/ICR mouse, Wistar Han and/or Sprague Dawley rat, cynomolgus monkey, and human liver microsomes, S9 fractions, and hepatocytes. ALC-0315 and ALC-0159 were stable (>82% remaining) over 120 min in liver microsomes and S9 fractions and over 240 min in hepatocytes in all species and test systems (Studies [01049-20008](#), [01049-20009](#), [01049-20010](#), [01049-20020](#), [01049-20021](#), and [01049-20022](#); [Tabulated Summaries 2.6.5.10A](#) and [2.6.5.10B](#)).

The metabolism of ALC-0315 and ALC-0159 was further evaluated (Study [PF-07302048_05Aug20_043725](#); [Tabulated Summaries 2.6.5.9](#), [2.6.5.10C](#), and [2.6.5.10D](#)) in vitro using blood, liver S9 fractions, and hepatocytes from CD-1 mice, Wistar Han rats, cynomolgus monkeys, and humans and in vivo using the rat plasma, urine, feces, and liver from the PK study ([Section 2.6.4.3](#)). This study determined ALC-0315 and ALC-0159 are

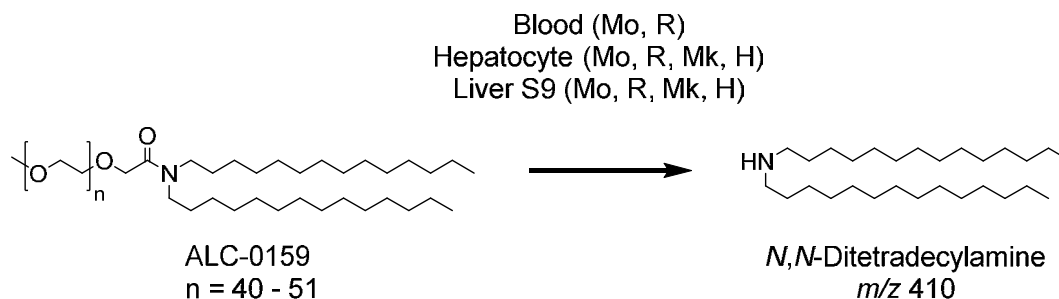
metabolized slowly and undergo hydrolytic metabolism of the ester and amide functionalities, respectively. This hydrolytic metabolism was observed across the species evaluated, as shown in Figure 2.6.4-3 and Figure 2.6.4-4.

Figure 2.6.4-3. Proposed Biotransformation Pathway of ALC-0315 in Various Species



Metabolism of ALC-0315 occurs via two sequential ester hydrolysis reactions, first yielding the monoester metabolite (m/z 528) followed by the doubly deesterified metabolite (m/z 290). Subsequent metabolism of the doubly deesterified metabolite resulted in a glucuronide metabolite (m/z 466), which was only observed in urine from the rat PK study. The acid product of both hydrolysis reactions of ALC-0315, 6-hexyldecanoic acid (m/z 255), was also identified.

090177e1950b5f8d\Approved\Approved On: 29-Sep-2020 20:20 (GMT)

Figure 2.6.4-4. Proposed Biotransformation Pathway of ALC-0159 in Various Species

The primary route of metabolism identified for ALC-0159 involves amide bond hydrolysis yielding *N,N*-ditetradecylamine (*m/z* 410). This metabolite was identified in mouse and rat blood, as well as hepatocytes and liver S9 from mouse, rat, monkey, and human. No metabolites of ALC-0159 were identified from in vivo samples.

The other two lipids in the LNP are naturally occurring (cholesterol and DSPC) and will be metabolized and excreted like other endogenous lipids. As the protein encoded by the mRNA in BNT162b2 is expected to be proteolytically degraded and RNA is degraded by cellular RNases and subjected to nucleic acid metabolism, no RNA or protein metabolism or excretion studies will be conducted.

2.6.4.6. Excretion

In the rat PK study (Section 2.6.4.3), there was no detectable excretion ALC-0315 and ALC-0159 in urine after IV administration of LNPs containing surrogate luciferase RNA at 1 mg/kg. The percent excreted unchanged in feces was ~1% for ALC-0315 and ~50% for ALC-0159. Metabolites of ALC-0315 were detected in the urine of rats (Figure 2.6.4-3). No excretion studies have been conducted with BNT162b2 for the reasons described in Section 2.6.4.5.

2.6.4.7. Pharmacokinetic Drug Interactions

No PK drug interaction studies have been conducted with BNT162b2.

2.6.4.8. Discussion and Conclusions

In the rat PK study, concentrations of ALC-0159 dropped approximately 8000- and >250-fold in plasma and liver, respectively, during this 2-week study. For ALC-0315, the elimination of the molecule from plasma and liver was slower, but concentrations fell approximately 7000- and 4-fold in two weeks for plasma and liver, respectively. Overall, the apparent terminal $t_{1/2}$ in plasma and liver were similar in both tissues and were 2-3 and 6-8 days for ALC-0159 and ALC-0315, respectively. The apparent terminal $t_{1/2}$ in plasma likely represents the re-distribution of the respective lipids from the tissues into which they have distributed as the LNP back to plasma where they are eliminated.

Overall, it appears that 50% of ALC-0159 was eliminated unchanged in feces. Metabolism played a role in the elimination of ALC-0315, as little to no unchanged material was detected

BNT162b2

Module 2.6.4. Pharmacokinetics Written Summary

in either urine or feces. Investigations of urine, feces and plasma from the rat PK study identified a series of ester cleavage products of ALC-0315; this likely represents the primary clearance mechanism acting on this molecule, although no quantitative data is available to confirm this hypothesis. In vitro, ALC-0159 was metabolized slowly by hydrolytic metabolism of the amide functionality.

The potential biodistribution of BNT162b2 was assessed using luciferase expression as a surrogate reporter. Protein expression was demonstrated at the site of injection and to a lesser extent, and more transiently, in the liver after BALB/c mice received an IM injection of RNA encoding luciferase in an LNP formulation like BNT162b2. Luciferase expression was identified at the injection site at 6 hours after injection and was not detected by 9 days. Expression in the liver was also present at 6 hours after injection and was not detected by 48 hours after injection.

2.6.4.9. References

1. [World Health Organization. Annex 1. Guidelines on the nonclinical evaluation of vaccines. In: WHO Technical Report Series No. 927, Geneva, Switzerland. World Health Organization; 2005:31-63.](#)
2. [World Health Organization. Annex 2. Guidelines on the nonclinical evaluation of vaccine adjuvants and adjuvanted vaccines. In: WHO Technical Report Series No. 987, Geneva, Switzerland. World Health Organization 2014:59-100.](#)

090177e1950b5f8d\Approved\Approved On: 29-Sep-2020 20:20 (GMT)

CONFIDENTIAL

Page 9

FDA-CBER-2021-4379-0000982

2.4 NONCLINICAL OVERVIEW

090177e1950c1a59\Approved\Approved On: 29-Sep-2020 23:37 (GMT)

CONFIDENTIAL

Page 1

FDA-CBER-2021-4379-0000939

TABLE OF CONTENTS

2.4 NONCLINICAL OVERVIEW	1
LIST OF ABBREVIATIONS AND DEFINITION OF TERMS	4
2.4.1. OVERVIEW OF NONCLINICAL TESTING STRATEGY	6
Table 2.4.1-1. Nomenclature of the Vaccine Candidates	6
Table 2.4.1-2. Nonclinical Studies	8
2.4.2. PHARMACOLOGY	9
2.4.2.1. Primary Pharmacodynamics	9
2.4.2.1.1. Summary	9
2.4.2.1.2. BNT162b2, A Lipid Nanoparticle Encapsulated RNA Vaccine Encoding the SARS-CoV-2 P2 S as a Vaccine Antigen.....	9
Figure 2.4.2-1. Schematic of the Organization of the SARS-CoV-2 S Glycoprotein	10
2.4.2.1.3. Immunogenicity of BNT162b2 (V9) in Mice	10
2.4.2.1.4. Evaluation of BNT162b2 (V9) Immunogenicity and Protection Against SARS-CoV-2 Challenge in Rhesus Macaques.....	11
2.4.2.1.5. Immunogenicity Testing After Weekly Immunization of Rats in GLP Compliant Repeat Dose Toxicology Studies.....	12
2.4.2.1.6. Secondary Pharmacodynamics	12
2.4.2.1.7. Safety Pharmacology	12
2.4.2.1.8. Pharmacodynamic Drug Interactions	13
2.4.3. PHARMACOKINETICS	14
2.4.3.1. Brief Summary	14
2.4.3.2. Methods of Analysis	14
2.4.3.3. Absorption	14
2.4.3.3.1. In Vitro Absorption	14
2.4.3.3.2. Single-Dose Pharmacokinetics	15
Table 2.4.3-1. PK of ALC-0315 and ALC-0159 in Wistar Han Rats After IV Administration of LNPs Containing Surrogate Luciferase RNA at 1 mg/kg.....	15
Figure 2.4.3-1. Plasma and Liver Concentrations of ALC-0315 and ALC-0159 in Wistar Han Rats After IV Administration of LNPs Containing Surrogate Luciferase RNA at 1 mg/kg.....	15
2.4.3.4. Distribution	15
Figure 2.4.3-2. Bioluminescence Emission in BALB/c Mice after IM Injection of an LNP Formulation of modRNA Encoding Luciferase.....	16

090177e1950c1a59\Approved\Approved On: 29-Sep-2020 23:37 (GMT)

2.4.3.5. Metabolism 16

Figure 2.4.3-3. Proposed Biotransformation Pathway of ALC-0315 in Various Species 17

Figure 2.4.3-4. Proposed Biotransformation Pathway of ALC-0159 in Various Species 18

2.4.3.6. Excretion 18

2.4.3.7. Pharmacokinetic Drug Interactions 18

2.4.4. TOXICOLOGY 19

2.4.4.1. Brief Summary 19

Table 2.4.4-1. Overview of Toxicity Testing Program 20

2.4.4.2. Single-Dose Toxicity 21

2.4.4.3. Repeat-Dose Toxicity 21

 2.4.4.3.1. Repeat-Dose Toxicity Study of Three LNP-Formulated RNA Platforms
 Encoding for Viral Proteins by Repeated Intramuscular Administration to Wistar Han
 Rats (Study 38166)..... 21

 2.4.4.3.2. 17-Day Intramuscular Toxicity Study of BNT162b2 (V9) in Wistar Han
 Rats with a 3-week Recovery (Study 20GR142, Ongoing)..... 24

2.4.4.4. Genotoxicity 25

2.4.4.5. Carcinogenicity 25

2.4.4.6. Reproductive and Developmental Toxicity 26

2.4.4.7. Local Tolerance 26

2.4.4.8. Other Toxicity Studies 26

 2.4.4.8.1. Phototoxicity 26

 2.4.4.8.2. Antigenicity 26

 2.4.4.8.3. Immunotoxicity 26

 2.4.4.8.4. Mechanistic Studies 26

 2.4.4.8.5. Dependence 26

 2.4.4.8.6. Studies on Metabolites 26

 2.4.4.8.7. Studies on Impurities 27

 2.4.4.8.8. Other Studies 27

2.4.4.9. Target Organ Toxicity 27

2.4.5. INTEGRATED OVERVIEW AND CONCLUSIONS 28

2.4.6. LIST OF LITERATURE REFERENCES 30

090177e1950c1a59\Approved\Approved On: 29-Sep-2020 23:37 (GMT)

LIST OF ABBREVIATIONS AND DEFINITION OF TERMS

A:G	Albumin:globulin ratio
ADME	Absorption, distribution, metabolism, excretion
ALC-0159	Proprietary PEG-lipid included as an excipient in the LNP formulation used in BNT162b2
ALC-0315	Proprietary amino-lipid included as an excipient in the LNP formulation used in BNT162b2
ALT	Alanine aminotransferase
aPTT	Activated partial thromboplastin time
AST	Aspartate aminotransferase
CAS	Chemical abstracts service
CBER	Center for Biologics Evaluation and Research
CD	Cluster of differentiation
COVID-19	Coronavirus Disease 2019
DART	Developmental and reproductive toxicity
DNA	Deoxyribonucleic acid
DSPC	1,2-distearoyl-sn-glycero-3-phosphocholine
ELISA	Enzyme-linked immunosorbent assay
GGT	Gamma-glutamyl transferase
GLP	Good Laboratory Practice
H	Human (in metabolite scheme)
IFN	Interferon
IgG	Immunoglobulin G
IL	Interleukin
IM	Intramuscular(ly)
IND	Investigational New Drug Application
IV	Intravenous(ly)
LNP	Lipid-nanoparticle
Luc	Luciferase (from firefly <i>Pyroactomena lucifera</i>)
LUC	Large unstained cells
Mk	Monkey (in metabolite scheme)
Mo	Mouse (in metabolite scheme)
modRNA	Nucleoside-modified mRNA
mRNA	Messenger RNA
NA	Not applicable
NHP	Nonhuman primate
OECD	Organisation for Economic Co-operation and Development
P2 S	Spike protein P2 mutant
PEG	Polyethylene glycol
PK	Pharmacokinetics
PT	Prothrombin time
QC	Quality control review
QW	Once weekly
R	Rat (in metabolite scheme)

090177e1950c1a59\Approved\Approved On: 29-Sep-2020 23:37 (GMT)

LIST OF ABBREVIATIONS AND DEFINITION OF TERMS

RBC	Red blood cell
RBD	Receptor binding domain
RdRp	RNA-dependent RNA-polymerase
RNA	Ribonucleic acid
RT-PCR	Reverse transcription-polymerase chain reaction
S	SARS-CoV-2 spike glycoprotein
S1	S1 domain of the SARS-CoV-2 spike glycoprotein
S9	Supernatant fraction obtained from liver homogenate by centrifuging at 9000 g
SARS	Severe Acute Respiratory Syndrome
SARS-CoV-2	Severe acute respiratory syndrome coronavirus 2; coronavirus causing COVID-19
Tfh	T follicular helper cell
Th1	Type 1 T helper cells
TK	Toxicokinetic
TNF	Tumor necrosis factor
V8	Variant 8; P2 S
V9	Variant 9; P2 S
WBC	White blood cell
WHO	World Health Organization

2.4.1. OVERVIEW OF NONCLINICAL TESTING STRATEGY

BNT162b2 (BioNTech code number BNT162, Pfizer code number PF-07302048) is an investigational vaccine intended to prevent COVID-19, which is caused by SARS-CoV-2. BNT162b2 is a nucleoside modified mRNA (modRNA) expressing full-length S with two proline mutations (P2) to lock the transmembrane protein in an antigenically optimal prefusion conformation (Pallesen et al, 2017; Wrapp et al, 2020). The vaccine is formulated in lipid nanoparticles (LNPs). The LNP is composed of 4 lipids: ALC-0315, ALC-0159, DSPC, and cholesterol. Other excipients in the formulation include sucrose, NaCl, KCL, Na₂HPO₄, and KH₂PO₄. The dose selected for BNT162b2, advanced to Phase 2/3 clinical evaluation and intended for commercial use, is 30 ug RNA administered IM on Days 1 and 22.

In nonclinical studies, two variants of BNT162b2 were tested; designated “variant 8” and “variant 9” (V8 and V9, respectively). The variants differ only in their codon optimization sequences which are designed to improve antigen expression, otherwise the amino acid sequences of the encoded antigens are identical. Only BNT162b2 (V9) has been evaluated in the clinic and is the subject of this marketing application. The characteristics of each variant is described in the table below (Table 2.4.1-1).

Table 2.4.1-1. Nomenclature of the Vaccine Candidates

Product Code	RNA Platform	Antigen Variant	Description/Translated Protein	Variant Code	GLP Tox Data	Clinical Candidate
BNT162b2	modRNA	V8 ^a	P2 S	RBP020.1	Yes	No
BNT162b2	modRNA	V9^a	P2 S	RBP020.2	Yes^b	Yes

- a. The V8 and V9 variants of the P2 S antigen have the same amino acid sequence. Different codon optimizations were used for their ribonucleotide sequences.
 - b. A repeat-dose toxicity study with BNT162b2 (V9) is currently ongoing. Interim dosing phase data are included in the toxicology summaries.
- Bold: BNT162b2 (V9) vaccine candidate submitted for licensure.

The primary pharmacology, distribution, metabolism, and safety of BNT162b2 were evaluated in nonclinical pharmacology, pharmacokinetic, and toxicity studies in vitro and in vivo (Table 2.4.1-2).

Immunogenicity of BNT162b2 (V9) was evaluated in mice (2.4.2.1.3) and nonhuman primates (2.4.2.1.4). Immunogenicity of BNT162b2(V8) was evaluated in rats (2.4.2.1.5). For assessment of serum antibody responses in mice and rats, S1 and RBD-binding IgG responses were tested by an ELISA. Functional antibody responses were tested by a SARS-CoV-2 pseudotype neutralization assay (pVNT). In nonhuman primate studies, S1-binding IgG responses were tested in a direct Luminex-based immunoassay (dLIA) and functional antibody responses were assessed in an authentic SARS-CoV-2 neutralization assay. S-specific T cell responses were assessed in mouse and nonhuman primate studies in an IFN γ ELISpot and by intracellular cytokine staining flow cytometry-based analysis of the Th1/Th2 profile using splenocytes. The immunological assays are described in Section 2.6.2.12.

090177e1950c1a59\Approved\Approved On: 29-Sep-2020 23:37 (GMT)

A SARS-CoV-2 challenge study in BNT162b2 (V9)-immunized nonhuman primates was also conducted to assess protection against infection and to demonstrate lack of disease enhancement (Section 2.4.2.1.4.2).

Platform properties that support BNT162b2 were initially demonstrated with non-SARS-CoV-2 antigens. Non-GLP in vivo testing of an LNP-formulated modRNA encoding luciferase examined biodistribution in BALB/c mice after IM injection (Section 2.4.3.4) and the PK of the two novel excipients in the LNP formulation, ALC-0315 and ALC-0159, in Wistar Han rats (Section 2.4.3.3). In addition, the metabolism of ALC-0315 and ALC-0159 was evaluated in mouse, rat, monkey, and human blood, liver microsomes, S9 fractions, and hepatocytes and in vivo in rat plasma, urine, feces, and liver samples from the PK study (Table 2.4.1-2; Section 2.4.3.5).

BNT162b2 (V8) and (V9) have been studied in GLP-compliant repeat-dose toxicity studies in rats (Table 2.4.1-2). A GLP repeat-dose toxicity study for BNT162b2 (V8) has been completed. A GLP repeat-dose toxicity study for BNT162b2 (V9) is ongoing. As described above, the differences between the two BNT162b2 variants are minor. Therefore, it is expected that the nonclinical toxicity findings in the ongoing study with BNT162b2 (V9) will be comparable to BNT162b2 (V8) and is supported by the data generated in the ongoing study to date. The study designs are described in Section 2.4.4 and are based on WHO guidelines for vaccine development (WHO, 2005). An ongoing DART study of BNT162b2 (V9) in rats will be completed during the review of the marketing application. No additional toxicity studies are planned for BNT162b2.

IM administration was chosen for the toxicity studies as this is the intended route of administration. Rats were chosen for toxicity assessments as they are a commonly used animal species for the evaluation of toxicity and they mount an antigen-specific immune response to vaccination with BNT162b2.

The repeat-dose toxicity studies and the DART study in rats were/are being conducted in accordance with Good Laboratory Practice for Nonclinical Laboratory Studies, Code of US Federal Regulations (21 CFR Part 58), in an OECD Mutual Acceptance of Data member state. The location of records for inspection will be included in the final study report.

BNT162b2

Module 2.4. Nonclinical Overview

Table 2.4.1-2. Nonclinical Studies

Study Number	Study Type	Species / Test System	Test Item	Dose [RNA]	Cross reference
Pharmacology - BNT162b2 studies					
R-20-0085	In vivo immunogenicity	BALB/c mice	BNT162b2 (V9)	0.2, 1, 5 µg	Section 2.4.2.1.3
R-20-0112	In vivo immunogenicity	BALB/c mice	BNT162a1, BNT162b1, BNT162b2 (V9), BNT162c2	5 µg	Section 2.4.2.1.3
R-20-0211	In vitro protein expression	Cell culture	BNT162b2 (V9)	varied	Section 2.6.2.3
VR-VTR-10671	In vivo immunogenicity and SARS-CoV-2 challenge	Rhesus macaques	BNT162b2 (V9)	30 and 100 µg	Section 2.4.2.1.4
ADME					
PF-07302048_06Jul20_072424	PK of ALC-0315 and ALC-0159	Wistar Han Rats	modRNA encoding luciferase formulated in LNP comparable to BNT162b2	1 mg/kg	Section 2.4.3.3
R-20-0072	In vivo distribution	BALB/c mice	modRNA encoding luciferase formulated in LNP comparable to BNT162b2	2 µg	Section 2.4.3.4
01049-20008	In vitro metabolism	CD-1/ICR mouse, Wistar Han and/or Sprague Dawley rat, cynomolgus monkey and human liver microsomes, S9 fraction, hepatocytes	ALC-0315	NA	Section 2.4.3.5
01049-20009					
01049-20010			ALC-0159	NA	
01049-20020					
01049-20021					
01049-20022					
PF-07302048_05Aug20_043725	In vitro and in vivo metabolism	Blood, liver S9 fractions and hepatocytes from CD-1 mouse, Wistar Han rat, cynomolgus monkey and human. In vivo samples from Wistar Han rat plasma, urine, feces, and liver	In vitro: ALC-0315 and ALC-0159 In vivo: modRNA encoding luciferase formulated in LNP comparable to BNT162b2	1 mg/kg modRNA (in vivo samples)	Section 2.4.3.5
Toxicology – Studies with BNT162b2 variants					
38166	Repeat-dose toxicity	Wistar Han Rats	BNT162b2 (V8)	100 µg	Section 2.4.4.3
20GR142	Repeat-dose toxicity	Wistar Han Rats	BNT162b2 (V9)	30 µg	Section 2.4.4.3
20256434	Reproductive and developmental	Wistar Han Rats	BNT162b2 (V9)	30 µg	Section 2.4.4.6

090177e1950c1a59\Approved\Approved On: 29-Sep-2020 23:37 (GMT)

2.4.2. PHARMACOLOGY

2.4.2.1. Primary Pharmacodynamics

2.4.2.1.1. Summary

BNT162b2 (V9) (BioNTech code number BNT162, Pfizer code number PF-07302048) is a nucleoside-modified mRNA (modRNA) vaccine that encodes the SARS-CoV-2 full-length spike glycoprotein (S). In some preclinical research, a different variant of BNT162b2 was used: BNT162b2 (V8), which has a different codon optimization but encodes a protein with the same amino acid sequence as BNT162b2 (V9). In this document, “BNT162b2” refers to BNT162b2 (V9), unless otherwise specified. The glycoprotein encoded by both BNT162b2 variants includes two amino acid substitutions to proline (P2 S) locking the transmembrane protein in an antigenically optimal prefusion conformation (Wrapp et al, 2020; Pallesen et al, 2017). The RNA is formulated with functional and structural lipids, which protect the RNA from degradation and enable transfection of the RNA into host cells after IM injection. S is a major target of virus neutralizing antibodies and is a key antigen for vaccine development. The well-resolved trimeric prefusion structure and the high affinity binding to ACE2 and human neutralizing antibodies demonstrate that the recombinant P2 S authentically presents the ACE2 binding site and other epitopes targeted by many SARS-CoV-2 neutralizing antibodies.

In vitro studies and in vivo studies in mice and nonhuman primates demonstrate the mechanism of action for this RNA-based vaccine, to encode SARS-CoV-2 S that induces an immune response characterized by both a strong neutralizing antibody response and Th1-type CD4⁺ and a IFN γ ⁺ CD8⁺ T-cell response. BNT162b2 immunization protected rhesus macaques from infectious SARS-CoV-2 challenge, with reduced detection of viral RNA in vaccine-immunized animals compared to saline-immunized animals and with no evidence of clinical exacerbation.

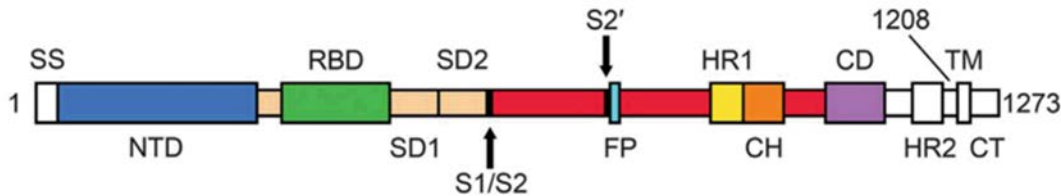
2.4.2.1.2. BNT162b2, A Lipid Nanoparticle Encapsulated RNA Vaccine Encoding the SARS-CoV-2 P2 S as a Vaccine Antigen

BNT162b2 is based on a nucleoside-modified mRNA (modRNA) platform technology (described in Section 2.6.2.1). Vaccination with modRNA formulated in LNPs is characterized by strong expansion of Th1-skewed antigen-specific T follicular helper (Tfh) cells, which stimulate and expand germinal center B cells, thereby resulting in particularly strong, long lived, high-affinity antibody responses (Sahin et al, 2014; Pardi et al, 2018). ModRNA vaccine candidates against other infectious diseases induce strong antibody responses and prime and expand multifunctional CD4⁺ and CD8⁺ T cells (Pardi et al, 2017; Pardi et al, 2018).

SARS-CoV-2 S is a large, trimeric glycoprotein that exists predominantly in a prefusion conformation on the virion (Ke et al, 2020). It is cleaved by furin into an N-terminal S1 and a C-terminal S2 fragment. S attaches to the host cell receptor, ACE2 by its receptor binding domain, which is contained in the S1 furin cleavage fragment. Spontaneously and during cell entry, the S1 fragment dissociates, and the S2 fragment undergoes a fold-back rearrangement

to the post-fusion conformation in a process that facilitates fusion of viral and host cell membranes. S is the main target of virus neutralizing antibodies (Zakhartchouk et al, 2007; Yong et al, 2019). Most of the antibodies with SARS-CoV-2 neutralizing activity are directed against the RBD (Jiang et al, 2020; Zost et al, 2020).

Figure 2.4.2-1. Schematic of the Organization of the SARS-CoV-2 S Glycoprotein



The S1 furin cleavage fragment includes the signal sequence (SS), the N terminal domain (NTD), the receptor binding domain (RBD, which binds the human cellular receptor, ACE-2), subdomain 1 (SD1), and subdomain 2 (SD2). The furin cleavage site (S1/S2) separates S1 from the S2 fragment, which contains the S2 protease cleavage site (S2') followed by a fusion peptide (FP), heptad repeats (HR1 and HR2), a central helix (CH) domain, the connector domain (CD), the transmembrane domain (TM) and a cytoplasmic tail (CT).
Source: modified from Wrapp et al, 2020.

BNT162b2 (V9) encodes a full-length P2 S transmembrane protein that contains two consecutive prolines introduced at amino acid positions 986 and 987, between the central helix (CH) and heptad repeat 1 (HR1) (Figure 2.4.2-1) (Wrapp et al, 2020; Pallesen et al, 2017). Two codon optimized forms of the coding sequence for this antigen were tested preclinically and were designated “variant 8” and “variant 9” (V8 and V9), with the vaccine candidate tested clinically and being proposed for licensure or authorization, V9, expressed from a codon optimized RNA gene with a higher content of cytosine ribonucleotides for increased protein expression. The RNA-expressed P2 S is membrane bound and elicits a potent humoral neutralizing antibody response and Th1-type CD4⁺ and CD8⁺ cellular response to block virus infection and kill virus infected cells, respectively.

Electron cryomicroscopy analysis of purified recombinant P2 S, expressed from DNA encoding the same S amino acid sequence as BNT162b2 RNA (except for the addition of a C-terminal tag for protein purification) revealed high similarity to previously reported structures (Cai et al, 2020). The well-resolved trimeric prefusion structure and the high affinity binding to ACE2 and human neutralizing antibodies demonstrate that the recombinant full-length P2 S protein authentically presents the ACE-2 binding site (Section 2.6.2.4).

2.4.2.1.3. Immunogenicity of BNT162b2 (V9) in Mice

BNT162b2 was highly immunogenic in mice with strong antigen-binding IgG and high titer neutralizing antibody responses together with a Th1-phenotype CD4⁺ response as well as an IFN γ ⁺, IL-2⁺ CD8⁺ T-cell response after a single immunization (described in Section 2.6.2.5). Total IgG ELISA showed that the vaccine induced a strong, dose-dependent IgG response

that recognizes S1 and the RBD and elicited high neutralizing titers in a pseudotype neutralization assay.

Stimulation of fresh splenocytes, collected 28 days after immunization, with an S protein-specific overlapping peptide pool demonstrated robust CD4⁺ and CD8⁺ T-cell IFN γ responses and a Th1-dominant profile was demonstrated in quantification of cytokines (IL-2 and IFN γ) in the corresponding culture supernatants (described in Section 2.6.2.5).

In summary, BNT162b2 induced a strong, neutralizing antibody response. CD4⁺ and CD8⁺ T-cell responses were detectable 12 and 28 days after one immunization and exhibited a Th1-dominant T cell response characteristic of RNA-based vaccines.

2.4.2.1.4. Evaluation of BNT162b2 (V9) Immunogenicity and Protection Against SARS-CoV-2 Challenge in Rhesus Macaques

BNT162b2 was assessed for immunogenicity and for protection against an infectious SARS-CoV-2 challenge in rhesus macaques. SARS-CoV-2 infection in humans manifests as both asymptomatic infection and as the disease COVID-19, with diverse signs, symptoms, and levels of severity. Based on published reports, SARS-CoV-2 challenged rhesus macaques develop an acute, transient infection in the upper and lower respiratory tract and have evidence of viral replication in the gastrointestinal tract, similar to humans (Zou et al, 2020; Kim et al, 2020). Varying degrees of pulmonary inflammation, primarily at the peak of infection at approximately Day 2 to 4 post-challenge, have been reported in the literature (Munster et al, 2020). The human and rhesus ACE-2 receptor have 100% amino acid identity at the critical binding residues, which may account for the fidelity of this SARS-CoV-2 animal model (Zhou et al, 2020).

2.4.2.1.4.1. Immunogenicity in Rhesus Macaques

Rhesus macaques immunized IM with 30 μ g or 100 μ g of BNT162b2 on Days 0 and 21 had readily detectable S1-binding IgG and SARS-CoV-2 neutralizing titers (NT50) as early as 14 days after a single immunization, with substantial increases following the second immunization (described in Section 2.6.2.6.1). On Day 28, seven days after Dose 2, at the 30 μ g dose level, the neutralizing geometric mean titer (GMT) reached 8-fold the GMT of a 38 member panel of human convalescent sera (HCS); at the 100 μ g dose level, the neutralizing GMT was 18-fold the HCS GMT. The HCS sera were drawn from SARS-CoV-2 infected individuals 18 to 83 years of age, at least 14 days after PCR-confirmed diagnosis and at a time when individuals were asymptomatic. The HCS panel provides a currently accessible benchmark to judge the quality of the humoral immune response to the vaccine. A decline of both S1-binding IgG levels and neutralizing titers was observed out to the latest measured time point (Day 56) but remained above the neutralizing GMT and the S1-binding geometric mean concentration (GMC) of the HCS.

As seen following mouse immunization, strong S-specific Th1-dominant IFN γ ⁺ T-cell responses were detected in all immunized rhesus macaques. By intracellular cytokine staining analysis, there was a dose-dependent increase in S-specific CD4⁺ T cell responses with a strong Th1-bias evidenced by high frequency of IFN γ ⁺, IL-2⁺, or TNF- α ⁺ cells.

Notably, CD8⁺ T-cell responses were also detectable in BNT162b2-immunized animals (summarized in Section 2.6.2.6.1).

2.4.2.1.4.2. SARS-CoV-2 Challenge of BNT162b2 (V9)-Immunized Nonhuman Primates

Groups of 2-4 year old male rhesus macaques that had received two IM immunizations with 100 µg BNT162b2 V9 (n=6) or saline (Control; n=3) 21 days apart were challenged 55 days after the second immunization with 1.05×10^6 plaque forming units of SARS-CoV-2 (strain USA-WA1/2020), split equally between the intranasal (IN) and intratracheal (IT) routes, as previously described (Singh et al, 2020). SARS-CoV-2 RNA was measured by reverse-transcription quantitative polymerase chain reaction (RT-qPCR) in bronchoalveolar lavage fluid, nasal swabs, and oropharyngeal swabs. The difference in viral RNA detection in BAL fluid between BNT162b2-immunised and control-immunised rhesus macaques after challenge is highly statistically significant (by a nonparametric test, p=0.0014). None of the challenged animals showed clinical signs of significant illness, indicating that the 2-4 years old male rhesus challenge model is primarily an infection model for SARS-CoV-2, not a COVID-19 disease model. No radiographic evidence of vaccine-elicited enhanced disease was observed (described in Section 2.6.2.6.2). In summary, BNT162b2 (V9) provided complete protection in the lungs and there was no evidence of vaccine-elicited disease enhancement.

2.4.2.1.5. Immunogenicity Testing After Weekly Immunization of Rats in GLP Compliant Repeat Dose Toxicology Studies

The nonclinical safety data package consists of two GLP-compliant repeat-dose rat toxicity studies where both BNT162b2 variants (V8 and V9) were evaluated (Section 2.4.4). In the first study (Study 38166), the immunogenicity of BNT162b2 (V8) was analyzed and results are described herein. The second GLP toxicology study (Study 20GR142) is ongoing and evaluates BNT162b2 (V9).

In Study 38166, rats received three weekly doses of BNT162b2 (V8). Serum samples were collected from main study animals on Day 17, two days after the 3rd dose, at the end of the dosing phase and on Day 38, at the end of a 3-week recovery phase.

The sera were analyzed by ELISA for IgG that bound S1 and RBD as well as for SARS-CoV-2-S pseudovirus neutralizing antibodies. The vaccine candidates elicited IgG that recognized S1 and RBD. After immunization, animals developed high titers of antigen-specific antibodies as well as pseudovirus neutralization titers (described in Section 2.6.2.7).

2.4.2.1.6. Secondary Pharmacodynamics

No secondary pharmacodynamics studies were conducted with BNT162b2.

2.4.2.1.7. Safety Pharmacology

No safety pharmacology studies were conducted with BNT162b2 as they are not considered necessary for the development of vaccines according to the WHO guideline (WHO, 2005).

2.4.2.1.8. Pharmacodynamic Drug Interactions

Nonclinical studies evaluating pharmacodynamic drug interactions with BNT162b2 were not conducted as they are generally not considered necessary to support development and licensure of vaccine products for infectious diseases ([WHO, 2005](#)).

090177e1950c1a59\Approved\Approved On: 29-Sep-2020 23:37 (GMT)

2.4.3. PHARMACOKINETICS

2.4.3.1. Brief Summary

Assessment of the ADME profile of BNT162b2 (BioNTech code number BNT162, Pfizer code number PF-07302048) included evaluating the PK and metabolism of two novel lipid excipients (ALC-0315 and ALC-0159) in the LNP and potential biodistribution of BNT162b2 using luciferase expression as a surrogate reporter. An intravenous rat PK study, using LNPs with the identical lipid composition as BNT162b2, demonstrated that ALC-0315 and ALC-0159 distribute from the plasma to the liver. While there was no detectable excretion of either lipid in the urine, the percent of dose excreted unchanged in feces was ~1% for ALC-0315 and ~50% for ALC-0159.

The biodistribution of BNT162b2 was evaluated using luciferase expression as a surrogate reporter in BALB/c mice. Mice were administered a luciferase expressing modRNA formulated like BNT162b2, with the identical lipid composition. Luciferase expression was measured in vivo following luciferin application. Luciferase expression was identified at the injection site at 6 hours after injection and was not detected after 9 days. Expression in the liver was also present to a lesser extent at 6 hours after injection and was not detected by 48 hours after injection.

The in vitro metabolism of ALC-0315 and ALC-0159 was evaluated in blood, liver microsomes, S9 fractions, and hepatocytes from mice, rats, monkeys, and humans. The in vivo metabolism was examined in rat plasma, urine, feces, and liver samples from the PK study. Metabolism of ALC-0315 and ALC-0159 appears to occur slowly in vitro and in vivo. ALC-0315 and ALC-0159 are metabolized by hydrolytic metabolism of the ester and amide functionalities, respectively, and this hydrolytic metabolism is observed across the species evaluated.

In summary, the nonclinical ADME studies indicate that the LNP distributes to the liver. Approximately 50% of ALC-0159 is excreted unchanged in feces, while metabolism played a role in the elimination of ALC-0315.

2.4.3.2. Methods of Analysis

No methods of analysis have been validated to support GLP TK studies of components of BNT162b2; however, a qualified LC/MS method was developed to support quantitation of the two novel LNP excipients for the non-GLP IV PK study in rats (Study [PF-07302048_06Jul20_072424](#)). Methods for immunogenicity and efficacy studies are described in Section [2.6.2.12](#).

2.4.3.3. Absorption

2.4.3.3.1. In Vitro Absorption

No absorption studies were conducted for BNT162b2, as the administration route is IM.

2.4.3.3.2. Single-Dose Pharmacokinetics

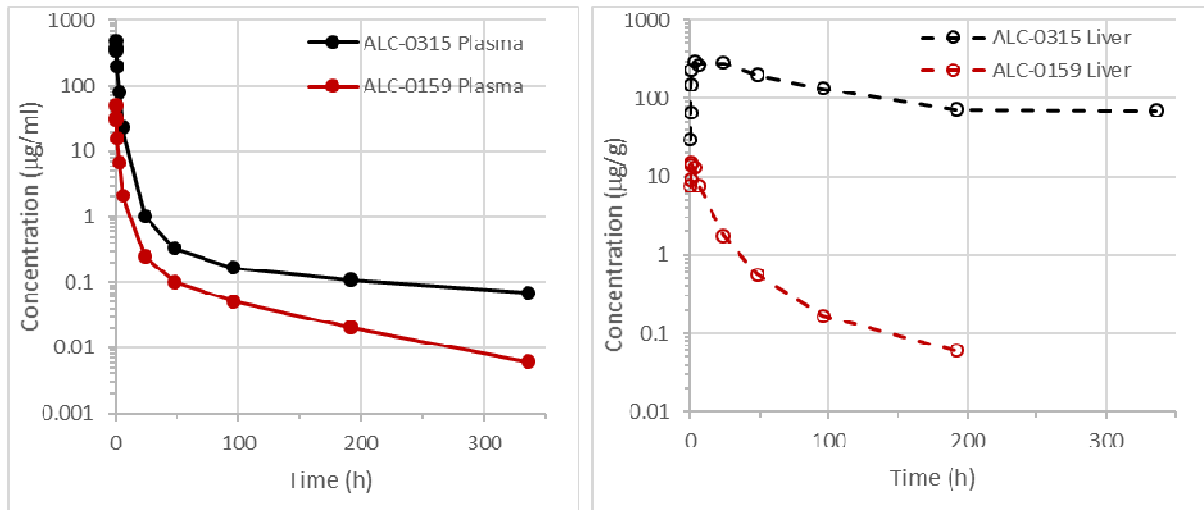
An intravenous rat PK study (PF-07302048_06Jul20_072424) was performed using LNPs containing surrogate luciferase RNA, with the identical lipid composition as BNT162b2, to explore the disposition of ALC-0315 and ALC-0159. The findings are depicted in Table 2.4.3-1, Tabulated Summary 2.6.5.3, and Figure 2.4.3-1.

Table 2.4.3-1. PK of ALC-0315 and ALC-0159 in Wistar Han Rats After IV Administration of LNPs Containing Surrogate Luciferase RNA at 1 mg/kg

Analyte	Dose of Analyte (mg/kg)	Gender /N	t _{1/2} (h)	AUC _{inf} (µg•h/mL)	AUC _{last} (µg•h/mL)	Estimated fraction of dose distributed to liver (%) ^a
ALC-0315	15.3	Male/3 ^b	139	1030	1020	60
ALC-0159	1.96	Male/3 ^b	72.7	99.2	98.6	20

a. Calculated as highest mean amount in the liver (µg)/total mean dose (µg) of ALC-0315 or ALC-0159.
b. 3 animals per timepoint; non-serial sampling.

Figure 2.4.3-1. Plasma and Liver Concentrations of ALC-0315 and ALC-0159 in Wistar Han Rats After IV Administration of LNPs Containing Surrogate Luciferase RNA at 1 mg/kg



Pharmacokinetic studies have not been conducted with BNT162b2 and are generally not considered necessary to support the development and licensure of vaccine products for infectious diseases (WHO, 2005; WHO, 2014).

2.4.3.4. Distribution

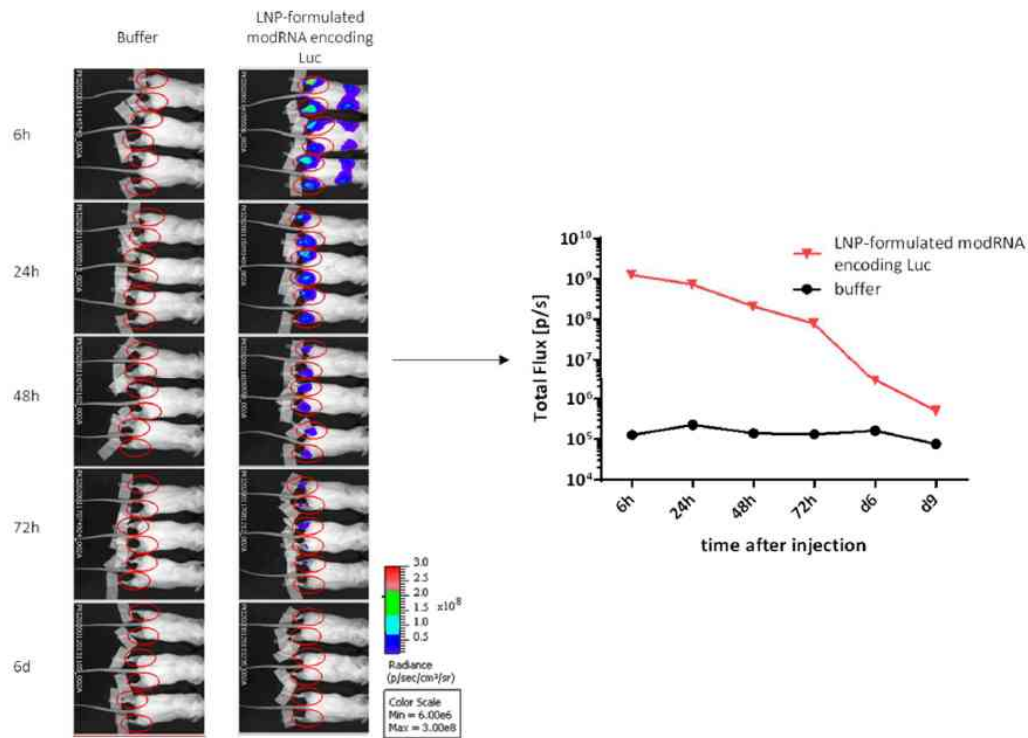
In an in vivo study (R-20-0072), biodistribution was assessed using luciferase as a surrogate marker protein, with RNA encoding luciferase formulated like BNT162b2, with the identical lipid composition. The LNP-formulated luciferase-encoding modRNA was administered to BALB/c mice by IM injection of 1 µg each in the right and left hind leg (for a total of 2 µg). Using in vivo bioluminescence after injection of luciferin substrate, luciferase protein

090177e1950c1a59\Approved\Approved On: 29-Sep-2020 23:37 (GMT)

expression was detected at different timepoints at the site of injection and to a lesser extent, and more transiently, in the liver (Figure 2.4.3-2, Tabulated Summary 2.6.5.5). Distribution to the liver is likely mediated by LNPs entering the blood stream. The luciferase expression at the injection sites dropped to background levels after 9 days. The repeat-dose toxicity study in rats showed no evidence of liver injury (Section 2.4.4.3.1).

The biodistribution of the antigen encoded by the RNA component of BNT162b2 is expected to be dependent on the LNP distribution and the results presented should be representative for the vaccine RNA platform, as the LNP-formulated luciferase-encoding modRNA had the same lipid composition.

Figure 2.4.3-2. Bioluminescence Emission in BALB/c Mice after IM Injection of an LNP Formulation of modRNA Encoding Luciferase



2.4.3.5. Metabolism

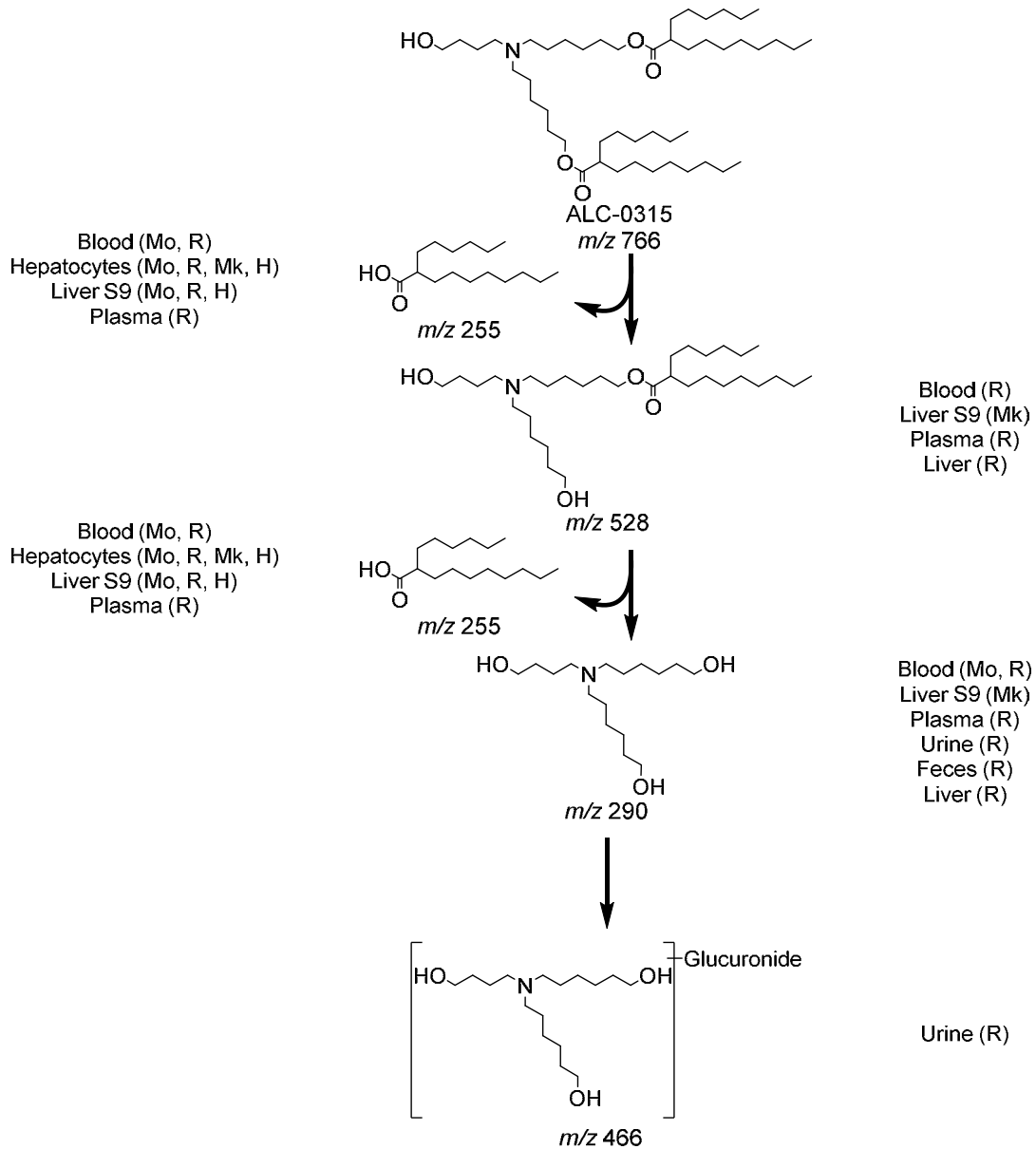
Of the four lipids used as excipients in the LNP formulation, two are naturally occurring (cholesterol and DSPC) and will be metabolized and excreted like their endogenous counterparts. The in vitro metabolic stability of the two novel lipids, ALC-0315 (aminolipid) and ALC-0159 (PEG-lipid), were evaluated in mouse, rat, monkey, and human liver microsomes, S9 fractions, and hepatocytes. ALC-0315 and ALC-0159 were stable (>82% remaining) over 120 min in liver microsomes and S9 fractions and over 240 min in hepatocytes in all species and test systems (Studies 01049-20008, 01049-20009,

090177e1950c1a59\Approved\Approved On: 29-Sep-2020 23:37 (GMT)

01049-20010, 01049-20020, 01049-20021, and 01049-20022; Tabulated Summary 2.6.5.10A and 2.6.5.10B).

Further study of the metabolism of ALC-0315 and ALC-0159 in vitro and in vivo evaluating the plasma, urine, feces, and liver from the rat PK study (Section 2.4.3.3.2) determined ALC-0315 and ALC-0159 are metabolized slowly (Study PF-07302048_05Aug20_043725; Tabulated Summaries 2.6.5.9, 2.6.5.10C, and 2.6.5.10D). ALC-0315 and ALC-0159 underwent hydrolytic metabolism of the ester and amide functionalities, respectively, and this hydrolytic metabolism was observed across the species evaluated (Figure 2.4.3-3 and Figure 2.4.3-4).

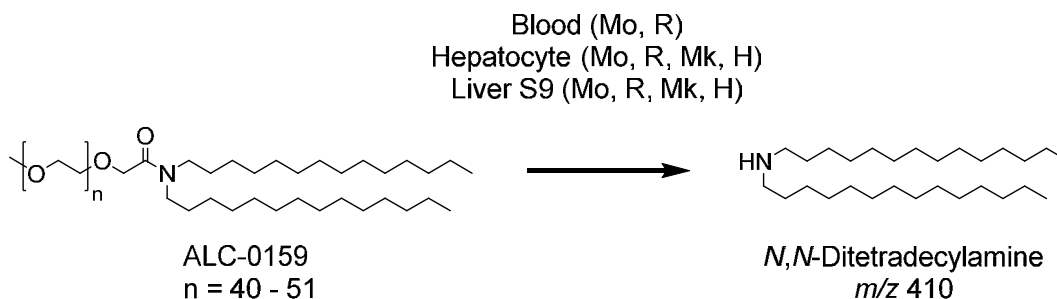
Figure 2.4.3-3. Proposed Biotransformation Pathway of ALC-0315 in Various Species



090177e1950c1a59\Approved\Approved On: 29-Sep-2020 23:37 (GMT)

Metabolism of ALC-0315 occurs via two sequential ester hydrolysis reactions, first yielding the monoester metabolite (m/z 528) followed by the doubly deesterified metabolite (m/z 290). Subsequent metabolism of the doubly deesterified metabolite resulted in a glucuronide metabolite (m/z 466), which was only observed in urine from the rat PK study. Additionally, 6-hexyldecanoic acid (m/z 255), the acid product of both hydrolysis reactions of ALC-0315, was identified.

Figure 2.4.3-4. Proposed Biotransformation Pathway of ALC-0159 in Various Species



The primary route of metabolism identified for ALC-0159 involves amide bond hydrolysis yielding *N,N*-ditetradecylamine (m/z 410).

The protein encoded by the RNA in BNT162b2 is expected to be proteolytically degraded like other endogenous proteins. RNA is degraded by cellular RNases and subjected to nucleic acid metabolism. Nucleotide metabolism occurs continuously within the cell, with the nucleoside being degraded to waste products and excreted or recycled for nucleotide synthesis. Therefore, no RNA or protein metabolism or excretion studies will be conducted.

2.4.3.6. Excretion

In the rat PK study (Section 2.4.3.3.2), there was no detectable excretion of ALC-0315 and ALC-0159 in urine after IV administration of LNPs containing surrogate luciferase RNA at 1 mg/kg. The percent excreted unchanged in feces was ~1% for ALC-0315 and ~50% for ALC-0159. Metabolites of ALC-0315 were detected in the urine of rats (Figure 2.4.3-3). No excretion studies have been conducted with BNT162b2 for the reasons described in Section 2.4.3.5.

2.4.3.7. Pharmacokinetic Drug Interactions

No PK drug interaction studies have been conducted with BNT162b2.

2.4.4. TOXICOLOGY

2.4.4.1. Brief Summary

The nonclinical toxicity assessment of BNT162b2 (BioNTech code number BNT162, Pfizer code number PF-07302048) includes 2 GLP-compliant repeat-dose toxicity studies and a developmental and reproductive toxicity (DART) study in Wistar Han rats outlined below in [Table 2.4.4-1](#). The nonclinical safety evaluation included 2 variants of BNT162b2: V8 and V9. BNT162b2 (V9), the candidate submitted for marketing application, differs from BNT162b2 (V8) only in the presence of optimized codons to improve antigen expression, but the amino acid sequences of the encoded antigens are identical. A GLP repeat-dose toxicity study for BNT162b2 (V8) has been completed (Study [38166](#)). A GLP repeat-dose toxicity study for BNT162b2 (V9) (Study [20GR142](#)) is ongoing and the study report will be provided during the marketing application review. It is expected that, based on the similarity of the variants, the nonclinical toxicity findings with BNT162b2 (V9) will not be different from BNT162b2 (V8). For the ongoing repeat-dose toxicity study, in-life parameters and clinical pathology (hematology, clinical chemistry, coagulation parameters, and acute phase proteins) as well as scheduled necropsy data (organ weights and macroscopic observations) are summarized in [Section 2.4.4.3.2](#). The remaining in-life parameters (serology) and microscopic pathology from the dosing phase as well as all endpoints collected during the recovery phase will be submitted during the marketing application review process. Likewise, the ongoing DART study with BNT162b2 (V9) will be completed and results will be available during the marketing application review.

The IM route of exposure was selected as it is the intended route of clinical administration. The selection of rats as the toxicology test species is consistent with the WHO guidance documents on nonclinical evaluation of vaccines ([WHO, 2005](#)), which recommend that vaccine toxicity studies be conducted in a species in which an immune response is induced by the vaccine. Generation of an immune response to BNT162b2 has been confirmed in rats in the first repeat-dose toxicity study. The Wistar Han rat is used routinely for regulatory toxicity studies, and there is an extensive historical safety database on this strain of rat.

Table 2.4.4-1. Overview of Toxicity Testing Program

Study ^a	Study (Sponsor) No.	Group/ Dose, µg RNA	Total Volume (µL) ^b	No. of Animals/ Group	Study Status
Repeat-Dose Toxicity					
17-Day, 2 or 3 Dose (1 Dose/Week) IM Toxicity With a 3 Week Recovery Phase in Rats ^{c,d}	38166	Control ^e , 0	200 ^f	15/sex	Completed
		BNT162b2 (V8), 100	200 ^f	15/sex	
17-Day, 3 Dose (1 Dose/Week) IM Toxicity With a 3 Week Recovery Phase in Rats ^g	20GR142	Saline ^h , 0	60	15/sex	Ongoing
		BNT162b2 (V9) ⁱ , 30	60	15/sex	
Reproductive & Developmental Toxicity					
Combined Fertility and Developmental Study (Including Teratogenicity and Postnatal Investigations) of BNT162b1, BNT162b2 and BNT162b3 by the IM route in Rats	20256434 (RN9391 R58)	Saline ^h , 0	60	44 F	Ongoing
		BNT162b2 (V9) ⁱ , 30	60	44 F	

a. All studies are GLP-compliant and were conducted in an OECD mutual acceptance of data-compliant member state.

b. Doses were administered as 1 application at 1 site unless otherwise indicated.

c. Study also evaluated the BNT162a1, BNT162b1 and BNT162c1 vaccine candidates.

d. QW x 3 (Days 1, 8, 15) for BNT162a1, BNT162b1, and BNT162b2 (V8); QW x 2 (Days 1, 8) for BNT162c1.

e. Phosphate buffered saline, 300 mM sucrose.

f. One application (100 µL) at 2 sites for a total dose volume of 200 µL.

g. Study also evaluated other vaccine candidates.

h. Sterile saline (0.9% NaCl).

i. BNT162b2 (V8) and BNT162b2 (V9) both encode the same amino acid sequence of the spike protein antigen with two prefusion conformation-stabilizing amino acids in the stalk.

Administration of BNT162b2 by IM injection to male and female Wistar Han rats once every week, for a total of 3 weekly cycles of dosing, was tolerated without evidence of systemic toxicity. Expected immune responses to the vaccine were evident such as edema and erythema at the injection sites, transient elevation in body temperature, and elevations in WBCs and acute phase reactants. Injection site reactions were common in all vaccine-administered animals and were greater after boost immunizations. Changes secondary to inflammation included slight and transient reduction in body weights and transient reduction in RETIC, PLT, and RBC mass parameters (Brooks, 2017; Kim 2014; Kim, 2016). All changes in clinical pathology parameters and acute phase proteins were similar to control at the end of the recovery phase for BNT162b2 (V8). Macroscopic pathology and organ weight

090177e1950c1a59\Approved\Approved On: 29-Sep-2020 23:37 (GMT)

changes were also consistent with immune activation and inflammatory response and included increased size and weight of draining iliac lymph nodes and spleen. Vaccine-related microscopic findings at the end of dosing for BNT162b2 (V8) were evident in injection sites and surrounding tissues, in the draining iliac lymph nodes, bone marrow, spleen, and liver. Microscopic findings at the end of the dosing phase were partially or completely recovered in all animals at the end of the recovery phase for BNT162b2 (V8). A robust immune response was elicited to the BNT162b2 (V8) vaccine antigen.

2.4.4.2. Single-Dose Toxicity

A separate single-dose toxicity study with BNT162b2 has not been conducted.

2.4.4.3. Repeat-Dose Toxicity

2.4.4.3.1. Repeat-Dose Toxicity Study of Three LNP-Formulated RNA Platforms Encoding for Viral Proteins by Repeated Intramuscular Administration to Wistar Han Rats (Study 38166)

The vaccine candidate BNT162b2 (V8), an LNP-formulated modified RNA vaccine expressing SARS-CoV-2 P2 S, was assessed in a GLP-compliant repeat-dose toxicity study in Wistar Han rats (Study 38166; Tabulated Summary 2.6.7.7A). This study also included assessment of 3 other LNP-formulated RNA vaccines, encoding either the SARS-CoV-2 P2 S or RBD antigens, which were not selected for market application. For the purpose of this submission, only the study findings from the 100 µg BNT162b2 (V8) vaccine group are summarized; findings from the other vaccine candidates were generally similar.

Administration of BNT162b2 (V8) via IM injections once weekly for 3 administrations to male and female Wistar Han rats was tolerated without evidence of systemic toxicity. The vaccine elicited a robust antigen-specific immune response and produced non-adverse macroscopic changes at the injection sites, spleen, and the draining lymph nodes, increased hematopoiesis in the bone marrow and spleen, liver vacuolation and clinical pathology changes consistent with an immune response. The findings in this study were fully recovered or showed evidence of recovery at the end of the 3-week recovery phase, and consistent with those typically associated with the IM administration of LNP-encapsulated mRNA vaccines (Hassett et al, 2019).

Body weights were lower 24 hours after each BNT162b2 (V8) vaccine administration compared with predose values (down to 0.92x versus baseline) with evidence of weight gain (1.22 to 1.37 versus baseline) by the end of recovery. Body weight gain between the administrations was comparable to the buffer control group. There were no noteworthy effects on body weight at the end of the recovery phase. There were no effects on food consumption.

BNT162b2 (V8)-administered animals generally had higher body temperatures compared with buffer control animals at 4 and 24 hours postdose. Group mean temperatures in rats administered the BNT162b2 (V8) vaccine were higher, but within approximately 1°C of the group mean body temperature of buffer-administered animals. Individual rats administered BNT162b2 (V8) did not have body temperatures >40.0°C after administration.

Local reactions were observed in male and female animals dosed IM with BNT162b2 (V8). The incidence and severity of the reactions were higher after the second or third injections compared with the first injection. The majority of animals had very slight edema or rarely slight erythema after the first dose. After the second or third dose, severities of edema and erythema increased up to moderate or rarely, severe. These observations resolved prior to the next injection or for recovery animals resolved during the 3-week recovery phase.

Most BNT162b2 (V8)-related changes in clinical pathology were consistent with an acute phase response and anticipated inflammation. Minor and variable alterations in other clinical pathology parameters were considered secondary effects of vaccination.

Expected immune responses to BNT162b2 (V8) were evident in hematology, such as elevations in mean neutrophil (up to 7.8x) and LUC counts (up to 7.7x controls) and were highest on Day 17, 48 hours after the last injection. White blood cells were higher (up to 2.2x controls) in the BNT162b2 (V8) vaccinated group on Day 17. Platelets were slightly decreased on Day 17 (down to 0.66x controls). A transient reduction in reticulocyte counts (down to 0.28x controls) was only observed after the administration of the first dose on Day 4. Decreased reticulocytes were similarly observed in rats treated with the licensed LNP-siRNA pharmaceutical Onpattro™ (NDA # 210922) but have not been observed in humans treated with this biotherapeutic (Kozauer et al, 2018), suggesting this is a species-specific effect. A slight reduction in red blood cell mass (HGB down to 0.87x controls) was observed on Day 17. Reticulocyte and RBC mass parameter decreases were likely secondary to the inflammation.

BNT162b2 (V8)-related changes in clinical chemistry included slightly higher GGT (a biomarker of biliary and not hepatocellular injury [Boone et al, 2005]) on Days 4 (up to 4.6x controls) and 17 (up to 4.2x controls) without evidence of microscopic changes in the biliary system or other hepatobiliary biomarkers. Additionally, higher GGT was not observed in the second repeat-dose toxicity study (20GR142). Albumin was slightly lower on Days 4 (down to 0.87x controls) and 17 (down to 0.89x controls) and globulin slightly higher on Day 17 (up to 1.2x controls). This resulted in the A:G ratio being slightly lower on Days 4 (down to 0.84x controls) and 17 (down to 0.76x controls). The effect on albumin and globulin were related to the vaccine-mediated inflammatory response as part of the negative and positive acute phase response, respectively (Sellers et al, 2020).

The acute phase proteins alpha-1-acid glycoprotein (up to 21x controls on Day 17) and alpha-2 macroglobulin (up to 217x controls on Day 17) were elevated in both males and females in the BNT162b2 (V8)-administered group on Days 4 and 17. Fibrinogen was higher in the vaccine-administered group (up to 3.1x controls), consistent with an acute phase response. Higher concentrations of acute phase proteins are an anticipated response to vaccination.

All changes in clinical pathology parameters and acute phase proteins were reversed at the end of the recovery phase.

090177e1950c1a59\Approved\Approved On: 29-Sep-2020 23:37 (GMT)

Compared with the buffer control, there were no test-article related differences in the concentration of serum cytokines evaluated, in urinalysis parameters, or in ophthalmoscopic or auditory parameters.

BNT162b2 (V8)-related higher absolute and relative spleen weights (up to 1.62x controls) were evident and correlated with the macroscopic observation of increased spleen size and the increased hematopoiesis. This is likely secondary to immune responses induced by the BNT162b2 (V8) vaccine.

The most common macroscopic observation in the BNT162b2 (V8) group was a thickened injection site and/or induration noted for nearly all animals (16/20) at necropsy. This finding correlated with microscopic inflammation at the injection site. Macroscopic findings at the injection site were resolved at the end of the recovery phase. Enlarged spleen and iliac lymph nodes were noted in several animals in the BNT162b2 (V8)-administered group. The effects on the lymphoid organs are consistent with immune responses to the BNT162b2 (V8).

Vaccine-related microscopic findings at the end of dosing were evident in injection sites and surrounding tissues, in the draining (iliac) lymph nodes, bone marrow, spleen, and liver.

The inflammation at the injection site was characterized by infiltrates of macrophages, granulocytes, and lymphocytes into the muscle, and variably into the dermis and subcutis. Injection site inflammation was associated with mostly mild myofiber degeneration, occasional muscle necrosis, and mostly mild fibrosis. Injection site findings were consistent with an immune/inflammatory response to an intramuscular vaccine administration.

In the draining (iliac) lymph node, increased cellularity of the follicular germinal centers and increased plasma cells (plasmacytosis) were variably present for all BNT162b2 (V8)-dosed animals. In addition, minimal to mild increases in the cellularity of bone marrow and hematopoiesis in the spleen likely related to increased granulopoiesis and correlated with increased circulating neutrophils (which correlated with increased spleen size and weight) were present in BNT162b2 (V8)-dosed animals.

Vacuolation of hepatocytes (minimal to mild) in the portal regions of the liver were present for all BNT162b2 (V8)-dosed animals. The liver findings were not associated with changes in markers of hepatocyte injury (eg, AST or ALT). While GGT was elevated in vaccine administered animals, it was not considered to be associated with the vacuolation of hepatocytes (Enmulat et al, 2010). Vacuolation of liver hepatocytes has been associated with hepatic clearance of the PEGylated lipid in the LNPs (Ivens et al, 2015).

Microscopic findings at the end of the dosing phase were partially or completely resolved in all animals at the end of the recovery phase. Inflammation at the injection site and surrounding tissues was less severe (minimal to mild) in animals administered BNT162b2 (V8) at the end of the 3-week recovery phase, indicating partial recovery. In the iliac lymph node, plasmacytosis was less severe, and macrophage infiltrates were present at the end of the 3-week recovery phase and reflect resolution of the inflammation noted at the end of the dosing phase.

All other observations in the bone marrow, spleen and liver were fully resolved at the end of the 3-week recovery phase.

The immune response to the vaccine antigen was evaluated by S1-binding IgG and RBD-binding IgG ELISAs, and a SARS-CoV-2 S pseudotype neutralization (pVNT) assay at Days 17 and 38 (Section 2.4.2.1.4). The data demonstrate that BNT162b2 (V8) elicited a SARS-CoV-2 S-specific antibody response with high neutralizing activity.

In conclusion, administration of BNT162b2 (V8) by IM injection to male and female Wistar Han rats once every week for 3 doses, was tolerated at 100 µg RNA without evidence of systemic toxicity.

2.4.4.3.2. 17-Day Intramuscular Toxicity Study of BNT162b2 (V9) in Wistar Han Rats with a 3-week Recovery (Study 20GR142, Ongoing)

The vaccine candidate BNT162b2 (V9), an LNP-formulated modified RNA vaccine expressing SARS-CoV-2 P2 S, was assessed in a GLP-compliant repeat-dose toxicity study in Wistar Han rats. This study also included assessment of another LNP-formulated RNA vaccine candidate (BNT162b3) that will not be included in the marketing application. For the purpose of this submission, the study findings from the BNT162b2 (V9) vaccine are summarized; findings from the BNT162b3 vaccine candidate also tested in this study were generally similar. BNT162b2 (V9) was administered at 30 µg once weekly administration for 3 doses (Days 1, 8, and 15) followed by a 3-week recovery phase (Tabulated Summary 2.6.7.7B).

For the ongoing repeat-dose study, in-life parameters and clinical pathology (hematology, clinical chemistry, coagulation parameters, and acute phase proteins) as well as scheduled necropsy data (organ weights and macroscopic observations) are summarized below. The remaining in-life parameters (serology) and microscopic pathology from the dosing phase as well as all endpoints collected during the recovery phase will be submitted during the marketing application review process.

All animals administered BNT162b2 (V9) survived to scheduled necropsy. There were no test article-related clinical signs or body weight changes noted. Test article-related reduced mean food consumption was noted on Days 4 and 11 (down to 0.83x controls). Test article-related higher mean body temperature (maximum increase post each dose) compared with control animals was noted on Day 1 (up to 0.54°C), Day 8 (up to 0.98°C), and Day 15 (up to 1.03°C) postdose.

BNT162b2 (V9)-related injection site edema and erythema were noted on Days 1 (maximum of slight edema and very slight erythema), 8 (maximum of moderate edema and very slight erythema) and 15 (maximum of moderate edema and very slight erythema). Test article-related erythema and edema fully resolved and was not noted prior to dose administration on Days 8 and 15.

All clinical pathology changes (type and magnitude) were generally consistent with expected immune responses to the vaccine or secondary to inflammation.

There were higher white blood cells (up to 2.95x controls), primarily involving neutrophils (up to 6.80x controls), monocytes (up to 3.30x controls), and LUC (up to 13.2x controls) and slightly higher eosinophils and basophils on Days 4 and 17. White blood cells were higher on Day 17 as compared with Day 4. There were transiently lower reticulocytes on Day 4 (down to 0.27x controls) in both sexes and higher reticulocytes on Day 17 (up to 1.31x controls) in females only. Lower RBC mass parameters (down to 0.90x controls) were present on Days 4 and 17.

There were lower A:G ratios (down to 0.82x) on Days 4 and 17. Higher fibrinogen levels were observed on Day 17 (up to 2.49x) when compared with control animals, consistent with an acute phase response. The acute phase proteins alpha-1-acid glycoprotein (up to 39x on Day 17) and alpha-2 macroglobulin (up to 71x on Day 17) were elevated in both males and females in the BNT162b2 (V9)-administered group on Days 4 and 17 with higher concentrations generally observed in males. All other changes in clinical pathology parameters were considered incidental. There were no changes in any of the urinalysis parameters evaluated.

Test article-related higher group mean absolute and relative spleen weights (to body and brain weight) were noted in BNT162b2 (V9) administered males (up to 1.42x) and females (up to 1.62x) relative to control group means. There were no other test article-related changes in organ weights.

Test article-related macroscopic findings included the observation of enlarged draining lymph nodes and pale/dark firm injection sites in animals administered BNT162b2 (V9). Macroscopically, enlarged draining lymph nodes (males: 1/10; females: 1/10), pale/dark injection sites (males: 2/10; females: 3/10) and firm injection sites (males: 2/10; females: 4/10) were observed.

In conclusion, administration of BNT162b2 (V9) via IM injections weekly for 3 administrations to male and female Wistar Han rats was tolerated without evidence of systemic toxicity. Dosing of BNT162b2 (V9) produced changes consistent with an inflammatory response and immune activation. The findings in this study are consistent with those typically associated with the IM administration of LNP-encapsulated mRNA vaccines.

2.4.4.4. Genotoxicity

No genotoxicity studies are planned for BNT162b2 as the components of the vaccine construct are lipids and RNA and are not expected to have genotoxic potential (WHO, 2005).

2.4.4.5. Carcinogenicity

Carcinogenicity studies with BNT162b2 have not been conducted as the components of the vaccine construct are lipids and RNA and are not expected to have carcinogenic or tumorigenic potential. Carcinogenicity testing is generally not considered necessary to support the development and licensure of vaccine products for infectious diseases (WHO, 2005).

2.4.4.6. Reproductive and Developmental Toxicity

Reproductive and developmental toxicity assessments are ongoing with BNT162b2 (V9) (Study 20256434) and the study report will be submitted during the licensure review.

Macroscopic and microscopic evaluation of male and female reproductive tissues from the repeat-dose toxicity study with BNT162b2 (V8) showed no evidence of toxicity (Section [2.4.4.3.1](#)).

2.4.4.7. Local Tolerance

Local tolerance of IM administration of BNT162b2 was evaluated by injection site observations and macroscopic and microscopic examination of injection sites in the repeat-dose toxicity studies and is described in Section [2.4.4.3](#).

2.4.4.8. Other Toxicity Studies

2.4.4.8.1. Phototoxicity

Phototoxicity studies with BNT162b2 have not been conducted.

2.4.4.8.2. Antigenicity

Immunogenicity was evaluated as part of the primary pharmacology studies (Section [2.4.2.1](#)). Serology data from the pivotal repeat-dose toxicity study (Study [38166](#)) shows a robust antigen-specific immune response to BNT162b2.

2.4.4.8.3. Immunotoxicity

Stand-alone immunotoxicity studies with BNT162b2 have not been conducted. However, immunotoxicological endpoints were collected as part of the repeat-dose toxicity studies; there were no adverse effects observed and no significant effects on measured cytokines (Section [2.6.6.3](#)).

2.4.4.8.4. Mechanistic Studies

Mechanistic studies with BNT162b2 have not been conducted.

2.4.4.8.5. Dependence

Dependence studies with BNT162b2 have not been conducted.

2.4.4.8.6. Studies on Metabolites

Stand-alone studies with administration of metabolites of BNT162b2 have not been conducted.

2.4.4.8.7. Studies on Impurities

Stand-alone studies with administration of impurities of BNT162b2 have not been conducted.

2.4.4.8.8. Other Studies

No other studies with BNT162b2 evaluated in this submission have been conducted.

2.4.4.9. Target Organ Toxicity

Based on data from the GLP repeat-dose toxicity studies (Section 2.4.4.3), administration of BNT162b2 was associated with local reactogenicity at the injection site and expected inflammatory responses. Microscopic findings within injection sites, which were partially reversed by the end of recovery, support this conclusion. Vacuolation of hepatocytes in the portal regions of the liver was considered vaccine-related and consistent with liver clearance of the PEG-lipid component of the LNP (Ivens et al, 2015). The liver finding was reversible, not associated with changes in markers of hepatocyte injury, and, was not adverse. The elevated levels of GGT were not attributed to the vacuolation (Ennulat et al, 2010).

2.4.5. INTEGRATED OVERVIEW AND CONCLUSIONS

The nonclinical program demonstrates that BNT162b2 variants are immunogenic in mice (variant V9), rats (variant V8), and nonhuman primates (variant V9), and the toxicity studies support the marketing application of this vaccine. Preclinical assessments in mice and nonhuman primates demonstrate that BNT162b2 (V9) elicits a rapid antibody response with measurable SARS-CoV-2 neutralizing titers after a single dose and substantial increases in titers after a second dose that exceed titers in sera from SARS-CoV-2/COVID-19-recovered patients. A Th1-dominant T cell response was evident in both mice and nonhuman primates. In a SARS-CoV-2 rhesus challenge model, BNT162b2 (V9) provided complete protection in the lungs and there was no evidence of vaccine-elicited disease enhancement.

An IV rat PK study, using an LNP with the identical lipid composition as BNT162b2, demonstrated that the novel lipid excipients in the LNP formulation, ALC-0315 and ALC-0159, distribute from the plasma to the liver. While there was no detectable excretion of either lipid in the urine, the percent of dose excreted unchanged in feces was ~1% for ALC-0315 and ~50% for ALC-0159. Further studies indicated metabolism played a role in the elimination of ALC-0315. Biodistribution was assessed using luciferase expression as a surrogate reporter formulated like BNT162b2, with the identical lipid composition. After IM injection of the LNP-formulated RNA encoding luciferase in BALB/c mice, luciferase protein expression was demonstrated at the site of injection 6 hours post dose and was not detected after 9 days. Luciferase was detected to a lesser extent in the liver; expression was present at 6 hours after injection and was not detected by 48 hours after injection. The metabolism of ALC-0315 and AL-0159 was evaluated in blood, liver microsomes, S9 fractions, and hepatocytes from mice, rats, monkeys, and humans. The in vivo metabolism was examined in rat plasma, urine, feces, and liver samples from the PK study. Metabolism of ALC-0315 and ALC-0159 appears to occur slowly in vitro and in vivo. ALC-0315 and ALC-0159 are metabolized by hydrolytic metabolism of the ester and amide functionalities, respectively, and this hydrolytic metabolism is observed across the species evaluated.

Administration of BNT162b2 (V8) and BNT162b2 (V9) by IM injection to male and female Wistar Han rats once every week for a total of 3 weekly cycles of dosing was tolerated without evidence of systemic toxicity in GLP-compliant repeat-dose toxicity studies. Expected inflammatory responses to the vaccine were evident such as edema and erythema at the injection sites, transient elevation in body temperature, and elevations in WBCs and acute phase reactants. Injection site reactions were common in all vaccine-administered animals and were greater after boost immunizations. Changes secondary to inflammation included slight and transient reduction in body weights and transient reduction in RETIC, PLT and RBC mass parameters. All changes in clinical pathology parameters and acute phase proteins were reversed at the end of the recovery phase for BNT162b2 (V8). Macroscopic pathology and organ weight changes were also consistent with immune activation and inflammatory response and included increased size of draining iliac lymph nodes and increased size and weight of spleen. Vaccine-related microscopic findings at the end of dosing phase for BNT162b2 (V8) were evident in injection sites and surrounding tissues, in the draining iliac lymph nodes, bone marrow, spleen, and liver. Microscopic findings at the end of the dosing phase were partially or completely recovered in all animals at the end of the recovery phase for BNT162b2 (V8). A robust immune response was elicited to the BNT162b2 (V8) antigen.

BNT162b2

Module 2.4. Nonclinical Overview

In summary, the nonclinical package summarized above and in the ongoing studies supports the licensure of BNT162b2 administered twice by IM injection at a dose of 30 µg RNA.

090177e1950c1a59\Approved\Approved On: 29-Sep-2020 23:37 (GMT)

CONFIDENTIAL

Page 29

FDA-CBER-2021-4379-0000967

2.4.6. LIST OF LITERATURE REFERENCES

Boone L, Meyer D, Cusick P, et al. Selection and interpretation of clinical pathology indicators of hepatic injury in preclinical studies. *Vet Clin Pathol* 2005;34(3):182-8.

Brooks MB, Turk JR, Guerrero A, et al. Non-Lethal Endotoxin Injection: A Rat Model of Hypercoagulability *PLoS ONE* 2017;12(1):e0169976.

Cai Y, Zhang J, Xiao T, et al. Distinct conformational states of SARS-CoV-2 spike protein. *Science* 2020;10.1126/science.abd4251.

Ennulat D, Magid-Slav M, Rehm S, et al. Diagnostic performance of traditional hepatobiliary biomarkers of drug-induced liver injury in the rat. *Toxicol Sci* 2010;116(2):397-412.

Hassett KJ, Benenato KE, Jacquinet E et al. Optimization of lipid nanoparticles for intramuscular administration of mRNA vaccines. *Molecular Therapy Nucleic acids* 2019;15:1-11.

Ivens I, Achanzar W, Bauman A, et al. PEGylated Biopharmaceuticals: Current experience and considerations for nonclinical development *Toxicol Path* 2015;43:959-83.

Jiang S, Hyllyer C, Du L. Neutralizing antibodies against SARS-CoV-2 and other human coronaviruses. *Science and society. Trends Immunol* 2020; 41(5)(May):355-9.

Ke Z, Oton J, Qu K, et al. Structures, conformations and distributions of SARS-CoV-2 spike protein trimers on intact virions. *Nature* 2020;10.1038/s41586-020-2665-2.

Kim A, Fung E, Parikh SG, et al. A mouse model of anemia of inflammation: complex pathogenesis with partial dependence on hepcidin. *Blood* 2014;123(8):1129-36.

Kim A, Fung E, Parikh SG, et al. Isocitrate treatment of acute anemia of inflammation in a mouse model. *Blood Cells, Molecules, and Diseases* 2016;56(1):31-6.

Kim JY, Ko JH, Kim Y, et al. Viral load kinetics of SARS-CoV-2 infection in first two patients in Korea. *J Korean Med Sci* 2020;35(7)(Feb):e86.

Kozauer NA, Dunn WH, Unger EF, et al. CBER multi-discipline review of Onpattro. NDA 210922. 10 Aug 2018. Available at:

https://www.accessdata.fda.gov/drugsatfda_docs/nda/2018/210922Orig1s000MultiR.pdf.
02 Aug 2020.

Munster VJ, Feldmann F, Williamson BN, et al. Respiratory disease and virus shedding in rhesus macaques inoculated with SARS-CoV-2. Available from:

<https://doi.org/10.1101/2020.03.21.001628>. Accessed: 24 Sep 2020

Pallesen J, Wang N, Corbett KS, et al. Immunogenicity and structures of a rationally designed prefusion MERS-CoV spike antigen. *Proc Natl Acad Sci USA* 2017;114(35):E7348-57.

090177e1950c1a59\Approved\Approved On: 29-Sep-2020 23:37 (GMT)

Pardi N, Hogan MJ, Pelc RS, et al. Zika virus protection by a single low-dose nucleoside-modified mRNA vaccination. *Nature* 2017;543(7644):248-51.

Pardi N, Parkhouse K, Kirkpatrick E, et al. Nucleoside-modified mRNA immunization elicits influenza virus hemagglutinin stalk-specific antibodies. *Nat Comm* 2018;9(1)(08):3361.

Sahin U, Karikó K, Türeci Ö. mRNA-based therapeutics - developing a new class of drugs. *Nat Rev Drug Discov* 2014;13(10):759-80.

Sellers RS, Nelson K, Bennet B, et al. Scientific and regulatory policy committee points to consider*: approaches to the conduct and interpretation of vaccine safety studies for clinical and anatomic pathologists. *Toxicol Pathol* 2020; 48(2):257-76.

Singh DK, SR Ganatra, B Singh et al. SARS-CoV-2 infection leads to acute infection with dynamic cellular and inflammatory flux in the lung that varies across nonhuman primate species. Available from: <https://doi.org/10.1101/2020.06.05.136481>. Accessed: 24 Sep 2020.

Study 20GR142 . Giovanelli M. 17-Day Intramuscular Toxicity Study of BNT162B2 (V9) and BNT162B3C in Wistar Han Rats with a 3-Week Recovery. Study ongoing.

World Health Organization. WHO guidelines on nonclinical evaluation of vaccines. Annex 1. In: World Health Organization. WHO technical report series, no. 927. Geneva, Switzerland; World Health Organization; 2005:31-63.

World Health Organization. Annex 2. Guidelines on the nonclinical evaluation of vaccine adjuvants and adjuvanted vaccines. In: WHO technical report series no. 987. Geneva, Switzerland: World Health Organization; 2014: p. 59-100.

Wrapp D, Wang N, Corbett KS, et al. Cryo-EM structure of the 2019-nCoV spike in the prefusion conformation. *Science* 2020;367(6483):1260-3.

Yong CY, Ong HK, Yeap SK, et al. Recent advances in the vaccine development against middle east respiratory syndrome-coronavirus. *Front Microbiol* 2019;10:1781.

Zakhartchouk AN, Sharon C, Satkunarajah M, et al. Immunogenicity of a receptor-binding domain of SARS coronavirus spike protein in mice: implications for a subunit vaccine. *Vaccine* 2007;25(1):136-43.

Zhou M, Zhang X, Qu J. Coronavirus disease 2019 (COVID-19): a clinical update. *Front Med* 2020(Apr):1-10.

Zost S, Gilchuk P, Chen R, et al. Rapid isolation and profiling of a diverse panel of human monoclonal antibodies targeting the SARS-CoV-2 spike protein. *BioRxiv* posted May13, 2020, www.biorxiv.org/content/10.1101/2020.05.12.091462v1.

Zou L, Ruan F, Huang M, et al. SARS-CoV-2 viral load in upper respiratory specimens of infected patients. *N Engl J Med* 2020;382(12)(03):1177-9.

2.4 NONCLINICAL OVERVIEW

090177e1934a5cff\Approved\Approved On: 21-Apr-2020 19:41 (GMT)

TABLE OF CONTENTS

2.4 NONCLINICAL OVERVIEW	1
LIST OF ABBREVIATIONS AND DEFINITION OF TERMS	6
2.4.1. OVERVIEW OF NONCLINICAL TESTING STRATEGY	8
Table 2.4.1-1. Nomenclature of the Vaccine Candidates	9
Table 2.4.1-2. Nonclinical Studies	10
2.4.2. PHARMACOLOGY	13
2.4.2.1. Primary Pharmacodynamics	13
2.4.2.1.1. Summary	13
2.4.2.1.2. RNA Vaccine Platforms	14
Figure 2.4.2-1. Overview of the Three RNA Platforms	14
2.4.2.1.3. Lipid Nanoparticles	16
Figure 2.4.2-2. Schematic Organization of a LNP	17
Table 2.4.2-1. Lipids in the Formulation	18
2.4.2.1.4. Immune Phenotype Elicited by LNP-Formulated RNA Vaccines	19
Table 2.4.2-2. Characteristics of the Adaptive Immune Response for the mRNA Platforms.....	19
2.4.2.1.5. SARS-CoV-2 S as a Vaccine Target	20
Figure 2.4.2-3. Replication Cycle of a Coronavirus	21
Figure 2.4.2-4. Schematic of the Organization of the SARS-CoV-2 S Glycoprotein	22
2.4.2.1.6. Serological and Virological Assays	22
2.4.2.1.7. Lack of Cell to Cell Spread of saRNA	23
Figure 2.4.2-5. Design of Assay to Test for saRNA Cell-to-Cell Spread	24
Figure 2.4.2-6. Flow Cytometry Detection of Cell Surface HA	24
2.4.2.1.8. In Vitro Expression of Antigens from COVID-19 vaccine RNA	25
Figure 2.4.2-7. Western Blot Detection of RBD and P2 S in RNA-Transfected Cells ...	25
Figure 2.4.2-8. Immunofluorescence Detection of RBD and P2 S in RNA Transfected Cells.....	26
2.4.2.1.9. Supportive Mouse Immunogenicity Studies	27
Figure 2.4.2-9. Influenza HA Binding and Virus Neutralization Elicited by Immunization of Mice with modRNA Encoding HA in the Clinical LNP Formulation..	27
Figure 2.4.2-10. CD4+ and CD8+ T Cell Response to LNP-Formulated modRNA Encoding Influenza HA by IFN- ELISpot.....	28

090177e1934a5cff\Approved\Approved On: 21-Apr-2020 19:41 (GMT)

Figure 2.4.2-11. IgG Response Recognizing S1 and RBD 7, 14, 21, and 28 d after Immunization with uRNA Encoding P2 S V8..... 29

Figure 2.4.2-12. Kinetics of the IgG Response Recognizing S1 and RBD after Immunization with uRNA Encoding P2 S V8..... 30

Figure 2.4.2-13. Pseudovirus Neutralization 14, 21 and 28 d after Immunization with uRNA Encoding P2 S V8..... 31

Figure 2.4.2-14. IgG Response Recognizing S1 and RBD 7, 14 and 21 d after Immunization with saRNA Encoding RBD V5..... 32

Figure 2.4.2-15. Pseudovirus Neutralization 14 d after Immunization with saRNA Encoding the RBD V5..... 33

Figure 2.4.2-16. IgG Response Recognizing S1 and RBD IgG 7, 14 and 21 d after Immunization with modRNA Encoding P2 S V8..... 34

Figure 2.4.2-17. Pseudovirus Neutralization 14 d after Immunization with modRNA Encoding P2 S V8..... 35

2.4.2.1.10. Mouse Immunogenicity Studies for COVID-19 Vaccine Candidates 35

Table 2.4.2-3. Design of Mouse Immunogenicity Studies for COVID-19 Vaccine Candidates..... 35

Figure 2.4.2-18. IgG Response Recognizing S1 and RBD 7, 14, 21 and 28 d after Immunization with uRNA Encoding RBD V5..... 37

Figure 2.4.2-19. Kinetics of the IgG Response Recognizing S1 and RBD after Immunization with uRNA Encoding RBD V5..... 38

Figure 2.4.2-20. Pseudovirus Neutralization Titers 7, 14, and 21 after Immunization with uRNA Encoding RBD V5..... 39

Figure 2.4.2-21. IgG Response Recognizing S1 and RBD 7, 14, 21 and 28 d after Immunization with modRNA Encoding RBD V5..... 40

Figure 2.4.2-22. Kinetics of the IgG Response Recognizing S1 and RBD after Immunization with modRNA Encoding RBD V5..... 41

Figure 2.4.2-23. Pseudovirus Neutralization 14, 21 and 28 d after Immunization with modRNA Encoding RBD V5..... 42

Figure 2.4.2-24. IgG Response Recognizing S1 and RBD 7 and 14 d after Immunization with modRNA Encoding P2 S V9..... 43

Figure 2.4.2-25. IgG Response Recognizing S1 and RBD 7, 14 and 21 d after Immunization with saRNA Encoding P2 S V9..... 44

Figure 2.4.2-26. Pseudovirus Neutralization 14 and 21 d after Immunization with saRNA Encoding P2 S V9..... 45

2.4.2.1.11. Immunogenicity Testing After Weekly Immunization of Rats in the GLP Compliant Repeat Dose Toxicology Study..... 45

Figure 2.4.2-27. IgG Responses Recognizing S1 after Repeated Immunization in the Rat Toxicology Study..... 46

090177e1934a5cff\Approved\Approved On: 21-Apr-2020 19:41 (GMT)

Figure 2.4.2-28. IgG Responses Recognizing RBD after Repeated Immunization in the Rat Toxicology Study.....	47
Table 2.4.2-4. IgG Concentrations Against S1 and RBD in Immunized Wistar Han Rats.....	47
Figure 2.4.2-29. Pseudovirus Neutralization Activity (pVN50) in Repeatedly Dosed Rats.....	48
2.4.2.1.12. Secondary pharmacodynamics	48
2.4.2.1.13. Safety pharmacology	48
2.4.2.1.14. Nonclinical pharmacology - Conclusions	48
2.4.3. PHARMACOKINETICS	50
2.4.3.1. Brief Summary	50
2.4.3.2. Methods of Analysis	50
2.4.3.3. In Vitro Absorption	50
2.4.3.4. Pharmacokinetics	50
2.4.3.5. Distribution	50
Figure 1. Bioluminescence Emission in BALB/c Mice after IM Injection of an LNP Formulation of modRNA Encoding Luciferase.....	51
2.4.3.6. Metabolism	51
2.4.3.7. Excretion	52
2.4.3.8. Pharmacokinetic Drug Interactions	52
2.4.4. TOXICOLOGY	53
2.4.4.1. Brief Summary	53
Table 2.4.4-1. Overview of Toxicity Testing Program	54
2.4.4.2. Single-Dose Toxicity	55
2.4.4.3. Repeat-Dose Toxicity	55
2.4.4.3.1. Repeat-Dose Toxicity Study of Three LNP-Formulated RNA Platforms Encoding for Viral Proteins by Repeated Intramuscular Administration to Wistar Han Rats.....	55
2.4.4.4. Genotoxicity	58
2.4.4.5. Carcinogenicity	59
2.4.4.6. Reproductive and Developmental Toxicity	59
2.4.4.7. Local Tolerance	59
2.4.4.8. Other Toxicity Studies	59
2.4.4.8.1. Phototoxicity	59

090177e1934a5cff\Approved\Approved On: 21-Apr-2020 19:41 (GMT)

COVID-19 Vaccine (BNT162, PF-07302048)

BB-IND 19736

Module 2.4. Nonclinical Overview

2.4.4.8.2. Antigenicity	59
2.4.4.8.3. Immunotoxicity	59
2.4.4.8.4. Mechanistic Studies	59
2.4.4.8.5. Dependence	60
2.4.4.8.6. Studies on Metabolites	60
2.4.4.8.7. Studies on Impurities	60
2.4.4.8.8. Other Studies	60
2.4.4.9. Target Organ Toxicity	60
IN-TEXT TABLES AND FIGURES	54
Table 2.4.4-1. Overview of Toxicity Testing Program	54
2.4.5. INTEGRATED OVERVIEW AND CONCLUSIONS	61
2.4.6. LIST OF LITERATURE REFERENCES	63

090177e1934a5cff\Approved\Approved On: 21-Apr-2020 19:41 (GMT)

LIST OF ABBREVIATIONS AND DEFINITION OF TERMS

ADCC	Antibody-dependent cellular cytotoxicity
aPTT	Activated partial thromboplastin time
CAS	Chemical abstracts service
CBER	Center for Biologics Evaluation and Research
CD	Cluster of differentiation
CoV	Coronavirus
COVID-19	Coronavirus Disease 2019
DDI	Drug drug interaction
dLIA	Direct binding Luminex immunoassay
DNA	Deoxyribonucleic acid
DSPC	1,2-distearoyl-sn-glycero-3-phosphocholine
ELISA	Enzyme-linked immunosorbent assay
ELISpot	Enzyme-linked immunosorbent spot assay
FIH	First-In-Human
GGT	Gamma-glutamyl transferase
GLP	Good Laboratory Practice
HA	Hemagglutinin
HAI	Hemagglutinin inhibition assay
HEK	Human embryonic kidney
IB	Investigator's Brochure
IFN	Interferon
IgG	Immunoglobulin G
IL	Interleukin
IM	Intramuscular(ly)
IND	Investigational New Drug Application
IV	Intravenous(ly)
kDa	Kilodalton
LLOQ	Lower limit of quantification
LNP	Lipid-nanoparticle
Luc	Luciferase (from firefly <i>Pyroactomena lucifera</i>)
LUC	Large unstained cells
MERS	Middle East respiratory syndrome
modRNA	Nucleoside-modified mRNA
mRNA	Messenger RNA
NHP	Nonhuman primate
NVA	Non-vaccine antigen
OECD	Organisation for Economic Co-operation and Development
ORF	Open reading frame
P2 S	Spike protein P2 mutant
PK	Pharmacokinetics
PT	Prothrombin time
pVNT	Pseudotype virus neutralization assay

COVID-19 Vaccine (BNT162, PF-07302048)

BB-IND 19736

Module 2.4. Nonclinical Overview

QC	Quality control review
QW	Once weekly
RBD	Receptor binding domain
RdRp	RNA-dependent RNA-polymerase
RNA	Ribonucleic acid
RT-PCR	Reverse transcription-polymerase chain reaction
S	SARS-CoV-2 spike glycoprotein
saRNA	Self-amplifying RNA
SARS	Severe Acute Respiratory Syndrome
SARS-CoV-2	Severe acute respiratory syndrome coronavirus 2; coronavirus causing COVID-19
SDS-PAGE	Sodium dodecyl sulfate-polyacrylamide gel electrophoresis
SEM	Standard error of the mean
siRNA	Small interfering RNA
Tfh	T follicular helper cell
Th1	Type 1 T helper cells
Th2	Type 2 T helper cells
TK	Toxicokinetic
TLR	Toll-like receptor
TNF	Tumor necrosis factor
ULOQ	Upper limit of quantification
uRNA	Unmodified mRNA
UTR	Untranslated region
V5	Variant 5; RBD
V8	Variant 8; P2 S
V9	Variant 9; P2 S
VEE	Venezuelan equine encephalitis virus
VLVs	Virus-like vesicles
VSV	Vesicular stomatitis virus
WHO	World Health Organization

090177e1934a5cff\Approved\Approved On: 21-Apr-2020 19:41 (GMT)

2.4.1. OVERVIEW OF NONCLINICAL TESTING STRATEGY

BioNTech and Pfizer are developing an investigational vaccine intended to prevent COVID-19, which is caused by SARS-CoV-2. The vaccine is referred to as COVID-19 vaccine (BioNTech code number BNT162; Pfizer reference number PF-07302048).

Each candidate for the vaccine contains RNA from one of three platforms:

- unmodified mRNA (uRNA)
- nucleoside modified mRNA (modRNA)
- self-amplifying RNA (saRNA)

The RNA is formulated in LNPs. Each of the RNAs expresses one of two antigens, which are based on SARS-CoV-2 spike glycoprotein (S):

- A trimerized receptor binding domain (RBD; [Kirchdoerfer et al, 2018](#)).
- The full-length, membrane-anchored glycoprotein with two introduced proline mutations (P2 S; [Pallesen et al, 2017](#); [Wrapp et al, 2020](#)).

The antigens have variants (V5 for the RBD and V8 or V9 for P2 S). Variants of the same antigen have the same amino acid sequence, but the RNAs that encode them differ in their codon optimization.

In the phase 1/2 clinical study, C4591001, four COVID-19 vaccine candidates will be evaluated:

- BNT162a1 (RBL063.3) - uRNA encoding RBD V5
- BNT162b1 (RBP020.3) - modRNA encoding RBD V5
- BNT162b2 (RBP020.2) - modRNA encoding P2 S V9
- BNT162c2 (RBS004.2) - saRNA encoding P2 S V9

Reference information on these clinical vaccine candidates and other constructs tested nonclinically is provided in [Table 2.4.1-1](#).

The primary pharmacology of the COVID-19 vaccine candidates and constructs expressing alternative antigens on the same vaccine platforms were evaluated in non-clinical pharmacology studies *in vitro* and *in vivo* ([Table 2.4.1-2](#)). *In vitro* testing demonstrated that saRNA does not spread from cell to cell ([Section 2.4.2.1.7](#)). Expression of the RBD and P2 S antigens from vaccine candidate RNAs was demonstrated in cultured cells ([Section 2.4.2.1.8](#)).

Platform properties that support the COVID-19 vaccines were demonstrated with non-SARS-CoV-2 antigens. Non-GLP *in vivo* testing of LNP-formulated modRNA encoding luciferase

examined biodistribution in BALB/c mice after IM injection ([Section 2.4.3.5](#)). A murine immunogenicity study of an LNP-formulated modRNA expressing influenza HA provided platform data against a target for which there are well-established immunogenicity benchmarks and data on cell-mediated responses ([Section 2.4.2.1.9.1](#)).

A series of mouse immunogenicity studies demonstrated that the vaccine candidates ([Section 2.4.2.1.10](#)) and additional constructs ([Section 2.4.2.1.9](#)) that are being tested in the GLP repeat-dose toxicity study rapidly elicit SARS-CoV-2 S antigen binding IgG and serum SARS-CoV-2 pseudovirus neutralizing responses. The mouse immunogenicity studies are in progress, and final study reports will be provided to the IND as they become available and prior to testing of the vaccine candidates in the Phase 1/2 trial. Immunogenicity data are also available from serum drawn 2 days after two or three weekly doses of vaccine candidates in the rat GLP repeat dose toxicity study ([Section 2.4.2.1.11](#)).

Table 2.4.1-1. Nomenclature of the Vaccine Candidates

Product Code	RNA Platform	Antigen Variant	Description/Translated Protein	Variant Code	GLP Tox Data	Phase 1/2 Candidate
PF-07302048	NA	NA	Pfizer code for any COVID-19 vaccine	NA	NA	NA
BNT-162	NA	NA	BioNTech code for any COVID-19 vaccine	NA	NA	NA
BNT162a1	uRNA	V5	RBD	RBL063.3	Yes	Yes
BNT162a2	uRNA	V8 ^a	P2 S	RBL063.1	No	No
BNT162b1	modRNA	V5	RBD	RBP020.3	Yes	Yes
BNT162b2	modRNA	V8	P2 S	RBP020.1	Yes	No
BNT162b2	modRNA	V9	P2 S	RBP020.2	No	Yes
BNT162c1	saRNA	V5	RBD	RBS004.3	Yes	No
BNT162c2	saRNA	V9	P2 S	RBS004.2	No	Yes

a. The V8 and V9 variants of the P2 S antigen have the same amino acid sequence. Different codon optimizations were used for their coding sequences.

In the mouse and rat immunogenicity studies of the vaccine candidates, antigen binding IgG responses are tested by an ELISA and functional antibody responses are tested by a SARS-CoV-2 pVNT. The serology assays are described in [Section 2.4.2.1.6](#).

A nonhuman primate immunogenicity study has been initiated to assess antigen-binding antibody, infectious SARS-CoV-2 neutralization, and Th1/Th2 T helper cell phenotypes elicited by the vaccine candidates in a species with immune responses more predictive of human responses. However, there are abundant data with non-COVID-19 vaccine candidates demonstrating that RNA platforms skew the immune response to a Th1 profile. Those data are summarized in [Section 2.4.2.1.4](#).

The potential toxicity of LNP-formulated uRNA, modRNA, and saRNA vaccine candidates encoding SARS-CoV-2 antigens administered IM is currently being studied in a GLP-compliant (pivotal) repeat-dose toxicity study in rats ([Study 38166](#)), which started dosing on 17 March 2020. The study design is described in [Section 2.4.4](#) and is based on WHO guidelines for vaccine development ([WHO, 2005](#)). Interim data from the dosing phase

090177e1934a5cff\Approved\Approved On: 21-Apr-2020 19:41 (GMT)

of the toxicity study are provided as part of the IND in support of FIH clinical studies, as agreed upon with CBER (Advice of April 6, 2020 in response to Pre-IND meeting request PS005569). The interim report will include all dosing phase mortality, clinical observations, body weight, food consumption, body temperature, injection site dermal scores, ophthalmoscopic and auditory endpoints, hematology, coagulation, clinical chemistry, urinalysis parameters, a subset of cytokine endpoints, serology, macroscopic findings and organ weights from the dosing phase animals. Remaining cytokine results and microscopic pathology from the dosing phase as well as all the recovery phase endpoints will be submitted in a final report as soon as it becomes available, but no later than 120 days after filing the IND.

Table 2.4.1-2. Nonclinical Studies

Study Number	Study Type	Species / Test System	Test Item	Dose [µg]	Results	Cross reference
BNT162 vaccine studies						
R-20-0074	In vitro antigen expression and localization	HEK293T cells	BNT162a1 (RBL063.3) BNT162b1 (RBP020.3) BNT162b2 (RBP020.1) BNT162c1 (RBS004.3)	2.5	All tested items expressed the encoded S protein derived antigen.	Section 2.4.2.1.8
R-20-0040	In vivo immunogenicity	Mice ^a	BNT162a1 (RBL063.3)	1, 5, 10	Immunogenicity was shown in all tested doses.	Section 2.4.2.1.10.1
R-20-0042	In vivo immunogenicity	Mice	BNT162b1 (RBP020.3)	0.2, 1, 5	Immunogenicity was shown in all tested doses.	Section 2.4.2.1.10.2
R-20-0085	In vivo immunogenicity	Mice	BNT162b2 (RBP020.2)	0.2, 1, 5	Immunogenicity was shown in all tested doses.	Section 2.4.2.1.10.3
R-20-0053	In vivo immunogenicity	Mice	BNT162c2 (RBS004.2)	0.2, 1, 5	Immunogenicity was shown in all tested doses.	Section 2.4.2.1.10.4
Supportive studies						
R-20-0073	In vivo immunogenicity	Mice	modRNA encoding influenza HA	1	HA delivered by LNP-formulated modRNA induced a strong antibody and antigen-specific T cell response.	Section 2.4.2.1.9.1

Table 2.4.1-2. Nonclinical Studies - Continued

Study Number	Study Type	Species / Test System	Test Item	Dose [µg]	Results	Cross reference
R-20-0052	In vivo immunogenicity	Mice	BNT162a2 (RBL063.1)	1, 5, 10	Immunogenicity was shown in all tested doses.	Section 2.4.2.1.9.2
R-20-0041	In vivo immunogenicity	Mice	BNT162c1 (RBS004.3)	0.2, 1, 5	Immunogenicity was shown in all tested doses.	Section 2.4.2.1.9.3
R-20-0054	In vivo immunogenicity	Mice	BNT162b2 (RBP020.1)	0.2, 1, 5	Immunogenicity was shown in all tested doses.	Section 2.4.2.1.9.4
R-20-0072	In vivo distribution	Mice	modRNA encoding luciferase	2	ModRNA expressed luciferase in mice with distribution in the muscle (injection site) and liver.	Section 2.4.3.5

a. All murine testing was conducted in BALB/c mice.

After initiation of GLP repeat-dose toxicity testing of the vaccine candidates, the antigen expression and mouse immunogenicity data presented here ([Section 2.4.2.1.8](#) and [Section 2.4.2.1.10](#)) were obtained. These data led to a re-evaluation of which vaccine candidates would be chosen for clinical testing in study C4591001. Two changes were made:

1. Based on higher expression levels, BNT162b2 (RBP020.2), a modRNA that expresses P2 S V9, was chosen for clinical testing in place of the BNT162b2 (RBP020.1), a modRNA that expresses P2 S V8 and is being tested in the GLP repeat dose toxicology study. Antigens P2 S V8 and P2 S V9 have the same amino acid sequence and differ only in codon optimization.
2. Based on greater immunogenicity in mice, BNT162c2 (RBS004.2), a saRNA that expresses P2 S V9, was chosen for clinical testing in place of BNT162c1 (RBS004.3), a saRNA that expresses RBD V5 and is being tested in the repeat dose GLP toxicity study. Both the saRNA platform and the expressed antigen of the clinical candidate BNT162c2 (RBS004.2) are being tested in the repeat dose toxicology study, though in different platform-antigen combinations.

These changes are considered minor and are not expected to have a safety impact; therefore, BioNTech/Pfizer do not plan to conduct additional toxicity studies to support clinical administration. For more details see [Section 2.4.5](#).

090177e1934a5cffApproved On: 21-Apr-2020 19:41 (GMT)

IM administration was chosen for the toxicity study as this is the intended route of administration in the clinic. Rats were chosen for toxicity assessments as they are a commonly used rodent species for the evaluation of toxicity and they mount an immune response to vaccination with the COVID-19 vaccine candidates.

The pivotal repeat-dose toxicity study in rats was conducted in accordance with Good Laboratory Practice for Nonclinical Laboratory Studies, Code of US Federal Regulations (21 CFR Part 58), in an OECD Mutual Acceptance of Data member state. The location of records for inspection will be included in the final study report.

090177e1934a5cff\Approved\Approved On: 21-Apr-2020 19:41 (GMT)

2.4.2. PHARMACOLOGY

2.4.2.1. Primary Pharmacodynamics

2.4.2.1.1. Summary

There is an urgent need for the development of a new prophylactic vaccine given the threat posed by the increasing number of globally distributed outbreaks of SARS-CoV-2 infection and its associated disease, COVID-19. There are currently no approved vaccines or antiviral drugs to prevent or treat infection with SARS-CoV-2 or its associated disease, COVID-19 (Habibzadeh and Stoneman, 2020). RNA-based vaccines encode a viral antigen that is translated by the vaccinated organism into protein to induce a protective immune response. There are three RNA platforms under development: unmodified mRNA (uRNA), nucleoside modified mRNA (modRNA), and self-amplifying mRNA (saRNA).

More than a dozen nonclinical good laboratory practice (GLP) safety studies and clinical safety data are available for uRNA and modRNA. These data have been obtained primarily with RNAs formulated with liposomes and LNPs that are related, but not identical, to those that will be used in the planned clinical trial C4591001.

The overall nonclinical toxicity data generated by BioNTech on their portfolio suggest a favorable safety profile for uRNA, modRNA, and saRNA formulated with different nanoparticles for various administration routes including for intravenous (IV) injection. The favorable safety profile after IV dosing is notable because IV injection results in a higher systemic exposure than the intramuscular (IM) injection planned in clinical trial C4591001. Overall, the findings were mild and mostly related to the mode-of-action and the RNA-intrinsic stimulation of innate immune sensors. No unsuspected target organs of toxicity were identified. The nonclinical safety profile of uRNA and modRNA in rodents was predictive of clinical safety.

The available interim nonclinical safety and toxicity data generated in a GLP-compliant repeat-dose toxicity study of the COVID-19 family of LNP-enveloped uRNA, modRNA, and saRNA vaccine platforms encoding SARS-CoV-2 antigens are included in this IND (Section 2.4.4.3) together with other preclinical data supporting the clinical use of the COVID-19 vaccine candidates. Given the urgency of this pandemic, additional data will be submitted to the IND at the times agreed upon with CBER.

There are currently no data available on the effects of any of the COVID-19 candidates in humans. However, a number of human studies for other RNA candidate vaccines seeking different indications have provided relevant data to support RNA as a vaccine platform and thus support the COVID-19 vaccine candidates. These data have shown that certain aspects of the immune responses to RNA translate well from animals to humans and are discussed in the Clinical Overview (Section 2.5.1.8).

The safety and immunogenicity of four COVID-19 vaccine candidates (BNT162a1/RBL063.3, BNT162b1/RBP020.3, BNT162b2/RBP020.2, and BNT162c2/RBS004.2) against SARS-CoV-2 will be investigated clinically, as part of a

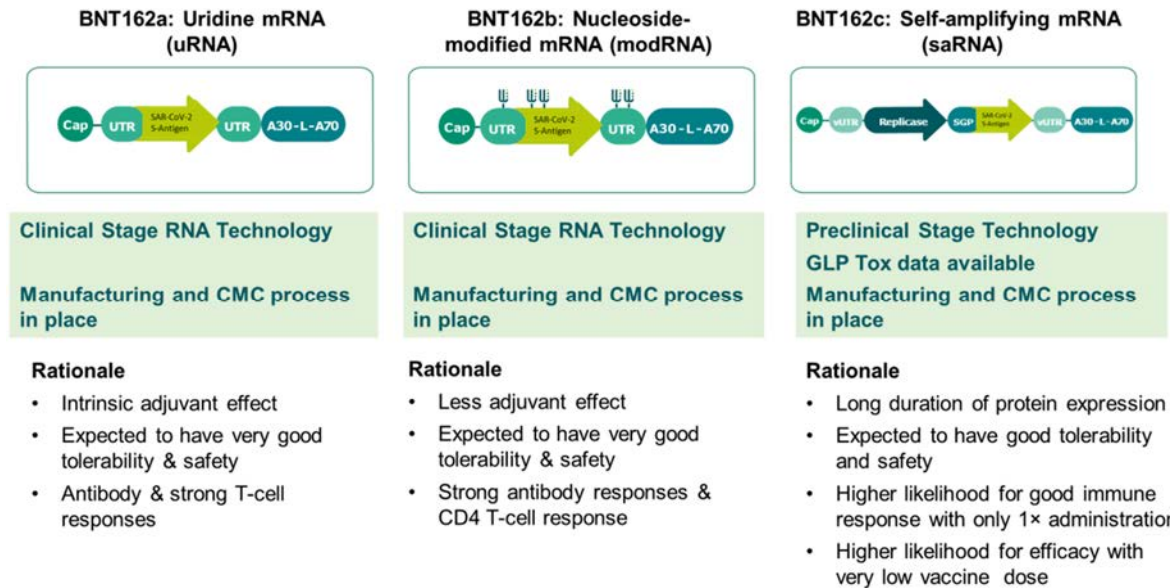
program to develop a prophylactic vaccine to prevent infection with SARS-CoV-2 and its associated disease COVID-19.

2.4.2.1.2. RNA Vaccine Platforms

BioNTech has longstanding and diversified expertise in utilizing messenger RNA (mRNA) to deliver genetic information to cells, where it is used to express proteins for a therapeutic effect. BioNTech has been working in the RNA field for more than a decade with emphasis in the oncology field. Biontech and Pfizer are developing a portfolio of RNA therapies that utilize different mRNA platforms to develop an optimized formulation for a given infectious disease indication with emphasis on preventing viral diseases such as COVID-19.

Biontech is evaluating three RNA platforms in human clinical trials for oncology indications, primarily as repeatedly IV administered therapeutic cancer vaccines, and over 613 patients have been dosed to date. This clinical experience includes many patients who have had long term exposure, i.e., who have received more than 8 IV administrations.

Figure 2.4.2-1. Overview of the Three RNA Platforms



The mRNA vaccine molecules are capped and contain ORFs, which are flanked by the UTRs, and polyA-tails at the 3' end. The ORF of the uRNA and modRNA vectors encode the vaccine antigen of interest. Self-amplifying RNA has two ORFs. The first ORF encodes an alphavirus-derived replicase which, upon translation, mediates self-amplification of the RNA. The second ORF encodes the vaccine antigen.

RNA is attractive as a vaccine platform as it enables timely and effective response to emerging infectious disease threats. RNA vaccines can mimic antigen expression during natural infection by directing expression of virtually any pathogen antigen with high precision and flexibility of antigen design. RNA occurs naturally in the body, is metabolized and eliminated by the body's natural mechanisms, does not integrate into the genome, is transiently expressed, and, therefore, is considered safe. Vaccination with RNA in general

090177e1934a5cffApproved On: 21-Apr-2020 19:41 (GMT)

generates robust immune responses as RNA not only delivers the vaccine antigen, but also has intrinsic adjuvant effects.

RNA vaccine platform approaches greatly simplify development and manufacturing, irrespective of the encoded pathogen antigens. Thus, RNA has the potential of rapid, cost-efficient, high-volume manufacturing and flexible stockpiling (long term storage of low-volume libraries of frozen plasmid and unformulated RNA, which can be rapidly formulated and distributed). BioNTech has expertise in production process development for various RNA chemistries and formulations. A LNP-formulated RNA-based vaccine would provide one of the most flexible, scalable, and fastest approaches to protect against new, fast spreading, virus infections (Rauch et al, 2018; Sahin et al, 2014).

RNA vaccines are molecularly defined, highly purified immunogens. Unlike live attenuated vaccines, RNA vaccines do not carry the risks associated with infection. RNA-based vaccines are manufactured using a cell-free in vitro transcription process, which allows an easy and rapid production and the prospect of producing high numbers of vaccine doses within a shorter time period than possible with conventional vaccine approaches. This capability is pivotal to enable the most effective response in outbreak scenarios.

In the COVID-19 vaccine candidates, RNA drug substances are formulated with lipids as RNA-LNP drug products. The vaccine candidates are supplied as buffered-liquid solutions for IM injection. The RNA drug substances are highly purified single-stranded, 5'-capped messenger mRNAs produced by in vitro transcription from the corresponding DNA templates, each encoding full-length or parts of the SARS-CoV-2 S glycoprotein.

The RNA components of the COVID-19 vaccine candidates are based on three platforms (Figure 2.4.2-1): unmodified mRNA (uRNA), nucleoside-modified mRNA (modRNA), and self-amplifying RNA (saRNA).

2.4.2.1.2.1. uRNA

uRNA is single-stranded, 5'-capped mRNA that is translated upon entering the cell. In addition to the open reading frame (ORF) encoding the SARS-CoV-2 antigen, each uRNA contains common structural elements optimized for increased stability and translational efficiency – a 5' cap, 5' untranslated region (UTR), 3' UTR, and poly(A)-tail.

2.4.2.1.2.1. modRNA

ModRNA is also a single-stranded, 5'-capped mRNA that is translated upon entering the cell. In addition to the ORF encoding the SARS-CoV-2 antigen, each modRNA contains common structural elements optimized for high efficacy of the RNA. Compared to the uRNA, modRNA contains a different 5' cap structure and a substitution of 1-methyl-pseudouridine for uridine. This substitution decreases recognition of the vaccine RNA by innate immune sensors, such as toll-like receptors (TLRs) 7 and 8, resulting in decreased innate immune activation and increased protein translation.

2.4.2.1.2.2. saRNA

SaRNA is a single-stranded 5'-capped RNA that self-amplifies upon entering the cell. The SARS-CoV-2 antigen is translated as the RNA self-amplifies. A 5' ORF encodes the Venezuelan equine encephalitis (VEE) virus RNA-dependent RNA polymerase (RDRP or replicase). A 3' ORF encodes the SARS-CoV-2 antigen, under control of a subgenomic promoter. The saRNA vector contains additional conserved sequence elements supporting replication and translation, including 5' and 3' UTRs and a poly A tail, but no other VEE virus coding sequences. When saRNA is introduced to the cytoplasm of a cell, ribosomes translate the replicase. The replicase, which also has a capping function, carries out negative strand RNA synthesis and then uses the negative strand copies of the positive strand vaccine RNA to synthesize new complete positive strand RNAs (for replication) and large quantities of the much shorter subgenomic mRNA, which encodes the antigen. The resulting "launch" of saRNA results in high level, intracellular expression of the antigen and innate immune activation to potentiate an adaptive immune response to the expressed antigen.

2.4.2.1.2.3. Summary

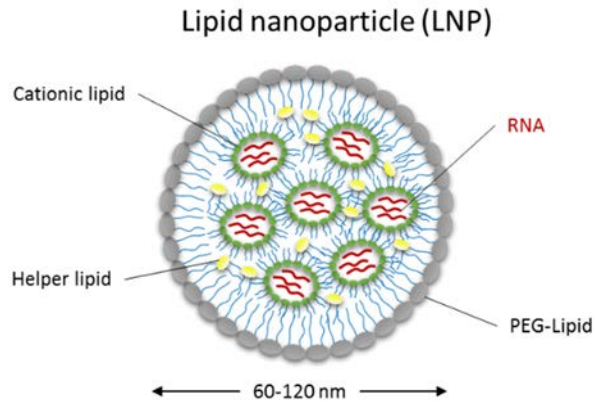
The three RNA platforms have complementary strengths: uRNA, with high intrinsic adjuvanticity; modRNA, with blunted innate immune sensor activating capacity and thus augmented expression of the target antigen; and saRNA, from which higher amounts of protein per injected RNA template can be produced.

The structural elements of the vector backbones of COVID-19 vaccine candidates are optimized for prolonged and strong translation of the antigen-encoding RNA component. The different COVID-19 vaccine RNA platforms exhibit distinct antigen expression profiles after IM injection. All RNA-encoded antigens are expressed transiently. For BNT162a1 (uRNA) and BNT162b1 and BNT162b2 (modRNA), the antigen expression peaks shortly after injection; for BNT162c2 (saRNA), the antigen expression peaks later and is more prolonged due to self-amplification. All vaccine candidates may be administered using prime/boost or prime-only administration regimens.

2.4.2.1.3. Lipid Nanoparticles

RNAs from each of the platforms are formulated with lipids, which protect the RNA from degradation and enable transfection of the RNA into host cells after IM injection. The same LNP formulation ([Figure 2.4.2-2](#)) is used for all of the COVID-19 vaccine candidates.

Figure 2.4.2-2. Schematic Organization of a LNP

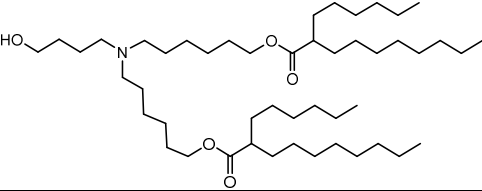
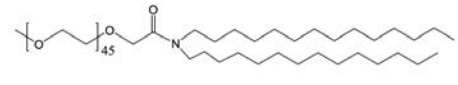
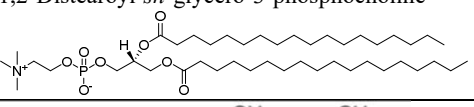
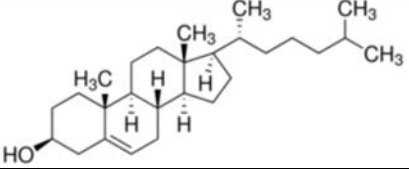


The LNPs are composed of four lipids in a defined ratio. During mixing of the RNA and the dissolved lipids, the lipids form the nanoparticles encapsulating the RNA. After injection, the LNPs are taken up by the cells, and the RNA is released into the cytosol. In the cytosol, the RNA is translated, and the encoded viral antigen is produced.

The formulation contains two functional lipids, ALC-0315 and ALC-01592, and two structural lipids DSPC (1,2-distearoyl-sn-glycero-3-phosphocholine) and cholesterol. The physicochemical properties and the structures of the four lipids are shown in [Table 2.4.2-1](#).

090177e1934a5cff\Approved\Approved On: 21-Apr-2020 19:41 (GMT)

Table 2.4.2-1. Lipids in the Formulation

Lipid (CAS number)	Molecular weight [Da]	Molecular formula	Physical state and storage condition	Chemical name (synonyms) and structure
ALC-0315 (not applicable)	766	C ₄₈ H ₉₅ NO ₅	Liquid (oil) -20°C	(4-hydroxybutyl)azanediylbis(hexane-6,1-diyl)bis(2-hexyldecanoate) 
ALC-0159 (1849616-42-7)	~2400-2600	C ₃₀ H ₆₀ NO(C ₂ H ₄ O) _n OCH ₃ n=45-50	Solid -20°C	2-[(polyethylene glycol)-2000]-N,N-ditetradecylacetamide 
DSPC (816-94-4)	790	C ₄₄ H ₈₈ NO ₈ P	Solid -20°C	1,2-Distearoyl- <i>sn</i> -glycero-3-phosphocholine 
Cholesterol (57-88-5)	387	C ₂₇ H ₄₆ O	Solid -20°C	

CAS = Chemical Abstracts Service; DSPC = 1,2-distearoyl-*sn*-glycero-3-phosphocholine.

090177e1934a5cff\Approved\Approved On: 21-Apr-2020 19:41 (GMT)

2.4.2.1.4. Immune Phenotype Elicited by LNP-Formulated RNA Vaccines

Due to RNA’s inherent adjuvant activity mediated by binding to innate immune sensors such as toll like receptors, RNA-LNP vaccines induce a robust neutralizing antibody response and a concomitant T-cell response resulting in protective immunization with minimal vaccine doses.

The utility of each of the RNA platforms used for development of the COVID-19 vaccine candidates is supported by various nonclinical studies that demonstrate the efficient induction of potent neutralizing antibody and T-cell responses against a variety of viral pathogens including influenza virus, Ebola virus, human immunodeficiency virus (HIV), and Zika virus (Vogel et al, 2018; Moyo et al, 2019; Pardi et al, 2017; Pardi et al, 2018). Unpublished immunogenicity data from RNA based vaccines against other viruses such as Marburg and Lassa virus indicate that the range of applications for anti-viral RNA vaccines is broad (data on file). Moreover, all the mRNA platforms confer strong prophylactic vaccine activity in murine influenza challenge models.

Table 2.4.2-2. Characteristics of the Adaptive Immune Response for the mRNA Platforms

	uRNA^a	modRNA^b	saRNA^c
CD4⁺ T cell response	<ul style="list-style-type: none"> • Induction of multifunctional strongly Th1+, skewed immune response with induction of IFN-γ+, TNF-α+, IL-2+ CD4+ T cells. • Strong expansion of follicular helper Tfh cells with an IFN-γ+, Tfh cells (mouse, human NHP). 	<ul style="list-style-type: none"> • Strong induction of multi-functional Th1 skewed immune response with induction of Th1+, IFN-γ+, TNF-α+, IL-2+ CD4+ T cells. • Strong expansion of follicular helper Tfh cells with an IFN-γ+, Tfh cells (mouse, human NHP). 	<ul style="list-style-type: none"> • Expansion of a strongly Th1 skewed immune response with, multifunctional Th1+, IFN-γ+, TNF-α+, IL-2+ CD4+ T cells (mouse).
CD8⁺ T cell response	<ul style="list-style-type: none"> • Expansion of multifunctional CD8 cytotoxic, effector and long lived memory T cells with an IFN-γ+, TNF-α+, CD107+ phenotype (mouse, human). 	<ul style="list-style-type: none"> • Expansion of multifunctional cytotoxic, effector and long lived memory CD8 T cells with an IFN-γ+, TNF-α+, CD107+ phenotype (mouse, human). 	<ul style="list-style-type: none"> • Strong expansion of long-lived effector and central memory CD8+ T cells with an IFN-γ+, TNF-α+, CD107+ phenotype (mouse).
Antibody response	<ul style="list-style-type: none"> • High-titer, high-affinity, long lived neutralizing antibody responses after prime only/boost (mouse, rats, NHP) • ADCC activity (rabbits). • Mouse IgG1 ~ IgG2a. 	<ul style="list-style-type: none"> • High-titer, high-affinity, long lived neutralizing antibody responses after prime/boost only (mouse, rats, NHP). • ADCC activity (rabbits) • Mouse IgG1 ~ IgG2a. 	<ul style="list-style-type: none"> • High-titer, neutralizing antibody responses after prime only (mouse, rats, pig, NHP). • Mouse IgG2a >>IgG1.

ADCC = Antibody-dependent cellular cytotoxicity; IgG = Immunoglobulin G; IL interleukin; IFN = Interferon; NHP = Non-human primate; Tfh = T follicular helper; TNF = Tumor necrosis factor; CD = cluster of differentiation.

a. Source: Pardi et al, 2017, 2018, 2019; Vogel et al, 2018, Kranz et al, 2016

b. Source: Vogel et al, 2018, Kranz et al, 2016, Pardi et al, 2017, 2018, 2019

c. Source: Vogel et al, 2018, Moyo et al, 2019

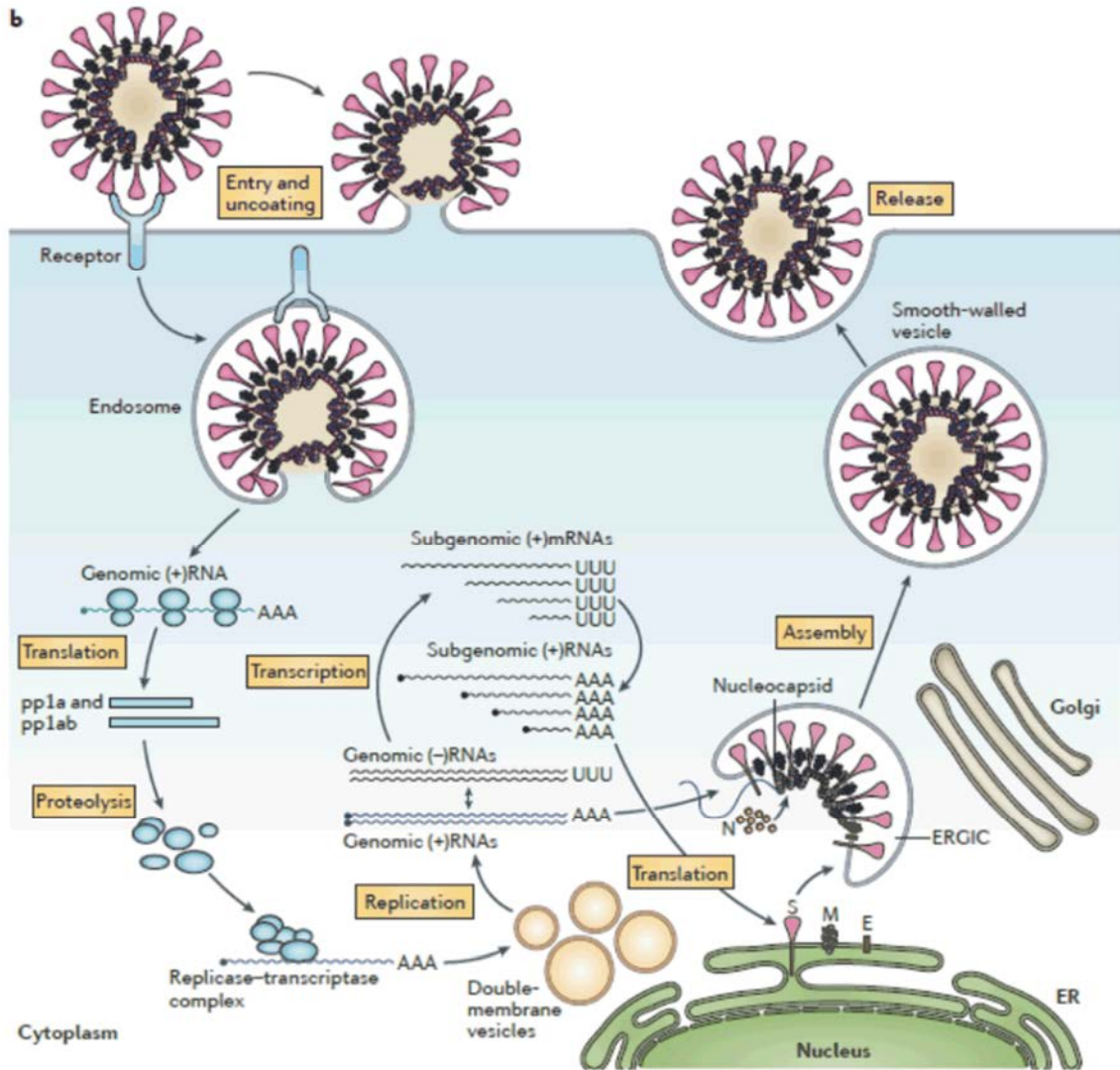
090177e1934a5cffApproved On: 21-Apr-2020 19:41 (GMT)

Vaccine candidates based on these mRNA platforms induce strong antibody responses and prime and expand multifunctional CD4 and CD8 positive T cells. The properties of antigen-specific immune responses induced by vaccination with these mRNA formats were studied in several species ([Table 2.4.2-2](#)). Vaccination with modRNA is characterized by the strong expansion of Th1-skewed antigen-specific T follicular helper (Tfh) cells, which stimulate and expand germinal center B cells, thereby resulting in particularly strong, long-lived, high-affinity antibody responses. The uRNA and saRNA formats exhibit a higher immune-stimulatory activity due to their TLR7/8 stimulatory capacity, thereby giving rise to a type-I interferon release, a strongly Th1 biased CD4+ T cell response as well as strong expansion of cytotoxic T cells ([Sahin et al, 2014](#)). Due to self-amplification and prolonged translation saRNA is able to induce strong CD4+ and CD8+ T cell responses by a prime only administration schedule ([Vogel et al, 2018](#)).

2.4.2.1.5. SARS-CoV-2 S as a Vaccine Target

Coronaviruses, like SARS-CoV-2, are members of a family of enveloped, positive sense, single-stranded RNA viruses ([Figure 2.4.2-3](#)). Coronaviruses encode four structural proteins. Of these, the spike glycoprotein (S) is the key target for vaccine development ([Figure 2.4.2-4](#)). Like influenza virus hemagglutinin (HA), coronavirus S is responsible for receptor-recognition, attachment to the cell, viral envelope fusion with a host cell membrane, and genomic release driven by the S protein conformation change leading to the fusion of viral and host cell membranes. S is cleaved by host proteases into the S1 and S2 fragments. While S2, which is membrane anchored, is responsible for membrane fusion, the S1 fragment, with its C-terminal receptor-binding domain (RBD), recognizes the host receptor and binds to the target host cell. SARS-CoV and SARS-CoV-2 have similar structural properties and bind to the same host cell receptor, angiotensin converting enzyme 2 (ACE-2) ([Zhou et al, 2020](#)).

Figure 2.4.2-3. Replication Cycle of a Coronavirus



Source: de Wit et al, 2016

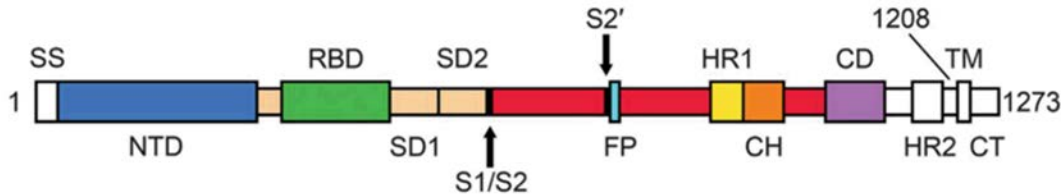
Coronavirus S is pivotal not only for host cell recognition and entry, but also for the induction of virus neutralizing antibodies by the host immune system (Zakhartchouk et al, 2007; Yong et al, 2019). Some monoclonal antibodies against S, particularly those directed against the RBD, neutralize SARS-CoV and Middle East respiratory syndrome (MERS-)CoV infection in vitro and in vivo (Hulswit et al, 2016). Targeting the S protein, as well as its S1 cleavage fragment, or the RBD alone, with vaccines is sufficient to induce neutralizing immune responses (Al-Amri et al, 2017).

The RBD forms membrane distal “heads” on the S protein that are connected to the body by a hinge. In the native S protein, when the RBD is in the “heads down” conformation, the

090177e1934a5cffApproved\Approved On: 21-Apr-2020 19:41 (GMT)

neutralizing epitopes at the receptor binding site are occluded. When the RBD is in the “heads up” conformation, the neutralizing epitopes at the receptor binding site are exposed. Therefore, a P2 mutant, “heads up” variant of S can elicit a stronger neutralizing antibody response than native S (Pallesen et al, 2017; Wrapp et al, 2020).

Figure 2.4.2-4. Schematic of the Organization of the SARS-CoV-2 S Glycoprotein



The S1 fragment includes the signal sequence (SS) and the receptor binding domain (RBD), which is the key subunit within the S protein that is relevant for binding to the human cellular receptor ACE2. The S2 subunit contains the S2 protease cleavage site (S2') followed by a fusion peptide (FP) for membrane fusion, heptad repeats (HR1 and HR2) with a central helix (CH) domain, the transmembrane domain (TM) and a cytoplasmic tail (CT). Source: modified from Wrapp et al, 2020.

The COVID-19 vaccine candidates selected for clinical testing feature the following vaccine antigens (Figure 2.4.2-4).

- A non-membrane anchored receptor binding domain from SARS-CoV-2 S, with a C-terminal T4 fibrin foldon domain added to trimerize the molecule, potentially increasing its immunogenicity (RBD; Kirchdoerfer et al, 2018). One codon optimized form of the coding sequence for this antigen is designated “variant 5” (V5).
- A membrane-anchored full-length S glycoprotein with the mutation of residues in the central helix proline to lock S in an antigenically optimal “heads up” conformation (Wrapp et al, 2020; Pallesen et al, 2017). Two codon optimized forms of the coding sequence for this antigen are designated “variant 8” and “variant 9” (V8 and V9).

The antigen may be incorporated into the cellular membrane or secreted into the extracellular environment and induce an adaptive immune response. In addition, as S protein is the antigen that recognizes and drives infection of the host cells, it is a key target of virus neutralizing antibodies. Furthermore, as RNA-expressed S protein is fragmented intracellularly, the resulting peptides can be presented at the cell surface, triggering a specific T cell-mediated immune response with activity against the virus.

2.4.2.1.6. Serological and Virological Assays

For preclinical immunogenicity studies, a pseudotype neutralization assay (pVNT) has been used as a surrogate of virus neutralization (which, for SARS-CoV-2, requires BSL3 containment). The pVNT is based on a vesicular stomatitis virus (VSV) vector that lacks the

090177e1934a5cff\Approved\Approved On: 21-Apr-2020 19:41 (GMT)

VSV G glycoprotein. The pseudotype virus instead bears the wild type SARS-CoV-2 S glycoprotein, which mediates entry of the pseudovirus into cells. The pseudovirus can be inactivated by the binding of neutralizing antibodies to the S glycoprotein. For both nonhuman primate preclinical studies and the clinical trial, an authentic SARS-CoV-2 neutralization assay rather than the pseudovirus neutralization assay is planned.

For preclinical studies, antigen-based direct immunoassays (ELISA and/or Luminex formats) measure S1-specific (S1 recombinant protein, Sino Biologics) and RBD-specific (recombinant RBD, Sino Biologics) IgG levels in serum samples. For clinical studies and nonhuman primate studies, a direct binding Luminex immunoassay (dLIA) is being developed to quantify S-specific serum antibodies, allowing comparison of SARS-CoV-2 neutralizing antibody titers to S1-binding or RBD-binding IgG levels as a measure of the quality of vaccine responses.

In addition, a SARS-CoV-2 non-vaccine antigen (NVA) assay is being developed to measure antibodies specific for SARS-CoV-2 antigens not present in any of the vaccine candidates being prepared for C4591001. The NVA will permit evaluation of serological responses to SARS-CoV-2 that are the result of natural exposure rather than vaccine-elicited responses.

To detect SARS-CoV-2 virus shedding, a sensitive reverse transcription-polymerase chain reaction (RT-PCR)-based assay will be used to test nasal swab specimens. An FDA-approved molecular diagnostic will be used for screening swabs for SARS-CoV-2 and may be used in further studies. In addition, we are developing a real time quantitative PCR assay that uses the industry's gold standard polymerase to amplify highly conserved regions of the N and E genes. All available genome sequences have been analyzed and suggest that these regions remain stable across the major sequence clades. The assay will be automated, if necessary, to allow for high throughput processing and testing over 100 samples per day.

2.4.2.1.7. Lack of Cell to Cell Spread of saRNA

The saRNA vector encodes the alphavirus RNA-dependant RNA polymerase and the vaccine antigen but lacks the genes encoding the alphavirus structural proteins required for virus particle formation, genome packaging and propagation from transfected cells to additional cells. Therefore, the saRNA vaccine lacks the capacity to cause a propagating infection. This inherent safety feature of saRNA vaccine design is confirmed by experimental data.

An infectivity assay was performed to test whether saRNA that expresses the Venezuelan equine encephalitis virus (VEE) RNA-dependent RNA polymerase from its 5' ORF and the HA of influenza virus (strain H1N1, A/California/07/2009) from its 3' ORF can spread cell to cell. In this assay, the HA-encoding saRNA was transfected into HEK cells (schematic of the experiment in [Figure 2.4.2-5](#)). After a 24 h incubation, the medium from the transfected cells was transferred onto new acceptor cells, which were then also incubated for 24 h. Surface HA expression on the transfected cells and the acceptor cells was measured by flow cytometry using HA-specific antibody-based staining. As a positive control, A/California/04/2009 influenza virus, which can spread cell to cell and express HA, was used in place of the saRNA in parallel experimental steps. Donor cells expressed HA on the cell

surface when transfected with saRNA encoding HA or infected with influenza virus (Figure 2.4.2-6). HA was not detected on recipient cells incubated with medium from the donor cells transfected with saRNA encoding HA, but HA was detected recipient cells incubated with medium from influenza virus-infected donor cells.

Figure 2.4.2-5. Design of Assay to Test for saRNA Cell-to-Cell Spread

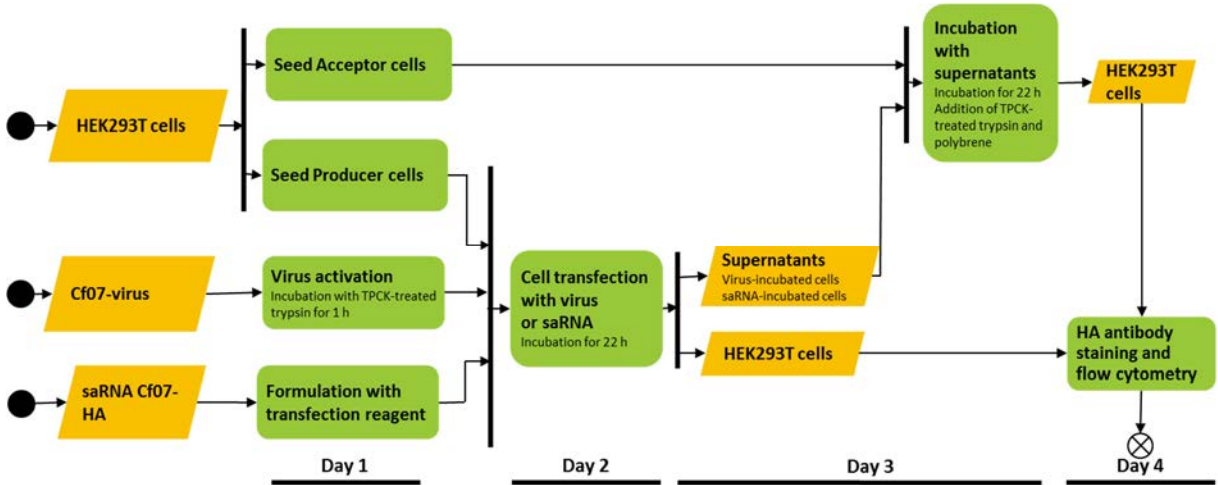
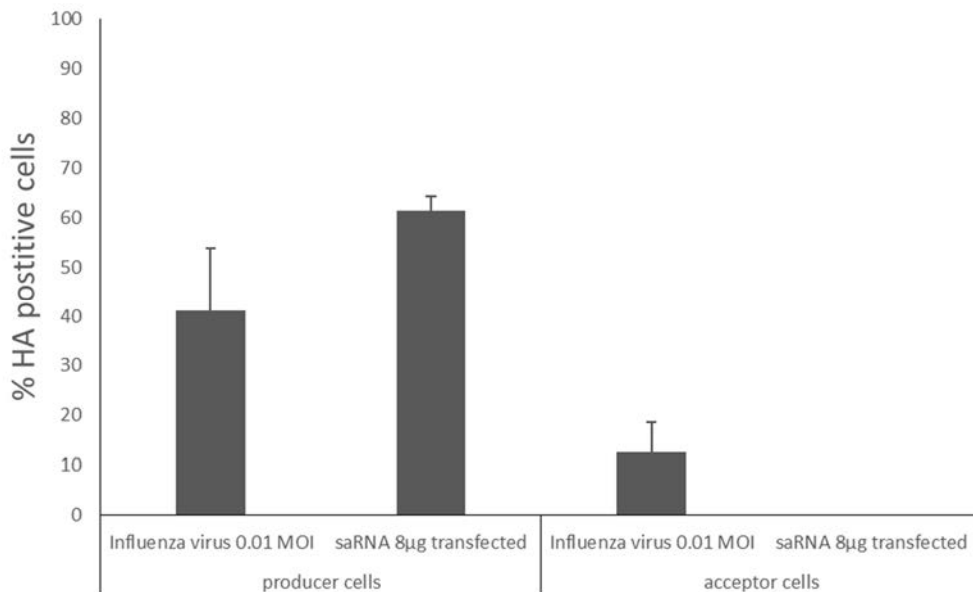


Figure 2.4.2-6. Flow Cytometry Detection of Cell Surface HA



Donor cells were analyzed for the presence of HA on the cell surface 24 h after infection or transfection (left). Acceptor cells were analyzed for the presence of HA on the cell surface 24 h after transfer of medium from the donor cells (right). Data give the mean ± SD of triplicate wells for the virus and quadruplicate wells for the saRNA.

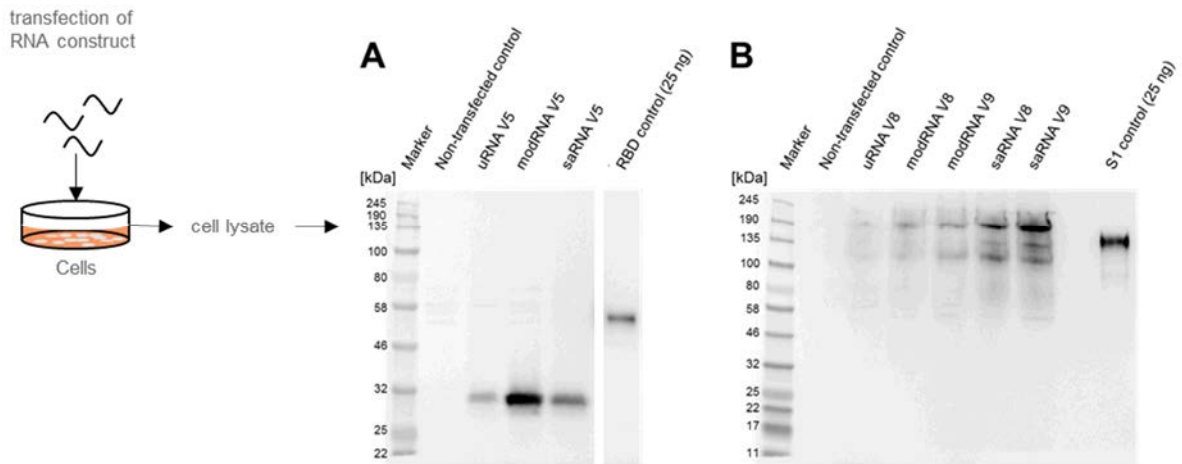
090177e1934a5cff\Approved\Approved On: 21-Apr-2020 19:41 (GMT)

This experiment demonstrates that saRNA encoding HA does not spread cell-to-cell under conditions in which infectious influenza virus does spread cell-to-cell. There is no plausible mechanism for a P2 “heads up” mutant SARS-CoV2 S antigen (Kirchdoerfer et al, 2018) or the RBD in the saRNA platform used for the BNT162c vaccine candidates to mediate cell to cell spread. Therefore, the data with HA-encoding saRNA establish that the saRNA platform does not support cell to cell spread.

2.4.2.1.8. In Vitro Expression of Antigens from COVID-19 vaccine RNA

To analyze whether RBD V5, P2 S V8, or P2 S V9 are expressed from the uRNA, modRNA, or saRNA drug substances, HEK 293T cells were transfected with the RNAs, and antigen expression was assessed by western blot (Figure 2.4.2-7), or immunofluorescence microscopy (Figure 2.4.2-8).

Figure 2.4.2-7. Western Blot Detection of RBD and P2 S in RNA-Transfected Cells

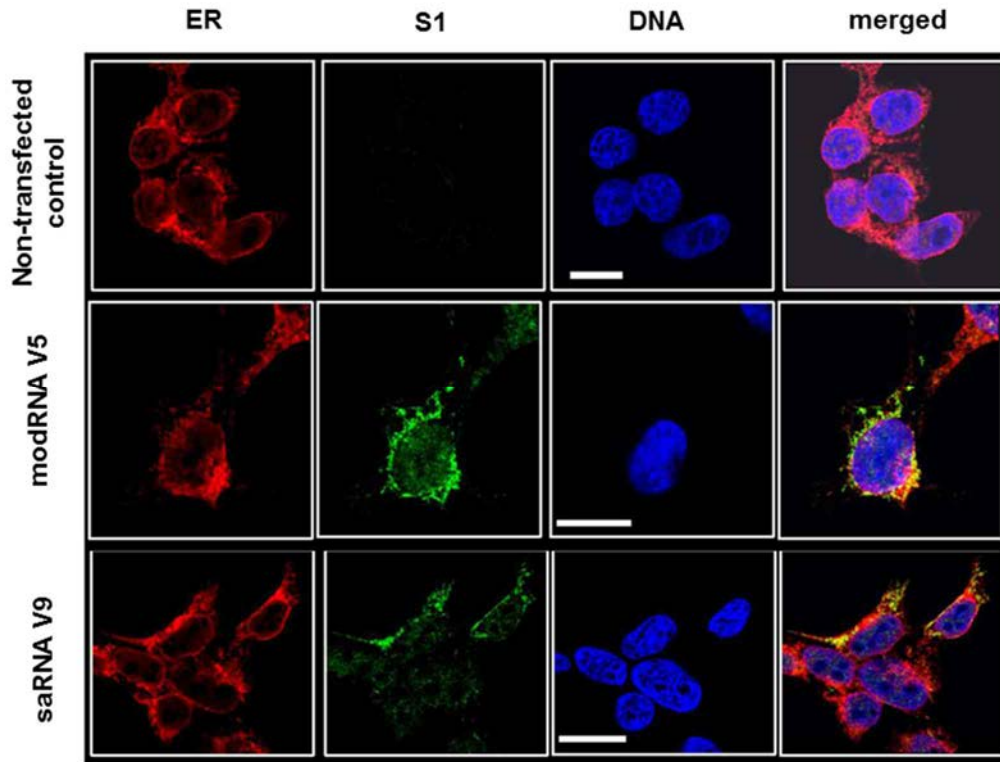


HEK 293T cells were transfected using RiboJuice™ mRNA transfection reagent (Merck Millipore) with 1 µg of the RNA drug substances (A) uRNA, modRNA, and saRNA encoding RBD V5 and (B) uRNA, modRNA, and saRNA encoding P2 S V8, and modRNA and saRNA encoding P2 S V9. 18 h after transfection, cell lysates were analyzed by a sodium dodecyl sulfate (SDS)–polyacrylamide gel electrophoresis (PAGE) system followed by western blot using a polyclonal antibody that recognizes SARS-CoV-2 S1. All samples showed specific antigen expression, and specific bands were detected for the RBD V5-encoding constructs at the expected apparent MW of 30 kDa and for the P2 S V8 and P2 S V9-encoding constructs at the expected apparent MW of 140 kDa. Recombinant proteins (50 ng RBD, expected apparent MW 52 kDa; 25 ng S1, expected apparent MW 102 kDa) were used as assay controls. RBD V5 was separated with a 10% polyacrylamide gel. P2 S V8 and V9 were separated with a 4–15% polyacrylamide gel.

RBD V5 has a predicted MW of 29.46 kDa, and P2 S V8 and V9 have a predicted MW of 141.14 kDa. Western blot confirmed the presence in lysates of HEK293T cells transfected with the RNA drug substances of proteins that had the expected apparent MWs of the antigens and were recognized by an anti-SARS-CoV-2 S1 polyclonal antibody. This finding confirms expression of the antigens from the RNAs. RBD V5 expression was greatest from the modRNA platform. P2 S expression was greatest from the saRNA platform, with greater expression for the V9 codon optimization variant than for the V8 codon optimization variant.

090177e1934a5cfffApproved On: 21-Apr-2020 19:41 (GMT)

Figure 2.4.2-8. Immunofluorescence Detection of RBD and P2 S in RNA Transfected Cells



HEK293T cells were transfected with 2.5 µg of modRNA encoding RBD V5 or saRNA encoding P2S V9 using RiboJuice™ RNA transfection reagent (Merck Millipore). After 18 h in culture, cells were fixed and stained for the endoplasmic reticulum (ER) with concanavalin A and an Alexa Fluor™ 594 conjugate (red). They were stained for RBD and P2 S with an anti-S1 polyclonal antiserum that recognizes both P2 S and RBD and Alexa Fluor® 488 (green). They were stained for DNA to visualize the nucleus with Hoechst (blue). The merged color panels show that the RBD V5 expressed by modRNA and the P2 S V9 expressed by saRNA each co-localize with the ER marker (scale: 10 µm). A control of non-transfected cells is shown in the top row.

Co-localization of the RBD and P2 S with an endoplasmic reticulum (ER) marker was shown by immunofluorescence microscopy of HEK293T cells transfected with BNT162b1 (modRNA encoding RBD V5) or BNT162c2 (saRNA encoding P2 S V9), respectively (Figure 2.4.2-8).

090177e1934a5cff\Approved\Approved On: 21-Apr-2020 19:41 (GMT)

2.4.2.1.9. Supportive Mouse Immunogenicity Studies

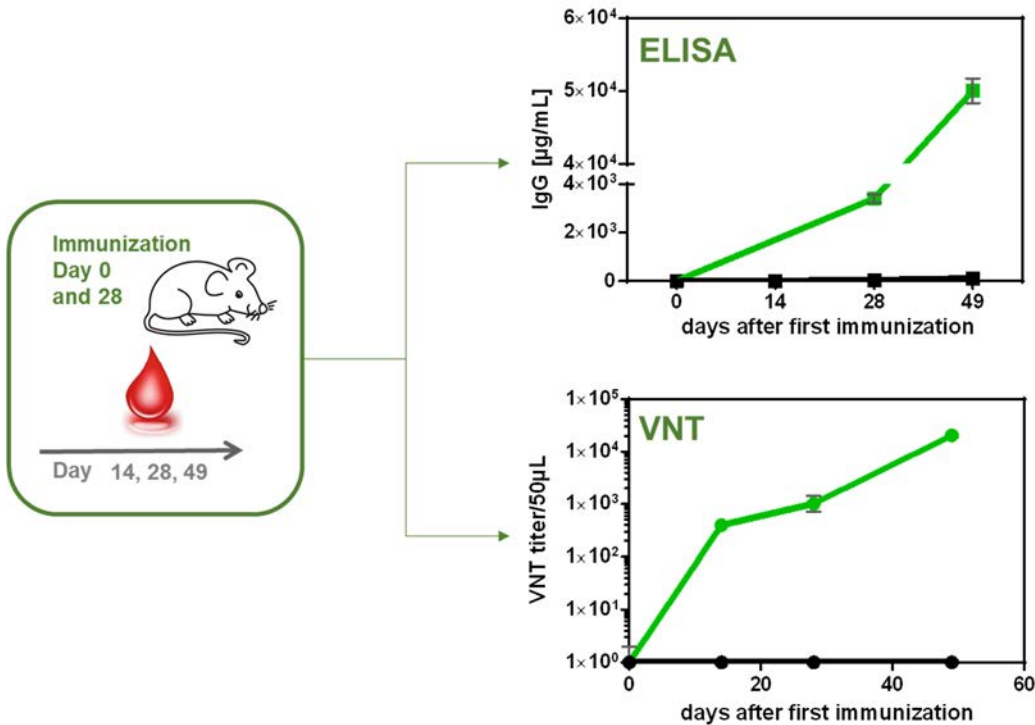
2.4.2.1.9.1. Immunogenicity of modRNA Encoding Influenza HA

Because of the extensive knowledge of immunity elicited by influenza HA, including decades of mass influenza immunization and an accepted serological correlate of protection, immunization with LNP-formulated modRNA that encodes influenza HA (H1 A/California/07/2009) provides a benchmark for the platform.

The modRNA was formulated with the same LNP composition that will be used in C4591001. BALB/c mice were immunized IM with 1 µg of the formulated RNA on days 0 and 28. ELISA of sera obtained on days 28 and 49 showed high levels of HA-specific IgG (Figure 2.4.2-9). Sera obtained as early as 14 days after the first dose had high neutralization titers against A/California/07/2009 influenza virus, and by day 49 (21 days after the second dose) serum influenza neutralization titers exceeded 1×10^4 .

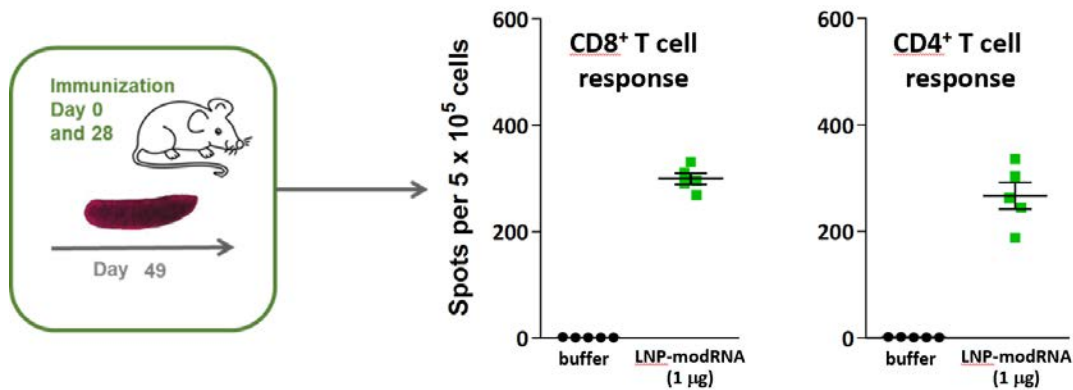
Hemagglutination inhibition (HAI) titers against A/California/07/2009 measured in sera drawn on day 49 were 1472 ± 279 (mean \pm SEM; data not graphed). This HAI titer greatly exceeds the titer of 40 that is generally accepted as protective against influenza.

Figure 2.4.2-9. Influenza HA Binding and Virus Neutralization Elicited by Immunization of Mice with modRNA Encoding HA in the Clinical LNP Formulation



BALB/c mice were immunized twice IM with 1 µg of the vaccine candidate. HA-specific IgG was measured by ELISA. The functionality of the antibodies was measured by influenza virus neutralization.

Figure 2.4.2-10. CD4⁺ and CD8⁺ T Cell Response to LNP-Formulated modRNA Encoding Influenza HA by IFN- γ ELISpot



BALB/c mice received two IM immunizations with 1 μg of modRNA encoding influenza HA. The T cell response was analyzed using antigen specific peptides to stimulate T cells recovered from the spleen. Interferon (IFN- γ) release was measured after peptide stimulation using an ELISpot assay.

IFN- γ ELISpot on splenocytes harvested on day 49 and stimulated with antigen-specific peptides showed strong CD4⁺ and CD8⁺ T cell responses (Figure 2.4.2-10). These data confirm that modRNA, formulated with the LNPs that will be used in C4591001 elicit Th1 phenotype T cell responses.

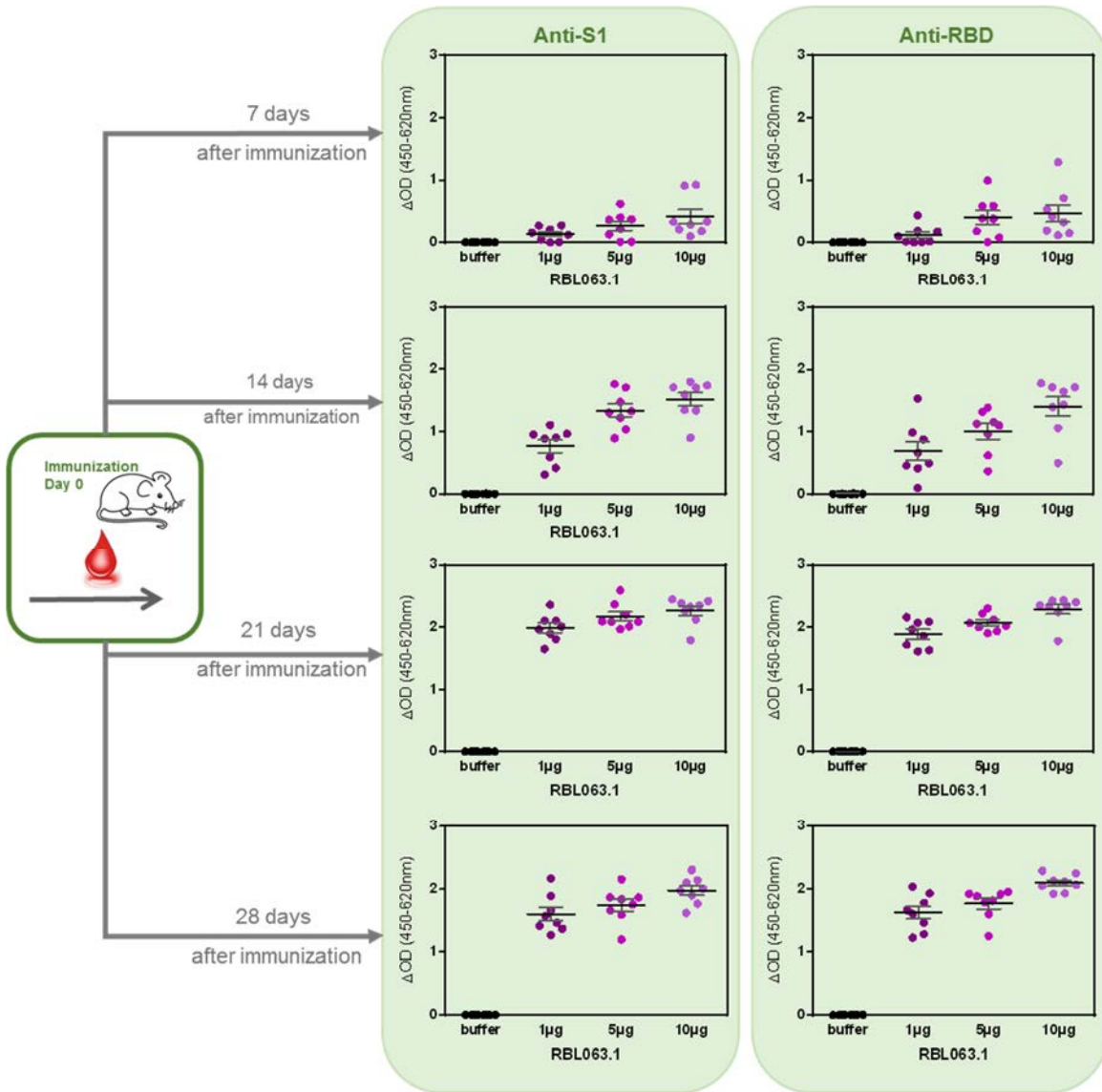
Various other immunogenicity studies in mice have documented the induction of neutralizing antibodies and antigen-specific Th1 type T cell responses with uRNA and saRNA vaccines encoding influenza HA (Vogel et al, 2018). These data were consistent across indications and models and document the immune response profile expected for RNA vaccines.

2.4.2.1.9.2. Immunogenicity of uRNA Encoding P2 S V8 (BNT162a2/RBL063.1)

Note that uRNA encoding RBD, not P2 S, is being prepared for clinical testing.

The immunogenicity of LNP-formulated uRNA encoding P2 S V8 was tested in mice (experimental details described in the legends to Figure 2.4.2-11 - Figure 2.4.2-13). ELISA data show an early, dose-dependent IgG response recognizing S1 and the RBD (Figure 2.4.2-11). Concentrations of IgG recognizing S1 (Figure 2.4.2-12A) and RBD (Figure 2.4.2-12B) increased over time. Sera obtained 14, 21 and 28 d after immunization showed dose-dependent SARS-CoV-2 pseudovirus neutralization (Figure 2.4.2-13). The study is ongoing.

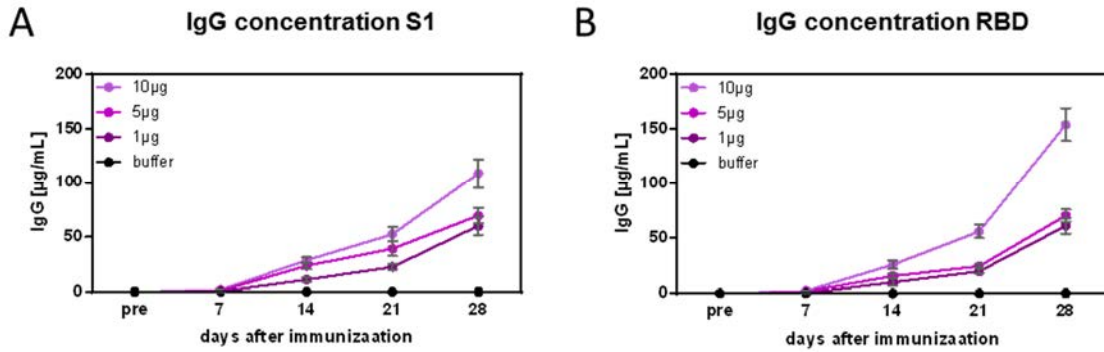
Figure 2.4.2-11. IgG Response Recognizing S1 and RBD 7, 14, 21, and 28 d after Immunization with uRNA Encoding P2 S V8



BALB/c mice were immunized IM once with 1, 5 or 10 μg of LNP-formulated RBL063.1. On 7, 14, 21 and 28 d after immunization, animals were bled, and the serum samples were analyzed for anti-S1 (left) and anti-RBD (right) antigen-specific IgG by ELISA. For day 7 (1:100), day 14 (1:100), day 21 (1:300) and d28 (1:900) results from different serum dilutions are depicted on the graphs. One point in the graph stands for one mouse. Every mouse serum was measured in duplicate. Group size n=8. Mean \pm SEM are depicted by the horizontal lines with whiskers for each group.

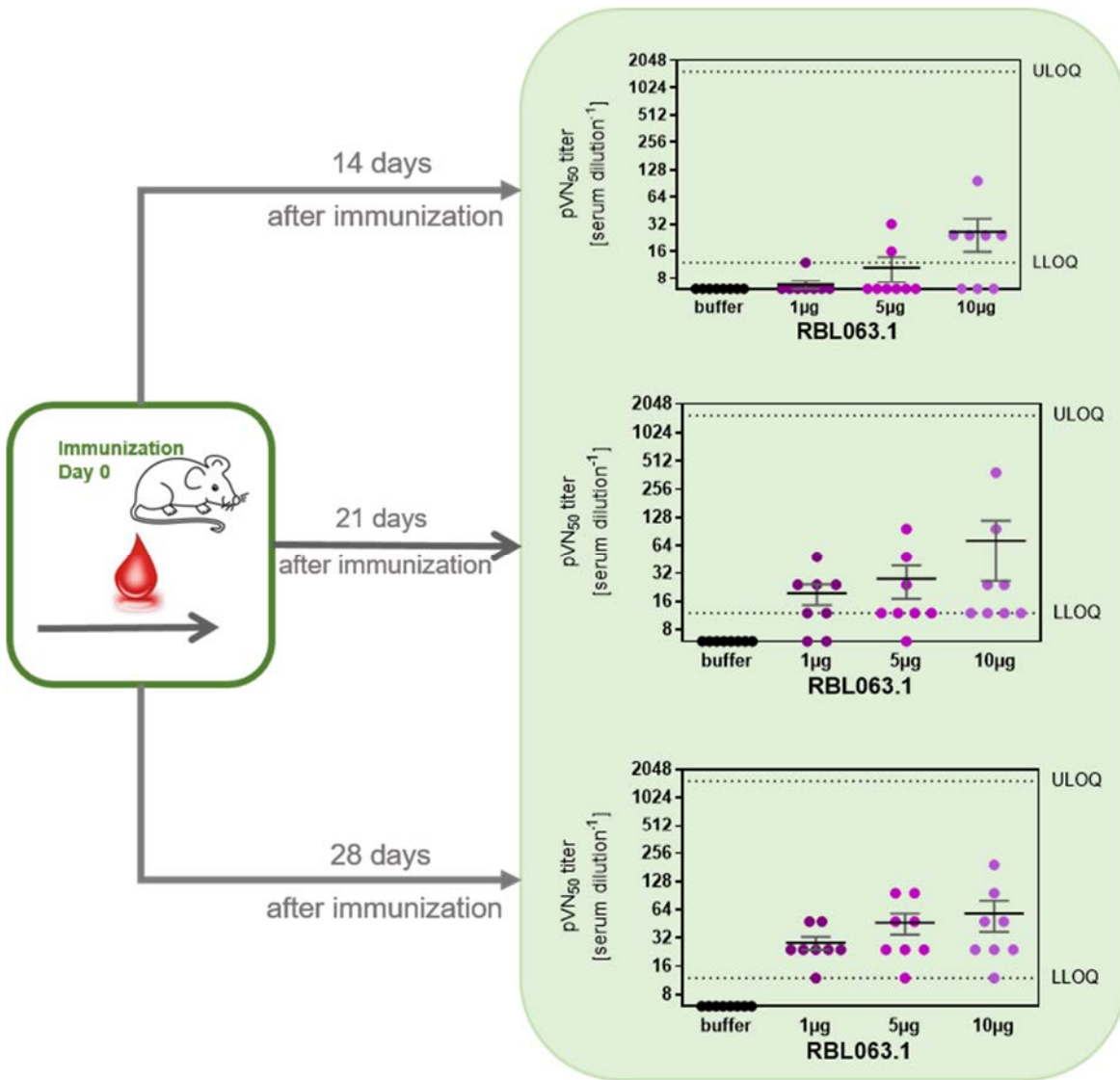
090177e1934a5cff\Approved\Approved On: 21-Apr-2020 19:41 (GMT)

Figure 2.4.2-12. Kinetics of the IgG Response Recognizing S1 and RBD after Immunization with uRNA Encoding P2 S V8



For individual Δ OD values, the antibody concentrations in the serum samples were calculated. The serum samples were tested against (A) the S1 protein and (B) RBD. Group mean antibody concentrations are shown (\pm SEM).

Figure 2.4.2-13. Pseudovirus Neutralization 14, 21 and 28 d after Immunization with uRNA Encoding P2 S V8



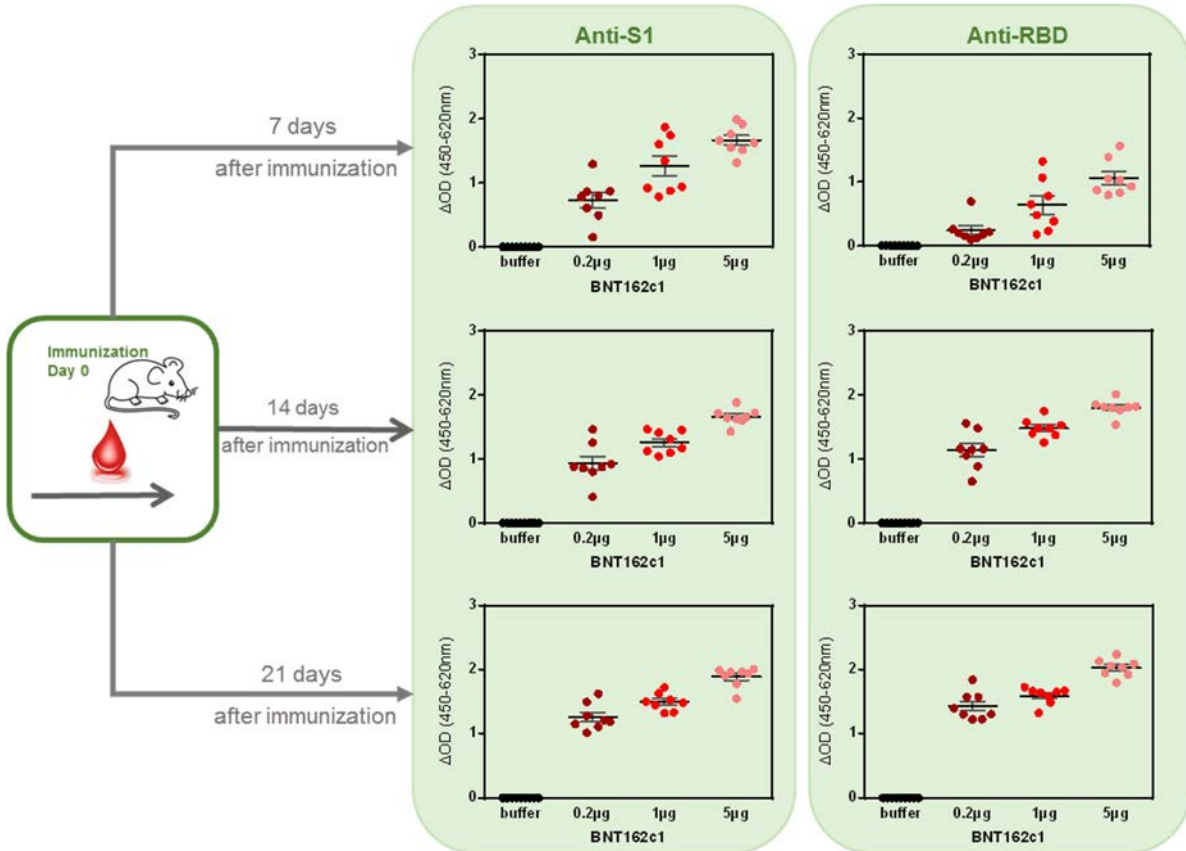
BALB/c mice were immunized IM once with 1, 5 or 10 µg of LNP-formulated RBL063.1. On 14, 21 and 28 d after immunization, animals were bled, and the sera were tested for SARS CoV-2 pseudovirus neutralization. Graphs depict pVN50 serum dilutions (50% reduction of infectious events, compared to positive controls without serum). One point in the graphs stands for one mouse. Every mouse sample was measured in duplicate. Group size n=8. Mean ± SEM is shown by horizontal bars with whiskers for each group. LLOQ, lower limit of quantification. ULOQ, upper limit of quantification.

090177e1934a5cff\Approved On: 21-Apr-2020 19:41 (GMT)

2.4.2.1.9.3. Immunogenicity of saRNA Encoding the RBD V5 (BNT162c1/RBL004.3)

The immunogenicity of LNP-formulated saRNA encoding RBD V5 was tested in mice (experimental details in the figure legends). ELISA data show an early, dose-dependent IgG response recognizing S1 and RBD (Figure 2.4.2-14). Pseudotype neutralizing titers are detected 14 d after immunization (Figure 2.4.2-15). The study is ongoing.

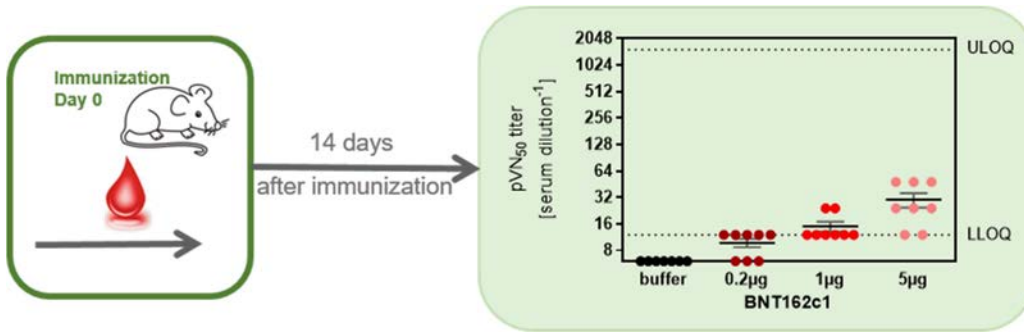
Figure 2.4.2-14. IgG Response Recognizing S1 and RBD 7, 14 and 21 d after Immunization with saRNA Encoding RBD V5



BALB/c mice were immunized IM once with 0.2, 1 or 5µg of LNP-formulated RBS004.3. 7, 14 and 21 d after immunization, animals were bled and the serum samples were analyzed for total amount of anti-S1 (left) and anti-RBD (right) antigen specific immunoglobulin G (IgG) measured via ELISA. For day 7 (1:100), day 14 (1:300) and days 21 (1:900) different serum dilution were included in the graph. One point in the graph stands for one mouse, every mouse sample was measured in duplicates (group size n=8; mean ± SEM is included for the groups).

090177e1934a5cff\Approved\Approved On: 21-Apr-2020 19:41 (GMT)

Figure 2.4.2-15. Pseudovirus Neutralization 14 d after Immunization with saRNA Encoding the RBD V5



BALB/c mice were immunized IM once with 0.2, 1 or 5 µg of LNP-formulated RBS004.3. On 14 d after immunization, animals were bled and the sera were tested for SARS CoV-2 pseudovirus neutralization. Graphs depict pVN₅₀ serum dilutions (50% reduction of infectious events, compared to positive controls without serum). One point in the graphs stands for one mouse. Every mouse sample was measured in duplicate. Group size n=8. Mean ± SEM is shown by horizontal bars with whiskers for each group. LLOQ, lower limit of quantification. ULOQ, upper limit of quantification.

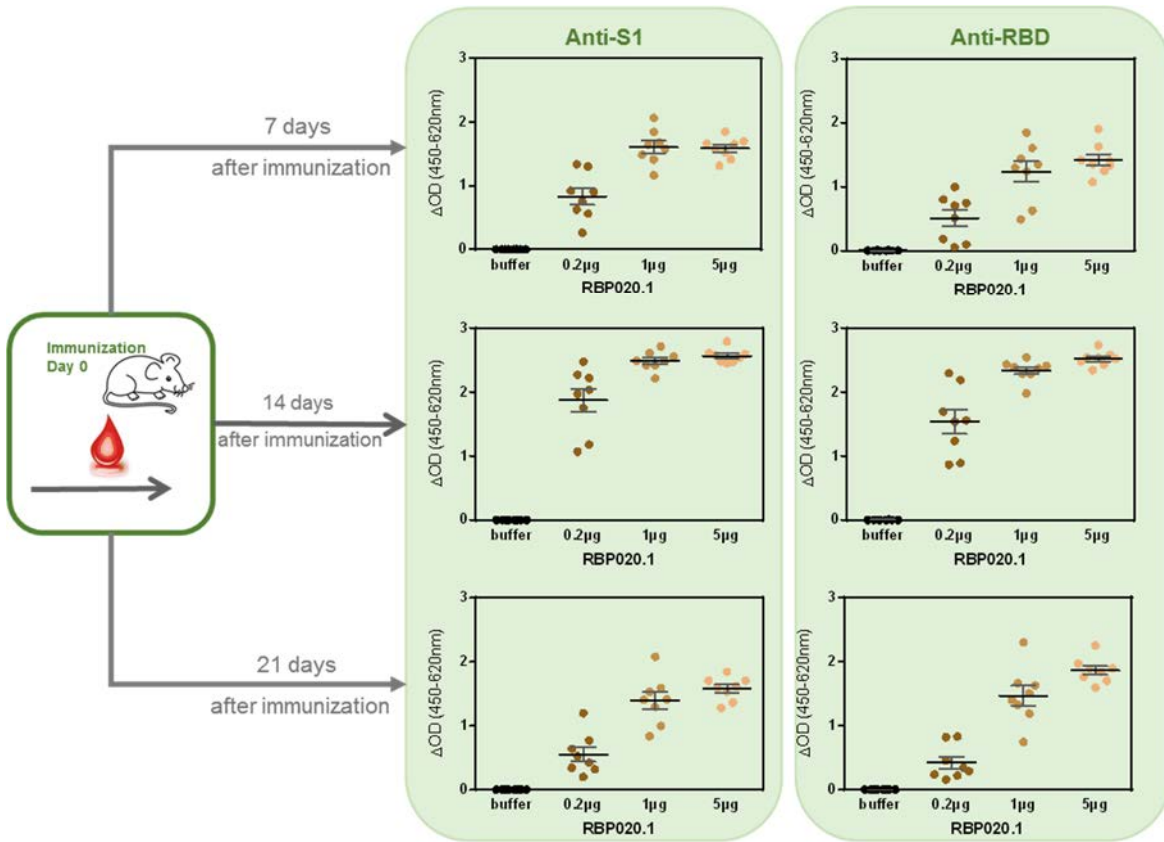
2.4.2.1.9.4. Immunogenicity of modRNA Encoding P2 S V8 (BNT162b2/RBP020.1)

Note that modRNA encoding P2 S V9, not P2 S V8, is being prepared for clinical testing.

The immunogenicity of LNP-formulated modRNA encoding P2 S V8 was tested in mice (experimental details in the figure legends). ELISA data show an early, dose-dependent IgG response recognizing S1 and RBD (Figure 2.4.2-16). Dose-dependent pseudotype neutralizing titers are detected 14 d after immunization (Figure 2.4.2-17). The study is ongoing.

090177e1934a5cff\Approved\Approved On: 21-Apr-2020 19:41 (GMT)

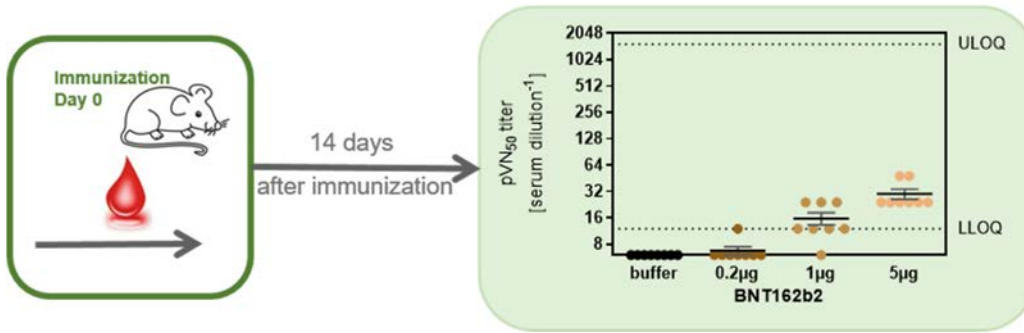
Figure 2.4.2-16. IgG Response Recognizing S1 and RBD IgG 7, 14 and 21 d after Immunization with modRNA Encoding P2 S V8



BALB/c mice were immunized IM once with 0.2, 1 or 5 μg of LNP-formulated modRNA RBP020.1. 7, 14 and 21 d after immunization, animals were bled and the serum samples were analyzed for total amount of anti-S1 (left) and anti-RBD (right) antigen specific immunoglobulin G (IgG) measured via ELISA. For day 7 (1:100), day 14 (1:300) and day 21 (1:1100) different serum dilution were included in the graph. One point in the graph stands for one mouse, every mouse sample was measured in duplicates (group size $n=8$; mean \pm SEM is included for the groups).

090177e1934a5cff\Approved\Approved On: 21-Apr-2020 19:41 (GMT)

Figure 2.4.2-17. Pseudovirus Neutralization 14 d after Immunization with modRNA Encoding P2 S V8



BALB/c mice were immunized IM once with 0.2, 1 or 5 µg of LNP-formulated modRNA RBP020.1. On 14 d after immunization, animals were bled and the sera were tested for SARS CoV-2 pseudovirus neutralization. Graphs depict pVN₅₀ serum dilutions (50% reduction of infectious events, compared to positive controls without serum). One point in the graphs stands for one mouse. Every mouse sample was measured in duplicate. Group size n=8. Mean ± SEM is shown by horizontal bars with whiskers for each group. LLOQ, lower limit of quantification. ULOQ, upper limit of quantification.

2.4.2.1.10. Mouse Immunogenicity Studies for COVID-19 Vaccine Candidates

Mouse immunogenicity studies are currently ongoing for all COVID-19 vaccine candidates: BNT162a1 (RBL063.3), BNT162b1 (RBP020.3), BNT162b2 (RBP020.2), and BNT162c2 (RBS004.2). Antigen-specific IgG binding levels and pseudovirus neutralizing titers from time points after a single dose of vaccine are available for all candidates and show immunogenicity for both RBD V5 and P2 S V9. Updates will be provided.

Table 2.4.2-3. Design of Mouse Immunogenicity Studies for COVID-19 Vaccine Candidates

Group no	No of animals	Vaccine dose	Immunization day	Dose volume [µL] / route	Blood collection day	End of in-life phase
1	8	Buffer	0	20 / IM	7, 14, 21, 28	28
2	8	Low	0	20 / IM	7, 14, 21, 28	28
3	8	Medium	0	20 / IM	7, 14, 21, 28	28
4	8	High	0	20 / IM	7, 14, 21, 28	28

2.4.2.1.10.1. Immunogenicity of uRNA Encoding RBD V5 (BNT162a1/RBL063.3)

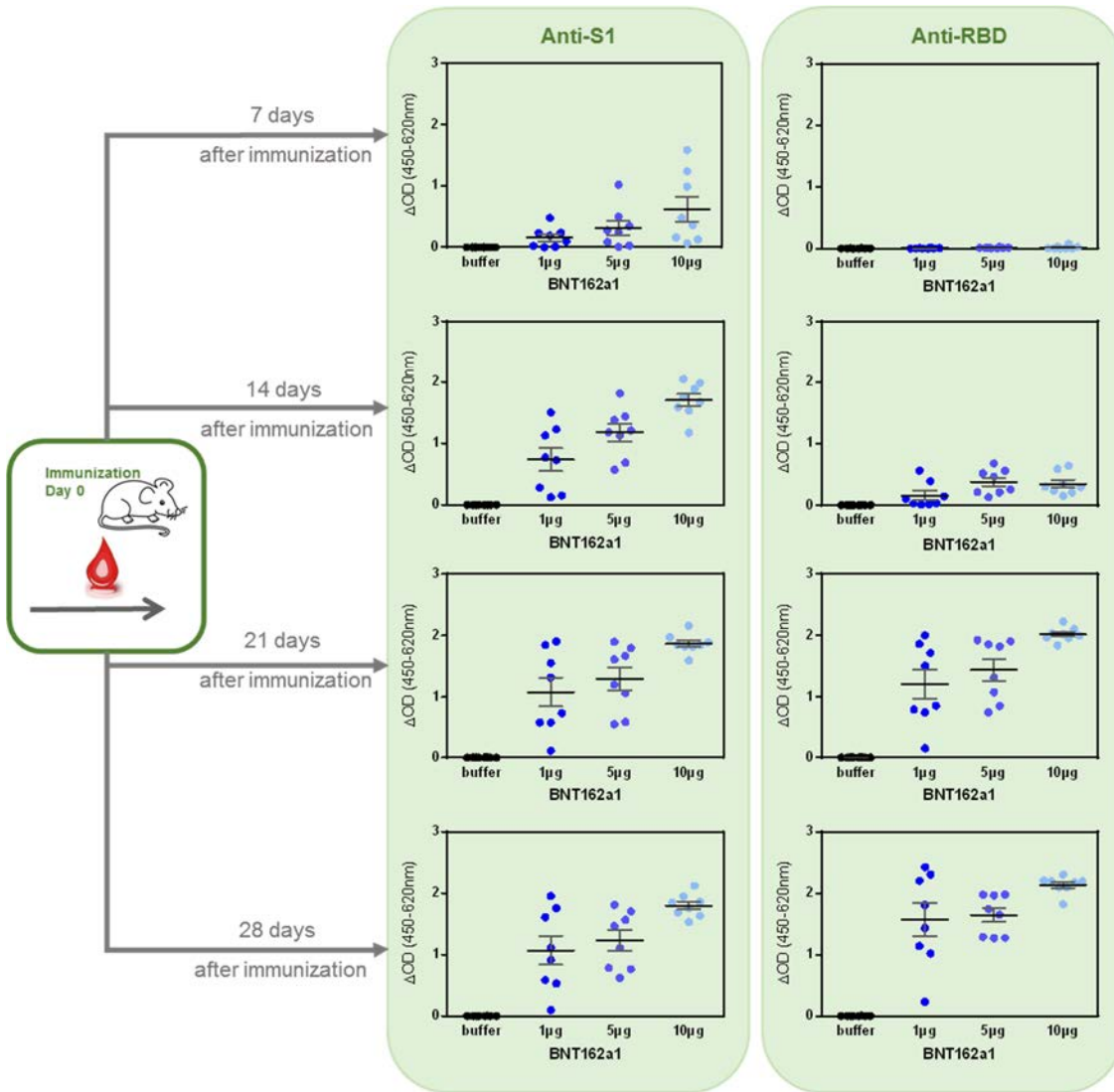
The immunogenicity of LNP-formulated uRNA encoding RBD V5 (vaccine candidate BNT162a1) was tested in mice (experimental details in Table 2.4.2-3 and the figure legends). ELISA data show an early, dose-dependent IgG response recognizing S1 and RBD (Figure 2.4.2-18). Antibody concentrations in the serum samples were calculated for the individual sampling days, and the kinetics of IgGs against S1 and RBD proteins are shown in Figure 2.4.2-19. Concentrations of IgG recognizing S1 increased in a dose-dependent manner to d21 and but did not increase further at d28 (Figure 2.4.2-19A). Concentrations of IgG recognizing RBD increased over time in a dose-dependent manner to D28

090177e1934a5cffApproved On: 21-Apr-2020 19:41 (GMT)

(Figure 2.4.2-19B). Sera obtained 14, 21 and 28 d after immunization showed minimal to no SARS-CoV-2 pseudovirus neutralization at any dose (Figure 2.4.2-20). The study is ongoing.

The lack of pseudovirus neutralization activity after a single dose of this vaccine candidate in mice contrasts with the pseudovirus neutralization titers elicited by this candidate after three weekly IM immunizations at the human dose levels in rats (Section 2.4.2.1.11). These findings suggest that the dose levels used in mice for this candidate may have been suboptimal, that more than one dose may be needed to elicit a response, or that the candidate is more immunogenic in rats.

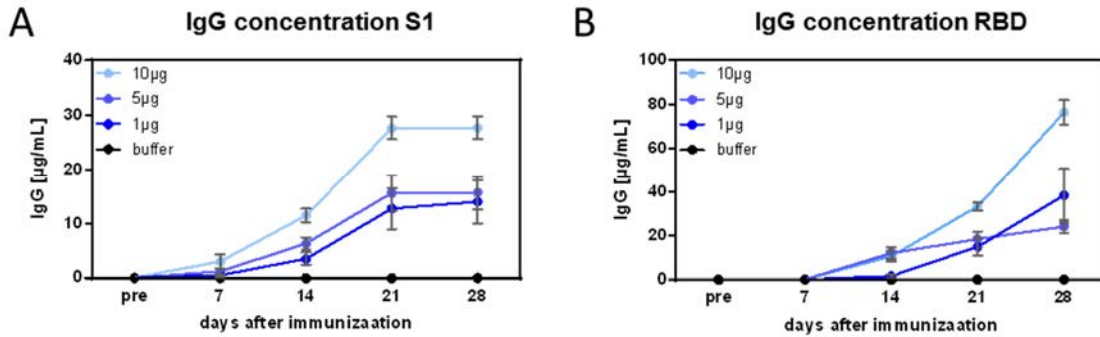
Figure 2.4.2-18. IgG Response Recognizing S1 and RBD 7, 14, 21 and 28 d after Immunization with uRNA Encoding RBD V5



BALB/c mice were immunized IM once with 1, 5 or 10 µg of LNP-formulated RBL063.3. On 7, 14, 21 and 28 d after immunization, animals were bled, and the sera were analyzed for anti-S1 (left) and anti-RBD (right) antigen-specific IgG by ELISA. On 7, 14, 21 and 28 d after immunization, animals were bled, and the sera were analyzed for anti-S1 (left) and anti-RBD (right) antigen-specific IgG by ELISA. For all time points, values for a serum dilution of 1:100 were included on the graphs. For all time points, values for a serum dilution of 1:100 were included on the graphs. One point in the graph stands for one mouse. Every mouse sample was measured in duplicate. Group size n=8. Mean ± SEM is depicted as a horizontal line with whiskers for each group.

090177e1934a5cff\Approved On: 21-Apr-2020 19:41 (GMT)

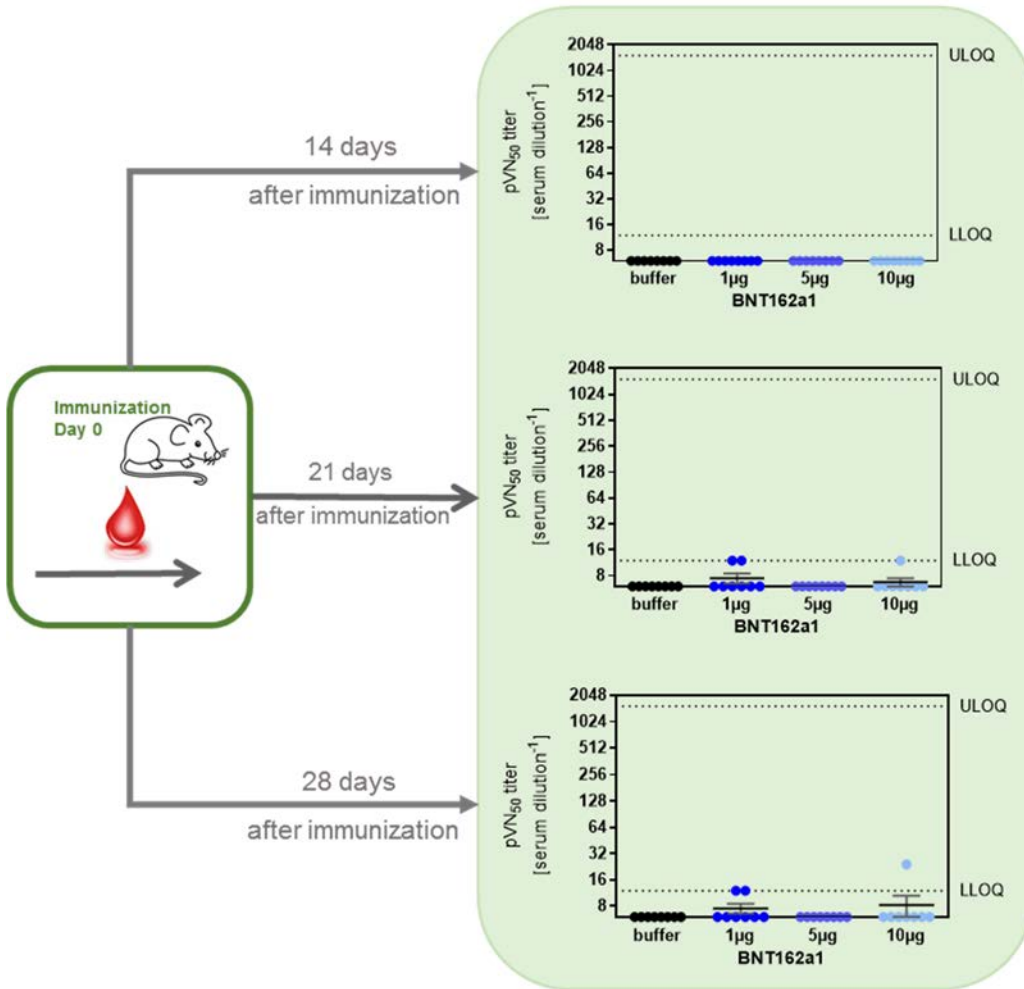
Figure 2.4.2-19. Kinetics of the IgG Response Recognizing S1 and RBD after Immunization with uRNA Encoding RBD V5



For individual Δ OD values, the antibody concentrations in the serum samples were calculated. The serum samples were tested against (A) the S1 protein and (B) RBD. Group mean antibody concentrations are shown (\pm SEM). Note that for the S1 and the RBD, 1 mg/mL protein were coated onto a 96 well plate. BNT162b2 encodes the RBD only. As the RBD is smaller than S1, more antibody binding sites are available in 1 mg/mL of RBD compared to S1 which could explain the higher antibody concentration calculated against RBD.

090177e1934a5cff\Approved\Approved On: 21-Apr-2020 19:41 (GMT)

Figure 2.4.2-20. Pseudovirus Neutralization Titers 7, 14, and 21 after Immunization with uRNA Encoding RBD V5



BALB/c mice were immunized IM once with 1, 5 or 10 µg of BNT162a1. On 14, 21 and 28 d after immunization, animals were bled, and the sera were tested for SARS CoV-2 pseudovirus neutralization. Graphs depict pVN₅₀ serum dilutions (50% reduction of infectious events, compared to positive controls without serum). One point in the graphs stands for one mouse. Every mouse sample was measured in duplicate. Group size n=8. Mean ± SEM is shown by horizontal bars with whiskers for each group. LLOQ, lower limit of quantification. ULOQ, upper limit of quantification.

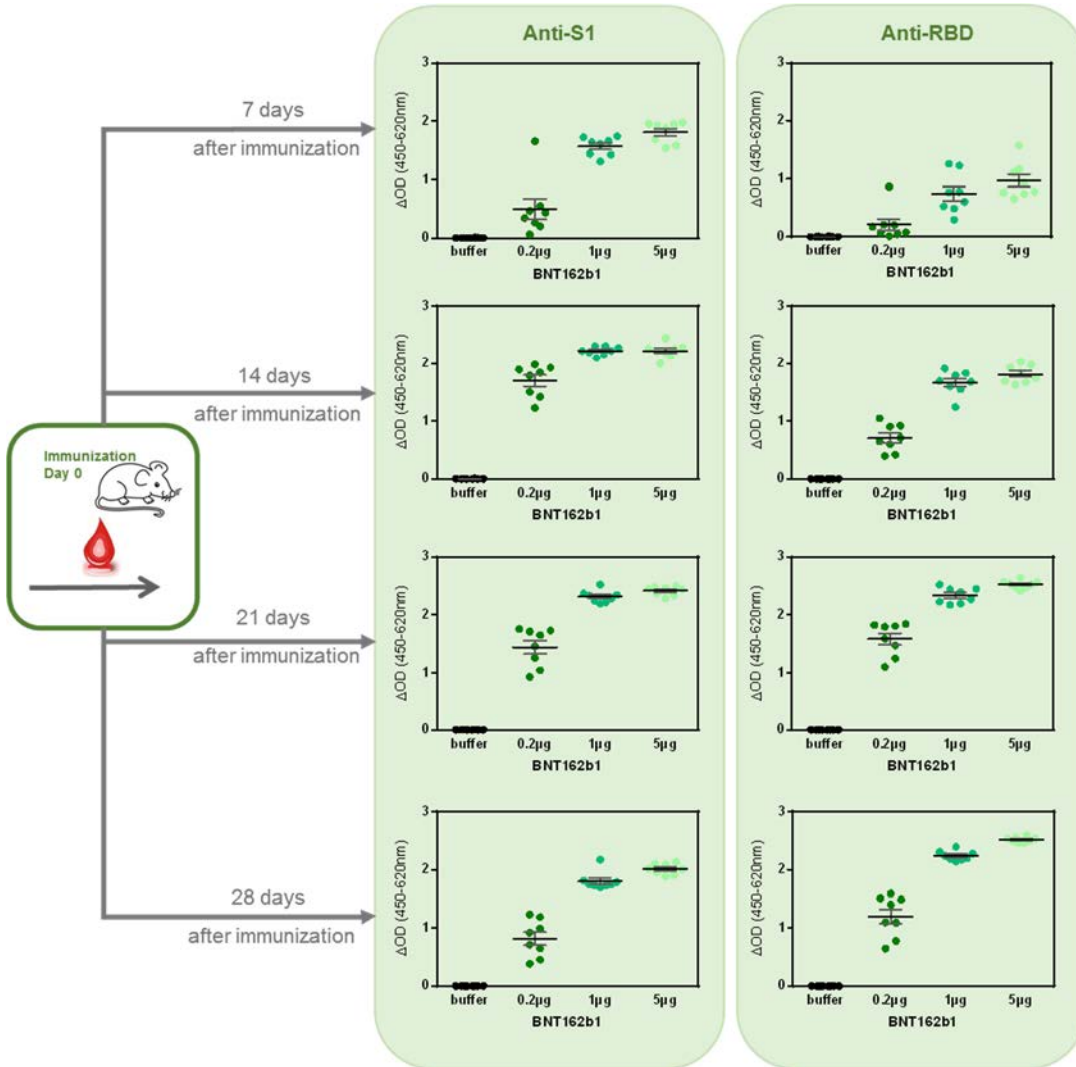
2.4.2.1.10.2. Immunogenicity of modRNA Encoding RBD V5 (BNT162b1/RBP020.3)

The immunogenicity of LNP-formulated modRNA encoding RBD V5 (vaccine candidate BNT162b1) was tested in mice (experimental details in Table 2.4.2-3 and the figure legends). ELISA data show an early, dose-dependent IgG response recognizing S1 and RBD (Figure 2.4.2-21). Antibody concentrations in the serum samples were calculated for the individual sampling days, and the kinetics of IgGs against S1 and RBD proteins are shown in Figure 2.4.2-22. Antibody concentrations against S1 (Figure 2.4.2-22A) and RBD (Figure 2.4.2-22B) increased in a dose-dependent manner over time. Sera obtained 14, 21

090177e1934a5cffApproved On: 21-Apr-2020 19:41 (GMT)

and 28 d after immunization show dose-dependent pseudovirus neutralization (Figure 2.4.2-23). The study is ongoing.

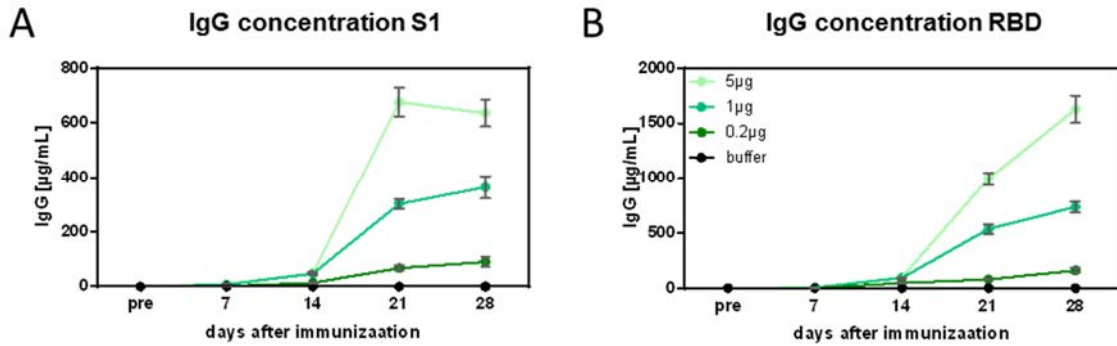
Figure 2.4.2-21. IgG Response Recognizing S1 and RBD 7, 14, 21 and 28 d after Immunization with modRNA Encoding RBD V5



BALB/c mice were immunized IM once with 0.2, 1 or 5 µg of LNP-formulated modRNA vaccine candidate encoding the RBD (BNT162b1). On 7, 14, 21 and 28 d after immunization, animals were bled, and the sera were analyzed for anti-S1 (left) and anti-RBD (right) antigen-specific IgG by ELISA. For day 7 (1:100), day 14 (1:300), day 21 (1:900) and day 28 (1:2700), data from different serum dilutions were included on the graphs. One point on the graphs stands for one mouse. Every serum sample was measured in duplicate. Group size n=8. Mean ± SEM is depicted by a horizontal line with whiskers for each group.

090177e1934a5cff\Approved\Approved On: 21-Apr-2020 19:41 (GMT)

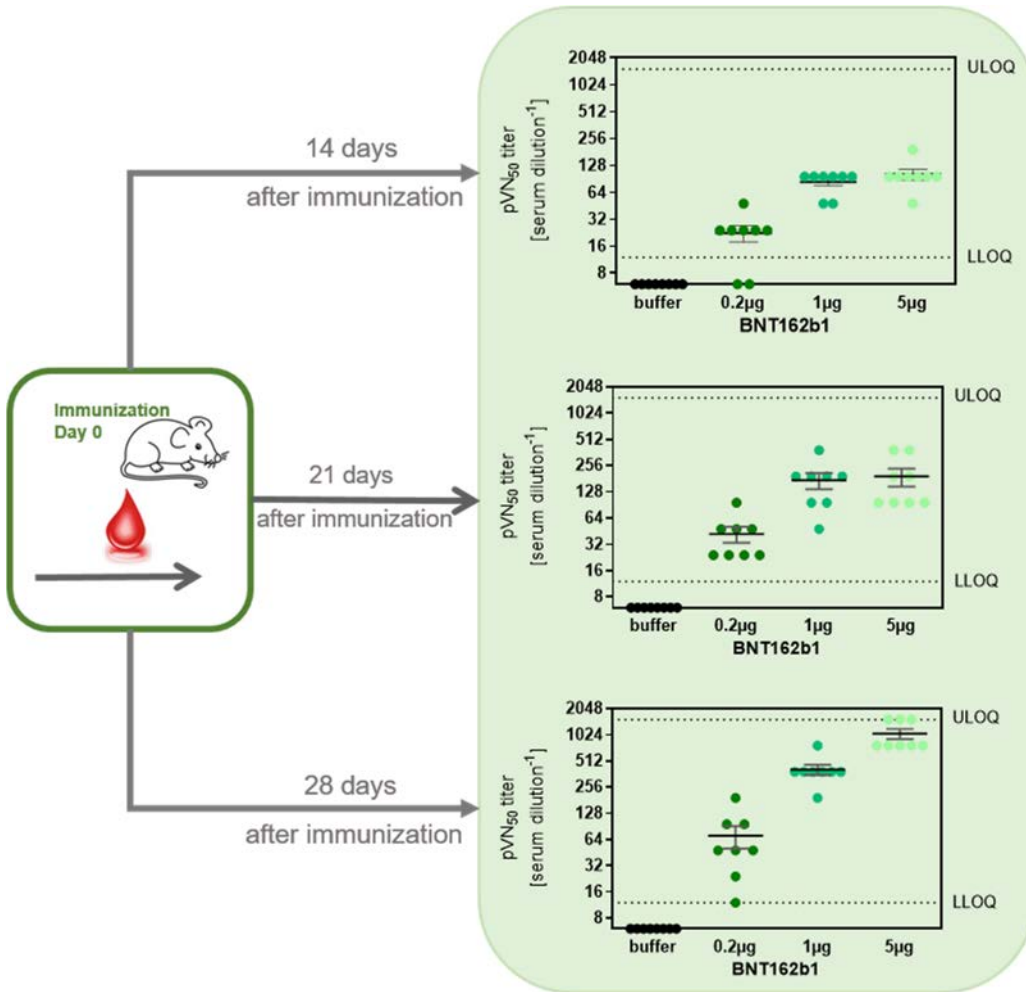
Figure 2.4.2-22. Kinetics of the IgG Response Recognizing S1 and RBD after Immunization with modRNA Encoding RBD V5



For individual Δ OD values, the antibody concentrations in the serum samples were calculated. The serum samples were tested against (A) the S1 protein and (B) RBD. Group mean antibody concentrations are shown (\pm SEM). Note that for the S1 and the RBD, 1mg/mL protein were coated onto a 96well plate. BNT162b2 encodes for the receptor binding domain only. As the RBD has a smaller size than the S1, more antibody binding sites are available within 1 mg/mL of RBD compared to S1 which could explain the higher antibody concentration calculated against RBD.

090177e1934a5cff\Approved\Approved On: 21-Apr-2020 19:41 (GMT)

Figure 2.4.2-23. Pseudovirus Neutralization 14, 21 and 28 d after Immunization with modRNA Encoding RBD V5



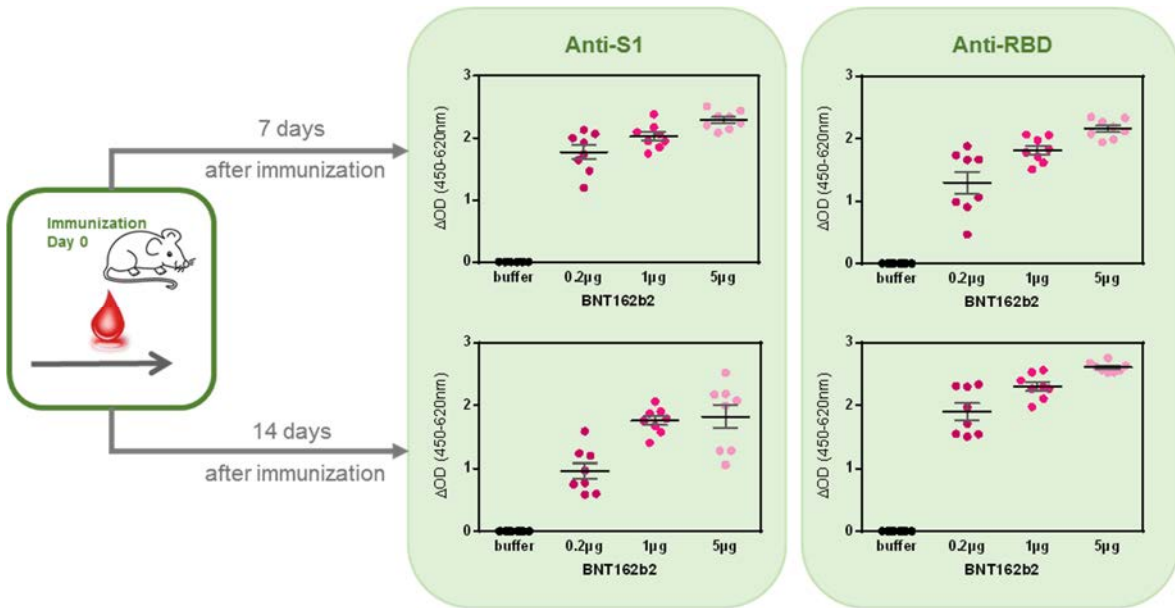
BALB/c mice were immunized IM once with 0.2, 1 or 5 µg of BNT162b1. On 14, 21 and 28 d after immunization, animals were bled, and the sera were tested for SARS CoV-2 pseudovirus neutralization. Graphs depict pVN₅₀ serum dilutions (50% reduction of infectious events, compared to positive controls without serum). One point in the graphs stands for one mouse. Every mouse sample was measured in duplicate. Group size n=8. Mean ± SEM is shown by horizontal bars with whiskers for each group. LLOQ, lower limit of quantification. ULOQ, upper limit of quantification.

090177e1934a5cff\Approved\Approved On: 21-Apr-2020 19:41 (GMT)

2.4.2.1.10.3. Immunogenicity of modRNA Encoding P2 S V9 (BNT162b2/RBP020.2)

The immunogenicity of LNP-formulated modRNA encoding P2S V9 (vaccine candidate BNT162b2) was tested in mice (experimental details in Table 2.4.2-3 and the figure legend). ELISA data show an early, dose-dependent IgG response recognizing S1 and RBD (Figure 2.4.2-24). The study is ongoing. Additional data including neutralization data will be provided before human dosing commences with this candidate.

Figure 2.4.2-24. IgG Response Recognizing S1 and RBD 7 and 14 d after Immunization with modRNA Encoding P2 S V9



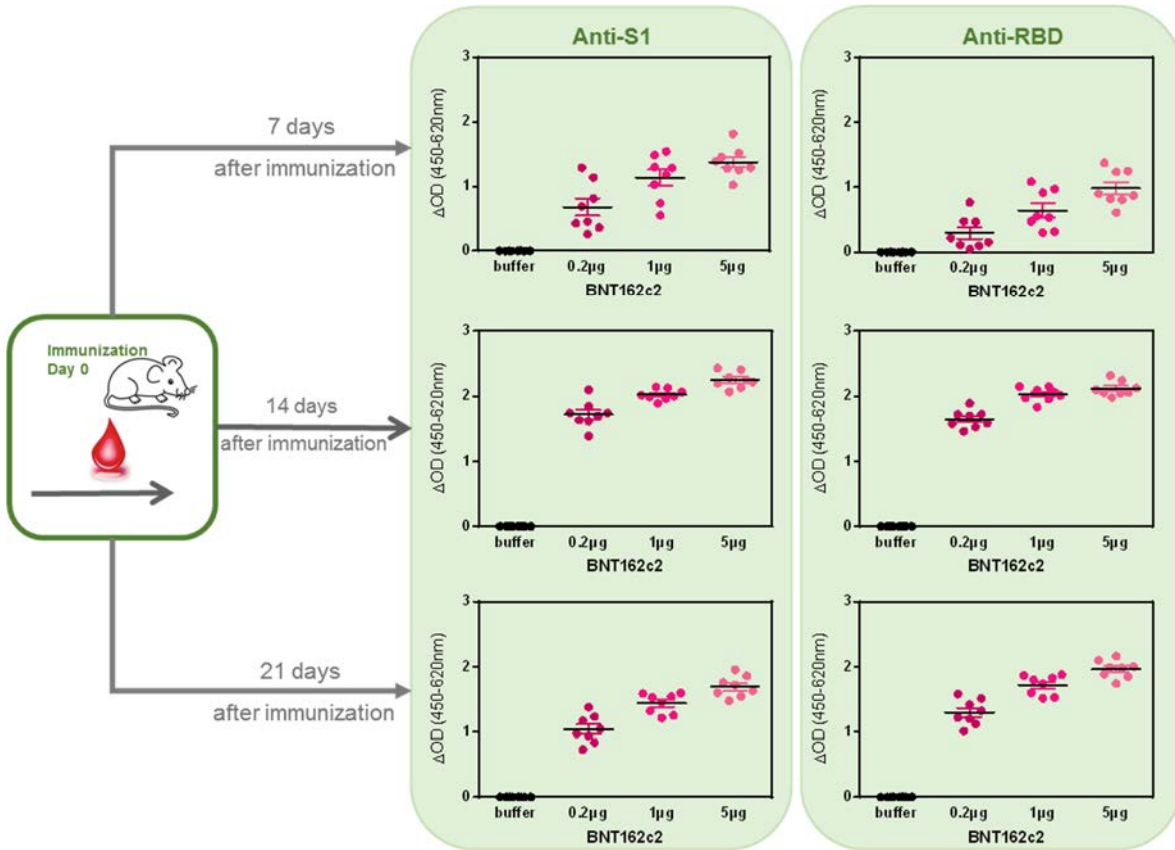
BALB/c mice were immunized IM once with 0.2, 1 or 5 μg of LNP-formulated modRNA vaccine candidate encoding the P2 S-V9 (BNT162b2). On 7 and 14 d after immunization, animals were bled, and the sera were analyzed for anti-S1 (left) and anti-RBD (right) antigen-specific IgG by ELISA. For day 7 (1:300) and day 14 (1:900), data from different serum dilutions were included on the graphs. One point on the graphs stands for one mouse. Every serum sample was measured in duplicate. Group size n=8. Mean ± SEM is depicted by a horizontal line with whiskers for each group.

090177e1934a5cff\Approved\Approved On: 21-Apr-2020 19:41 (GMT)

2.4.2.1.10.4. Immunogenicity of saRNA Encoding P2 S V9 (BNT162c2/RBS004.2)

The immunogenicity of LNP-formulated saRNA encoding P2 S V9 (vaccine candidate BNT162c2) was tested in mice (experimental details in Table 2.4.2-3 and the figure legends). ELISA data show an early, dose-dependent IgG response recognizing S1 and RBD (Figure 2.4.2-25). Sera obtained 14 and 21 d after immunization show dose-dependent pseudovirus neutralization (Figure 2.4.2-26). The study is ongoing.

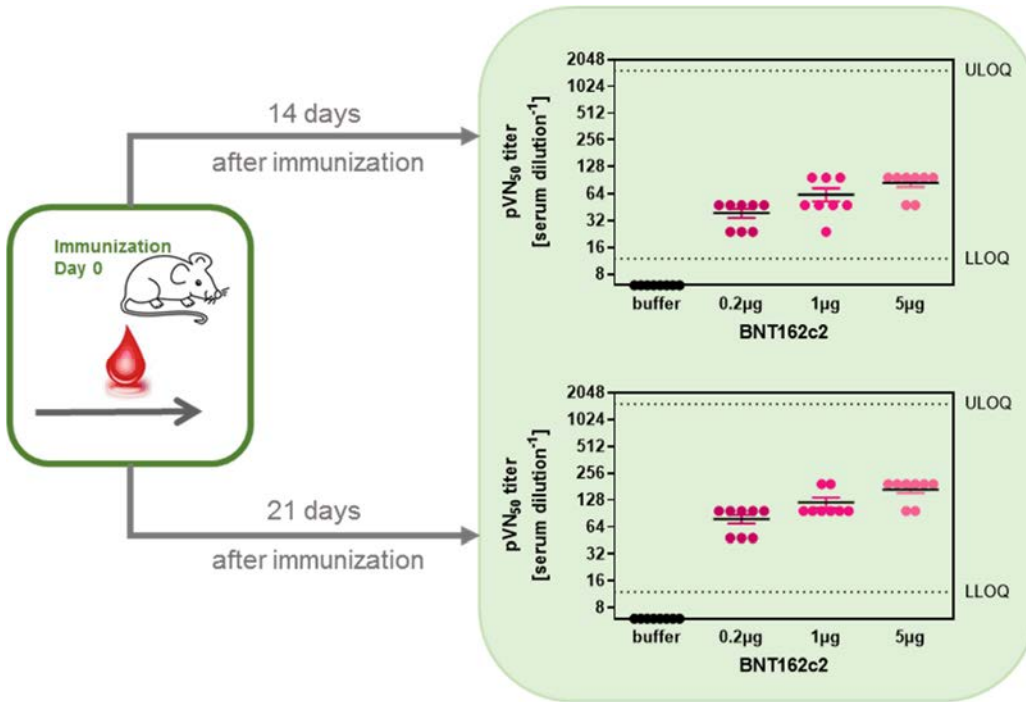
Figure 2.4.2-25. IgG Response Recognizing S1 and RBD 7, 14 and 21 d after Immunization with saRNA Encoding P2 S V9



BALB/c mice were immunized IM once with 0.2, 1 or 5 µg of LNP-formulated saRNA vaccine candidate encoding the P2 S-V9 (BNT162c2). 7, 14 and 21 d after immunization, animals were bled and the serum samples were analyzed for total amount of anti-S1 (left) and anti-RBD (right) antigen specific immunoglobulin G (IgG) measured via ELISA. For day 7 (1:100), day 14 (1:300) and day 21 (1:900) different serum dilutions were included in the graph. One point in the graph stands for one mouse, every mouse sample was measured in duplicates (group size n=8; mean ± SEM is included for the groups).

090177e1934a5cff\Approved\Approved On: 21-Apr-2020 19:41 (GMT)

Figure 2.4.2-26. Pseudovirus Neutralization 14 and 21 d after Immunization with saRNA Encoding P2 S V9



BALB/c mice were immunized IM once with 0.2, 1 or 5 µg of Bnt162c2. On 14, and 21 d after immunization, animals were bled, and the sera were tested for SARS CoV-2 pseudovirus neutralization. Graphs depict pVN₅₀ serum dilutions (50% reduction of infectious events, compared to positive controls without serum). One point in the graphs stands for one mouse. Every mouse sample was measured in duplicate. Group size n=8. Mean ± SEM is shown by horizontal bars with whiskers for each group. LLOQ, lower limit of quantification. ULOQ, upper limit of quantification.

2.4.2.1.11. Immunogenicity Testing After Weekly Immunization of Rats in the GLP Compliant Repeat Dose Toxicology Study

The immunogenicity of COVID-19 vaccine candidates BNT162a1, BNT162b1, BNT162b2 (RBP020.1), and BNT162c1 in the GLP compliant repeat-dose rat toxicity study (Study 38166) was analyzed. Experimental details are in the figure legends. The rats received two weekly doses of saRNA candidate (BNT162c1) or three weekly doses of the uRNA candidate (BNT162a1) and modRNA candidates (BNT162b1 and BNT162b2/RBP020.1). Serum samples were collected from main study animals on day 10 (BNT162c1) or day 17 (BNT162a1, BNT162b1, and BNT162b2) after the first immunization. These blood draws correspond to 3 days post second dose and 3 days post third dose, respectively.

The sera were analyzed by ELISA for IgG that bound S1 (Figure 2.4.2-27) and RBD (Figure 2.4.2-28) and for SARS-CoV2-S pseudovirus neutralization (Figure 2.4.2-29). Each of the vaccine candidates elicited IgG that recognized S1 and RBD. Comparisons between the candidates' immunogenicity are complicated by the differences in dose level and number

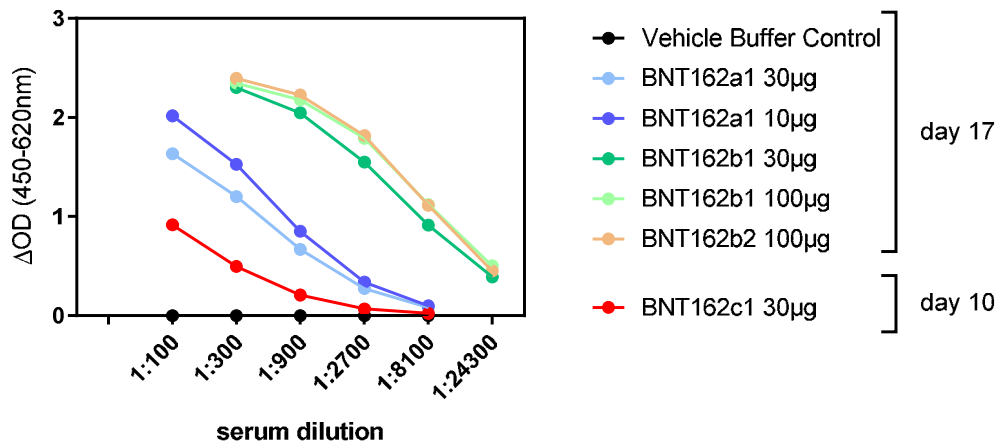
090177e1934a5cffApproved On: 21-Apr-2020 19:41 (GMT)

of doses, as well timing of blood draws between the RNA platforms and antigens. The rank order of the antigen-binding IgG responses was the same regardless of whether the target antigen in the ELISA was S1 or RBD. The analysis showed the lowest IgG responses to two doses of 30 µg of saRNA encoding the RBD at day 10 after the first immunization, middle IgG responses to three doses of 10 or 30 µg of uRNA encoding the RBD (BNT162a1) at day 17, and the highest antibody responses to three doses of 30 or 100 µg of modRNA encoding RBD (BNT162b1) or of 100 µg of RNA encoding P2 S V8 (BNT162b2/RBP020.1) at day 17. Comparison of the two modRNAs that had the same dosing level and regimen but encoded different antigens (the RBD for B162b1 and P2 S for B162b2/RBP020.1) showed equivalent IgG responses to both target antigens (S1 and RBD) by ELISA.

Antibody concentrations were calculated for the individual serum samples and the concentrations of IgG recognizing S1 and RBD are given in Table 2.4.2-4. Antibody concentrations against S1 and RBD were, as expected, slightly higher for the higher dose of modRNA encoding RBD (BNT162b1) but slightly lower for the higher dose of uRNA expressing RBD (BNT162a1).

Pseudovirus neutralization results paralleled the antigen binding results (Figure 2.4.2-27). The highest neutralizing titers were elicited by three doses of 30 or 100 µg of the modRNAs at day 17, middle neutralizing titers were elicited by three doses of 10 or 30 µg of uRNA at day 17, and minimal to no detectable neutralizing titers were elicited by two doses of 30 µg of saRNA at day 10.

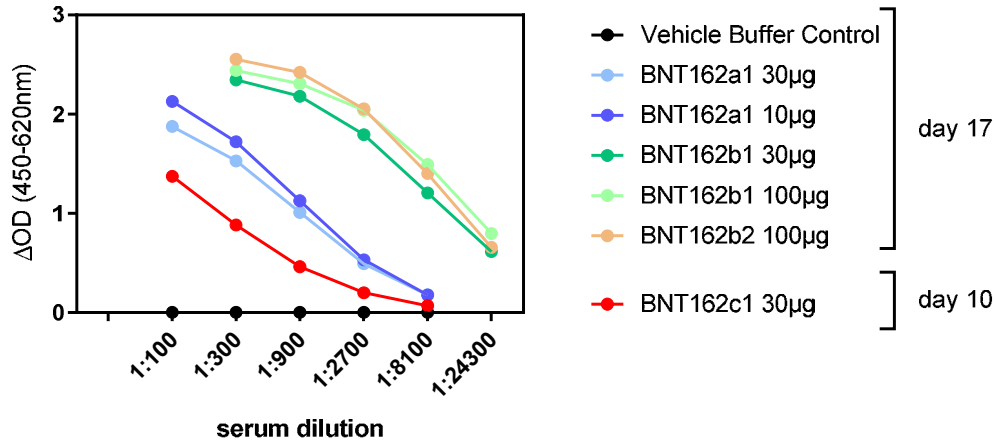
Figure 2.4.2-27. IgG Responses Recognizing S1 after Repeated Immunization in the Rat Toxicology Study



Wistar Han rats were immunized IM with three weekly injections of 10 or 30 µg BNT162a1, 30 or 100 µg BNT162b1, 100 µg BNT162b2 (RBP020.1), or two weekly injections of 30 µg BNT162c1. On day 10 (BNT162c1) or day 17 (all other cohorts) animals were bled and the sera were tested for total amount of anti-S1 antigen specific immunoglobulin G (IgG) measured via ELISA. Different serum dilutions were tested ranging from 1:100 to 1:24300. One point in the graph stands for the ΔOD group mean value at a particular given serum dilution (group size n=20).

090177e1934a5cff\Approved\Approved On: 21-Apr-2020 19:41 (GMT)

Figure 2.4.2-28. IgG Responses Recognizing RBD after Repeated Immunization in the Rat Toxicology Study



Wistar Han rats were immunized IM with three weekly injections of 10 or 30 μg BNT162a1, 30 or 100 μg BNT162b1, 100 μg BNT162b2 (RBP020.1), or two weekly injections of 30 μg BNT162c1. On day 10 (BNT162c1) or day 17 (all other cohorts) animals were bled and the sera were tested for total amount of anti-RBD antigen specific immunoglobulin G (IgG) measured via ELISA. Different serum dilutions were tested ranging from 1:100 to 1:24300. One point in the graph stands for the ΔOD group mean value at a particular given serum dilution (group size n=20).

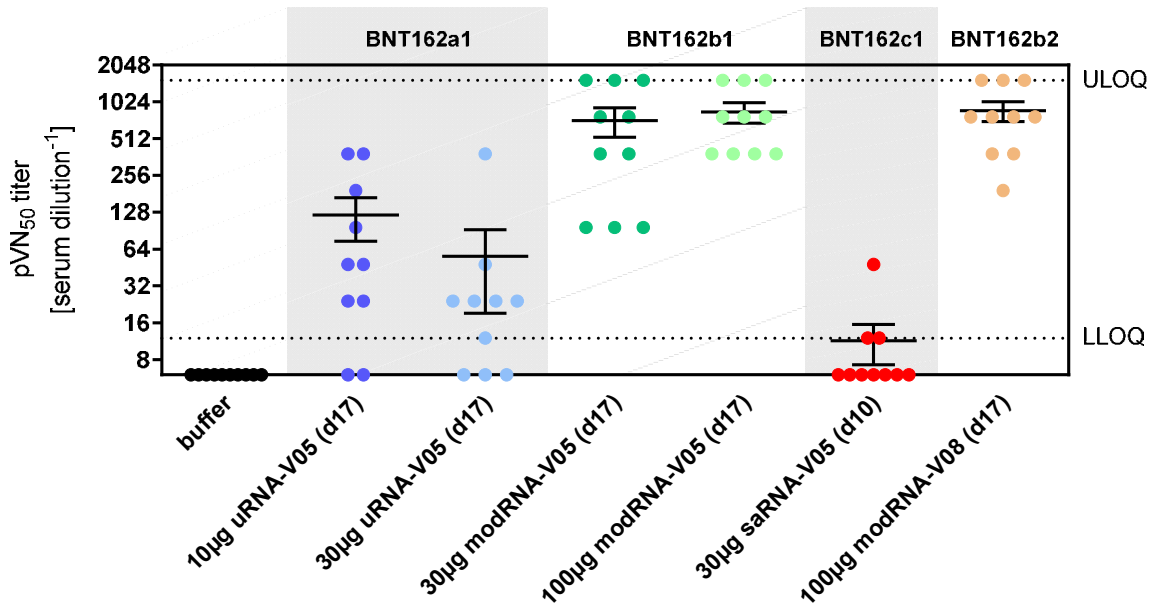
Table 2.4.2-4. IgG Concentrations Against S1 and RBD in Immunized Wistar Han Rats

IgG total [μg/mL]	17 d after first immunization					10 d after first immunization
	BNT162a1 30 μg	BNT162a1 10 μg	BNT162b1 100 μg	BNT162b1 30 μg	BNT162b2 100 μg	BNT162c1 30 μg
Against S1	83.0 ± 13.6	149.8 ± 24.6	1844.2 ± 243.4	1502.9 ± 269.9	1755.9 ± 164.1	19.3 ± 3.7
Against RBD	192.6 ± 35.2	208.3 ± 28.9	2632.6 ± 270.9	2017.0 ± 257.1	2331.4 ± 185.1	56.3 ± 12.0

For individual ΔOD values, the antibody concentrations in the serum samples were calculated. The serum samples were tested against the S1 protein and RBD. Group mean antibody concentrations are shown (±SEM) that were graphed in Figure 2.4.2-27 and Figure 2.4.2-28.

090177e1934a5cff\Approved\Approved On: 21-Apr-2020 19:41 (GMT)

Figure 2.4.2-29. Pseudovirus Neutralization Activity (pVN₅₀) in Repeatedly Dosed Rats



Wistar Han rats were immunized IM with three weekly injections of 10 or 30 µg BNT162a1, 30 or 100 µg BNT162b1, 100 µg BNT162b2 (RBP020.1), or two weekly injections of 30 µg BNT162c1. On day 10 (BNT162c1) or day 17 (all other cohorts) animals were bled and the sera were tested for SARS CoV-2 pseudovirus neutralization. Graphs depict pVN₅₀ serum dilutions (50% reduction of infectious events, compared to positive controls without serum). One point in the graphs stands for one rat. Every rat sample was measured in duplicate. Group size n=5 male and n=5 female rats. Mean ± SEM is shown by horizontal bars with whiskers for each group. LLOQ, lower limit of quantification. ULOQ, upper limit of quantification.

2.4.2.1.12. Secondary pharmacodynamics

No secondary pharmacodynamics studies were conducted for the COVID-19 vaccine candidates.

2.4.2.1.13. Safety pharmacology

No safety pharmacology studies were conducted as they are not considered necessary according to the WHO guideline (WHO, 2005).

2.4.2.1.14. Nonclinical pharmacology - Conclusions

All nonclinical pharmacology studies and their analysis are ongoing.

The currently available data demonstrate that vaccines based on each of the three RNA platforms (uRNA, modRNA, and saRNA) in conjunction with both the trimerized RBD V5 and P2 S V8 and V9, including the clinical vaccine candidates, BNT162a1, BNT162b1, BNT162b2 (RBP020.1), and BNT162c2, are capable of inducing robust immune responses in mice and rats. In mice, antigen-binding IgG responses were detected as soon as 7 d

090177e1934a5cff\Approved\Approved On: 21-Apr-2020 19:41 (GMT)

post-immunization. Immune responses measured by SARS-CoV-2 pseudovirus neutralization are detectable 14 d post-immunization in mice immunized with intermediate doses. Similar results indicating immunogenicity were obtained in an accessory study to the GLP-compliant repeat-dose toxicology study in rats ([Study 38166](#)).

As both antigen variants, RBD and P2 S, elicit antigen-binding antibodies and pseudovirus-neutralizing serum titers, and all three RNA platforms have proven immunogenic for other viral antigens, these preliminary data support the clinical testing of each of these vaccine candidates.

Differences in results obtained in mice and rats, such as the lack of pseudovirus neutralizing titers elicited in mice ([Section 2.4.2.1.10.1](#)) but robust neutralizing titers elicited in rats ([Section 2.4.2.1.11](#)) by uRNA encoding the RBD, point to complexities in interpretation of results in rodent models. Rather than trying to optimize timing, dose level, and regimen in mice to appropriately describe the immune profiles, which is very time consuming and may not be relevant to the human situation (especially given species-specific innate immune mechanisms), such results provide the rationale for our desire to assess the humoral and cellular immune response to COVID-19 vaccine candidates as quickly as possible in the human sentinel cohorts.

090177e1934a5cff\Approved\Approved On: 21-Apr-2020 19:41 (GMT)

2.4.3. PHARMACOKINETICS

2.4.3.1. Brief Summary

Currently, no nonclinical methods of analysis, absorption, PK, TK, metabolism, excretion, or DDI studies have been conducted for the COVID-19 vaccine candidates (BNT162 [PF-07302048]) described in [Section 2.4.1](#).

The biodistribution of the COVID-19 vaccine platform after IM administration was assessed in BALB/c mice. Mice were administered a luciferase expressing modRNA formulated like the COVID-19 vaccine candidates. Luciferase expression was measured in vivo by luciferin application. Luciferase expression was identified at the injection site at 6 hours after injection and was gone by 9 days. Liver expression was also present to a lesser extent at 6 hours after injection and was gone by 48 hours after injection. These data are consistent with the biodistribution that has been observed for RNA platform vaccine candidates that have been already evaluated clinically and have shown a good safety profile (as described in Section 2.4.3.5 below).

2.4.3.2. Methods of Analysis

No nonclinical PK or TK methods of analysis have been developed for the components of the COVID-19 vaccines.

2.4.3.3. In Vitro Absorption

No absorption studies were conducted for the COVID-19 vaccines, as the administration route is IM.

2.4.3.4. Pharmacokinetics

Pharmacokinetic studies have not been conducted with the COVID-19 vaccine candidates and are generally not considered necessary to support the development and licensure of vaccine products for infectious diseases ([WHO, 2005](#); [WHO, 2014](#)).

2.4.3.5. Distribution

To date, whole body distribution studies have not been conducted with the COVID-19 vaccine candidates. In an in vivo study ([Study R-20-0072](#)), the biodistribution was assessed using luciferase as a surrogate marker protein, using RNA encoding luciferase formulated like the COVID-19 vaccine candidates (using LNP8). The RNA was administered to BALB/c mice by IM injection in the right and left hind leg, each with 1 µg of LNP-formulated modRNA encoding luciferase. Luciferase protein expression was detected at different timepoints, by measuring the in vivo bioluminescence after injection of the luciferin substrate, at the site of injection and to a lesser extent in the liver ([Figure 1](#)). Distribution to the liver is likely mediated by the LNPs entering the blood stream. The luciferase expression dropped to background levels after 9 days.

The biodistribution of the antigen encoded by the RNA component of the COVID-19 vaccines is expected to be dependent on the LNP distribution. Therefore, the modRNA encoding luciferase results should be representative for COVID-19 vaccine RNA platforms. BioNTech has safely tested RNAs, formulated in lipoplexes that are similar to LNPs and also show biodistribution to the liver, at higher doses non-clinically and clinically by IV administration. Although liver function tests will be carefully monitored during the clinical development of these vaccines, BioNTech’s prior clinical experience indicates that the distribution to the liver does not pose a safety concern. These previous clinical and non-clinical studies conducted by BioNTech are summarized in the included Investigator’s Brochure (April 2020 Investigator’s Brochure, Section 2.5 and 4.3.1).

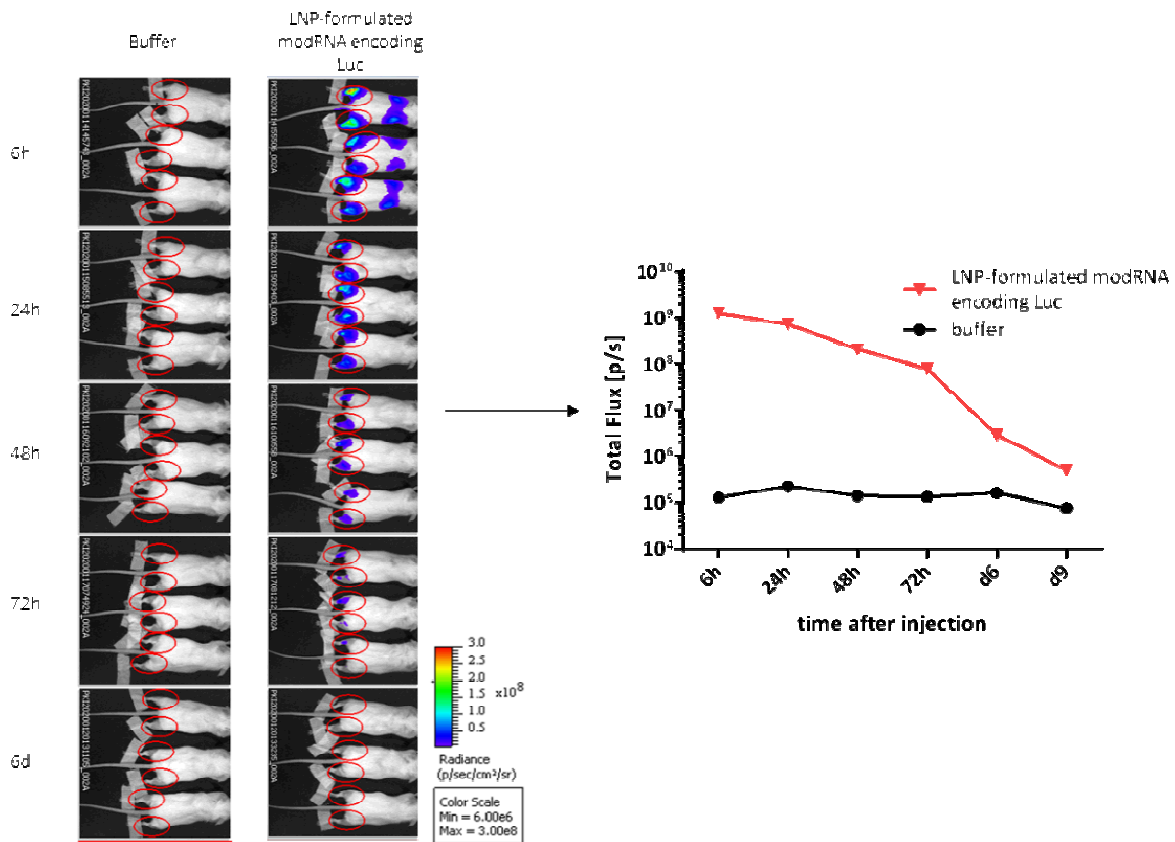


Figure 1. Bioluminescence Emission in BALB/c Mice after IM Injection of an LNP Formulation of modRNA Encoding Luciferase

2.4.3.6. Metabolism

Proteins encoded by the RNA in the COVID-19 vaccine candidates are expected to be proteolytically degraded like other endogenous proteins. RNA, including pseudouridine modified RNA and saRNA, is degraded by cellular RNases and subjected to nucleic acid metabolism. Nucleotide metabolism occurs continuously within the cell, with the nucleoside being degraded to waste products and excreted or recycled for nucleotide synthesis.

090177e1934a5cff\Approved\Approved On: 21-Apr-2020 19:41 (GMT)

COVID-19 Vaccine (BNT162, PF-07302048)

BB-IND 19736

Module 2.4. Nonclinical Overview

Therefore, no RNA or protein metabolism or excretion studies will be conducted. Of the four lipids used as excipients in the LNP formulation, two are naturally occurring (cholesterol and DSPC) and will be metabolized and excreted like other endogenous lipids. The PK profile of the two novel lipids (ALC-0315 and ALC-0159) will be characterized at a later stage of nonclinical development.

2.4.3.7. Excretion

No excretion studies have been conducted with the COVID-19 vaccine candidates for the reasons described in [Section 2.4.3.6](#).

2.4.3.8. Pharmacokinetic Drug Interactions

No PK drug interaction studies have been conducted with the COVID-19 vaccine candidates.

090177e1934a5cff\Approved\Approved On: 21-Apr-2020 19:41 (GMT)

2.4.4. TOXICOLOGY

2.4.4.1. Brief Summary

A GLP-compliant repeat-dose toxicity study in Wistar Han rats is ongoing to support the nonclinical toxicity assessment of the COVID-19 vaccine candidates (BNT162; PF-07302048) (outlined in [Table 2.4.4-1](#)).

The IM route of exposure was selected as it is the intended route of clinical administration. The selection of rats as the toxicology test species is consistent with the WHO guidance documents on nonclinical evaluation of vaccines ([WHO, 2005](#)), which recommend that vaccine toxicity studies be conducted in a species in which an immune response is induced by the vaccine antigen. Mice have developed an immune response to the COVID-19 vaccine candidates, and immunogenicity has been confirmed in rats in the ongoing repeat-dose toxicity study. The Wistar Han rat is used routinely for regulatory toxicity studies, and there is an extensive historical safety database on this strain of rat.

The non-QC, unaudited interim study report ([Study 38166](#)) includes results of dosing phase mortality, clinical signs, body weight, food consumption, body temperature, injection site dermal scores, ophthalmoscopic and auditory endpoints, hematology, coagulation, clinical chemistry, and urinalysis parameters, a subset of cytokine endpoints, serology, organ weights and macroscopic pathology from dosing phase animals. Remaining cytokine results and microscopic pathology from the dosing phase as well as all the recovery phase endpoints will be submitted in a final report as soon as it becomes available, but no later than 120 days after submission of the IND.

Initial results following administration of COVID-19 vaccine candidates by IM injection to male and female Wistar Han rats once every week, for a total of 2 or 3 weekly cycles of dosing, suggest the COVID-19 vaccine candidates were tolerated without evidence of systemic toxicity.

Table 2.4.4-1. Overview of Toxicity Testing Program

Study ^{a,b}	Dose Group	Dose/Week (µg RNA)	Total Volume (µL)	Tabulated Summary
Repeat-Dose Toxicity				
21-Day, 2 or 3 Dose (1 Dose/Week) ^c IM Toxicity in Rats With a 3-Week Recovery Period (Study 38166)	Control (Buffer ^d)	0	200 (2 x 100 µL) ^e	2.6.7.7A
	BNT162a1 (RBL063.3) (uRNA-LNP RBD V5)	30	60 (1 x 60 µL) ^f	
	BNT162a1 (RBL063.3) (uRNA-LNP RBD V5)	10	20 (1 x 20 µL) ^f	
	BNT162b1 (RBP020.3) (modRNA-LNP RBD V5)	30	60 (1 x 60 µL) ^f	
	BNT162b1 (RBP020.3) (modRNA-LNP RBD V5)	100	200 (2 x 100 µL) ^e	
	BNT162c1 (RBS004.3) (saRNA-LNP RBD V5)	30	70 (1 x 70 µL) ^f	
	BNT162b2 (RBP020.1) (modRNA-LNP SP2 V8)	100	200 (2 x 100 µL) ^e	

a. The repeat-dose toxicity study was GLP-compliant and was conducted in an OECD mutual acceptance of data-compliant member state.

b. The repeat-dose toxicity study was conducted with male and female animals.

c. QW x 3 (Days 1, 8, 15) for BNT162a1, BNT162b1, and BNT162b2; QW x 2 (Days 1, 8) for BNT162c1.

d. Phosphate buffered saline, 300 mM sucrose.

e. One application (100 µL) at 2 sites for a total dose volume of 200 µL.

f. One application at 1 site.

Expected inflammatory responses to the vaccine candidates were evident, such as edema and erythema at the injection sites, transient elevation in body temperature, slight and transient reduction in body weights, elevations in mean neutrophil, monocyte, and LUC counts, and elevations in acute phase reactants. Injection site reactions were common in all vaccine-administered animals and were greater after boost immunizations, which was attributable to the pharmacologically relevant progression of the elicited immune response. Decreased reticulocytes were observed in rats treated with the licensed LNP-siRNA pharmaceutical Onpattro™ (NDA # 210922) but have not been observed in humans treated with this biotherapeutic (Kozauer et al, 2018) suggesting this is a species-specific effect. Decreased platelet counts were noted after repeat administration but based on their small magnitude, no disruptions in hemostasis would be anticipated. Test article-related changes in clinical pathology were consistent with an acute phase response and anticipated low-level systemic inflammation. Macroscopic pathology and organ weight changes were also consistent with an inflammatory response. By the end of the dosing phase, an immune response was elicited from all COVID-19 vaccine candidate groups.

2.4.4.2. Single-Dose Toxicity

A separate single-dose toxicity study with the COVID-19 vaccine candidates has not been conducted.

2.4.4.3. Repeat-Dose Toxicity

2.4.4.3.1. Repeat-Dose Toxicity Study of Three LNP-Formulated RNA Platforms Encoding for Viral Proteins by Repeated Intramuscular Administration to Wistar Han Rats

The objective of this pivotal repeat-dose toxicity study was to determine the potential toxicity of three LNP-formulated RNA vaccine platforms, encoding SARS-CoV-2 P2 S or RBD, administered once weekly by IM administration to rats and to assess the reversibility of any effects after a 3-week recovery period (Study 38166; Tabulated Summary 2.6.7.7A). The LNP formulation is the same for the three RNA platforms administered in this study.

Wistar Han rats (15/sex/group) were administered COVID-19 vaccine via IM injection at doses of 0 (buffer), 30 and 10 (BNT162a1/RBL063.3), 30 and 100 (BNT162b1/RBP020.3), 30 (BNT162c1/RBS004.3), or 100 (BNT162b2/RBP020.1) μg RNA/dose per animal. Doses were administered once a week for 2 weeks (Days 1, 8) for BNT162c1 or once a week for 3 weeks (Days 1, 8, 15) for BNT162a1, BNT162b1, and BNT162b2. Dose volume ranged from 20 to 100 μL /application site. Following the dosing period, 10 animals/sex from each group were euthanized 2 days post last immunization for post-mortem assessments. The remaining 5 animals/sex/group were euthanized following a 3-week recovery period. Additional satellite animals (3/sex/group) were used for blood sampling for cytokine analysis.

Clinical signs of toxicity were assessed twice daily throughout the study. Body weights were recorded twice weekly during the dosing and the recovery phase. Food consumption was evaluated once weekly. Local tolerance (injection site dermal assessment) was evaluated 4, 24, 48, 96, and 144 hours after each administration, and body temperatures were evaluated at 4 and 24 hours after each administration. Additional body temperature measurements were taken at 48 hours if an animal had a body temperature $>40^{\circ}\text{C}$. A limited set of serum cytokines (IFN- γ , TNF- α , IL-1- β , IL-6, IL-10) were evaluated prior to and 6 hours post each dose and at the end of the dosing phase. Clinical pathology (hematology and clinical chemistry parameters as well as acute phase proteins) was evaluated 3 days after the first administration and at the end of the dosing and recovery phases. Urine analysis, coagulation parameters, auditory and ophthalmological parameters, serology, organ weights, macroscopic and microscopic pathology were evaluated at the end of dosing and recovery phases.

Interim results from this pivotal repeat-dose toxicity study are summarized below and are also provided in an interim non-QC, unaudited study report (Study 38166). As agreed with CBER via the Pre-IND Meeting - Request for Written Feedback (Section 1.12.1 Correspondence Regarding Pre-IND Meeting), interim data submitted in this IND include all dosing phase mortality, clinical signs, body weight, food consumption, body temperature, injection site observations, ophthalmoscopic and auditory endpoints, a subset of serum

cytokine endpoints, hematology, coagulation, clinical chemistry, urinalysis parameters, organ weights and macroscopic pathology as well as serology data from animals at the end of the dosing phase. Remaining cytokine results and microscopic pathology from the dosing phase as well as all the recovery phase endpoints will be submitted in a final report as soon as it becomes available, and no later than 120 days after submission of the IND.

At the interim phase of reporting, all test articles were tolerated, and all animals survived to the end of the dosing phase. Test article-related in-life findings included injection site reactions, transient body weight loss the day after dosing, and slightly higher body temperature at 4 and 24 hours postdose.

Body weights decreased 24 hours after each COVID-19 vaccine administration compared to predose values (<10%). No reduction was noted for the buffer control. Body weight gain between the administrations was comparable to the buffer control group.

Vaccine-administered animals generally had higher body temperatures compared to buffer control animals at 4 and 24 hours postdose. Group mean temperatures in COVID-19 vaccine-administered rats were within approximately 1°C of the group mean body temperature of buffer-administered animals. In rare cases, individual COVID-19 vaccine-administered rats had body temperatures up to 40.2°C, which decreased to <40°C within 24 hours after administration.

Slightly lower (0.77x to 0.97x) food consumption was seen in COVID-19 vaccine-administered animals compared to the buffer control group during Week 1, which was not apparent during Week 2.

There were no changes observed in either the ophthalmic or auditory examinations.

Expected inflammatory responses to the vaccine candidates were evident at the injection sites. Injection site reactions consisted primarily of transient edema and erythema, which resolved prior to the subsequent vaccine administration. Injection site reactions were more frequent and severe after the second and third vaccine administrations. The occurrence of higher severity injection site reactions after boost vaccinations is attributable to the pharmacologically relevant progression of the elicited immune response.

After the first vaccine administration, very slight (Grade 1) or slight (Grade 2) edema was noted in some animals across vaccine-administered groups 24 hours post administration. The reaction generally resolved within the following 24 to 48 hours and was resolved in all animals by 144 hours post administration. After the second vaccine administration, the local reaction was more pronounced (Grade 1 to Grade 3 [moderate]) and present in more, though not in all, animals. In animals administered 30 µg BNT162a1, eschar formation at the injection site was apparent for some animals after the second vaccine administration and appeared painful, but resolved. Of note, no Grade 3 or Grade 4 (severe) local reactions occurred after the first administration. The occurrence of higher severity local reactions after the second vaccine administration is attributed to the short dosing interval (once weekly).

Reversible very slight (Grade 1) erythema was noted from 48 to 96 hours post first vaccine administration in some animals in all vaccine-administered groups, except 30 µg BNT162b1.

After the second vaccine administration, very slight (Grade 1) to well-defined (Grade 2) erythema was noted in some animals from 24 to 48 hours (30 µg BNT162a1, 30 µg BNT162b1, 100 µg BNT162b2), and was resolved by 96 hours post administration. However, 144 hours post the second administration, severe (Grade 4) erythema was observed in some vaccine-administered animals (10 µg BNT162a1, 100 µg BNT162b1, 100 µg BNT162b2), but the observation was resolved within the following 24 hours.

Test article-related changes in clinical pathology were consistent with an acute phase response and anticipated systemic inflammation. Minor and variable alterations in other clinical pathology parameters were considered secondary effects of vaccination, including inflammation and injection site tissue changes.

Changes in hematology included lower mean reticulocyte and platelet counts, and higher mean white blood cell, neutrophil, monocyte, and LUC counts compared to control rats.

The transient reduction in reticulocyte counts (0.24x to 0.74x) was only observed after the first dose administration on Day 4 and was not accompanied by a reduction in red blood cell counts or hemoglobin content. Mean reticulocyte decreases were comparable across treatment groups and were likely related to the acute phase response.

Lower platelet counts (0.58x to 0.85x) were observed in all vaccine-administered groups except BNT162b2 at Days 10 or 17 and is likely inflammation-related platelet consumption. These decreases would not be anticipated to result in bleeding based on their small magnitude; there were no clinical findings consistent with disruptions in hemostasis.

Expected inflammatory responses to the vaccine candidates were evident, such as elevations in mean neutrophil (3.7x to 7.8x), monocyte (1.6x to 2.3x), and LUC counts (2.7x to 13x). White blood cells (1.5x to 2.2x) (neutrophils, monocytes, and/or LUC) were higher in all vaccinated groups compared to buffer controls and were higher at Days 10 and 17 than Day 4.

Test article-related changes in clinical chemistry included slightly higher GGT (1.9x to 4.6x) in all treatment groups on Day 4 and Days 10 or 17. This change may be secondary to an inflammatory response ([Singh, 1986](#)).

The acute phase proteins alpha-1-acid glycoprotein (4.1x to 7.2x) and alpha-2 macroglobulin (3.2x to 91x) were elevated in both males and females in all vaccine-administered groups on Day 4. Fibrinogen was higher (2.4x to 3.1x) in both males and females in all vaccine-administered groups on Day 10 or 17. There were no apparent sex related differences in these effects. Higher concentrations of acute phase proteins are an anticipated response to vaccination.

Coagulation parameters PT, aPTT, and fibrinogen were measured at the end of the in-life phase. As noted above, fibrinogen was higher in all vaccine-administered groups

approximately 3X compared to control, consistent with an acute phase response. aPTT was slightly prolonged (up to 1.2x) in all groups except in the 30 µg BNT162b1 group compared to the control group. This increase is likely secondary to inflammation and the low magnitude is not anticipated to cause clinical alterations in hemostasis.

Compared with buffer control, there were no test-article related difference in the concentration of serum cytokines evaluated.

At Days 10 or 17, lower urine volume (as low as 0.67x) and higher urine specific gravity (up to 1.02x) was observed in vaccine-administered groups, likely secondary to dehydration. This correlated with systemic evidence of dehydration in some groups (increases in blood urea nitrogen, creatine, and phosphorus).

Test-article related higher (1.1x to 1.6x) absolute spleen weights were evident in most vaccine administered groups and correlated with the macroscopic observation of increased spleen size. This is likely secondary to immune responses induced by the COVID-19 vaccine candidates.

The most common macroscopic observation in all treatment groups was a thickened injection site and/or induration at the injected muscle. This finding was test-item related and was caused by the local inflammation process. Enlarged spleen and iliac lymph nodes were noted in several animals in the COVID-19 vaccine-administered groups. The effects on the lymphoid organs are consistent with immune responses to the COVID-19 vaccine candidates.

Administration of the vaccine candidates elicited antibody immune responses was evaluated by S1 domain and RBD sub-domain specific ELISA, as well as SARS-CoV-2 S pVNT by Day 10 or 17. The data demonstrates that all COVID-19 vaccine candidates elicited a SARS-CoV-2 S protein specific antibody response directed against the S1 domain and the RBD sub-domain. Antibody responses detected via ELISA directly translated into neutralizing activity as seen in the VSV/SARS-CoV-2 S pVNT. COVID-19 vaccine candidates showing higher antigen-specific antibody titers also displayed more pronounced virus neutralization effect. Additional details on the serology data from Study 38166 are provided in [Section 2.4.2.1.11](#).

In conclusion, administration of COVID-19 vaccine candidates by IM injection to male and female Wistar Han rats once every week, for a total of 2 or 3 weekly cycles of dosing, were tolerated up to 100 µg RNA without evidence of systemic toxicity to any of the COVID-19 vaccine candidates evaluated. Immune responses were generated to all of the vaccine candidates.

2.4.4.4. Genotoxicity

No genotoxicity studies are planned for the COVID-19 vaccine candidates, as the components of all vaccine constructs are lipids and RNA that are not expected to have genotoxic potential ([WHO, 2005](#)).

2.4.4.5. Carcinogenicity

Carcinogenicity studies with the COVID-19 vaccine candidates have not been conducted as the components of all vaccine constructs are lipids and RNA that are not expected to have carcinogenic or tumorigenic potential. Carcinogenicity testing is generally not considered necessary to support the development and licensure of vaccine products for infectious diseases ([WHO, 2005](#); [WHO, 2014](#)).

2.4.4.6. Reproductive and Developmental Toxicity

Reproductive or developmental toxicity assessments have not been conducted with the COVID-19 vaccine candidates.

Macroscopic and microscopic evaluation of male and female reproductive tissues will be included in the final report of the pivotal repeat-dose toxicity study ([Study 38166](#)).

2.4.4.7. Local Tolerance

Local tolerance of IM administration of the COVID-19 vaccine candidates was evaluated by injection site observations, macroscopic, and microscopic examination of injection sites in the pivotal repeat-dose toxicity study and described above ([Section 2.4.4.3.1](#)).

2.4.4.8. Other Toxicity Studies

2.4.4.8.1. Phototoxicity

Phototoxicity studies with the COVID-19 vaccine candidates have not been conducted.

2.4.4.8.2. Antigenicity

Immunogenicity was evaluated as part of the primary pharmacology studies ([Section 2.4.2.1](#)). In general, all three RNA platforms and both antigens generated a robust immune response in non-GLP mouse studies. Interim, serology data from the pivotal repeat-dose toxicity study shows a robust immune response to the COVID-19 vaccine candidates.

2.4.4.8.3. Immunotoxicity

Stand-alone immunotoxicity studies with the COVID-19 vaccine candidates have not been conducted. However, immunotoxicological endpoints have been collected as part of the pivotal repeat-dose toxicity study.

2.4.4.8.4. Mechanistic Studies

Mechanistic studies with the COVID-19 vaccine candidates have not been conducted.

2.4.4.8.5. Dependence

Dependence studies with the COVID-19 vaccine candidates have not been conducted.

2.4.4.8.6. Studies on Metabolites

Stand-alone studies with administration of metabolites of the COVID-19 vaccine candidates have not been conducted.

2.4.4.8.7. Studies on Impurities

Stand-alone studies with administration of impurities of the COVID-19 vaccine candidates have not been conducted.

2.4.4.8.8. Other Studies

No other studies with the proposed COVID-19 vaccine candidates evaluated in this submission have been conducted.

However, all three RNA platforms have been tested previously using RNAs expressing different genes of interest for other disease targets in several nonclinical GLP safety studies in mice and NHP. These studies have been performed with naked RNAs or RNAs formulated with lipids similar, but not identical, to the lipid nanoparticles to be used in the proposed COVID-19 clinical trial. The nonclinical toxicity data suggest a favorable safety profile for uRNA, modRNA, and saRNA formulated with different lipid vehicles for various administration routes, including IV injection. These studies were conducted by BioNTech and are summarized in the included IB ([Section 4.3.1, Version 3.0, 17 April 2020](#)).

Review of studies conducted with the non-COVID vaccine uRNA in mice and cynomolgus monkeys showed the uRNA/LNP platform to be tolerated. The safety profile of the systemically administered RNA formulation in these studies was characterized by mild findings, which were mostly related to the mode of action and the formulated RNA-intrinsic stimulation of innate immune sensors (eg, transient cytokine increase, hematological changes, and effects on lymphoid organs). IV doses of up to 60 µg/animal of uRNA in mice (Study 28864) and 88.6 µg/animal in cynomolgus monkeys (Study 29928) were tested without any signs of unexpected overstimulation of the immune system.

The data from these studies will not be submitted as part of the IND package as the studies did not use the final clinical candidates and are for background information purposes only.

2.4.4.9. Target Organ Toxicity

Based on interim data from the dosing phase of the GLP repeat-dose toxicity study ([Section 2.4.4.3.1](#)), administration of COVID-19 vaccines were associated with local reactogenicity at the injection site and expected acute phase hematological responses. Microscopic findings from this study will be added upon availability.

090177e1934a5c5cf\Approved\Approved On: 21-Apr-2020 19:41 (GMT)

2.4.5. INTEGRATED OVERVIEW AND CONCLUSIONS

The nonclinical program demonstrates that the vaccine candidates are immunogenic in mice and rats, and the toxicity study supports the clinical administration of COVID-19 vaccines up to two (saRNA) or three (uRNA and modRNA) doses at up to 30 µg (uRNA and saRNA) or 100 µg (modRNA). Preclinical assessments in mice demonstrate that COVID-19 vaccine candidates elicit a rapid antibody response that is also functional. Because some mouse studies are still ongoing, additional data will be available prior to human dosing with each vaccine candidate. The data provide proof-of-concept that COVID-19 vaccine candidates can elicit an anti-SARS-CoV-2 immune response and support further investigation of the candidates in humans. Additional characterization of the immune response will be assessed in the ongoing non-human primate immunogenicity study.

The potential biodistribution of the COVID-19 vaccine candidates was assessed using luciferase expression as a surrogate reporter. Protein expression was demonstrated at the site of injection and to a lesser extent in the liver after BALB/c mice received an IM injection of RNA encoding luciferase in a LNP formulation like the COVID-19 vaccine candidates. Luciferase expression was identified at the injection site at 6 hours after injection and was gone by 9 days. Liver expression was also present at 6 hours after injection and was gone by 48 hours after injection consistent with other vaccine candidates that have already been evaluated clinically and shown to be safe.

Based on previous nonclinical and clinical experience with the three RNA platforms, a beneficial safety profile is anticipated, and may include transient local reactions (such as swelling/edema or redness) and body temperature increases. Preliminary data available from the ongoing GLP compliant repeat-dose toxicity study supports this expectation. At the end of the dosing phase, there was no mortality or adverse clinical observations. Transient increases in vaccine-related injection site reactions, inflammatory markers in the blood, and increased body temperature have been observed. These findings are an expected physiological response to an RNA vaccine and were not considered adverse. An immune response to the COVID-19 vaccine candidates was observed at the end of the dosing phase. Given the lack of adverse findings in the interim GLP repeat dose study results, the nonclinical toxicity program supports the clinical administration of COVID-19 vaccines up to 2 (saRNA) or 3 (uRNA and modRNA) doses at up to 30 µg (uRNA, saRNA) or 100 µg (modRNA) per dose.

After initiation of the GLP repeat-dose toxicity study, the decision was made to clinically evaluate BNT162a1 and BNT162b1 in Study C4591001 as planned, but to evaluate 2 alternate vaccine candidates in the place of BNT162b2 (RBP020.1) and BNT162c1 (RBS004.3).

One of the new vaccine candidates for C4591001, BNT162b2 (RBP020.2), encodes P2 S V9. BNT162b2 (RBP020.1), which was tested in the GLP toxicity study, encodes P2 S V8. The 2 antigens, P2 S V8 and P2 S V9, have the same amino acid sequence but different codon optimizations of the antigen's coding sequence. The new codon optimization is anticipated

to increase antigen expression. The new codon optimization is not anticipated to impact the innate response to the RNA.

The other new vaccine candidate for C4591001, BNT162c2 (RBS004.2), is an saRNA-based vaccine candidate that encodes P2 S V9. BNT162c1 (RBS004.3), which is being tested in the ongoing rat GLP repeat dose toxicity study, is an saRNA that encodes the RBD. Both the saRNA platform and P2 S antigen are being evaluated in the ongoing rat GLP repeat-dose toxicity study. These changes are considered to have no safety impact and do not presently require additional toxicity studies to support clinical administration.

Administration of these 2 new vaccine candidates in the clinic is supported by 1) platform safety in multiple GLP toxicity studies and clinical studies with uRNA, modRNA, and saRNA-based vaccines using different lipid vehicles ([Section 2.4.4.8.8](#) and [IB Version 3, 17 April 2020](#)), 2) the interim results of the GLP repeat-dose toxicity study with uRNA (BNT162a1/RBL063.3), modRNA (BNT162b1/RBP020.3 and BNT162b2/RBP020.1), and saRNA (BNT162c1/RBS004.3) candidates, and 3) the similarity of the BNT162b2 variants, with no anticipated changes in safety profile, and 4) in vivo pharmacology studies in rodents showing immunogenicity similar to other candidates and toleration.

Furthermore, the use of these 2 alternative candidates in clinical trials is supported by the 2018 WHO Ebola guidance ([WHO, 2018](#)), which allows for no nonclinical toxicity evaluation with clinical candidates providing adequate nonclinical toxicity testing of the platform, as well as the safety experience with the RNA-LNP platform and ongoing repeat-dose toxicity study with the vaccine antigens.

090177e1934a5cff\Approved\Approved On: 21-Apr-2020 19:41 (GMT)

2.4.6. LIST OF LITERATURE REFERENCES

Al-Amri SS, Abbas AT, Siddiq LA, et al. Immunogenicity of candidate MERS-CoV DNA vaccines based on the spike protein. *Sci Rep* 2017;7:44875.

de Wit E, N van Doremalen, D Falzarano, et al. SARS and MERS: Recent insights into emerging coronaviruses. *Nat Rev Microbiol* 2016;14:523-34.

Habibzadeh P, Stoneman EK. The novel coronavirus: a bird's eye view. *Int J Occup Environ Med* 2020;11(2):65-71.

Hulswit RJ, de Haan CA, Bosch B-J. Coronavirus spike protein and tropism changes. *Adv Virus Res* 2016;96:29-57.

Kirchdoerfer RN, Wang N, Pallesen J, et al. Stabilized coronavirus spikes are resistant to conformational changes induced by receptor recognition or proteolysis. *Sci Rep* 2018;8(1):15701.

Kozauer NA, Dunn WH, Unger EF, et al. CBER multi-discipline review of Onpattro. NDA 210922. 10 Aug 2018.

Kranz LM, Diken M, Haas H, et al. Systemic RNA delivery to dendritic cells exploits antiviral defence for cancer immunotherapy. *Nature* 2016;534:396-401.

Moyo N, Vogel AB, Buus S, et al. Efficient induction of T cells against conserved HIV-1 regions by mosaic vaccines delivered as self-amplifying mRNA. *Mol Ther Methods Clin Dev* 2019;12:32-46.

Pallesen J, Wang N, Corbett KS, et al. Immunogenicity and structures of a rationally designed prefusion MERS-CoV spike antigen. *Proc Natl Acad Sci USA* 2017;114(35):E7348-57.

Pardi N, Hogan MJ, Pelc RS, et al. Zika virus protection by a single low-dose nucleoside-modified mRNA vaccination. *Nature* 2017;543(7644):248-51.

Pardi N, Parkhouse K, Kirkpatrick E, et al. Nucleoside-modified mRNA immunization elicits influenza virus hemagglutinin stalk-specific antibodies. *Nat Comm* 2018;9(1):3361.

Pardi N, LaBranche CC, Ferrari G, et al. Characterization of HIV-1 nucleoside-modified mRNA vaccines in rabbits and rhesus macaques. *Mol Ther Nucleic Acids* 2019;15:36-47.

Rauch S, Jasny E, Schmidt KE, et al. New vaccine technologies to combat outbreak situations. *Front Immunol* 2018;9:1963.

Sahin U, Karikó K, Türeci Ö. mRNA-based therapeutics - developing a new class of drugs. *Nat Rev Drug Discov* 2014;13(10):759-80.

COVID-19 Vaccine (BNT162, PF-07302048)

BB-IND 19736

Module 2.4. Nonclinical Overview

Singh J, Chander J, Singh S, et al. γ -Glutamyl transpeptidase: a novel biochemical marker in inflammation. *Biochem Pharmacol* 1986;35(21):3753-60.

Study 28864. 6-Week repeated dose toxicity study of RBL001.1, RBL002.2, RBL003.1, and RBL004.1 by intravenous administration to C57BL/6 mice. 11 October 2013. Available upon request.

Study 29928. Pilot pharmacokinetic and pharmacodynamic study of RBL001.1, RBL002.2, RBL003.1 and RBL004.1 after intravenous administration to cynomolgus monkeys.

07 November 2013. Available upon request.

Vogel AB, Lambert L, Kinnear E, et al. Self-amplifying RNA vaccines give equivalent protection against influenza to mRNA vaccines but at much lower doses. *Mol Ther* 2018;26(2):446-55.

World Health Organization. WHO guidelines on nonclinical evaluation of vaccines. Annex 1. In: World Health Organization. WHO technical report series, no. 927. Geneva, Switzerland; World Health Organization; 2005:31-63.

World Health Organization. Annex 2. Guidelines on the nonclinical evaluation of vaccine adjuvants and adjuvanted vaccines. In: WHO technical report series no. 987. Geneva, Switzerland: World Health Organization; 2014: p. 59-100.

WHO Expert Committee on Biological Standardization. Annex 2. Guidelines on the quality, safety and efficacy of Ebola vaccines. In: WHO technical report series, no. 1011. Geneva, Switzerland: World Health Organization; 2018: p. 87-179. Available upon request.

Wrapp D, Wang N, Corbett KS, et al. Cryo-EM structure of the 2019-nCoV spike in the prefusion conformation. *Science* 2020;367(6483):1260-63.

Yong CY, Ong HK, Yeap SK, et al. Recent advances in the vaccine development against middle east respiratory syndrome-coronavirus. *Front Microbiol* 2019;10:1781.

Zakhartchouk AN, Sharon C, Satkunarajah M, et al. Immunogenicity of a receptor-binding domain of SARS coronavirus spike protein in mice: implications for a subunit vaccine. *Vaccine* 2007;25(1):136-43.

Zhou M, X Zhang, J Qu et al. Coronavirus disease 2019 (COVID-19): a clinical update. *Front Med* 2020; <https://doi.org/10.1007/s11684-020-0767-8>.

090177e1934a5c5cf\Approved\Approved On: 21-Apr-2020 19:41 (GMT)

(b) (4)

FINAL REPORT

Test Facility Study No. 185350
Sponsor Reference No. ALC-NC-0552

**A Tissue Distribution Study of a [³H]-Labelled Lipid Nanoparticle-mRNA
Formulation Containing ALC-0315 and ALC-0159 Following
Intramuscular Administration in Wistar Han Rats**

TEST FACILITY:

(b) (4)

SPONSOR:

Acuitas Therapeutics Inc.
6190 Agronomy Road, Suite 402
Vancouver, British Columbia
V6T 1Z3 Canada

TABLE OF CONTENTS

1 COMPLIANCE STATEMENT 6

2 QUALITY ASSURANCE STATEMENT 7

3 RESPONSIBLE PERSONNEL 8

4 SUMMARY 9

5 INTRODUCTION..... 11

5.1 Study Location..... 11

5.2 Study Dates 11

5.3 Archiving..... 12

6 EXPERIMENTAL PROCEDURE..... 12

6.1 Test Item 12

6.2 Other Materials 13

6.3 Animals and Husbandry..... 14

6.4 Specific Activity..... 14

6.5 Dose Formulation 14

6.6 Dose Administration and Determination..... 15

6.7 Collection of Biological Samples 15

6.8 Sample Storage 16

6.9 Preparation of Samples for Total Radioactivity Analysis..... 16

6.9.1 Dose Formulation 16

6.9.2 Blood and Plasma 16

6.9.3 Tissues 16

6.9.4 Urine, Faeces and Cage Wash..... 17

6.10 Quantification of Radioactivity..... 17

090177e195794698\Approved\Approved On: 09-Nov-2020 21:23 (GMT)

6.10.1 Liquid Scintillation Counting 17

6.10.2 Data Presentation 17

6.11 Protocol Deviations 18

7 RESULTS 19

7.1 Clinical Observations..... 19

7.2 Body Weights..... 19

7.3 Tissue Distribution Following Intramuscular Administration 19

8 CONCLUSIONS 22

9 TABLES..... 23

10 APPENDICES 28

090177e195794698\Approved\Approved On: 09-Nov-2020 21:23 (GMT)

LIST OF TABLES

Table 1 Mean (Sexes-Combined) Concentration and Recovery of Total Radioactivity in Whole Blood, Plasma and Tissues Following Single Intramuscular Administration of [³H]-08-A01-C01 to Wistar Han Rats 23

Table 2 Mean Concentration of Total Radioactivity in Whole Blood, Plasma and Tissues Following Single Intramuscular Administration of [³H]-08-A01-C01 to Wistar Han Rats 25

Table 3 Mean Recovery of Total Radioactivity in Tissues Following Single Intramuscular Administration of [³H]-08-A01-C01 to Wistar Han Rats 27

090177e195794698\Approved\Approved On: 09-Nov-2020 21:23 (GMT)

LIST OF APPENDICES

Appendix 1 Certificates of Analysis for [³H]-08-A01-C01 and [³H]-CHE 28
Appendix 2 Individual Animal Dosing Summary 30
Appendix 3 Urine and Faeces Sample Weights 33
Appendix 4 Individual Male Concentration Data 36
Appendix 5 Individual Female Concentration Data 43
Appendix 6 Individual Male Recovery Data 50
Appendix 7 Individual Female Recovery Data 57
Appendix 8 Individual Male 100 µg mRNA data 64

090177e195794698\Approved\Approved On: 09-Nov-2020 21:23 (GMT)

1 COMPLIANCE STATEMENT

Study Title: A Tissue Distribution Study of a [³H]-Labelled Lipid Nanoparticle-mRNA Formulation Containing ALC-0315 and ALC-0159 Following Intramuscular Administration in Wistar Han Rats

GLP regulations are not applicable to studies of this nature therefore no claim of GLP compliance is made. Nevertheless, as Study Director, I confirm that this study was conducted in a GLP compliant facility and that the practices and procedures adopted during its conduct were consistent with the OECD Principles of Good Laboratory Practice as incorporated into the United Kingdom Statutory Instrument for GLP.

The study was conducted according to the procedures herein described and this report represents a true and accurate record of the results obtained.

DocuSigned by: (b) (4)
 Signer Name: (b) (4)
Signing Reason: I approve this document
Signing Time: 05-Nov-2020 11:52:33 EST
CD262FA0424043DEB85DE525652AC3BD

(b) (4)
Study Director

090177e195794698\Approved\Approved On: 09-Nov-2020 21:23 (GMT)

2 QUALITY ASSURANCE STATEMENT

Study Title: A Tissue Distribution Study of a [³H]-Labelled Lipid Nanoparticle-mRNA Formulation Containing ALC-0315 and ALC-0159 Following Intramuscular Administration in Wistar Han Rats

This study has not been subjected to any study specific Quality Assurance procedures.

3 RESPONSIBLE PERSONNEL

Study Director: [REDACTED] (b) (4)

Sponsor Representative: [REDACTED] (b) (6)

Test Facility Management: [REDACTED] (b) (4)

090177e195794698\Approved\Approved On: 09-Nov-2020 21:23 (GMT)

4 SUMMARY

The test item, 08-A01-C01, is an aqueous dispersion of lipid nanoparticles (LNP), comprised of a proprietary mixture of lipid components (including ALC-0315, ALC-0159, distearoylphosphatidylcholine, and cholesterol) and mRNA. The mRNA encodes a model protein (luciferase) and is not pharmacologically active. The test item contains trace amounts of radiolabelled [Cholesteryl-1,2-³H(N)]-Cholesteryl Hexadecyl Ether (³H)-CHE), a non-exchangeable, non-metabolisable lipid marker used to monitor the disposition of the lipid nanoparticles (containing encapsulated mRNA). Once intracellular, the [³H]-CHE does not recirculate and therefore allows assessment of distribution of the particles.

The objectives of this study were to:

1. Characterise the disposition of 08-A01-C01 containing a radiolabelled lipid marker in male and female Wistar Han rats following a single intramuscular administration.
2. Determine the concentration and content of radioactivity in blood, plasma and tissues of rats (expressed as µg lipid eq/mL (or per g for tissue), and % administered (injected dose)/tissue, where appropriate).

Wistar Han rats (21 male and 21 female) each received a single intramuscular dose of [³H]-08-A01-C01 at a target mRNA total dose of 50 µg/animal (1.29 mg/animal total lipid dose). The content and concentration of total radioactivity in blood, plasma and tissues were determined at pre-defined time points following administration.

Whole blood and tissue samples were collected at 0.25, 1, 2, 4, 8, 24 and 48 hours post-dose (three animals/sex/timepoint) and plasma was subsequently separated from blood by centrifugation. The concentration of total radioactivity was measured by liquid scintillation counting (LSC).

Following intramuscular administration of [³H]-08-A01-C01 to male and female Wistar Han rats at a target dose level of 50 µg/animal (1.29 mg/animal total lipid dose), the greatest mean concentration was found remaining in the injection site at each time point in both sexes. Outside the injection site, low levels of radioactivity were detected in most tissues, with the greatest levels in plasma observed 1-4 hours post-dose. Over 48 hours, [³H]-08-A01-C01 distributed mainly to liver, adrenal glands, spleen and ovaries, with maximum concentrations observed at 8-48 hours post-dose. Total recovery (% of injected dose) of [³H]-08-A01-C01 outside the injection site was greatest in the liver (up to 21.5%) and was much less in spleen (≤1.1%), adrenal glands (≤0.1%) and ovaries (≤0.1%). The mean concentrations and tissue distribution pattern were broadly similar between the sexes.

Blood:plasma ratios were generally between 0.5-0.6, indicating that the majority of the total radioactivity is associated with the plasma fraction and that [³H]-08-A01-C01 does not undergo appreciable accumulation in red blood cells.

In conclusion, the distribution of [³H]-08-A01-C01 (monitoring the [³H]-CHE lipid label) in blood, plasma and selected tissues was determined in male and female Wistar Han rats over 48 hours after a single intramuscular injection at 50 µg mRNA/animal (1.29 mg/animal lipid dose). The concentrations of [³H]-08-A01-C01 were greatest in the injection site at all time points, with levels peaking in the plasma by 1-4 hours post-dose and distribution mainly into liver, adrenal glands, spleen and ovaries over 48 hours. Total recovery of radioactivity outside of the injection site was greatest in the liver, with much lower total recovery in spleen, and very little recovery in adrenals glands and ovaries. The mean plasma, blood and tissue concentrations and tissue distribution patterns were broadly similar between the sexes and [³H]-08-A01-C01 did not associate with red blood cells.

090177e195794698\Approved\Approved On: 09-Nov-2020 21:23 (GMT)

5 INTRODUCTION

The objectives of this study were to:

1. Characterise the disposition of 08-A01-C01 containing a radiolabelled lipid marker in male and female Wistar Han rats following a single intramuscular administration
2. Determine the concentration and content of radioactivity in blood, plasma and tissues of rats (expressed as µg lipid eq/g (or per mL for plasma) and % injected dose/tissue, where appropriate)

The Wistar Han rat was chosen as the animal model for this study as it is an accepted rodent species for preclinical toxicity testing by regulatory agencies and has been used in all regulatory toxicology studies by the Sponsor.

The study was designed to be appropriate for submission to regulatory authorities. However, it is recognised that no detailed test guidelines for the conduct of drug distribution and pharmacokinetic studies are currently available.

Initially, 21 male rats were dosed at 100 µg mRNA/animal. Some adverse clinical signs were observed after approximately 24 hours post-dose and a subsequent review of the data showed concentrations were well detected in tissues. After discussions with the Sponsor, the target dose level was lowered to 50 µg mRNA/animal by amendment for the remainder of the study. Reference is made to the 100 µg mRNA /animal group in some sections of the report, however, the results are not discussed.

5.1 Study Location

The study was carried out at (b) (4) according to (b) (4) Protocol No. 185350 and Amendments 1 and 2.

5.2 Study Dates

The study was conducted according to the following timetable:

Study Initiation:	16 July 2020
Experimental Start Date:	17 July 2020
Experimental Completion Date:	24 September 2020
Study Completion Date:	See compliance page for date of Study Director's signature.

090177e195794698\Approved\Approved On: 09-Nov-2020 21:23 (GMT)

5.3 Archiving

All raw data generated and recorded during this study will be stored in the Scientific Archive of (b) (4) for 2 years after issue of the final report. After the 2-year period the Sponsor will be consulted regarding the disposal, transfer, or continued storage of the raw data. Electronic data generated by the Test Facility were archived as noted above, except reporting files stored on Shared Document Management System (SDMS), which were archived at the (b) (4)

The original signed copy of the final report will be stored indefinitely in the Scientific Archive of (b) (4)

The residual [³H]-08-A01-C01 dose (approximately 5 MBq) will be retained and stored in a fridge set to maintain 4°C at (b) (4)

Biological samples generated during the course of this study were held deep frozen until issue of the final report. (b) (4) will contact the Sponsor to discuss the fate of the samples (disposal, return or retain at (b) (4)) on issue of the final report. Samples will be disposed of unless (b) (4) receives written instruction regarding shipment of the samples to the Sponsor or continued storage at (b) (4)

6 EXPERIMENTAL PROCEDURE

6.1 Test Item

Identification:	[³ H]-08-A01-C01
Supplier:	Acuitas Therapeutics Inc
Lot Number:	NC-0552-1
Expiration Date:	July 7, 2021
Physical Description:	White to off-white, homogenous, opalescent liquid; no foreign particles
Concentration (mRNA):	1.0 mg/mL
Radioactive Concentration	0.864 mCi/mL, 1,900,000 dpm/μL

090177e195794698\Approved\Approved On: 09-Nov-2020 21:23 (GMT)

Concentration (Total Lipid)	25.7 mg/mL
Molecular weight	Not applicable for LNP
Purity:	94%
Radiochemical Purity	>97%
Specific Activity (mRNA):	0.864 mCi/mg (32.0 MBq/mg)
Correction Factor	None
Storage Conditions:	Frozen (-60°C to -90°C)

The test item contains trace amounts of radiolabelled [Cholesteryl-1,2-³H(N)]-Cholesteryl Hexadecyl Ether (³H)-CHE), a non-exchangeable, non-metabolisable lipid marker used to monitor the disposition of the lipid nanoparticles (containing encapsulated mRNA). Per the manufacturer's information, the radiochemical purity of [³H]-CHE was found to be >97% and the rate of decomposition is initially 2% for 6 months from the date of purification (16 December 2019). No radiochemical purity assessments were made as part of this study.

The Certificates of Analysis for [³H]-08-A01-C01 and [³H]-CHE are presented in [Appendix 1](#).

6.2 Other Materials

AquaSafe 500 Plus liquid scintillation fluid was obtained from Zinsser Inc.

Monophase® was used in conjunction with the Perkin Elmer Model 307 Automatic Sample Oxidiser and was supplied by Perkin Elmer Life Science and Analytical Instruments Inc, UK.

Spec-Chec™-³H used to estimate efficiencies of combustion was also obtained from Perkin Elmer Life Science and Analytical Instruments Inc, UK.

All other materials and chemicals used were of analytical grade where available and supplied by standard commercial suppliers.

6.3 Animals and Husbandry

Forty-two male and 21 female Wistar Han rats (8-11 weeks and body weight 179-270 g at the time of dosing) were used in the study and were supplied by (b) (4). The animals were acclimatised to the experimental unit for at least 5 days prior to use on the study. During the acclimatisation periods, the animals were closely observed by the animal technicians to ensure that they were in good health and suitable for inclusion in the study. During the study period the animals were closely observed twice daily by the animal technicians to ensure that they were in good health.

During the study period, the rats were housed in groups in polycarbonate and stainless steel cages with wire mesh floors. Animals used for excretion collection were housed singly in all-glass metabolism cages for the separate collection of urine and faeces.

A standard laboratory diet of known formulation (SDS Rat and Rat Maintenance Diet No.1, Special Diet Services, 1 Stepfield, Witham, Essex) and domestic mains tap water were available *ad libitum*.

Holding and study areas had automatic control of light cycles and temperature. Automatic 12 hours light and 12 hours dark. Ranges of temperature and humidity measured during the study were 21-23°C and 44-67%, respectively, with the exception of 31 July 2020 where the room temperature reached a maximum of 25°C.

6.4 Specific Activity

The specific activity value of 1.24 MBq/mg lipid (as calculated from the 0.864 mCi/mg mRNA specific activity value supplied and converted to per mg lipid) was used to calculate the amount of [³H]-08-A01-C01 dispensed in the dose formulation.

6.5 Dose Formulation

[³H]-08-A01-C01 was provided in PBS/sucrose buffer at the required dose concentration (1 mg mRNA/mL). No dilutions were therefore required. Four dose formulation vials were provided (3 x 1.5 mL and 1 x 1.2 mL).

The appropriate number of vials for each dosing occasion were defrosted for at least 30 minutes prior to dosing. Prior to use, each vial was inverted 3 times to mix. Once dosing was complete, each vial was stored in a fridge within 4 hours of removal from the -80°C freezer.

The radioactive concentration of the supplied dose formulation was determined by the removal of triplicate aliquots (50 µL) prior to and after the first dosing occasion. Appropriate

dilutions of each aliquot were prepared in distilled water and duplicate aliquots of each dilution were analysed by liquid scintillation counting (LSC).

The radioactive concentration determined by LSC was within 10% of the target value provided in the supplied Certificate of Analysis and was used in the dose determination calculations.

6.6 Dose Administration and Determination

Each animal received a single (one site) intramuscular administration of [³H]-08-A01-C01 at either 50 or 100 µL volume for the 50 and 100 µg mRNA/animal dose groups, respectively (target doses of 1.29 or 2.57 mg total lipid/animal, respectively).

The actual dose received by each animal was determined with reference to the dose concentration, the volume of dose administered and the specific activity of [³H]-08-A01-C01 in the formulated dose. Any undosed residue was also taken in to account. The actual dose received by each animal is documented in [Appendix 2](#).

6.7 Collection of Biological Samples

Three male and three female rats were sacrificed at the following times:

0.25, 1, 2, 4, 8, 24 and 48 hours post dose

From each animal, a terminal blood sample (*ca.* 5-10 mL) was collected by cardiac puncture into heparinised tubes. A portion (*ca.* 0.5 mL) was retained and plasma separated from the remainder of each sample by centrifugation (3000 rpm for 10 minutes in a centrifuge set to maintain a temperature of 4°C). Blood cells were discarded.

The following tissues were collected (where relevant for sex):

Adipose tissue	Ovaries
Adrenal glands	Pancreas
Bladder	Pituitary gland
Bone (femur)	Prostate
Bone marrow (femur)	Salivary glands
Brain	Skin
Eyes	Muscle
Heart	Small intestine
Injection site	Spinal cord
Kidneys	Spleen
Large intestine	Stomach
Liver	Testes
Lung	Thymus
Lymph node (mandibular)	Thyroid

Lymph node (mesenteric)

Uterus

Additionally, for animals 043M, 045M, 046M, 048M, 051M, 052M, 055M and 058M, the tibia/fibula bone was also collected but not analysed (refer to Section 6.11).

6.8 Sample Storage

Samples not analysed immediately were stored frozen in a freezer set to maintain a temperature of -20°C until taken for analysis, with the exception of urine and faeces samples which were stored at -80°C. After analysis, samples were returned to storage in a freezer set to maintain a temperature of -20°C.

Samples of cage wash, dose determinations and dose residues were stored at room temperature prior to and following analysis. These samples were discarded at the Study Director's discretion following acceptance of the study results.

6.9 Preparation of Samples for Total Radioactivity Analysis

Volumes or weights of all samples were measured where appropriate

6.9.1 Dose Formulation

Duplicate aliquots (0.1 mL) of each dilution of the dose formulation were diluted with water and dissolved in scintillation fluid (Aquasafe 500 Plus, Zinsser Inc.) and analysed directly by liquid scintillation counting.

6.9.2 Blood and Plasma

Duplicate weighed aliquots of whole blood (2 x *ca.* 0.15 g) were taken and then combusted using a Perkin Elmer Model 307 Sample Oxidiser. The resultant $^3\text{H}_2\text{O}$ generated was collected by absorption in Monophase® (15 mL).

Duplicate aliquots (100 µL) of plasma were allowed to air dry, diluted with water and dissolved in scintillation fluid (Aquasafe 500 Plus, Zinsser Inc.) and analysed directly by LSC.

6.9.3 Tissues

Tissue samples were finely chopped with scissors and duplicate, where appropriate, portions were combusted using a Perkin Elmer Model 307 Sample Oxidiser. Smaller tissues were aliquoted directly. The resultant $^3\text{H}_2\text{O}$ generated was collected by absorption in Monophase® S (15 mL).

Combustion of standards showed that recovery efficiencies were in excess of 95% throughout.

6.9.4 Urine, Faeces and Cage Wash

Urine, faeces and cage wash samples were collected but not analysed for total radioactivity. Urine and faeces sample weights were taken prior to storage. Urine and faeces samples were retained at -80°C for possible analysis of specific lipids by LC-MS/MS conducted and reported separately. The sample weights are presented in [Appendix 3](#).

6.10 Quantification of Radioactivity

6.10.1 Liquid Scintillation Counting

All samples prepared in scintillation fluid were subjected to liquid scintillation counting for 5 min, together with representative blank samples, using a Liquid Scintillation Analyser with automatic quench correction by an external standard method. Prior to analysis, samples were allowed to stabilise with regard to light and temperature. Self-normalisation and calibration (SNC) were conducted once a day. An unquenched tritium standard was used to initially calibrate the system to obtain optimal performance by adjusting the voltage on the photomultiplier tubes. Representative blank sample values were subtracted from sample count rates to give net disintegrations per minute (dpm) per sample. A limit of reliable measurement of 30 counts per minute (cpm) above background was instituted in these laboratories. Any results arising from data below the limit of reliable measurement were noted in the Results section of the report. Sample repeat analysis were in accordance with Standard Operating Procedures.

6.10.2 Data Presentation

Levels of radioactivity in all samples were quantified by LSC and the data captured into DEBRA® management software, Version 5.7 (LabLogic Ltd, UK). Plasma, blood and tissues concentrations of radioactivity in dpm/g and mass eq/g were calculated based on the measured specific activity (1.24 MBq/mg lipid) of radiolabelled test item in the dose formulation.

Individual and mean data were tabulated. The following information was reported:

- Radioactive content in tissues where a total organ weight is applicable was calculated as % administered (injected) dose
- Radioactive content in tissues, whole blood and plasma as µg equiv/g (or mL).
- Blood/plasma ratio

Data presented in results tables are computer generated in DEBRA and rounded appropriately for inclusion in the report. As a consequence, calculation of individual and mean values from data presented will, in some instances, yield slight differences from the results presented.

6.11 Protocol Deviations

Due to the unavailability of rats within specification at (b) (4) the rat supplier used in this study was Envigo, UK, deviating from Section 11 of the Protocol. In the opinion of the Study Director this had no impact on the study outcome since the correct age and strain of rats were used on this study.

In error, tibia/fibula bone were collected at necropsy for animals 043M, 045M, 046M, 048M, 051M, 052M, 055M, and 058M instead of femur bone, deviating from Section 14.1 of the Protocol. Once noticed, the femur bone was retrieved from the residual carcass stored in the -20°C freezer pending disposal and analysed after discussions with the Sponsor. The results appeared similar to the other animals in each timepoint and therefore this had no impact on the study outcome.

7 RESULTS

7.1 Clinical Observations

In the 100 µg mRNA male group, approximately 24 h following administration, animal 021M was noted to have decreased activity, ungroomed, brown staining on muzzle and irregular respiration. A decrease in bodyweight was noted in all remaining animals (approximately 16 g, equivalent to *ca.* 7% reduction of bodyweight) and food hoppers appeared untouched. By approximately 30 hours post-dose, animal 021M was also piloerect, hunched, and was hypersensitive to noise stimulus. Animal 021M was humanely killed and the diagnostic necropsy carried out showed one finding in the liver (prominent lobular architecture). Additionally, animals 019M and 020M were hunched and piloerect from approximately 30 h post-dose onwards.

In the 50 µg mRNA male group, following administration and for the duration of the study, no adverse effects were noted in any animal.

In the 50 µg mRNA female group, approximately 30 h following administration, animal 042F was noted to have decreased activity, and irregular respiration. At 48 h post dose animal 042F was additionally hunched and piloerect.

7.2 Body Weights

At the time of dosing, body weights were in the range of 217-270 g (males) and 179-224 g (females).

7.3 Tissue Distribution Following Intramuscular Administration

The mean (sex combined) concentration and recovery of total radioactivity in whole blood, plasma, injection site and tissues following a single intramuscular administration of [³H]-08-A01-C01 to Wistar Han rats at a target dose level of 50 µg mRNA/animal (1.29 mg/animal lipid) is presented in [Table 1](#). The mean concentration of total radioactivity in whole blood, plasma, injection site and tissues following a single intramuscular administration of [³H]-08-A01-C01 to male and female Wistar Han rats at a target dose level of 50 µg mRNA/animal (1.29 mg/animal lipid) is presented in [Table 2](#). The mean recovery in male and female individual tissues is presented in [Table 3](#).

Individual male and female concentration data is presented in [Appendix 4](#) and [Appendix 5](#), respectively. Individual male and female recovery data is presented in [Appendix 6](#) and [Appendix 7](#), respectively. The male 100 µg data is presented in [Appendix 8](#).

When analysing the injection site, there was often high inter-animal variability in concentration and % injected dose values at each time point. This may have been due to

difficulty in collecting the entirety of this sample since the total area that the injected bolus dose migrated to within the muscle was not visible. When dosing the male 50 µg mRNA group, the injection site was circled using a marker pen to help aid dissection of the injection area. The overall injection site concentrations and % dose values were higher in males than in females. Since concentrations in other tissues were broadly similar between the sexes, it is likely that the higher injection site values in males were a result of its more consistent identification and collection in males.

Following a single intramuscular administration of [³H]-08-A01-C01, the greatest mean tissue concentration and, in most instances, % of injected dose was found remaining in the injection site at each time point in both sexes. The injection site mean concentration and equivalent % dose values are presented in the table below.

Timepoint (h)	Injection site (µg equiv lipid/g)		Injection site (% dose)	
	Male	Female	Male	Female
0.25	219.940	36.566	32.887	6.815
1	587.670	199.950	68.829	36.411
2	529.210	93.144	39.053	24.094
4	619.850	56.227	47.710	9.056
8	299.590	125.930	18.731	24.993
24	267.170	122.540	31.957	26.295
48	268.770	61.088	32.823	16.426

The highest mean recovery of total radioactivity observed was 68.8% of the administered dose at 1-hour post-dose in males.

Low levels of radioactivity were detected in most tissues from the first time point (0.25 h), with the greatest level found circulating in plasma between 1-4 hours post-dose. The plasma and blood mean concentrations and blood:plasma ratios are presented in the table below.

Timepoint (h)	Blood (µg equiv lipid/g)		Plasma (µg equiv lipid/mL)		Blood:plasma ratio	
	Male	Female	Male	Female	Male	Female
0.25	3.003	0.936	6.035	1.894	0.48	1.15
1	2.809	5.928	5.379	10.884	0.49	0.54
2	4.028	6.773	8.714	9.091	0.46	0.64
4	3.400	2.698	8.755	4.251	0.42	0.60
8	2.000	0.628	3.573	1.147	0.56	0.55
24	1.274	0.544	2.621	0.945	0.49	0.57
48	0.535	0.305	1.085	0.524	0.50	0.58

Mean plasma concentrations peaked by 4 hours post-dose in males (8.755 µg equiv lipid/mL) and by 1 hour post-dose in females (10.884 µg equiv lipid/mL), before steadily decreasing. Concentrations were higher in plasma than in blood, with mean blood:plasma ratios generally

ca. 0.5-0.6, indicating that the majority of the total radioactivity is associated with the plasma fraction.

Over 48 hours, [³H]-08-A01-C01 distributed from the injection site to most tissues, with the majority of tissues exhibiting low levels of radioactivity. The highest mean concentrations observed, and the equivalent % dose, are presented in the tables below.

Timepoint (h)	Values expressed as µg equiv lipid/g)						
	Liver		Spleen		Adrenal glands		Ovaries
	Male	Female	Male	Female	Male	Female	Female
0.25	1.151	0.323	0.354	0.313	0.302	0.240	0.104
1	4.006	5.244	2.140	2.801	0.580	2.388	1.339
2	9.574	12.370	5.255	10.213	1.206	4.232	1.638
4	18.525	14.569	8.945	11.646	2.569	3.206	2.341
8	27.916	25.172	24.434	19.747	6.387	7.218	3.088
24	23.360	15.119	22.819	17.341	19.948	7.595	5.240
48	18.164	30.411	19.550	27.155	21.476	14.942	12.261

=Mean includes results calculated from data less than 30 cpm above background

Timepoint (h)	Liver		Spleen		Adrenal glands		Ovaries
	Male	Female	Male	Female	Male	Female	Female
0.25	0.995	0.209	0.014	0.011	0.001	0.001	0.001
1	2.834	2.907	0.087	0.098	0.002	0.012	0.009
2	7.629	7.030	0.232	0.418	0.005	0.015	0.008
4	15.027	8.699	0.351	0.419	0.012	0.018	0.016
8	21.519	14.580	1.118	0.845	0.026	0.043	0.025
24	19.901	10.977	0.957	0.685	0.083	0.049	0.037
48	13.953	18.357	0.914	1.146	0.104	0.108	0.095

=Mean includes results calculated from data less than 30 cpm above background

Maximum concentrations (C_{max}) in liver and spleen were observed at 8 hours post-dose in males and 48 hours post dose in females, but were broadly similar and appeared to plateau at 8 hours post-dose when considering variability. The greatest mean concentration outside the injection site was observed in the liver, with values of 27.916 µg equiv lipid/g (equivalent to 21.5 % dose) in males and 30.411 µg equiv lipid/g (equivalent to 18.4 % dose) in females. In the spleen the highest concentrations were 24.434 µg equiv lipid/g in males and 27.155 µg equiv lipid/g (equivalent to 1.1% dose in both sexes).

In the adrenal glands and ovaries, the highest mean concentrations were observed at 48 hours post-dose. The highest mean concentrations in the adrenal glands were 21.476 and 14.942 µg equiv lipid/g in males and females, respectively (equivalent to 0.1% dose in both sexes). The highest mean ovaries concentration was 12.261 µg equiv lipid/g (equivalent to 0.1 % dose).

090177e195794698\Approved\Approved On: 09-Nov-2020 21:23 (GMT)

8 CONCLUSIONS

In conclusion, the distribution of [³H]-08-A01-C01 (monitoring the [³H]-CHE lipid label) in blood, plasma and selected tissues was determined in male and female Wistar Han rats over 48 hours after a single intramuscular injection at 50 µg mRNA/animal (1.29 mg/animal lipid dose). The concentrations of [³H]-08-A01-C01 were greatest in the injection site at all time points, with levels peaking in the plasma by 1-4 hours post-dose and distribution mainly into liver, adrenal glands, spleen and ovaries over 48 hours. Total recovery of radioactivity outside of the injection site was greatest in the liver, with much lower total recovery in spleen, and very little recovery in adrenals glands and ovaries. The mean plasma, blood and tissue concentrations and tissue distribution patterns were broadly similar between the sexes and [³H]-08-A01-C01 did not associate with red blood cells.

9 TABLES

Table 1 Mean (Sexes-Combined) Concentration and Recovery of Total Radioactivity in Whole Blood, Plasma and Tissues Following Single Intramuscular Administration of [³H]-08-A01-C01 to Wistar Han Rats

Target Dose Level: 50 µg mRNA/Animal; 1.29 mg Total Lipid/Animal

Results expressed as total lipid concentration (µg lipid equiv/g (mL)) and % of administered dose

Sample	Total Lipid Concentration (µg lipid equiv/g (or mL))							% of Administered Dose						
	0.25 min	1 h	2 h	4 h	8 h	24 h	48 h	0.25 min	1 h	2 h	4 h	8 h	24 h	48 h
Adipose tissue	0.057	0.100	0.126	0.128	0.093	0.084	0.181	-	-	-	-	-	-	-
Adrenal glands	0.271	1.484	2.719	2.888	6.803	13.772	18.209	0.001	0.007	0.010	0.015	0.035	0.066	0.106
Bladder	0.041	0.130	0.146	0.167	0.148	0.247	0.365	0.000	0.001	0.001	0.001	0.001	0.002	0.002
Bone (femur)	0.091	0.195	0.266	0.276	0.340	0.342	0.687	-	-	-	-	-	-	-
Bone marrow (femur)	0.479	0.960	1.237	1.236	1.836	2.492	3.771	-	-	-	-	-	-	-
Brain	0.045	0.100	0.138	0.115	0.073	0.069	0.068	0.007	0.013	0.020	0.016	0.011	0.010	0.009
Eyes	0.010	0.035	0.052	0.067	0.059	0.091	0.112	0.000	0.001	0.001	0.002	0.002	0.002	0.003
Heart	0.282	1.029	1.402	0.987	0.790	0.451	0.546	0.018	0.056	0.084	0.060	0.042	0.027	0.030
Injection site	128.253	393.810	311.177	338.039	212.760	194.855	164.929	19.851	52.620	31.574	28.383	21.862	29.126	24.625
Kidneys	0.391	1.161	2.046	0.924	0.590	0.426	0.425	0.050	0.124	0.211	0.109	0.075	0.054	0.057
Large intestine	0.013	0.048	0.093	0.287	0.649	1.104	1.338	0.008	0.025	0.065	0.192	0.405	0.692	0.762
Liver	0.737	4.625	10.972	16.547	26.544	19.240	24.288	0.602	2.871	7.330	11.863	18.050	15.439	16.155
Lung	0.492	1.210	1.834	1.497	1.151	1.039	1.093	0.052	0.101	0.178	0.169	0.122	0.101	0.101
Lymph node (man)	0.064	0.189	0.290	0.408	0.534	0.554	0.727	-	-	-	-	-	-	-
Lymph node (mes)	0.050	0.146	0.530	0.489	0.689	0.985	1.366	-	-	-	-	-	-	-
Muscle	0.021	0.061	0.084	0.103	0.096	0.095	0.192	-	-	-	-	-	-	-
Ovaries (females)	0.104	1.339	1.638	2.341	3.088	5.240	12.261	0.001	0.009	0.008	0.016	0.025	0.037	0.095
Pancreas	0.081	0.207	0.414	0.380	0.294	0.358	0.599	0.003	0.007	0.014	0.015	0.015	0.011	0.019
Pituitary gland	0.339	0.645	0.868	0.854	0.405	0.478	0.694	0.000	0.001	0.001	0.001	0.000	0.000	0.001
Prostate (males)	0.061	0.091	0.128	0.157	0.150	0.183	0.170	0.001	0.001	0.002	0.003	0.003	0.004	0.003
Salivary glands	0.084	0.193	0.255	0.220	0.135	0.170	0.264	0.003	0.007	0.008	0.008	0.005	0.006	0.009
Skin	0.013	0.208	0.159	0.145	0.119	0.157	0.253	-	-	-	-	-	-	-

- =Partial tissue taken therefore not applicable

090177e195794698\Approved\Approved On: 09-Nov-2020 21:23 (GMT)

Table 1 Mean (Sexes-Combined) Concentration of Total Radioactivity in Whole Blood, Plasma and
 (Continued) Tissues Following Single Intramuscular Administration of [³H]-08-A01-C01 to Wistar Han Rats

Target Dose Level: 50 µg mRNA/Animal; 1.29 mg Total Lipid/Animal

Results expressed as total lipid concentration (µg lipid equiv/g (mL)) and % of administered dose

Sample	Total Lipid Concentration (µg lipid equiv/g (or mL))							% of Administered Dose						
	0.25 min	1 h	2 h	4 h	8 h	24 h	48 h	0.25 min	1 h	2 h	4 h	8 h	24 h	48 h
Small intestine	0.030	0.221	0.476	0.879	1.279	1.302	1.472	0.024	0.130	0.319	0.543	0.776	0.906	0.835
Spinal cord	0.043	0.097	0.169	0.250	0.106	0.085	0.112	0.001	0.002	0.002	0.003	0.001	0.001	0.001
Spleen	0.334	2.471	7.734	10.296	22.091	20.080	23.353	0.013	0.093	0.325	0.385	0.982	0.821	1.030
Stomach	0.017	0.065	0.115	0.144	0.268	0.152	0.215	0.006	0.019	0.034	0.030	0.040	0.037	0.039
Testes (males)	0.031	0.042	0.079	0.129	0.146	0.304	0.320	0.007	0.010	0.017	0.030	0.034	0.074	0.074
Thymus	0.088	0.243	0.340	0.335	0.196	0.207	0.331	0.004	0.007	0.010	0.012	0.008	0.007	0.008
Thyroid	0.155	0.536	0.842	0.851	0.544	0.578	1.000	0.000	0.001	0.001	0.001	0.001	0.001	0.001
Uterus (females)	0.043	0.203	0.305	0.140	0.287	0.289	0.456	0.002	0.011	0.015	0.008	0.016	0.018	0.022
Whole blood	1.970	4.369	5.401	3.049	1.314	0.909	0.420	-	-	-	-	-	-	-
Plasma	3.965	8.132	8.903	6.503	2.360	1.783	0.805	-	-	-	-	-	-	-
Blood:plasma ratio	0.815	0.515	0.550	0.510	0.555	0.530	0.540	-	-	-	-	-	-	-

- =Partial tissue taken therefore not applicable/not applicable

090177e195794698\Approved\Approved On: 09-Nov-2020 21:23 (GMT)

Table 2 Mean Concentration of Total Radioactivity in Whole Blood, Plasma and Tissues Following Single Intramuscular Administration of [³H]-08-A01-C01 to Wistar Han Rats

Target Dose Level: 50 µg mRNA/Animal; 1.29 mg Total Lipid/Animal

Results expressed as µg lipid equiv/g (mL)

Sample	0.25 min		1 h		2 h		4 h		8 h		24 h		48 h	
	Male	Female	Male	Female	Male	Female	Male	Female	Male	Female	Male	Female	Male	Female
Adipose tissue	0.040	°0.073	0.050	0.149	0.070	0.182	0.093	0.163	0.116	0.069	0.126	0.042	0.129	0.232
Adrenal glands	0.302	°0.240	0.580	2.388	1.206	4.232	2.569	3.206	6.387	7.218	19.948	7.595	21.476	14.942
Bladder	0.049	°0.033	0.095	0.165	0.137	0.155	0.227	0.106	0.211	0.085	0.323	0.171	0.340	0.389
Bone (femur)	0.126	0.056	0.148	0.241	0.235	0.296	0.335	0.217	0.502	0.177	0.504	0.180	0.520	0.854
Bone marrow (femur)	0.761	°0.196	0.910	1.010	1.136	1.337	1.557	0.915	2.397	1.274	3.579	1.405	3.690	3.851
Brain	0.073	°0.016	0.083	0.117	0.143	0.133	0.155	0.075	0.101	0.045	0.090	0.047	0.083	0.052
Eyes	0.014	°0.006	0.027	0.043	0.046	0.058	0.095	0.038	0.088	0.030	0.129	0.052	0.127	0.097
Heart	0.419	°0.144	0.631	1.426	1.122	1.682	1.049	0.925	1.189	0.391	0.583	0.318	0.672	0.420
Injection site	219.940	36.566	587.670	199.950	529.210	93.144	619.850	56.227	299.590	125.930	267.170	122.540	268.770	61.088
Kidneys	0.511	0.271	0.630	1.692	1.124	2.967	1.033	0.814	0.837	0.342	0.504	0.348	0.482	0.368
Large intestine	0.017	°0.008	0.031	0.065	0.080	0.106	0.350	0.224	0.690	0.608	1.741	0.466	1.426	1.249
Liver	1.151	0.323	4.006	5.244	9.574	12.370	18.525	14.569	27.916	25.172	23.360	15.119	18.164	30.411
Lung	0.737	0.247	0.845	1.574	1.594	2.074	1.772	1.222	1.674	0.628	1.316	0.762	1.288	0.898
Lymph node (man)	0.090	°0.038	0.154	0.223	0.217	0.362	0.424	0.391	0.695	0.372	0.744	0.363	0.820	0.633
Lymph node (mes)	0.052	°0.048	0.095	0.196	0.229	0.831	0.441	0.536	0.649	0.729	1.106	0.863	1.057	1.675
Muscle	°0.029	0.012	0.039	0.082	0.067	0.100	0.075	0.130	0.101	0.091	0.098	0.092	0.280	0.104
Ovaries (females)	-	°0.104	-	1.339	-	1.638	-	2.341	-	3.088	-	5.240	-	12.261
Pancreas	0.125	0.037	0.153	0.261	0.423	0.404	0.361	0.398	0.349	0.239	0.396	0.320	0.587	0.611
Pituitary gland	0.537	°0.141	0.446	0.844	0.781	0.955	1.249	0.458	0.669	0.141	0.656	0.300	0.543	0.845
Prostate (males)	0.061	-	0.091	-	0.128	-	0.157	-	0.150	-	0.183	-	0.170	-
Salivary glands	0.114	°0.054	0.148	0.237	0.214	0.295	0.270	0.169	0.176	0.094	0.243	0.096	0.297	0.231
Skin	°0.016	0.010	0.028	0.387	0.054	0.263	0.085	0.204	0.122	0.116	0.195	0.118	0.209	0.297

°=Mean includes results calculated from data less than 30 cpm above background

090177e195794698\Approved\Approved On: 09-Nov-2020 21:23 (GMT)

Table 2 Mean Concentration of Total Radioactivity in Whole Blood, Plasma and Tissues Following Single (Continued) Intramuscular Administration of [³H]-08-A01-C01 to Wistar Han Rats

Target Dose Level: 50 µg mRNA/Animal; 1.29 mg Total Lipid/Animal

Results expressed as µg lipid equiv/g (mL)

Sample	0.25 min		1 h		2 h		4 h		8 h		24 h		48 h	
	Male	Female	Male	Female	Male	Female	Male	Female	Male	Female	Male	Female	Male	Female
Small intestine	0.038	°0.021	0.194	0.247	0.471	0.481	0.919	0.838	1.525	1.033	1.878	0.726	1.630	1.314
Spinal cord	0.061	°0.024	0.072	0.122	0.166	0.172	0.375	0.124	0.168	0.044	0.121	0.048	0.162	0.062
Spleen	0.354	°0.313	2.140	2.801	5.255	10.213	8.945	11.646	24.434	19.747	22.819	17.341	19.550	27.155
Stomach	0.018	°0.015	0.039	0.091	0.104	0.126	0.186	0.101	0.410	0.126	0.222	0.081	0.235	0.195
Testes (males)	0.031	-	0.042	-	0.079	-	0.129	-	0.146	-	0.304	-	0.320	-
Thymus	0.106	°0.069	0.187	0.298	0.220	0.459	0.461	0.209	0.292	0.100	0.255	0.159	0.296	0.366
Thyroid	0.217	°0.093	0.391	0.680	0.575	1.109	1.097	0.604	0.781	0.307	0.820	0.335	1.344	0.655
Uterus (females)	-	°0.043	-	0.203	-	0.305	-	0.140	-	0.287	-	0.289	-	0.456
Whole Blood	3.003	0.936	2.809	5.928	4.028	6.773	3.400	2.698	2.000	0.628	1.274	0.544	0.535	0.305
Plasma	6.035	1.894	5.379	10.884	8.714	9.091	8.755	4.251	3.573	1.147	2.621	0.945	1.085	0.524
Blood:plasma ratio	0.48	1.15	0.49	0.54	0.46	0.64	0.42	0.60	0.56	0.55	0.49	0.57	0.50	0.58

°=Mean includes results calculated from data less than 30 cpm above background

090177e195794698\Approved\Approved On: 09-Nov-2020 21:23 (GMT)

Table 3 Mean Recovery of Total Radioactivity in Tissues Following Single Intramuscular Administration of [³H]-08-A01-C01 to Wistar Han Rats

Target Dose Level: 50 µg mRNA/Animal; 1.29 mg Total Lipid/Animal

Results expressed as % administered dose

Sample	0.25 min		1 h		2 h		4 h		8 h		24 h		48 h	
	Male	Female	Male	Female	Male	Female	Male	Female	Male	Female	Male	Female	Male	Female
Adrenal glands	0.001	°0.001	0.002	0.012	0.005	0.015	0.012	0.018	0.026	0.043	0.083	0.049	0.104	0.108
Bladder	0.000	°0.000	0.001	0.001	0.001	0.001	0.001	0.001	0.002	0.000	0.002	0.001	0.002	0.002
Brain	0.011	°0.002	0.010	0.016	0.021	0.019	0.021	0.011	0.014	0.007	0.012	0.007	0.011	0.007
Eyes	0.000	°0.000	0.000	0.001	0.001	0.001	0.002	0.001	0.002	0.001	0.002	0.001	0.003	0.002
Heart	0.028	°0.008	0.032	0.079	0.065	0.102	0.067	0.052	0.061	0.022	0.035	0.018	0.039	0.020
Injection site	32.887	6.815	68.829	36.411	39.053	24.094	47.710	9.056	18.731	24.993	31.957	26.295	32.823	16.426
Kidneys	0.069	0.030	0.077	0.171	0.149	0.272	0.136	0.082	0.109	0.040	0.068	0.039	0.071	0.042
Large intestine	0.011	°0.004	0.018	0.032	0.054	0.075	0.236	0.148	0.463	0.346	1.091	0.293	0.810	0.714
Liver	0.995	0.209	2.834	2.907	7.629	7.030	15.027	8.699	21.519	14.580	19.901	10.977	13.953	18.357
Lung	0.082	0.022	0.085	0.117	0.189	0.167	0.226	0.112	0.180	0.064	0.136	0.065	0.131	0.070
Ovaries (females)	-	°0.001	-	0.009	-	0.008	-	0.016	-	0.025	-	0.037	-	0.095
Pancreas	0.005	0.001	0.006	0.008	0.015	0.012	0.013	0.017	0.014	0.016	0.013	0.009	0.015	0.023
Pituitary gland	0.000	°0.000	0.000	0.001	0.000	0.001	0.001	0.000	0.000	0.000	0.000	0.000	0.000	0.001
Prostate (males)	0.001	-	0.001	-	0.002	-	0.003	-	0.003	-	0.004	-	0.003	-
Salivary glands	0.004	°0.002	0.005	0.008	0.007	0.009	0.009	0.006	0.007	0.003	0.008	0.003	0.010	0.007
Small intestine	0.032	°0.015	0.124	0.135	0.353	0.285	0.623	0.462	0.972	0.580	1.275	0.536	0.971	0.698
Spinal cord	0.001	°0.000	0.001	0.002	0.001	0.002	0.003	0.002	0.001	0.001	0.001	0.001	0.001	0.001
Spleen	0.014	°0.011	0.087	0.098	0.232	0.418	0.351	0.419	1.118	0.845	0.957	0.685	0.914	1.146
Stomach	0.008	°0.003	0.016	0.022	0.033	0.035	0.037	0.022	0.055	0.024	0.054	0.020	0.049	0.029
Testes (males)	0.007	-	0.010	-	0.017	-	0.030	-	0.034	-	0.074	-	0.074	-
Thymus	0.005	°0.002	0.006	0.008	0.008	0.012	0.018	0.006	0.012	0.003	0.009	0.004	0.008	0.007
Thyroid	0.000	°0.000	0.000	0.001	0.001	0.001	0.001	0.001	0.001	0.000	0.001	0.000	0.001	0.001
Uterus (females)	-	°0.002	-	0.011	-	0.015	-	0.008	-	0.016	-	0.018	-	0.022

°=Mean includes results calculated from data less than 30 cpm above background

090177e195794698\Approved\Approved On: 09-Nov-2020 21:23 (GMT)

10 APPENDICES

Appendix 1 Certificates of Analysis for [³H]-08-A01-C01 and [³H]-CHE

Confidential



R&D Formulation Characterization Report

Batch ID	LNP ID	Specific Activity	[Lipid]	Encaps	Encapsulated mRNA	Yield	mRNA/Lipid Ratio	Particle Diameter	Poly-dispersity
		dpm/uL	mg/mL	%	mg/mL	mg	mg/mg	nm	
NC-0552-1	08-A01-C01	1,900,000	25.7	94	1.0	6.05	0.039	89	0.062

Notes

Formulated July 6, 2020 for NC-0552 using BioNTech mRNA (AnSo luc 1041 CorVac) and trace labeled with 3H-CHE. Endotoxin below detection limit (<0.5 EU/mL). Sterile filtered using 0.2 µm pore-size filters.

Stored at -70°C. Thaw at room temperature and dilute on the day of use.

(b) (6)

(b) (6)

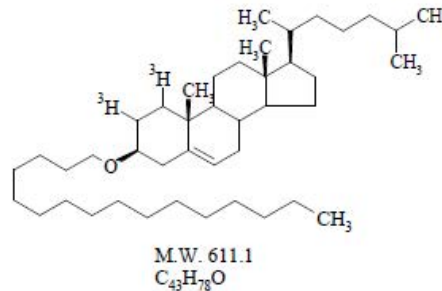
08-July-20
Date

Appendix 1 Certificates of Analysis for [³H]-08-A01-C01 and [³H]-CHE
(continued)

TECHNICAL DATA SHEET	³ H
Research Use Only. Not for use in diagnostic procedures	
CHOLESTERYL HEXADECYL ETHER, [CHOLESTERYL-1,2-³H(N)]-	
Product Number: NET859	

LOT SPECIFIC INFORMATION

Lot Number:	2656317
Specific Activity:	51.9 Ci/mmol
	1920 GBq/mmol
Production Date:	16-Dec-2019



PACKAGING: 1.0 mCi/ml (37 MBq/ml) in toluene, under argon in an ampoule. Shipped on dry ice.

STABILITY AND STORAGE RECOMMENDATIONS: When cholesteryl hexadecyl ether, [cholesteryl-1,2-³H(N)]- is stored at -20°C in its original solvent and at its original concentration, the rate of decomposition is initially 2% for 6 months from date of purification. Stability is nonlinear and not correlated to isotope half-life. Lot to lot variation may occur.

SPECIFIC ACTIVITY RANGE: 40-60 Ci/mmol (1480-2220 GBq/mmol)

RADIOCHEMICAL PURITY: This product was initially found to be greater than 97% when determined by the following methods. The rate of decomposition can accelerate. It is advisable to check purity prior to use:

High pressure liquid chromatography on a Zorbax C-8 column using the following mobile phase:
acetonitrile : isopropanol, (35:65).

Thin layer chromatography on silica gel using the following solvent system:
toluene : hexane, (1:9).

QUALITY CONTROL: The radiochemical purity of cholesteryl hexadecyl ether, [cholesteryl-1,2-³H(N)]- is checked at appropriate intervals using the first listed chromatography method.

The precursor used in the synthesis of NET-859 is synthetic.

HAZARD INFORMATION: WARNING: This product contains a chemical known to the state of California to cause cancer.

PerkinElmer, Inc.
549 Albany Street
Boston, MA 02118 USA
P: (800) 762-4000 or (+1) 203-925-4602
www.perkinelmer.com/en/radiochemicals
For a complete listing of our global offices, visit www.perkinelmer.com/ContactUs
Copyright ©2010, PerkinElmer, Inc. All rights reserved. PerkinElmer® is a registered trademark of PerkinElmer, Inc.
All other trademarks are the property of their respective owners.
NET859-REV-02



Appendix 2 Individual Animal Dosing Summary

Males

Target Dose Level: 50 µg mRNA/Animal; 1.29 mg Total Lipid/Animal

Animal ID	Body weight (g)	Dose Received		
		mg mRNA	mg lipid	MBq
043M	270	0.0514	1.32	1.63
044M	264	0.0518	1.33	1.65
045M	244	0.0521	1.34	1.66
046M	263	0.0525	1.35	1.68
047M	232	0.0514	1.32	1.64
048M	228	0.0525	1.35	1.67
049M	259	0.0514	1.32	1.64
050M	249	0.0518	1.33	1.66
051M	257	0.0533	1.37	1.70
052M	258	0.0521	1.34	1.66
053M	249	0.0529	1.36	1.69
054M	235	0.0525	1.35	1.68
055M	247	0.0502	1.29	1.60
056M	256	0.0514	1.32	1.64
057M	266	0.0521	1.34	1.66
058M	263	0.0521	1.34	1.66
059M	243	0.0525	1.35	1.67
060M	248	0.0518	1.33	1.65
061M	240	0.0521	1.34	1.66
062M	259	0.0521	1.34	1.66
063M	238	0.0521	1.34	1.66

090177e195794698\Approved\Approved On: 09-Nov-2020 21:23 (GMT)

**Appendix 2 Individual Animal Dosing Summary
(continued)****Females****Target Dose Level: 50 µg mRNA/Animal; 1.29 mg Total Lipid/Animal**

Animal ID	Body weight (g)	Dose Received		
		mg mRNA	mg lipid	MBq
022F	215	0.0521	1.34	1.66
023F	206	0.0529	1.36	1.68
024F	206	0.0514	1.32	1.64
025F	212	0.0533	1.37	1.70
026F	213	0.0525	1.35	1.68
027F	207	0.0529	1.36	1.69
028F	198	0.0529	1.36	1.68
029F	208	0.0529	1.36	1.69
030F	214	0.0518	1.33	1.64
031F	204	0.0537	1.38	1.71
032F	207	0.0533	1.37	1.70
033F	209	0.0521	1.34	1.66
034F	224	0.0510	1.31	1.62
035F	179	0.0482	1.24	1.53
036F	211	0.0467	1.20	1.49
037F	205	0.0506	1.30	1.61
038F	225	0.0502	1.29	1.60
039F	213	0.0525	1.35	1.67
040F	199	0.0533	1.37	1.69
041F	218	0.0529	1.36	1.69
042F	193	0.0533	1.37	1.70

090177e195794698\Approved\Approved On: 09-Nov-2020 21:23 (GMT)

**Appendix 2 Individual Animal Dosing Summary
 (continued)**

Males

Target Dose Level: 100 µg mRNA/Animal; 2.57 mg Total Lipid/Animal

Animal ID	Body weight (g)	Dose Received		
		mg mRNA	mg lipid	MBq
001M	240	0.104	2.66	3.30
002M	243	0.106	2.73	3.38
003M	277	0.107	2.74	3.40
004M	247	0.106	2.72	3.37
005M	243	0.107	2.76	3.42
006M	237	0.107	2.74	3.39
007M	245	0.107	2.75	3.41
008M	237	0.106	2.73	3.39
009M	248	0.106	2.73	3.39
010M	227	0.101	2.60	3.22
011M	267	0.105	2.71	3.36
012M	237	0.106	2.72	3.37
013M	241	0.105	2.69	3.34
014M	264	0.107	2.76	3.42
015M	264	0.105	2.71	3.36
043M	241	0.106	2.73	3.39
017M	252	0.106	2.73	3.39
018M	263	0.105	2.70	3.35
019M	248	0.106	2.72	3.37
020M	246	0.106	2.73	3.39
021M	217	0.107	2.75	3.41

090177e195794698\Approved\Approved On: 09-Nov-2020 21:23 (GMT)

Appendix 3 Urine and Faeces Sample Weights

Males

Target Dose Level: 50 µg mRNA/Animal; 1.29 mg Total Lipid/Animal

Results expressed in g

Sample	Timepoint	061M	062M	063M
Urine	Pre-dose	6.860	18.617	14.228
	6 h	6.139	8.101	8.153
	24 h	21.208	29.766	40.276
	48 h	28.317	28.566	36.902
Faeces	Pre-dose	11.324	7.893	6.070
	24 h	4.716	14.327	8.659
	48 h	6.968	8.398	7.007

**Appendix 3 Urine and Faeces Sample Weights
 (continued)**

Females

Target Dose Level: 50 µg mRNA/Animal; 1.29 mg Total Lipid/Animal

Results expressed in g

Sample	Timepoint	040F	041F	042F
Urine	Pre-dose	3.963	9.453	7.513
	6 h	4.844	5.664	9.719
	24 h	20.736	29.176	21.294
	48 h	30.371	33.928	23.141
Faeces	Pre-dose	6.110	2.679	6.010
	24 h	8.887	9.193	5.619
	48 h	4.565	6.139	4.834

090177e195794698\Approved\Approved On: 09-Nov-2020 21:23 (GMT)

**Appendix 3 Urine and Faeces Sample Weights
 (continued)**

Males

Target Dose Level: 100 µg mRNA/Animal; 2.57 mg Total Lipid/Animal

Results expressed in g

Sample	Timepoint	019M	020M	021M
Urine	Pre-dose	7.519	4.094	13.159
	6 h	8.883	8.835	10.517
	24 h	29.916	22.983	12.664
	48 h	37.860	35.653	*6.931
Faeces	Pre-dose	9.491	9.292	4.882
	24 h	11.197	14.005	8.769
	48 h	6.950	8.229	*2.449

Note that for animal 021M the collection period was approximately 24-31 h.

Appendix 4 Individual Male Concentration Data**Concentration of Total Radioactivity in Whole Blood, Plasma and Tissues 0.25 min Following Single Intramuscular Administration of [³H]-08-A01-C01 to Male Wistar Han Rats****Target Dose Level: 50 µg mRNA/Animal; 1.29 mg Total Lipid/Animal****Results expressed as µg lipid equiv/g (mL)**

Sample	043M	044M	045M	Mean	SD
Adipose tissue	0.056	0.045	0.019	0.040	0.019
Adrenal glands	0.380	0.480	0.046	0.302	0.227
Bladder	0.096	0.045	0.007	0.049	0.045
Bone (femur)	0.172	0.085	0.119	0.126	0.044
Bone marrow (femur)	0.775	0.326	1.182	0.761	0.428
Brain	0.093	0.092	0.033	0.073	0.034
Eyes	0.025	0.013	0.005	0.014	0.010
Heart	0.710	0.474	0.074	0.419	0.322
Injection site	436.090	159.310	64.429	219.940	193.100
Kidneys	0.808	0.600	0.123	0.511	0.351
Large intestine	0.020	0.027	0.003	0.017	0.012
Liver	2.035	1.226	0.193	1.151	0.923
Lung	1.050	0.826	0.334	0.737	0.366
Lymph node (Man)	0.152	0.069	0.049	0.090	0.055
Lymph node (Mes)	0.087	0.054	0.016	0.052	0.036
Muscle	0.049	0.035	*0.003	°0.029	°0.024
Pancreas	0.156	0.201	0.019	0.125	0.095
Pituitary gland	0.962	0.535	0.115	0.537	0.424
Prostate	0.098	0.074	0.012	0.061	0.044
Salivary glands	0.169	0.145	0.028	0.114	0.076
Skin	0.030	0.015	*0.002	°0.016	°0.014
Small intestine	0.064	0.043	0.008	0.038	0.028
Spinal cord	0.108	0.063	0.013	0.061	0.047
Spleen	0.519	0.450	0.094	0.354	0.228
Stomach	0.022	0.027	0.005	0.018	0.012
Testes	0.053	0.036	0.006	0.031	0.024
Thymus	0.119	0.169	0.030	0.106	0.071
Thyroid	0.292	0.307	0.053	0.217	0.142
Whole Blood	5.631	2.526	0.852	3.003	2.425
Plasma	9.854	6.519	1.732	6.035	4.083
Blood:plasma ratio	0.57	0.39	0.49	0.48	0.09

* = Results calculated from data less than 30 cpm above background

° = Mean includes results calculated from data less than 30 cpm above background

Appendix 4 Individual Male Concentration Data
(continued)**Concentration of Total Radioactivity in Whole Blood, Plasma and Tissues 1 hour Following Single Intramuscular Administration of [³H]-08-A01-C01 to Male Wistar Han Rats****Target Dose Level: 50 µg mRNA/Animal; 1.29 mg Total Lipid/Animal****Results expressed as µg lipid equiv/g (mL)**

Sample	046M	047M	048M	Mean	SD
Adipose tissue	0.037	0.073	0.040	0.050	0.020
Adrenal glands	0.293	0.647	0.800	0.580	0.260
Bladder	0.111	0.087	0.088	0.095	0.013
Bone (femur)	0.115	0.085	0.246	0.148	0.085
Bone marrow (femur)	0.561	1.150	1.021	0.910	0.310
Brain	0.033	0.108	0.107	0.083	0.043
Eyes	0.014	0.019	0.049	0.027	0.019
Heart	0.266	0.780	0.847	0.631	0.318
Injection site	503.490	593.230	666.280	587.670	81.536
Kidneys	0.322	0.710	0.857	0.630	0.276
Large intestine	0.026	0.032	0.037	0.031	0.005
Liver	2.667	3.571	5.780	4.006	1.602
Lung	0.428	1.203	0.903	0.845	0.391
Lymph node (Man)	0.151	0.166	0.145	0.154	0.011
Lymph node (Mes)	0.076	0.100	0.109	0.095	0.017
Muscle	0.030	0.036	0.050	0.039	0.010
Pancreas	0.076	0.189	0.193	0.153	0.067
Pituitary gland	0.202	0.502	0.634	0.446	0.221
Prostate	0.063	0.105	0.105	0.091	0.024
Salivary glands	0.084	0.151	0.208	0.148	0.062
Skin	0.020	0.027	0.039	0.028	0.010
Small intestine	0.144	0.214	0.223	0.194	0.043
Spinal cord	0.062	0.070	0.084	0.072	0.011
Spleen	3.314	1.388	1.720	2.140	1.029
Stomach	0.024	0.043	0.049	0.039	0.013
Testes	0.026	0.041	0.057	0.042	0.015
Thymus	0.201	0.133	0.226	0.187	0.048
Thyroid	0.126	0.599	0.448	0.391	0.241
Whole Blood	0.873	4.534	3.018	2.809	1.840
Plasma	2.937	6.047	7.153	5.379	2.186
Blood:plasma ratio	0.30	0.75	0.42	0.49	0.23

090177e195794698\Approved\Approved On: 09-Nov-2020 21:23 (GMT)

Appendix 4 Individual Male Concentration Data
 (continued)

Concentration of Total Radioactivity in Whole Blood, Plasma and Tissues 2 hours Following Single Intramuscular Administration of [³H]-08-A01-C01 to Male Wistar Han Rats

Target Dose Level: 50 µg mRNA/Animal; 1.29 mg Total Lipid/Animal

Results expressed as µg lipid equiv/g (mL)

Sample	049M	050M	051M	Mean	SD
Adipose tissue	0.084	0.034	0.090	0.070	0.031
Adrenal glands	1.809	0.584	1.226	1.206	0.613
Bladder	0.152	0.080	0.179	0.137	0.051
Bone (femur)	0.250	0.180	0.273	0.235	0.048
Bone marrow (femur)	1.526	0.559	1.323	1.136	0.510
Brain	0.220	0.088	0.121	0.143	0.069
Eyes	0.036	0.023	0.077	0.046	0.028
Heart	1.782	0.682	0.901	1.122	0.582
Injection site	445.930	1052.800	88.843	529.210	487.370
Kidneys	1.467	0.785	1.120	1.124	0.341
Large intestine	0.074	0.056	0.109	0.080	0.027
Liver	12.023	5.816	10.885	9.574	3.304
Lung	2.397	0.968	1.419	1.594	0.730
Lymph node (Man)	0.328	0.112	0.210	0.217	0.108
Lymph node (Mes)	0.312	0.180	0.194	0.229	0.073
Muscle	0.083	0.060	0.057	0.067	0.014
Pancreas	0.296	0.179	0.792	0.423	0.325
Pituitary gland	1.175	0.405	0.764	0.781	0.385
Prostate	0.150	0.095	0.139	0.128	0.029
Salivary glands	0.279	0.113	0.251	0.214	0.089
Skin	0.083	0.032	0.048	0.054	0.026
Small intestine	0.455	0.458	0.500	0.471	0.025
Spinal cord	0.184	0.150	0.163	0.166	0.017
Spleen	6.771	2.590	6.403	5.255	2.315
Stomach	0.121	0.059	0.133	0.104	0.040
Testes	0.120	0.039	0.077	0.079	0.040
Thymus	0.248	0.146	0.265	0.220	0.065
Thyroid	0.749	0.361	0.615	0.575	0.197
Whole Blood	4.913	2.788	4.384	4.028	1.106
Plasma	10.623	6.177	9.341	8.714	2.288
Blood:plasma ratio	0.46	0.45	0.47	0.46	0.01

090177e195794698\Approved\Approved On: 09-Nov-2020 21:23 (GMT)

**Appendix 4 Individual Male Concentration Data
(continued)****Concentration of Total Radioactivity in Whole Blood, Plasma and
Tissues 4 hours Following Single Intramuscular Administration of
[³H]-08-A01-C01 to Male Wistar Han Rats****Target Dose Level: 50 µg mRNA/Animal; 1.29 mg Total Lipid/Animal****Results expressed as µg lipid equiv/g (mL)**

Sample	052M	053M	054M	Mean	SD
Adipose tissue	0.062	0.092	0.124	0.093	0.031
Adrenal glands	2.252	1.999	3.456	2.569	0.779
Bladder	0.207	0.239	0.234	0.227	0.017
Bone (femur)	0.264	0.234	0.506	0.335	0.149
Bone marrow (femur)	1.318	1.364	1.987	1.557	0.374
Brain	0.136	0.112	0.217	0.155	0.055
Eyes	0.084	0.133	0.067	0.095	0.034
Heart	0.993	0.669	1.484	1.049	0.411
Injection site	445.970	1001.000	412.620	619.850	330.480
Kidneys	0.967	0.737	1.395	1.033	0.334
Large intestine	0.413	0.311	0.327	0.350	0.055
Liver	14.739	16.391	24.445	18.525	5.193
Lung	2.047	1.003	2.265	1.772	0.675
Lymph node (Man)	0.283	0.564	0.426	0.424	0.140
Lymph node (Mes)	0.287	0.258	0.780	0.441	0.293
Muscle	0.064	0.057	0.104	0.075	0.025
Pancreas	0.277	0.413	0.393	0.361	0.073
Pituitary gland	0.933	2.418	0.397	1.249	1.047
Prostate	0.161	0.121	0.190	0.157	0.035
Salivary glands	0.232	0.197	0.380	0.270	0.097
Skin	0.073	0.052	0.131	0.085	0.041
Small intestine	0.822	0.698	1.235	0.919	0.281
Spinal cord	0.193	0.745	0.188	0.375	0.320
Spleen	6.146	11.159	9.529	8.945	2.557
Stomach	0.324	0.058	0.176	0.186	0.134
Testes	0.105	0.098	0.185	0.129	0.049
Thymus	0.210	0.371	0.800	0.461	0.305
Thyroid	1.055	1.301	0.936	1.097	0.186
Whole Blood	3.547	2.519	4.133	3.400	0.817
Plasma	8.820	4.802	12.644	8.755	3.922
Blood:plasma ratio	0.40	0.52	0.33	0.42	0.10

090177e195794698\Approved\Approved On: 09-Nov-2020 21:23 (GMT)

Appendix 4 Individual Male Concentration Data
(continued)**Concentration of Total Radioactivity in Whole Blood, Plasma and Tissues 8 hours Following Single Intramuscular Administration of [³H]-08-A01-C01 to Male Wistar Han Rats****Target Dose Level: 50 µg mRNA/Animal; 1.29 mg Total Lipid/Animal****Results expressed as µg lipid equiv/g (mL)**

Sample	055M	056M	057M	Mean	SD
Adipose tissue	0.076	0.163	0.109	0.116	0.044
Adrenal glands	4.440	4.886	9.835	6.387	2.995
Bladder	N.S.	0.198	0.224	0.211	N.A.
Bone (femur)	0.510	0.355	0.639	0.502	0.142
Bone marrow (femur)	3.050	1.943	2.199	2.397	0.579
Brain	0.105	0.096	0.103	0.101	0.005
Eyes	N.S.	0.071	0.104	0.088	N.A.
Heart	1.418	1.008	1.142	1.189	0.209
Injection site	181.620	497.270	219.870	299.590	172.260
Kidneys	0.934	0.795	0.783	0.837	0.084
Large intestine	0.735	0.665	0.672	0.690	0.039
Liver	23.158	22.178	38.412	27.916	9.103
Lung	1.679	1.643	1.701	1.674	0.029
Lymph node (Man)	0.432	1.053	0.601	0.695	0.321
Lymph node (Mes)	0.444	0.609	0.892	0.649	0.226
Muscle	0.082	0.096	0.127	0.101	0.023
Pancreas	0.352	0.418	0.276	0.349	0.071
Pituitary gland	0.635	0.477	0.894	0.669	0.211
Prostate	0.184	0.127	0.139	0.150	0.030
Salivary glands	0.170	0.157	0.202	0.176	0.023
Skin	0.138	0.111	0.117	0.122	0.014
Small intestine	1.423	1.518	1.634	1.525	0.106
Spinal cord	0.146	0.119	0.239	0.168	0.063
Spleen	21.122	24.073	28.107	24.434	3.507
Stomach	0.345	0.107	0.777	0.410	0.340
Testes	0.153	0.107	0.179	0.146	0.037
Thymus	0.317	0.278	0.282	0.292	0.021
Thyroid	0.940	0.611	0.792	0.781	0.165
Whole Blood	2.215	1.968	1.817	2.000	0.201
Plasma	3.978	3.465	3.275	3.573	0.364
Blood:plasma ratio	0.56	0.57	0.55	0.56	0.01

N.S. = No sample due to oxidiser failure

N.A. = Not applicable

Appendix 4 Individual Male Concentration Data
(continued)**Concentration of Total Radioactivity in Whole Blood, Plasma and Tissues 24 hours Following Single Intramuscular Administration of [³H]-08-A01-C01 to Male Wistar Han Rats****Target Dose Level: 50 µg mRNA/Animal; 1.29 mg Total Lipid/Animal****Results expressed as µg lipid equiv/g (mL)**

Sample	058M	059M	060M	Mean	SD
Adipose tissue	0.079	0.116	0.182	0.126	0.053
Adrenal glands	10.795	21.060	27.988	19.948	8.650
Bladder	0.211	0.394	0.365	0.323	0.099
Bone (femur)	0.456	0.408	0.649	0.504	0.127
Bone marrow (femur)	2.286	3.625	4.824	3.579	1.270
Brain	0.049	0.099	0.124	0.090	0.038
Eyes	0.098	0.113	0.178	0.129	0.042
Heart	0.640	0.590	0.520	0.583	0.060
Injection site	178.010	330.550	292.960	267.170	79.471
Kidneys	0.522	0.407	0.584	0.504	0.090
Large intestine	0.592	1.611	3.019	1.741	1.219
Liver	17.750	21.966	30.365	23.360	6.422
Lung	0.942	1.334	1.672	1.316	0.365
Lymph node (Man)	0.577	0.689	0.965	0.744	0.200
Lymph node (Mes)	0.905	1.040	1.373	1.106	0.241
Muscle	0.092	0.068	0.133	0.098	0.033
Pancreas	0.294	0.382	0.513	0.396	0.110
Pituitary gland	0.489	0.768	0.711	0.656	0.147
Prostate	0.150	0.183	0.215	0.183	0.032
Salivary glands	0.168	0.243	0.317	0.243	0.075
Skin	0.134	0.166	0.287	0.195	0.081
Small intestine	0.971	1.994	2.670	1.878	0.855
Spinal cord	0.091	0.144	0.127	0.121	0.027
Spleen	19.140	15.796	33.523	22.819	9.419
Stomach	0.110	0.168	0.386	0.222	0.145
Testes	0.234	0.286	0.392	0.304	0.080
Thymus	0.163	0.235	0.368	0.255	0.104
Thyroid	0.721	0.660	1.081	0.820	0.228
Whole Blood	1.473	1.237	1.112	1.274	0.183
Plasma	2.584	2.935	2.345	2.621	0.297
Blood:plasma ratio	0.57	0.42	0.47	0.49	0.08

090177e195794698\Approved\Approved On: 09-Nov-2020 21:23 (GMT)

**Appendix 4 Individual Male Concentration Data
(continued)****Concentration of Total Radioactivity in Whole Blood, Plasma and
Tissues 48 hours Following Single Intramuscular Administration of
[³H]-08-A01-C01 to Male Wistar Han Rats****Target Dose Level: 50 µg mRNA/Animal; 1.29 mg Total Lipid/Animal****Results expressed as µg lipid equiv/g (mL)**

Sample	061M	062M	063M	Mean	SD
Adipose tissue	0.104	0.162	0.121	0.129	0.030
Adrenal glands	13.913	35.091	15.424	21.476	11.815
Bladder	0.274	0.447	0.298	0.340	0.094
Bone (femur)	0.344	0.577	0.639	0.520	0.155
Bone marrow (femur)	2.566	5.049	3.455	3.690	1.258
Brain	0.051	0.112	0.087	0.083	0.031
Eyes	0.100	0.121	0.160	0.127	0.031
Heart	0.418	0.955	0.642	0.672	0.270
Injection site	292.370	196.910	317.030	268.770	63.446
Kidneys	0.309	0.673	0.463	0.482	0.182
Large intestine	0.998	1.235	2.045	1.426	0.549
Liver	17.734	20.580	16.177	18.164	2.233
Lung	0.809	1.885	1.170	1.288	0.548
Lymph node (Man)	0.728	1.078	0.656	0.820	0.226
Lymph node (Mes)	0.924	1.620	0.626	1.057	0.510
Muscle	0.078	0.115	0.647	0.280	0.318
Pancreas	0.291	0.506	0.964	0.587	0.344
Pituitary gland	0.431	0.610	0.588	0.543	0.098
Prostate	0.110	0.265	0.135	0.170	0.083
Salivary glands	0.286	0.370	0.234	0.297	0.069
Skin	0.177	0.267	0.183	0.209	0.051
Small intestine	1.178	2.030	1.681	1.630	0.428
Spinal cord	0.089	0.129	0.267	0.162	0.093
Spleen	12.073	25.689	20.887	19.550	6.906
Stomach	0.122	0.315	0.268	0.235	0.101
Testes	0.214	0.471	0.275	0.320	0.134
Thymus	0.226	0.362	0.299	0.296	0.068
Thyroid	0.830	1.797	1.406	1.344	0.486
Whole Blood	0.594	0.473	0.536	0.535	0.060
Plasma	1.021	1.003	1.230	1.085	0.126
Blood:plasma ratio	0.58	0.47	0.44	0.50	0.08

090177e195794698\Approved\Approved On: 09-Nov-2020 21:23 (GMT)

Appendix 5 Individual Female Concentration Data**Concentration of Total Radioactivity in Whole Blood, Plasma and Tissues 0.25 min Following Single Intramuscular Administration of [³H]-08-A01-C01 to Female Wistar Han Rats****Target Dose Level: 50 µg mRNA/Animal; 1.29 mg Total Lipid/Animal****Results expressed as µg lipid equiv/g (mL)**

Sample	022F	023F ^A	024F	Mean	SD
Adipose tissue	0.203	*0.002	0.015	°0.073	°0.113
Adrenal glands	0.578	*0.000	0.143	°0.240	°0.301
Bladder	0.050	*0.000	0.048	°0.033	°0.029
Bone (femur)	0.146	0.003	0.019	0.056	0.079
Bone marrow (femur)	N.S.	0.264	*0.128	°0.196	N.A.
Brain	0.036	*0.002	0.011	°0.016	°0.018
Eyes	0.015	*0.000	0.004	°0.006	°0.008
Injection site	27.519	77.480	4.697	36.566	37.225
Heart	0.310	*0.001	0.121	°0.144	°0.156
Kidneys	0.544	0.126	0.143	0.271	0.236
Large intestine	0.019	*0.001	0.004	°0.008	°0.010
Liver	0.635	0.018	0.316	0.323	0.309
Lung	0.550	0.012	0.177	0.247	0.275
Lymph node (Man)	0.088	*0.000	0.025	°0.038	°0.045
Lymph node (Mes)	0.127	*0.000	0.018	°0.048	°0.069
Muscle	0.024	0.006	0.007	0.012	0.010
Ovaries	0.206	*0.000	0.106	°0.104	°0.103
Pancreas	0.072	0.008	0.030	0.037	0.033
Pituitary gland	0.310	*0.000	0.113	°0.141	°0.157
Salivary glands	0.133	*0.000	0.028	°0.054	°0.070
Skin	0.018	0.004	0.009	0.010	0.007
Small intestine	0.051	*0.001	0.010	°0.021	°0.026
Spinal cord	0.057	*0.000	0.016	°0.024	°0.029
Spleen	0.366	*0.004	0.570	°0.313	°0.287
Stomach	0.032	*0.001	0.013	°0.015	°0.016
Thymus	0.159	*0.003	0.047	°0.069	°0.080
Thyroid	0.181	*0.000	0.097	°0.093	°0.091
Uterus	0.090	*0.000	0.037	°0.043	°0.045
Whole Blood	2.016	0.013	0.778	0.936	1.011
Plasma	4.189	0.005	1.487	1.894	2.121
Blood:plasma ratio	0.48	2.43	0.52	1.15	1.12

N.S. = No sample due to analysis error (the bone marrow was not able to be removed from the bone since the bone was initially crushed for analysis)

A = Animal 023F appeared to have a slow distribution compared with the other animals

* = Results calculated from data less than 30 cpm above background

° = Mean includes results calculated from data less than 30 cpm above background

Appendix 5 Individual Female Concentration Data
 (continued)

Concentration of Total Radioactivity in Whole Blood, Plasma and Tissues 1 hour Following Single Intramuscular Administration of [³H]-08-A01-C01 to Female Wistar Han Rats

Target Dose Level: 50 µg mRNA/Animal; 1.29 mg Total Lipid/Animal

Results expressed as µg lipid equiv/g (mL)

Sample	025F	026F	027F	Mean	SD
Adipose tissue	0.145	0.234	0.069	0.149	0.083
Adrenal glands	1.779	2.131	3.254	2.388	0.770
Bladder	0.123	0.206	0.166	0.165	0.042
Bone (femur)	0.216	0.285	0.223	0.241	0.038
Bone marrow (femur)	0.886	1.219	0.926	1.010	0.182
Brain	0.096	0.139	0.115	0.117	0.022
Eyes	0.052	0.052	0.027	0.043	0.015
Heart	1.273	1.884	1.120	1.426	0.404
Injection site	31.021	202.720	366.100	199.950	167.560
Kidneys	1.568	2.396	1.112	1.692	0.651
Large intestine	0.060	0.065	0.070	0.065	0.005
Liver	6.342	4.717	4.674	5.244	0.951
Lung	1.455	1.954	1.313	1.574	0.336
Lymph node (Man)	0.226	0.266	0.176	0.223	0.045
Lymph node (Mes)	0.207	0.226	0.155	0.196	0.037
Muscle	0.080	0.093	0.072	0.082	0.011
Ovaries	1.630	1.650	0.736	1.339	0.522
Pancreas	0.208	0.343	0.234	0.261	0.072
Pituitary gland	0.607	1.114	0.810	0.844	0.255
Salivary glands	0.245	0.327	0.140	0.237	0.094
Skin	0.056	0.956	0.148	0.387	0.495
Small intestine	0.281	0.223	0.235	0.247	0.031
Spinal cord	0.111	0.119	0.137	0.122	0.013
Spleen	2.423	2.626	3.355	2.801	0.490
Stomach	0.085	0.118	0.070	0.091	0.025
Thymus	0.248	0.483	0.164	0.298	0.165
Thyroid	0.510	0.997	0.533	0.680	0.275
Uterus	0.194	0.251	0.164	0.203	0.044
Whole Blood	5.057	8.484	4.243	5.928	2.251
Plasma	9.655	14.318	8.680	10.884	3.014
Blood:plasma ratio	0.52	0.59	0.49	0.54	0.05

090177e195794698\Approved\Approved On: 09-Nov-2020 21:23 (GMT)

**Appendix 5 Individual Female Concentration Data
(continued)****Concentration of Total Radioactivity in Whole Blood, Plasma and Tissues 2 hours Following Single Intramuscular Administration of [³H]-08-A01-C01 to Female Wistar Han Rats****Target Dose Level: 50 µg mRNA/Animal; 1.29 mg Total Lipid/Animal****Results expressed as µg lipid equiv/g (mL)**

Sample	028F	029F	030F	Mean	SD
Adipose tissue	0.110	0.274	0.162	0.182	0.084
Adrenal glands	1.429	8.981	2.285	4.232	4.135
Bladder	0.062	0.289	0.114	0.155	0.119
Bone (femur)	0.132	0.566	0.189	0.296	0.236
Bone marrow (femur)	0.575	1.722	1.714	1.337	0.660
Brain	0.063	0.241	0.095	0.133	0.095
Eyes	0.034	0.117	0.023	0.058	0.051
Heart	0.554	3.221	1.272	1.682	1.380
Injection site	0.092	1.744	277.600	93.144	159.740
Kidneys	0.623	2.870	5.408	2.967	2.394
Large intestine	0.027	0.198	0.092	0.106	0.086
Liver	5.209	21.794	10.108	12.370	8.521
Lung	0.908	4.000	1.313	2.074	1.681
Lymph node (Man)	0.198	0.701	0.188	0.362	0.293
Lymph node (Mes)	1.473	0.640	0.381	0.831	0.571
Muscle	0.045	0.140	0.114	0.100	0.049
Ovaries	0.474	2.683	1.756	1.638	1.109
Pancreas	0.116	0.825	0.270	0.404	0.373
Pituitary gland	0.414	1.853	0.599	0.955	0.783
Salivary glands	0.141	0.562	0.182	0.295	0.232
Skin	0.040	0.263	0.486	0.263	0.223
Small intestine	0.305	0.664	0.473	0.481	0.180
Spinal cord	0.109	0.289	0.118	0.172	0.102
Spleen	2.066	23.785	4.788	10.213	11.832
Stomach	0.088	0.211	0.077	0.126	0.074
Thymus	0.109	1.108	0.160	0.459	0.562
Thyroid	0.371	1.791	1.163	1.109	0.711
Uterus	0.169	0.568	0.178	0.305	0.228
Whole Blood	2.194	14.470	3.655	6.773	6.706
Plasma	4.442	15.480	7.350	9.091	5.721
Blood:plasma ratio	0.49	0.93	0.50	0.64	0.25

090177e195794698\Approved\Approved On: 09-Nov-2020 21:23 (GMT)

Appendix 5 Individual Female Concentration Data
 (continued)

Concentration of Total Radioactivity in Whole Blood, Plasma and Tissues 4 hours Following Single Intramuscular Administration of [³H]-08-A01-C01 to Female Wistar Han Rats

Target Dose Level: 50 µg mRNA/Animal; 1.29 mg Total Lipid/Animal

Results expressed as µg lipid equiv/g (mL)

Sample	031F	032F	033F	Mean	SD
Adipose tissue	0.134	0.061	0.296	0.163	0.121
Adrenal glands	1.879	3.483	4.255	3.206	1.212
Bladder	0.043	0.101	0.175	0.106	0.066
Bone (femur)	0.136	0.194	0.321	0.217	0.095
Bone marrow (femur)	0.448	0.818	1.480	0.915	0.522
Brain	0.033	0.058	0.133	0.075	0.052
Eyes	0.022	0.046	0.048	0.038	0.015
Heart	0.296	0.746	1.734	0.925	0.735
Injection site	8.920	103.630	56.133	56.227	47.355
Kidneys	0.328	0.627	1.486	0.814	0.601
Large intestine	0.165	0.222	0.283	0.224	0.059
Liver	8.503	14.685	20.519	14.569	6.009
Lung	0.610	1.159	1.898	1.222	0.646
Lymph node (Man)	0.173	0.454	0.546	0.391	0.194
Lymph node (Mes)	0.316	0.598	0.695	0.536	0.197
Muscle	0.033	0.057	0.301	0.130	0.148
Ovaries	0.555	2.916	3.552	2.341	1.579
Pancreas	0.358	0.270	0.568	0.398	0.153
Pituitary gland	0.251	0.317	0.805	0.458	0.303
Salivary glands	0.087	0.156	0.262	0.169	0.088
Skin	0.043	0.371	0.197	0.204	0.164
Small intestine	0.684	0.739	1.089	0.838	0.220
Spinal cord	0.073	0.061	0.236	0.124	0.098
Spleen	9.910	11.442	13.587	11.646	1.847
Stomach	0.050	0.113	0.141	0.101	0.047
Thymus	0.130	0.267	0.231	0.209	0.071
Thyroid	0.225	0.718	0.867	0.604	0.336
Uterus	0.080	0.096	0.246	0.140	0.091
Whole Blood	1.090	1.981	5.022	2.698	2.062
Plasma	2.037	3.442	7.274	4.251	2.711
Blood:plasma ratio	0.53	0.58	0.69	0.60	0.08

090177e195794698\Approved\Approved On: 09-Nov-2020 21:23 (GMT)

Appendix 5 Individual Female Concentration Data
(continued)**Concentration of Total Radioactivity in Whole Blood, Plasma and Tissues 8 hours Following Single Intramuscular Administration of [³H]-08-A01-C01 to Female Wistar Han Rats****Target Dose Level: 50 µg mRNA/Animal; 1.29 mg Total Lipid/Animal****Results expressed as µg lipid equiv/g (mL)**

Sample	034F	035F	036F	Mean	SD
Adipose tissue	0.095	0.041	0.072	0.069	0.027
Adrenal glands	7.562	6.554	7.538	7.218	0.575
Bladder	0.047	0.080	0.127	0.085	0.040
Bone (femur)	0.243	0.143	0.144	0.177	0.057
Bone marrow (femur)	1.262	1.350	1.210	1.274	0.071
Brain	0.047	0.030	0.058	0.045	0.014
Eyes	0.046	0.013	0.032	0.030	0.016
Heart	0.532	0.193	0.448	0.391	0.177
Injection site	30.227	174.950	172.620	125.930	82.890
Kidneys	0.416	0.239	0.372	0.342	0.092
Large intestine	0.679	0.381	0.764	0.608	0.201
Liver	22.242	25.442	27.834	25.172	2.806
Lung	0.661	0.378	0.846	0.628	0.236
Lymph node (Man)	0.315	0.251	0.551	0.372	0.158
Lymph node (Mes)	0.790	0.481	0.915	0.729	0.223
Muscle	0.040	0.160	0.075	0.091	0.062
Ovaries	2.960	1.276	5.029	3.088	1.880
Pancreas	0.390	0.087	0.241	0.239	0.151
Pituitary gland	0.169	0.099	0.157	0.141	0.037
Salivary glands	0.124	0.074	0.082	0.094	0.027
Skin	0.137	0.057	0.155	0.116	0.052
Small intestine	1.162	0.839	1.098	1.033	0.171
Spinal cord	0.051	0.021	0.060	0.044	0.020
Spleen	19.387	16.090	23.763	19.747	3.849
Stomach	0.243	0.040	0.094	0.126	0.105
Thymus	0.111	0.086	0.102	0.100	0.013
Thyroid	0.395	0.131	0.395	0.307	0.152
Uterus	0.584	0.055	0.223	0.287	0.270
Whole Blood	0.731	0.319	0.833	0.628	0.272
Plasma	1.421	0.574	1.447	1.147	0.496
Blood:plasma ratio	0.51	0.56	0.58	0.55	0.03

090177e195794698\Approved\Approved On: 09-Nov-2020 21:23 (GMT)

Appendix 5 Individual Female Concentration Data
 (continued)

Concentration of Total Radioactivity in Whole Blood, Plasma and Tissues 24 hours Following Single Intramuscular Administration of [³H]-08-A01-C01 to Female Wistar Han Rats

Target Dose Level: 50 µg mRNA/Animal; 1.29 mg Total Lipid/Animal

Results expressed as µg lipid equiv/g (mL)

Sample	037F	038F	039F	Mean	SD
Adipose tissue	0.031	0.042	0.053	0.042	0.011
Adrenal glands	9.718	3.981	9.084	7.595	3.145
Bladder	0.141	0.135	0.235	0.171	0.056
Bone (femur)	0.158	0.105	0.278	0.180	0.089
Bone marrow (femur)	1.180	1.058	1.978	1.405	0.500
Brain	0.040	0.039	0.063	0.047	0.014
Eyes	0.063	0.037	0.057	0.052	0.014
Heart	0.342	0.259	0.355	0.318	0.052
Injection site	2.568	202.540	162.510	122.540	105.810
Kidneys	0.270	0.412	0.361	0.348	0.072
Large intestine	0.561	0.370	0.465	0.466	0.095
Liver	13.368	10.520	21.469	15.119	5.681
Lung	0.519	0.822	0.945	0.762	0.219
Lymph node (Man)	0.259	0.242	0.589	0.363	0.195
Lymph node (Mes)	0.944	0.550	1.095	0.863	0.281
Muscle	0.028	0.114	0.133	0.092	0.056
Ovaries	4.091	5.266	6.363	5.240	1.136
Pancreas	0.176	0.362	0.422	0.320	0.128
Pituitary gland	0.309	0.213	0.379	0.300	0.083
Salivary glands	0.084	0.083	0.119	0.096	0.021
Skin	0.047	0.156	0.151	0.118	0.062
Small intestine	0.748	0.661	0.769	0.726	0.057
Spinal cord	0.047	0.034	0.064	0.048	0.015
Spleen	15.606	12.977	23.440	17.341	5.443
Stomach	0.094	0.054	0.096	0.081	0.024
Thymus	0.154	0.190	0.135	0.159	0.028
Thyroid	0.302	0.294	0.410	0.335	0.065
Uterus	0.307	0.207	0.354	0.289	0.075
Whole Blood	0.475	0.380	0.779	0.544	0.208
Plasma	0.930	0.681	1.223	0.945	0.271
Blood:plasma ratio	0.51	0.56	0.64	0.57	0.06

090177e195794698\Approved\Approved On: 09-Nov-2020 21:23 (GMT)

Appendix 5 Individual Female Concentration Data
 (continued)

Concentration of Total Radioactivity in Whole Blood, Plasma and Tissues 48 hours Following Single Intramuscular Administration of [³H]-08-A01-C01 to Female Wistar Han Rats

Target Dose Level: 50 µg mRNA/Animal; 1.29 mg Total Lipid/Animal

Results expressed as µg lipid equiv/g (mL)

Sample	040F	041F	042F	Mean	SD
Adipose tissue	0.081	0.201	0.414	0.232	0.168
Adrenal glands	12.979	15.142	16.707	14.942	1.872
Bladder	0.234	0.640	0.293	0.389	0.219
Bone (femur)	0.299	1.911	0.351	0.854	0.916
Bone marrow (femur)	2.096	1.993	7.463	3.851	3.129
Brain	0.038	0.046	0.072	0.052	0.018
Eyes	0.064	0.105	0.121	0.097	0.029
Heart	0.352	0.369	0.539	0.420	0.103
Injection site	93.643	27.547	62.073	61.088	33.059
Kidneys	0.314	0.378	0.412	0.368	0.050
Large intestine	1.210	1.507	1.031	1.249	0.241
Liver	24.416	20.707	46.111	30.411	13.722
Lung	0.921	0.719	1.053	0.898	0.168
Lymph node (Man)	0.600	0.516	0.784	0.633	0.137
Lymph node (Mes)	1.557	1.669	1.800	1.675	0.122
Muscle	0.126	0.068	0.119	0.104	0.032
Ovaries	9.305	13.544	13.933	12.261	2.567
Pancreas	0.364	0.298	1.170	0.611	0.485
Pituitary gland	0.910	0.816	0.810	0.845	0.056
Salivary glands	0.200	0.204	0.288	0.231	0.049
Skin	0.303	0.173	0.416	0.297	0.122
Small intestine	1.142	1.461	1.339	1.314	0.161
Spinal cord	0.043	0.075	0.069	0.062	0.017
Spleen	19.456	16.775	45.234	27.155	15.714
Stomach	0.154	0.197	0.233	0.195	0.040
Thymus	0.314	0.248	0.536	0.366	0.151
Thyroid	0.584	0.870	0.512	0.655	0.190
Uterus	0.267	0.521	0.581	0.456	0.167
Whole Blood	0.258	0.338	0.320	0.305	0.042
Plasma	0.429	0.598	0.546	0.524	0.087
Blood:plasma ratio	0.60	0.57	0.59	0.58	0.02

090177e195794698\Approved\Approved On: 09-Nov-2020 21:23 (GMT)

Appendix 6 Individual Male Recovery Data

Recovery of Total Radioactivity in Tissues 0.25 min Following Single Intramuscular Administration of [³H]-08-A01-C01 to Male Wistar Han Rats

Target Dose Level: 50 µg mRNA/Animal; 1.29 mg Total Lipid/Animal

Results expressed as % administered dose

Sample	043M	044M	045M	Mean	SD
Adrenal glands	0.002	0.002	0.000	0.001	0.001
Bladder	0.001	0.000	0.000	0.000	0.000
Brain	0.013	0.014	0.005	0.011	0.005
Eyes	0.001	0.000	0.000	0.000	0.000
Heart	0.056	0.024	0.004	0.028	0.026
Injection site	82.460	6.097	10.103	32.887	42.978
Kidneys	0.103	0.087	0.016	0.069	0.046
Large intestine	0.012	0.018	0.002	0.011	0.008
Liver	1.735	1.083	0.167	0.995	0.787
Lung	0.133	0.082	0.031	0.082	0.051
Pancreas	0.004	0.010	0.001	0.005	0.005
Pituitary gland	0.001	0.000	0.000	0.000	0.000
Prostate	0.002	0.002	0.000	0.001	0.001
Salivary glands	0.007	0.005	0.001	0.004	0.003
Small intestine	0.051	0.040	0.005	0.032	0.024
Spinal cord	0.002	0.001	0.000	0.001	0.001
Spleen	0.020	0.019	0.003	0.014	0.009
Stomach	0.008	0.013	0.002	0.008	0.006
Testes	0.012	0.008	0.001	0.007	0.005
Thymus	0.005	0.010	0.001	0.005	0.005
Thyroid	0.000	0.000	0.000	0.000	0.000

090177e195794698\Approved\Approved On: 09-Nov-2020 21:23 (GMT)

**Appendix 6 Individual Male Recovery Data
 (continued)**

**Recovery of Total Radioactivity in Tissues 1 hour Following Single
 Intramuscular Administration of [³H]-08-A01-C01 to Male Wistar Han
 Rats**

Target Dose Level: 50 µg mRNA/Animal; 1.29 mg Total Lipid/Animal

Results expressed as % administered dose

Sample	046M	047M	048M	Mean	SD
Adrenal glands	0.001	0.003	0.002	0.002	0.001
Bladder	0.001	0.001	0.000	0.001	0.000
Brain	0.005	0.014	0.013	0.010	0.005
Eyes	0.000	0.000	0.001	0.000	0.000
Heart	0.015	0.036	0.045	0.032	0.015
Injection site	74.148	46.614	85.725	68.829	20.090
Kidneys	0.047	0.086	0.098	0.077	0.027
Large intestine	0.016	0.017	0.021	0.018	0.002
Liver	2.218	2.607	3.676	2.834	0.755
Lung	0.043	0.131	0.081	0.085	0.044
Pancreas	0.004	0.009	0.006	0.006	0.003
Pituitary gland	0.000	0.000	0.000	0.000	0.000
Prostate	0.001	0.002	0.001	0.001	0.001
Salivary glands	0.003	0.005	0.006	0.005	0.002
Small intestine	0.102	0.133	0.136	0.124	0.019
Spinal cord	0.001	0.000	0.001	0.001	0.000
Spleen	0.115	0.063	0.082	0.087	0.026
Stomach	0.007	0.019	0.023	0.016	0.008
Testes	0.007	0.009	0.013	0.010	0.003
Thymus	0.008	0.004	0.007	0.006	0.002
Thyroid	0.000	0.001	0.000	0.000	0.000

090177e195794698\Approved\Approved On: 09-Nov-2020 21:23 (GMT)

**Appendix 6 Individual Male Recovery Data
(continued)****Recovery of Total Radioactivity in Tissues 2 hours Following Single Intramuscular Administration of [³H]-08-A01-C01 to Male Wistar Han Rats****Target Dose Level: 50 µg mRNA/Animal; 1.29 mg Total Lipid/Animal****Results expressed as % administered dose**

Sample	049M	050M	051M	Mean	SD
Adrenal glands	0.006	0.003	0.005	0.005	0.001
Bladder	0.001	0.001	0.001	0.001	0.000
Brain	0.033	0.013	0.016	0.021	0.011
Eyes	0.001	0.000	0.002	0.001	0.001
Heart	0.109	0.036	0.051	0.065	0.039
Injection site	53.157	53.477	10.525	39.053	24.707
Kidneys	0.203	0.096	0.148	0.149	0.054
Large intestine	0.063	0.035	0.063	0.054	0.016
Liver	10.166	4.262	8.460	7.629	3.038
Lung	0.313	0.094	0.160	0.189	0.113
Pancreas	0.011	0.006	0.028	0.015	0.012
Pituitary gland	0.000	0.000	0.000	0.000	0.000
Prostate	0.002	0.002	0.003	0.002	0.000
Salivary glands	0.010	0.004	0.008	0.007	0.003
Small intestine	0.418	0.305	0.336	0.353	0.058
Spinal cord	0.001	0.001	0.002	0.001	0.001
Spleen	0.296	0.101	0.299	0.232	0.114
Stomach	0.034	0.017	0.047	0.033	0.015
Testes	0.027	0.008	0.017	0.017	0.009
Thymus	0.010	0.005	0.008	0.008	0.002
Thyroid	0.001	0.001	0.000	0.001	0.000

**Appendix 6 Individual Male Recovery Data
 (continued)**

Recovery of Total Radioactivity in Tissues 4 hours Following Single Intramuscular Administration of [³H]-08-A01-C01 to Male Wistar Han Rats

Target Dose Level: 50 µg mRNA/Animal; 1.29 mg Total Lipid/Animal

Results expressed as % administered dose

Sample	052M	053M	054M	Mean	SD
Adrenal glands	0.013	0.009	0.014	0.012	0.002
Bladder	0.001	0.002	0.001	0.001	0.000
Brain	0.019	0.015	0.029	0.021	0.007
Eyes	0.002	0.002	0.001	0.002	0.001
Heart	0.071	0.033	0.096	0.067	0.032
Injection site	61.619	36.450	45.061	47.710	12.792
Kidneys	0.151	0.088	0.169	0.136	0.042
Large intestine	0.271	0.219	0.216	0.236	0.031
Liver	12.655	13.898	18.528	15.027	3.095
Lung	0.356	0.080	0.241	0.226	0.139
Pancreas	0.007	0.020	0.011	0.013	0.007
Pituitary gland	0.001	0.001	0.000	0.001	0.000
Prostate	0.003	0.002	0.003	0.003	0.001
Salivary glands	0.009	0.007	0.012	0.009	0.002
Small intestine	0.632	0.499	0.737	0.623	0.120
Spinal cord	0.002	0.004	0.002	0.003	0.001
Spleen	0.309	0.410	0.334	0.351	0.052
Stomach	0.053	0.027	0.033	0.037	0.013
Testes	0.028	0.021	0.039	0.030	0.009
Thymus	0.010	0.011	0.033	0.018	0.013
Thyroid	0.001	0.001	0.001	0.001	0.000

090177e195794698\Approved\Approved On: 09-Nov-2020 21:23 (GMT)

**Appendix 6 Individual Male Recovery Data
 (continued)**

Recovery of Total Radioactivity in Tissues 8 hours Following Single Intramuscular Administration of [³H]-08-A01-C01 to Male Wistar Han Rats

Target Dose Level: 50 µg mRNA/Animal; 1.29 mg Total Lipid/Animal

Results expressed as % administered dose

Sample	055M	056M	057M	Mean	SD
Adrenal glands	0.013	0.023	0.042	0.026	0.015
Bladder	N.S.	0.001	0.002	0.002	N.A.
Brain	0.014	0.013	0.014	0.014	0.001
Eyes	N.S.	0.001	0.002	0.002	N.A.
Heart	0.071	0.051	0.061	0.061	0.010
Injection site	18.863	19.984	17.346	18.731	1.324
Kidneys	0.114	0.107	0.108	0.109	0.004
Large intestine	0.536	0.424	0.430	0.463	0.063
Liver	17.280	17.862	29.414	21.519	6.844
Lung	0.226	0.146	0.169	0.180	0.042
Pancreas	0.010	0.021	0.012	0.014	0.006
Pituitary gland	0.000	0.000	0.001	0.000	0.000
Prostate	0.004	0.002	0.001	0.003	0.001
Salivary glands	0.008	0.006	0.007	0.007	0.001
Small intestine	0.850	1.034	1.031	0.972	0.106
Spinal cord	0.001	0.001	0.001	0.001	0.000
Spleen	1.037	1.022	1.293	1.118	0.152
Stomach	0.043	0.026	0.097	0.055	0.037
Testes	0.034	0.022	0.045	0.034	0.012
Thymus	0.013	0.010	0.012	0.012	0.001
Thyroid	0.001	0.001	0.001	0.001	0.000

N.S. = No sample due to oxidiser failure

N.A. = Not applicable

090177e195794698\Approved\Approved On: 09-Nov-2020 21:23 (GMT)

**Appendix 6 Individual Male Recovery Data
 (continued)**

Recovery of Total Radioactivity in Tissues 24 hours Following Single Intramuscular Administration of [³H]-08-A01-C01 to Male Wistar Han Rats

Target Dose Level: 50 µg mRNA/Animal; 1.29 mg Total Lipid/Animal

Results expressed as % administered dose

Sample	058M	059M	060M	Mean	SD
Adrenal glands	0.052	0.059	0.137	0.083	0.047
Bladder	0.002	0.002	0.002	0.002	0.000
Brain	0.006	0.013	0.017	0.012	0.006
Eyes	0.002	0.002	0.004	0.002	0.001
Heart	0.051	0.026	0.026	0.035	0.014
Injection site	39.854	26.623	29.394	31.957	6.978
Kidneys	0.075	0.053	0.075	0.068	0.012
Large intestine	0.332	0.895	2.045	1.091	0.873
Liver	14.444	16.303	28.957	19.901	7.897
Lung	0.109	0.118	0.179	0.136	0.038
Pancreas	0.007	0.017	0.015	0.013	0.005
Pituitary gland	0.000	0.000	0.000	0.000	0.000
Prostate	0.003	0.004	0.005	0.004	0.001
Salivary glands	0.005	0.008	0.012	0.008	0.004
Small intestine	0.693	1.198	1.934	1.275	0.624
Spinal cord	0.001	0.002	0.002	0.001	0.001
Spleen	0.977	0.660	1.234	0.957	0.287
Stomach	0.021	0.033	0.107	0.054	0.046
Testes	0.057	0.058	0.105	0.074	0.028
Thymus	0.007	0.010	0.009	0.009	0.002
Thyroid	0.001	0.001	0.001	0.001	0.000

090177e195794698\Approved\Approved On: 09-Nov-2020 21:23 (GMT)

**Appendix 6 Individual Male Recovery Data
(continued)****Recovery of Total Radioactivity in Tissues 48 hours Following Single Intramuscular Administration of [³H]-08-A01-C01 to Male Wistar Han Rats****Target Dose Level: 50 µg mRNA/Animal; 1.29 mg Total Lipid/Animal****Results expressed as % administered dose**

Sample	061M	062M	063M	Mean	SD
Adrenal glands	0.078	0.157	0.078	0.104	0.046
Bladder	0.001	0.002	0.002	0.002	0.000
Brain	0.006	0.016	0.012	0.011	0.005
Eyes	0.002	0.003	0.003	0.003	0.000
Heart	0.024	0.055	0.037	0.039	0.016
Injection site	49.053	18.355	31.059	32.823	15.425
Kidneys	0.045	0.104	0.063	0.071	0.031
Large intestine	0.541	0.624	1.264	0.810	0.395
Liver	12.962	17.164	11.734	13.953	2.848
Lung	0.088	0.173	0.133	0.131	0.043
Pancreas	0.010	0.013	0.023	0.015	0.007
Pituitary gland	0.000	0.000	0.000	0.000	0.000
Prostate	0.002	0.004	0.004	0.003	0.001
Salivary glands	0.010	0.012	0.008	0.010	0.002
Small intestine	0.635	1.258	1.020	0.971	0.314
Spinal cord	0.001	0.001	0.002	0.001	0.001
Spleen	0.544	1.271	0.926	0.914	0.364
Stomach	0.027	0.065	0.056	0.049	0.019
Testes	0.053	0.109	0.060	0.074	0.030
Thymus	0.004	0.012	0.009	0.008	0.004
Thyroid	0.001	0.002	0.001	0.001	0.001

Appendix 7 Individual Female Recovery Data**Recovery of Total Radioactivity in Tissues 0.25 min Following Single Intramuscular Administration of [³H]-08-A01-C01 to Female Wistar Han Rats****Target Dose Level: 50 µg mRNA/Animal; 1.29 mg Total Lipid/Animal****Results expressed as % administered dose**

Sample	022F	023F	024F	Mean	SD
Adrenal glands	0.003	*0.000	0.001	°0.001	°0.002
Bladder	0.000	*0.000	0.000	°0.000	°0.000
Brain	0.005	*0.000	0.002	°0.002	°0.002
Eyes	0.000	*0.000	0.000	°0.000	°0.000
Heart	0.017	*0.000	0.006	°0.008	°0.008
Injection site	8.145	11.578	0.723	6.815	5.549
Kidneys	0.063	0.012	0.014	0.030	0.028
Large intestine	0.010	*0.000	0.002	°0.004	°0.005
Liver	0.435	0.010	0.180	0.209	0.214
Lung	0.051	0.001	0.013	0.022	0.026
Ovaries	0.002	*0.000	0.001	°0.001	°0.001
Pancreas	0.002	0.000	0.001	0.001	0.001
Pituitary gland	0.000	*0.000	0.000	°0.000	°0.000
Salivary glands	0.004	*0.000	0.001	°0.002	°0.002
Small intestine	0.038	*0.001	0.005	°0.015	°0.020
Spinal cord	0.000	*0.000	0.000	°0.000	°0.000
Spleen	0.014	*0.000	0.017	°0.011	°0.009
Stomach	0.007	*0.000	0.002	°0.003	°0.003
Thymus	0.005	*0.000	0.002	°0.002	°0.002
Thyroid	0.000	*0.000	0.000	°0.000	°0.000
Uterus	0.004	*0.000	0.002	°0.002	°0.002

* = Results calculated from data less than 30 cpm above background

° = Mean includes results calculated from data less than 30 cpm above background

**Appendix 7 Individual Female Recovery Data
(continued)****Recovery of Total Radioactivity in Tissues 1 hour Following Single Intramuscular Administration of [³H]-08-A01-C01 to Female Wistar Han Rats****Target Dose Level: 50 µg mRNA/Animal; 1.29 mg Total Lipid/Animal****Results expressed as % administered dose**

Sample	025F	026F	027F	Mean	SD
Adrenal glands	0.010	0.011	0.015	0.012	0.003
Bladder	0.001	0.001	0.001	0.001	0.000
Brain	0.013	0.019	0.015	0.016	0.003
Eyes	0.001	0.001	0.001	0.001	0.000
Heart	0.066	0.109	0.062	0.079	0.026
Injection site	10.609	47.776	50.847	36.411	22.398
Kidneys	0.162	0.250	0.102	0.171	0.074
Large intestine	0.030	0.035	0.029	0.032	0.003
Liver	3.586	2.713	2.421	2.907	0.606
Lung	0.112	0.131	0.106	0.117	0.013
Ovaries	0.012	0.010	0.004	0.009	0.004
Pancreas	0.009	0.009	0.007	0.008	0.001
Pituitary gland	0.000	0.001	0.001	0.001	0.000
Salivary glands	0.008	0.009	0.006	0.008	0.002
Small intestine	0.153	0.130	0.121	0.135	0.017
Spinal cord	0.002	0.002	0.001	0.002	0.001
Spleen	0.082	0.099	0.112	0.098	0.015
Stomach	0.024	0.021	0.023	0.022	0.002
Thymus	0.007	0.013	0.004	0.008	0.005
Thyroid	0.001	0.001	0.001	0.001	0.000
Uterus	0.008	0.010	0.015	0.011	0.004

**Appendix 7 Individual Female Recovery Data
(continued)****Recovery of Total Radioactivity in Tissues 2 hours Following Single Intramuscular Administration of [³H]-08-A01-C01 to Female Wistar Han Rats****Target Dose Level: 50 µg mRNA/Animal; 1.29 mg Total Lipid/Animal****Results expressed as % administered dose**

Sample	028F	029F	030F	Mean	SD
Adrenal glands	0.010	0.022	0.012	0.015	0.006
Bladder	0.000	0.001	0.001	0.001	0.001
Brain	0.008	0.034	0.014	0.019	0.014
Eyes	0.001	0.003	0.000	0.001	0.001
Heart	0.028	0.201	0.077	0.102	0.089
Injection site	0.018	0.236	72.027	24.094	41.511
Kidneys	0.056	0.264	0.497	0.272	0.221
Large intestine	0.018	0.142	0.065	0.075	0.063
Liver	3.203	12.436	5.452	7.030	4.815
Lung	0.080	0.311	0.110	0.167	0.125
Ovaries	0.003	0.012	0.009	0.008	0.004
Pancreas	0.003	0.022	0.010	0.012	0.010
Pituitary gland	0.000	0.002	0.000	0.001	0.001
Salivary glands	0.005	0.015	0.007	0.009	0.006
Small intestine	0.205	0.367	0.283	0.285	0.081
Spinal cord	0.002	0.004	0.001	0.002	0.002
Spleen	0.063	1.010	0.180	0.418	0.516
Stomach	0.027	0.057	0.022	0.035	0.019
Thymus	0.003	0.028	0.004	0.012	0.014
Thyroid	0.000	0.002	0.001	0.001	0.001
Uterus	0.008	0.025	0.011	0.015	0.009

**Appendix 7 Individual Female Recovery Data
(continued)****Recovery of Total Radioactivity in Tissues 4 hours Following Single Intramuscular Administration of [³H]-08-A01-C01 to Female Wistar Han Rats****Target Dose Level: 50 µg mRNA/Animal; 1.29 mg Total Lipid/Animal****Results expressed as % administered dose**

Sample	031F	032F	033F	Mean	SD
Adrenal glands	0.011	0.019	0.023	0.018	0.006
Bladder	0.000	0.001	0.001	0.001	0.000
Brain	0.005	0.007	0.020	0.011	0.008
Eyes	0.001	0.001	0.001	0.001	0.000
Heart	0.013	0.046	0.097	0.052	0.042
Injection site	2.619	19.042	5.508	9.056	8.768
Kidneys	0.031	0.062	0.154	0.082	0.064
Large intestine	0.111	0.136	0.198	0.148	0.045
Liver	5.207	8.846	12.045	8.699	3.421
Lung	0.054	0.093	0.188	0.112	0.069
Ovaries	0.003	0.022	0.022	0.016	0.011
Pancreas	0.016	0.009	0.027	0.017	0.009
Pituitary gland	0.000	0.000	0.001	0.000	0.000
Salivary glands	0.003	0.005	0.011	0.006	0.005
Small intestine	0.354	0.435	0.596	0.462	0.123
Spinal cord	0.001	0.001	0.003	0.002	0.001
Spleen	0.390	0.421	0.447	0.419	0.028
Stomach	0.014	0.022	0.029	0.022	0.008
Thymus	0.004	0.007	0.006	0.006	0.002
Thyroid	0.000	0.001	0.001	0.001	0.000
Uterus	0.005	0.004	0.016	0.008	0.007

**Appendix 7 Individual Female Recovery Data
(continued)****Recovery of Total Radioactivity in Tissues 8 hours Following Single Intramuscular Administration of [³H]-08-A01-C01 to Female Wistar Han Rats****Target Dose Level: 50 µg mRNA/Animal; 1.29 mg Total Lipid/Animal****Results expressed as % administered dose**

Sample	034F	035F	036F	Mean	SD
Adrenal glands	0.048	0.031	0.051	0.043	0.011
Bladder	0.000	0.000	0.001	0.000	0.000
Brain	0.007	0.004	0.009	0.007	0.002
Eyes	0.001	0.000	0.001	0.001	0.000
Heart	0.029	0.010	0.027	0.022	0.011
Injection site	10.296	26.182	38.500	24.993	14.139
Kidneys	0.056	0.022	0.042	0.040	0.017
Large intestine	0.409	0.233	0.397	0.346	0.098
Liver	13.264	12.033	18.443	14.580	3.402
Lung	0.089	0.028	0.074	0.064	0.031
Ovaries	0.022	0.010	0.042	0.025	0.016
Pancreas	0.034	0.002	0.011	0.016	0.016
Pituitary gland	0.000	0.000	0.000	0.000	0.000
Salivary glands	0.005	0.002	0.003	0.003	0.001
Small intestine	0.718	0.308	0.714	0.580	0.235
Spinal cord	0.001	0.000	0.001	0.001	0.000
Spleen	0.853	0.601	1.082	0.845	0.241
Stomach	0.043	0.005	0.023	0.024	0.019
Thymus	0.004	0.002	0.003	0.003	0.001
Thyroid	0.001	0.000	0.001	0.000	0.000
Uterus	0.030	0.004	0.014	0.016	0.013

**Appendix 7 Individual Female Recovery Data
 (continued)**

Recovery of Total Radioactivity in Tissues 24 hours Following Single Intramuscular Administration of [³H]-08-A01-C01 to Female Wistar Han Rats

Target Dose Level: 50 µg mRNA/Animal; 1.29 mg Total Lipid/Animal

Results expressed as % administered dose

Sample	037F	038F	039F	Mean	SD
Adrenal glands	0.064	0.032	0.050	0.049	0.016
Bladder	0.001	0.001	0.001	0.001	0.000
Brain	0.005	0.006	0.009	0.007	0.002
Eyes	0.001	0.001	0.001	0.001	0.000
Heart	0.019	0.014	0.020	0.018	0.003
Injection site	0.444	39.677	38.765	26.295	22.392
Kidneys	0.029	0.053	0.035	0.039	0.013
Large intestine	0.334	0.283	0.263	0.293	0.037
Liver	9.112	9.776	14.042	10.977	2.675
Lung	0.053	0.071	0.072	0.065	0.010
Ovaries	0.031	0.038	0.043	0.037	0.006
Pancreas	0.005	0.007	0.014	0.009	0.004
Pituitary gland	0.000	0.000	0.000	0.000	0.000
Salivary glands	0.003	0.003	0.004	0.003	0.001
Small intestine	0.575	0.601	0.432	0.536	0.091
Spinal cord	0.001	0.001	0.001	0.001	0.000
Spleen	0.591	0.508	0.955	0.685	0.237
Stomach	0.019	0.011	0.029	0.020	0.009
Thymus	0.003	0.005	0.003	0.004	0.001
Thyroid	0.000	0.000	0.001	0.000	0.000
Uterus	0.027	0.009	0.017	0.018	0.009

090177e195794698\Approved\Approved On: 09-Nov-2020 21:23 (GMT)

**Appendix 7 Individual Female Recovery Data
 (continued)**

Recovery of Total Radioactivity in Tissues 48 hours Following Single Intramuscular Administration of [³H]-08-A01-C01 to Female Wistar Han Rats

Target Dose Level: 50 µg mRNA/Animal; 1.29 mg Total Lipid/Animal

Results expressed as % administered dose

Sample	040F	041F	042F	Mean	SD
Adrenal glands	0.085	0.126	0.114	0.108	0.021
Bladder	0.001	0.004	0.002	0.002	0.001
Brain	0.005	0.006	0.010	0.007	0.002
Eyes	0.001	0.003	0.003	0.002	0.001
Heart	0.018	0.017	0.024	0.020	0.004
Injection site	20.139	5.852	23.287	16.426	9.292
Kidneys	0.036	0.045	0.044	0.042	0.005
Large intestine	0.570	0.928	0.644	0.714	0.189
Liver	15.122	13.811	26.137	18.357	6.770
Lung	0.066	0.066	0.076	0.070	0.006
Ovaries	0.075	0.113	0.097	0.095	0.019
Pancreas	0.011	0.007	0.050	0.023	0.024
Pituitary gland	0.001	0.001	0.000	0.001	0.000
Salivary glands	0.007	0.005	0.009	0.007	0.002
Small intestine	0.540	0.825	0.729	0.698	0.145
Spinal cord	0.001	0.002	0.001	0.001	0.000
Spleen	0.772	0.848	1.818	1.146	0.583
Stomach	0.023	0.028	0.035	0.029	0.006
Thymus	0.007	0.005	0.009	0.007	0.002
Thyroid	0.001	0.001	0.001	0.001	0.000
Uterus	0.010	0.031	0.025	0.022	0.010

090177e195794698\Approved\Approved On: 09-Nov-2020 21:23 (GMT)

Appendix 8 Individual Male 100 µg mRNA data

Concentration of Total Radioactivity in Whole Blood, Plasma and Tissues 0.25 min Following Single Intramuscular Administration of [³H]-08-A01-C01 to Male Wistar Han Rats

Target Dose Level: 100 µg mRNA/Animal; 2.57 mg Total Lipid/Animal

Results expressed as µg lipid equiv/g (mL)

Sample	001M	002M	003M	Mean	SD
Adipose tissue	0.075	0.108	0.018	0.067	0.046
Adrenal glands	0.193	0.192	0.184	0.190	0.005
Bladder	0.035	0.079	0.026	0.047	0.028
Bone (femur)	0.195	0.054	0.044	0.098	0.085
Bone marrow (femur)	0.312	0.163	0.229	0.234	0.075
Brain	0.050	0.047	0.046	0.048	0.002
Eyes	0.015	0.021	0.007	0.014	0.007
Heart	0.394	0.365	0.460	0.406	0.048
Injection site	16.832	24.313	179.840	73.662	92.030
Kidneys	0.576	0.552	0.273	0.467	0.169
Large intestine	0.016	0.012	0.051	0.026	0.022
Liver	0.963	0.503	0.670	0.712	0.233
Lung	0.689	0.497	0.410	0.532	0.143
Lymph node (Man)	0.043	0.046	0.042	0.044	0.002
Lymph node (Mes)	0.045	0.020	0.018	0.028	0.015
Muscle	0.035	0.040	0.285	0.120	0.143
Pancreas	0.088	0.068	0.068	0.075	0.012
Pituitary gland	0.787	0.796	0.225	0.603	0.327
Prostate	0.035	0.045	0.047	0.042	0.006
Salivary glands	0.087	0.087	0.049	0.074	0.022
Skin	2.094	3.233	12.691	6.499	6.668
Small intestine	0.046	0.030	0.016	0.031	0.015
Spinal cord	0.091	0.064	0.068	0.074	0.015
Spleen	0.426	1.463	0.221	0.704	0.666
Stomach	0.032	0.026	*0.007	°0.022	°0.013
Testes	0.033	0.030	0.020	0.028	0.007
Thymus	0.121	0.161	0.216	0.166	0.048
Thyroid	0.175	0.498	0.105	0.259	0.209
Whole Blood	2.291	2.426	1.678	2.132	0.398
Plasma	5.640	5.530	3.924	5.031	0.960
Blood:plasma ratio	0.41	0.44	0.43	0.42	0.02

*=Results calculated from data less than 30 cpm above background

°=Mean includes results calculated from data less than 30 cpm above background

090177e195794698\Approved\Approved On: 09-Nov-2020 21:23 (GMT)

Appendix 8 Individual Male 100 µg mRNA Data
 (continued)

Concentration of Total Radioactivity in Whole Blood, Plasma and Tissues 1 hour Following Single Intramuscular Administration of [3H]-08-A01-C01 to Male Wistar Han Rats

Target Dose Level: 100 µg mRNA/Animal; 2.57 mg Total Lipid/Animal

Results expressed as µg lipid equiv/g (mL)

Sample	004M	005M	006M	Mean	SD
Adipose tissue	0.193	0.307	0.350	0.283	0.081
Adrenal glands	1.775	1.877	2.208	1.953	0.227
Bladder	0.224	0.098	0.264	0.195	0.086
Bone (femur)	1.102	0.530	0.566	0.733	0.320
Bone marrow (femur)	2.111	4.732	2.456	3.100	1.424
Brain	0.253	0.297	0.296	0.282	0.025
Eyes	0.229	0.070	0.093	0.131	0.086
Heart	1.948	3.461	2.496	2.635	0.766
Injection site	152.370	78.654	150.890	127.300	42.139
Kidneys	3.017	3.096	3.170	3.094	0.077
Large intestine	0.090	0.091	0.152	0.111	0.035
Liver	13.805	10.906	16.323	13.678	2.711
Lung	3.523	3.532	2.901	3.319	0.362
Lymph node (Man)	0.366	0.379	0.437	0.394	0.038
Lymph node (Mes)	0.268	0.412	0.389	0.356	0.077
Muscle	0.184	0.213	0.195	0.198	0.015
Pancreas	0.335	0.375	0.469	0.393	0.069
Pituitary gland	1.389	1.810	1.717	1.639	0.221
Prostate	0.328	0.363	0.380	0.357	0.027
Salivary glands	0.471	0.613	0.493	0.526	0.076
Skin	3.043	0.407	1.179	1.543	1.355
Small intestine	0.393	3.191	3.563	2.382	1.733
Spinal cord	0.216	0.356	0.303	0.292	0.071
Spleen	4.066	4.402	4.868	4.445	0.402
Stomach	0.332	2.377	8.099	3.603	4.026
Testes	0.185	0.196	0.486	0.289	0.171
Thymus	0.332	0.343	0.596	0.424	0.149
Thyroid	1.219	1.909	1.266	1.465	0.385
Whole Blood	7.985	11.835	10.357	10.059	1.942
Plasma	23.703	26.782	26.070	25.518	1.612
Blood:plasma ratio	0.34	0.44	0.40	0.39	0.05

090177e195794698\Approved\Approved On: 09-Nov-2020 21:23 (GMT)

Appendix 8 Individual Male 100 µg mRNA Data
(continued)**Concentration of Total Radioactivity in Whole Blood, Plasma and Tissues 2 hours Following Single Intramuscular Administration of [³H]-08-A01-C01 to Male Wistar Han Rats****Target Dose Level: 100 µg mRNA/Animal; 2.57 mg Total Lipid/Animal****Results expressed as µg lipid equiv/g (mL)**

Sample	007M	008M	009M	Mean	SD
Adipose tissue	0.311	0.211	0.486	0.336	0.140
Adrenal glands	3.152	3.337	2.559	3.016	0.406
Bladder	0.310	0.241	0.479	0.343	0.122
Bone (femur)	0.835	0.462	0.385	0.561	0.241
Bone marrow (femur)	3.322	2.694	2.057	2.691	0.632
Brain	0.348	0.310	0.250	0.302	0.049
Eyes	0.126	0.104	0.064	0.098	0.031
Heart	2.866	3.359	3.481	3.235	0.326
Injection site	6.971	61.485	30.751	33.069	27.331
Kidneys	2.887	2.858	2.679	2.808	0.113
Large intestine	0.283	0.125	0.148	0.185	0.085
Liver	33.320	24.542	22.034	26.632	5.926
Lung	3.839	2.982	3.769	3.530	0.476
Lymph node (Man)	0.784	0.413	0.474	0.557	0.199
Lymph node (Mes)	0.859	0.503	0.333	0.565	0.268
Muscle	0.220	0.182	0.189	0.197	0.020
Pancreas	0.595	0.512	0.557	0.554	0.041
Pituitary gland	1.998	1.921	1.729	1.883	0.139
Prostate	0.458	0.354	0.461	0.424	0.061
Salivary glands	0.740	0.597	0.539	0.625	0.104
Skin	0.524	0.353	0.454	0.444	0.086
Small intestine	1.147	0.887	0.755	0.930	0.199
Spinal cord	0.396	0.373	0.360	0.377	0.018
Spleen	14.103	8.227	7.803	10.044	3.521
Stomach	0.234	0.142	0.143	0.173	0.053
Testes	0.239	0.402	0.317	0.320	0.081
Thymus	0.447	0.424	0.371	0.414	0.039
Thyroid	1.906	1.397	1.481	1.595	0.273
Whole Blood	11.413	10.005	10.736	10.718	0.704
Plasma	25.479	22.927	22.340	23.582	1.669
Blood:plasma ratio	0.45	0.44	0.48	0.45	0.02

090177e195794698\Approved\Approved On: 09-Nov-2020 21:23 (GMT)

**Appendix 8 Individual Male 100 µg mRNA Data
 (continued)**

**Concentration of Total Radioactivity in Whole Blood, Plasma and
 Tissues 4 hours Following Single Intramuscular Administration of
 [³H]-08-A01-C01 to Male Wistar Han Rats**

Target Dose Level: 100 µg mRNA/Animal; 2.57 mg Total Lipid/Animal

Results expressed as µg lipid equiv/g (mL)

Sample	010M	011M	012M	Mean	SD
Adipose tissue	0.222	0.262	0.105	0.196	0.082
Adrenal glands	5.481	2.469	2.491	3.480	1.732
Bladder	0.237	0.151	0.156	0.181	0.048
Bone (femur)	1.452	1.249	0.348	1.016	0.588
Bone marrow (femur)	1.880	3.875	1.459	2.405	1.291
Brain	0.373	0.123	0.090	0.195	0.155
Eyes	0.095	0.056	0.042	0.065	0.027
Heart	1.233	1.095	1.064	1.131	0.090
Injection site	55.286	464.630	257.860	259.260	204.680
Kidneys	2.190	1.607	1.007	1.601	0.591
Large intestine	0.180	0.713	0.338	0.410	0.274
Liver	38.606	14.955	19.426	24.329	12.565
Lung	1.255	3.060	1.398	1.904	1.003
Lymph node (Man)	0.694	0.271	0.242	0.402	0.253
Lymph node (Mes)	0.970	0.427	0.502	0.633	0.294
Muscle	0.129	0.076	0.085	0.097	0.029
Pancreas	0.189	0.419	0.299	0.302	0.115
Pituitary gland	0.870	0.599	0.480	0.649	0.200
Prostate	0.244	0.133	0.133	0.170	0.064
Salivary glands	0.334	0.192	0.170	0.232	0.089
Skin	0.931	0.178	2.172	1.094	1.007
Small intestine	0.758	1.381	1.189	1.110	0.319
Spinal cord	0.154	0.094	0.111	0.120	0.031
Spleen	9.286	27.731	9.780	15.599	10.510
Stomach	0.057	0.131	0.302	0.163	0.125
Testes	0.397	0.134	0.110	0.214	0.159
Thymus	0.164	0.229	0.185	0.193	0.033
Thyroid	1.256	0.565	0.742	0.854	0.359
Whole Blood	4.741	2.416	2.502	3.220	1.318
Plasma	11.200	5.253	5.862	7.438	3.272
Blood:plasma ratio	0.42	0.46	0.43	0.44	0.02

090177e195794698\Approved\Approved On: 09-Nov-2020 21:23 (GMT)

Appendix 8 Individual Male 100 µg mRNA Data
 (continued)

Concentration of Total Radioactivity in Whole Blood, Plasma and Tissues 8 hours Following Single Intramuscular Administration of [3H]-08-A01-C01 to Male Wistar Han Rats

Target Dose Level: 100 µg mRNA/Animal; 2.57 mg Total Lipid/Animal

Results expressed as µg lipid equiv/g (mL)

Sample	013M	014M	015M	Mean	SD
Adipose tissue	0.134	0.147	0.269	0.184	0.075
Adrenal glands	6.445	9.564	32.615	16.208	14.294
Bladder	0.741	0.264	0.499	0.501	0.238
Bone (femur)	0.835	0.274	0.855	0.655	0.330
Bone marrow (femur)	1.920	1.495	2.225	1.880	0.367
Brain	0.165	0.120	0.214	0.166	0.047
Eyes	0.188	0.146	0.229	0.188	0.041
Heart	2.084	1.104	2.398	1.862	0.675
Injection site	126.340	106.800	2.416	78.521	66.629
Kidneys	2.145	1.122	1.472	1.580	0.520
Large intestine	1.713	1.199	1.781	1.564	0.318
Liver	34.463	41.789	61.002	45.751	13.706
Lung	2.999	1.707	3.360	2.689	0.869
Lymph node (Man)	1.158	0.644	1.099	0.967	0.282
Lymph node (Mes)	1.076	1.409	1.701	1.395	0.313
Muscle	0.158	0.096	0.196	0.150	0.051
Pancreas	0.433	0.326	0.579	0.446	0.127
Pituitary gland	0.858	0.517	0.994	0.790	0.246
Prostate	0.314	0.176	0.386	0.292	0.107
Salivary glands	0.242	0.168	0.386	0.265	0.111
Skin	0.295	0.285	0.547	0.376	0.148
Small intestine	2.012	1.963	1.865	1.946	0.075
Spinal cord	0.185	0.148	0.252	0.195	0.053
Spleen	24.956	16.693	35.344	25.664	9.345
Stomach	0.113	0.187	2.187	0.829	1.177
Testes	0.269	0.328	0.361	0.319	0.047
Thymus	0.110	0.295	0.481	0.295	0.185
Thyroid	1.544	0.885	2.170	1.533	0.642
Whole Blood	3.450	2.106	4.202	3.253	1.062
Plasma	7.541	4.597	8.168	6.768	1.907
Blood:plasma ratio	0.46	0.46	0.51	0.48	0.03

090177e195794698\Approved\Approved On: 09-Nov-2020 21:23 (GMT)

**Appendix 8 Individual Male 100 µg mRNA Data
 (continued)**

**Concentration of Total Radioactivity in Whole Blood, Plasma and
 Tissues 24 hours Following Single Intramuscular Administration of
 [³H]-08-A01-C01 to Male Wistar Han Rats**

Target Dose Level: 100 µg mRNA/Animal; 2.57 mg Total Lipid/Animal

Results expressed as µg lipid equiv/g (mL)

Sample	016M	017M	018M	Mean	SD
Adipose tissue	0.268	0.219	0.261	0.249	0.027
Adrenal glands	63.795	42.538	52.924	53.085	10.629
Bladder	0.609	0.643	0.373	0.542	0.147
Bone (femur)	1.254	2.075	0.950	1.426	0.582
Bone marrow (femur)	5.002	4.711	7.513	5.742	1.541
Brain	0.186	0.221	0.255	0.221	0.034
Eyes	0.342	0.247	0.360	0.316	0.061
Heart	1.613	1.877	1.760	1.750	0.132
Injection site	50.606	70.405	268.240	129.750	120.340
Kidneys	1.971	1.774	2.460	2.068	0.353
Large intestine	5.083	2.282	3.210	3.525	1.427
Liver	51.485	71.224	45.827	56.179	13.334
Lung	3.831	3.615	3.360	3.602	0.236
Lymph node (Man)	3.227	1.555	1.570	2.117	0.961
Lymph node (Mes)	5.835	3.496	3.765	4.366	1.279
Muscle	0.208	0.263	0.247	0.239	0.028
Pancreas	0.767	0.966	0.781	0.838	0.111
Pituitary gland	1.320	1.362	1.603	1.428	0.152
Prostate	0.407	0.446	0.481	0.445	0.037
Salivary glands	0.617	0.561	0.701	0.626	0.071
Skin	0.833	0.937	0.645	0.805	0.148
Small intestine	3.736	3.157	3.433	3.442	0.289
Spinal cord	0.229	0.200	0.326	0.252	0.066
Spleen	47.746	74.940	44.431	55.706	16.739
Stomach	0.572	0.802	0.489	0.621	0.162
Testes	0.638	0.502	0.616	0.585	0.073
Thymus	0.473	0.568	0.506	0.516	0.048
Thyroid	1.845	1.890	2.651	2.129	0.453
Whole Blood	2.448	1.756	3.404	2.536	0.827
Plasma	5.639	5.297	8.191	6.376	1.581
Blood:plasma ratio	0.43	0.33	0.42	0.39	0.05

090177e195794698\Approved\Approved On: 09-Nov-2020 21:23 (GMT)

Appendix 8 Individual Male 100 µg mRNA Data
 (continued)

Concentration of Total Radioactivity in Whole Blood, Plasma and Tissues 48 hours Following Single Intramuscular Administration of [3H]-08-A01-C01 to Male Wistar Han Rats

Target Dose Level: 100 µg mRNA/Animal; 2.57 mg Total Lipid/Animal

Results expressed as µg lipid equiv/g (mL)

Sample	019M	020M	Mean
Adipose tissue	0.276	0.234	0.255
Adrenal glands	52.496	45.684	49.090
Bladder	0.779	0.849	0.814
Bone (femur)	0.639	0.867	0.753
Bone marrow (femur)	3.233	2.890	3.062
Brain	0.477	0.173	0.325
Eyes	0.239	0.260	0.249
Heart	1.132	1.158	1.145
Injection site	48.800	59.876	54.338
Kidneys	0.971	1.131	1.051
Large intestine	4.144	2.190	3.167
Liver	48.512	36.690	42.601
Lung	1.853	2.477	2.165
Lymph node (Man)	2.418	1.157	1.788
Lymph node (Mes)	5.067	3.297	4.182
Muscle	0.166	0.926	0.546
Pancreas	0.540	0.701	0.620
Pituitary gland	0.987	0.884	0.936
Prostate	0.308	0.285	0.296
Salivary glands	0.488	0.588	0.538
Skin	0.640	0.699	0.670
Small intestine	3.644	3.750	3.697
Spinal cord	0.212	0.237	0.224
Spleen	35.545	33.899	34.722
Stomach	0.794	1.011	0.903
Testes	0.523	0.555	0.539
Thymus	0.514	0.655	0.584
Thyroid	1.604	1.523	1.564
Whole Blood	0.967	1.011	0.989
Plasma	1.451	1.493	1.472
Blood:plasma ratio	0.67	0.68	0.67

090177e195794698\Approved\Approved On: 09-Nov-2020 21:23 (GMT)

**Appendix 8 Individual Male 100 µg mRNA Data
(continued)****Recovery of Total Radioactivity in Tissues 0.25 min Following Single Intramuscular Administration of [³H]-08-A01-C01 to Male Wistar Han Rats****Target Dose Level: 100 µg mRNA/Animal; 2.57 mg Total Lipid/Animal****Results expressed as % administered dose**

Sample	001M	002M	003M	Mean	SD
Adrenal glands	0.000	0.000	0.000	0.000	0.000
Bladder	0.000	0.000	0.000	0.000	0.000
Brain	0.003	0.003	0.003	0.003	0.000
Eyes	0.000	0.000	0.000	0.000	0.000
Heart	0.011	0.009	0.017	0.013	0.004
Injection site	1.865	3.345	18.252	7.821	9.064
Kidneys	0.037	0.033	0.019	0.030	0.010
Large intestine	0.006	0.004	0.018	0.009	0.008
Liver	0.368	0.185	0.278	0.277	0.091
Lung	0.028	0.017	0.023	0.023	0.005
Pancreas	0.001	0.001	0.002	0.001	0.000
Pituitary gland	0.000	0.000	0.000	0.000	0.000
Prostate	0.000	0.000	0.000	0.000	0.000
Salivary glands	0.001	0.002	0.001	0.001	0.000
Small intestine	0.016	0.009	0.006	0.010	0.005
Spinal cord	0.001	0.001	0.000	0.001	0.000
Spleen	0.010	0.026	0.006	0.014	0.011
Stomach	0.005	0.004	*0.002	°0.003	°0.002
Testes	0.004	0.003	0.003	0.003	0.001
Thymus	0.003	0.003	0.004	0.003	0.001
Thyroid	0.000	0.000	0.000	0.000	0.000

* = Results calculated from data less than 30 cpm above background

° = Mean includes results calculated from data less than 30 cpm above background

**Appendix 8 Individual Male 100 µg mRNA Data
(continued)****Recovery of Total Radioactivity in Tissues 1 hour Following Single
Intramuscular Administration of [³H]-08-A01-C01 to Male Wistar Han
Rats****Target Dose Level: 100 µg mRNA/Animal; 2.57 mg Total Lipid/Animal****Results expressed as % administered dose**

Sample	004M	005M	006M	Mean	SD
Adrenal glands	0.005	0.003	0.004	0.004	0.001
Bladder	0.001	0.000	0.001	0.001	0.000
Brain	0.019	0.020	0.020	0.019	0.001
Eyes	0.002	0.001	0.001	0.001	0.001
Heart	0.049	0.103	0.074	0.075	0.027
Injection site	15.619	13.609	16.094	15.107	1.319
Kidneys	0.191	0.176	0.188	0.185	0.008
Large intestine	0.024	0.027	0.050	0.034	0.014
Liver	5.198	3.856	5.564	4.873	0.899
Lung	0.148	0.159	0.103	0.137	0.030
Pancreas	0.004	0.006	0.007	0.006	0.002
Pituitary gland	0.000	0.000	0.000	0.000	0.000
Prostate	0.003	0.003	0.003	0.003	0.000
Salivary glands	0.007	0.009	0.011	0.009	0.002
Small intestine	0.132	1.003	1.062	0.732	0.521
Spinal cord	0.001	0.003	0.001	0.002	0.001
Spleen	0.090	0.087	0.089	0.089	0.001
Stomach	0.075	0.362	1.259	0.565	0.618
Testes	0.020	0.021	0.057	0.033	0.021
Thymus	0.007	0.005	0.006	0.006	0.001
Thyroid	0.001	0.001	0.001	0.001	0.000

**Appendix 8 Individual Male Recovery Data
 (continued)**

Recovery of Total Radioactivity in Tissues 2 hours Following Single Intramuscular Administration of [³H]-08-A01-C01 to Male Wistar Han Rats

Target Dose Level: 100 µg mRNA/Animal; 2.57 mg Total Lipid/Animal

Results expressed as % administered dose

Sample	007M	008M	009M	Mean	SD
Adrenal glands	0.008	0.006	0.007	0.007	0.001
Bladder	0.001	0.001	0.001	0.001	0.000
Brain	0.024	0.021	0.018	0.021	0.003
Eyes	0.001	0.001	0.001	0.001	0.000
Heart	0.078	0.095	0.115	0.096	0.019
Injection site	0.598	9.070	3.532	4.400	4.302
Kidneys	0.180	0.148	0.160	0.163	0.016
Large intestine	0.088	0.038	0.055	0.061	0.025
Liver	11.802	8.114	8.654	9.523	1.992
Lung	0.147	0.112	0.153	0.137	0.022
Pancreas	0.008	0.007	0.011	0.009	0.002
Pituitary gland	0.001	0.000	0.000	0.000	0.000
Prostate	0.003	0.004	0.004	0.004	0.001
Salivary glands	0.012	0.010	0.013	0.011	0.002
Small intestine	0.434	0.294	0.281	0.336	0.085
Spinal cord	0.003	0.004	0.002	0.003	0.001
Spleen	0.271	0.155	0.192	0.206	0.059
Stomach	0.036	0.023	0.026	0.028	0.007
Testes	0.025	0.045	0.036	0.035	0.010
Thymus	0.010	0.008	0.007	0.008	0.001
Thyroid	0.001	0.001	0.001	0.001	0.000

090177e195794698\Approved\Approved On: 09-Nov-2020 21:23 (GMT)

Appendix 8 Individual Male Recovery Data
 (continued)

Recovery of Total Radioactivity in Tissues 4 hours Following Single Intramuscular Administration of [³H]-08-A01-C01 to Male Wistar Han Rats

Target Dose Level: 100 µg mRNA/Animal; 2.57 mg Total Lipid/Animal

Results expressed as % administered dose

Sample	010M	011M	012M	Mean	SD
Adrenal glands	0.010	0.005	0.005	0.007	0.003
Bladder	0.001	0.000	0.000	0.001	0.000
Brain	0.027	0.009	0.006	0.014	0.011
Eyes	0.001	0.001	0.000	0.001	0.000
Heart	0.031	0.043	0.033	0.036	0.007
Injection site	5.231	59.191	24.168	29.530	27.377
Kidneys	0.141	0.101	0.058	0.100	0.041
Large intestine	0.062	0.258	0.123	0.147	0.100
Liver	13.675	6.428	7.436	9.180	3.926
Lung	0.079	0.141	0.069	0.096	0.039
Pancreas	0.003	0.008	0.006	0.006	0.003
Pituitary gland	0.000	0.000	0.000	0.000	0.000
Prostate	0.002	0.001	0.001	0.001	0.001
Salivary glands	0.005	0.003	0.003	0.004	0.001
Small intestine	0.234	0.614	0.356	0.401	0.194
Spinal cord	0.001	0.001	0.001	0.001	0.000
Spleen	0.177	0.530	0.167	0.291	0.207
Stomach	0.007	0.035	0.043	0.028	0.019
Testes	0.048	0.017	0.012	0.026	0.019
Thymus	0.003	0.005	0.003	0.003	0.001
Thyroid	0.001	0.000	0.001	0.001	0.000

090177e195794698\Approved\Approved On: 09-Nov-2020 21:23 (GMT)

**Appendix 8 Individual Male Recovery Data
 (continued)**

Recovery of Total Radioactivity in Tissues 8 hours Following Single Intramuscular Administration of [³H]-08-A01-C01 to Male Wistar Han Rats

Target Dose Level: 100 µg mRNA/Animal; 2.57 mg Total Lipid/Animal

Results expressed as % administered dose

Sample	013M	014M	015M	Mean	SD
Adrenal glands	0.025	0.021	0.080	0.042	0.033
Bladder	0.002	0.001	0.001	0.001	0.001
Brain	0.012	0.009	0.014	0.012	0.003
Eyes	0.002	0.001	0.002	0.002	0.001
Heart	0.058	0.035	0.081	0.058	0.023
Injection site	8.806	17.803	0.313	8.974	8.746
Kidneys	0.134	0.073	0.091	0.099	0.031
Large intestine	0.511	0.398	0.634	0.514	0.118
Liver	11.864	16.293	24.504	17.553	6.414
Lung	0.192	0.129	0.197	0.172	0.038
Pancreas	0.005	0.006	0.012	0.007	0.004
Pituitary gland	0.000	0.000	0.000	0.000	0.000
Prostate	0.002	0.001	0.003	0.002	0.001
Salivary glands	0.004	0.003	0.008	0.005	0.003
Small intestine	0.585	0.529	0.633	0.582	0.052
Spinal cord	0.002	0.001	0.002	0.002	0.000
Spleen	0.560	0.369	0.848	0.592	0.241
Stomach	0.021	0.019	0.288	0.109	0.155
Testes	0.031	0.036	0.038	0.035	0.004
Thymus	0.002	0.004	0.007	0.004	0.002
Thyroid	0.001	0.001	0.001	0.001	0.000

090177e195794698\Approved\Approved On: 09-Nov-2020 21:23 (GMT)

**Appendix 8 Individual Male Recovery Data
 (continued)**

Recovery of Total Radioactivity in Tissues 24 hours Following Single Intramuscular Administration of [³H]-08-A01-C01 to Male Wistar Han Rats

Target Dose Level: 100 µg mRNA/Animal; 2.57 mg Total Lipid/Animal

Results expressed as % administered dose

Sample	016M	017M	018M	Mean	SD
Adrenal glands	0.137	0.095	0.106	0.113	0.022
Bladder	0.003	0.002	0.001	0.002	0.001
Brain	0.012	0.015	0.019	0.015	0.003
Eyes	0.004	0.002	0.004	0.003	0.001
Heart	0.038	0.052	0.051	0.047	0.008
Injection site	3.590	15.406	29.435	16.144	12.938
Kidneys	0.107	0.104	0.165	0.125	0.034
Large intestine	1.668	0.752	0.996	1.139	0.475
Liver	22.736	26.544	20.865	23.382	2.894
Lung	0.170	0.160	0.226	0.185	0.036
Pancreas	0.010	0.016	0.012	0.013	0.003
Pituitary gland	0.000	0.000	0.000	0.000	0.000
Prostate	0.003	0.004	0.004	0.004	0.000
Salivary glands	0.011	0.010	0.011	0.010	0.001
Small intestine	1.194	0.896	1.321	1.137	0.218
Spinal cord	0.002	0.001	0.002	0.002	0.001
Spleen	1.003	1.590	1.111	1.234	0.312
Stomach	0.066	0.099	0.065	0.077	0.019
Testes	0.070	0.056	0.075	0.067	0.010
Thymus	0.007	0.009	0.007	0.008	0.002
Thyroid	0.001	0.001	0.001	0.001	0.000

090177e195794698\Approved\Approved On: 09-Nov-2020 21:23 (GMT)

**Appendix 8 Individual Male Recovery Data
(continued)****Recovery of Total Radioactivity in Tissues 48 hours Following Single Intramuscular Administration of [³H]-08-A01-C01 to Male Wistar Han Rats****Target Dose Level: 100 µg mRNA/Animal; 2.57 mg Total Lipid/Animal****Results expressed as % administered dose**

Sample	019M	020M	Mean
Adrenal glands	0.155	0.112	0.134
Bladder	0.002	0.002	0.002
Brain	0.034	0.012	0.023
Eyes	0.002	0.003	0.002
Heart	0.030	0.031	0.030
Injection site	2.978	10.414	6.696
Kidneys	0.063	0.076	0.070
Large intestine	1.070	0.719	0.894
Liver	17.436	16.159	16.797
Lung	0.071	0.132	0.102
Pancreas	0.007	0.006	0.006
Pituitary gland	0.000	0.000	0.000
Prostate	0.003	0.002	0.003
Salivary glands	0.008	0.009	0.008
Small intestine	0.790	1.021	0.905
Spinal cord	0.002	0.002	0.002
Spleen	0.886	0.649	0.768
Stomach	0.044	0.047	0.046
Testes	0.064	0.054	0.059
Thymus	0.006	0.005	0.006
Thyroid	0.001	0.001	0.001

2.4 NONCLINICAL OVERVIEW

090177e1962c108d\Approved\Approved On: 08-Feb-2021 15:26 (GMT)

TABLE OF CONTENTS

2.4 NONCLINICAL OVERVIEW	1
LIST OF ABBREVIATIONS AND DEFINITION OF TERMS	4
2.4.1. OVERVIEW OF NONCLINICAL TESTING STRATEGY	6
Table 2.4.1-1. Nomenclature of the Vaccine Candidates	6
Table 2.4.1-2. Nonclinical Studies	8
2.4.2. PHARMACOLOGY	10
2.4.2.1. Primary Pharmacodynamics	10
2.4.2.1.1. Summary	10
2.4.2.1.2. BNT162b2, A Lipid Nanoparticle Encapsulated RNA Vaccine Encoding the SARS-CoV-2 P2 S as a Vaccine Antigen.....	10
Figure 2.4.2-1. Schematic of the Organization of the SARS-CoV-2 S Glycoprotein	11
2.4.2.1.3. Immunogenicity of BNT162b2 (V9) in Mice	11
2.4.2.1.4. Evaluation of BNT162b2 (V9) Immunogenicity and Protection Against SARS-CoV-2 Challenge in Rhesus Macaques.....	12
2.4.2.1.5. Immunogenicity Testing After Weekly Immunization of Rats in GLP Compliant Repeat Dose Toxicology Studies and a Developmental and Reproductive Toxicity Study.....	13
2.4.2.2. Secondary Pharmacodynamics	14
2.4.2.3. Safety Pharmacology	14
2.4.2.4. Pharmacodynamic Drug Interactions	14
2.4.3. PHARMACOKINETICS	15
2.4.3.1. Brief Summary	15
2.4.3.2. Methods of Analysis	15
2.4.3.3. Absorption	16
2.4.3.3.1. In Vitro Absorption	16
2.4.3.3.2. Single-Dose Pharmacokinetics	16
Table 2.4.3-1. PK of ALC-0315 and ALC-0159 in Wistar Han Rats After IV Administration of LNPs Containing Surrogate Luciferase RNA at 1 mg/kg.....	16
Figure 2.4.3-1. Plasma and Liver Concentrations of ALC-0315 and ALC-0159 in Wistar Han Rats After IV Administration of LNPs Containing Surrogate Luciferase RNA at 1 mg/kg.....	16
2.4.3.4. Distribution	17
Figure 2.4.3-2. Bioluminescence Emission in BALB/c Mice after IM Injection of an LNP Formulation of modRNA Encoding Luciferase.....	17

BNT162b2

Module 2.4. Nonclinical Overview

2.4.3.5. Metabolism 18

Figure 2.4.3-3. Proposed Biotransformation Pathway of ALC-0315 in Various Species 19

Figure 2.4.3-4. Proposed Biotransformation Pathway of ALC-0159 in Various Species 20

2.4.3.6. Excretion 20

2.4.3.7. Pharmacokinetic Drug Interactions 20

2.4.4. TOXICOLOGY 21

2.4.4.1. Brief Summary 21

Table 2.4.4-1. Overview of Toxicity Testing Program 22

2.4.4.2. Single-Dose Toxicity 23

2.4.4.3. Repeat-Dose Toxicity 23

 2.4.4.3.1. Repeat-Dose Toxicity Study of Three LNP-Formulated RNA Platforms
 Encoding for Viral Proteins by Repeated Intramuscular Administration to Wistar Han
 Rats..... 23

 2.4.4.3.2. 17-Day Intramuscular Toxicity Study of BNT162b2 (V9) in Wistar Han
 Rats with a 3-week Recovery..... 26

2.4.4.4. Genotoxicity 29

2.4.4.5. Carcinogenicity 29

2.4.4.6. Reproductive and Developmental Toxicity 29

2.4.4.7. Local Tolerance 30

2.4.4.8. Other Toxicity Studies 30

 2.4.4.8.1. Phototoxicity 30

 2.4.4.8.2. Antigenicity 30

 2.4.4.8.3. Immunotoxicity 30

 2.4.4.8.4. Mechanistic Studies 30

 2.4.4.8.5. Dependence 31

 2.4.4.8.6. Studies on Metabolites 31

 2.4.4.8.7. Studies on Impurities 31

 2.4.4.8.8. Other Studies 31

2.4.4.9. Target Organ Toxicity 31

2.4.5. INTEGRATED OVERVIEW AND CONCLUSIONS 32

2.4.6. LIST OF LITERATURE REFERENCES 34

090177e1962c108d\Approved\Approved On: 08-Feb-2021 15:26 (GMT)

LIST OF ABBREVIATIONS AND DEFINITION OF TERMS

A:G	Albumin:globulin ratio
ACE	Angiotension-converting enzyme
ADME	Absorption, distribution, metabolism, excretion
ALC-0159	Proprietary PEG-lipid included as an excipient in the LNP formulation used in BNT162b2
ALC-0315	Proprietary amino-lipid included as an excipient in the LNP formulation used in BNT162b2
ALT	Alanine aminotransferase
AST	Aspartate aminotransferase
BAL	Bronchoalveolar lavage
CAS	Chemical abstracts service
CBER	Center for Biologics Evaluation and Research
CD	Cluster of differentiation
COVID-19	Coronavirus Disease 2019
DART	Developmental and reproductive toxicity
DNA	Deoxyribonucleic acid
DSPC	1,2-distearoyl-sn-glycero-3-phosphocholine
ELISA	Enzyme-linked immunosorbent assay
EUA	Emergency Use Authorization
F0	Parental generation administered vaccine
F1	First generation offspring of F0 generation
GD	Gestation day
GGT	Gamma-glutamyl transferase
GLP	Good Laboratory Practice
H	Human (in metabolite scheme)
[³ H]-CHE	Radiolabeled [Cholesteryl-1,2- ³ H(N)]-Cholesteryl Hexadecyl Ether
HGB	Hemoglobin
IFN	Interferon
IgG	Immunoglobulin G
IL	Interleukin
IM	Intramuscular(ly)
IND	Investigational New Drug Application
IV	Intravenous(ly)
LC/MS	Liquid chromatography-tandem mass spectrometry
LD	Lactation day
LNP	Lipid-nanoparticle
Luc	Luciferase (from firefly <i>Pyroactomena lucifera</i>)
LUC	Large unstained cell
Mk	Monkey (in metabolite scheme)
Mo	Mouse (in metabolite scheme)
modRNA	Nucleoside-modified mRNA
mRNA	Messenger RNA
NA	Not applicable

090177e1962c108d\Approved\Approved On: 08-Feb-2021 15:26 (GMT)

LIST OF ABBREVIATIONS AND DEFINITION OF TERMS - CONTINUED

NHP	Nonhuman primate
OECD	Organisation for Economic Co-operation and Development
P2 S	Spike protein P2 mutant
PEG	Polyethylene glycol
PK	Pharmacokinetics
PLT	Platelet
PND	Postnatal day
PT	Prothrombin time
QC	Quality control review
QW	Once weekly
R	Rat (in metabolite scheme)
RBC	Red blood cell
RBD	Receptor binding domain
RdRp	RNA-dependent RNA-polymerase
RDW	Red cell distribution width
RETIC	Reticulocyte
RNA	Ribonucleic acid
RT-PCR	Reverse transcription-polymerase chain reaction
S	SARS-CoV-2 spike glycoprotein
S1	S1 domain of the SARS-CoV-2 spike glycoprotein
S9	Supernatant fraction obtained from liver homogenate by centrifuging at 9000 g
SARS	Severe Acute Respiratory Syndrome
SARS-CoV-2	Severe acute respiratory syndrome coronavirus 2; coronavirus causing COVID-19
Tfh	T follicular helper cell
Th1	Type 1 T helper cells
TK	Toxicokinetic
TNF	Tumor necrosis factor
V8	Variant 8; P2 S
V9	Variant 9; P2 S
WBC	White blood cell
WHO	World Health Organization

2.4.1. OVERVIEW OF NONCLINICAL TESTING STRATEGY

BNT162b2 (BioNTech code number BNT162, Pfizer code number PF-07302048) is an investigational vaccine intended to prevent COVID-19, which is caused by SARS-CoV-2. BNT162b2 is a nucleoside modified mRNA (modRNA) expressing full-length S with two proline mutations (P2) to lock the transmembrane protein in an antigenically optimal prefusion conformation (Pallesen et al, 2017; Wrapp et al, 2020). The vaccine is formulated in lipid nanoparticles (LNPs). The LNP is composed of 4 lipids: ALC-0315, ALC-0159, DSPC, and cholesterol. Other excipients in the formulation include sucrose, NaCl, KCl, Na₂HPO₄, and KH₂PO₄. The dose selected for BNT162b2, with efficacy demonstrated in Phase 2/3 clinical evaluation and intended for commercial use, is 30 µg administered IM as two doses given 21 days apart.

In nonclinical studies, two variants of BNT162b2 were tested; designated “variant 8” and “variant 9” (V8 and V9, respectively). The variants differ only in their codon optimization sequences which are designed to improve antigen expression, otherwise the amino acid sequences of the encoded antigens are identical. Only BNT162b2 (V9) has been evaluated in the clinic, is currently authorized under EUA, and is the subject of this BLA application. The characteristics of each variant are described in the table below (Table 2.4.1-1).

Table 2.4.1-1. Nomenclature of the Vaccine Candidates

Product Code	RNA Platform	Antigen Variant	Description/Translated Protein	Variant Code	GLP Tox Data	Clinical Candidate
BNT162b2	modRNA	V8 ^a	P2 S	RBP020.1	Yes	No
BNT162b2	modRNA	V9^a	P2 S	RBP020.2	Yes	Yes

a. The V8 and V9 variants of the P2 S antigen have the same amino acid sequence. Different codon optimizations were used for their ribonucleotide sequences.

Bold: BNT162b2 (V9) vaccine candidate submitted for licensure.

The primary pharmacology, distribution, metabolism, and safety of BNT162b2 were evaluated in nonclinical pharmacology, pharmacokinetic, and toxicity studies in vitro and in vivo (Table 2.4.1-2).

Immunogenicity of BNT162b2 was evaluated in mice (2.4.2.1.3), rats (2.4.2.1.5) and nonhuman primates (2.4.2.1.4). For assessment of serum antibody responses in mice and rats, S1 and RBD-binding IgG responses were tested by an ELISA. Functional antibody responses were tested by a SARS-CoV-2 pseudotype neutralization assay (pVNT). In nonhuman primate studies, S1-binding IgG responses were tested in a direct Luminex-based immunoassay (dLIA) and functional antibody responses were assessed in a SARS-CoV-2 neutralization assay. S-specific T cell responses were assessed in mouse and nonhuman primate studies in an IFNγ ELISpot and by intracellular cytokine staining flow cytometry-based analysis of the Th1/Th2 profile using splenocytes.

A SARS-CoV-2 challenge study in BNT162b2 (V9)-immunized nonhuman primates was also conducted to assess protection against infection and to demonstrate lack of disease enhancement (Section 2.4.2.1.4.2).

Platform properties that support BNT162b2 were initially demonstrated with non-SARS-CoV-2 antigens. Non-GLP in vivo testing of an LNP-formulated modRNA encoding luciferase examined biodistribution in BALB/c mice and Wistar Han rats after IM injection (Section 2.4.3.4) and the PK of the two novel excipients in the LNP formulation, ALC-0315 and ALC-0159, in Wistar Han rats (Section 2.4.3.3). In addition, the metabolism of ALC-0315 and ALC-0159 was evaluated in mouse, rat, monkey, and human blood, liver microsomes, S9 fractions, and hepatocytes and in vivo in rat plasma, urine, feces, and liver samples from the PK study (Table 2.4.1-2; Section 2.4.3.5).

BNT162b2 (V8) and (V9) have been studied in GLP-compliant repeat-dose toxicity studies in rats (Table 2.4.1-2). Two GLP repeat-dose toxicity studies for BNT162b2 (V8) and BNT162b2 (V9), one study for each variant, have been completed. The study designs are described in Section 2.4.4 and are based on WHO guidelines for vaccine development (WHO, 2005). A DART study with BNT162b2 (V9) in rats has also been completed. No additional toxicity studies are planned for BNT162b2.

IM administration was chosen for the toxicity studies as this is the intended route of administration. Rats were chosen for toxicity assessments as they are a commonly used animal species for the evaluation of toxicity, and they mount an antigen-specific immune response to vaccination with BNT162b2.

The design of the nonclinical repeat-dose toxicity studies was consistent with the WHO Guidelines on Nonclinical Evaluation of Vaccines, the EMA Note for Guidance on Preclinical Pharmacological and Toxicological Testing of Vaccines, and Japan guidance on the nonclinical safety assessment of vaccines. In addition, the 2020 CBER guidance on “Development and Licensure of Vaccines to Prevent COVID-19” (US FDA, 2020) was considered when assembling the nonclinical safety licensure package as well as feedback from regulatory agencies. All GLP-compliant studies were conducted in accordance with Good Laboratory Practice for Nonclinical Laboratory Studies, Code of US Federal Regulations (21 CFR Part 58), in an OECD Mutual Acceptance of Data member state. All nonclinical studies described herein were conducted by or for Pfizer Inc or BioNTech RNA Pharmaceuticals GmbH. The location of records for inspection is included in each final study report.

090177e1962c108d\Approved\Approved On: 08-Feb-2021 15:26 (GMT)

Table 2.4.1-2. Nonclinical Studies

Study Number	Study Type	Species / Test System	Test Item	Dose [RNA]	Cross reference
Pharmacology - BNT162b2 studies					
R-20-0085	In vivo immunogenicity	BALB/c mice	BNT162b2 (V9)	0.2, 1, 5 µg	Section 2.4.2.1.3
R-20-0112	In vivo immunogenicity	BALB/c mice	BNT162a1, BNT162b1, BNT162b2 (V9), BNT162c2	5 µg	Section 2.4.2.1.3
R-20-0211	In vitro protein expression	Cell culture	BNT162b2 (V9)	varied	Section 2.4.2.1.2
VR-VTR-10741	In vitro protein expression	Cell culture	BNT162b2 (V9)	varied	Section 2.4.2.1.2
VR-VTR-10671	In vivo immunogenicity and SARS-CoV-2 challenge	Rhesus macaques	BNT162b2 (V9)	30 and 100 µg	Section 2.4.2.1.4
ADME					
PF-07302048_06Jul20_072424	PK of ALC-0315 and ALC-0159	Wistar Han Rats	modRNA encoding luciferase formulated in LNP comparable to BNT162b2	1 mg/kg	Section 2.4.3.3
R-20-0072	In vivo distribution	BALB/c mice	modRNA encoding luciferase formulated in LNP comparable to BNT162b2	2 µg	Section 2.4.3.4
185350	In vivo distribution	Wistar Han Rats	modRNA encoding luciferase formulated in LNP comparable to BNT162b2 with trace amounts of [³ H]-CHE as non-diffusible label	50 µg	Section 2.4.3.4
01049-20008	In vitro metabolism	CD-1/ICR mouse, Wistar Han and/or Sprague Dawley rat, cynomolgus monkey and human liver microsomes, S9 fraction, hepatocytes	ALC-0315	NA	Section 2.4.3.5
01049-20009					
01049-20010					
01049-20020			ALC-0159	NA	
01049-20021					
01049-20022					

090177e1962c108d\Approved\Approved On: 08-Feb-2021 15:26 (GMT)

BNT162b2

Module 2.4. Nonclinical Overview

Table 2.4.1-2. Nonclinical Studies - Continued

Study Number	Study Type	Species / Test System	Test Item	Dose [RNA]	Cross reference
PF-07302048 _05Aug20_043725	In vitro and in vivo metabolism	Blood, liver S9 fractions and hepatocytes from CD-1 mouse, Wistar Han rat, cynomolgus monkey and human. In vivo samples from Wistar Han rat plasma, urine, feces, and liver	In vitro: ALC-0315 and ALC-0159 In vivo: modRNA encoding luciferase formulated in LNP comparable to BNT162b2	1 mg/kg modRNA (in vivo samples)	Section 2.4.3.5
Toxicology – Studies with BNT162b2 variants					
38166	Repeat-dose toxicity	Wistar Han Rats	BNT162b2 (V8)	100 µg	Section 2.4.4.3
20GR142	Repeat-dose toxicity	Wistar Han Rats	BNT162b2 (V9)	30 µg	Section 2.4.4.3
20256434	Development and Reproductive Toxicity	Wistar Han Rats	BNT162b2 (V9)	30 µg	Section 2.4.4.6

090177e1962c108d\Approved\Approved On: 08-Feb-2021 15:26 (GMT)

2.4.2. PHARMACOLOGY

2.4.2.1. Primary Pharmacodynamics

2.4.2.1.1. Summary

BNT162b2 (BioNTech code number BNT162, Pfizer code number PF-07302048) is a nucleoside-modified mRNA (modRNA) vaccine that encodes the SARS-CoV-2 full-length spike glycoprotein (S). The glycoprotein encoded by both BNT162b2 variants includes two amino acid substitutions to proline (P2 S) locking the transmembrane protein in an antigenically optimal prefusion conformation (Wrapp et al, 2020; Pallesen et al, 2017). The RNA is formulated with functional and structural lipids, which protect the RNA from degradation and enable transfection of the RNA into host cells after IM injection. S is a major target of virus neutralizing antibodies and is a key antigen for vaccine development. The well-resolved trimeric prefusion structure and the high affinity binding to ACE2 and human neutralizing antibodies demonstrate that the recombinant P2 S authentically presents the ACE2 binding site and other epitopes targeted by many SARS-CoV-2 neutralizing antibodies.

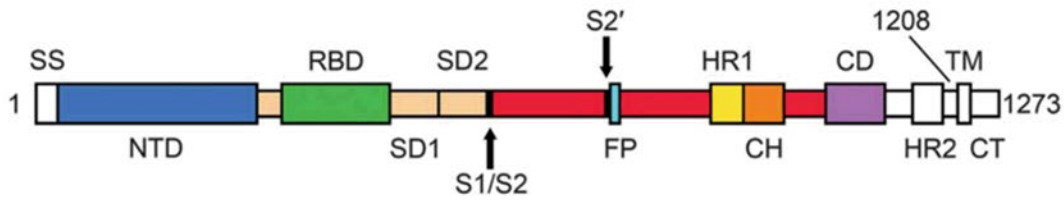
In vitro studies and in vivo studies in mice and nonhuman primates demonstrate the mechanism of action for this RNA-based vaccine, which is to encode SARS-CoV-2 S that induces an immune response characterized by both a strong neutralizing antibody response and Th1-type CD4⁺ and an IFN γ ⁺ CD8⁺ T-cell response. BNT162b2 immunization protected rhesus macaques from infectious SARS-CoV-2 challenge, with reduced detection of viral RNA in vaccine-immunized animals compared to saline-immunized animals and with no evidence of clinical exacerbation.

2.4.2.1.2. BNT162b2, A Lipid Nanoparticle Encapsulated RNA Vaccine Encoding the SARS-CoV-2 P2 S as a Vaccine Antigen

BNT162b2 is based on a nucleoside-modified mRNA (modRNA) platform technology. Vaccination with modRNA formulated in LNPs is characterized by strong expansion of Th1-skewed antigen-specific T follicular helper (Tfh) cells, which stimulate and expand germinal center B cells, thereby resulting in particularly strong, long lived, high-affinity antibody responses (Sahin et al, 2014; Pardi et al, 2018). ModRNA vaccine candidates against other infectious diseases induce strong antibody responses and prime and expand multifunctional CD4⁺ and CD8⁺ T cells (Pardi et al, 2017; Pardi et al, 2018).

SARS-CoV-2 S is a large, trimeric glycoprotein that exists predominantly in a prefusion conformation on the virion (Ke et al, 2020). It is cleaved by furin into an N-terminal S1 and a C-terminal S2 fragment. S attaches to the host cell receptor, ACE2, by its receptor binding domain which is contained in the S1 furin cleavage fragment. Spontaneously and during cell entry, the S1 fragment dissociates, and the S2 fragment undergoes a fold-back rearrangement to the post-fusion conformation in a process that facilitates fusion of viral and host cell membranes. S is the main target of virus neutralizing antibodies (Zakhartchouk et al, 2007; Yong et al, 2019). Most of the antibodies with SARS-CoV-2 neutralizing activity are directed against the RBD (Jiang et al, 2020; Zost et al, 2020).

090177e1962c108d\Approved\Approved On: 08-Feb-2021 15:26 (GMT)

Figure 2.4.2-1. Schematic of the Organization of the SARS-CoV-2 S Glycoprotein

The S1 furin cleavage fragment includes the signal sequence (SS), the N terminal domain (NTD), the receptor binding domain (RBD, which binds the human cellular receptor, ACE-2), subdomain 1 (SD1), and subdomain 2 (SD2). The furin cleavage site (S1/S2) separates S1 from the S2 fragment, which contains the S2 protease cleavage site (S2') followed by a fusion peptide (FP), heptad repeats (HR1 and HR2), a central helix (CH) domain, the connector domain (CD), the transmembrane domain (TM) and a cytoplasmic tail (CT).

Source: modified from [Wrapp et al, 2020](#).

BNT162b2 (V9) encodes a full-length P2 S transmembrane protein that contains two consecutive prolines introduced at amino acid positions 986 and 987, between the central helix (CH) and heptad repeat 1 (HR1) (Figure 2.4.2-1) ([Wrapp et al, 2020](#); [Pallesen et al, 2017](#)). Two codon optimized forms of the coding sequence for this antigen were tested preclinically and were designated “variant 8” and “variant 9” (V8 and V9), with the vaccine candidate tested clinically and being proposed for licensure or authorization, V9, expressed from a codon optimized RNA gene with a higher content of cytosine ribonucleotides for increased protein expression. The RNA-expressed P2 S is membrane bound and elicits a potent humoral neutralizing antibody response and Th1-type CD4⁺ and CD8⁺ cellular response to block virus infection and kill virus infected cells, respectively.

Efficient in vitro expression of the P2 S protein was demonstrated following in vitro transfection of cells with BNT162b2 RNA drug substance and BNT162b2 drug product. Electron cryomicroscopy analysis of purified recombinant P2 S, expressed from DNA encoding the same S amino acid sequence as BNT162b2 RNA (except for the addition of a C-terminal tag for protein purification) revealed high similarity to previously reported structures ([Cai et al, 2020](#)). The well-resolved trimeric prefusion structure and the high affinity binding to ACE2 and human neutralizing antibodies demonstrate that the recombinant full-length P2 S protein authentically presents the ACE-2 binding site.

2.4.2.1.3. Immunogenicity of BNT162b2 (V9) in Mice

BNT162b2 was highly immunogenic in mice with strong antigen-binding IgG and high titer neutralizing antibody responses together with a Th1-phenotype CD4⁺ response as well as an IFN γ ⁺, IL-2⁺ CD8⁺ T-cell response after a single immunization. Total IgG ELISA showed that the vaccine induced a strong, dose-dependent IgG response that recognizes S1 and the RBD and elicited high neutralizing titers in a pseudotype neutralization assay.

Stimulation of fresh splenocytes, collected 28 days after immunization, with an S protein specific overlapping peptide pool demonstrated robust CD4⁺ and CD8⁺ T-cell IFN γ responses and a Th1-dominant profile was demonstrated in quantification of cytokines (IL-2 and IFN γ) in the corresponding culture supernatants.

In summary, BNT162b2 induced a strong, neutralizing antibody response. CD4⁺ and CD8⁺ T-cell responses were detectable 12 and 28 days after one immunization and exhibited a Th1-dominant T cell response characteristic of RNA-based vaccines.

2.4.2.1.4. Evaluation of BNT162b2 (V9) Immunogenicity and Protection Against SARS-CoV-2 Challenge in Rhesus Macaques

BNT162b2 was assessed for immunogenicity and for protection against an infectious SARS-CoV-2 challenge in rhesus macaques. SARS-CoV-2 infection in humans manifests as both asymptomatic infection and as the disease COVID-19, with diverse signs, symptoms, and levels of severity. Based on published reports, SARS-CoV-2 challenged rhesus macaques develop an acute, transient infection in the upper and lower respiratory tract and have evidence of viral replication in the gastrointestinal tract, similar to humans (Zou et al, 2020; Kim et al, 2020). Varying degrees of pulmonary inflammation, primarily at the peak of infection at approximately Day 2 to 4 post-challenge, have been reported in the literature (Munster et al, 2020). The human and rhesus ACE-2 receptor have 100% amino acid identity at the critical binding residues, which may account for the fidelity of this SARS-CoV-2 animal model (Zhou et al, 2020).

2.4.2.1.4.1. Immunogenicity in Rhesus Macaques

Rhesus macaques immunized IM with 30 µg or 100 µg of BNT162b2 on Days 0 and 21 had readily detectable S1-binding IgG and SARS-CoV-2 neutralizing titers (NT50) as early as 14 days after a single immunization, with substantial increases following the second immunization. On Day 28, seven days after Dose 2 at the 30 µg dose level, the neutralizing geometric mean titer (GMT) reached 8-fold the GMT of a 38 member panel of human convalescent sera (HCS); at the 100 µg dose level, the neutralizing GMT was 18-fold the HCS GMT. The HCS sera were drawn from SARS-CoV-2 infected individuals 18 to 83 years of age, at least 14 days after PCR-confirmed diagnosis and at a time when individuals were asymptomatic. The HCS panel provides a currently accessible benchmark to judge the quality of the humoral immune response to the vaccine. A decline of both, S1-binding IgG levels and neutralizing titers, was observed out to the latest measured time point (Day 56) but remained above the neutralizing GMT and the S1-binding geometric mean concentration (GMC) of the HCS.

As seen following mouse immunization, strong S-specific Th1-dominant IFN γ ⁺ T-cell responses were detected in all immunized rhesus macaques. By intracellular cytokine staining analysis, there was a dose-dependent increase in S-specific CD4⁺ T cell responses with a strong Th1-bias evidenced by high frequency of IFN γ ⁺, IL-2⁺, or TNF- α ⁺ cells. Notably, CD8⁺ T-cell responses were also detectable in BNT162b2-immunized animals.

2.4.2.1.4.2. SARS-CoV-2 Challenge of BNT162b2 (V9)-Immunized Nonhuman Primates

Groups of 2-4 year old male rhesus macaques that had received two IM immunizations with 100 µg BNT162b2 V9 (n=6) or saline (Control; n=3) 21 days apart were challenged 55 days after the second immunization with 1.05×10^6 plaque forming units of SARS-CoV-2 (strain USA-WA1/2020), split equally between the intranasal (IN) and intratracheal (IT) routes, as

090177e1962c108d\Approved\Approved On: 08-Feb-2021 15:26 (GMT)

previously described (Singh et al, 2020) (VR-VTR-10671). SARS-CoV-2 RNA was measured by reverse transcription- quantitative polymerase chain reaction (RT-qPCR) in bronchoalveolar lavage fluid, nasal swabs, and oropharyngeal swabs. The difference in viral RNA detection in BAL fluid between BNT162b2-immunised and control-immunised rhesus macaques after challenge is highly statistically significant (by a nonparametric test, $p=0.0014$). None of the challenged animals showed clinical signs of significant illness, indicating that the 2-4 years old male rhesus challenge model is primarily an infection model for SARS-CoV-2, not a COVID-19 disease model. No radiographic or histological evidence of vaccine-elicited enhanced disease was observed. In summary, BNT162b2 provided complete protection from the presence of detectable viral RNA in the lungs compared to the saline control with no evidence of vaccine-elicited disease enhancement.

2.4.2.1.5. Immunogenicity Testing After Weekly Immunization of Rats in GLP Compliant Repeat Dose Toxicology Studies and a Developmental and Reproductive Toxicity Study

The nonclinical safety data package consists of two GLP-compliant repeat-dose rat toxicity studies, in which both BNT162b2 variants (V8 and V9) were evaluated, and a DART study, in which BNT162b2 (V9) was evaluated (Section 2.4.4). In all studies, Study 38166 (evaluating V8) as well as Study 20GR142 and Study 20256434 (evaluating V9), the vaccine candidates were immunogenic.

In Study 38166, male and female rats received three weekly IM doses of BNT162b2 (V8). Serum samples were collected from main study animals on Day 17 (two days after the third dose) at the end of the dosing phase and on Day 38 at the end of a 3-week recovery phase. The sera were analyzed by ELISA for IgG that bound S1 and RBD as well as for SARS-CoV-2-S pseudovirus neutralizing antibodies. The vaccine candidates elicited IgG that recognized S1 and RBD. After immunization, animals developed high titers of antigen-specific antibodies as well as pseudovirus neutralization titers.

In Study 20GR142, male and female rats received three weekly IM doses of BNT162b2 (V9). Serum samples were collected from study animals prior to vaccine administration, at the end of the dosing phase on Day 17 (two days after the third dose), and at the end of the 3-week recovery phase on Recovery Phase Day 21. Sera were analyzed for SARS-CoV-2 neutralizing antibodies. After immunization, BNT162b2 (V9) elicited SARS-CoV-2 neutralizing antibody responses in males and females at the end of the dosing and recovery phases of the study. SARS-CoV-2 neutralizing antibody responses were not observed in animals prior to vaccine administration or in saline-administered control animals.

In Study 20256434, female rats were administered 4 total IM doses of BNT162b2 (V9) 21 and 14 days prior to mating and on GD9 and GD20. Serum samples were collected from females prior to vaccine administration, just prior to mating (M0), at the end of gestation (GD21), and at the end of lactation (LD21) and offspring (fetuses on GD21 and pups on PND21). Sera were analyzed for SARS-CoV-2 neutralizing antibodies. After immunization, SARS-CoV-2 neutralizing titers were detected in all maternal females as well as in their offspring (fetuses and pups). SARS-CoV-2 neutralizing antibody titers were not observed in animals prior to vaccine administration or in saline-administered control animals.

2.4.2.2. Secondary Pharmacodynamics

No secondary pharmacodynamics studies were conducted with BNT162b2.

2.4.2.3. Safety Pharmacology

No safety pharmacology studies were conducted with BNT162b2 as they are not considered necessary for the development of vaccines according to the WHO guideline ([WHO, 2005](#)).

2.4.2.4. Pharmacodynamic Drug Interactions

Nonclinical studies evaluating pharmacodynamic drug interactions with BNT162b2 were not conducted as they are generally not considered necessary to support development and licensure of vaccine products for infectious diseases (WHO, 2005).

2.4.3. PHARMACOKINETICS

2.4.3.1. Brief Summary

Assessment of the ADME profile of BNT162b2 (BioNTech code number BNT162, Pfizer code number PF-07302048) included evaluating the PK and metabolism of two novel lipid excipients (ALC-0315 and ALC-0159) in the LNP and potential biodistribution of BNT162b2 using luciferase expression as a surrogate reporter. The luciferase reporter was used as it was a readily available reporter that has been widely used to develop an understanding of protein/organ expression (Chen et al, 2020; Elia et al, 2020; Fukuchi et al, 2020; Hassett et al, 2019; Truong et al, 2019; Barry et al, 2012; Jeon et al, 2006). An intravenous rat PK study, using LNPs with the identical lipid composition as BNT162b2, demonstrated that ALC-0315 and ALC-0159 distribute from the plasma to the liver. While there was no detectable excretion of either lipid in the urine, the percent of dose excreted unchanged in feces was ~1% for ALC-0315 and ~50% for ALC-0159.

The biodistribution of BNT162b2 was evaluated using luciferase expression as a surrogate reporter in BALB/c mice. Mice were administered a luciferase expressing modRNA formulated like BNT162b2, with the identical lipid composition. Luciferase expression was measured in vivo following luciferin application. Luciferase expression was identified at the injection site at 6 hours after injection and was not detected after 9 days. Expression in the liver was also present to a lesser extent at 6 hours after injection and was not detected by 48 hours after injection. The distribution was also examined in male and female Wistar Han rats using LNPs with a comparable lipid composition to BNT162b2 but with a surrogate luciferase RNA and containing trace amounts of radiolabeled [³H]-CHE, a non-exchangeable, non-metabolizable lipid marker. The greatest mean concentration of LNP was found remaining in the injection site in both sexes. Total recovery (% of injected dose) of LNP outside the injection site was greatest in the liver and was much less in the spleen, adrenal glands, and ovaries.

The in vitro metabolism of ALC-0315 and ALC-0159 was evaluated in blood, liver microsomes, S9 fractions, and hepatocytes from mice, rats, monkeys, and humans. The in vivo metabolism was examined in rat plasma, urine, feces, and liver samples from the PK study. Metabolism of ALC-0315 and ALC-0159 appears to occur slowly in vitro and in vivo. ALC-0315 and ALC-0159 are metabolized by hydrolytic metabolism of the ester and amide functionalities, respectively, and this hydrolytic metabolism is observed across the species evaluated.

In summary, the nonclinical ADME studies indicate that the LNP distributes to the liver. Approximately 50% of ALC-0159 is excreted unchanged in feces, while metabolism played a role in the elimination of ALC-0315.

2.4.3.2. Methods of Analysis

No methods of analysis have been validated to support GLP TK studies of components of BNT162b2; however, a qualified LC/MS method was developed to support quantitation of the two novel LNP excipients for the non-GLP IV PK study in rats

090177e1962c108d\Approved\Approved On: 08-Feb-2021 15:26 (GMT)

(Study PF-07302048_06Jul20_072424). Methods for immunogenicity and efficacy studies are described in Section 2.6.2.12.

2.4.3.3. Absorption

2.4.3.3.1. In Vitro Absorption

No absorption studies were conducted for BNT162b2, as the administration route is IM.

2.4.3.3.2. Single-Dose Pharmacokinetics

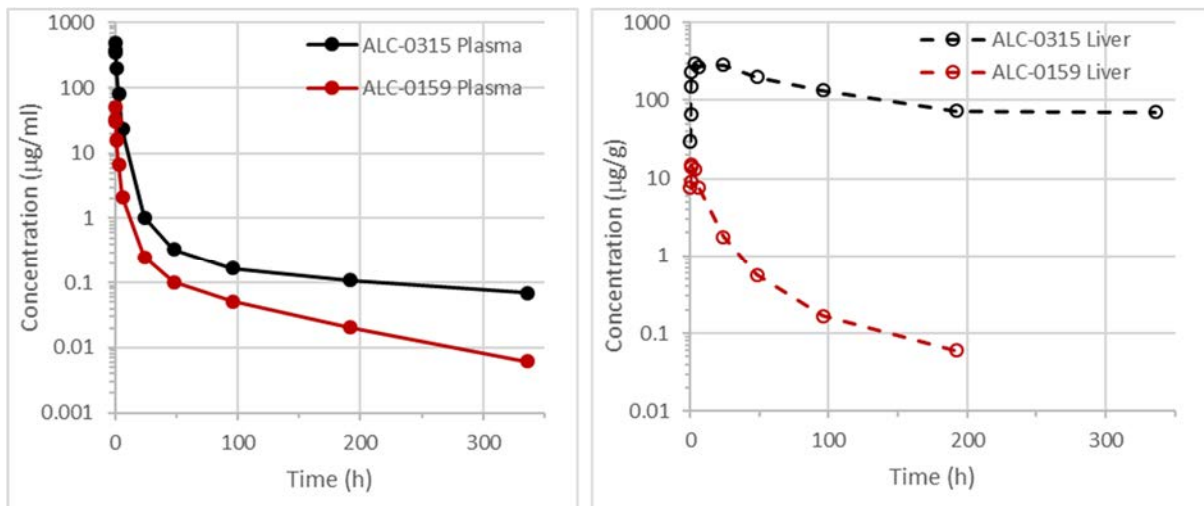
An intravenous rat PK study (PF-07302048_06Jul20_072424; [Tabulated Summary 2.6.5.3](#)) was performed using LNPs containing surrogate luciferase RNA, with the identical lipid composition as BNT162b2. This study was conducted to explore the disposition of ALC-0315 and ALC-0159 that had reached the systemic circulation following IM administration; thus, the IV route was felt to be appropriate. The findings are depicted in Table 2.4.3-1 and Figure 2.4.3-1.

Table 2.4.3-1. PK of ALC-0315 and ALC-0159 in Wistar Han Rats After IV Administration of LNPs Containing Surrogate Luciferase RNA at 1 mg/kg

Analyte	Dose of Analyte (mg/kg)	Gender /N	t _{1/2} (h)	AUC _{inf} (µg•h/mL)	AUC _{last} (µg•h/mL)	Estimated fraction of dose distributed to liver (%) ^a
ALC-0315	15.3	Male/3 ^b	139	1030	1020	60
ALC-0159	1.96	Male/3 ^b	72.7	99.2	98.6	20

a. Calculated as highest mean amount in the liver (µg)/total mean dose (µg) of ALC-0315 or ALC-0159.
b. 3 animals per timepoint; non-serial sampling.

Figure 2.4.3-1. Plasma and Liver Concentrations of ALC-0315 and ALC-0159 in Wistar Han Rats After IV Administration of LNPs Containing Surrogate Luciferase RNA at 1 mg/kg



090177e1962c108d\Approved\Approved On: 08-Feb-2021 15:26 (GMT)

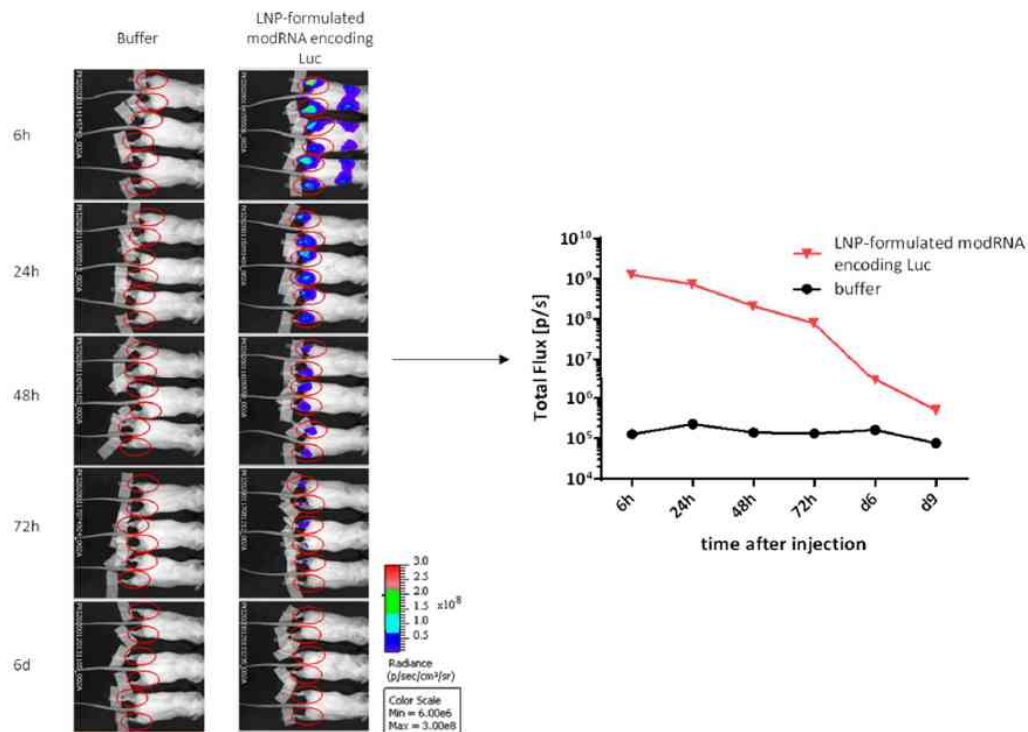
Pharmacokinetic studies have not been conducted with BNT162b2 and are generally not considered necessary to support the development and licensure of vaccine products for infectious diseases (WHO, 2005; WHO, 2014).

2.4.3.4. Distribution

In an in vivo study (R-20-0072; Tabulated Summary 2.6.5.5A), biodistribution was assessed using luciferase as a surrogate marker protein, with RNA encoding luciferase formulated like BNT162b2, with the identical lipid composition. The LNP-formulated luciferase-encoding modRNA was administered to BALB/c mice by IM injection of 1 µg each in the right and left hind leg (for a total of 2 µg). Using in vivo bioluminescence after injection of luciferin substrate, luciferase protein expression was detected at different timepoints at the site of injection and to a lesser extent, and more transiently, in the liver (Figure 2.4.3-2. Distribution to the liver is likely mediated by LNPs entering the blood stream. The luciferase expression at the injection sites dropped to background levels after 9 days. The repeat-dose toxicity study in rats showed no evidence of liver injury (Section 2.4.4.3).

The biodistribution of the antigen encoded by the RNA component of BNT162b2 is expected to be dependent on the LNP distribution and the results presented should be representative for the vaccine RNA platform, as the LNP-formulated luciferase-encoding modRNA had the same lipid composition.

Figure 2.4.3-2. Bioluminescence Emission in BALB/c Mice after IM Injection of an LNP Formulation of modRNA Encoding Luciferase



090177e1962c108d\Approved\Approved On: 08-Feb-2021 15:26 (GMT)

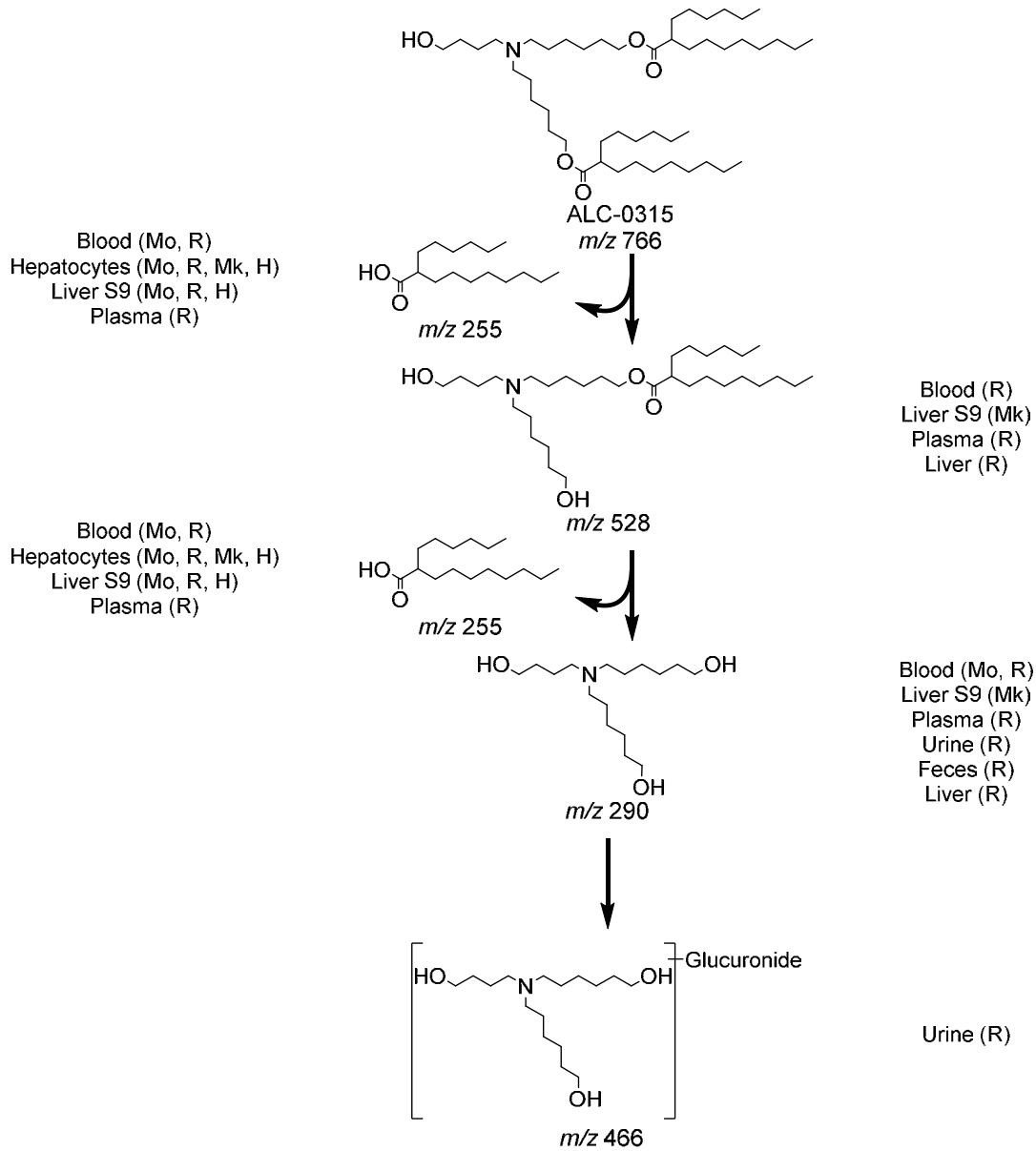
The distribution of a LNP with a comparable lipid composition to BNT162b2 but with a surrogate luciferase RNA (monitoring the ^3H -CHE lipid label), was investigated in blood, plasma and selected tissues in male and female Wistar Han rats over 48 hours after a single IM injection at 50 μg mRNA/animal ([Study 185350](#); [Tabulated Summary 2.6.5.5B](#)). The greatest mean concentration of LNP was found remaining in the injection site at each time point in both sexes. Outside the injection site, low levels of radioactivity were detected in most tissues, with the greatest levels in plasma observed 1-4 hours post-dose. Over 48 hours, the LNP distributed mainly to liver, adrenal glands, spleen and ovaries, with maximum concentrations observed at 8-48 hours post-dose. Total recovery (% of injected dose) of LNP, for combined male and female animals, outside of the injection site was greatest in the liver (up to 18%) and was much less in the spleen ($\leq 1.0\%$), adrenal glands ($\leq 0.11\%$) and ovaries ($\leq 0.095\%$). The mean concentrations and tissue distribution pattern were broadly similar between the sexes.

2.4.3.5. Metabolism

Of the four lipids used as excipients in the LNP formulation, two are naturally occurring (cholesterol and DSPC) and will be metabolized and excreted like their endogenous counterparts. The in vitro metabolic stability of the two novel lipids, ALC-0315 (aminolipid) and ALC-0159 (PEG-lipid), were evaluated in mouse, rat, monkey, and human liver microsomes, S9 fractions, and hepatocytes. ALC-0315 and ALC-0159 were stable ($>82\%$ remaining) over 120 min in liver microsomes and S9 fractions and over 240 min in hepatocytes in all species and test systems ([Studies 01049-20008](#), [01049-20009](#), [01049-20010](#), [01049-20020](#), [01049-20021](#), and [01049-20022](#); [Tabulated Summaries 2.6.5.10A](#) and [2.6.5.10B](#)).

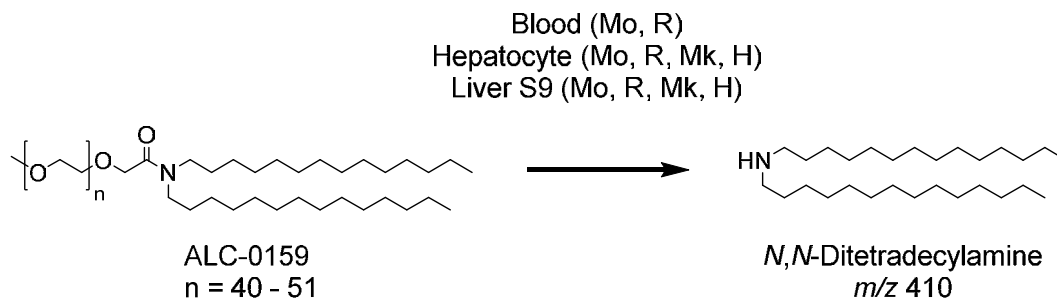
Further study of the metabolism of ALC-0315 and ALC-0159 in vitro and in vivo evaluating the plasma, urine, feces, and liver from the rat PK study ([Section 2.4.3.3.2](#)) determined ALC-0315 and ALC-0159 are metabolized slowly ([Study PF-07302048_05Aug20_043725](#); [Tabulated Summaries 2.6.5.9](#), [2.6.5.10C](#), and [2.6.5.10D](#)). ALC-0315 and ALC-0159 underwent hydrolytic metabolism of the ester and amide functionalities, respectively, and this hydrolytic metabolism was observed across the species evaluated ([Figure 2.4.3-3](#) and [Figure 2.4.3-4](#)).

Figure 2.4.3-3. Proposed Biotransformation Pathway of ALC-0315 in Various Species



Metabolism of ALC-0315 occurs via two sequential ester hydrolysis reactions, first yielding the monoester metabolite (m/z 528) followed by the doubly deesterified metabolite (m/z 290). Subsequent metabolism of the doubly deesterified metabolite resulted in a glucuronide metabolite (m/z 466), which was only observed in urine from the rat PK study. Additionally, 6-hexyldecanoic acid (m/z 255), the acid product of both hydrolysis reactions of ALC-0315, was identified.

090177e1962c108d\Approved\Approved On: 08-Feb-2021 15:26 (GMT)

Figure 2.4.3-4. Proposed Biotransformation Pathway of ALC-0159 in Various Species

The primary route of metabolism identified for ALC-0159 involves amide bond hydrolysis yielding *N,N*-ditetradecylamine (*m/z* 410).

The protein encoded by the RNA in BNT162b2 is expected to be proteolytically degraded like other endogenous proteins. RNA is degraded by cellular RNases and subjected to nucleic acid metabolism. Nucleotide metabolism occurs continuously within the cell, with the nucleoside being degraded to waste products and excreted or recycled for nucleotide synthesis. Therefore, no RNA or protein metabolism or excretion studies will be conducted.

2.4.3.6. Excretion

In the rat PK study ([Section 2.4.3.3.2](#)), there was no detectable excretion of ALC-0315 and ALC-0159 in urine after IV administration of LNPs containing surrogate luciferase RNA at 1 mg/kg. The percent excreted unchanged in feces was ~1% for ALC-0315 and ~50% for ALC-0159. Metabolites of ALC-0315 were detected in the urine of rats ([Figure 2.4.3-3](#)). No excretion studies have been conducted with BNT162b2 for the reasons described in [Section 2.4.3.5](#).

2.4.3.7. Pharmacokinetic Drug Interactions

No PK drug interaction studies have been conducted with BNT162b2.

2.4.4. TOXICOLOGY

2.4.4.1. Brief Summary

The nonclinical toxicity assessment of BNT162b2 (BioNTech code number BNT162, Pfizer code number PF-07302048) includes 2 GLP-compliant repeat-dose toxicity studies and a developmental and reproductive toxicity (DART) study in Wistar Han rats, outlined below in [Table 2.4.4-1](#). The nonclinical safety evaluation included 2 variants of BNT162b2: V8 and V9. BNT162b2 (V9), the candidate submitted for licensure, differs from BNT162b2 (V8) only in the presence of optimized codons to improve antigen expression, but the amino acid sequences of the encoded antigens are identical. Two GLP repeat-dose toxicity studies for BNT162b2 (V8) and BNT162b2 (V9), one study for each variant, have been completed. In both studies, the nonclinical toxicology findings were similar between BNT162b2 (V9) and BNT162b2 (V8). BNT162b2 (V9) was assessed for development and reproductive toxicity in rats.

The IM route of exposure was selected as it is the intended route of clinical administration. The selection of rats as the toxicology test species is consistent with the WHO guidance documents on nonclinical evaluation of vaccines ([WHO, 2005](#)), which recommend that vaccine toxicity studies be conducted in a species in which an immune response is induced by the vaccine. Generation of an immune response to BNT162b2 has been confirmed in rats in both repeat-dose toxicity studies and the DART study. The Wistar Han rat is used routinely for regulatory toxicity studies, and there is an extensive historical safety database on this strain of rat.

Table 2.4.4-1. Overview of Toxicity Testing Program

Study ^a	Study (Sponsor) No.	Group/ Dose, µg RNA	Total Volume (µL) ^b	No. of Animals/ Group	Study Status
Repeat-Dose Toxicity					
17-Day, 2 or 3 Dose (1 Dose/Week) IM Toxicity With a 3 Week Recovery Phase in Rats ^{c,d}	38166	Control ^e , 0	200 ^f	15/sex	Completed
		BNT162b2 (V8) ⁱ , 100	200 ^f	15/sex	
17-Day, 3 Dose (1 Dose/Week) IM Toxicity With a 3 Week Recovery Phase in Rats ^g	20GR142	Saline ^h , 0	60	15/sex	Completed
		BNT162b2 (V9) ⁱ , 30	60	15/sex	
Developmental and Reproductive Toxicity					
Combined Fertility and Developmental Study (Including Teratogenicity and Postnatal Investigations) by the IM route in Rats ^j	20256434 (RN9391 R58)	Saline ^h , 0	60	44 F	Completed
		BNT162b2 (V9) ⁱ , 30	60	44 F	

a. All studies are GLP-compliant and were conducted in an OECD mutual acceptance of data-compliant member state.

b. Doses were administered as 1 application at 1 site unless otherwise indicated.

c. Study also evaluated the BNT162a1, BNT162b1, and BNT162c1 vaccine candidates.

d. QW x 3 (Days 1, 8, 15) for BNT162a1, BNT162b1, and BNT162b2 (V8); QW x 2 (Days 1, 8) for BNT162c1.

e. Phosphate buffered saline, 300 mM sucrose.

f. One application (100 µL) at 2 sites for a total dose volume of 200 µL.

g. Study also evaluated BNT162b3.

h. Sterile saline (0.9% NaCl).

i. BNT162b2 (V8) and BNT162b2 (V9) both encode the same amino acid sequence of the spike protein antigen with two prefusion conformation-stabilizing amino acids in the stalk.

j. Study also evaluated BNT162b1 and BNT162b3.

Administration of BNT162b2 by IM injection to male and female Wistar Han rats once every week for a total of 3 weekly cycles of dosing was tolerated without evidence of systemic toxicity in GLP-compliant repeat-dose toxicity studies. Expected inflammatory responses to the vaccine were evident such as edema and erythema at the injection sites, transient elevation in body temperature, elevations in WBCs and acute phase reactants, and lower A:G ratios. A transient elevation in GGT was noted in animals vaccinated with BNT162b2 (V8) in Study 38166 without evidence of microscopic changes in the biliary system or other hepatobiliary biomarkers but was not recapitulated in Study 20GR142. Injection site reactions were common in all vaccine-administered animals and were greater after boost immunizations. Changes secondary to inflammation included slight and transient reduction in body weights and transient reductions in RETIC, PLT, and RBC mass parameters. All changes in clinical pathology parameters and acute phase proteins were reversed at the end of

the recovery phase for BNT162b2 with the exception of higher RDW, higher globulins, and lower A:G ratios in animals administered BNT162b2 (V9). The higher RDW reflects prior RETIC increases. The higher A:G is due to low magnitude increases in globulins, which is an expected immune response to vaccine administration (Sellers et al, 2020).

Macroscopic pathology and organ weight changes were also consistent with immune activation and inflammatory response and included increased size of draining iliac lymph nodes and increased size and weight of spleen. Vaccine-related microscopic findings at the end of the dosing phase consisted of edema and inflammation in injection sites and surrounding tissues; increased cellularity in the draining (iliac) lymph nodes, bone marrow, and spleen; and hepatocyte vacuolation in the liver. Periportal vacuolation of hepatocytes was not associated with any microscopic evidence of hepatic injury or alterations in liver function tests and is interpreted to reflect hepatocyte uptake of the LNP lipids (Sedic et al, 2018). Microscopic findings at the end of the dosing phase were partially or completely recovered in all animals at the end of the recovery phase for BNT162b2. A robust immune response was elicited to the BNT162b2 antigen.

In the DART study, administration of BNT162b2 to female rats twice before the start of mating and twice during gestation at the human clinical dose (30 µg RNA/dosing day) was associated with nonadverse effects (body weight, food consumption, and localized effects in the injection site) after each dose administration. There were no effects of BNT162b2 administration on mating performance, fertility, or any ovarian or uterine parameters in the F0 female rats nor on embryo-fetal or postnatal survival, growth, or development in the F1 offspring through the end of lactation. A SARS-CoV-2 neutralizing antibody response to the vaccine was confirmed in F0 female rats prior to mating, at the end of gestation, and at the end of lactation and these neutralizing antibodies were also detectable in the F1 offspring (fetuses and pups).

2.4.4.2. Single-Dose Toxicity

A separate single-dose toxicity study with BNT162b2 has not been conducted.

2.4.4.3. Repeat-Dose Toxicity

2.4.4.3.1. Repeat-Dose Toxicity Study of Three LNP-Formulated RNA Platforms Encoding for Viral Proteins by Repeated Intramuscular Administration to Wistar Han Rats

The vaccine candidate BNT162b2 (V8), an LNP-formulated modified RNA vaccine expressing SARS-CoV-2 P2 S, was assessed in a GLP-compliant repeat-dose toxicity study in Wistar Han rats (Study 38166). This study also included assessment of 3 other LNP-formulated RNA vaccines, encoding either the SARS-CoV-2 P2 S or RBD antigens, which were not selected for licensure. For the purpose of this submission, only the study findings from the 100 µg BNT162b2 (V8) vaccine group are summarized; findings from the other vaccine candidates were generally similar.

Administration of BNT162b2 (V8) via IM injections once weekly for 3 administrations to male and female Wistar Han rats was tolerated without evidence of systemic toxicity. The

vaccine elicited a robust antigen-specific immune response and produced nonadverse macroscopic changes at the injection sites, spleen, and the draining lymph nodes; increased hematopoiesis in the bone marrow and spleen; periportal hepatocyte vacuolation; and clinical pathology changes consistent with an immune response. The findings in this study were fully recovered or showed evidence of ongoing recovery at the end of the 3-week recovery phase, and were consistent with those typically associated with the IM administration of LNP-encapsulated mRNA vaccines (Hassett et al, 2019).

Body weights were lower 24 hours after each BNT162b2 (V8) vaccine administration compared with predose values (down to 0.92x versus baseline) with evidence of weight gain (1.22x to 1.37x versus baseline) by the end of recovery. Body weight gain between the administrations was comparable to the buffer control group. There were no noteworthy effects on body weight at the end of the recovery phase. There were no effects on food consumption.

BNT162b2 (V8)-administered animals generally had higher body temperatures compared with buffer control animals at 4 and 24 hours postdose. Group mean temperatures in rats administered the BNT162b2 (V8) vaccine were higher, but within approximately 1°C of the group mean body temperature of buffer-administered animals. Individual rats administered BNT162b2 (V8) did not have body temperatures >40.0°C after administration.

Local reactions were observed in male and female animals dosed IM with BNT162b2 (V8). The incidence and severity of the reactions were higher after the second or third injections compared with the first injection. The majority of animals had very slight edema or rarely slight erythema after the first dose. After the second or third dose, the severity of edema and erythema increased up to moderate or rarely, severe grades. These observations resolved prior to the next injection or for recovery animals resolved during the 3-week recovery phase.

Most BNT162b2 (V8)-related changes in clinical pathology were consistent with an acute phase response and anticipated inflammation. Minor and variable alterations in other clinical pathology parameters were considered secondary effects of vaccination.

Expected immune responses to BNT162b2 (V8) were evident in hematology, such as elevations in mean neutrophil (up to 7.8x) eosinophil (up to 5.1x controls), basophil (1.47x controls), and LUC counts (up to 7.7x controls) and were highest on Day 17, 48 hours after the last injection. WBCs were higher (up to 2.2x controls) in the BNT162b2 (V8) vaccinated group on Day 17. PLT counts were slightly decreased on Day 17 (down to 0.66x controls). A transient reduction in RETIC counts (down to 0.28x controls) was only observed after the administration of the first dose on Day 4. Decreased RETICs were similarly observed in rats treated with the licensed LNP-siRNA pharmaceutical Onpattro™ (NDA # 210922) but have not been observed in humans treated with this biotherapeutic (Kozauer et al, 2018), suggesting this is a species-specific effect. A slight reduction in red blood cell mass (HGB down to 0.87x controls) was observed on Day 17. RETIC and RBC mass parameter decreases were likely secondary to the inflammation.

BNT162b2 (V8)-related changes in clinical chemistry included slightly higher GGT (a biomarker of biliary and not hepatocellular injury [Boone et al, 2005]) on Days 4 (up to 4.6x

controls) and 17 (up to 4.2x controls) without evidence of microscopic changes in the biliary system or other hepatobiliary biomarkers. Additionally, higher GGT was not observed in the second repeat-dose toxicity study (20GR142), conducted with the clinical candidate submitted for licensure. Albumin was slightly lower on Days 4 (down to 0.87x controls) and 17 (down to 0.89x controls) and globulin slightly higher on Day 17 (up to 1.2x controls). This resulted in the A:G ratio being slightly lower on Days 4 (down to 0.84x controls) and 17 (down to 0.76x controls). The effect on albumin and globulin were related to the vaccine-mediated inflammatory response as part of the negative and positive acute phase response, respectively (Sellers et al, 2020).

The acute phase proteins alpha-1-acid glycoprotein (up to 21x controls on Day 17) and alpha-2-macroglobulin (up to 217x controls on Day 17) were elevated in both males and females in the BNT162b2 (V8)-administered group on Days 4 and 17. Fibrinogen was higher in the vaccine-administered group (up to 3.1x controls), consistent with an acute phase response. Higher concentrations of acute phase proteins are an anticipated response to vaccination.

All changes in clinical pathology parameters and acute phase proteins were reversed at the end of the recovery phase.

Compared with the buffer control, there were no test-article related differences in the concentration of serum cytokines evaluated, in urinalysis parameters, or in ophthalmoscopic or auditory parameters.

BNT162b2 (V8)-related higher absolute and relative (to body) spleen weights (up to 1.62x controls) were evident and correlated with the macroscopic observation of increased spleen size and the increased hematopoiesis. This is likely secondary to immune responses induced by the BNT162b2 (V8) vaccine.

The most common macroscopic observation in the BNT162b2 (V8) group was a thickened injection site and/or induration noted for nearly all animals (16/20) at necropsy. This finding correlated with microscopic inflammation at the injection site. Macroscopic findings at the injection site were resolved at the end of the recovery phase. Enlarged spleen and iliac lymph nodes were noted in several animals in the BNT162b2 (V8)-administered group, which correlated microscopically to expansion of lymphoid and/or hematopoietic cells. The effects on the lymphoid organs are consistent with immune responses to the BNT162b2 (V8).

Vaccine-related microscopic findings at the end of dosing were evident in injection sites and surrounding tissues, in the draining (iliac) lymph nodes, bone marrow, spleen, and liver.

The inflammation at the injection site was characterized by infiltrates of macrophages, granulocytes, and lymphocytes into the muscle, and variably into the dermis and subcutis. Injection site inflammation was associated with moderate edema, mild myofiber degeneration, occasional muscle necrosis, and mild fibrosis. Injection site findings were consistent with an immune/inflammatory response to an IM vaccine administration.

In the draining (iliac) lymph node, increased cellularity of the follicular germinal centers and increased plasma cells (plasmacytosis) were variably present for all BNT162b2 (V8)-dosed animals. In addition, minimal to mild increases in the cellularity of bone marrow and

hematopoiesis in the spleen likely related to increased granulopoiesis and correlated with increased circulating neutrophils (which correlated with increased spleen size and weight) were present in BNT162b2 (V8)-dosed animals.

Vacuolation of hepatocytes (minimal to mild) in the portal regions of the liver were present for all BNT162b2 (V8)-dosed animals. The liver findings were not associated with changes in markers of hepatocyte injury (eg, AST or ALT). While GGT was elevated in vaccine-administered animals, it was not considered to be associated with the vacuolation of hepatocytes (Enmulat et al, 2010). The microscopic observation of liver vacuolation is believed to be associated with hepatocyte uptake of the LNP lipids (Section 2.4.3.4; Sedic et al, 2018).

Microscopic findings at the end of the dosing phase were partially or completely resolved in all animals at the end of the recovery phase. Inflammation at the injection site and surrounding tissues was less severe (minimal to mild) in animals administered BNT162b2 (V8) at the end of the 3-week recovery phase, indicating partial recovery. In the iliac lymph node, plasmacytosis was less severe, and macrophage infiltrates were present at the end of the 3-week recovery phase and reflect resolution of the inflammation noted at the end of the dosing phase.

All other observations in the bone marrow, spleen, and liver were fully resolved at the end of the 3-week recovery phase.

The immune response to the vaccine antigen was evaluated by S1-binding IgG and RBD-binding IgG ELISAs, and a SARS-CoV-2 S pseudotype neutralization (pVNT) assay on Days 17 and 38 (Section 2.4.2.1.4). The data demonstrate that BNT162b2 (V8) elicited a SARS-CoV-2 S-specific antibody response with high neutralizing activity.

In conclusion, administration of BNT162b2 (V8) by IM injection to male and female Wistar Han rats once every week for 3 doses, was tolerated at 100 µg RNA/dosing day without evidence of systemic toxicity.

2.4.4.3.2. 17-Day Intramuscular Toxicity Study of BNT162b2 (V9) in Wistar Han Rats with a 3-week Recovery

The vaccine candidate BNT162b2 (V9), an LNP-formulated modified RNA vaccine expressing SARS-CoV-2 P2 S, was assessed in a GLP-compliant repeat-dose toxicity study in Wistar Han rats (Study 20GR142). This study also included assessment of another LNP-formulated RNA vaccine candidate (BNT162b3) that will not be included in the licensure application. For the purpose of this submission, the study findings from the BNT162b2 (V9) vaccine are summarized; findings from the BNT162b3 vaccine candidate also tested in this study were generally similar. BNT162b2 (V9) was administered at 30 µg once weekly for 3 doses (Days 1, 8, and 15) followed by a 3-week recovery phase.

Administration of BNT162b2 (V9) via IM injections once weekly for 3 administrations to male and female Wistar Han rats was tolerated without evidence of systemic toxicity. The vaccine elicited a robust antigen-specific immune response and produced nonadverse macroscopic changes at the injection sites, spleen, and the draining lymph nodes; increased

hematopoiesis in the bone marrow and spleen; liver vacuolation; and clinical pathology changes consistent with an immune response. The findings in this study were either fully recovered or showed evidence of ongoing recovery at the end of the 3-week recovery phase, and were consistent with those typically associated with the IM administration of LNP-encapsulated mRNA vaccines (Hassett et al, 2019).

All animals administered BNT162b2 (V9) survived to scheduled necropsy. There were no test article-related clinical signs or body weight changes noted. Test article-related reduced mean food consumption was noted on Days 4 and 11 (down to 0.83x controls). Test article-related higher mean body temperature (maximum increase post each dose) compared with control animals was noted on Day 1 (up to 0.54°C), Day 8 (up to 0.98°C), and Day 15 (up to 1.03°C) postdose.

BNT162b2 (V9)-related injection site edema and erythema were noted on Days 1 (up to slight edema and very slight erythema), 8 (up to moderate edema and very slight erythema), and 15 (up to moderate edema and very slight erythema). The incidence and severity of the reactions were higher after the second or third injections compared with the first injection. Test article-related erythema and edema fully resolved prior to dose administration on Days 8 and 15. Injection site erythema and edema were fully resolved at the end of the recovery phase.

All clinical pathology changes (type and magnitude) were generally consistent with expected immune responses to the vaccine or secondary to inflammation.

There were higher WBCs (up to 2.95x controls), primarily involving neutrophils (up to 6.60x controls), monocytes (up to 3.30x controls), and LUC (up to 13.2x controls) and slightly higher eosinophils and basophils on Days 4 and 17. WBCs were higher on Day 17 as compared with Day 4. There were transiently lower RETICs on Day 4 (down to 0.27x controls) in both sexes and higher RETICs on Day 17 (up to 1.31x controls) in females only. Lower RBC mass parameters (down to 0.90x controls) were present on Days 4 and 17. All test article-related hematology and coagulation changes noted in the dosing phase were fully reversed after a 3-week recovery phase, with the exception of higher red cell distribution width (up to 1.21x controls) in animals administered BNT162b2 (V9). The higher RDW reflects prior reticulocyte increases.

There were lower A:G ratios (down to 0.82x) on Days 4 and 17. Higher fibrinogen levels were observed on Day 17 (up to 2.49x) when compared with control animals, consistent with an acute phase response. The acute phase proteins alpha-1-acid glycoprotein (up to 39x on Day 17) and alpha-2-macroglobulin (up to 71x on Day 17) were elevated in both males and females in the BNT162b2 (V9)-administered group on Days 4 and 17 with higher concentrations generally observed in males. All other changes in clinical pathology parameters were considered incidental. All test article-related clinical chemistry changes noted in the dosing phase were fully reversed after a 3-week recovery phase, except higher globulins (up to 1.08x controls) in animals administered BNT162b2 (V9) and lower A:G ratio (down to 0.91x controls) in females administered BNT162b2 (V9), reflecting vaccine-related immune response.

Test article-related higher group mean absolute and relative spleen weights (compared to body weight) were noted in males that had received BNT162b2 (V9) (up to 1.42x) and females (up to 1.59x) relative to control group means. There were no other test article-related changes in organ weights. At the end of the recovery phase, spleen weights were within normal limits.

Test article-related macroscopic findings included the observation of enlarged draining lymph nodes (2/20 animals) and pale/dark (5/20 animals) or firm (6/20 animals) injection sites in animals administered BNT162b2 (V9). These changes fully recovered, except for partial recovery of enlarged draining nodes, suggesting recovery in progress.

Test article-related microscopic pathology findings were observed at the injection site and in the draining (iliac) and inguinal lymph nodes, spleen, bone marrow, and liver for both vaccine candidates. All microscopic findings were nonadverse, as there was no evidence of systemic toxicity or clinical signs of illness or lameness.

At the end of the dosing phase, test article-related mixed cell inflammation (mild to moderate) and edema (mild to moderate) at the injection site were consistent with findings typically associated with the IM administration of LNP-encapsulated mRNA vaccines (Hassett et al, 2019). These findings correlated with macroscopic observations of abnormal color (dark/pale) and consistency (firm). At the end of the 3-week recovery phase, there was full recovery for injection site edema and partial recovery for injection site inflammation, suggesting recovery in progress.

At the end of the dosing phase, test article-related findings in the draining (iliac) and inguinal lymph nodes (up to moderately increased cellularity of plasma cells and germinal centers), spleen (minimally increased cellularity of hematopoietic cells and germinal centers), and the bone marrow (minimal increased cellularity of hematopoietic cells) were present. These changes are secondary to immune activation and/or inflammation at the injection site. The presence of plasma cells (interpreted as plasmablasts) in the draining (iliac) and inguinal lymph nodes is consistent with a robust immunological response to the vaccines. These observations correlated with macroscopic observations of abnormal size (enlarged) in the lymph nodes and spleen and increased spleen weights. At the end of the 3-week recovery phase, full recovery of increased cellularity of hematopoietic cells in the spleen and bone marrow, with partial recovery (recovery in progress) of increased cellularity of plasma cells and germinal centers in the draining and inguinal lymph nodes, and increased cellularity of the germinal centers in the spleen.

At the end of the dosing phase, the test article-related microscopic finding of minimal periportal hepatocyte vacuolation was not associated with hepatocellular damage or alterations in liver function tests. The liver vacuolation is believed to be associated with hepatocyte uptake of the LNP lipids (Section 2.4.3.4; Sedic et al, 2018). At the end of 3-week recovery phase, this finding was completely recovered.

Administration of 3 once weekly doses of BNT162b2 (V9) elicited SARS-CoV-2 neutralizing antibody responses in males and females at the end of the dosing (Day 17) and recovery phases (Day 21) of the study. SARS-CoV-2 neutralizing antibody responses were

090177e1962c108d\Approved\Approved On: 08-Feb-2021 15:26 (GMT)

not observed in animals prior to vaccine administration or in saline-administered control animals.

In conclusion, administration of BNT162b2 (V9) at 30 µg RNA/dosing day via IM injections weekly for 3 administrations to male and female Wistar Han rats was tolerated without evidence of systemic toxicity. Dosing of BNT162b2 (V9) produced changes consistent with an inflammatory response and immune activation. The findings in this study are consistent with those typically associated with the IM administration of LNP-encapsulated mRNA vaccines.

2.4.4.4. Genotoxicity

No genotoxicity studies are planned for BNT162b2 as the components of the vaccine construct are lipids and RNA and are not expected to have genotoxic potential (WHO, 2005).

2.4.4.5. Carcinogenicity

Carcinogenicity studies with BNT162b2 have not been conducted as the components of the vaccine construct are lipids and RNA and are not expected to have carcinogenic or tumorigenic potential. Carcinogenicity testing is generally not considered necessary to support the development and licensure of vaccine products for infectious diseases (WHO, 2005).

2.4.4.6. Reproductive and Developmental Toxicity

Reproductive and developmental toxicity assessments were made with BNT162b2 (V9) (Study 20256434). BNT162b2 was administered by IM injection at the human clinical dose (30 µg RNA/dosing day) to 44 female Wistar Han rats (F0) 21 and 14 days prior to mating with untreated males and on GD 9 and 20, for a total of 4 dosing days. A separate control group of 44 F0 females received saline by the same route and regimen.

Following completion of a mating phase with untreated males, 22 rats/group underwent caesarean-section on GD 21 and were submitted to routine embryo-fetal development evaluations. The remaining 22 rats/group were allowed to litter and development of the offspring was observed until PND 21.

There were no BNT162b2-related deaths during the study. IM administration of BNT162b2 before and during gestation to female Wistar rats resulted in nonadverse clinical signs and macroscopic findings localized to the injection site as well as transient, nonadverse body weight and food consumption effects after each dose administration. These maternal findings are all consistent with administration of a vaccine and an inflammatory/immune response.

There were no BNT162b2-related effects on any mating or fertility parameters. There were no BNT162b2-related effects on any ovarian, uterine, or litter parameters, including embryo-fetal survival, growth, or external, visceral, or skeletal malformations, anomalies, or variations. There were no effects of BNT162b2 administration on postnatal offspring (F1) development, including postnatal growth, physical development (pinna unfolding and eye

opening), reflex ontogeny (pre-weaning auditory and visual function tests), macroscopic observations, and survival.

All F0 females administered BNT162b2 developed SARS-CoV-2 neutralizing antibodies and these antibodies were also detectable in all fetuses and pups from the caesarean and littering groups, respectively. The animals in the saline control group did not exhibit an immune response to BNT162b2.

In conclusion, administration of BNT162b2 to female rats twice before the start of mating and twice during gestation at the human clinical dose was associated with nonadverse effects (body weight, food consumption, and effects localized to the injection site) after each dose administration. However, there were no effects of BNT162b2 administration on mating performance, fertility, or any ovarian or uterine parameters in the F0 female rats nor on embryo-fetal or postnatal survival, growth, or development in the F1 offspring. An immune response was confirmed in F0 female rats following administration of each vaccine candidate and these responses were also detectable in the F1 offspring (fetuses and pups).

Macroscopic and microscopic evaluation of male and female reproductive tissues from the repeat-dose toxicity studies with BNT162b2 showed no evidence of toxicity.

2.4.4.7. Local Tolerance

Local tolerance of IM administration of BNT162b2 was evaluated by injection site observations and macroscopic and microscopic examination of injection sites in the repeat-dose toxicity studies and is described in [Section 2.4.4.3](#).

2.4.4.8. Other Toxicity Studies

2.4.4.8.1. Phototoxicity

Phototoxicity studies with BNT162b2 have not been conducted.

2.4.4.8.2. Antigenicity

Immunogenicity was evaluated as part of the primary pharmacodynamic studies ([Section 2.4.2.1](#)). Serology data from the repeat-dose toxicity studies shows a robust antigen-specific immune response to BNT162b2.

2.4.4.8.3. Immunotoxicity

Stand-alone immunotoxicity studies with BNT162b2 have not been conducted. However, immunotoxicological endpoints were collected as part of the repeat-dose toxicity studies; there were no adverse effects observed and no significant effects on measured cytokines.

2.4.4.8.4. Mechanistic Studies

Mechanistic studies with BNT162b2 have not been conducted.

2.4.4.8.5. Dependence

Dependence studies with BNT162b2 have not been conducted.

2.4.4.8.6. Studies on Metabolites

Stand-alone studies with administration of metabolites of BNT162b2 have not been conducted.

2.4.4.8.7. Studies on Impurities

Stand-alone studies with administration of impurities of BNT162b2 have not been conducted.

2.4.4.8.8. Other Studies

No other studies with BNT162b2 evaluated in this submission have been conducted.

2.4.4.9. Target Organ Toxicity

Based on data from the GLP repeat-dose toxicity studies ([Section 2.4.4.3](#)), administration of BNT162b2 was well tolerated without any evidence of systemic toxicity. BNT162b2 administration was associated with local reactogenicity at the injection site and expected inflammatory responses, including increases in lymphoid cells in draining lymph nodes and spleen. Microscopic findings within injection sites, which were partially reversed by the end of recovery, support this conclusion. The liver finding was reversible, not associated with changes in markers of hepatocyte injury and not considered adverse. The elevated levels of GGT in [Study 38166](#) were not recapitulated in [Study 20GR142](#) and were not associated with hepatobiliary changes microscopically. Elevated GGT was not attributed to the hepatocyte vacuolation ([Enmulat et al, 2010](#)).

090177e1962c108d\Approved\Approved On: 08-Feb-2021 15:26 (GMT)

2.4.5. INTEGRATED OVERVIEW AND CONCLUSIONS

The nonclinical program demonstrates that BNT162b2 is immunogenic in mice, rats, and nonhuman primates, and the toxicity studies support the licensure of this vaccine. Preclinical assessments in mice and nonhuman primates demonstrate that BNT162b2 elicits a rapid antibody response with measurable SARS-CoV-2 neutralizing titers after a single dose and substantial increases in titers after a second dose that exceed titers in sera from SARS-CoV-2/COVID-19-recovered patients. A Th1-dominant T cell response was evident in both mice and nonhuman primates. In a SARS-CoV-2 rhesus challenge model, BNT162b2 provided complete protection in the lungs, as determined by lack of detectable viral RNA, and there was no evidence of vaccine-elicited disease enhancement.

An IV rat PK study, using an LNP with the identical lipid composition as BNT162b2, demonstrated that the novel lipid excipients in the LNP formulation, ALC-0315 and ALC-0159, distribute from the plasma to the liver. While there was no detectable excretion of either lipid in the urine, the percent of dose excreted unchanged in feces was ~1% for ALC-0315 and ~50% for ALC-0159. Further studies indicated metabolism played a role in the elimination of ALC-0315. Biodistribution was assessed using luciferase expression as a surrogate reporter formulated like BNT162b2, with the identical lipid composition. After IM injection of the LNP-formulated RNA encoding luciferase in BALB/c mice, luciferase protein expression was demonstrated at the site of injection 6 hours post dose and was not detected after 9 days. Luciferase was detected to a lesser extent in the liver; expression was present at 6 hours after injection and was not detected by 48 hours after injection. After IM administration of a radiolabeled LNP-mRNA formulation containing ALC-0315 and ALC-0159 to rats, the percent of administered dose was also greatest at the injection site. Outside of the injection site, total recovery of radioactivity was greatest in the liver and much lower in the spleen, with very little recovery in the adrenal glands and ovaries. The metabolism of ALC-0315 and ALC-0159 was evaluated in blood, liver microsomes, S9 fractions, and hepatocytes from mice, rats, monkeys, and humans. The *in vivo* metabolism was examined in rat plasma, urine, feces, and liver samples from the PK study. Metabolism of ALC-0315 and ALC-0159 appears to occur slowly *in vitro* and *in vivo*. ALC-0315 and ALC-0159 are metabolized by hydrolytic metabolism of the ester and amide functionalities, respectively, and this hydrolytic metabolism is observed across the species evaluated.

Administration of BNT162b2 by IM injection to male and female Wistar Han rats once every week for a total of 3 weekly cycles of dosing was tolerated without evidence of systemic toxicity in GLP-compliant repeat-dose toxicity studies. Expected immune responses to the vaccine were evident such as edema and erythema at the injection sites, transient elevation in body temperature, elevations in WBCs and acute phase reactants, and decreased A:G ratios. Injection site reactions were common in all vaccine-administered animals and were greater after boost immunizations. Changes secondary to inflammation included slight and transient reductions in body weights and transient reductions in RETIC, PLT, and RBC mass parameters. All changes in hematology parameters and acute phase proteins were similar to control at the end of the recovery phase for BNT162b2 with the exception of higher RDW and lower A:G ratios in animals administered BNT162b2 (V9). Macroscopic pathology and organ weight changes were also consistent with immune activation and inflammatory response and included increased size of draining iliac lymph nodes and increased size and

090177e1962c108d\Approved\Approved On: 08-Feb-2021 15:26 (GMT)

BNT162b2

Module 2.4. Nonclinical Overview

weight of spleen. Vaccine-related microscopic findings at the end of dosing for BNT162b2 were evident in injection sites and surrounding tissues, in the draining iliac lymph nodes, bone marrow, spleen, and liver. Microscopic findings at the end of the dosing phase were partially (recovery in progress) or completely recovered in all animals at the end of the recovery phase for BNT162b2. A robust immune response was elicited to the BNT162b2 vaccine antigen.

Administration of BNT162b2 to female rats twice before the start of mating and twice during gestation at the human clinical dose (30 µg RNA/dosing day) was associated with nonadverse effects (body weight, food consumption and effects localized to the injection site) after each dose administration. There were no effects of BNT162b2 administration on mating performance, fertility, or any ovarian or uterine parameters in the F0 female rats nor on embryo-fetal or postnatal survival, growth, or development in the F1 offspring. An immune response was confirmed in F0 female rats following administration of BNT162b2 and this response was also detectable in the F1 offspring (fetuses and pups).

In summary, the nonclinical package summarized above supports the BLA of BNT162b2 administered twice by IM injection at a dose of 30 µg RNA.

090177e1962c108d\Approved\Approved On: 08-Feb-2021 15:26 (GMT)

2.4.6. LIST OF LITERATURE REFERENCES

Barry MA, May S, Weaver EA. Imaging luciferase-expressing viruses. *Methods Mol Biol* 2012;797:79-87.

Boone L, Meyer D, Cusick P, et al. Selection and interpretation of clinical pathology indicators of hepatic injury in preclinical studies. *Vet Clin Pathol* 2005;34(3):182-8.

Cai Y, Zhang J, Xiao T, et al. Distinct conformational states of SARS-CoV-2 spike protein. *Science* 2020;10.1126/science.abd4251.

Chen C-Y, Tran DM, Cavedon A, et al. Treatment of Hemophilia A Using Factor VIII Messenger RNA Lipid Nanoparticles. *Mol Ther Nucleic Acids* 2020;20:534-44.

Elia U, Ramishetti S, Dammes N, et al. Design of SARS-CoV-2 RBD mRNA Vaccine Using Novel Ionizable Lipids. *bioRxiv* 2020.10.15.341537.

Ennulat D, Magid-Slav M, Rehm S, et al. Diagnostic performance of traditional hepatobiliary biomarkers of drug-induced liver injury in the rat. *Toxicol Sci* 2010;116(2):397-412.

Fukuchi M, Saito R, Maki S, et al. Visualization of activity-regulated BDNF expression in the living mouse brain using non-invasive near-infrared bioluminescence imaging. *Mol Brain* 2020;13(1):122.

Hassett KJ, Benenato KE, Jacquinet E et al. Optimization of lipid nanoparticles for intramuscular administration of mRNA vaccines. *Molecular Therapy Nucleic Acids* 2019;15:1-11.

Jeon YH, Choi Y, Kang JH, et al. In vivo monitoring of DNA vaccine gene expression using firefly luciferase as a naked DNA. *Vaccine* 2006;24(16):3057-62.

Jiang S, Hyllyer C, Du L. Neutralizing antibodies against SARS-CoV-2 and other human coronaviruses. *Science and society. Trends Immunol* 2020;41(5)(May):355-9.

Ke Z, Oton J, Qu K, et al. Structures, conformations and distributions of SARS-CoV-2 spike protein trimers on intact virions. *Nature* 2020;10.1038/s41586-020-2665-2.

Kim JY, Ko JH, Kim Y, et al. Viral load kinetics of SARS-CoV-2 infection in first two patients in Korea. *J Korean Med Sci* 2020;35(7)(Feb):e86.

Kozauer NA, Dunn WH, Unger EF, et al. CBER multi-discipline review of Onpattro. NDA 210922. 10 Aug 2018. Available at: https://www.accessdata.fda.gov/drugsatfda_docs/nda/2018/210922Orig1s000MultiR.pdf. 02 Aug 2020.

Munster VJ, Feldmann F, Williamson BN, et al. Respiratory disease in rhesus macaques inoculated with SARS-CoV-2. *Nature* 2020 (May). Available from: <https://doi.org/10.1101/2020.03.21.001628>. Accessed: 24 Sep 2020.

Pallesen J, Wang N, Corbett KS, et al. Immunogenicity and structures of a rationally designed prefusion MERS-CoV spike antigen. *Proc Natl Acad Sci USA* 2017;114(35):E7348-57.

Pardi N, Hogan MJ, Pelc RS, et al. Zika virus protection by a single low-dose nucleoside-modified mRNA vaccination. *Nature* 2017;543(7644):248-51.

Pardi N, Parkhouse K, Kirkpatrick E, et al. Nucleoside-modified mRNA immunization elicits influenza virus hemagglutinin stalk-specific antibodies. *Nat Comm* 2018;9(1)(08):3361.

Sahin U, Karikó K, Türeci Ö. mRNA-based therapeutics - developing a new class of drugs. *Nat Rev Drug Discov* 2014;13(10):759-80.

Sedic M, Senn J, Lynn A, et al. Safety Evaluation of Lipid Nanoparticle-Formulated Modified mRNA in the Sprague- Dawley Rat and Cynomolgus Monkey. *Vet Path* 2018;55(2):341-54.

Sellers RS, Nelson K, Bennet B, et al. Scientific and regulatory policy committee points to consider*: approaches to the conduct and interpretation of vaccine safety studies for clinical and anatomic pathologists. *Toxicol Pathol* 2020;48(2):257-76.

Singh DK, Ganatra SR, Singh B, et al. SARS-CoV-2 infection leads to acute infection with dynamic cellular and inflammatory flux in the lung that varies across nonhuman primate species. *bioRxiv* 2020:06.05.136481. Accessed: 24 Sep 2020.

Truong B, Allegri G, Liu X-B, et al. Lipid nanoparticle-targeted mRNA therapy as a treatment for the inherited metabolic liver disorder arginase deficiency. *Proc Natl Acad Sci USA* 2019;116(42):21150-9.

US Department of Health and Human Services, Food and Drug Administration, Center for Biologics Evaluation and Research. Development and licensure of vaccines to prevent COVID-19. In: *Guidance for industry*. Rockville, MD: Food and Drug Administration; 2020: 21 pages.

World Health Organization. WHO guidelines on nonclinical evaluation of vaccines. Annex 1. In: *World Health Organization. WHO technical report series, no. 927*. Geneva, Switzerland; World Health Organization; 2005:31-63.

World Health Organization. Annex 2. Guidelines on the nonclinical evaluation of vaccine adjuvants and adjuvanted vaccines. In: *WHO technical report series no. 987*. Geneva, Switzerland: World Health Organization; 2014: p. 59-100.

Wrapp D, Wang N, Corbett KS, et al. Cryo-EM structure of the 2019-nCoV spike in the prefusion conformation. *Science* 2020;367(6483):1260-3.

Yong CY, Ong HK, Yeap SK, et al. Recent advances in the vaccine development against middle east respiratory syndrome-coronavirus. *Front Microbiol* 2019;10:1781.

090177e1962c108d\Approved\Approved On: 08-Feb-2021 15:26 (GMT)

Zakhartchouk AN, Sharon C, Satkunarajah M, et al. Immunogenicity of a receptor-binding domain of SARS coronavirus spike protein in mice: implications for a subunit vaccine. *Vaccine* 2007;25(1):136-43.

Zhou M, Zhang X, Qu J. Coronavirus disease 2019 (COVID-19): a clinical update. *Front Med* 2020(Apr):1-10.

Zost S, Gilchuk P, Chen R, et al. Rapid isolation and profiling of a diverse panel of human monoclonal antibodies targeting the SARS-CoV-2 spike protein. *BioRxiv* posted May13, 2020, www.biorxiv.org/content/10.1101/2020.05.12.091462v1.

Zou L, Ruan F, Huang M, et al. SARS-CoV-2 viral load in upper respiratory specimens of infected patients. *N Engl J Med* 2020;382(12)(03):1177-9.

MODULE 2.6.4. PHARMACOKINETICS WRITTEN SUMMARY

This document contains confidential information belonging to BioNTech/Pfizer. Except as may be otherwise agreed to in writing, by accepting or reviewing these materials, you agree to hold such information in confidence and not to disclose it to others (except where required by applicable law), nor to use it for unauthorized purposes. In the event of actual or suspected breach of this obligation, BioNTech/Pfizer should be promptly notified.

090177e1961d1c83\Approved\Approved On: 08-Feb-2021 17:49 (GMT)

TABLE OF CONTENTS

LIST OF ABBREVIATIONS AND DEFINITION OF TERMS3

2.6.4. PHARMACOKINETICS WRITTEN SUMMARY4

 2.6.4.1. Brief Summary4

 2.6.4.2. Methods of Analysis.....4

 2.6.4.3. Absorption4

 2.6.4.4. Distribution.....5

 2.6.4.5. Metabolism.....7

 2.6.4.6. Excretion9

 2.6.4.7. Pharmacokinetic Drug Interactions9

 2.6.4.8. Discussion and Conclusions9

 2.6.4.9. References10

090177e1961d1c83\Approved\Approved On: 08-Feb-2021 17:49 (GMT)

LIST OF ABBREVIATIONS AND DEFINITION OF TERMS

ADME	Absorption, distribution, metabolism, excretion
ALC-0159	Proprietary PEG-lipid included as an excipient in the LNP formulation used in BNT162b2
ALC-0315	Proprietary amino-lipid included as an excipient in the LNP formulation used in BNT162b2
[³ H]-CHE	Radiolabeled [Cholesteryl-1,2- ³ H(N)]-Cholesteryl Hexadecyl Ether
DSPC	1,2-distearoyl-sn-glycero-3-phosphocholine
GLP	Good Laboratory Practice
H	Human (in metabolite scheme)
IM	Intramuscular(ly)
IV	Intravenous(ly)
LNP	Lipid-nanoparticle
Luc	Luciferase (from firefly <i>Pyroactomena lucifera</i>)
Mk	Monkey (in metabolite scheme)
Mo	Mouse (in metabolite scheme)
modRNA	Nucleoside-modified mRNA
mRNA	Messenger RNA
PEG	Polyethylene glycol
PK	Pharmacokinetics
R	Rat (in metabolite scheme)
RNA	Ribonucleic acid
S9	Supernatant fraction obtained from liver homogenate by centrifuging at 9000 g
WHO	World Health Organization

2.6.4. PHARMACOKINETICS WRITTEN SUMMARY

2.6.4.1. Brief Summary

The ADME profile of BNT162b2 (BioNTech code number BNT162, Pfizer code number PF-07302048) included evaluation of the PK and metabolism of two novel lipid excipients (ALC-0315 and ALC-0159) in the LNP and potential biodistribution using luciferase expression as a surrogate reporter or a radiolabeled lipid marker. The PK study showed the LNP distributes from the blood to the liver, ~1% of ALC-0315 and ~50% of ALC-0159 were excreted unchanged in feces, and there was no detectable excretion of unchanged ALC-0315 and ALC-0159 in the urine.

In a mouse biodistribution study, protein expression was demonstrated at the site of injection and to a lesser extent in the liver after BALB/c mice received an IM injection of modRNA encoding luciferase in an LNP formulation, with the identical lipid composition as BNT162b2. Luciferase expression was identified at the injection site at 6 hours after injection and was not detected after 9 days. Liver expression was also present at 6 hours after injection and was no longer detected by 48 hours after injection. A quantitative biodistribution study was also carried out in Wistar Han rats using a radiolabeled lipid marker and a luciferase modRNA in the same LNP formulation as BNT162b2. Following IM administration, the greatest mean concentration remained at the injection site, while up to 18% of the administered dose was found in the liver.

The metabolism of ALC-0315 (aminolipid) and ALC-0159 (PEG-lipid) was evaluated in vitro using blood, liver microsomes, S9 fractions, and hepatocytes from mice, rats, monkeys, and humans. The in vivo metabolism was examined in rat plasma, urine, feces, and liver samples collected during the PK study. In vitro and in vivo studies indicated ALC-0315 and ALC-0159 are metabolized slowly by hydrolytic metabolism of the ester and amide functionalities, respectively, across the species evaluated.

2.6.4.2. Methods of Analysis

No methods of analysis have been validated to support GLP TK studies of components of BNT162b2; however, a qualified LC/MS method was developed to support quantitation of the two novel LNP excipients for the non-GLP IV PK study in rats ([PF-07302048_06Jul20_072424](#)). Methods for immunogenicity and efficacy studies are described in [Section 2.6.2.12](#).

2.6.4.3. Absorption

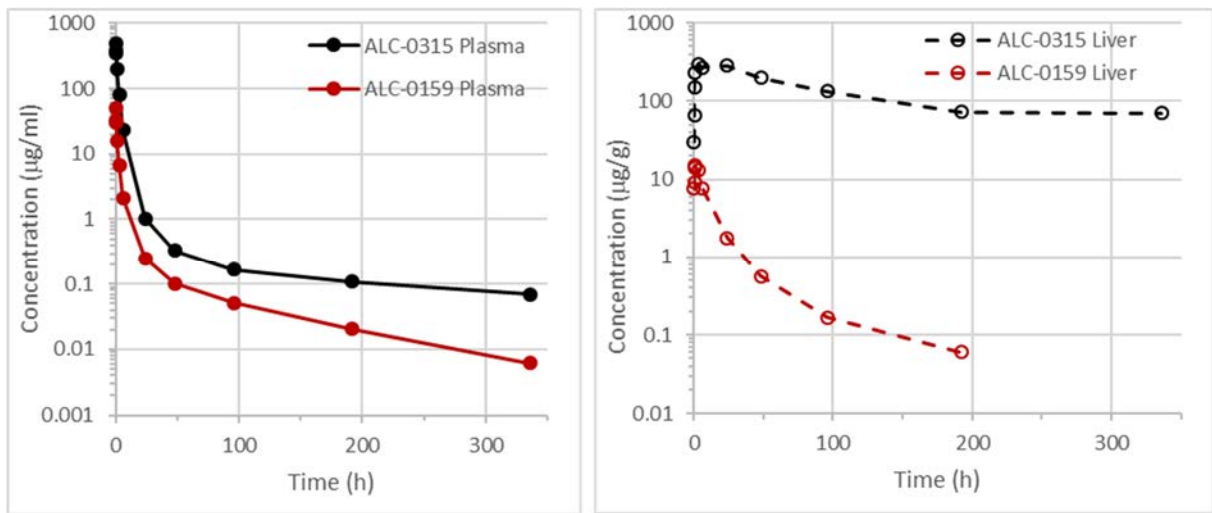
An intravenous rat PK study was performed using LNPs containing surrogate luciferase RNA, with the identical lipid composition as BNT162b2, to explore the disposition of ALC-0159 and ALC-0315 ([Table 2.6.4-1](#), Study [PF-07302048_06Jul20_072424](#); [Tabulated Summary 2.6.5.3](#)). The distribution of the LNP from the blood to the liver was rapid and essentially complete by 24 h, with <1% of the maximum observed plasma concentrations remaining ([Figure 2.6.4-1](#)). The liver appears to be the major site of drug uptake from the blood.

Table 2.6.4-1. PK of ALC-0315 and ALC-0159 in Wistar Han Rats After IV Administration of LNPs Containing Surrogate Luciferase RNA at 1 mg/kg

Analyte	Dose of Analyte (mg/kg)	Gender /N	t _{1/2} (h)	AUC _{inf} (µg•h/mL)	AUC _{last} (µg•h/mL)	Estimated fraction of dose distributed to liver (%) ^a
ALC-0315	15.3	Male/3 ^b	139	1030	1020	60
ALC-0159	1.96	Male/3 ^b	72.7	99.2	98.6	20

a. Calculated as highest mean amount in the liver (µg)/total mean dose (µg) of ALC-0315 or ALC-0159.
b. 3 animals per timepoint; non-serial sampling.

Figure 2.6.4-1. Plasma and Liver Concentrations of ALC-0315 and ALC-0159 in Wistar Han Rats After IV Administration of LNPs Containing Surrogate Luciferase RNA at 1 mg/kg



No absorption studies were conducted for BNT162b2, as the administration route is IM. Pharmacokinetic studies have not been conducted with BNT162b2 and are generally not considered necessary to support the development and licensure of vaccine products for infectious diseases (WHO, 2005; WHO, 2014).

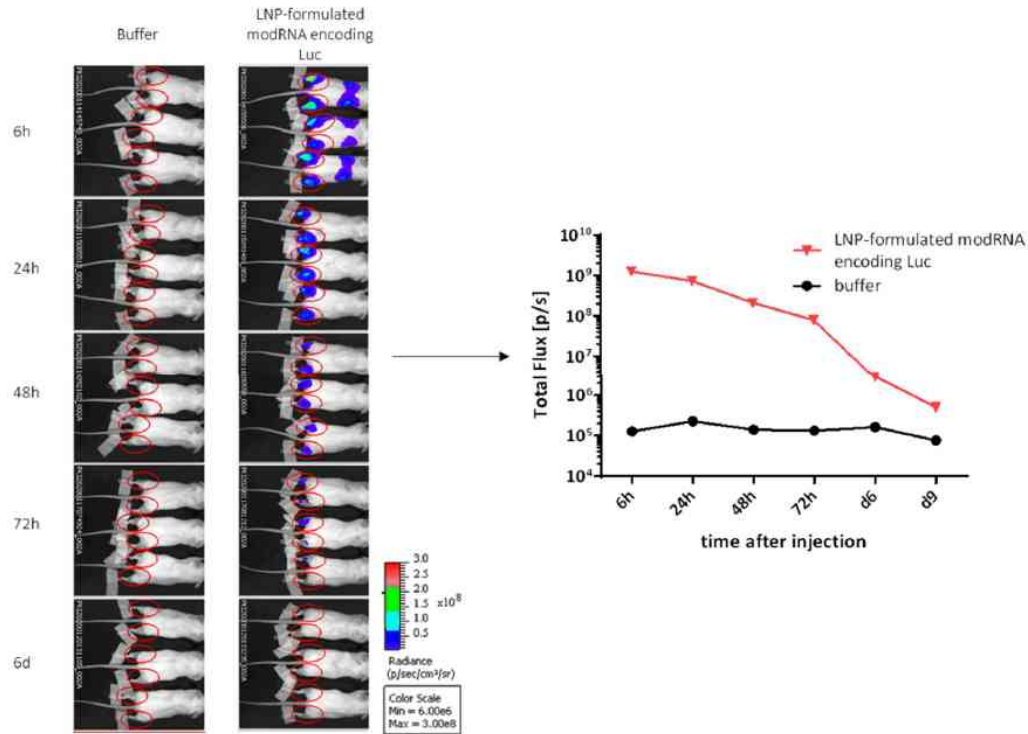
2.6.4.4. Distribution

In an in vivo study in BALB/c mice (Study R-20-0072; Tabulated Summary 2.6.5.5A), the biodistribution of BNT162b2 was assessed using luciferase as a surrogate marker protein. RNA encoding luciferase was formulated like BNT162b2, with the identical lipid composition, and mice received IM injections of 1 µg each in the right and left hind leg (for a total of 2 µg) of LNP-formulated modRNA encoding luciferase. Luciferase protein expression was detected at different timepoints, by measuring the in vivo bioluminescence (Figure 2.6.4-2) after injection of luciferin substrate, at the site of injection and to a lesser extent in the liver. Distribution to the liver is likely mediated by LNPs entering the blood stream. The repeat-dose toxicity studies in rats showed no evidence of liver injury (Section 2.6.6.3). The luciferase expression at the injection site, the tissue with the highest

090177e1961d1c83\Approved\Approved On: 08-Feb-2021 17:49 (GMT)

bioluminescence, dropped to background levels after 9 days. As detailed in Section 2.6.4.3, following systemic (IV) administration the liver appears to be the major organ into which the LNPs distribute, this is consistent with the observations made following IM administration.

Figure 2.6.4-2. Bioluminescence Emission in BALB/c Mice after IM Injection of an LNP Formulation of modRNA Encoding Luciferase



These qualitative data are supported by a biodistribution study (Study 185350; [Tabulated Summary 2.6.5.5B](#)) carried out with LNPs with a comparable lipid composition as BNT162b2 but with a luciferase mRNA and a [³H]-CHE lipid radiolabel. Following IM administration to male and female Wistar Han rats at a dose of 50 µg (1.29 mg total lipid), the greatest mean concentration was found remaining in the injection site at each time point in both sexes. Outside the injection site, the highest levels of radioactivity were observed in plasma at 1-4 hours post-dose. Over 48 hours, the radiolabel distributed mainly to the liver, adrenal glands, spleen and ovaries, with maximum concentrations observed at 8-48 hours post-dose. Total recovery of radioactivity (% of injected dose) outside the injection site was greatest in the liver (up to 18%) and was much less in the spleen (≤1.0%), adrenal glands (≤0.11%) and ovaries (≤0.095%). The mean concentrations and tissue distribution pattern were broadly similar between sexes.

The biodistribution of the expression of the antigen encoded by the RNA component of BNT162b2 is expected to be dependent on the LNP distribution. Therefore, results of these biodistribution studies should be representative for BNT162b2, as the LNP-formulated luciferase-encoding modRNA had the same lipid composition.

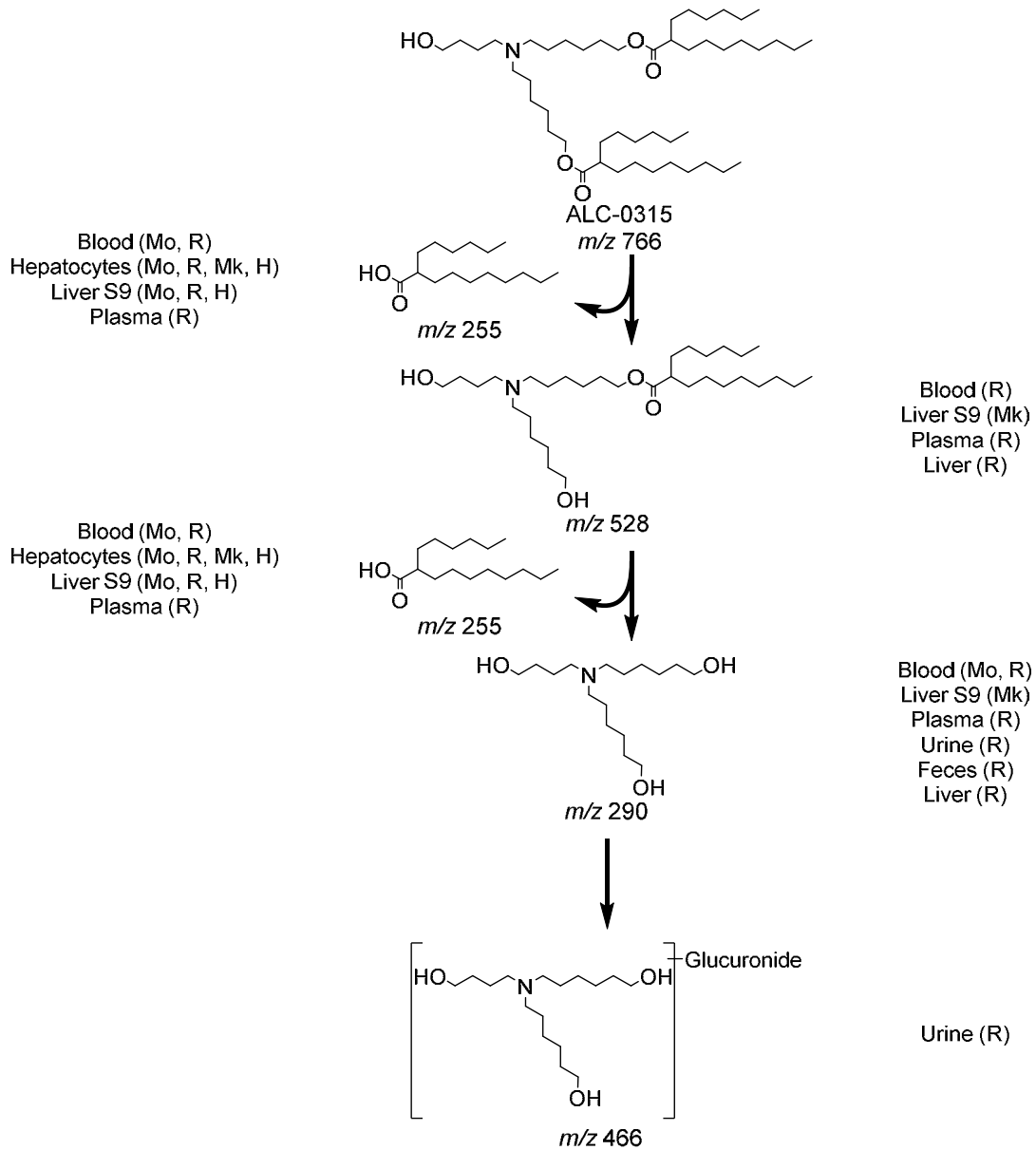
090177e1961d1c83\Approved\Approved On: 08-Feb-2021 17:49 (GMT)

2.6.4.5. Metabolism

Metabolism studies were conducted to evaluate ALC-0315 (aminolipid) and ALC-0159 (PEG-lipid). These novel lipids were evaluated for in vitro metabolic stability in CD-1/ICR mouse, Wistar Han and/or Sprague Dawley rat, cynomolgus monkey, and human liver microsomes, S9 fractions, and hepatocytes. ALC-0315 and ALC-0159 were stable (>82% remaining) over 120 min in liver microsomes and S9 fractions and over 240 min in hepatocytes in all species and test systems (Studies [01049-20008](#), [01049-20009](#), [01049-20010](#), [01049-20020](#), [01049-20021](#), and [01049-20022](#); [Tabulated Summaries 2.6.5.10A](#) and [2.6.5.10B](#)).

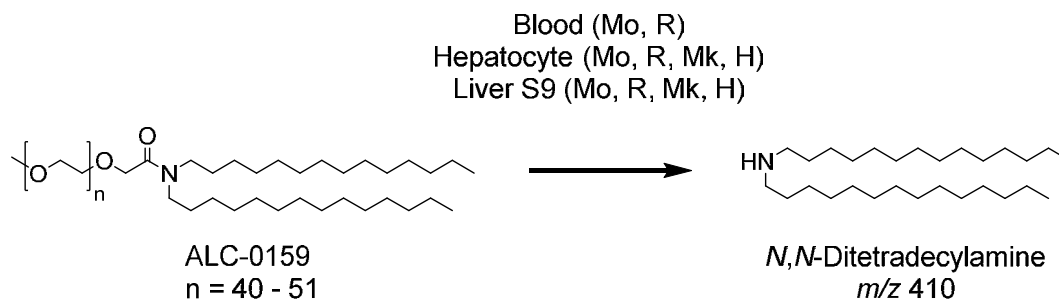
The metabolism of ALC-0315 and ALC-0159 was further evaluated (Study [PF-07302048_05Aug20_043725](#); [Tabulated Summaries 2.6.5.9](#), [2.6.5.10C](#), and [2.6.5.10D](#)) in vitro using blood, liver S9 fractions, and hepatocytes from CD-1 mice, Wistar Han rats, cynomolgus monkeys, and humans and in vivo using the rat plasma, urine, feces, and liver from the PK study ([Section 2.6.4.3](#)). This study determined ALC-0315 and ALC-0159 are metabolized slowly and undergo hydrolytic metabolism of the ester and amide functionalities, respectively. This hydrolytic metabolism was observed across the species evaluated, as shown in [Figure 2.6.4-3](#) and [Figure 2.6.4-4](#).

Figure 2.6.4-3. Proposed Biotransformation Pathway of ALC-0315 in Various Species



Metabolism of ALC-0315 occurs via two sequential ester hydrolysis reactions, first yielding the monoester metabolite (m/z 528) followed by the doubly deesterified metabolite (m/z 290). Subsequent metabolism of the doubly deesterified metabolite resulted in a glucuronide metabolite (m/z 466), which was only observed in urine from the rat PK study. The acid product of both hydrolysis reactions of ALC-0315, 6-hexyldecanoic acid (m/z 255), was also identified.

090177e1961d1c83\Approved\Approved On: 08-Feb-2021 17:49 (GMT)

Figure 2.6.4-4. Proposed Biotransformation Pathway of ALC-0159 in Various Species

The primary route of metabolism identified for ALC-0159 involves amide bond hydrolysis yielding *N,N*-ditetradecylamine (*m/z* 410). This metabolite was identified in mouse and rat blood, as well as hepatocytes and liver S9 from mouse, rat, monkey, and human. No metabolites of ALC-0159 were identified from in vivo samples.

The other two lipids in the LNP are naturally occurring (cholesterol and DSPC) and will be metabolized and excreted like other endogenous lipids. As the protein encoded by the mRNA in BNT162b2 is expected to be proteolytically degraded and RNA is degraded by cellular RNases and subjected to nucleic acid metabolism, no RNA or protein metabolism or excretion studies will be conducted.

2.6.4.6. Excretion

In the rat PK study (Section 2.6.4.3), there was no detectable excretion ALC-0315 and ALC-0159 in urine after IV administration of LNPs containing surrogate luciferase RNA at 1 mg/kg. The percent excreted unchanged in feces was ~1% for ALC-0315 and ~50% for ALC-0159. Metabolites of ALC-0315 were detected in the urine of rats (Figure 2.6.4-3). No excretion studies have been conducted with BNT162b2 for the reasons described in Section 2.6.4.5.

2.6.4.7. Pharmacokinetic Drug Interactions

No PK drug interaction studies have been conducted with BNT162b2.

2.6.4.8. Discussion and Conclusions

In the rat PK study, concentrations of ALC-0159 dropped approximately 8000- and >250-fold in plasma and liver, respectively, during this 2-week study. For ALC-0315, the elimination of the molecule from plasma and liver was slower, but concentrations fell approximately 7000- and 4-fold in two weeks for plasma and liver, respectively. Overall, the apparent terminal $t_{1/2}$ in plasma and liver were similar in both tissues and were 2-3 and 6-8 days for ALC-0159 and ALC-0315, respectively. The apparent terminal $t_{1/2}$ in plasma likely represents the re-distribution of the respective lipids from the tissues into which they have distributed as the LNP back to plasma where they are eliminated.

Overall, it appears that 50% of ALC-0159 was eliminated unchanged in feces. Metabolism played a role in the elimination of ALC-0315, as little to no unchanged material was detected in either urine or feces. Investigations of urine, feces and plasma from the rat PK study

identified a series of ester cleavage products of ALC-0315; this likely represents the primary clearance mechanism acting on this molecule, although no quantitative data is available to confirm this hypothesis. In vitro, ALC-0159 was metabolized slowly by hydrolytic metabolism of the amide functionality.

The potential biodistribution of BNT162b2 was assessed using luciferase expression as a surrogate reporter. Protein expression was demonstrated at the site of injection and to a lesser extent, and more transiently, in the liver after BALB/c mice received an IM injection of RNA encoding luciferase in an LNP formulation like BNT162b2. Luciferase expression was identified at the injection site at 6 hours after injection and was not detected by 9 days. Expression in the liver was also present at 6 hours after injection and was not detected by 48 hours after injection. These findings are supported by a quantitative biodistribution study in Wistar Han rats. After IM administration of a radiolabeled lipid marker and a luciferase modRNA in the same LNP formulation as BNT162b2 to rats, the percent of administered dose was greatest at the injection site. Outside of the injection site, total recovery of radioactivity was highest in the liver and much lower in the spleen, with very little recovery in the adrenal glands and ovaries.

2.6.4.9. References

1. World Health Organization. Annex 1. Guidelines on the nonclinical evaluation of vaccines. In: WHO Technical Report Series No. 927, Geneva, Switzerland. World Health Organization; 2005:31-63.
2. World Health Organization. Annex 2. Guidelines on the nonclinical evaluation of vaccine adjuvants and adjuvanted vaccines. In: WHO Technical Report Series No. 987, Geneva, Switzerland. World Health Organization 2014:59-100.

MODULE 2.6.5. PHARMACOKINETICS TABULATED SUMMARY

This document contains confidential information belonging to BioNTech/Pfizer. Except as may be otherwise agreed to in writing, by accepting or reviewing these materials, you agree to hold such information in confidence and not to disclose it to others (except where required by applicable law), nor to use it for unauthorized purposes. In the event of actual or suspected breach of this obligation, BioNTech/Pfizer should be promptly notified.

CONFIDENTIAL

Page 1

BNT162b2

2.6.5 Pharmacokinetics Tabulated Summary

2.6.5.1. PHARMACOKINETICS OVERVIEW

Test Article: BNT162b2

Type of Study	Test System	Test item	Method of Administration	Testing Facility	Report Number
Single Dose Pharmacokinetics					
Single Dose Pharmacokinetics and Excretion in Urine and Feces of ALC-0159 and ALC-0315	Rat (Wistar Han)	modRNA encoding luciferase formulated in LNP comparable to BNT162b2	IV bolus	Pfizer Inc ^a	PF-07302048_06Jul20_072424
Distribution					
In Vivo Distribution	Mice (BALB/c)	modRNA encoding luciferase formulated in LNP comparable to BNT162b2	IM Injection	BioNTech ^b	R-20-0072
In Vivo Distribution	Rat (Wistar Han)	modRNA encoding luciferase formulated in LNP comparable to BNT162b2 with trace amounts of [³ H]-CHE as non-diffusible label	IM Injection	(b) (4)	185350
Metabolism					
In Vitro and In Vivo Metabolism					
In Vitro Metabolic Stability of ALC-0315 in Liver Microsomes	Mouse (CD-1/ICR), rat (Sprague Dawley and Wistar Han), monkey (Cynomolgus), and human liver microsomes	ALC-0315	In vitro	(b) (4)	01049-20008
In Vitro Metabolic Stability of ALC-0315 in Liver S9	Mouse (CD-1/ICR), rat (Sprague Dawley), monkey (Cynomolgus), and human S9 liver fractions	ALC-0315	In vitro	(b) (4)	01049-20009

CONFIDENTIAL

Page 2

BNT162b2

2.6.5 Pharmacokinetics Tabulated Summary

2.6.5.1. PHARMACOKINETICS OVERVIEW

Test Article: BNT162b2

Type of Study	Test System	Test item	Method of Administration	Testing Facility	Report Number
In Vitro Metabolic Stability of ALC-0315 in Hepatocytes	Mouse (CD-1/ICR), rat (Sprague Dawley and Wistar Han), monkey (Cynomolgus), and human hepatocytes	ALC-0315	In vitro	(b) (4)	01049-20010
In Vitro Metabolic Stability of ALC-0159 in Liver Microsomes	Mouse (CD-1/ICR), rat (Sprague Dawley and Wistar Han), monkey (Cynomolgus), and human liver microsomes	ALC-0159	In vitro	(b) (4)	01049-20020
In Vitro Metabolic Stability of ALC-0159 in Liver S9	Mouse (CD-1/ICR), rat (Sprague Dawley), monkey (Cynomolgus), and human S9 fractions	ALC-0159	In vitro	(b) (4)	01049-20021
In Vitro Metabolic Stability of ALC-0159 in Hepatocytes	Mouse (CD-1/ICR), rat (Sprague Dawley and Wistar Han), monkey (Cynomolgus), and human hepatocytes	ALC-0159	In vitro	(b) (4)	01049-20022
Biotransformation of ALC-0159 and ALC-0315 In Vitro and In Vivo in Rats	In vitro: CD-1 mouse, Wistar Han rat, cynomolgus monkey, and human blood, liver S9 fractions and hepatocytes In vivo: male Wistar Han rats	ALC-0315 and ALC-0159	In vitro or IV (in vivo in rats)	Pfizer Inc ^e	PF-07302048_05Aug20_043725

090177e196137069\Approved\Approved On: 21-Jan-2021 23:22 (GMT)

BNT162b2

2.6.5 Pharmacokinetics Tabulated Summary

2.6.5.1. PHARMACOKINETICS OVERVIEW

Test Article: BNT162b2

Type of Study	Test System	Test item	Method of Administration	Testing Facility	Report Number
<p>ALC-0159 = 2-[(polyethylene glycol)-2000]-N,N-ditetradecylacetamide), a proprietary polyethylene glycol-lipid included as an excipient in the LNP formulation used in BNT162b2; ALC-0315 = (4-hydroxybutyl)azanediylbis(hexane-6,1-diyl)bis(2-hexyldecanoate), a proprietary aminolipid included as an excipient in the LNP formulation used in BNT162b2; [³H]-CHE = radiolabeled [cholesteryl-1,2-³H(N)]-cholesteryl hexadecyl ether; IM = Intramuscular; IV = Intravenous; LNP = lipid nanoparticles; S9 = Supernatant fraction obtained from liver homogenate by centrifuging at 9000 g.</p> <p>a. La Jolla, California.</p> <p>b. Mainz, Germany.</p> <p>(b) (4)</p> <p>e. Groton, Connecticut.</p>					

090177e196137069\Approved\Approved On: 21-Jan-2021 23:22 (GMT)

BNT162b2

2.6.5 Pharmacokinetics Tabulated Summary

**2.6.5.3. PHARMACOKINETICS:
PHARMACOKINETICS AFTER A SINGLE DOSE**

**Test Article: modRNA encoding luciferase in LNP
Report Number: PF-07302048_06Jul20_072424**

Species (Strain)	Rat (Wistar Han)	
Sex/Number of Animals	Male/ 3 animals per timepoint ^a	
Feeding Condition	Fasted	
Method of Administration	IV	
Dose modRNA (mg/kg)	1	
Dose ALC-0159 (mg/kg)	1.96	
Dose ALC-0315 (mg/kg)	15.3	
Sample Matrix	Plasma, liver, urine and feces	
Sampling Time Points (h post dose):	Predose, 0.1, 0.25, 0.5, 1, 3, 6, 24, 48, 96, 192, 336	
Analyte	ALC-0315	ALC-0159
PK Parameters:	Mean ^b	Mean ^b
AUC _{inf} (µg•h/mL) ^c	1030	99.2
AUC _{last} (µg•h/mL)	1020	98.6
Initial t _{1/2} (h) ^d	1.62	1.74
Terminal elimination t _{1/2} (h) ^e	139	72.7
Estimated fraction of dose distributed to liver (%) ^f	59.5	20.3
Dose in Urine (%)	NC ^g	NC ^g
Dose in Feces (%) ^h	1.05	47.2

ALC-0159 = 2-[(polyethylene glycol)-2000]-N,N-ditetradecylacetamide), a proprietary polyethylene glycol-lipid included as an excipient in the LNP formulation used in BNT162b2; ALC-0315 = (4-hydroxybutyl)azanediylbis(hexane-6,1-diyl)bis(2-hexyldecanoate), a proprietary aminolipid included as an excipient in the LNP formulation used in BNT162b2; AUC_{inf} = Area under the plasma drug concentration-time curve from 0 to infinite time; AUC_{last} = Area under the plasma drug concentration-time curve from 0 to the last quantifiable time point; BLQ = Below the limit of quantitation; LNP = Lipid nanoparticle; modRNA = Nucleoside modified messenger RNA; PK = Pharmacokinetics; t_{1/2} = Half-life.

- a. Non-serial sampling, 36 animals total.
- b. Only mean PK parameters are reported due to non-serial sampling.
- c. Calculated using the terminal log-linear phase (determined using 48, 96, 192, and 336 h for regression calculation).
- d. ln(2)/initial elimination rate constant (determined using 1, 3, and 6 h for regression calculation).
- e. ln(2)/terminal elimination rate constant (determined using 48, 96, 192, and 336 h for regression calculation).
- f. Calculated as follows: highest mean amount in the liver (µg)/total mean dose (µg) of ALC-0315 or ALC-0159.
- g. Not calculated due to BLQ data.
- h. Fecal excretion, calculated as: (mean µg of analyte in feces/ mean µg of analyte administered) × 100

BNT162b2

2.6.5 Pharmacokinetics Tabulated Summary

2.6.5.5A. PHARMACOKINETICS: ORGAN DISTRIBUTION

Test Article: modRNA encoding luciferase in LNP
Report Number: R-20-0072

Species (Strain):	Mice (BALB/c)
Sex/Number of Animals:	Female/3 per group
Feeding Condition:	Fed ad libitum
Vehicle/Formulation:	Phosphate-buffered saline
Method of Administration:	Intramuscular injection
Dose (mg/kg):	1 µg/hind leg in gastrocnemius muscle (2 µg total)
Number of Doses:	1
Detection:	Bioluminescence measurement
Sampling Time (hour):	6, 24, 48, 72 hours; 6 and 9 days post-injection

Time point	Total Mean Bioluminescence signal (photons/second)		Mean Bioluminescence signal in the liver (photons/second)
	Buffer control	modRNA Luciferase in LNP	modRNA Luciferase in LNP
6 hours	1.28×10 ⁵	1.26×10 ⁹	4.94×10 ⁷
24 hours	2.28×10 ⁵	7.31×10 ⁸	2.4×10 ⁶
48 hours	1.40×10 ⁵	2.10×10 ⁸	Below detection ^a
72 hours	1.33×10 ⁵	7.87×10 ⁷	Below detection ^a
6 days	1.62×10 ⁵	2.92×10 ⁶	Below detection ^a
9 days	7.66×10 ⁴	5.09×10 ⁵	Below detection ^a

LNP = Lipid nanoparticle; modRNA = Nucleoside modified messenger RNA.

a. At or below the background level of the buffer control.

090177e196137069\Approved\Approved On: 21-Jan-2021 23:22 (GMT)

BNT162b2

2.6.5 Pharmacokinetics Tabulated Summary

2.6.5.5B. PHARMACOKINETICS: ORGAN DISTRIBUTION CONTINUED

**Test Article: [³H]-Labelled LNP-mRNA formulation containing ALC-0315 and ALC-0159
Report Number: 185350**

Species (Strain):	Rat (Wistar Han)
Sex/Number of Animals:	Male and female/3 animals/sex/timepoint (21 animals/sex total for the 50 µg dose)
Feeding Condition:	Fed ad libitum
Method of Administration:	Intramuscular injection
Dose:	50 µg [³ H]-08-A01-C0 (lot # NC-0552-1)
Number of Doses:	1
Detection:	Radioactivity quantitation using liquid scintillation counting
Sampling Time (hour):	0.25, 1, 2, 4, 8, 24, and 48 hours post-injection

Sample	Mean total lipid concentration (µg lipid equivalent/g (or mL) (males and females combined))							% of administered dose (males and females combined)						
	0.25 min	1 h	2 h	4 h	8 h	24 h	48 h	0.25 min	1 h	2 h	4 h	8 h	24 h	48 h
Adipose tissue	0.057	0.100	0.126	0.128	0.093	0.084	0.181	--	--	--	--	--	--	--
Adrenal glands	0.271	1.48	2.72	2.89	6.80	13.8	18.2	0.001	0.007	0.010	0.015	0.035	0.066	0.106
Bladder	0.041	0.130	0.146	0.167	0.148	0.247	0.365	0.000	0.001	0.001	0.001	0.001	0.002	0.002
Bone (femur)	0.091	0.195	0.266	0.276	0.340	0.342	0.687	--	--	--	--	--	--	--
Bone marrow (femur)	0.479	0.960	1.24	1.24	1.84	2.49	3.77	--	--	--	--	--	--	--
Brain	0.045	0.100	0.138	0.115	0.073	0.069	0.068	0.007	0.013	0.020	0.016	0.011	0.010	0.009
Eyes	0.010	0.035	0.052	0.067	0.059	0.091	0.112	0.000	0.001	0.001	0.002	0.002	0.002	0.003
Heart	0.282	1.03	1.40	0.987	0.790	0.451	0.546	0.018	0.056	0.084	0.060	0.042	0.027	0.030
Injection site	128	394	311	338	213	195	165	19.9	52.6	31.6	28.4	21.9	29.1	24.6
Kidneys	0.391	1.16	2.05	0.924	0.590	0.426	0.425	0.050	0.124	0.211	0.109	0.075	0.054	0.057
Large intestine	0.013	0.048	0.093	0.287	0.649	1.10	1.34	0.008	0.025	0.065	0.192	0.405	0.692	0.762
Liver	0.737	4.63	11.0	16.5	26.5	19.2	24.3	0.602	2.87	7.33	11.9	18.1	15.4	16.2
Lung	0.492	1.21	1.83	1.50	1.15	1.04	1.09	0.052	0.101	0.178	0.169	0.122	0.101	0.101

090177e196137069Approved\Approved On: 21-Jan-2021 23:22 (GMT)

BNT162b2

2.6.5 Pharmacokinetics Tabulated Summary

2.6.5.5B. PHARMACOKINETICS: ORGAN DISTRIBUTION CONTINUED

**Test Article: [³H]-Labelled LNP-mRNA formulation containing ALC-0315 and ALC-0159
Report Number: 185350**

Sample	Total Lipid concentration (µg lipid equivalent/g [or mL]) (males and females combined)							% of Administered Dose (males and females combined)						
	0.25 min	1 h	2 h	4 h	8 h	24 h	48 h	0.25 min	1 h	2 h	4 h	8 h	24 h	48 h
Lymph node (mandibular)	0.064	0.189	0.290	0.408	0.534	0.554	0.727	--	--	--	--	--	--	--
Lymph node (mesenteric)	0.050	0.146	0.530	0.489	0.689	0.985	1.37	--	--	--	--	--	--	--
Muscle	0.021	0.061	0.084	0.103	0.096	0.095	0.192	--	--	--	--	--	--	--
Ovaries (females)	0.104	1.34	1.64	2.34	3.09	5.24	12.3	0.001	0.009	0.008	0.016	0.025	0.037	0.095
Pancreas	0.081	0.207	0.414	0.380	0.294	0.358	0.599	0.003	0.007	0.014	0.015	0.015	0.011	0.019
Pituitary gland	0.339	0.645	0.868	0.854	0.405	0.478	0.694	0.000	0.001	0.001	0.001	0.000	0.000	0.001
Prostate (males)	0.061	0.091	0.128	0.157	0.150	0.183	0.170	0.001	0.001	0.002	0.003	0.003	0.004	0.003
Salivary glands	0.084	0.193	0.255	0.220	0.135	0.170	0.264	0.003	0.007	0.008	0.008	0.005	0.006	0.009
Skin	0.013	0.208	0.159	0.145	0.119	0.157	0.253	--	--	--	--	--	--	--
Small intestine	0.030	0.221	0.476	0.879	1.28	1.30	1.47	0.024	0.130	0.319	0.543	0.776	0.906	0.835
Spinal cord	0.043	0.097	0.169	0.250	0.106	0.085	0.112	0.001	0.002	0.002	0.003	0.001	0.001	0.001
Spleen	0.334	2.47	7.73	10.3	22.1	20.1	23.4	0.013	0.093	0.325	0.385	0.982	0.821	1.03
Stomach	0.017	0.065	0.115	0.144	0.268	0.152	0.215	0.006	0.019	0.034	0.030	0.040	0.037	0.039
Testes (males)	0.031	0.042	0.079	0.129	0.146	0.304	0.320	0.007	0.010	0.017	0.030	0.034	0.074	0.074
Thymus	0.088	0.243	0.340	0.335	0.196	0.207	0.331	0.004	0.007	0.010	0.012	0.008	0.007	0.008
Thyroid	0.155	0.536	0.842	0.851	0.544	0.578	1.00	0.000	0.001	0.001	0.001	0.001	0.001	0.001
Uterus (females)	0.043	0.203	0.305	0.140	0.287	0.289	0.456	0.002	0.011	0.015	0.008	0.016	0.018	0.022
Whole blood	1.97	4.37	5.40	3.05	1.31	0.909	0.420	--	--	--	--	--	--	--
Plasma	3.97	8.13	8.90	6.50	2.36	1.78	0.805	--	--	--	--	--	--	--
Blood:Plasma ratio ^a	0.815	0.515	0.550	0.510	0.555	0.530	0.540	--	--	--	--	--	--	--

090177e196137069\Approved\Approved On: 21-Jan-2021 23:22 (GMT)

BNT162b2

2.6.5 Pharmacokinetics Tabulated Summary

**2.6.5.5B. PHARMACOKINETICS: ORGAN
DISTRIBUTION CONTINUED**

**Test Article: [³H]-Labelled LNP-mRNA formulation containing
ALC-0315 and ALC-0159
Report Number: 185350**

-- = Not applicable, partial tissue taken; [³H]-08-A01-C0 = An aqueous dispersion of LNPs, including ALC-0315, ALC-0159, distearoylphosphatidylcholine, cholesterol, mRNA encoding luciferase and trace amounts of radiolabeled [Cholesteryl-1,2-3H(N)]-Cholesteryl Hexadecyl Ether, a nonexchangeable, non-metabolizable lipid marker used to monitor the disposition of the LNPs; ALC-0159 = 2-[(polyethylene glycol)-2000]-N,N--ditetradecylacetamide), a proprietary polyethylene glycol-lipid included as an excipient in the LNP formulation used in BNT162b2; ALC-0315 = (4--hydroxybutyl)azanediyl)bis(hexane-6,1-diyl)bis(2-hexyldecanoate), a proprietary aminolipid included as an excipient in the LNP formulation used in BNT162b2; LNP = Lipid nanoparticle; mRNA = messenger RNA.

a. The mean male and female blood:plasma values were first calculated separately and this value represents the mean of the two values.

090177e196137069\Approved\Approved On: 21-Jan-2021 23:22 (GMT)

BNT162b2

2.6.5 Pharmacokinetics Tabulated Summary

2.6.5.9. PHARMACOKINETICS: METABOLISM IN VIVO, RAT

Test Article: modRNA encoding luciferase in LNP
Report Number: PF-07302048_05Aug20_043725

Species (Strain): Rat (Wistar Han)
 Sex/ Number of animals: Male/ 36 animals total for plasma and liver, 3 animals for urine and feces
 Method of Administration: Intravenous
 Dose (mg/kg): 1
 Test System: Plasma, Urine, Feces, Liver
 Analysis Method: Ultrahigh performance liquid chromatography/ mass spectrometry

Biotransformation	m/z	Metabolites of ALC-0315 Detected			
		Plasma	Urine	Feces	Liver
N-dealkylation, oxidation	102.0561 ^a	ND	ND	ND	ND
N-Dealkylation, oxidation	104.0706 ^b	ND	ND	ND	ND
N-dealkylation, oxidation	130.0874 ^a	ND	ND	ND	ND
N-Dealkylation, oxidation	132.1019 ^b	ND	ND	ND	ND
N-dealkylation, hydrolysis, oxidation	145.0506 ^a	ND	ND	ND	ND
Hydrolysis (acid)	255.2330 ^a	+	ND	ND	ND
Hydrolysis, hydroxylation	271.2279 ^a	ND	ND	ND	ND
Bis-hydrolysis (amine)	290.2690 ^b	+	+	+	+
Hydrolysis, glucuronidation	431.2650 ^a	ND	ND	ND	ND
Bis-hydrolysis (amine), glucuronidation	464.2865 ^a	ND	ND	ND	ND
Bis-hydrolysis (amine), glucuronidation	466.3011 ^b	ND	+	ND	ND
Hydrolysis (amine)	528.4986 ^b	+	ND	ND	+
Hydrolysis (amine), Glucuronidation	704.5307 ^b	ND	ND	ND	ND
Oxidation to acid	778.6930 ^a	ND	ND	ND	ND
Oxidation to acid	780.7076 ^b	ND	ND	ND	ND
Hydroxylation	782.7232 ^b	ND	ND	ND	ND
Sulfation	844.6706 ^a	ND	ND	ND	ND
Sulfation	846.6851 ^b	ND	ND	ND	ND
Glucuronidation	940.7458 ^a	ND	ND	ND	ND
Glucuronidation	942.7604 ^b	ND	ND	ND	ND

Note: Both theoretical and observed metabolites are included.

m/z = mass to charge ratio; ND = Not detected; + = minor metabolite as assessed by ultraviolet detection.

a. Negative ion mode.

b. Positive ion mode.

CONFIDENTIAL

Page 10

090177e196137069Approved\Approved On: 21-Jan-2021 23:22 (GMT)

BNT162b2

2.6.5 Pharmacokinetics Tabulated Summary

2.6.5.10A. PHARMACOKINETICS: METABOLISM IN VITRO

Test Article: ALC-0315
Report Numbers: 01049-20008
01049-20009
01049-20010

Type of Study:	Liver Microsomes + NADPH		Stability of ALC-0315 In Vitro S9 Fraction + NADPH, UDPGA, and alamethicin		Hepatocytes
Study System:					
ALC-0315 Concentration:	1 µM		1 µM		1 µM
Duration of Incubation (min):	120 min		120 min		240 min
Analysis Method:	Ultra-high performance liquid chromatography-tandem mass spectrometry				

Incubation time (min)	Percent ALC-0315 remaining													
	Liver Microsomes					Liver S9 Fraction				Hepatocytes				
	Mouse (CD-1/ICR)	Rat (SD)	Rat (WH)	Monkey (Cyno)	Human	Mouse (CD-1/ICR)	Rat (SD)	Monkey (Cyno)	Human	Mouse (CD-1/ICR)	Rat (SD)	Rat (WH)	Monkey (Cyno)	Human
0	100.00	100.00	100.00	100.00	100.00	100.00	100.00	100.00	100.00	100.00	100.00	100.00	100.00	100.00
15	98.77	94.39	96.34	97.96	100.24	97.69	98.85	99.57	95.99	--	--	--	--	--
30	97.78	96.26	97.32	96.18	99.76	97.22	99.62	96.96	97.32	101.15	97.75	102.70	96.36	100.72
60	100.49	99.73	98.54	100.00	101.45	98.61	99.62	99.13	94.98	100.77	98.50	102.32	97.82	101.44
90	97.78	98.66	94.15	97.96	100.48	98.15	98.85	98.70	98.33	101.92	99.25	103.09	100.0	100.36
120	96.54	95.99	93.66	97.71	98.31	96.76	98.46	99.57	99.33	98.85	97.38	99.61	96.36	100.72
180	--	--	--	--	--	--	--	--	--	101.15	98.88	103.47	95.64	98.92
240	--	--	--	--	--	--	--	--	--	99.62	101.12	100.00	93.82	99.64
t½ (min)	>120	>120	>120	>120	>120	>120	>120	>120	>120	>240	>240	>240	>240	>240

-- = Data not available; ALC-0315 = (4-hydroxybutyl)azanediylbis(hexane-6,1-diyl)bis(2-hexyldecanoate), a proprietary aminolipid included as an excipient in the lipid nanoparticle formulation used in BNT162b2; Cyno = Cynomolgus; NADPH = Reduced form of nicotinamide adenine dinucleotide phosphate; NC = not calculated; SD = Sprague Dawley; t½ = half-life; WH = Wistar-Han; UDPGA= uridine-diphosphate-glucuronic acid trisodium salt.

090177e196137069\Approved On: 21-Jan-2021 23:22 (GMT)

BNT162b2

2.6.5 Pharmacokinetics Tabulated Summary

2.6.5.10B. PHARMACOKINETICS: METABOLISM IN VITRO CONTINUED

Test Article: ALC-0159
 Report Numbers: **01049-20020**
01049-20021
01049-20022

Type of Study:	Liver Microsomes + NADPH		Stability of ALC-0159 In Vitro S9 Fraction + NADPH, UDPGA, and alamethicin		Hepatocytes
Study System:	Liver Microsomes + NADPH		Stability of ALC-0159 In Vitro S9 Fraction + NADPH, UDPGA, and alamethicin		Hepatocytes
ALC-0159 Concentration:	1 µM		1 µM		1 µM
Duration of Incubation (min):	120 min		120 min		240 min
Analysis Method:	Ultra-high performance liquid chromatography-tandem mass spectrometry				

Incubation time (min)	Percent ALC-0159 remaining													
	Liver Microsomes					Liver S9 Fraction				Hepatocytes				
	Mouse (CD-1/ICR)	Rat (SD)	Rat (WH)	Monkey (Cyno)	Human	Mouse (CD-1/ICR)	Rat (SD)	Monkey (Cyno)	Human	Mouse (CD-1/ICR)	Rat (SD)	Rat (WH)	Monkey (Cyno)	Human
0	100.00	100.00	100.00	100.00	100.00	100.00	100.00	100.00	100.00	100.00	100.00	100.00	100.00	100.00
15	82.27	101.24	112.11	100.83	99.59	98.93	84.38	91.30	106.73	--	--	--	--	--
30	86.40	93.78	102.69	85.12	92.28	91.10	90.87	97.96	107.60	100.85	93.37	113.04	90.23	106.34
60	85.54	98.34	105.38	86.36	95.53	102.85	97.97	105.56	104.97	94.92	91.81	105.07	92.93	101.58
90	85.41	95.44	100.90	94.63	97.97	90.75	93.51	108.33	109.36	94.28	90.25	112.80	94.59	92.67
120	95.87	97.10	108.97	93.39	93.09	106.76	92.70	105.74	119.59	87.08	89.47	104.11	97.51	96.04
180	--	--	--	--	--	--	--	--	--	94.92	93.96	102.90	89.81	93.66
240	--	--	--	--	--	--	--	--	--	102.75	94.93	98.79	92.93	102.57
t½ (min)	>120	>120	>120	>120	>120	>120	>120	>120	>120	>240	>240	>240	>240	>240

-- = Data not available; ALC-0159 = 2-[(polyethylene glycol)-2000]-N,N-ditetradecylacetamide), a proprietary polyethylene glycol-lipid included as an excipient in the lipid nanoparticle formulation used in BNT162b2; Cyno = Cynomolgus; NADPH = Reduced form of nicotinamide adenine dinucleotide phosphate; NC = not calculated; SD = Sprague Dawley; WH = Wistar-Han; UDPGA= uridine-diphosphate-glucuronic acid trisodium salt.

090177e196137069\Approved On: 21-Jan-2021 23:22 (GMT)

BNT162b2

2.6.5 Pharmacokinetics Tabulated Summary

**2.6.5.10C. PHARMACOKINETICS: METABOLISM
IN VITRO CONTINUED**

**Test Article: ALC-0315
Report Number: PF-07302048_05Aug20_043725**

Type of study		Metabolism of ALC-0315 In Vitro											
Study system		Blood				Hepatocytes				Liver S9 Fraction			
ALC-0315 concentration		10 µM				10 µM				10 µM			
Duration of incubation		24 h				4 h				24 h			
Analysis Method:		Ultrahigh performance liquid chromatography/ mass spectrometry											
Biotransformation	m/z	Blood				Hepatocytes				Liver S9 Fraction			
		Mouse	Rat	Monkey	Human	Mouse	Rat	Monkey	Human	Mouse	Rat	Monkey	Human
<i>N</i> -dealkylation, oxidation	102.0561 ^a	ND	ND	ND	ND	ND	ND	ND	ND	ND	ND	ND	ND
<i>N</i> -Dealkylation, oxidation	104.0706 ^b	ND	ND	ND	ND	ND	ND	ND	ND	ND	ND	ND	ND
<i>N</i> -dealkylation, oxidation	130.0874 ^a	ND	ND	ND	ND	ND	ND	ND	ND	ND	ND	ND	ND
<i>N</i> -Dealkylation, oxidation	132.1019 ^b	ND	ND	ND	ND	ND	ND	ND	ND	ND	ND	ND	ND
<i>N</i> -dealkylation, hydrolysis, oxidation	145.0506 ^a	ND	ND	ND	ND	ND	ND	ND	ND	ND	ND	ND	ND
Hydrolysis (acid)	255.2330 ^a	+	+	ND	ND	+	+	+	+	+	+	ND	+
Hydrolysis, hydroxylation	271.2279 ^a	ND	ND	ND	ND	ND	ND	ND	ND	ND	ND	ND	ND
Bis-hydrolysis (amine)	290.2690 ^b	+	+	ND	ND	ND	ND	ND	ND	ND	ND	+	ND
Hydrolysis, glucuronidation	431.2650 ^a	ND	ND	ND	ND	ND	ND	ND	ND	ND	ND	ND	ND
Bis-hydrolysis (amine), glucuronidation	464.2865 ^a	ND	ND	ND	ND	ND	ND	ND	ND	ND	ND	ND	ND
Bis-hydrolysis (amine), glucuronidation	466.3011 ^b	ND	ND	ND	ND	ND	ND	ND	ND	ND	ND	ND	ND
Hydrolysis (amine)	528.4986 ^b	ND	+	ND	ND	ND	ND	ND	ND	ND	ND	+	ND
Hydrolysis (amine), glucuronidation	704.5307 ^b	ND	ND	ND	ND	ND	ND	ND	ND	ND	ND	ND	ND
Oxidation to acid	778.6930 ^a	ND	ND	ND	ND	ND	ND	ND	ND	ND	ND	ND	ND
Oxidation to acid	780.7076 ^b	ND	ND	ND	ND	ND	ND	ND	ND	ND	ND	ND	ND
Hydroxylation	782.7232 ^b	ND	ND	ND	ND	ND	ND	ND	ND	ND	ND	ND	ND
Sulfation	844.6706 ^a	ND	ND	ND	ND	ND	ND	ND	ND	ND	ND	ND	ND
Sulfation	846.6851 ^b	ND	ND	ND	ND	ND	ND	ND	ND	ND	ND	ND	ND
Glucuronidation	940.7458 ^a	ND	ND	ND	ND	ND	ND	ND	ND	ND	ND	ND	ND
Glucuronidation	942.7604 ^b	ND	ND	ND	ND	ND	ND	ND	ND	ND	ND	ND	ND

Note: Both theoretical and observed metabolites are included.
 m/z = mass to charge ratio; ND = Not detected; + = metabolite present.
 a. Negative ion mode.
 b. Positive ion mode.

090177e196137069\Approved\Approved On: 21-Jan-2021 23:22 (GMT)

BNT162b2

2.6.5 Pharmacokinetics Tabulated Summary

**2.6.5.10D. PHARMACOKINETICS: METABOLISM
IN VITRO CONTINUED**

Test Article: ALC-0159
Report Number: PF-07302048_05Aug20_043725

Type of study		Metabolism of ALC-0159 In Vitro											
Study system		Blood				Hepatocytes				Liver S9 Fraction			
ALC-0159 concentration		10 µM				10 µM				10 µM			
Duration of incubation		24 h				4 h				24 h			
Analysis Method:		Ultrahigh performance liquid chromatography/ mass spectrometry											
Biotransformation	m/z	Blood				Hepatocytes				Liver S9 Fraction			
		Mouse	Rat	Monkey	Human	Mouse	Rat	Monkey	Human	Mouse	Rat	Monkey	Human
<i>O</i> -Demethylation, <i>O</i> -dealkylation	107.0703 ^b	ND	ND	ND	ND	ND	ND	ND	ND	ND	ND	ND	ND
<i>O</i> -Demethylation, <i>O</i> -dealkylation	151.0965 ^b	ND	ND	ND	ND	ND	ND	ND	ND	ND	ND	ND	ND
<i>O</i> -Demethylation, <i>O</i> -dealkylation	195.1227 ^b	ND	ND	ND	ND	ND	ND	ND	ND	ND	ND	ND	ND
Hydrolysis, <i>N</i> -Dealkylation	214.2529 ^b	ND	ND	ND	ND	ND	ND	ND	ND	ND	ND	ND	ND
<i>N</i> -Dealkylation, oxidation	227.2017 ^a	ND	ND	ND	ND	ND	ND	ND	ND	ND	ND	ND	ND
Hydrolysis (amine)	410.4720 ^b	+	+	ND	ND	+	+	+	+	+	+	+	+
<i>N,N</i> -Didealkylation	531.5849 ^b	ND	ND	ND	ND	ND	ND	ND	ND	ND	ND	ND	ND
<i>N</i> -Dealkylation	580.6396 ^b	ND	ND	ND	ND	ND	ND	ND	ND	ND	ND	ND	ND
<i>O</i> -Demethylation, oxidation	629.6853 ^b	ND	ND	ND	ND	ND	ND	ND	ND	ND	ND	ND	ND
Hydroxylation	633.6931 ^b	ND	ND	ND	ND	ND	ND	ND	ND	ND	ND	ND	ND
ω -Hydroxylation, Oxidation	637.1880 ^b	ND	ND	ND	ND	ND	ND	ND	ND	ND	ND	ND	ND
Hydrolysis (acid)	708.7721 ^b	ND	ND	ND	ND	ND	ND	ND	ND	ND	ND	ND	ND

Note: Both theoretical and observed metabolites are included.
 m/z = mass to charge ratio; ND = Not detected; + = metabolite present.
 a. Negative ion mode.
 b. Positive ion mode.

090177e196137069\Approved\Approved On: 21-Jan-2021 23:22 (GMT)